A Large-Scale Investigation of the Molecular Epidemiology and Phylogenetics of Vancomycin-Resistant *Enterococcus faecium* from Irish Hospitals: A Microbial Genomics Approach

Nicole Kavanagh

August 2024

A thesis submitted to the University of Dublin, Trinity College in fulfilment of the requirements for the degree of Doctor of Philosophy

Microbiology Research Unit,
Division of Oral Biosciences,
Dublin Dental University Hospital,
Trinity College Dublin

Declaration

I declare that this thesis has not been submitted as an exercise for a degree at this or any other university and it is entirely my own work, except where duly acknowledged in the text.

I agree to deposit this thesis in the University's open access institutional repository or allow the library to do so on my behalf, subject to Irish Copyright Legislation and Trinity College Library conditions of use and acknowledgement.

I consent to the examiner retaining a copy of the thesis beyond the examining period, should they so wish (EU GDPR May 2018).

_____

Nicole Kavanagh

Summary

Enterococcus faecium is a commensal bacterium of the human gastrointestinal tract that has emerged as an important opportunistic pathogen, particularly in immunocompromised patients. Multi-drug resistant strains, notably vancomycin resistant *E. faecium* (VREfm), constitute a substantial burden of disease globally. For over a decade, the Republic of Ireland reported some of the highest rates of resistant invasive enterococcal infection in Europe, ranging from 28.4-45.8%. Despite this, little is known about the epidemiology, population structure or transmission dynamics of *E. faecium* in Irish hospitals. Conventional bacterial typing methods, such as pulsed field gel electrophoresis (PFGE), often lack the discriminatory powers necessary to resolve complex transmission networks. However, in recent years advances in high-throughput whole-genome sequencing (WGS) technology have revolutionised investigations into the evolution, genetic diversity, and transmission of VREfm in healthcare settings. The work described in this thesis utilised high-resolution short- and long-read WGS to comprehensively investigate the VREfm population structure in seven Irish hospitals and the association of endemic, clonal lineages in the context of a protracted, retrospectively identified, silent outbreak.

The first part of this study (Chapter 3) investigated the population biology of *E. faecium* from seven Irish hospitals (H1-H7) in various geographical locations. Between June 2017 and August 2022, a total of 1,028 *E. faecium* isolates (894 screening, 102 bloodstream infection (BSI), 12 urine and 20 'other' clinical specimens) from individual patients were investigated, with the majority of isolates (73%, 753/1028) from a large Dublin acute hospital (H1). Short-read WGS and core-genome multi-locus sequence typing (cgMLST) based on 1,423 core loci using the Ridom SeqShere+ software suite (version 8.5.1, Ridom GmbH, Germany) were used to assess epidemiology. A previously published threshold of ≤20 allelic differences was used to infer genetic relationships and to deem isolates as closely related. The majority (979/1028; 95.2%) were vancomycin resistant, of which 963/978 (98.3%) harboured the *vanA* transposon (vancomycin MIC>4 mg/L). A small proportion (1.5%, 15/979) of isolates harboured both a plasmid-mediated *vanA* and a chromosomal *vanB*. All isolates belonged to hospital-adapted Clade A1, and the majority (732/1028; 72.3%) belonged to multi locus sequence type (MLST) sequence type (ST) 80. The population within major STs was highly polyclonal, with cgMLST further segregating isolates into 65 related isolate clonal complex (CT) groups and 60 singletons with an average cluster size of 15 (median: 5, range: 2-145). The most frequent CTs identified were CT2933 (*N*=145), CT1916 (*N*=116), CT1598 (*N*=64), CT1599 (*N*=58) and CT1511 (*N*=58), accounting for 43% (439/1028) of all isolates, with the three major CTs belonging to ST80. Inter and intra-hospital dissemination of highly-related clones was evident over extended time periods (up to 47 months). Additionally, the recovery of closely related (≤20 allelic differences) vancomycin susceptible *E. faecium* (VSEfm) and VREfm demonstrated the potential for the emergence of novel VREfm clones by the loss/gain of the *vanA* transposon.

Comparison of the 1,028 Irish isolates with 1,325 Clade A1 international isolates from 30 countries across six continents between 1986-2016 using cgMLST revealed very little overlap. The majority of Irish isolates (98.5%) clustered independently on distinct network branches on a cgMLST-based minimum spanning tree (MST) indicating that local evolution plays a significant role in the epidemiology of VREfm. The extrachromosomal *vanA*-regions of seven Irish VREfm representing a variety of ST and CTs (SJ10 [ST789, CT1601], SJ11 [ST1478, CT24], BSI_SJ40 [ST80, CT1598], SJ82 [ST203, CT20], SJ245 [ST117, CT2929], RC-19-039 [ST17, CT2934] and RC_19_023 [ST80, CT1916]) were fully resolved by hybrid assembly of short-read and long-read WGS sequences. The *vanA* regions varied in size and differed from the prototype Tn*1546 vanA* operon from VREfm BM4147. Differences included multiple orientations of the *vanA* operon genes, a cadmium efflux accessory protein gene insertion and additional non-coding DNA sequences including repeat regions. The SJ11*vanA* region was used as a reference for comparison against the corresponding *vanA* regions of all Irish VREfm (*N*=979) isolates; 86.3% (845/979) of isolates harboured a *vanA* region with >90% sequence identity to the SJ11*vanA*. Six of the *vanA* regions examined harboured deletions in the *tnpA* transposase gene, mainly in the 3′ end, the extent of which varied. The seven closed VREfm harboured *vanA* regions located on a diverse array of circular and linear plasmids. Linear plasmids are a novel finding in *E. faecium*, and have been previously identified in VREfm from Japan, Switzerland, and India. Linear topology of plasmids was confirmed using S1 nuclease treatment followed by PFGE. Both circular and linear plasmids harbouring *vanA* were shown to be conjugative by filter mating with a plasmid-free VSEfm recipient strain.

The second part of this study (Chapter 4) investigated the transmission and persistence of VREfm in two critical care wards (WA and WB) of H1 over 39-months using WGS. Rectal screening (*N*=330, September 2019-December 2022) and environmental (*N*=48, November 2022-December 2022) *E. faecium* were investigated using short-read WGS. Isolate relatedness was assessed by cgMLST and core-genome single nucleotide polymorphism (cgSNP) analysis. Likely transmission chains were identified using the SeqTrack algorithm (https://graphsnp.fordelab.com) based on cgSNP data and recovery location. Well-characterized *E. faecium* (*N*=908) from seven Irish hospitals including H1 (June 2017-July 2022) were also investigated. In total, 378 *E. faecium* isolates recovered over 39 months from wards WA and WB of H1 were analysed, including 330 rectal screening isolates (WA, 109 (33%); WB, 221 (67%)). Twenty-eight environmental isolates were recovered from 3/13 handwash basin drains (19 from two WA drains and nine from one WB drain). An additional 20 environmental isolates were recovered from surface sampling of near-patient high-touch ward sites. All patient isolates were *vanA*-encoding VREfm. The majority (43/48, 89%) of environmental isolates

were VSEfm and five were *vanA*-encoding VREfm. cgMLST identified three predominant ST80 CTs (CT2933, CT2932 and CT1916) (55% of isolates) of related isolates (≤20 allelic differences). cgSNP analysis differentiated these CTs into multiple distinct closely related genomic clusters (≤10 cgSNPs). Parsimonious network construction identified 55 likely inter- and intra-ward transmissions with epidemiological support (≤30 days) between patients involving 73 isolates (≤10 cgSNPs) from seven genomic clusters. Numerous other likely transmissions over longer time periods without evident epidemiological links were identified, suggesting persistence and unidentified reservoirs contribute to dissemination. The three CTs predominated among *E. faecium* (*N*=1286) in seven hospitals, highlighting inter-hospital spread and cross-institutional dominance without known epidemiological links. *In silico* analysis using ABRicate v.0.9.8 (https://github.com/tseemann/abricate) of VSEfm short-reads identified four environmental isolates harbouring *vanA* operon remnants including the *vanZ* and *vanY* genes, but lacking the *vanHAX* and *vanRS* genes. One isolate (JHE024) was fully closed by hybrid assembly, which identified *vanZ* and *vanY* on an 88,110 bp circular plasmid. The organization of the *van* remnant and adjacent sequences were similar to *vanA* regions on plasmids in Irish VREfm, indicating the VSEfm may have arisen from a VREfm ancestor. These findings highlight that VSEfm carriage should be considered in Infection Prevention and Control (IPC) surveillance policies.

The final part of this study (Chapter 5) hypothesised that within-patient diversity and the presence of multiple VREfm and VSEfm co-colonising strains could complicate transmission analysis and explain the diverse array of Tn*1546*-like *vanA* transposon iterations found in Chapter 3. A total of 150 VREfm colonies were sequenced from rectal screens from 10 patients (15 isolates per patient, P1-P10) on seven H1 wards (W1 *N*=1, W2 *N*=1, W3 *N*=4, W9 *N*=1, W18 *N*=1, W20 *N*=1, WE *N*=1). The majority (70%, 7/10) of patients harboured a diverse colonising population, consisting of two (*N*=4), three (*N*=2) or four (*N*=1) unique VREfm CTs. A high level of genomic variation was observed between isolate pairs from different CTs within the same patient using split *k*-mer analysis suggesting distinct VREfm acquisition events. The cgMLST-based MST revealed three CTs (CT2933, CT6489 and CT6738) each consisting of closely related (<20 allelic differences) VREfm from multiple patients recovered between October 2022-Janurary 2023 (105 days) suggesting possible direct and/or indirect transmission. Further analysis of the VREfm (*N*=150) with an additional 622 isolates from Chapter 3 from individual patients and environmental sites (VREfm *N*=579, VSEfm *N*=43) from the same seven H1 wards (W1 *N*=107, W2 *N*=156, W3 *N*=327, W9 *N*=7, W18 *N*=22 and W20 *N*=3), provided further evidence for the persistence of highly-related minority subpopulations across multiple H1 wards. These findings highlight the limitations of single-colony sampling strategies used currently in outbreak investigations.

Plasmid sequences from a representative subset of 39 rectal screening VREfm from the 10 patients (P1 *N*=6, P2 *N*=2, P3 *N*=3, P4 *N*=4, P5 *N*=5, P6 *N*=4, P7 *N*=4, P8 *N*=7, P9 *N*=2 and P10 *N*=2) were fully resolved by hybrid assembly of short-read and long-read WGS sequences. A total of 193 plasmids were identified in the 39 VREfm. Pairwise plasmid genetic relatedness (*N*=193) was assessed using a reference-free approach based on Mash distances (https://github.com/marbl/Mash). Using a mash threshold of ≤0.0001, equivalent to ≥99.5% average nucleotide identity, near-identical plasmids were identified in genetically divergent *E. faecium* subtypes, both within the same patient and multiple patients. Among the 39 within-patient VREfm investigated in detail from patients P1-P10, 72% (28/39) harboured *vanA* on linear plasmids belonging to a discrete cluster, suggesting acquisition of *vanA* is an important factor driving the evolution of linear plasmids in Irish VREfm. Examination of the structural organisation of the *van* operon from the 39 VREfm revealed the presence of identical *vanA* regions (≥99.9% average nucleotide identity) in clonally divergent CTs within the same patient. There were also many examples of distinct iterations of the *van* transposon carried by multiple diverse CTs within the same patient. These findings serve to highlight the promiscuous nature of the Tn*1546*-like *vanA* transposon and its ability to utilise a variety of plasmid types to facilitate dissemination.

Finally, four of the VREfm-positive rectal swabs (patients P1, P3, P5 and P8) were selected to provide a snap-shot of VSEfm carriage in the patient cohort. Thirty VSEfm were identified among 80 colonies screened. All 30 VSEfm belonged to Clade A1, the majority belonged to ST80 (25/30) with the remainder belonging to ST203. An MST based on cgMLST analysis of the study VREfm (*N*=150) and VSEfm (*N*=30) revealed two distinct CT clusters (≤20 allelic differences) comprising mixtures of VSEfm and VREfm from the same patient. Hybrid assembly of four representative VSEfm from distinct CTs revealed highly similar plasmidomes compared to VREfm. However, in some cases, genetically closely related VSEfm and VREfm from the same patient exhibited plasmidome differences.

In conclusion, this study constitutes the first comprehensive investigation of the epidemiology and population structure of clade A1 *E. faecium* from hospital patients in the Republic of Ireland using a WGS approach. The study revealed that ST80 has emerged as the predominant endemic *E. faecium* lineage in Ireland. A diverse and polyclonal population was identified within the major STs including ST80, which were segregated further into genetically distinct sub-lineages using cgSNP or SKA analysis. Irish VREfm were found to harbour multiple distinct iterations of the *vanA* TN*1546*-like transposon enriched with IS*1216E* elements which likely facilitate spread. Large linear plasmids were found to be the major vehicle of *vanA* dissemination in Irish VREfm. The diversity of VREfm clones identified and their widespread intra- and inter-hospital dissemination, highlight the need for improved surveillance and review of national IPC guidelines. The extensive within-patient VREfm diversity identified warrants the urgent development of novel screening tests to rapidly identify co-colonized patients to inform outbreak investigations.

Table of Contents

Acknowledgements ..... **i**
Index of Tables ..... **iii**
Index of Figures ..... **xii**
Abbreviations ..... **xx**
Publications ..... **xxv**
Chapter 1 General Introduction **1**
1.1 *Enterococcus* species 2
1.2 *E. faecium* colonisation and hospital transmission 3
1.3 *E. faecium*: a promiscuous bacterium living in a plastic world 6
1.3.1 The core genome: attack of the clones 6
1.3.2 The accessory genome 8
1.3.2.1 Plasmids 10
1.3.2.2 Transposable elements 10
1.4 Mechanisms of antimicrobial resistance 13
1.4.1 β-lactam resistance 13
1.4.2 Aminoglycoside resistance 14
1.4.3 Glycopeptide resistance 16
1.4.4 Linezolid resistance 22
1.5 Prevalence of VREfm in Ireland 23
1.6 Clinical burden of VREfm 26
1.7 Economic burden of VREfm 29
1.8 Traditional molecular typing methods 30
1.8.1 PFGE 32
1.8.2 MLST 32
1.9 Whole-genome sequencing 34
1.9.1 Second generation sequencing 34
1.9.2 Third generation sequencing 35
1.10 Applying a WGS approach to VREfm surveillance 38
1.10.1 Comparative genomics 38
1.10.1.1 cgMLST 38
1.10.1.2 wgMLST 39
1.10.1.3 Analysis of single nucleotide polymorphisms 39
1.10.1.4 The *k*-mer revolution 40
1.10.2 Accessory genome analysis 42
1.11 Project aims 43
Chapter 2 General Materials and Methods **44**
2.1 Bacterial isolates 45
2.1.1 Ethical approval 45
2.2 General microbiological methods 45
2.2.1 Microbial culture and long-term storage 45

2.2.2 Chemicals, reagents, and buffers 45
2.3 Isolate identification and antimicrobial susceptibility testing 48
2.3.1 Conventional culture and identification 48
2.3.2 Antimicrobial susceptibility testing 48
2.4 DNA extraction for whole-genome sequencing 50
2.4.1 Qiagen DNeasy Blood and Tissue 50
2.4.2 Qiagen HMW MagAttract 50
2.4.3 Quality assurance of extracted DNA 51
2.5 Whole-genome sequencing 51
2.5.1 Second generation sequencing 51
2.5.1.1 Library preparation 52
2.5.1.1.1 Tagmentation and clean-up 52
2.5.1.1.2 Amplification of tagmented libraries 52
2.5.1.1.3 PCR clean-up 52
2.5.1.2 Quantification of library preparation concentrations 53
2.5.1.3 Library denaturation and MiSeq loading 53
2.5.1.4 Post run quality assurance and processing 53
2.5.2 Third generation WGS 54
2.5.2.1 Library preparation 54
2.5.2.1.1 DNA repair and end-prep 54
2.5.2.1.2 Native barcode ligation 55
2.5.2.1.3 Adapter ligation and clean-up 55
2.5.2.2 Priming and loading the SpotON flow cell 56
2.5.2.3 Post sequencing processing 56
2.6 Bioinformatic Analysis 56
2.6.1 Second generation WGS 56
2.6.1.1 Data export and read trimming 56
2.6.1.2 *de novo* assembly 57
2.6.1.3 Molecular typing 57
2.6.1.4 Whole-genome multi-locus sequence typing (wgMLST) 57
2.6.1.5 Core-genome multi-locus sequence typing (cgMLST) 58
2.6.1.6 Genotyping 58
2.6.1.7 Quality assurance 58
2.6.1.8 Phylogenetic tree analysis 58
2.7 Hybrid assembly 59
2.8 Analysis of plasmid profiles 59
2.8.1 Plasmid profile determination 59
2.8.2 Genetic organisation of *vanA*-encoding regions and plasmids 59
2.8.3 Pulse-Field Gel Electrophoresis 60
2.8.4 Filter mating 60
Chapter 3 Genomic analysis of vancomycin-resistant *Enterococcus faecium* from Irish hospitals reveals a high prevalence of ST80 and spread of similar *vanA* regions via IS*1216E* and plasmid transfer in diverse genetic lineages 62
3.1 Introduction 63

3.2 Materials and Methods 65
3.2.1 Isolate collection 65
3.2.1.1 Patient isolates 65
3.2.1.2 International comparator reference isolates 66
3.2.2 Phenotypic susceptibility testing 66
3.2.3 Second generation Illumina short-read sequencing 66
3.2.3.1 Genomic DNA Extraction 66
3.2.3.2 Short-read sequencing 66
3.2.4 Third generation MinION long-read sequencing 66
3.2.4.1 Genomic DNA Extraction 66
3.2.4.2 Long-read sequencing 66
3.2.5 Bioinformatic analysis 67
3.2.5.1 *de novo* assembly 67
3.2.5.2 MLST 67
3.2.5.3 wgMLST and cgMLST 67
3.2.5.4 Genotyping 67
3.2.5.5 Phylogenetic trees 67
3.2.5.5.1 Neighbour joining tree 67
3.2.6 Hybrid assembly 67
3.2.7 Plasmid analysis 68
3.2.7.1 Plasmid profile determination 68
3.2.7.2 Genetic organisation of *vanA*-encoding regions and plasmids 68
3.2.8 Filter mating 68
3.3 Results 69
3.3.1 Genomic epidemiology of Irish hospital *E. faecium* 69
3.3.2 Irish, global and Danish *E. faecium* comparison 85
3.3.3 Structural organization of the *van* region in Irish VREfm 97
3.3.4 Transmission of *vanA* via IS*1216E*-mediated transposition and circular plasmid conjugation 105
3.3.5 Identification of novel linear plasmids encoding *vanA* 120
3.3.6 Conjugative ability of linear plasmids encoding *vanA* 130
3.3.7 Final confirmation of linear topology using PFGE analysis 138
3.4 Discussion 140
Chapter 4 Protracted transmission and persistence of ST80 vancomycin-resistant *Enterococcus faecium* clonal complex types CT2933, CT2932 and CT1916 in a large Irish hospital: a 39-month genomic study 147
4.1 Introduction 148
4.2 Materials and methods 150
4.2.1 Isolate collection 150
4.2.1.1 Patient isolates 150
4.2.1.2 Environmental isolates 150
4.2.1.3 Irish comparator reference isolates 155
4.2.2 Infection control procedures and antimicrobial stewardship 156
4.2.3 Phenotypic susceptibility testing 156
4.2.4 Second generation Illumina short-read sequencing 156

4.2.4.1 Genomic DNA Extraction 156
4.2.4.2 Short-read sequencing 156
4.2.5 Third generation MinION long-read sequencing 157
4.2.5.1 Genomic DNA Extraction 157
4.2.5.1.1 Wizard HMW DNA Extraction 157
4.2.5.2 Long-read sequencing 158
4.2.5.2.1 Library preparation (Native Barcoding Kit 24 v14) 159
4.2.5.3 Priming and loading the SpotON flow cell 160
4.2.5.4 Post sequencing processing 160
4.2.6 Bioinformatic analysis 161
4.2.6.1 *de novo* assembly 161
4.2.6.2 MLST 161
4.2.6.3 wgMLST and cgMLST 161
4.2.6.4 Genotyping 161
4.2.6.5 Core-genome SNP analysis 161
4.2.6.6 Phylogenetic trees 162
4.2.6.6.1 Neighbour joining tree 162
4.2.6.6.2 Maximum likelihood tree 162
4.2.6.6.3 Parsimonious transmission tree 162
4.2.7 Hybrid assembly 163
4.3 Results 164
4.3.1 Isolate description 164
4.3.2 Major cgMLST clusters of *E. faecium* 164
4.3.3 cgSNP analysis identifies closely related *E. faecium* subclusters 168
4.3.3.1 CT Cluster CI 171
4.3.3.2 CT Cluster CII 178
4.3.3.3 CT Cluster CIII 184
4.3.4 VRE transmission and persistence 190
4.3.4.1 CI 190
4.3.4.2 CII and CIII 197
4.3.5 Inter-hospital VRE transmission 202
4.3.6 VSEfm harbouring *van* remnants 227
4.4 Discussion 230
Chapter 5 Multi-strain gastrointestinal carriage of genetically diverse vancomycin-resistant Clade A1 *Enterococcus faecium* amongst Irish patients with frequent health-care exposure – one pick to represent them all! 235
5.1 Introduction 236
5.2 Materials and Methods 237
5.2.1 Isolate collection 237
5.2.1.1 Patient isolates 237
5.2.2 Phenotypic susceptibility testing 237
5.2.3 Second generation Illumina short-read sequencing 237
5.2.3.1 Genomic DNA Extraction 237
5.2.3.2 Short-read sequencing 238

5.2.4 Third generation MinION long-read sequencing 238
5.2.5 Bioinformatic analysis 238
5.2.5.1 *de novo* assembly 238
5.2.5.2 MLST 238
5.2.5.3 wgMLST and cgMLST 238
5.2.5.4 Genotyping 238
5.2.5.5 Split *k*-mer analysis 239
5.2.5.6 Phylogenetic trees 239
5.2.5.6.1 Neighbour joining tree 239
4.2.5.6.2 Maximum likelihood tree 239
5.2.6 Hybrid assembly 239
5.2.7 Plasmid analysis 239
5.2.7.1 Plasmid profile determination 239
5.2.8 Filter mating 240
5.2.9 PFGE 240
5.3 Results 241
5.3.1 Isolate description 241
5.3.2 Heterogeneity of within-patient VREfm colonisation 241
5.3.3 Whole-genome comparisons reveal potential transmission of minor frequency strains 255
5.3.4 Heterogeneity of VREfm colonisation: do minor frequency strains represent an unsampled 'hidden highway' of transmission? 257
5.3.5 Exploring the complex plasmidome dynamics of VREfm strains from patients co-colonised with multiple strains 262
5.3.6 Pairwise Mash distance-based clustering of plasmids 271
5.3.7 Linear plasmids as key vehicles of *vanA* dissemination 276
5.3.8 Analysis of the impact of within-patient VREfm diversity on the Tn*1546*-like *vanA* transposon 282
5.3.9 Analysis of Tn*1546*-like *vanA* regions within diverse *E. faecium* clonal lineages reveals no association between transposon iterations and complex type 286
5.3.10 A snap-shot of VSEfm carriage 291
5.4 Discussion 300
5.5 Appendix 308
Chapter 6 General Discussion 360
6.1 VREfm in Ireland: a game of clones 361
6.2 Out of sight, not out of existence: is it time to rethink VRE surveillance? 363
6.2.1 Cost-benefit ratio 364
6.2.2 Resource requirements 368
6.2.3 Suboptimal infrastructure 369
6.2.4 Environmental screening 371
6.2.5 VSEfm surveillance 372
6.3 Implications of unprecedented VREfm transmission: enterococcal plasmids, here and there, or absolutely everywhere? 373
6.3.1 Better the devil you know than the devil you don't – interspecies dissemination of vancomycin resistance and pan-resistant *E. faecium* 374
6.4 The application of WGS-based typing methods in *E. faecium* 376
6.5 Future work 377

6.6 Concluding remarks 378
Bibliography 380
Appendix 1 425
Appendix 2 526

Acknowledgements

First and foremost, I would like to express my sincere thanks to my supervisor, Professor David Coleman, for his invaluable advice, continuous support, endless patience and encouragement throughout this PhD project. I have learned so much from your expertise and I am truly grateful to have had the opportunity to work under your supervision. Thank you for all the wonderful opportunities you have given me over the last number of years. I would also like to thank Dr. Brenda McManus for her thoughtful comments, constructive criticism and valuable insights throughout this experience – thank you for taking me under your wing as your adopted student. I will always be grateful for your guidance. I would also like to thank Dr. Peter Kinnevey for his guidance and encouragement (particularly during the horrors of our first paper submission).

I wish to express my sincere gratitude to the Health Research Board of Ireland for providing the funding for this project (ILP-POR-2019-010). Also, a huge thank you to the Microbiology Research Unit, Dublin Dental University Hospital for the additional financial support. I would also like to acknowledge and thank Dr. Mary O'Donnell for her work as laboratory manager. I always appreciated the afternoon chats about all things makeup, skincare and of course the cute pictures of your kittens. I will really miss the Christmas drinks in the common room.

I wish to thank the staff at the National MRSA Reference Laboratory who assisted me greatly in this research and to all their service users who contributed samples throughout this project. In particular, I would like to thank Dr. Gráinne Brennan and Dr. Brian O'Connell for their invaluable support. Additionally, I would like to express my gratitude to Professor Fidelma Fitzpatrick and the staff in Beaumont Microbiology laboratory for their valuable contributions and willingness to always help. A massive thank you to Professor Richard Goering and the staff in the Medical Microbiology and Immunology department in Creighton University (USA) – I am very grateful for all of the PFGE data and technical guidance.

A huge thank you to all the staff and students in the Microbiology Research unit, both past and present. Thank you all for making me feel so welcome and for all the support, friendship and most importantly the laughs. A very special thank you to Dr. Claire Crowley for being the most amazing support and friend I could have ever imagined – thank you for sharing a brain-cell with me, for the unhinged turbo-common room coffees (T-CRC) at 5pm and the 4am text messages. I could write another thesis about how much I appreciate you,

but instead I will just say one thing – slay! A massive shout-out to Dr. Bisola Aloba (my bae-bay) and Dr. Emily Deasy for the constant ridiculous conversations, never-ending laughs, 4pm karaoke sessions and most importantly for being the best people I could have asked for to share this experience with. A big thank you to Liam, James, AJ, Melvin, Michaela and Ross for all the chats, Fika Fridays, Kilkenny breakfasts, ice-cream breaks, Lincoln chicken strips and for being the most fun, supportive and encouraging friends. A massive thank you to the past lab members (Dr. Megan Earles, Dr. Elaine Moloney and Dr. Jessica Fletcher). To Dr. Sarah Egan thank you for your guidance, patience and helping me find my feet in the lab when I first started.

To my friends, particularly Beka, Lea and Cliodhna, thank you for always cheering me on and picking me up when I am down. I am forever grateful for our friendship and can't wait to navigate the next chapter of our lives together.

Most importantly, I am extremely thankful to my family, whose unwavering support and encouragement have been the foundation of my thesis journey. To my parents, Loraine and Edward, thank you for showing me the value of hard work, perseverance and curiosity. Your constant belief in my abilities and your endless love have been a constant source of strength. To my Nanna, I never forgot our promise – I hope I am doing you proud. To my older sister, Michelle, thank you for always being there to listen, support me and provide much needed perspective during challenging times. I'm lucky to have you as both a sister and best friend. To my wonderful nieces and nephews; Harry, Charlie, Eoghan, Cillian and Aoíbhin, for always putting a smile on my face and giving the best cuddles.

Saving the very best and most important for last - a very special thank you to my fiancé Conor. I cannot put in to words my gratitude for your patience, understanding and unwavering belief in me, particularly during the many late nights, weekends and moments of doubts. You have been my rock, my motivator and my biggest supporter, and I am so fortunate to have you by my side. Thank you for believing in me when I struggled to believe in myself and this honestly would not have been possible without you. I look forward to all the future holds for us.

Index of Tables

Table	Title	Page
1.1	Overview of the phenotypic and genotypic characteristics of the nine glycopeptide resistance operons identified in enterococci.	**18**
1.2	Molecular typing methods available for investigation and discrimination of VREfm	**31**
2.1	Details of the 2,911 *E. faecium* isolates investigated in the present study	**47**
2.2	Antimicrobial agents and antimicrobial susceptibility MIC breakpoints used in the present study	**49**
3.1a	Detailed metadata and distance matrices based on cgMLST analysis of global cluster 1 identified in a minimum spanning tree (MST) based on Irish Clade A1 *E. faecium* (*N*=1,028) and global Clade A1 *E. faecium* (*N*=1,325) (Figure 3.7)	**89**
3.1b	Detailed metadata and distance matrices based on cgMLST analysis of global cluster 2 identified in a minimum spanning tree (MST) based on Irish Clade A1 *E. faecium* (*N*=1,028) and global Clade A1 *E. faecium* (*N*=1,325) (Figure 3.7)	**90**
3.1c	Detailed metadata and distance matrices based on cgMLST analysis of global cluster 3 identified in a minimum spanning tree (MST) based on Irish Clade A1 *E. faecium* (*N*=1,028) and global Clade A1 *E. faecium* (*N*=1,325) (Figure 3.7)	**91**
3.1d	Detailed metadata and distance matrices based on cgMLST analysis of global cluster 4 identified in a minimum spanning tree (MST) based on Irish Clade A1 *E. faecium* (*N*=1,028) and global Clade A1 *E. faecium* (*N*=1,325) (Figure 3.7)	**92**
3.1e	Detailed metadata and distance matrices based on cgMLST analysis of global cluster 5 identified in a minimum spanning tree (MST) based on Irish Clade A1 *E. faecium* (*N*=1,028) and global Clade A1 *E. faecium* (*N*=1,325) (Figure 3.7)	**93**
3.1f	Detailed metadata and distance matrices based on cgMLST analysis of global cluster 6 identified in a minimum spanning tree (MST) based on	**94**

Table	Title	Page
	Irish Clade A1 *E. faecium* (*N*=1,028) and global Clade A1 *E. faecium* (*N*=1,325) (Figure 3.7)	
3.2	Coding sequences of linear plasmid pELF_BSI_SJ40 (131,341 bp) from *E. faecium* isolate BSI_SJ40 (ST80, CT1598) with putative protein products annotated with RAST, Prokka and EGGNOG mapper pipelines	**123**
3.3	Coding sequences of linear plasmid pELF_SJ11 (116,749 bp) from *E. faecium* isolate SJ11 (non-typeable by conventional MLST, CT24) with putative protein products annotated with RAST, Prokka and EGGNOG mapper pipelines	**126**
4.1	Detailed metadata on isolates recovered from positive environmental sites in Ward A and Ward B (*N*=48)	**154**
4.2	Detailed descriptions of three major complex types (CI, CII, CIII), subclusters and their related isolate groups (RIGs) identified using cgMLST and cgSNP analysis of 378 clade A1 *Enterococcus faecium* isolates from two critical care wards (W1 and W2) of a large Dublin acute hospital recovered between September 2019 and December 2022	**169**
4.3a	Detailed metadata and distance matrices based on pairwise cgSNP analysis of related isolate group CIA1 identified in sub-cluster CIA from CI (ST80/CT2933 lineage)	**174**
4.3b	Detailed metadata and distance matrices based on pairwise cgSNP analysis of related isolate group CIA2 identified in sub-cluster CIA from CI (ST80/CT2933 lineage)	**175**
4.3c	Detailed metadata and distance matrices based on pairwise cgSNP analysis of related isolate group CIA3 identified in sub-cluster CIA from CI (ST80/CT2933 lineage)	**176**
4.4a	Detailed metadata and distance matrices based on cgSNP analysis of related isolate group CIIA1 identified in sub-cluster CIIA from CII (ST80/CT2932 lineage)	**181**
4.4b	Detailed metadata and distance matrices based on cgSNP analysis of related isolate group CIIA2 identified in sub-cluster CIIA from CII (ST80/CT2932 lineage)	**182**

Table	Title	Page
4.4c	Detailed metadata and distance matrices based on cgSNP analysis of related isolate group CIIB1 identified in sub-cluster CIIA from CII (ST80/CT2932 lineage)	**183**
4.5a	Detailed metadata and distance matrices based on cgSNP analysis of related isolate group CIIIB1 identified in sub-cluster CIIIB from CIII (ST80/CT1916 lineage)	**187**
4.5b	Detailed metadata and distance matrices based on cgSNP analysis of related isolate group CIIIB2 identified in sub-cluster CIIIB from CIII (ST80/CT1916 lineage)	**188**
4.5c	Detailed metadata and distance matrices based on cgSNP analysis of related isolate group CIIIB2 identified in sub-cluster CIIIB from CIII (ST80/CT1916 lineage)	**189**
4.6a	Detailed metadata and distance matrices based on pairwise cgSNP analysis of RIG CIA1 identified in sub-cluster CIA from CI (ST80/CT2933 lineage) with additional isolates from database	**206**
4.6b	Detailed metadata and distance matrices based on pairwise cgSNP analysis of RIG CIA2 identified in sub-cluster CIA from CI (ST80/CT2933 lineage) with additional isolates from database	**207**
4.6c	Detailed metadata and distance matrices based on pairwise cgSNP analysis of RIG CIA3 identified in sub-cluster CIA from CI (ST80/CT2933 lineage) with additional isolates from database	**208**
4.6d	Detailed metadata and distance matrices based on pairwise cgSNP analysis of RIG CIA4 identified in sub-cluster CIA from CI (ST80/CT2933 lineage) with additional isolates from database	**209**
4.6e	Detailed metadata and distance matrices based on pairwise cgSNP analysis of RIG CIA5 identified in sub-cluster CIA from CI (ST80/CT2933 lineage) with additional isolates from database	**210**
4.6f	Detailed metadata and distance matrices based on pairwise cgSNP analysis of RIG CIB1 identified in sub-cluster CIB from CI (ST80/CT2933 lineage) with additional isolates from database	**211**
4.7a	Detailed metadata and distance matrices based on pairwise cgSNP analysis of RIG CIIA1 identified in sub-cluster CIIA from CII (ST80/CT2932 lineage) with additional isolates from database	**214**

Table	Title	Page
4.7b	Detailed metadata and distance matrices based on pairwise cgSNP analysis of RIG CIIA2 identified in sub-cluster CIIA from CII (ST80/CT2932 lineage) with additional isolates from database	**215**
4.7c	Detailed metadata and distance matrices based on pairwise cgSNP analysis of RIG CIIA3 identified in sub-cluster CIIA from CII (ST80/CT2932 lineage) with additional isolates from database	**216**
4.7d	Detailed metadata and distance matrices based on pairwise cgSNP analysis of RIG CIIB1 identified in sub-cluster CIIB from CII (ST80/CT2932 lineage) with additional isolates from database	**217**
4.8a	Detailed metadata and distance matrices based on pairwise cgSNP analysis of RIG CIIIB1 identified in sub-cluster CIIIB from CIII (ST80/CT1916 lineage) with additional isolates from database	**220**
4.8b	Detailed metadata and distance matrices based on pairwise cgSNP analysis of RIG CIIIB2 identified in sub-cluster CIIIB from CIII (ST80/CT1916 lineage) with additional isolates from database	**221**
4.8c	Detailed metadata and distance matrices based on pairwise cgSNP analysis of RIG CIIIB3 identified in sub-cluster CIIIB from CIII (ST80/CT1916 lineage) with additional isolates from database	**222**
4.8d	Detailed metadata and distance matrices based on pairwise cgSNP analysis of RIG CIIIB4 identified in sub-cluster CIIIB from CIII (ST80/CT1916 lineage) with additional isolates from database	**223**
4.8e	Detailed metadata and distance matrices based on pairwise cgSNP analysis of RIG CIIIB5 identified in sub-cluster CIIIB from CIII (ST80/CT1916 lineage) with additional isolates from database	**224**
5.1	Detailed metadata and distribution of complex types (CT)s for 150 Clade A1 VREfm isolates recovered from a single rectal screening swab from each of 10 separate patients	**244**
5.2a	Pairwise single nucleotide polymorphism (SNP) distance matrix based on split *k*-mer analysis (SKA) of 15 isolates recovered from patient P1	**252**
5.2b	Pairwise single nucleotide polymorphism (SNP) distance matrix based on split *k*-mer analysis (SKA) of 15 isolates recovered from patient two (P2)	**306**

Table	Title	Page
5.2c	Pairwise single nucleotide polymorphism (SNP) distance matrix based on split *k*-mer analysis (SKA) of 15 isolates recovered from patient three (P3)	**307**
5.2d	Pairwise single nucleotide polymorphism (SNP) distance matrix based on split *k*-mer analysis (SKA) of 15 isolates recovered from patient four (P4)	**308**
5.2e	Pairwise single nucleotide polymorphism (SNP) distance matrix based on split *k*-mer analysis (SKA) of 15 isolates recovered from patient five (P5)	**309**
5.2f	Pairwise single nucleotide polymorphism (SNP) distance matrix based on split *k*-mer analysis (SKA) of 15 isolates recovered from patient six (P6)	**310**
5.2g	Pairwise single nucleotide polymorphism (SNP) distance matrix based on split *k*-mer analysis (SKA) of 15 isolates recovered from patient seven (P7)	**311**
5.2h	Pairwise single nucleotide polymorphism (SNP) distance matrix based on split *k*-mer analysis (SKA) of 15 isolates recovered from patient eight (P8)	**312**
5.2i	Pairwise single nucleotide polymorphism (SNP) distance matrix based on split *k*-mer analysis (SKA) of 15 isolates recovered from patient nine (P9)	**313**
5.2j	Pairwise single nucleotide polymorphism (SNP) distance matrix based on split *k*-mer analysis (SKA) of 15 isolates recovered from patient ten (P10)	**314**
5.3a	Pairwise single nucleotide polymorphism (SNP) distance matrix based on split *k*-mer analysis (SKA) of VREfm belonging to complex type (CT) 1898 identified using core-genome multi-locus sequence type (cgMLST) analysis of 150 Clade A1 VREfm isolates recovered from a single rectal screening swab from each of 10 separate patients (Figure 5.1)	**254**
5.3b	Pairwise single nucleotide polymorphism (SNP) distance matrix based on split *k*-mer analysis (SKA) of eleven VREfm belonging to complex type (CT) 1916 identified using core-genome multi-locus sequence type (cgMLST) analysis of 150 Clade A1 VREfm isolates recovered	**315**

Table	Title	Page
	from a single rectal screening swab from each of 10 separate patients (Figure 5.1)	
5.3d	Pairwise single nucleotide polymorphism (SNP) distance matrix based on split *k*-mer analysis (SKA) of eight VREfm belonging to complex type (CT) 2932 identified using core-genome multi-locus sequence type (cgMLST) analysis of 150 clade A1 VREfm isolates recovered from a single rectal screening swab from each of 10 separate patients (Figure 5.1)	**317**
5.3e	Pairwise single nucleotide polymorphism (SNP) distance matrix based on split *k*-mer analysis (SKA) of 48 VREfm belonging to complex type (CT) 6489 identified using core-genome multi-locus sequence type (cgMLST) analysis of 150 clade A1 VREfm isolates recovered from a single rectal screening swab from each of 10 separate patients (Figure 5.1)	**318**
5.3f	Pairwise single nucleotide polymorphism (SNP) distance matrix based on split *k*-mer analysis (SKA) of 11 VREfm belonging to complex type (CT) 6738 identified using core-genome multi-locus sequence type (cgMLST) analysis of 150 clade A1 VREfm isolates recovered from a single rectal screening swab from each of 10 separate patients (Figure 5.1)	**319**
5.3g	Pairwise single nucleotide polymorphism (SNP) distance matrix based on split *k*-mer analysis (SKA) of 15 VREfm belonging to complex type (CT) 7537 identified using core-genome multi-locus sequence type (cgMLST) analysis of 150 clade A1 VREfm isolates recovered from a single rectal screening swab from each of 10 separate patients (Figure 5.1)	**320**
5.3h	Pairwise single nucleotide polymorphism (SNP) distance matrix based on split *k*-mer analysis (SKA) of five VREfm belonging to complex type (CT) 7567 identified using core-genome multi-locus sequence type (cgMLST) analysis of 150 clade A1 VREfm isolates recovered from a single rectal screening swab from each of 10 separate patients (Figure 5.1)	**321**
5.4a	Pairwise single nucleotide polymorphism (SNP) distance matrix based on split *k*-mer analysis (SKA) of *E. faecium* isolates (*N*=151)	**259**

Table	Title	Page
	belonging to complex type (CT) 2933 identified using core-genome multi-locus sequence type (cgMLST) analysis of 43 Clade A1 VREfm recovered from patients P1 (*N*=10), P4 (*N*=5), P6 (*N*=13), P7 (*N*=14) and P7 (*N*=1) with additional isolates from database (*N*=108) (Figure 5.4)	
5.4b	Pairwise single nucleotide polymorphism (SNP) distance matrix based on split *k*-mer analysis (SKA) of *E. faecium* isolates (*N*=80) belonging to complex type (CT) 2932 identified using core-genome multi-locus sequence type (cgMLST) analysis of eight Clade A1 VREfm recovered from patient P8 with additional isolates from database (*N*=72)	**322**
5.4c	Pairwise single nucleotide polymorphism (SNP) distance matrix based on split *k*-mer analysis (SKA) of *E. faecium* isolates (*N*=81) belonging to complex type (CT) 1916 identified using core-genome multi-locus sequence type (cgMLST) analysis of 11 Clade A1 VREfm recovered from patient P5 with additional isolates from database (*N*=70) (Figure 5.4	**323**
5.4d	Pairwise single nucleotide polymorphism (SNP) distance matrix based on split *k*-mer analysis (SKA) of *E. faecium* isolates (*N*=56) belonging to complex type (CT) 6489 identified using core-genome multi-locus sequence type (cgMLST) analysis of 48 Clade A1 VREfm recovered from patient P1 (*N*=5), P2 (*N*=14), P3 (*N*=12), P6 (*N*=2) and P9 (*N*=15) with additional isolates from database (*N*=8) (Figure 5.4)	**324**
5.4e	Pairwise single nucleotide polymorphism (SNP) distance matrix based on split *k*-mer analysis (SKA) of *E. faecium* isolates belonging to complex type (CT) 6738 identified using core-genome multi-locus sequence type (cgMLST) analysis of eleven Clade A1 VREfm recovered from patient P1 (*N*=1) and P4 (*N*=10) (Figure 5.4)	**325**
5.4f	5.4f. Pairwise single nucleotide polymorphism (SNP) distance matrix based on split *k*-mer analysis (SKA) of *E. faecium* (*N*=9) isolates belonging to complex type (CT) 1898 identified using core-genome multi-locus sequence type (cgMLST) analysis of three clade A1 VREfm recovered from patient P3 with additional isolates from database1 (*N*=6) (Figure 5.4)	**326**

Table	Title	Page
5.4g	Pairwise single nucleotide polymorphism (SNP) distance matrix based on split *k*-mer analysis (SKA) of *E. faecium* isolates (*N*=4) belonging to complex type (CT) 3395 identified using core-genome multi-locus sequence type (cgMLST) analysis of two clade A1 VREfm recovered from patient P5 with additional isolates from database1 (*N*=2) (Figure 5.4)	**327**
5.4h	Pairwise single nucleotide polymorphism (SNP) distance matrix based on split *k*-mer analysis (SKA) of *E. faecium* isolates (*N*=18) belonging to complex type (CT) 1921 identified using core-genome multi-locus sequence type (cgMLST) analysis of one Clade A1 VREfm recovered from patient P7 with additional isolates from database (*N*=17) (Figure 5.4)	**328**
5.4i	Pairwise single nucleotide polymorphism (SNP) distance matrix based on split *k*-mer analysis (SKA) of *E. faecium* isolates (*N*=6) belonging to complex type (CT) 7567 identified using core-genome multi-locus sequence type (cgMLST) analysis of five clade A1 VREfm recovered from patient P8 with additional isolates from database1 (*N*=1) (Figure 5.4)	**329**
5.5	Plasmid profiles and antimicrobial resistance gene repertoire of VREfm isolates closed by hybrid assembly (*N*=39)	**261**
5.6a	Detailed metadata and pairwise distance matrices based on MASH distance estimation of plasmid cluster C1	**273**
5.6b	Detailed metadata and pairwise distance matrices based on MASH distance estimation of plasmid cluster C2	**330**
5.6c	Detailed metadata and pairwise distance matrices based on MASH distance estimation of plasmid cluster C3	**331**
5.6d	Detailed metadata and pairwise distance matrices based on MASH distance estimation of plasmid cluster C4	**332**
5.6e	Detailed metadata and pairwise distance matrices based on MASH distance estimation of plasmid cluster C5	**333**
5.6f	Detailed metadata and pairwise distance matrices based on MASH distance estimation of plasmid cluster C6	**334**
5.6g	Detailed metadata and pairwise distance matrices based on MASH distance estimation of plasmid cluster C7	**335**

Table	Title	Page
5.6h	Detailed metadata and pairwise distance matrices based on MASH distance estimation of plasmid cluster C8	**336**
5.6i	Detailed metadata and pairwise distance matrices based on MASH distance estimation of plasmid cluster C9	**337**
5.6j	Detailed metadata and pairwise distance matrices based on MASH distance estimation of plasmid cluster C10	**338**
5.6k	Detailed metadata and pairwise distance matrices based on MASH distance estimation of plasmid cluster C11	**339**
5.6l	Detailed metadata and pairwise distance matrices based on MASH distance estimation of plasmid cluster C12	**340**
5.6m	Detailed metadata and pairwise distance matrices based on MASH distance estimation of plasmid cluster C13	**341**
5.6n	Detailed metadata and pairwise distance matrices based on MASH distance estimation of plasmid cluster C14	**342**
5.6o	Detailed metadata and pairwise distance matrices based on MASH distance estimation of plasmid cluster C15	**343**
5.6p	Detailed metadata and pairwise distance matrices based on MASH distance estimation of plasmid cluster C16	**344**
5.7	Detailed metadata and distribution of complex types (CT)s for 30 Clade A1 VSEfm isolates recovered from a single rectal screening swab from each of four separate patients	**290**
1	Phenotypic and genotypic characteristics and whole-genome sequencing data analysis of 1,028 clade A1 *Enterococcus faecium* isolates recovered from Irish hospitals between June 2017-August 2022	**423**
2	Details of the publicly available short-read sequencing data of global Clade A1 *Enterococcus faecium* isolates (*N*=1,325) from NCBI used to contextualise Irish *E. faecium*	**465**

Index of Figures

Figure	Title	Page
1.1	*E. faecium* gastrointestinal colonisation, hyper-proliferation, and subsequent infection.	**4**
1.2	Major routes of nosocomial transmission of hospital-adapted *E. faecium*.	**5**
1.3	Horizontal gene transfer between bacteria.	**9**
1.4	Schematic representation of the genetic composition of transposon types found in enterococci.	**12**
1.5	Schematic overview of the mechanism of vancomycin resistance mediated by the *vanA/B* operon.	**21**
1.6	The relationship between the total number of infections, attributable deaths and DALYS for clinically important antibiotic resistant bacteria in Irish public acute hospitals in 201	**28**
1.7	Overview of the key steps in the Unicycler hybrid assembly approach.	**37**
3.1	Neighbour-joining tree (NJT) based on cgMLST of 1,038 clade A1 *E. faecium isolates*, recovered between June 2017 and August 2022 from seven Irish hospitals	**72**
3.2	Minimum spanning tree (MST) based on core-genome multi-locus sequence typing (cgMLST) analysis of the 1,038 Clade A1 *E. faecium isolates* recovered between June 2017 and August 2022 from seven Irish hospitals	**73**
3.3	Neighbour-joining tree (NJT) based on cgMLST of 743 ST80 clade A1 *E. faecium* isolates, recovered between June 2017-August 2022 from seven Irish hospitals	**78**
3.4	Minimum spanning tree (MST) based on core-genome multi-locus sequence typing (cgMLST) analysis of 1,423 defined core loci for the 145 ST80/CT2933 isolates (referred to as CI) recovered from seven Irish hospitals over a 43-month period (October 2018-June 2022).	**80**
3.5	Minimum spanning tree (MST) based on core-genome multi-locus sequence typing (cgMLST) analysis of 1,423 defined core loci for	**82**

Figure	Title	Page
	the 127 ST80/CT1916/2023/2953/3175/3385 isolates (referred to as CII) recovered from six Irish hospitals over a 47-month period (December 2017-November 2021)	
3.6	Minimum spanning tree (MST) based on core-genome multi-locus sequence typing (cgMLST) analysis of 1,423 defined core loci for the 64 ST80/CT1598 isolates (referred to as CIII) recovered from five Irish hospitals over a 28-month period (July 2017-December 2019	**84**
3.7	Minimum spanning tree of Irish Clade A1 *E. faecium* (N=1,028) isolated between June 2017 and August 2022 and global Clade A1 *E. faecium* (*N*=1,325) [786 VREfm (521 vanA, 265 vanB) and 539 VSEfm) originating from 30 countries, spanning a 30-year period (1986-2016) from the study of van Hal *et al* and Raven *et al*.	**88**
3.8	Minimum spanning tree of Irish Clade A1 *E. faecium* (*N*=640) isolated between June 2017 and December 2019 and Danish VREfm (*N*=989) isolates between 2017 and 2018.	**96**
3.9	Schematic diagram showing the structural organization of *vanA* transposon regions closed by hybrid assembly from VREfm isolates from Irish hospitals.	**99**
3.10	Schematic diagram showing the extent of deletions and other mutations in the *tnpA* transposase gene within the *vanA* region closed by hybrid assembly from VREfm isolates from Irish hospitals.	**100**
3.11	Schematic diagram showing the structural organization of *vanB* transposon regions closed by hybrid assembly from VREfm isolates from Irish hospitals.	**104**
3.12	Schematic diagram of the structural organisation of plasmid pSJ82*vanA* from the VREfm screening isolate SJ82 encoding vanA resolved by hybrid assembly of paired-end Illumina MiSeq short reads with Oxford Nanopore Technologies long reads.	**107**
3.13	Schematic diagram of the structural organisation of plasmid pSJ245*vanA* from the VREfm screening isolate SJ245 encoding *vanA* resolved by hybrid assembly of paired-end Illumina MiSeq short reads with Oxford Nanopore Technologies long reads.	**109**

Figure	Title	Page
3.14	Schematic diagram of the structural organisation of plasmid JH022*vanA* from the VREfm screening isolate JH022 encoding *vanA* resolved by hybrid assembly of paired-end Illumina MiSeq short reads with Oxford Nanopore Technologies long reads	**111**
3.15	Schematic diagram of the structural organisation of plasmid pRC_19_039*vanA* from the VREfm screening isolate RC_19_039 encoding *vanA* resolved by hybrid assembly of paired-end Illumina MiSeq short reads with Oxford Nanopore Technologies long reads.	**113**
3.16	Comparative genetic organization of circular plasmids pJH022 and pJH022_TC1.	**115**
3.17	Schematic diagrams of the structural organization of (a) plasmids pSJ82_B and pSJ82*vanA* from VREfm donor strain SJ82, and (b) the vancomycin resistance plasmid pSJ82_TC from the transconjugant SJ82_TC1.	**116**
3.18	Comparative genetic organization of circular plasmids pSJ82*vanA*, pSJ82*vanA* _TC1 and pSJ82_B	**118**
3.19	Schematic diagram of the structural organisation of plasmid pRC_19_036*vanA* from the VSEfm BSI isolate RC_19_36 encoding *vanA*-remnant resolved by hybrid assembly of paired-end Illumina MiSeq short reads with Oxford Nanopore Technologies long reads.	**119**
3.20	Comparative genetic organization of linear plasmids pELF_SJ11 and pELF_BSI_SJ40 from Irish VREfm previously described linear plasmids from Japanese (pELF1 and pELF2) and Swiss (pELF_USZ) VREfm.	**122**
3.21	Comparative genetic organization of linear plasmids pELF_SJ11 and pELF_BSI_SJ40 from Irish VREfm and the *vanA*-encoding contig from Irish VREfm isolate SJ10.	**129**
3.22	Schematic diagram showing the structural organisation of linear plasmids pELF_SJ11 and pELF_SJ11_TC1 resolved by hybrid assembly of paired-end Illumina MiSeq short reads with Oxford Nanopore Technologies long reads.	**132**
3.23	Schematic diagram of the structural organisation of linear plasmids pELF_BSI_SJ40 and pELF_BSI_SJ40_TC1 resolved by hybrid	**133**

Figure	Title	Page
	assembly of paired-end Illumina MiSeq short reads with Oxford Nanopore Technologies long reads.	
3.24	Comparative genetic organization of linear plasmids pELF_SJ11 and pELF_SJ11_TC1.	**134**
3.25	Comparative genetic organization of linear plasmids pELF_BSI_SJ40 and pELF_BSI_SJ40_TC1.	**135**
3.26	Schematic diagram of the structural organisation of linear plasmids pELF_JH127 and pELF_JH127 _TC1 resolved by hybrid assembly of paired-end Illumina MiSeq short reads with Oxford Nanopore Technologies long reads.	**136**
3.27	Comparative genetic organization of linear plasmids linear plasmids pELF_JH127 and pELF_JH127 _TC1.	**137**
3.28	Pulse field gel electrophoresis (PFGE) analysis of undigested and S1 nuclease-treated DNA of eight representative vancomycin-resistant Enterococcus faecium isolates harbouring linear plasmids.	**139**
4.1	Schematic diagram pertaining to the laboratory processing of environmental isolates (*N*=48) from two critical care wards of a large Dublin acute hospital.	**152**
4.2	Neighbour joining tree (NJT) based on core-genome multilocus sequence type (cgMLST) analysis of 1,423 target genes for 378 clade A1 *Enterococcus faecium* isolates from two critical care wards (WA and WB) of a large Dublin acute hospital recovered between September 2019 and December 2022.	**166**
4.3	MLT based on phylogenetic analysis of 366 core-genome single nucleotide polymorphisms (cgSNPs) for the 96 clade A1 *Enterococcus faecium* isolates belonging to CT2933 identified by cgMLST of isolates from wards WA and WA.	**173**
4.4	MLT based on phylogenetic analysis of 220 cgSNPs for the 58 clade A1 *Enterococcus faecium* isolates from clonal complex CT12932 (referred to as CII) identified by cgMLST of isolates from two wards of a large Dublin acute hospital between September 2019 and December 2022.	**180**
4.5	MLT based on phylogenetic analysis of 341 cgSNPs for the 52 clade A1 *Enterococcus faecium* isolates from clonal complex CT1916	**186**

Figure	Title	Page
	(referred to as CTIII) identified by cgMLST of isolates from two wards of a large Dublin acute hospital between September 2019 and December 2022.	
4.6	Parsimonious transmission tree based on cgSNP distance and collection date of 96 clade A1 *Enterococcus faecium* isolates from the ST80/CT2933 lineage (referred to as CI) recovered from wards WA and WB between September 2019 and December 2022.	**192**
4.7	Parsimonious transmission tree based on cgSNP distance and collection time of 58 clade A1 *Enterococcus faecium* isolates from the ST80/CT2932 lineage (referred to as CII) recovered from Wards A and B between September 2019 and December 2022.	**197**
4.8	Parsimonious transmission tree based on cgSNP distance and collection time of 52 clade A1 *Enterococcus faecium* isolates from the ST80/CT1916 lineage (referred to as CIII) recovered from Wards A & B between September 2019 and December 2022.	**199**
4.9	Neighbour joining tree (NJT) based on core-genome multi locus sequence type (cgMLST) analysis of 1,423 target genes for 1,286 clade A1 *Enterococcus faecium* isolates recovered from seven Irish hospitals between June 2017 and December 2022.	**201**
4.10	MLT based on phylogenetic analysis of 731 cgSNPs for 215 clade A1 *Enterococcus faecium* belonging to CT2933 (referred to as CI) identified by cgMLST of isolates from six Irish hospitals between October 2018 and December 2022.	**204**
4.11	MLT based on phylogenetic analysis of 315 cgSNPs for the 88 clade A1 *Enterococcus faecium* isolates CT2932 (referred to as CII) identified by cgMLST of isolates from three Irish hospitals between October 2018 and December 2022.	**213**
4.12	MLT based on phylogenetic analysis of 728 cgSNPs for the 137 clade A1 *Enterococcus faecium* isolates CT1916 (referred to as CIII) identified by cgMLST of isolates from five Irish hospitals between June 2018 and December 2022.	**219**
4.13	Schematic diagram showing the comparative structural organisation of *vanA*- and *van* remnant-encoding plasmids closed by hybrid	**227**

Figure	Title	Page
	assembly from clinical and environmental *Enterococcus faecium* isolates from Irish hospitals.	
5.1	Minimum spanning tree (MST) based on core genome multi-locus sequence typing (cgMLST) analysis of 1,423 loci for 150 clade A1 VREfm isolates recovered from a single rectal screening swab from each of 10 separate patients.	**241**
5.2	Minimum spanning tree (MST) based on core genome multi-locus sequencing typing (cgMLST) analysis of 1,4234 loci of Irish Clade A1 *E. faecium* (*N*=1,444) isolated between June 2017 and December 2022 and global Clade A1 E. faecium (*N*=1,356) from 30 countries, spanning a 30-year time period (1986-2016) from the study of van Hal *et al*., 2021 and Raven *et al*., 2016.	**243**
5.3	Maximum likelihood tree (MLT) based on phylogenetic analysis of 150 Clade A1 vancomycin-resistant *Enterococcus faecium* (VREfm) isolates recovered from a single rectal screening swab from each of 10 separate patients	**251**
5.4	Figure 5.4. Neighbour joining tree (NJT) based on core-genome multi locus sequence type (cgMLST) analysis of 1,423 target genes for 772 Clade A1 *E. faecium* isolates recovered from W1, W2, W3, W9, W18, W20 and WE in Hospital 1 between June 2017 and December 2022.	**158**
5.5	Pairwise Mash distance-based clustering of plasmids (*N*=193) from 39 representative VREfm investigated from 10 patient rectal screening samples.	**271**
5.6	Pulse field gel electrophoresis (PFGE) analysis of undigested and S1 nuclease-treated DNA of four representative vancomycin-resistant *Enterococcus faecium* isolates harbouring vanA-encoding linear plasmids.	**275**
5.7	Comparative genetic organization of linear plasmids pELF_JHM5-6, pELF_JHM5-6_TC1, pELF_JHM5-13 and pELF_JHM5-13 from parental Irish vancomycin-resistant *Enterococcus faecium* (VREfm) and transconjugants derivatives of *E. faecium* 64/3 obtained following filter-mating experiments	**277**

Figure	Title	Page
5.8	Comparative genetic organisation of *vanA* transposon regions closed by hybrid assembly of VREfm isolates belonging to two complex types (CTs) from patient one.	**283**
5.9	Comparative genetic organisation of *vanA* transposon regions closed by hybrid assembly of VREfm isolates belonging to two complex types (CTs) from patient one.	**345**
5.10	Comparative genetic organisation of *vanA* transposon regions closed by hybrid assembly of VREfm isolates belonging to one complex type (CT) from patient P3.	**346**
5.11	Comparative genetic organisation of *vanA* transposon regions closed by hybrid assembly of four VREfm isolates belonging to two complex types (CTs) from patient P4.	**348**
5.12	Comparative genetic organisation of *vanA* transposon regions closed by hybrid assembly of five VREfm isolates belonging to three complex types (CTs) from patient P5.	**350**
5.13	Comparative genetic organisation of *vanA* transposon regions closed by hybrid assembly of four VREfm isolates belonging to two complex types (CTs) from patient P6	**352**
5.14	Comparative genetic organisation of *vanA* transposon regions closed by hybrid assembly of three VREfm isolates belonging to two complex types (CTs) from patient P7.	**353**
5.15	Comparative genetic organisation of *vanA* transposon regions closed by hybrid assembly of seven VREfm isolates belonging to three complex types (CTs) from patient P8.	**354**
5.16	Comparative genetic organisation of *vanA* transposon regions closed by hybrid assembly of two VREfm isolates belonging to one complex type (CT) from patient P9.	**356**
5.17	Comparative genetic organisation of *vanA* transposon regions closed by hybrid assembly of two VREfm isolates belonging to one complex type (CT) from patient P10.	**357**
5.18	Comparative genetic organisation of *vanA* transposon regions closed by hybrid assembly of VREfm isolates belonging to complex type (CT) 2933 from five patients.	**286**

Figure	Title	Page
5.19	Comparative genetic organisation of *vanA* transposon regions closed by hybrid assembly of VREfm isolates belonging to complex type (CT) 6489 from five patients.	**287**
5.20	Minimum spanning tree (MST) based on core genome multi-locus sequence typing (cgMLST) analysis of 1,423 loci for 150 clade A1 VREfm isolates recovered from a single rectal screening swab from each of 10 separate patients and 30 VSEfm isolates recovered from a single rectal swab from each of four separate patients.	**291**
5.21	Visual representation of the complete plasmidome assembly of VSEfm isolate JHMS8-4 and VREfm isolate JHM8-4 from complex type (CT) 2933 generated using Bandage.	**294**
5.22	Visual representation of the complete plasmidome assembly of VSEfm isolate JHMS1-1 and VREfm isolate JHM8-1 from complex type (CT) 2932 generated using Bandage.	**295**
5.23	Visual representation of the complete plasmidome assembly of VSEfm isolates JHMS3-4 (CT2950) and JHMS5-15 (CT2940) generated using Bandage.	**296**
5.24	Schematic diagram of the structural organisation of plasmid pELF_JHMS3-5 from the VSEfm rectal isolate JHMS3-5 (ST80/CT2950) from patient P3 encoding a vanA-remnant resolved by hybrid assembly of paired-end Illumina MiSeq short reads with Oxford Nanopore Technologies long reads.	**297**

Abbreviations

ABC	ATP-binding cassette
AFLP	Amplified fragment length polymorphism analysis
AMR	Antimicrobial resistance
BAPs	Bayesian analysis of population structure
BCL	Base call files
BED	Browser extensible data
BHIA	Brain heart infusion agar
BHIB	Brain heart infusion broth
BLAST	Basic Local Alignment Search Tool
BLT	Bead linked transposome
BSI	Bloodstream infection
Bp	Base pair
BWA	Burrows-Wheel aligner
CBA	Columbia blood agar
CC	Clonal complex
CD	Coding sequence
CDC	Centre for Disease Control and Prevention
cgMLST	Core-genome multilocus sequence type
cgSNP	Core-genome single nucleotide polymorphism
cgSNV	Core-genome single nucleotide variation
cm	Centimetre
CPU	Central processing unit
CRE	Carbapenem resistant *Enterobacterales*
CRISPR	Clustered regularly interspaced short palindromic repeats
CT	Complex type
C	Cluster
D-Ala D-Ala	D-Alanine D-Alanine
D-Ala D-Lac	D-Alanine D-Lactate
D-Ala D-Ser	D-Alanine D-Serine
DALYs	Disability-adjusted life years
DDS	Defined daily doses
DNA	Deoxyribonucleic acid

dNTPs	Deoxyribonucleotide triphosphate
e.g.	*Exempli gratia*; for example
EARS-net	European Antimicrobial Resistance Surveillance Network-Net
eBURST	Extended Based Upon Related Sequence Types
ECDC	European Centre for Disease Prevention and Control
EDTA	Ethylenediaminetetraacetic acid
et al.	*Et alia*; and others
etc.	*Et cetera*; and the rest
EU	European Union
EUCAST	European Committee on Antimicrobial Susceptibility testing
FLB	Flush buffer
FLT	Flush tether
fmol	Fentimolar
g	Gravitational force
GC	Guanine-cytosine
GFF	General feature format
GIT	Gastrointestinal tract
GP	General practitioner
GTR	General time reversible
h	Hours
H	Hospital
HDU	High dependency unit
HGT	Horizontal gene transfer
HIQA	Health Information and Quality Authority
HIV	Human immunodeficiency virus
HLR	High-level resistance
HMW	High molecular weight
HPSC	Health Protection Surveillance Centre
HRB	Health Research Board Ireland
HSE	Health Service Executive
HT1	Hybridisation buffer
I	Intermediate
ICE	Integrative conjugative elements
ICER	Incremental cost-effective ratio
ICU	Intensive care unit

Indels	Insertions and deletions
IPC	Infection prevention and control
IS	Insertion sequence
Kbp	Kilobase pair
L	Litre
M	Molar
MALDI-TOF	Matrix-Assisted Laser Desorption Ionization-Time of Flight Mass Spectrometry system
Mb	Mega base
Mbp	Mega base pairs
MDR	Multidrug resistance
Mg	Milligram
MGE	Mobile genetic element
MIC	Minimum inhibitory concentration
min	Minute
ml	Millilitre
MLST	Multilocus sequence typing
MLT	Maximum likelihood tree
mm	Millimetre
MRSA	Methicillin-resistant *Staphylococcus aureus*
MST	Minimum spanning tree
N/A	Not applicable
NaOH	Sodium hydroxide
NCBI	National Centre for Biotechnology Information
ng	nanogram
NGS	Next generation sequencing
NHSN	National Healthcare Safety Network
NJT	Neighbour-joining tree
nM	Nanometre
NT	Non-typeable
ONT	Oxford Nanopore Technologies
P	Patient
PacBio	Pacific Biosciences
PBP	Penicillin binding protein
PBS	Phosphate buffered saline

PCR	Polymerase chain reaction
PFGE	Pulsed-field gel electrophoresis
pH	Potential Hydrogen
pM	Picomolar
PTC	Potential transmission chain
Q	Quality score
QALY	Quality-adjusted life years
R	Resistant
RAPD	Random amplified polymorphic DNA
Rep	Replication initiator protein
RIG	Related isolate group
RNA	Ribonucleic acid
rRNA	Ribosomal ribonucleic acid
RSB	Resuspension buffer
S	Susceptible
SARI	Strategy for the Control of Antimicrobial Resistance in Ireland
SBS	Sequencing by synthesis
SPBs	Sample purification beads
SKA	Split *k*-mer analysis
SNP	Single nucleotide polymorphism
SRA	Sequence Read Archive
ST	Sequence type
TA	Toxin-antitoxin
TB1	Tagmentation buffer
TBE	Tris-borate/EDTA
TEs	Transposable elements
Tn	Transposon
TSB	Tagment stop buffer
TWB	Tagment wash buffer

UK	United Kingdom
USA	United States of America
v	Version
v/v	Volume per volume
VRE	Vancomycin-resistant enterococci
VREfm	Vancomycin-resistant *Enterococcus faecium*
VREfs	Vancomycin-resistant *Enterococcus faecalis*
VRSA	Vancomycin-resistant *Staphylococcus aureus*
VSE	Vancomycin-susceptible enterococci
VSEfm	Vancomycin-susceptible *Enterococcus faecium*
W	Ward
w/v	Weight per volume
wgMLST	Whole-genome multilocus sequence typing
WGS	Whole genome sequencing
WHO	World Health Organisation
µg	Microgram
µl	Microlitre
%	Percentage
°C	Degrees Celsius
‘	Prime
+	Positive
<	Less than
>	Greater than
~	Tilde; approximately
≤	Less than or equal to
≥	Greater than or equal to
α	Alpha
ß	Beta

Publications

Some of the work presented in this thesis has been published international peer-reviewed journals, as listed below. Offprints of the publications are included in Appendix 2.

Egan, S.A., Kavanagh, N.L., Shore, A.C., Mollerup, S., Samaniego Castruita, J.A., O'Connell, B., McManus, B.A., Brennan, G.I., Pinholt, M., Westh, H. and Coleman, D.C. (2022) Genomic analysis of 600 vancomycin-resistant *Enterococcus faecium* reveals a high prevalence of ST80 and spread of similar *vanA* regions via IS *1216E* and plasmid transfer in diverse genetic lineages in Ireland, *Journal of Antimicrobial Chemotherapy*, 77(2), pp. 320–330. Available at: https://doi.org/10.1093/jac/dkab393.

Kavanagh, N. L., Kinnevey, P. M., Egan, S. A., McManus, B. A., O'Connell, B., Brennan, G. I., & Coleman, D. C. (2024) Protracted transmission and persistence of ST80 vancomycin-resistant *Enterococcus faecium* clonal complex types CT2933, CT2932 and CT1916 in a large Irish hospital: a 39-month whole-genome sequencing study, *Journal of Hospital Infection*, 151, pp. 11–20. Available at: https://doi.org/10.1016/j.jhin.2024.06.002

Chapter 1

General Introduction

1.1 *Enterococcus* species

The genus *Enterococcus* comprises a group of robust Gram-positive, facultatively anaerobic bacterial species that are characterised by their remarkable versatility and non-fastidious nature. Formerly classified in the genus *Streptococcus*, enterococci are differentiated based on their ability to grow and survive under harsh conditions, including a wide range of temperatures (10°C-45°C), high salt concentrations and various pH levels (4.5-10). These properties facilitate their survival, persistence, and widespread dissemination in a diverse array of environmental and biological habitats including soil, open waters, grassland, and aquatic vegetation (Arias and Murray, 2012; Byappanahalli *et al.*, 2012). To date, >50 species of *Enterococcus* have been described in the literature, with the largest reservoir thought to be the gastrointestinal tract (GIT) of humans and other mammals, birds, reptiles, and insects (Mundt, 1963; Gilmore *et al.*, 2013; Parte, 2018; Parte *et al.*, 2020). Enterococci account for up to 1% of all endogenous human intestinal flora (Dubin and Palmer, 2014). The highly evolved role of enterococci in the gut consortium has been shown to involve conferring colonisation resistance, which significantly curtails opportunities for invasion of the gut tissues by more pathogenic microorganisms (Lebreton *et al.*, 2017; Arredondo-Alonso *et al.*, 2020).

Despite their commensal nature and low pathogenic potential, enterococci have emerged as significant nosocomial opportunistic pathogens that are of both medical and public health importance. The most clinically significant members of the *Enterococcus* genus and the causative agents of the vast majority of infections in humans are *Enterococcus faecium* and *Enterococcus faecalis*. The spectrum of disease caused by these organisms include endocarditis, urinary tract-, blood stream-, intra-abdominal-, burn and surgical site wound- and biliary tract infections (García-Solache and Rice, 2019). Up until the 1970s, *E. faecalis* was considered the primary species driving nosocomial enterococcal infection globally, accounting for approximately 90-95% of clinical enterococcal isolates (Arias and Murray, 2012). However, over the past two decades, the proportion of infections caused by *E. faecium* have rapidly increased, with rates of up to 40% reported, coinciding with the global emergence and dissemination of vancomycin resistance (Willems and van Schaik, 2009; Arias and Murray, 2012; García-Solache and Rice, 2019). This dynamic shift in the epidemiology of nosocomial enterococcal infection has constituted a substantial public-health concern as infections caused by *E. faecium* are associated with higher mortality, more complex patient management and increased length of hospital stay (Willems and van Schaik, 2009; Arias and Murray, 2012). As a result, the World Health Organisation has listed vancomycin-resistant *E. faecium* (VREfm) as a high-priority pathogen requiring urgent,

comprehensive research to understand its epidemiology, resistance mechanisms and transmission dynamics to inform effective patient management and infection prevention and control (IPC) strategies (WHO, 2017).

1.2 *E. faecium* colonisation and hospital transmission

As stated above, *Enterococcus spp.* constitute a small proportion of the human intestinal flora, accounting for approximately 10^5-10^7 colony-forming units per gram of faeces (Fiore *et al.,* 2019). High-density colonisation of the GIT with multi-drug resistant strains of *E. faecium*, such as VREfm, has been shown to be an important risk-factor preceding clinical infection, particularly in multimorbid or medically vulnerable patients. This is facilitated by antimicrobial-induced depletion of important commensal organisms within the GIT resulting in a deficiency in innate host immunity. This allows enterococci to establish dominance, invade through the intestinal barrier and translocate to other anatomical sites resulting in endogenous infection (Figure 1.1) (Brandl *et al.,* 2008; Archambaud *et al.,* 2019).

Asymptomatic patients colonised with VREfm can serve as an important silent reservoir for exogenous infection via direct patient-to-patient transmission and environmental contamination through faecal shedding (Figure 1.2). It has been demonstrated that for one hospitalised patient with clinically evident enterococcal infection, there are approximately 2-10 unidentified rectal carriers (Cattoir and Leclercq, 2013). Indirect *E. faecium* transmission and acquisition may also occur through patient contact with a contaminated environmental intermediary, such as shared bathroom facilities and high-touch near patient areas including beds, lockers, door handles, other communal surfaces and contaminated equipment (Lee *et al.,* 2018; Gouliouris *et al.,* 2020). This is in line with a recent study which demonstrated that environmental strains recovered from the near-patient environment may serve as a good alternative surveillance strategy and can be informative of the colonisation strains in circulation (Cassone *et al.,* 2018; Gouliouris *et al.,* 2020). The remarkable ability of *E. faecium* to persist in the hospital environment has been extensively documented, with some studies suggesting enterococci may survive for up to four months on inanimate objects in the absence of appropriate decontamination protocols (Kramer *et al.,* 2006). Transient carriage of enterococci by healthcare workers or visitors has also been indicated as an important route of transmission, with one studying suggesting that enterococci can survive up to 60 minutes on an individual's hands (Kramer *et al.,* 2006).

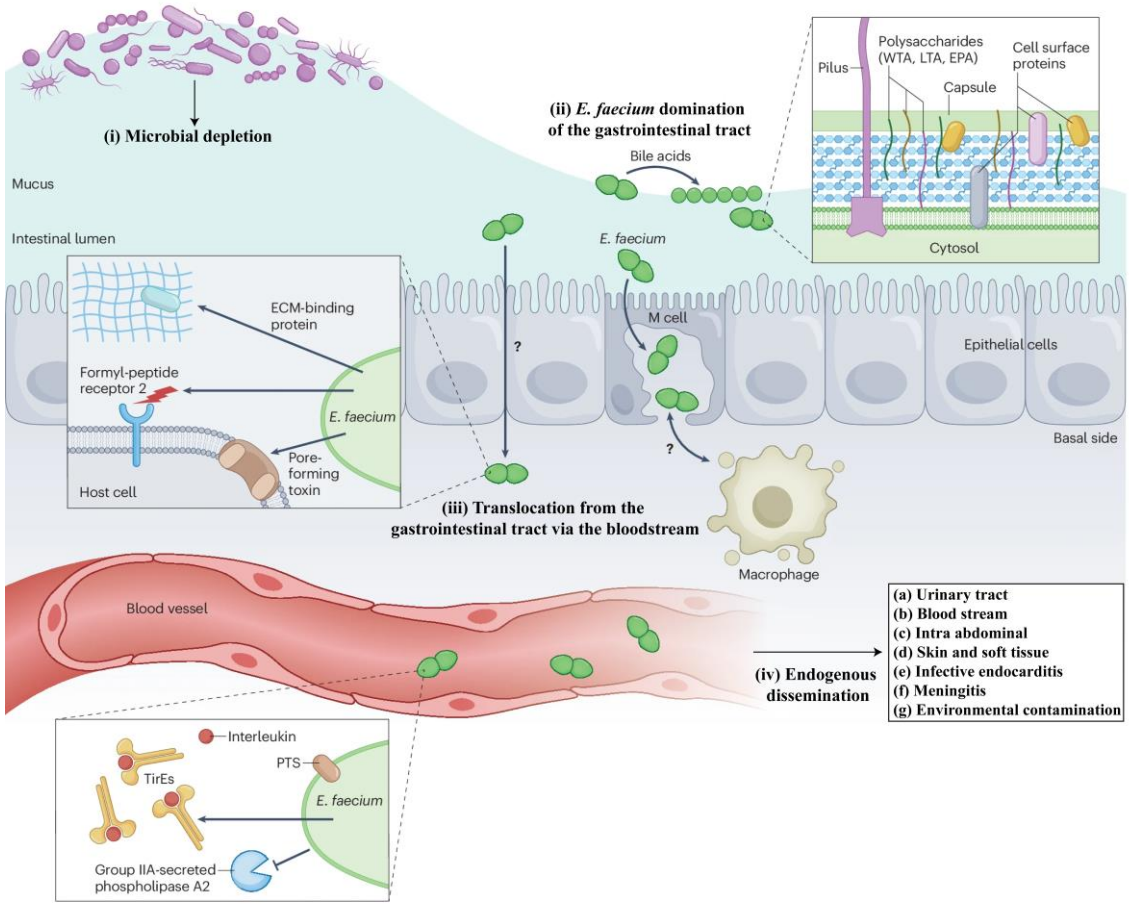

Figure 1.1 ***E. faecium*** **gastrointestinal colonisation, hyper-proliferation, and subsequent infection. (i)** The administration of broad-spectrum antimicrobials may deplete the normal healthy microflora and result in a decrease in innate host immunity. **(ii)** *E. faecium* may survive antibiotic treatment, selectively proliferate and establish intestinal dominance. **(iii)** Following intestinal over-growth, *E. faecium* may translocate into the deeper tissues of the GIT through direct penetration or via M cells thus gaining access to the bloodstream. **(iv)** Dissemination of *E. faecium* to other anatomical sites may occur via translocation through the bloodstream. Adapted from Wei *et al.*,2024.

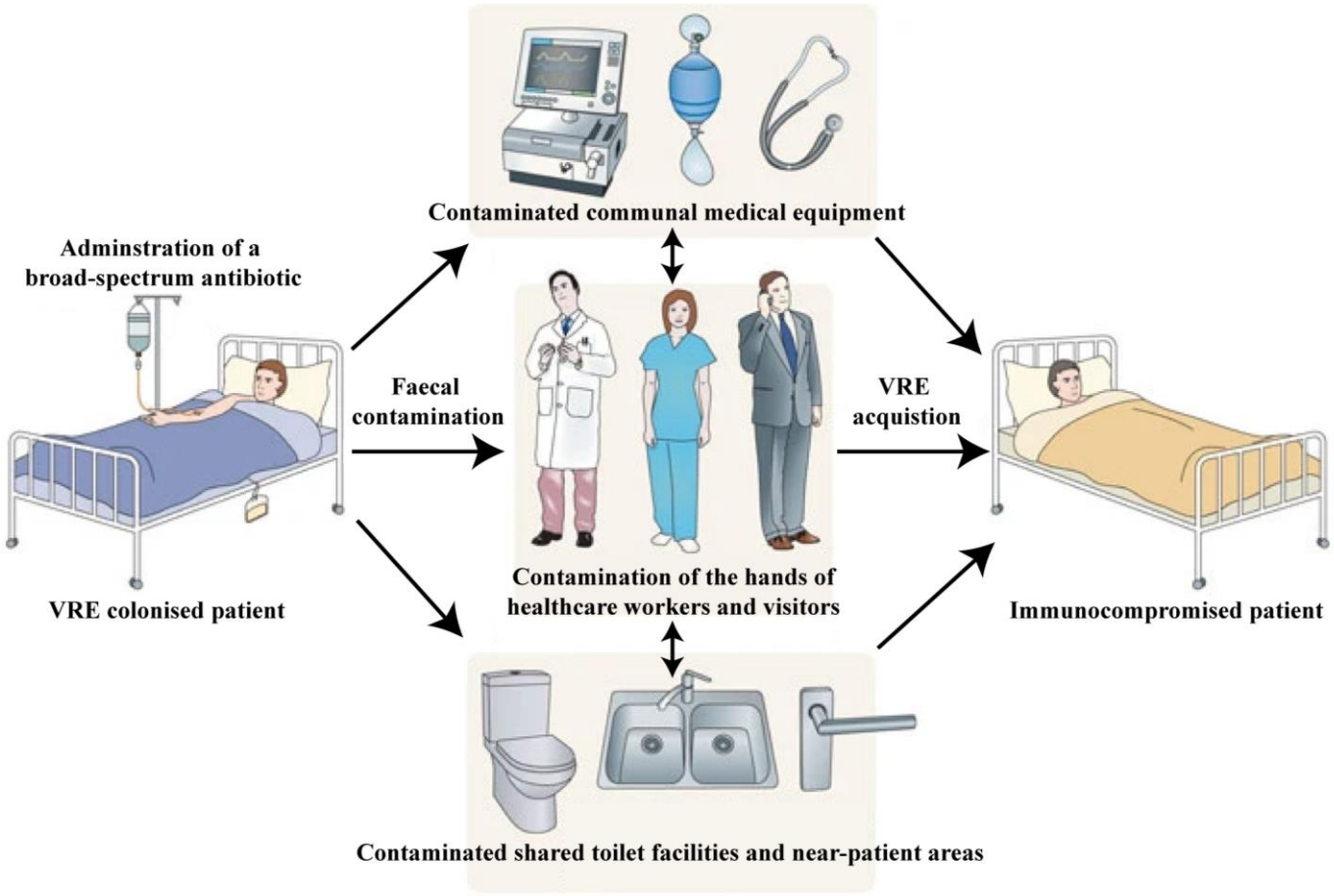

Figure 1.2 Major routes of nosocomial transmission of hospital-adapted *E. faecium*. A patient colonised with *E. faecium* may require broad-spectrum antimicrobials which results in depletion of the normal gastrointestinal flora and selective proliferation of more resistant organisms such as VREfm. This increases the likelihood of resulting translocation and infection with *E. faecium* within the host and also subsequent shedding into the hospital environment. Following contamination of medical equipment, high-touch areas such as door handles, bed rails or other communal surfaces, shared-bathroom facilities or the hands of health care workers, *E. faecium* may be acquired via the oral-faecal route by patients in close physical proximity to the colonised patient. Adapted from Arias and Murray, 2012.

1.3 *E. faecium*: a promiscuous bacterium living in a plastic world

Hospital-adapted *E. faecium* strains exhibit a substantial, open pangenome characterised by extensive plasticity and genome flexibility. This arises from the dynamic acquisition/loss and rearrangement of genes through a combination of *de novo* horizontal gene transfer (HGT) and recombination. The unique evolutionary trajectory and specialist adaptation of *E. faecium* strains within the hospital niche, often referred to as genetic capitalism, has resulted in a diverse and expansive gene pool allowing the consistent accumulation of novel adaptive traits that can confer a selective advantage (Baquero, 2004; van Schaik *et al.,* 2010; Freitas *et al.,* 2021). This phenomenon is sustained by the absence of genomic defence mechanisms such as clustered regularly interspaced short palindromic repeats (CRISPR) and type IV restriction modification systems, which prevent the entry and integration of foreign exogenous DNA (van Schaik *et al.,* 2010; Lebreton *et al.,* 2013).

Comparative *in silico* analysis of publicly available, hospital adapted *E. faecium* strains revealed a median genome size of ~2.92 mega base pairs (Mbp), a mean GC content of 37.8% and approximately 2,762 protein-coding sequences (https://www.ncbi.nlm.nih.gov/genome/?term=Enterococcus +faecium). These findings algin with previous studies, which indicate that clinical *E. faecium* isolates possess larger genomes associated with a higher number of genes and accessory elements compared to non-clinical strains (Kim and Marco, 2014; Arredondo-Alonso *et al.,* 2020; Mlaga *et al.,* 2021; Sanderson *et al.,* 2022). The *E. faecium* pangenome can be divided into two main segments: the core-genome and the accessory genome.

1.3.1 The core genome: attack of the clones

The *E. faecium* core genome comprises conserved core-stable genes which encode important house-keeping functions that are essential for growth, maintenance, and survival (Martin and Beiko, 2010). In recent years, comparative molecular analysis has identified significant differences in the core-genome of subpopulations of *E. faecium* dependent on their ecological niche. For example, clinical or hospital-adapted *E. faecium* are characterised by ampicillin and quinolone resistance, the acquisition of specific genetic elements such as pathogenicity islands encoding the *esp* gene and a putative hyaluronidase gene (*hyl*) both essential for biofilm formation, a phosphotransferase system promoting intestinal colonisation and integration of specific insertion element families such as IS*16* (Coque, 2002; Heikens *et al.,* 2007; Hendrick *et al.,* 2007, 2008, 2009; Leavis *et al.,* 2007; Heikens *et al.,* 2008, 2011; Galloway-Peña *et al.,* 2009; Leendertse *et al.,* 2009). The acquisition of

these key genetic elements has significantly contributed to the evolution and adaptation of a distinct clonal population with an increased fitness in hospitalised patients. This host-specific lineage was initially designated as 'C1' based on systematic amplified fragment length polymorphism analysis (AFLP) (Willems *et al.,* 2000). However it was later renamed as clonal complex (CC) 17 on the basis of a combination of multi-locus sequence typing (MLST) and the Based Upon Related Sequence Types (eBURST) algorithm. CC17 was subsequently found to be globally dispersed, with a variety of additional conserved core-gene adaptive traits reported, and deemed to have originated from a specific founder termed sequence type (ST) 17 (Willems *et al.,* 2005; Guzman Prieto *et al.,* 2016). However, it was later recognised that the designation of all nosocomial *E. faecium* into a single CC genetic subpopulation resulted in an over-simplification of host-specific lineages due to the highly recombinant nature of the genome (Willems *et al.,* 2012).

Bayesian analysis of population structure (BAPs) based on multilocus sequence type (MLST) revealed that the majority of nosocomial *E. faecium* strains (>80%) clustered into three major clonal lineages, ST17, ST18 and ST78, suggesting a convergent evolution of different constituent groups (Willems *et al.,* 2012). Interestingly, the authors in this study demonstrated that clinical *E. faecium* subpopulations display a high proportion of admixture, particularly within the MLST key house keeping genes (discussed in detail in Section 1.8.2), indicating that approximately 14% of the MLST loci originated from *E. faecium* strains from other ecological niches (Willems *et al.,* 2012). Subsequent implementation of whole-genome sequencing (WGS) technologies further supported a division in hospital adapted clones and proposed the presence of two sub-populations or clades, termed Clade A (hospital-associated) and Clade B (commensal), respectively (Galloway-Peña *et al.,* 2012; Palmer *et al.,* 2012). This divergence is estimated to have occurred >300,00 years ago (Galloway-Peña *et al.,* 2012). Further phylogenomic studies using core-genome single nucleotide variations (cgSNVs) revealed a secondary evolutionary split within Clade A isolates, which occurred more recently (~75 years ago) and segregated isolates into Clade A1 (human-derived clinical isolates) and Clade A2 (animal-associated isolates) (Lebreton *et al.,* 2013; Gouliouris *et al.,* 2018; Rios *et al.,* 2020). This suggests that hospital-adapted *E. faecium* evolved from an animal-derived ancestor that diverged prior to the clonal expansion of nosocomial lineages, with the hospital associated population emerging at a significantly accelerated pace (Rios *et al.,* 2020; Freitas *et al.,* 2021).

Notably, evidence suggests that when Clade A1 *E. faecium* became adapted to the hospital niche, the core-genome became relatively stable and recombination with other populations significantly declined (Willems *et al.,* 2012). Genetic variability within the core

genome of Clade A1 strains typically occurs in genetic hot-spots with specific regions more prone to the accumulation of genetic mutations such as single nucleotide polymorphisms (SNPs), homologous recombination or the integration of novel genomic segments (Martin and Beiko, 2010; de Been *et al.*, 2013; Howden *et al.*, 2013). In fact, it has been demonstrated that five out of the seven key loci in the MLST scheme are subject to homologous recombination (discussed in Section 1.8.2) (Howden *et al.*, 2013; Pinholt *et al.*, 2015; Carter *et al.*, 2016; Raven *et al.*, 2016). Notably, it has been reported that highly related *E. faecium* strains with stable core genomes may vary substantially in their accessory genome (Leavis *et al.*, 2007; van Schaik *et al.*, 2010; Lebreton *et al.*, 2013). These findings suggest that the development and establishment of endemic clonal lineages occurs globally with subsequent genomic expansion, with significant genetic diversity primarily arising due to HGT within the accessory genome.

1.3.2 The accessory genome

The accessory genome, often referred to as the mobilome, constitutes a significant proportion of the *E. faecium* pangenome, accounting for ~25-37% (van Schaik *et al.*, 2010; Lam *et al.*, 2012; Qin *et al.*, 2012). This can be defined as genes associated with 'non-essential' functions that may confer a selective advantage such as antimicrobial resistance or putative virulence determinants (de Been *et al.*, 2015; van Hal *et al.*, 2021). These genes are typically encoded on mobile genetic elements (MGEs), which serve as important vehicles of DNA transfer, and are often transferred horizontally between bacterial cells via conjugation, transformation, or transduction (Figure 1.3). Clade A1 strains have been shown to contain twice the number of MGEs when compared with non-clinical strains (Kim and Marco, 2014). Five distinct types of MGEs have been described in hospital-adapted *E. faecium* including plasmids, transposons, insertion sequences (IS), bacteriophages and genomic islands (Werner *et al.*, 2008; Hegstad *et al.*, 2010; Huddleston, 2014).

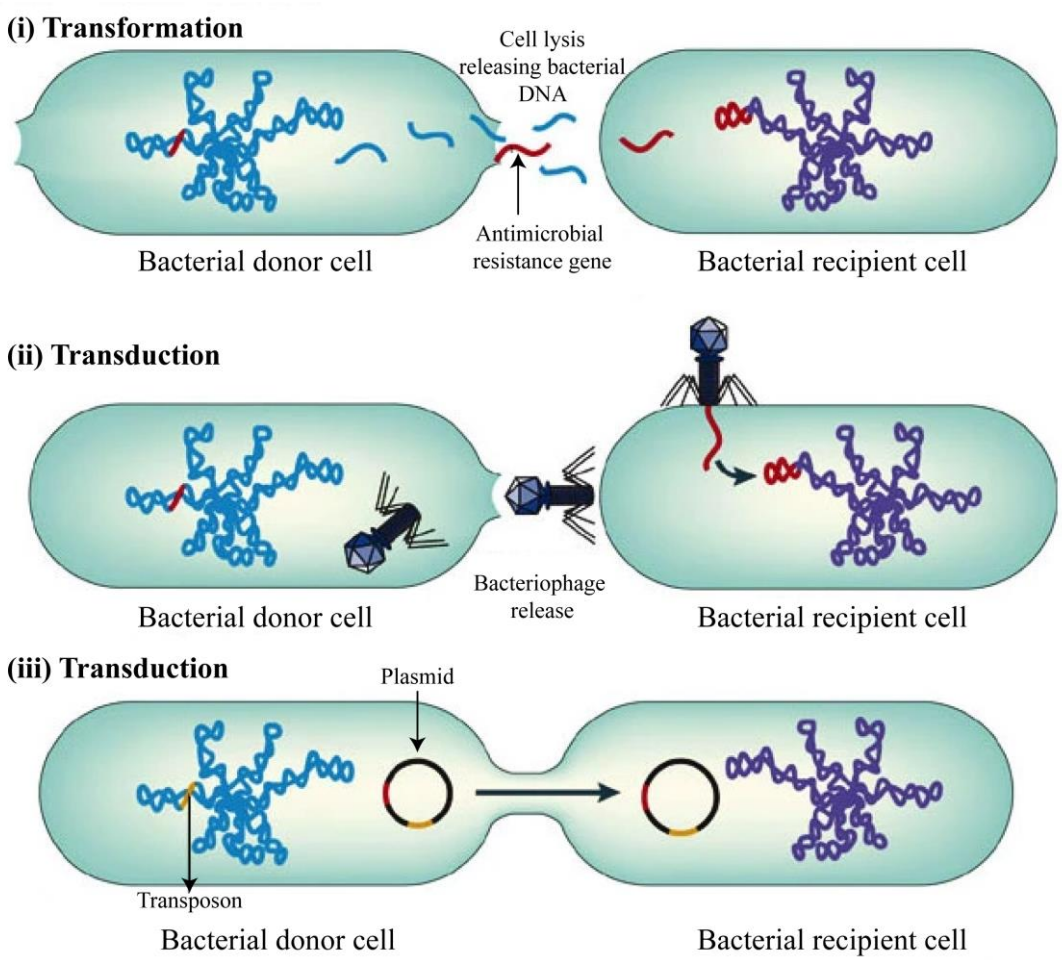

Figure 1.3. Horizontal gene transfer between bacteria. (i) Transformation occurs when exogenous DNA is taken up by a competent bacterial cell following lysis of a donor cell. The DNA can be subsequently integrated into the bacterial chromosome or on to a mobile genetic element such as a plasmid via recombination or transposition. **(ii)** Transduction occurs when donor cell DNA is packaged by bacteriophages during phage replication and release and the subsequent integration of the DNA into a recipient cell's genome following bacteriophage infection. **(ii)** During bacterial conjugation, DNA segments encoded on extrachromosomal elements called plasmids are exchanged via direct contact as a result of the formation of a mating bridge between a donor and recipient cell. The exchange of transposable elements is frequently facilitated by exchange of plasmids harbouring integrated transposable elements. Adapted from Furuya and Lowy, 2006.

1.3.2.1 Plasmids

Plasmids are circular or linear extrachromosomal DNA elements that are capable of semi-autonomous replication (Thomas, 2014). A wide spectrum of diverse plasmid types have been described in *Enterococcus* spp., encoding functional modalities responsible for plasmid replication, conjugative transfer, antimicrobial resistance, virulence factors and bacteriocins (Hasman and Aarestrup, 2002; Hancock *et al.,* 2014). Plasmids are considered abundant in VREfm, with one study indicating that clinical strains may harbour from 1-7 distinct plasmids in a single bacterial cell (Rosvoll *et al.,* 2010). In fact, it has been demonstrated that the plasmidome constitutes a substantial portion of the total genome size observed in clade A1 *E. faecium*, with vast heterogeneity observed in the literature with respect to plasmid length, with reports of <2 kilobase pairs (kbp) to >30 kb (Hegstad *et al.*, 2010; Palmer *et al.*, 2010; Rosvoll *et al.,* 2010, 2012; Hancock *et al.*, 2014; Sadowy, 2018). Interestingly, a study by Freitas and colleagues in 2016 suggested the presence of a species-specific plasmid pool in *E. faecium,* which notably was not shared with other enterococcal spp. such as *E. faecalis.*

Plasmids in enterococci are generally classified as conjugative (pheromone-responsive and non-pheromone responsive) or non-conjugative (rolling-circle replicating and mosaic). However, some non-conjugative plasmids in *E. faecium* have been shown to encode mobilisation and relaxosome components but lack the genes required for mating bridge formation. This plasmid type has been termed ‘mobilisable’ and can readily exploit the genetic machinery of conjugative plasmids also present in the bacterial cell which can facilitate horizontal dissemination (Norman *et al.,* 2009). Enterococcal plasmids have been further characterised on the basis of sequence homology against replication initiator proteins (*rep*) and have been grouped into four main family types including RepA_N, Inc18, RCR and Rep_3 (Arredondo-Alonso *et al.,* 2020). It is important to note that plasmids within clinical enterococci often exhibit extensive mosaicism and will display features from a variety of the main families referred to above due to the high level of recombination between multiple MGEs (Arredondo-Alonso *et al.,* 2020). Plasmids remain important vehicles of antimicrobial resistance in enterococci.

1.3.2.2 Transposable elements

Transposable elements (TEs) are segments of DNA that are capable of translocating from one genetic location to another in the same bacterial cell (Bennett, 2004; Martin and Beiko, 2010). IS are the simplest form of TE and are considered widespread in hospital-adapted *E.*

faecium (Werner *et al.*,2011). They are defined as a small segment of genetic material which encode only the enzyme(s) responsible for transposition. IS elements are also flanked on either side by inverted repeats which allows for insertion and recombination within the bacterial genome (Hegstad *et al.,* 2010). The most frequently encountered IS families in enterococcal isolates include IS*3*, IS*6*, IS*16*, IS*30*, IS*256* and IS*L3* (Leavis *et al.,* 2007; Hegstad *et al.,* 2010). The enrichment of *E. faecium* with IS elements can impact gene expression, contribute to genome plasticity, and mediate the further acquisition of novel adaptive mechanisms (Leavis *et al.,* 2007).

Transposons are larger TEs (2.5-21 kb) often encoding both the enzymes required for transposition and an additional adaptive marker such as an antimicrobial resistance gene(s) (Martin and Beiko, 2010). There are three main forms found in enterococci including composite transposons, Tn*3* family transposons and conjugative transposons (Figure 1.4) (Hegstad *et al.,* 2010). IS elements can form composite transposons when inserted on either side of an antimicrobial resistance gene (Bennett, 2004). The IS elements may comprise either inverted or direct repeats and facilitate mobilisation to other regions in the genome. In enterococci, composite transposons are typically associated with high-level aminoglycoside (gentamicin) or glycopeptide resistance (Hodel-Christian and Murray, 1991; Thal *et al.,* 1994; Handwerger and Skoble, 1995; Rice *et al.,* 1995; Quintiliani and Courvalin, 1996; Rice and Carias, 1998). The Tn*3* family of transposons are capable of intracellular transposition mediated by a transposase (*tnpA*) and a resolvase (*tnpR*) gene. They are associated with the widespread dissemination of high-level *vanA*-mediated vancomycin resistance by Tn*1546* (Hegstad *et al.,* 2010). Conjugative transposons are defined as integrative conjugative elements (ICE) that are capable of intercellular excision, conjugation, and integration through formatting of a mating-bridge (Hegstad *et al.,* 2010). They are frequently associated with resistance to tetracyclines, macrolides and *vanB2*-mediated vancomycin resistance such as Tn*1549* in *E. faecium*. Notably, conjugative transposons have been demonstrated to contribute to the intracellular co-transfer of other plasmids and transposons and facilitate the mobilisation of large chromosomal fragments between bacterial strains (Hegstad *et al.,* 2010).

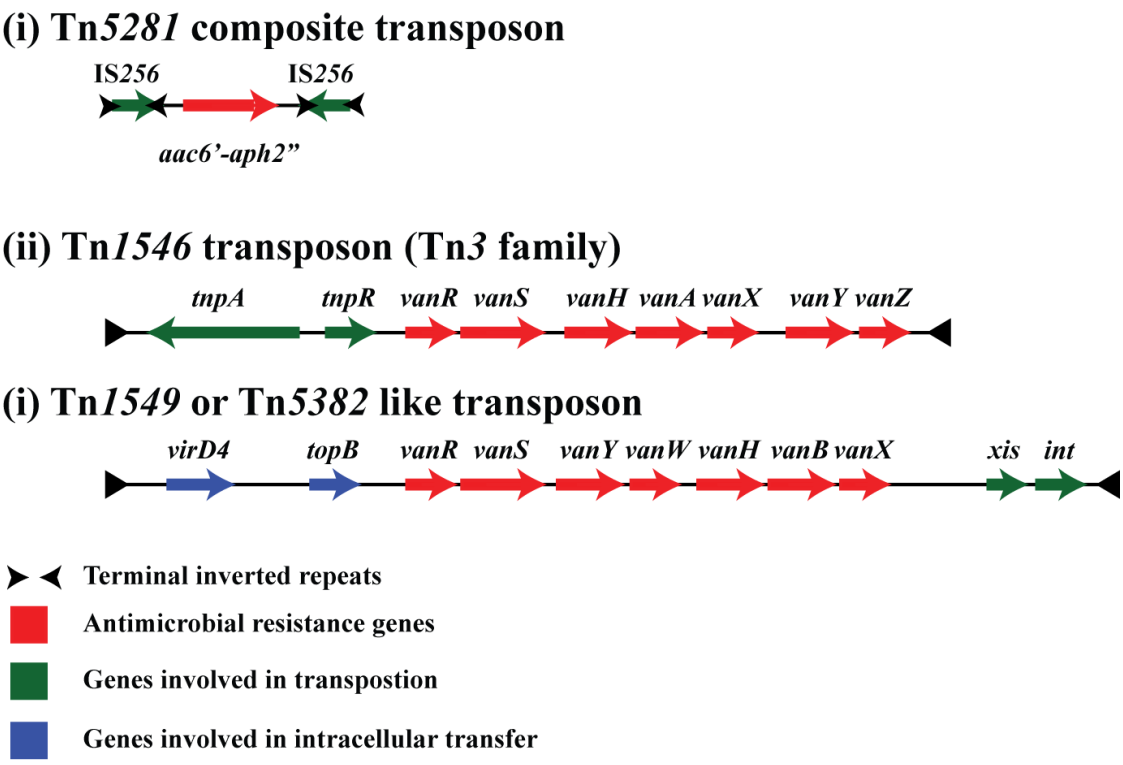

Figure 1.4 Schematic representation of the genetic composition of transposon types found in enterococci. Adapted from Hegstad *et al.*,2010.

1.4 Mechanisms of antimicrobial resistance

The transition of enterococci from commensal organisms to major nosocomial pathogen is in part attributable to their intrinsic resistance to a wide variety of antimicrobial agents. Additionally, the plasticity or malleable genome of enterococci allows the easy acquisition and dissemination of additional acquired resistant determinants via HGT of MGE such as plasmids, transposons, and insertions sequences (Crank and O'Driscoll, 2015; Guzman Prieto *et al.*, 2016). The occurrence of point-mutations that may alter both gene expression and drug target binding sites also contributes to resistance. *Enterococcus* spp. are potentially capable of developing resistance to all currently available antimicrobial agents with significant public health and healthcare budget implications. It is important, therefore, to discuss enterococci in the context of their antimicrobial resistance patterns to fully establish the impact and burden on a local, national, and global scale. A brief overview of the most clinically relevant antibiotics and the associated resistance mechanisms is provided below.

1.4.1 β-lactam resistance

It is well established that the mode of action of β-lactam antimicrobials involves inhibition of bacterial cell wall formation via covalent linkage of the cytoplasmic transpeptidase enzymes known as the penicillin binding proteins (PBPs). These pentapeptide precursors are involved in peptidoglycan cross-linking and interfering with their activity ultimately disrupts the integrity of the bacterial cell membrane resulting in programmed cell death due to the production of reactive oxygen species (Kohanski *et al.*, 2007; Zapun, Contreras-Martel and Vernet, 2008; Hollenbeck and Rice, 2012). Enterococci tend to exhibit low-level intrinsic resistance to β-lactam antibiotics due to the expression of modified or alternative PBPs with low affinity binding to the drug molecule. This tolerance, with reports of minimum inhibitory concentrations (MICs) of >32 μg/mL in the literature, ensures that the bactericidal activity of the antibiotic is hindered and a bacteriostatic effect is seen, which is dosage dependent. In cases of severe infection, such as endocarditis, where bactericidal activity is required, combination therapy is often employed by adopting a synergistic approach with both a β-lactam and an aminoglycoside (Moellering and Weinberg, 1971; Arias *et al.*, 2010).

Resistance to β-lactam antimicrobials, particularly ampicillin, is characteristically associated with *E. faecium*, where it is reported to be 4-16 times less susceptible than *E. faecalis* (Murray, 1990). The most commonly reported and significant resistance determinant for low-level intrinsic β-lactam resistance in *E. faecium* is the production of PBP5. This property has occurred in the absence of antimicrobial exposure, with strains

isolated from the pre-antibiotic era and from geographically isolated populations in the Soloman Islands displaying low-level resistance to the β-lactams (Murray, 1990). High-level resistance (HLR) to ampicillin, with MICs of >256 mg/L, has also been extensively reported in *E. faecium* and has been found to arise due to overproduction of PBP5 in combination with the acquisition of point-mutations in the C-terminal transpeptidase domain that further decrease affinity (Rybkine *et al.,* 1998; Arias *et al.,* 2010). In fact, it is thought that approximately 90% of *E. faecium* isolates encountered in a healthcare setting are fully resistant to ampicillin, whilst it is considered rare in *E. faecalis* (Arias and Murray, 2012). It should be noted that whilst the PBPs are primarily chromosomally encoded, HLR ampicillin resistance can be disseminated via both HGT and clonal expansion of strains with mutated genes (Dahl *et al.,* 2000; Hanrahan *et al.,* 2000; Rice *et al.,* 2005). This is of particular concern, as often ampicillin is considered the treatment of choice for infections caused by susceptible enterococci.

The presence of β-lactamase enzymes, such as *blaZ*, has been described in both *E. faecium* and *E. faecalis*; however expression is generally considered constitutive and low-level (Rice and Murray, 1995). This is of significance, particularly in routine laboratory susceptibility testing, where an inoculum effect may be observed. Generally, *Enterococcus* spp. may appear susceptible at concentrations used during MIC determination. However, at a higher bacterial inoculum, as in active infection, the proportion of enzyme produced may lead to increased levels of antimicrobial resistance. The presence of these enzymes, once identified, is generally not considered of clinical significance as the use of a β-lactamase inhibitor such as sulbactam during a treatment regime tends to re-establish susceptibility (Miller *et al.,* 2014).

1.4.2 Aminoglycoside resistance

The aminoglycosides are concentration-dependent, bactericidal antimicrobials that function by binding to the 30s bacterial ribosomal subunit and disrupting protein synthesis resulting in the production of impaired proteins (Miller *et al.,* 2014). Enterococci, particularly *E. faecium* and *E. faecalis*, exhibit low-level intrinsic tolerance to clinically attainable levels of aminoglycosides. This is due to a combination of facultative anaerobic metabolism and the poor permeability of the enterococcal cell envelope which limits the passage and uptake of the antimicrobial into the cellular space and therefore hinders activity (Aslangul *et al.,* 2006). Additionally, the presence of chromosomally encoded enzymes, which inactivate the aminoglycoside molecule via covalent modification of the ribosomal target, further increases the MIC and contributes to low-level inherent resistance. This is particularly evident in *E.*

faecium, with two intrinsic enzymes (N-acetyltransferase (*AAC(6')-Ii*) and 3'-aminoglycoside O-phosphotransferase type III (*APH(3')-IIIa*)) considered ubiquitous amongst hospital acquired clones. The presence of these enzymes confer resistance to tobramycin, sisomicin, kanamycin, netilmicin and amikacin (Costa *et al.*, 1993). In addition, many *E. faecium* clinical isolates possess a ribosomal RNA (rRNA) methyltransferase, termed EfmM, that modifies a cytidine residue on the 16S rRNA subunit thus further preventing the activity of both kanamycin and tobramycin (Galimand *et al.*, 2011). In a clinical setting, this phenomenon is often overcome by aminoglycoside-penicillin combination therapy, particularly in the case of severe infection, which has been shown to improve uptake and increase intracellular drug concentration which achieves an over-all bactericidal effect (Geraci and Martin, 1954; Hollenbeck and Rice, 2012). However, due to the resistance mechanisms employed by *E. faecium*, the selection of aminoglycoside antimicrobials that can be used reliably is severely limited and is often restricted to streptomycin and gentamicin which are not significantly affected by intrinsic enzyme production (Miller *et al.*, 2014).

As a result of selective pressure, acquired high-level aminoglycoside resistance has been documented in both *E. faecium* and *E. faecalis*, with MICs of up to 128,000 mg/L reported (Murray, 1990). This is of particular concern, with the acquisition of additional modifying enzymes or point-mutations potentially negating the clinical utility of combination treatment in severe infection. HLR to streptomycin may arise due to ribosomal mutations or via enzymatic inactivation as a result of acquisition of an adenyl transferase gene encoding *ant(6')-Ia* or *ant(3")-Ia* (Hollingshead and Vapnek, 1985; Chow, 2000). High level gentamicin resistance is associated with the gain of a composite transposon carrying a gene encoding a bifunctional enzyme, termed *APH(2")-Ia-AAC(6')-Ie*, that modifies the 2'hydrox position on the aminoglycoside and results in loss of target binding (Courvalin *et al.*, 1980; Ferretti *et al.*, 1986; Chow, 2000). Other genes that confer gentamicin resistance such as *aph(2")-Ic*, *aph(2")-Id* and *aph(2")-Ib* result in varying MICs as low as 256 mg/L, which may be missed in diagnostic microbiology laboratories when testing for HLR at cut-off concentrations of 500-1000 mg/L (Courvalin *et al.*, 1980; Chow *et al.*, 1997; Tsai *et al.*, 1998; Alam *et al.*, 2005). It is important to note that although these enzymes are considered minor contributors to over-all gentamicin resistance, their presence is still considered clinically relevant as the use of combination synergistic therapy will result in treatment failure (Chow, 2000).

1.4.3 Glycopeptide resistance

Glycopeptide antibiotics, such as vancomycin and teicoplanin, are typically considered the gold standard or treatment of choice for the management of patients with severe infections caused by multi-drug resistant (MDR) pathogens such as methicillin resistant *Staphylococcus aureus* (MRSA), penicillin resistant *Streptococcus pneumoniae*, *Clostridiodes difficle* and ampicillin- or aminoglycoside-resistant *Enterococcus* spp. (Bruniera *et al.*, 2015). Glycopeptides are cell-wall-active agents that compromise the overall integrity of the cell envelope by interfering with mature peptidoglycan formation resulting in osmotic stress and eventually cell death. This bactericidal effect is due to the binding of the drug molecule to the C-terminal D-Alanine D-Alanine (D-Ala D-Ala) moiety of the pentapeptide precursors thus inhibiting polymerisation, transglycosylation and ultimately peptidoglycan cross-linking (Miller *et al.*, 2014; Stogios and Savchenko, 2020). Glycopeptides, after their introduction into clinical practice, appeared exempt from the growing levels of antibiotic resistance observed with other classes of antimicrobials. This was thought to be as a result of their alternative underlying mechanism of action which involves binding directly to the cell wall of the microorganism, rather than a protein target contained within the cytoplasm. However, after 30 years in clinical use, the acquisition of both low-level (MIC of 4-32 mg/L) and high-level (MIC of >64 mg/L) vancomycin resistance was documented in enterococci and continues to remain a significant epidemiological and healthcare burden in modern day medicine (Courvalin, 2006).

The emergence and associated mechanisms involved in vancomycin resistance in *Enterococcus* spp. has been extensively described in the literature (Courvalin, 2006). Briefly, resistance is mediated by target modification, in which an alternation in the terminal amino acid of the pentapeptide precursor is observed, thus decreasing the affinity of binding of the antibiotic (García-Solache and Rice, 2019). The extent of resistance is dependent on the amino acid change, with low-level resistance associated with a modification of the terminal D-Alanine D-Alanine (D-Ala D-Ala) to D-Alanine D-Serine (D-Ala D-Ser). High-level vancomycin resistance is associated with a substitution of the terminal peptide to D-Alanine D-Lactate (D-Ala D-Lac), resulting in a decrease in affinity by approximately 1000-fold as a result of an elimination of a hydrogen bond required for drug binding (Courvalin, 2006; Miller *et al.*, 2014). The ability of vancomycin resistant enterococci (VRE) to modify the terminal pentapeptide amino acid is related to both chromosomally encoded properties of certain species such as *Enterococcus gallinarum* and *Enterococcus casseliflavus* and the acquisition of resistance gene clusters (denoted as *van*) harboured on MGEs such as plasmids. To date, nine glycopeptide resistance operons have been described (*vanA*, -B, -C,

-D, -E, -G, -L, -M and N) in *Enterococcus* spp. (Ahmed and Baptiste, 2018). An overview of the resistance properties and transferability conferred by each *van* operon is shown in Table 1.1.

Table 1.1 Overview of the phenotypic and genotypic characteristics of the nine glycopeptide resistance operons identified in enterococci

Strain characteristic	Phenotype								
	vanA	*vanB*	*vanC*	*vanD*	*vanE*	*vanG*	*vanL*	*vanM*	*vanN*
Common carrier spp.	*E. faecium* *E. faecalis*	*E. faecalis* *E. faecium*	*E. gallinarum* *E. casseliflavus* *E. flavescens*	*E. faecium*	*E. faecalis*	*E. faecalis*	*E. faecalis*	*E. faecium*	*E. faecium*
Resistance determinant	Acquired	Acquired	Intrinsic	Acquired	Acquired	Acquired	Acquired	Acquired	Acquired
Expression	Inducible	Inducible	Constitutive inducible	Constitutive inducible	Inducible	Inducible	Inducible	Inducible	Constitutive
Resistance level (vancomycin)	High	Variable	Low	Moderate	Low	Low	Low	High	Low
Vancomycin MIC (µg/mL)	64->1,000	4-1,024	2-32	128	16	16	8	>256	16
Teicoplanin MIC (µg/mL)	16-512	≤-0.5	≤-0.5	4	≤-0.5	≤-0.5	≤-0.5	0.65->256	0.5
Amino acid modification	D-Ala-D-Lac	D-Ala-D-Lac	D-Ala-D-Ser	D-Ala-D-Lac	D-Ala-D-Ser	D-Ala-D-Ser	D-Ala-D-Ser	D-Ala-D-Lac	D-Ala-D-Ser
References	[1]	[2]	[3]	[4]	[5]	[6]	[7]	[8]	[9]

[1](Arthur and Courvalin, 1993; Courvalin, 2006), [2](Dahl *et al.*, 1999, 2003; Arthur and Quintiliani R., 2001; Courvalin, 2006), [3](Dutta and Reynolds, 2002; Reynolds and Courvalin, 2005; Miller *et al.*, 2020), [4](Perichon *et al*., 1997; Depardieu *et al*., 2003, 2004), [5](Arthur and Courvalin, 1993; Fines *et al.*, 1999; Courvalin, 2006), [6](McKessar *et al.*, 2000), [7](Boyd *et al.*, 2008), [8](Xu *et al.*, 2010), [9](Lebreton *et al.*, 2011).

The most commonly encountered mediators of vancomycin resistance in enterococci, and therefore the most clinically relevant, are the *vanA* and *vanB* operons (Figure 1.5). The prevalence of each glycopeptide resistant genotype varies depending on geographical location, with *vanA* extensively reported amongst VREfm isolates from Europe and North America, whilst *vanB* is considered endemic in Australia (Bonten *et al.,* 2001; Werner *et al.,* 2008; Coombs *et al.,* 2014; Guzman Prieto *et al.,* 2016).

The most commonly encountered mediator of vancomycin resistance in Ireland is *vanA*. The operon is frequently carried on a Tn3-family Tn*1546*-type transposon, which exhibits a high level of heterogeneity as a result of the potential for point-mutations, insertion sequences and deletions due to its relative plasticity (Arthur and Courvalin, 1993; Willems *et al.,* 1999; Novais *et al.,* 2008; da Silva *et al.,* 2012; Hollenbeck and Rice, 2012; Kuo *et al.,* 2014; Wardal *et al.,* 2014). A recent study from Denmark reported multiple variants of Tn*1546* carrying *vanA* amongst clinical isolates of VREfm, with a total of five Tn*1546*-like transposons characterised (Pinholt *et al.,* 2017). In addition to the *van* resistance operon, each variant of Tn*1546* also harbours two genes involved in the transposition of the element, a transposase (*orf1*) and a resolvase (*orf2*) (Woodford *et al.,* 1995; Hegstad *et al.,* 2010; Werner *et al.,* 2011).

Dissemination of the *vanA* transposon typically occurs through HGT and has been found on both conjugative and non-conjugative plasmids. The most prevalent plasmid families associated with the transfer of *vanA* type glycopeptide resistance in *E. faecium* are the pRUM and Inc18 group, with a predominance of Inc18 noted in Europe (Hegstad *et al.,* 2010; Rosvoll *et al.,* 2010; Freitas *et al.,* 2016). Interestingly, both of these plasmid types have been noted to use a toxin-antitoxin system as a maintenance mechanism, which allows plasmid survival even in the absence of antibiotic selection (Hegstad *et al.,* 2010). Additionally, Inc18 group plasmids and mosaic plasmids consisting of a combination of Inc18/pRUM have been shown to exhibit a high recombination rate and are associated not only with isolates from healthcare settings but also with animal and waste-water isolates (Tomita *et al.,* 2002; Freitas *et al.,* 2013). Despite the apparent success of InC18 and pRUM plasmid types in almost the exclusive dissemination of *vanA* amongst global VREfm, recent studies have reported that any enterococcal plasmid may be a vehicle of Tn*1546* (Freitas *et al.,* 2016). This highlights the promiscuity of the *van* transposon and in-part explains the success of the *vanA* genotype in establishing itself as the main driver of glycopeptide resistance observed in enterococcal populations worldwide.

Enterococcus spp. carrying *vanB* exhibit variable vancomycin resistance, ranging from moderate to high-level (MICs of 4 to >256 µg/mL) and are typically susceptible to

teicoplanin (Crank and O'Driscoll, 2015). The operon is most commonly carried by Tn*916* family transposons such as Tn*1547*, Tn*5382* and Tn*1549* (Arthur and Courvalin, 1993; Carias *et al.,* 1998; Launay *et al.,* 2006; López *et al.,* 2009). MGEs such as transposons carrying *vanB* have been found in both the chromosome and on transferable pheromone-sensitive and conjugative plasmids (Hegstad *et al.,* 2010; Palmer *et al.,* 2010).

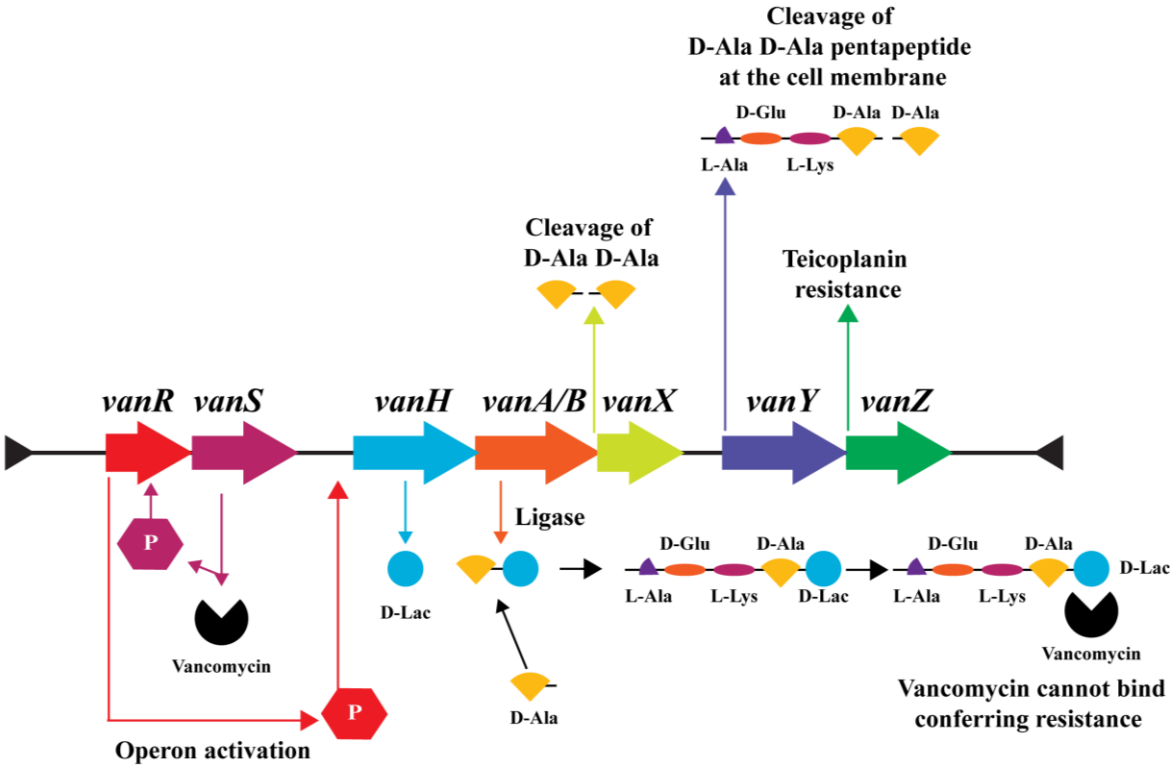

Figure 1.5. Schematic overview of the mechanism of vancomycin resistance mediated by the *vanA/B* operon. The operon consists of a two-component regulatory system (denoted by *vanR* and *vanS*) which responds to the presence of vancomycin and/or disruption at the cell membrane. The detection of the stimuli results in signal transduction to the cytoplasmic catalytic domain of *vanS*, which in turn causes kinase stimulation via phosphorylation of a histidine residue and transfer of a phosphoryl group to the response regulator *vanR*. This results in transcriptional activation of the down-stream regulatory and resistance genes. Briefly, a dipeptidase enzyme, *vanX*, hydrolyses D-Ala-D-Ala repeats in the growing pentapeptide precursor chains and *vanH*, a dehydrogenase, reduces pyruvate to D-Lac. A variable ligase gene, which is denoted as *vanA/B*, catalyses the formation of an ester bond to produce D-Ala-D-Lac pentapeptides, thus resulting in a modified target and a decrease in the affinity of target binding of vancomycin. *vanY* is a carboxypeptidase that can cleave D-Ala terminal peptides of late peptidoglycan precursors that were not eliminated by *vanX*. Finally, *vanZ*, which is associated with *vanA* genotypes, confers resistance to teicoplanin via an unknown mechanism. Adapted from Faron *et al.*, 2016.

1.4.4 Linezolid resistance

Linezolid, an oxazolidinone antibiotic, is a bacteriostatic agent with broad spectrum activity against clinically important MDR Gram-positive bacteria including VRE. It is considered a drug of last resort and was first approved for clinical use in 2000. Linezolid functions by inhibiting the transfer of the aminoacyl-tRNA to the A site of the bacterial ribosome via binding within the peptidyl transferase centre in the V domain of the 23S rRNA component of the 50s ribosomal subunit. The binding blocks the formation of a functional initiation complex and prevents the translation of mRNA, thus inhibiting protein synthesis (Shinabarger *et al.,* 1997; Leach *et al.,* 2007). As linezolid is synthetically produced, there are very limited natural reservoirs of resistance genes found within the general environment which has resulted in the slow and sporadic emergence of oxazolidinone resistance in a background of prolonged selective pressure (Meka and Gold, 2004). Mutations in the 23S rRNA binding site of the 50S subunit or the ribosomal proteins L3 and/or L4 are the most frequently observed mechanisms associated with linezolid resistance, with a G2576T transition most prevalent (Bi *et al.,* 2018). It should be noted that a variety of mutations have been documented in clinical isolates, including G2447T and T2504A transitions, which demonstrates that resistance often occurs via spontaneous *de novo* mutations rather than via HGT (Prystowsky *et al.,* 2001; Flamm *et al.,* 2012; Bialvaei *et al.,* 2017). Enterococci carry multiple copies of the 23s rRNA gene, with *E. faecium* reported to have a total of six copies, and unsurprisingly the level of expressed resistance correlates directly with the number of mutated alleles (Marshall *et al.,* 2002). Gene conversion, a process in which homologous recombination allows further genes to acquire the same mutation once a single allele is changed, is commonly observed with prolonged exposure to linezolid which can lead to HLR (García-Solache and Rice, 2019). For example, a mutation in one copy of an *E. faecium* rRNA gene was shown to confer an MIC of 8-16 mg/L, whilst >3 mutated genes conferred an MIC of between 64-128 mg/L (Marshall *et al.,* 2002).

Enterococcus spp. may also confer resistance to linezolid through the acquisition of plasmid-encoded genes such as the multidrug resistance-encoding methyltransferase gene *cfr*, the ATP-binding cassette (ABC)-F transporter encoding gene *poxtA* and/or the ABC transporter-encoding gene *optrA* (Wang *et al.,* 2015; Antonelli *et al.,* 2018; Bi *et al.,* 2018). The proportion of enterococcal isolates reported globally to harbour these mobile resistance genes is relatively low and sporadic in nature, however more recently a pronounced increase in the prevalence of *optrA* and *poxtA* has been observed (Mendes *et al.,* 2016, 2018). For example, a study by Egan and colleagues highlighted an increase in the spread and

proportion of plasmid-encoded *optrA* and *poxtA* among linezolid-resistant enterococci in Irish hospital with the highest rates in Europe reported to date of 22.7% (Egan *et al.*, 2020a). This increased acquisition and subsequent dissemination of plasmid-located linezolid-resistance via HGT poses a significant threat to public health, with the potential for transmission to VREfm and/or to other MDR Gram-positive organisms such as MRSA. This could give rise to pan-resistant derivatives, for which treatment options would be extremely limited and patient management significantly complicated. Unfortunately, this has been documented in several instances in the literature to date, with one study reporting 26.3% of linezolid-resistant enterococcal isolates harbouring both a *poxtA*-encoding plasmid and a *vanA* encoding-plasmid (Egan *et al.*, 2020a).

1.5 Prevalence of VREfm in Ireland

Understanding the molecular epidemiology, population biology and evolutionary genetics of VREfm is essential for surveillance as it provides an insight into patient management and potential infection prevention and control practices. The prevalence of VREfm-associated infections vary depending on geographical location, patient population and healthcare setting. Unfortunately, there is a significant lack of up-to-date, precise information regarding VREfm prevalence and population biology in Ireland in the literature. The majority of published studies used out-dated and unreliable typing methods which complicates the assessment of the true burden of disease and the over-all prevalence of infection and/or colonisation within both healthcare settings and the general population. Ireland has contributed resistance data for invasive enterococcal infections to the European Antimicrobial Resistance Surveillance Network-Net (EARS-net) since 2002 with all clinical microbiology laboratories participating. In quarter one of 2019, 38.4% of invasive *E. faecium* bloodstream infection (BSI) isolates recovered in Ireland were vancomycin resistant. In fact, VREfm invasive infection rates in Ireland are among the highest in Europe over a 10-year period (2008-2018) (ECDC, 2020). These reported numbers are limited to BSIs only, and therefore the true burden of disease caused by VRE in Irish hospitals is likely to be significantly greater than that reflected in these figures.

A study in an Irish tertiary referral centre in 2015 attempted to characterise the molecular epidemiology and population biology of VRE isolates recovered from BSIs between 2009 and 2012. A total of 75 patients with VRE BSI were identified, 95% of which were VREfm invasive isolates, with an overall rate of 0.12 VRE BSI per 1000 bed days. Interestingly, 77% of these patients were screened for VRE prior to a positive blood culture and 64% (48/75) were found to be colonised. VRE was also isolated from an additional

clinical specimen in 14 of these patients (including peritoneal drain fluid, intra-abdominal tissues, and superficial wound swabs). Using a combination of pulse-field gel electrophoresis (PFGE) and conventional MLST, the authors reported four dominant CC17 STs including ST17, ST18, ST78 and ST203 and suggested an over-all polyclonal pattern as a result of horizontal transmission in conjunction with the influx of new clones (Ryan *et al.,* 2015). However, this study is limited by the traditional genotyping methods employed, which are now considered insufficient for epidemiological typing and outbreak management.

A study conducted in 2014 in an acute Irish hospital in Cork attempted to determine the prevalence of VRE carriage and identified that 19.1% (67/350) of patient faecal samples tested were positive for VREfm, with a predominance of *vanA* noted. The authors also employed random amplified polymorphic DNA (RAPD) fingerprinting which highlighted a heterogenous CC17 population (Whelton *et al.,* 2016). Interestingly, this study also investigated 29 (8.2%) faecal samples from a community setting, none of which yielded VRE suggesting that VRE is predominantly acquired in a hospital-based setting in Ireland (Whelton *et al.,*2016). This is in contrast with other findings from Europe, with a study in France highlighting a large community reservoir of VRE with a prevalence rate of 11.8%, which was associated with the significant usage of avoparcin historically in animal husbandry (Gambarotto *et al.,* 2000; Mascini and Bonten, 2005). Additional studies from Germany and The Netherlands reported VRE colonisation rates of 6-12% in the community (Klare *et al.,* 1995; Endtz *et al.,* 1997). In contrast, an additional Irish study by Ryan and colleagues anonymously screened 100 faecal samples from patients attending the emergency department of an Irish hospital and reported a prevalence rate of 1%, compared to 38% with hospital inpatients (Ryan *et al.,* 2015). While these findings may indicate a difference in the ecology of Irish VREfm compared to other European countries, it is impossible to make accurate deductions on the VRE colonisation rates in the general Irish population based on the limited sample size of these studies. Furthermore, the majority of community samples tested were from elderly individuals which may have introduced an age-based bias. Further investigations are required to provide clear insights into the role of the community, animal husbandry and the food chain in the epidemiology of VREfm in Ireland.

Additional studies on the colonisation rate or prevalence of VREfm in Ireland are limited in their inclusion criteria and comprise only high-risk patients in critical areas such as augmented care and therefore any conclusions should be interpreted with that in mind. For example, a study in 2018 found that 19% (30/157) of patients screened for VRE within the intensive care unit (ICU) were colonised (McDermott *et al.,*2018). This is in keeping with European surveillance studies conducted by the EARS-net and National Healthcare

Safety Network (NHSN) with variable rates of colonisation reported in hospitalised patients and key differences observed depending on geographical location and associated patient immune status (ECDC, 2020, 2023, 2024). For example, rates as low as <2% were reported from Finland in contrast to 34% reported from Ireland (Orsi and Ciorba, 2013). It is important to note that a finding of VRE colonisation in any patient, irrespective of associated ward or immune status, is clinically significant as they may serve as reservoir of infection via environmental shedding, which could result in spread and aid dissemination. The study conducted by McDermott and colleagues, mentioned above, investigated the contribution of the near-patient environment to VRE transmission and found that 6.5% of all environmental sites tested were positive for VREfm, with 61% considered 'high-touch' in nature including drip-stands, chart holders and bed control panels. PFGE typing revealed a heterogenous population amongst patient isolates, while environmental isolates showed a more distinct clonal relationship (McDermott *et al.,* 2018). Environmental persistence of enterococci in hospitals has been extensively documented despite vigorous infection prevention and control cleaning regimens, which is due in-part to their tolerance to subclinical concentrations of various disinfectants, including some alcohol preparations and chlorhexidine (Guzmán Prieto *et al.,* 2017). A study from the United Kingdom, the closest geographical neighbour of Ireland, reported that 48% of environmental swabs taken in two haematology wards over a six-month period were positive for VREfm and 20% of bedroom/bathroom areas remained positive following routine cleaning after patient discharge. When deep cleaning was implemented, it was shown that approximately half of sample sites yielded *E. faecium* within three days of patients reoccupying the ward (Goulíouris *et al.,* 2018). It is not unreasonable to conclude that persistent contamination and colonisation of the direct patient environment with VREfm has provided extensive reservoirs which may have contributed to the rapid spread in Irish hospitals. Further studies utilising more up to date methodology are required to truly discern and confirm the role of the environment in a healthcare setting in the epidemiology of Irish VREfm.

A single study conducted by Raven and colleagues in 2016 remains the only available scientific literature to date that utilised WGS-based methods to investigate *E. faecium* population dynamics in Ireland. A total of 495 *E. faecium* (VREfm and vancomycin susceptible *E. faecium* (VSEfm)) BSI isolates recovered over a ten-year period (2001-2011) from 40 hospital microbiology laboratories were investigated. The majority of isolates 95.8% (*N*=474) were from the United Kingdom, whilst the remaining 4.2% (*N*=21) were from Ireland (Raven *et al.,* 2016). The study demonstrated a polyclonal VREfm population structure, with evidence of transmission between different hospital networks both within and

outside referral/country limits. Two clusters were highlighted that were geographically restricted to both the Republic of Ireland and Northern Ireland, with an additional finding of a unique *vanA* transposon region with deletions in the transposase, resolvase and *vanZ* genes within Irish isolates. This suggests a local source and evolution of *vanA* amongst Irish VREfm isolates (Raven *et al.,* 2016). Whilst this study utilised more discriminatory technology with high resolving power than previous Irish studies, in relation to Irish VREfm it is still limited by its small sample size (i.e., *N*=21).

Limited literature currently exists evaluating the true prevalence and molecular epidemiology of VREfm in Ireland and it is evident that there is an urgent requirement for robust, comprehensive surveillance and epidemiological typing studies. This would provide an insight into the emergence, evolution and spread of infection which would likely inform evidence-based recommendations to guide infection, prevention and control strategies which could significantly impact the further rise of VRE.

1.6 Clinical burden of VREfm

VREfm carriage and associated infection represent a major surveillance and therapeutic challenge for clinicians due to the urgent need to implement contact precautions and select appropriate therapy in a timely manner to reduce morbidity and mortality and curtail further transmission. Despite improvements in standard of care, patient management, and therapeutics, VREfm remains a high priority pathogen with the WHO highlighting the urgent need to invest in increased research and development of novel antimicrobials to address the growing resistance problem. Few studies currently accurately evaluate the global burden of disease caused by antimicrobial resistant pathogens, however a European-based study published in 2019 estimated that the age adjusted median disability-adjusted life years (DALYs) due to VRE infection (VREfm and vancomycin resistant *E. faecalis* (VREfs)) was 5.49 per 100,000 of the population with a median number of attributable deaths of 1081 per 100,000. Interestingly, the authors also emphasised that a higher proportion of the burden estimates for Ireland were due to VREfm and VREfs than in other countries (Cassini *et al.,*2019). Another study on the impact of infectious disease in Europe reported that the burden of antimicrobial resistant bacterial infections is comparable to that of tuberculosis, HIV/AIDS and influenza combined. It was also shown that 75% of the burden quantified by the DALYs was due to healthcare-associated infections and this could be diminished through the implementation of stringent infection prevention and control methods in conjunction with improved antimicrobial stewardship (Cassini *et al.,* 2018).

In July of 2021, the Health Information and Quality Authority (HIQA) in collaboration with the Health Research Board Ireland (HRB) published a report on the economic burden of antimicrobial resistance in Ireland and found that the total number of deaths attributable to 16 key antibiotic-resistant bacteria in public acute hospitals in Ireland in 2019 was 215, with resistant strains of *E. faecium and E. faecalis* accounting for 25.5% of deaths. In fact, according to this study the associated mortality rate due to VREfm and VREfs was reported as 1.11 per 100,000 population. The incidence of antimicrobial resistance due to VRE was estimated as 27.96 per 100,000 population and the overall total number of attributable DALYs was 25.70 per 100,000 population (Figure 1.6) (HIQA, 2021). Considering the potential for treatment failures in patients with VREfm, which can significantly impact prognosis, the cost of treatment and the length of hospital stay, it is likely that the link between morbidity and mortality associated with VRE infection is significant. It is clear based on the limited studies to date that VREfm constitutes a significant disease burden on patients, clinicians, the Irish healthcare system, and society.

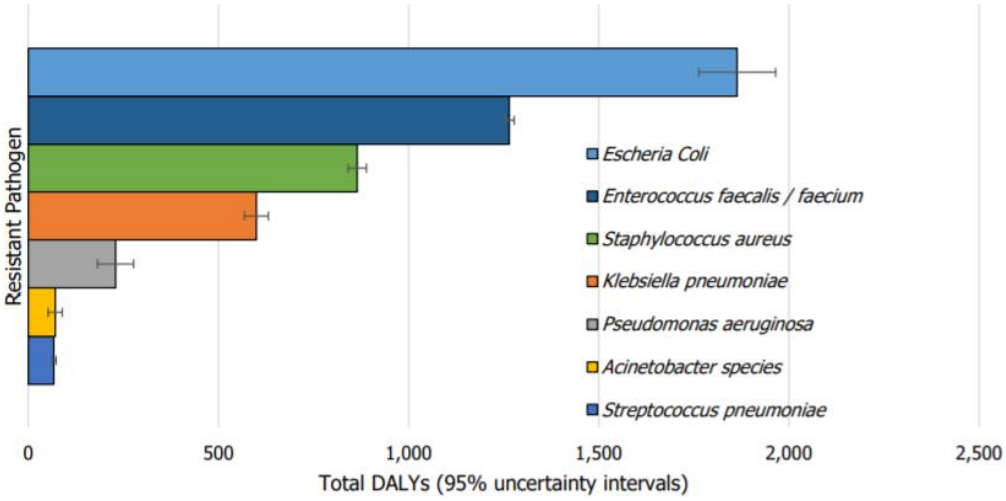

Figure 1.6. The relationship between the total number of infections, attributable deaths and DALYS for clinically important antibiotic resistant bacteria in Irish public acute hospitals in 2019. This graph highlights the high burden of disease associated with third-generation cephalosporin-resistant bacteria, VRE and MRSA (HIQA, 2021).

1.7 Economic burden of VREfm

The significant clinical burden of VREfm should always be considered in the context of the financial implications associated with the management of infection, with reports of substantial economic burden quoted throughout the literature. For example, it has been reported that infections caused by VRE are associated with an increased length of hospital stay, more complex antimicrobial therapy and a high proportion of additional invasive procedures which all contribute to extensive hospital-associated costs (Stosor *et al.,* 1998; Carmeli *et al.,* 2002; Pelz *et al.,* 2002; Song *et al.,* 2003; Kaye *et al.,* 2004; Butler *et al.,* 2010). In the USA, a significant variation on the financial burden attributed to VRE infections has been reported, ranging between $9,949 and $124,257 per episode, depending on the site of infection and underlying patient comorbidities. In these studies, the authors compared the cost of infection associated with a patient with VRE, a patient with a vancomycin susceptible enterococci (VSE) and a patient without enterococcal infection and found costs from $33,224 to $124,257, $20,895 to $56,707, and $8,192 und $18,863, respectively, (Stosor *et al.,* 1998; Pelz *et al.,* 2002; Song *et al.,* 2003; Butler *et al.,* 2010). In fact, one study highlighted an independent association of VRE infection with a 1.4-fold increase in total cost per patient (Kaye *et al.,* 2004; Puchter *et al.,* 2018).

Similar trends are evident in Europe, with one German hospital calculating the hospital costs directly attributed to VRE as €13,157 per patient. This study also highlighted that the presence of VRE alone significantly influences costs, with detailed analysis highlighting the differences between VRE and VSE patients after the onset of infection with variances observed in the costs of pharmacy, nursing staff, medical products, and assistant medical technicians – €37,971 vs €23,025, respectively (Puchter *et al.,* 2018). In Ireland, it was estimated by HIQA that the median economic burden of antimicrobial resistance due to VREfm and VREfs infection was approximately €3,070,201 in 2019 (95% Confidence Interval) (HIQA, 2021). It should be noted that these figures are estimates and are not actual costs calculated in real-time and only reflect additional costs accrued due to increased length of hospital stay. However, they do provide some insight into the major economic consequences of infection and highlight that VRE is perhaps often underestimated and overlooked in the context of other more closely monitored resistant organisms such as carbapenem resistant *Enterobacterales* (CRE) or MRSA.

1.8 Traditional molecular typing methods

The ability to accurately discriminate and determine the genetic relatedness of VREfm isolates is fundamental in local and national surveillance, population biology analysis and outbreak management. Molecular typing can be utilised to identify transmission pathways and environmental reservoirs, monitor emergence and epidemiological spread, gauge prevalence and identify circulating antimicrobial resistance determinants. There are a variety of available techniques described in the literature which vary in their discriminatory power, ease of use, inter- and intra-laboratory comparability, and cost-effectiveness. A brief summary of the repertoire of molecular typing platforms utilised in the characterisation and differentiation of *E. faecium* isolates is shown in Table 1.2. The value and application of PFGE and MLST is discussed in detail in the following sections.

Table 1.2 Molecular typing methods available for investigation and discrimination of VREfm

Method	Principle	Discrimination	Reproducibility	Data exchange	Applications
Ribotyping	Hybridisation of digested genomic bacterial DNA with labelled ribosomal-DNA probes	Moderate	Good	Difficult	Short-term epidemiological studies
RAPID/repPCR	PCR based amplification of non-coding repetitive sequences	Moderate	Poor	Difficult	Small 'in-house' hospital-based outbreak studies
AFLP	PCR based selective amplification of restriction fragments from digested bacterial genomic DNA	Moderate	Good	Difficult	Initial, first-in-line screening method to rule out isolate relatedness
PFGE	Macro restriction of bacterial DNA and clonal assignment based on fragment banding patterns	Moderate	Poor	Difficult	Historical gold standard for outbreak investigation. Lacks discrimination and unsuitable for long-term epidemiological analysis
MLST	DNA sequence comparison of fragments of seven house-keeping genes	Moderate	Excellent	Easy	Limited population-based analysis but lacks discrimination for outbreak analysis
Plasmid typing	Variety of available schemes that look at backbone loci associated with replication (rep tying) or plasmid mobility (mob typing) using PCR-based methods	Poor	Good	Moderate	Epidemiology of plasmid-based antibiotic resistance
WGS	Analysis of the entire bacterial genome	High	Excellent	Easy	Short- and long-term epidemiological studies and population-based analysis

Table adapted from Werner, 2013.
Abbreviations: AFLP, Amplified-Fragment Length Polymorphisms; PFGE, Pulsed Field Gel Electrophoresis MLST, Multi-locus Sequence Typing.

1.8.1 PFGE

Historically, PFGE was considered the gold standard and method of choice to investigate genetic relatedness and establish epidemiological links between enterococcal organisms recovered in an outbreak setting. The principle of this technique involves the enzymatic digestion of bacterial DNA using endonucleases that cleave DNA infrequently with subsequent DNA fragment separation by pulsed field gel electrophoresis followed by assignment of isolate relatedness based on banding patterns obtained (Patterson and Kelly, 1998). However, PFGE is technically demanding and requires a high degree of expertise for both procedure performance and data interpretation. In addition, downstream data evaluation is subjective and lacks standardisation and therefore intra-laboratory reproducibility and comparability is challenging (Werner, 2013). *Enterococcus* spp. are also characterised by an extremely plastic or malleable genome, with some studies suggesting that up to 44% of the core genome of *E. faecium* may be subject to recombination, which can result in a high proportion of DNA banding pattern polymorphisms amongst isolates when using PFGE (Leavis *et al.,* 2006; Howden *et al.,* 2013). A recent Danish study highlighted the lack of discriminatory power of PFGE with hospital-associated outbreak strains of *E. faecium* compared with WGS. The errors or misclassifications in phylogenetic analysis when using PFGE may be due to the low resolving power of the method which results in difficulty in separating bands of similar sizes and the fact that identical size bands does not necessarily equate to identical DNA content (Pinholt *et al.,* 2015). PFGE, therefore, is unsuitable and out-dated for epidemiological surveillance and population-based studies of *E. faecium.*

1.8.2 MLST

MLST is a more reproducible and standardised scheme for the discrimination of *E. faeciu*m based on polymerase chain reactions (PCR) amplification and subsequent Sanger sequencing of internal gene fragments from seven well-conserved house-keeping gene loci and was first described in the early 2000s (Homan *et al.,* 2002). When using an MLST based approach, isolates are assigned distinct allele numbers based on observed variations within the nucleotide sequences of each of the seven house-keeping genes. The allele numbers at each locus are then combined to define the allelic profile or genotype of the organism which is subsequently followed by ST assignment. An algorithm, termed eBURST, is then applied which allows the division of MLST data into groups of related ST isolates. This tool assigns distinct CC types, which is typically composed of a single predominant ST or genotype with several less common close descendants or relatives (Feil *et al.,* 2004). STs which differ by

only one allele out of the seven house-keeping genes are defined by the same CC type (Willems *et al.,* 2005). A MLST based international database (https://pubmlst.org/organisms/enterococcus-faecium) is publicly available for *E. faecium* and allows submission of novel allelic profiles for ST assignment as well as comparison against isolates on a global scale.

There are several advantages to employing an MLST approach compared to PFGE, including more standardisation, less subjective downstream data interpretation, and the ability to compare surveillance data reproducibly and accurately across laboratories. However, due to the high recombination rate associated with the enterococcal genome discussed previously, several studies have indicated that the resolving power of conventional MLST is insufficient for surveillance, outbreak assignment and can result in errors in phylogenetic analysis when compared with WGS approaches (de Been *et al.,* 2015; Pinholt *et al.,* 2015, 2017; Guzman Prieto *et al.,* 2016; Raven *et al.,* 2016). In fact, the significantly high proportion of rearrangement has been shown to include five of the seven house-keeping genes, which further indicates that establishing genetic relatedness based on MLST alone can give rise to misleading results (Howden *et al.,* 2013). In addition, the emergence of VREfm isolates that are considered non-typeable by conventional MLST schemes due to the loss of one of the house-keeping alleles (*pstS* gene) have been reported (Carter *et al.,* 2016; van Hal *et al.,* 2018). These factors serve to highlight and further add to the limitations associated with MLST for the monitoring of *E. faecium* in an outbreak setting and preclude the recommendation of this method as a solitary tool in the surveillance algorithm in infection prevention and control strategies

1.9 Whole-genome sequencing

High-throughput WGS has revolutionised surveillance and infection prevention and control strategies in healthcare settings by enabling high-resolution typing of clinically important antibiotic resistant bacteria. The significant improvement in the discriminatory power of the technology ensures highly accurate outbreak investigation, elucidation of complex transmission routes and environmental sources and monitoring of the emergence and spread of MDR organisms in real-time. In addition, the genome-wide approach circumvents the limitations of more traditional methods associated with high recombination rates and genetic diversity such as occur with VREfm. Sequencing technologies can be divided into three main categories depending on the underlying method and principle: first generation, second generation and third generation sequencing (Kchouk *et al.,* 2017). This study is mainly concerned with the applications of second and third generation sequencing to bacterial typing and have been outlined in brief below.

1.9.1 Second generation sequencing

Second generation sequencing-based technologies are characterised by the parallel production of millions of short reads (50-500 bp) of DNA with a more cost-effective and improved turn-around-time in comparison to previous generations and the absence of downstream electrophoresis-based detection methods. There are a variety of commercially available second generation WGS platforms including Roche 454, ABI's SOLid, Ion Torrent and Illumina. These short-read sequencing platforms can be further divided into two main categories based on their underlying sequencing chemistry and engineering: sequencing by ligation and sequencing by synthesis (Kchouk *et al.,* 2017).

The most frequently utilised platform for bacterial strain genotyping involves Illumina technology, which is based on a sequencing by synthesis approach with cyclic reversible termination (Besser *et al.,* 2018). Briefly, clonal template libraries are prepared in which high molecular weight bacterial genomic DNA is sheared and subsequently adapters are annealed or ligated to both ends of each fragment in a process termed tagmentation (Goodwin *et al.,* 2016; Kchouk *et al.,* 2017; Besser *et al.,* 2018; Feng *et al.,* 2018). The adapters can then selectively bind to complementary oligonucleotide sequences immobilised on the surface of a patterned flow cell. The free end of each strand can then interact with other primers nearby, which forms a bridge like structure. Each bound fragment on the solid flow cell is subsequently amplified, in a process known as PCR bridge amplification, which generates identical copies of each sequence and eventually results in 100-200 million distinct

clonal clusters (Kchouk *et al.,* 2017). Following solid-phase template enrichment, modified nucleotides, primers and DNA polymerase are added to the flow cell. Each nucleotide is labelled with a base-specific, cleavable fluorophore and contains an inactive 3'-hydroxyl blocking group. A sequencing cycle is then initiated, in which a single fluorescently labelled nucleotide is added to the fragments in each cluster, with the blocked 3' group preventing additional base incorporation. The flow cell is subsequently imaged using internal reflection fluorescence microscopy and the emitted signal determines the identity of the nucleotide base incorporated into the cluster. The 3'-hydrodxyl group, which also serves as a reaction terminator, is cleaved post-detection and the next cycle of incorporation, elongation and detection commences (Goodwin *et al.,* 2016; Kchouk *et al.,* 2017).

There are a variety of available platforms in the Illumina suite which include the MiSeq, HiSeq, NovaSeq, NextSeq and MiniSeq. Whilst each instrument may differ in terms of throughput, read length output and laboratory space requirements, the underlying sequencing biochemistry outlined above is identical (Besser *et al.,* 2018). The MiSeq is the most frequently utilised system in the Illumina family for microbial WGS research and outbreak investigation due to its high-quality output (0.1% for >90% of base calling), affordable run cost and reasonable turn-around-times in comparison to the other available instruments (Quainoo *et al.,* 2017).

1.9.2 Third generation sequencing

Despite the pioneering role of second generation WGS in bacterial genomics, technologies such as Illumina may produce a highly fragmented bacterial genome, which following assembly is spread across multiple contigs, many of which are short (<300 bp). This is due to the difficulty in resolving repetitive genomic regions, the presence of copy number alterations and significant structural variation (Goodwin *et al.,* 2016). Whilst this is sufficient for high-resolution population biology analysis and outbreak investigation, it significantly complicates the formation of a fully assembled bacterial genome, which prevents detailed analysis of accessory components such as MGEs, detection of HGT events and discovery of microbiologically important genes (Klassen and Currie, 2012). The development of third generation sequencing, also referred to as long-read sequencing, has helped to overcome this issue by negating the need to fragment the bacterial genome by base calling on a nucleotide level from a single continuous long strand of DNA (Goodwin *et al.,* 2016; Kchouk *et al.,* 2017; Besser *et al.,* 2018). The most widely utilised platforms in third generation sequencing are available from Pacific Biosciences (PacBio, California, USA) and Oxford Nanopore Technologies (ONT, Oxford, UK). The MinION instrument developed by ONT is

considered the most readily accessible, cost efficient and portable device currently available on the market, which can easily be used on a computer with basic central processing unit (CPU) performance (Goodwin *et al.,* 2016; Kchouk *et al.,* 2017; Besser *et al.,* 2018). The underlying sequencing chemistry of this technology involves passing an ionic current through a protein nanopore (nanoscale hole) present on a flow cell. The bacterial genomic DNA is then moved through the pore by action of a motor protein which generates a change in the ionic current. The degree of variation in the ionic current can be then utilised to identify the underlying sequence (i.e., determine the nucleotide base) (Kchouk *et al.,* 2017).

Whilst the MinION can improve the contiguity of *de novo* assembly by generating reads exceeding 150 kb, it is also associated with a high error rate of ~30% per base call and 0.1 in >75% of base calls (Quainoo *et al.,* 2017). Some studies have suggested an overall error rate of ~12% with 3% accounting for mismatches, 4% for insertions and 5% for deletions (Jain *et al.,* 2017). The significant potential for error in third generation sequencing has prompted its use in combination with other WGS platforms. For example, to overcome the limitations associated with both ONT and Illumina, a hybrid assembly-based approach using sequences generated by both is often employed. This involves using the ONT long reads as a scaffold to resolve ambiguities in assembly graphs that cannot be elucidated by Illumina short reads alone (Chen *et al.,* 2020). There are a variety of hybrid assembly pipelines available including Unicycler, SPAdes and MaSuRCA, however Unicycler is considered the superior approach for genomic analysis of bacterial pathogens (Zimin, 2014; Chen *et al.,* 2020). Briefly, Illumina short reads are first placed into a highly accurate assembly graph and ONT MinION reads are then used to build bridges to resolve the gaps present in the genome. By using the Illumina short reads first, a lower proportion of long reads are required which leads to lower misassembly rates and negates the high error rate associated with ONT (Chen *et al.,* 2020). An overview of the hybrid assembly approach employed by the bioinformatic Unicycler tool is shown in Figure 1.7.

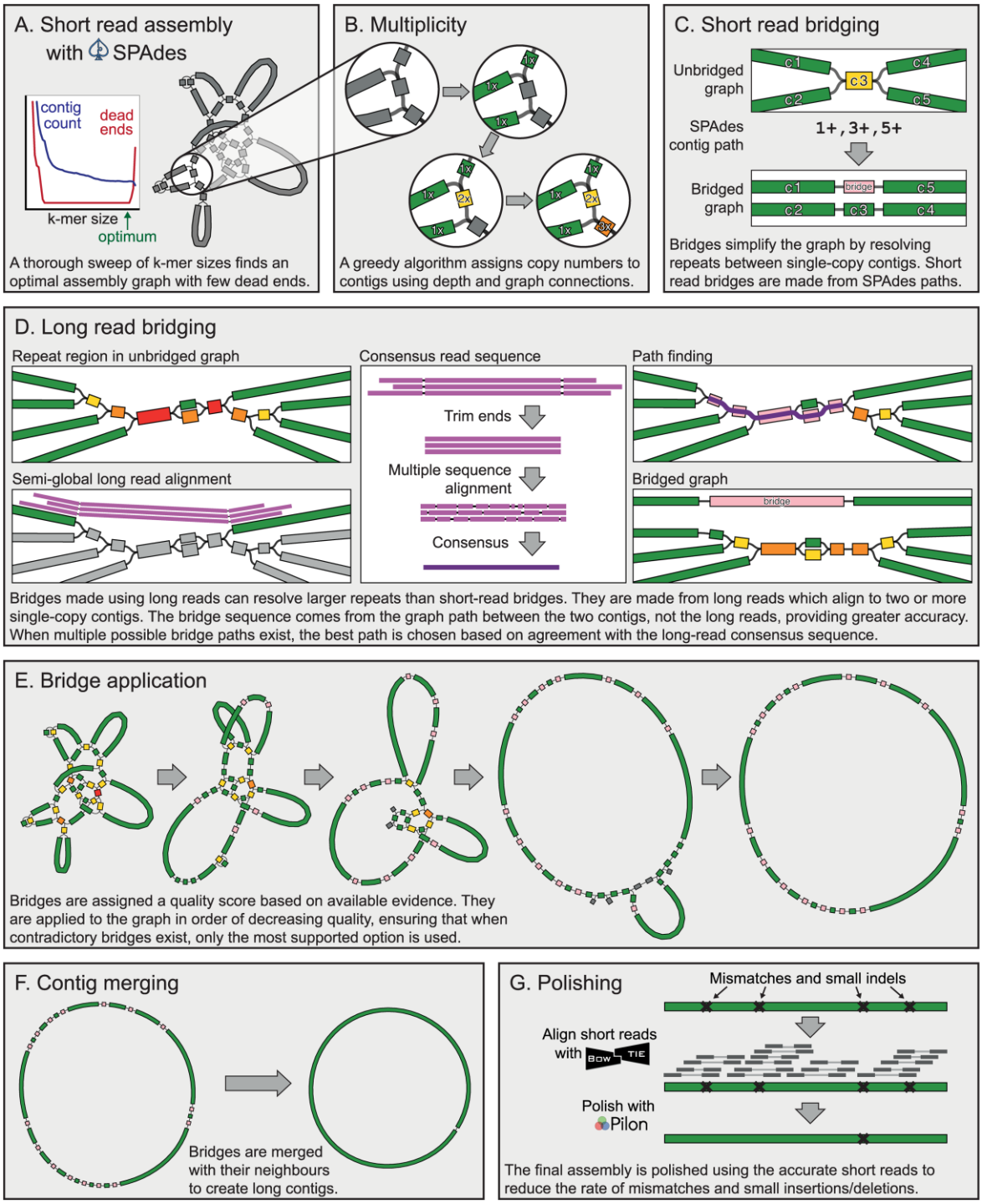

Figure 1.7 Overview of the key steps in the Unicycler hybrid assembly approach. Adapted from Wick *et al.*,2017.

1.10 Applying a WGS approach to VREfm surveillance

A large quantity of complex data is produced when a WGS based approach is used to study the molecular epidemiology and population structure of VREfm. A host of bioinformatic tools have been developed to extract and fully exploit relevant genomic information and allow the meaningful analysis and interpretation of sequencing data. Unfortunately, many of these tools are only available using command-line interfaces and require substantial skill and extensive knowledge of computer programming for operation and troubleshooting. However, there are a subset of commercially available and user-friendly platforms that require little bioinformatic background or knowledge and include software packages such as BioNumerics (Applied Maths, Ghent, Belgium) and SeqSphere + (Ridom GmbH, Germany).

1.10.1 Comparative genomics

A gene-by-gene allele calling and/or a variant mapping approach may be utilised downstream of WGS to establish epidemiological links and identify transmission events in VREfm surveillance. The main approaches used, to date, involve the discrimination of isolates based on core-genome MLST (cgMLST), whole-genome MLST (wgMLST), core-genome single nucleotide polymorphism (cgSNP) analysis and split *k*-mer analysis (SKA).

1.10.1.1 cgMLST

Whilst classical MLST has helped to overcome the intra- and inter-laboratory comparison issues associated with PFGE, its resolving power is considered insufficient in an outbreak setting and lacks appropriate discrimination. Additionally, as stated previously, the high level of genome plasticity exhibited in *E. faecium* that results in a high degree of DNA banding pattern polymorphisms when using PFGE, further complicates epidemiological investigations when using classical MLST (de Been *et al.*, 2015). In 2015, a cgMLST scheme was developed by de Been and colleagues to help overcome these limitations. This method utilises a genome-wide gene-by-gene comparison approach, as with classical MLST, but with an extension of the number of analysed genes from seven to 1,423 stable single-copy coding genes from the core-genome of *E. faecium* (de Been *et al.*, 2015). According to this scheme, it was deemed that isolates with ≤20 allele differences between genes are considered genetically indistinguishable, closely related, and most likely belonging to the same outbreak. Isolates with 21-40 allelic differences should be considered as possibly belonging to the same outbreak and should be interpreted in conjunction with relevant epidemiological and patient movement data (de Been *et al.*, 2015). This well-established

scheme has been successfully employed in a variety of studies for rapid, high-resolution outbreak investigation, to establish epidemiological patterns and to inform national surveillance systems (Pinholt *et al.*, 2015, 2017; Hammerum *et al.*, 2017, 2019; Egan *et al.*, 2020a, 2020b). In fact, it has been shown that cgMLST is equally as discriminatory as SNP-based phylogenetic approaches with the added advantage of allowing potential storage of allelic data in a central database (de Been *et al.*, 2015). This permits the comparison of isolates on a global scale and long-term epidemiological studies with a universal, standardised nomenclature.

1.10.1.2 wgMLST

A wgMLST scheme developed and curated by BioNumerics in 2018 expands on the cgMLST alleles to include both core and accessory genes with a total of 5,489 loci. It has been long established that hospital acquired clones of VREfm tend to be enriched with MGEs, insertion sequences and pathogenicity islands and therefore the inclusion of the accessory gene loci ensures that any significant genomic evidence is not overlooked during comparative analysis of highly similar isolates (Lebreton *et al.*, 2013; Gouliouris *et al.*, 2018).

1.10.1.3 Analysis of single nucleotide polymorphisms

Sequence read alignment to a study-specific reference isolate and subsequent variant calling may be utilised to infer genetic relatedness within a bacterial population. This commonly involves the identification and assessment of genetic variation, such as SNPs, nucleotide insertions and deletions (indels), between a reference sequence and query genome(s). These variations most frequently occur due to point mutations at single base positions within the bacterial genome which accumulate over time at a constant rate. For example, current studies on *in-vivo* evolution of *E. faecium* has suggested annual within-patient diversification rates of 6-122 cgSNPs (Pinholt *et al.*, 2015; Raven *et al.*, 2017; Gouliouris *et al.*, 2020; Higgs *et al.*, 2022). A consensus sequence, generated from the core genome alignments from reference positions covered by all query genomes, is utilised to identify SNPs between isolates and determine genetic relatedness. Reference mapping typically requires the use of specific filters, such as recombination masking, prior to SNP distance calculation to provide a true estimation of genomic epidemiology and isolate relatedness. This is due to the presence of regions associated with high recombinogenic potential such as MGEs which can introduce multiple SNPs in a single genomic event due to homologous recombination (Coll, 2021). However, more recent studies have suggested that masking recombination and

prophages in *E. faecium* isolates which are recently diverged and therefore highly related had little to no effect on pairwise distance calculations (Gouliouris *et al.,* 2020; Gorrie *et al.,* 2021; Higgs *et al.,* 2022).

The most important determinant of high resolution and reliable SNP calling is the choice of an appropriate reference genome (Bush *et al.,* 2020; Gorrie *et al.,* 2021; Higgs *et al.,* 2022). If a reference is genetically unrelated to the strains under investigation, lineage-specific regions comprising informative SNPs within the query genome(s) may be excluded from variant calling, referred to as hard reference bias. A study by Gorrie and colleagues in 2021 demonstrated that using a closely related reference genome to isolates being compared resulted in a larger core-genome alignment which significantly improved the resolution and discriminatory value of reference mapping. In fact, a recent study which sought to optimise approaches in outbreak investigation for health-care adapted *E. faecium* suggested the use of cgMLST analysis to initially broadly group isolates together and to identify cluster-specific reference genomes for use in subsequent reference mapping-based analysis (Higgs *et al.,* 2022). From a practical perspective, it is recognised that the identification of SNPs is time-consuming, costly and relies on complex, computationally intensive pipelines that require bioinformatic expertise. Additionally, the use of a study-specific reference precludes the inter-study comparison of *E. faecium* strains.

1.10.1.4 The k-mer revolution

In recent years, a number of novel techniques have been developed in order to overcome the limitations associated with reference-based and core genome approaches. This includes the use of direct whole-genome comparison tools, such as *k*-mer based analysis, which involves inferring genetic relatedness by examining the frequency and distribution of short sequences of DNA of length *k* (referred to as *k*-mers) across a bacterial population. The length of the *k*-mer is determined based on the size of the bacterial genome under analysis, with a range of 4-31 available. A sliding window of the selected *k*-mer size across the bacterial genome sequence, on the basis of raw reads or genome assemblies, is utilised to extract and count the *k*-mers. The resulting *k*-mer frequency profiles of the query genomes can then be compared using single-linkage clustering based on a variety of distance matrices such as Euclidean distance, Manhattan distance or Jaccard index to determine phylogenetic relations. This methodology has the added advantage that it is an alignment-free algorithm, meaning it does not require a reference sequence thus avoiding reference bias (Uelze *et al.,* 2020). Additionally, this method is extremely fast and scalable to thousands of bacterial genomes.

An open-sourced software described recently, termed split *k*-mer analysis (SKA), utilises this approach (Harris, 2018). This method involves the detection of structures called 'split k-mers' in short-read fastq files, in which odd-length k-mers are divided into two smaller fragments separate by a single variable middle base (Gardner and Hall, 2013; Harris, 2018). The left and right segments of the *k*-mer can then be utilised as a reference point to determine the position of the middle base. For example, if the same combination of left-right *k*-mer is identified in another bacterial genome, but with a different middle base, the variation can be interpreted as a SNP. A recent study investigating the accuracy and resolution of different bioinformatic approaches for outbreak resolution in VREfm proposed the optimal use of a combination of cgMLST clustering to first broadly group genetically similar isolates together and the subsequent use of SKA to inform transmission pathways (Higgs *et al.*, 2022). The authors demonstrated that the use of SKA with a cut-off of ≤7 SKA SNPs to infer genetic relatedness was highly comparable to the gold standard method of pairwise direct comparisons using *de novo* references in bacterial comparisons, however it required minimal computation resources and was relatively stable over-time when diverse samples were investigated. Additionally, this tool lends itself to automation which is an important consideration for implementation in a routine diagnostic surveillance capacity. Notably, the absence of a reference sequence allows samples to be compared across different hospital networks and on a global scale to better inform screening and IPC practices (Harris, 2018; Higgs *et al.*, 2022; Maechler *et al.*, 2023).

1.10.2 Accessory genome analysis

Despite the significant role of accessory elements in the transmission of antimicrobial resistance genes in a hospital setting, surveillance and outbreak analysis are often limited to strain tracing based on gene-by-gene comparison approaches such as cgMLST or SNPs. Whilst this approach is highly discriminatory, it may be unsuitable when utilised unaided by accessory genome analysis, particularly with highly recombinant organisms such as VREfm in which plasmid conjugation and translocation of resistance genes by transposition are frequent (Liu *et al.*, 2016; Sheppard *et al.*, 2016; Schürch *et al.*, 2018). In order to fully elucidate transmission events and highlight the impact of HGT in an outbreak setting, plasmid epidemiology should be investigated in conjunction with gene-by-gene comparative methods (Conlan *et al.*, 2014, 2016).

There are a variety of low-resolution techniques for accessory genome analysis which involve plasmid purification and subsequent PCR-based detection techniques, however they are not applicable or scalable to large collections of isolates (Schürch *et al.*, 2018). WGS approaches with downstream hybrid assembly as described in Section 1.7.2 allow the comparative sequence analysis of MGEs present in isolates, particularly those harbouring antimicrobial resistance genes, which can be used in combination with cgMLST and epidemiological data. This can lead to better insights into highly complex transmission routes during VREfm outbreaks, particularly when cgMLST alone can result in inaccurate and misleading results if HGT occurs between genetically unrelated clones during an outbreak event (Zhou *et al.*, 2018). Plasmid and transposon analysis only aid to further increase the discriminatory power of WGS by allowing investigation of clonal spread and the accompanying transmission of MGEs. For example, several studies have highlighted the importance of *van* transposon investigation with VREfm isolates that are deemed genetically identical by cgMLST acquiring dissimilar *van*-encoding transposons *de novo*, which may be incorrectly epidemiologically linked based on cgMLST alone (Howden *et al.*, 2013; Brodrick *et al.*, 2016; Zhou *et al.*, 2018). It is important to note, that isolates deemed indistinguishable by cgMLST can also harbour the same transposon and therefore can be deemed to belong to the same outbreak cluster (Sivertsen *et al.*, 2014; Wardal *et al.*, 2014; Brodrick *et al.*, 2016; Zhou *et al.*, 2018). A study conducted in Denmark utilising comparative sequence analysis of MGEs found that 82% of genetically related and unrelated VREfm isolates harboured an identical *vanA* plasmid (Pinholt *et al.*, 2017). This highlights the significant importance of including accessory genome analysis when adopting a WGS approach to VREfm surveillance.

1.11 Project aims

VREfm are of significant medical and public health importance with a capacity to adapt and persist within a wide range of environments, allowing them to both acquire and transmit a variety of antimicrobial resistant determinants, which has significant implications for patient management. For over a decade, the clinical and financial burden of VREfm nosocomial infections in Irish hospitals have been substantial, however little is known about the epidemiology, population biology and transmission dynamics of Irish VREfm. This thesis describes a genomic-based investigation of the success and expansion of *E. faecium* in Irish hospitals.

- The first research chapter (Chapter 3) of this project aimed to use WGS to comprehensively investigate for the first time the population biology and epidemiology of VREfm from hospital networks across the Republic of Ireland, to explore the diversity of the Tn*1546*-like *vanA* transposon in circulation and to identify potential characteristic features associated with Irish isolates in order to identify key factors that may contribute to spread. This study also sought to contextualise Irish isolates by comparison with international strains to help identify and evaluate geographical segregation of clusters and assess key differences in population biology.
- The second research chapter (Chapter 4) sought to utilise and expand on methods employed in Chapter 3 of this project to undertake an in-depth investigation of the transmission and persistence of VREfm clonal lineages in two critical care wards of a large Irish hospital using a combination of epidemiological analysis and a genomics approach over 39-months. This objective of this study also aimed to use WGS to provide some insights into the role of the environment as a reservoir for transmission in VREfm during the outbreak. It was hypothesised that, given the hyperendemicity of VREfm in Ireland, extensive transmission and persistence of VREfm clonal lineages could be mediated by both extensive direct patient-to-patient transmission and indirect dissemination via previously unidentified reservoirs such as the near patient ward environment and bathroom facilities.
- Following on from Chapter 4, it was hypothesised that within-patient diversity and intestinal carriage of multiple diverse VREfm strains in an individual patient could significantly impact and hinder transmission network elucidation and could potentially in-part explain the expansive pool of TN*1546*-like *vanA* transposons in circulation identified in Chapter 3. The final research chapter (Chapter 5) of this project aimed to investigate the level of diversity of found within the VREfm rectal colonising population and provide a comprehensive systematic analysis of the plasmidome carried by co-colonising strains.

Chapter 2

General Materials and Methods

2.1 Bacterial isolates

A total of 2,911 *E. faecium isolates* were investigated in the present study. This included isolates recovered in (i) Ireland between 2017 and 2022 (VREfm *N*=1,464 and VSEfm *N*=122) and (ii) isolates recovered internationally between 1986 and 2016 (VREfm *N*=786 and VSEfm *N*=539). Table 2.1 provides a detailed breakdown of all isolates investigated.

2.1.1 Ethical approval

Ethical approval for this project was granted by the Trinity College Dublin Dental School Research Ethics Committee (DSREC); reference number DSREC2020-01-02.

2.2 General microbiological methods

2.2.1 Microbial culture and long-term storage

All isolates were cryogenically preserved on beads in individual vials using the Microbank cryovial system (Pro-Lab Diagnostics, Toronto, Ontario, Canada) and stored at -80°C. Unless otherwise stated, routine culture was performed by aseptically inoculating a single cryogenic bead on Columbia Blood Agar (CBA; Fannin LTD., Dublin, Ireland), followed by incubation at 37°C for 18-24 h in a static incubator (Gallenkamp, Leicester, UK). For liquid culture, a single bacterial colony was picked from CBA, inoculated in 8 mL of Brain Heart Infusion Broth (BHIB) (Merck Ireland Ltd., Wicklow, Ireland), and incubated at 37°C for 18-24 h in an orbital incubator (Gallenkamp) at 200 rpm.

2.2.2 Chemicals, reagents, and buffers

All chemicals used in this study, unless otherwise stated, were of molecular biology grade and were purchased from Sigma-Aldrich [Merck] (Wicklow, Ireland). Oligonucleotide primers were custom synthesised by Sigma-Aldrich [Merck] at a stock concentration of 100 µM. Reagents required for PCR including deoxyribonucleotide triphosphate (dNTPs), Go Taq G2 Flexi DNA polymerase, corresponding flexi buffer, loading dye and 100 base pair (bp) DNA molecular size ladders were purchased from the Promega Corporation (Madison, WI, USA). PCR amplimers were visualised in horizontal agarose gels (1.0% w/v) by conventional gel electrophoresis at 100 V for 60 min with 0.5x Tris-borate/EDTA (TBE) buffer using the Galileo Bioscience Horizontal Gel System (Galileo Bioscience, Cambridge, MA, USA). Agarose gels were supplemented with 1 µl GelRed nucleic acid stain purchased from Biotium (Fermont, CA, USA) for fluorescent staining of PCR amplimers. Following electrophoresis, gels were visualised using The Alpha Innotech Alpha Imager Mini (Cell

Biosciences, Medical Supply Company Ltd., Dublin, Ireland) transilluminator. Ultra-purified water obtained from the Milli Q Biocel system (Merck-Millipore, Co Cork, Ireland) was used in the preparation of all buffers and other solutions as required. TBE buffer, used for agarose gel preparation and as an electrophoresis buffer, was prepared at stock concentration of 5x consisting of 0.45 M Trizma base, 0.45 boric acid and 0.01 M Ethylenediaminetetraacetic acid (EDTA) (pH 8) and diluted to 0.5x using Ultrapure Milli Q Biocel water.

Table 2.1. Details of the 2,911 *E. faecium* isolates investigated in the present study

Chapter	Study chapter	Number of isolates		Period of isolation	Country of Isolation
		VREfm	**VSEfm**		
3	Genomic analysis of vancomycin-resistant *Enterococcus faecium* from Irish hospitals reveals a high prevalence of ST80 and spread of similar *vanA* regions via IS*1216E* and plasmid transfer in diverse genetic lineages	1,765[1]	588[1]	1986-2022	Argentina, Australia, Belgium, Brazil, Canada, Chile, Denmark, Finland, France, Germany, Greece, Hungary, Ireland, Israel, Italy, Japan, Latvia, Luxembourg, Netherlands, Norway, Paraguay, Poland, Portugal, Saudi Arabia, Slovenia, Spain, Switzerland, Tanzania, Tunisia, United Kingdom, USA
4	Protracted transmission and persistence of ST80 vancomycin-resistant *Enterococcus faecium* clonal complex types CT2933, CT2932 and CT1916 in a large Irish hospital: a 39-month genomic study	1,192[2]	92[2]	2017-2022	Ireland
5	Multi-strain gastrointestinal carriage of genetically diverse vancomycin-resistant Clade A1 *Enterococcus faecium* amongst Irish patients with frequent health-care exposure – one pick to represent them all!	1,515[1,3]	612[1,3]	2022	Ireland

Abbreviations: VREfm, vancomycin-resistant *E. faecium*; VSEfm, vancomycin-susceptible *E. faecium.*
[1] Includes 1,325 previously described isolates (Raven *et al.,* 2016; van Hal *et al.,* 2021).
[2] Includes 908 isolates from Chapter 3.
[3] Includes 622 isolates from Chapter 3.

2.3 Isolate identification and antimicrobial susceptibility testing

2.3.1 Conventional culture and identification

Unless otherwise stated, all isolates investigated in this study were recovered and identified as VREfm or VSEfm in the clinical microbiology laboratory of the hospital where the clinical sample was originally collected. Briefly, screening specimens were initially inoculated on to chromID VRE chromogenic agar (bioMérieux, Marcy, L'Étoile, France) and incubated aerobically at 37°C for 24 h. Any specimens showing minimal or scanty growth were re-incubated for up to 48 h. Violet colonies indicative of VREfm were selected, purified by subculture on the same medium and definitively identified using the Vitek MS Matrix-Assisted Laser Desorption Ionization-Time of Flight Mass Spectrometry system (MALDI-TOF) (bioMérieux) as per the manufacturer's instructions. Blood cultures that flagged positive on the BacT/ALERT Virtuo Blood Culture Machine (bioMérieux) or the BD BACTEC Automated Blood Culture System (Becton, Dickinson and Company, NJ, USA) were inoculated onto a series of agar plates (including Columbia chocolate agar, CBA and MacConkey agar (Fannin Ltd., Dublin, Ireland)) as per the local laboratory standard operation procedure guidelines and incubated at 37°C for 24 h under aerobic, anaerobic and 5% (v/v) CO2 conditions. Selected colonies were then picked and identified using the Vitek MS MALDI-TOF or the BD Bruker MALDI Biotyper (Beton, Dickinson and Compan, NJ, USA) as per the manufacturer's instructions.

2.3.2 Antimicrobial susceptibility testing

Antimicrobial susceptibility testing was performed using the VITEK-2 (bioMérieux) P-622 identification card and interpreted using the European Committee on Antimicrobial Susceptibility testing (EUCAST) guidelines for MIC assay clinical breakpoints (EUCAST, 2023). A brief overview of the antimicrobial agents tested and relevant breakpoints are shown in Table 2.2. All isolates were then stored using the Microbank cryovial system (Pro-Lab Diagnostics) at -80°C.

Table 2.2: Antimicrobial agents and antimicrobial susceptibility MIC breakpoints used in the present study

Antimicrobial agent	MIC breakpoint (mg/L)			Reference
	Susceptible ≤	ATU[1]	Resistant >	
Ampicillin	4[2]	-	8[2]	(EUCAST, 2023)
Gentamicin[3]	N/A[4]	-	N/A[5]	(EUCAST, 2023)
Linezolid	4	-	4	(EUCAST, 2023)
Quinupristin-dalfopristin	1	-	4	(EUCAST, 2023)
Teicoplanin	2	-	2	(EUCAST, 2023)
Vancomycin	4	-	4	(EUCAST, 2023)

[1]Area of technical uncertainty.
[2] Susceptibility to amoxicillin and piperacillin (with and without beta-lactamase inhibitor) can be inferred from ampicillin.
[3] Gentamicin was used to screen for high-level aminoglycoside resistance (HLAR).
[4] Isolates with a gentamicin MIC of ≤128 mg/L indicated low-level intrinsic resistance and therefore a negative HLAR screen.
[5] Isolates with a gentamicin MIC of >128 mg/L indicated HLAR.

2.4 DNA extraction for whole-genome sequencing

2.4.1 Qiagen DNeasy Blood and Tissue

Genomic DNA was extracted from confirmed VREfm and VSEfm isolates using the Qiagen DNeasy Tissue and Blood kit (Qiagen, Crawley, United Kingdom), which was preceded by a modified pre-treatment lysis step for Gram-positive bacteria as recommended by the manufacturer. Isolates were initially reactivated from Microbank cryogenic storage beads on CBA and incubated for 24 h at 37°C. A single colony was then selected and inoculated into eight ml of BHIB and incubated overnight in a shaking incubator at 37°C and 200 rpm. The broth was subsequently centrifuged at 2,376 × *g* for five min. In order to encourage bacterial cell lysis, the supernatant was discarded, and the resulting pellet was resuspended in 200 µl of lysis buffer A1 and transferred into a fresh tube containing lyophilised lysis enhancer A2, both buffers supplied by Inter Array fzmb GmbH (Bad Langensalza, Germany). The solution was then incubated at 37°C for 2-3 h on an Eppendorf Thermomixer Comfort (Eppendorf, Hamburg, Germany) thermomixer at 300 rpm. Following lysis, the DNeasy Blood and Tissue kit extraction protocol was followed according to the manufacturer's instructions. Briefly, 25 µl of proteinase K and 200 µl of AL buffer (both supplied with the Qiagen kit) were added to the mixture and incubated for one h at 70°C on a heating block (Grant Instruments Cambridge Ltd., Shepreth, UK) to ensure degradation of contaminating proteins. Following incubation, 200 µl of chilled 100% (v/v) EtOH was added to encourage precipitation and improve DNA yield. DNeasy mini-spin column collection tubes (supplied with the Qiagen kit) were then utilised to selectively bind nucleic acids through a series of centrifugation steps coupled with the addition of 500 µl AW1 and AW2 wash buffers (supplied with Qiagen kit). Purified DNA was eluted into 50 µl of pre-warmed molecular biology-grade water and stored at -20°C prior to library preparation for WGS.

2.4.2 Qiagen HMW MagAttract

Template DNA for third generation sequencing was extracted using the commercially available Qiagen High-Molecular Weight MagAttract kit (Qiagen) with a modified pre-treatment step for Gram-positive bacteria. Samples were reactivated from Microbank cryogenic storage beads on to CBA and incubated for 24 h at 37°C. A single colony was then selected and inoculated into eight ml of BHIB and incubated overnight in a shaking incubator at 37°C and 200 rpm. Following incubation, each culture was centrifuged at 2,376 × g for five min, the supernatant discarded and the pellet resuspended in 200 µl of lysis buffer A1 and transferred into a fresh tube containing lyophilised lysis enhancer A2 buffer

(Inter Array). The solution was then incubated at 37°C for 2-3 h on the Eppendorf Thermomixer Comfort at 300 rpm. The remaining steps were followed as per the manufacturer's guidelines. Briefly, 20 µl of proteinase K, 150 µl of AL buffer and 4 µl of RNase A solution (all supplied with the MagAttract Qiagen kit) were added to the 200 µl mixture and incubated for 30 min at room temperature. Following incubation, 15 µl of MagAttract Suspension G and 280 µl of Buffer MB were added to each sample and incubated on a shaking thermomixer (Eppendorf) at room temperature for 3 min at 1400 rpm. Magnetic beads were utilised to selectively bind and purify nucleic acids through a series of silica-based purification steps coupled with the addition of wash buffers (Buffer MW1 and Buffer PE (supplied with the MagAttract Qiagen kit) to remove contaminants and PCR inhibitors. To allow for bead separation and supernatant removal, samples were placed on a magnetic separation rack (NEBNext New England BioLabs, MA, USA) for 1 min. Purified DNA was eluted into 100 µl of molecular grade water and stored at -20°C prior to library preparation for third generation WGS.

2.4.3 Quality assurance of extracted DNA

The concentration and quality of extracted enterococcal DNA was measured by UV absorption using the NanoDrop 2000 spectrophotometer (Thermo Fisher Scientific, Waltham, MA, USA). DNA was considered pure and adequate for WGS if the sample exhibited absorbance ratios of 1.8-2.0 and 2.0-2.2 at 260/280 nm and 230/260 nm wavelengths, respectively. Measurements obtained outside these parameters indicated the presence of contamination with interfering substances such as proteins, chaotropic salts and non-ionic detergents and therefore required repeated DNA extraction. Additionally, samples with absorbance ratios falling moderately outside (within one or two decimal places) the accepted limits were incubated at 70°C with the lids of the Eppendorf tubes open for up to one h to allow evaporation of potential volatile contaminants and subsequently rechecked.

2.5 Whole-genome sequencing

2.5.1 Second generation sequencing

Genomic DNA was extracted using the Qiagen DNeasy Tissue and Blood kit as detailed in Section 2.5.1. Second generation WGS was performed using the Illumina MiSeq bench-top sequencer in conjunction with both the MiSeq V2 500 cycle reagent kit and the MiSeq V3 600 cycle kit (Illumina, Eindhoven, Netherlands). In total, 428 isolates were sequenced using

the V2 kit, whilst 1,158 isolates were processed using the V3 kit. Libraries were scaled to yield a minimum coverage of 50x coverage per isolate.

2.5.1.1 Library preparation

Libraries were prepared for second generation sequencing using the Illumina DNA Prep (M) Tagmentation kit.

2.5.1.1.1 Tagmentation and clean-up

For each bacterial isolate, tagmentation was performed by mixing 15 µl of diluted genomic DNA (input concentration 250-300 ng), 5 µl of Bead-Linked Transposome (Illumina) and 5 µl of Tagmentation Buffer (Illumina) in a 0.2 ml PCR Tube (Fisher Scientific™, Dublin, Ireland). The amplicon tagmentation mix was then incubated at 55°C for 15 min in a PCR thermal cycler (Biometra Tone, Thistle Scientific Ltd., Glasgow, UK). Tagmentation was stopped by the addition of 5 µl of Tagment Stop Buffer (Illumina) and subsequent incubation at 37°C for 15 min. The contents of each tube were then transferred into individual wells of a 96-well polycarbonate PCR plate (Thermo Fisher Scientific) and placed on a magnetic stand (Thermo Fisher Scientific) for 3 min. Post separation from the bead pellet, the supernatant was discarded and the 96-well plate was removed from the magnetic stand. Each pellet was resuspended in 50 µl of Tagment Wash Buffer (Illumina), placed back on the magnet and allowed to separate for 3 min. The supernatant was then discarded and the wash process was repeated three times.

2.5.1.1.2 Amplification of tagmented libraries

Following tagmentation clean-up, the remaining Tagment Wash Buffer was removed and the libraries were immediately resuspended in 20 µl of master mix (10 µl Enhanced PCR Mix (Illumina) and 10 µl of nuclease free water). Each sample was then transferred to new 0.2 ml PCR tubes and 5 µl of a unique index adapter (Illumina Nextera DNA CD Indexes, 96 Index Plate) was added. PCR amplification was carried out on a thermocycler using the following conditions: 68°C for 3 min, 98°C for 3 min, 6 cycles of 98°C for 45 s, 62°C for 30 s and 68°C for 2 min, followed by a final step of 68°C for 1 min.

2.5.1.1.3 PCR clean-up

PCR clean-up was performed using sample purification beads (SPBs) supplied in the Illumia tagmentation kit and was based on size-selection. Following amplification, each PCR

product was transferred into individual wells of a 96-well 0.8 mL polypropyelene PCR plate (Abegene/Thermo Fisher Scientific, NH, USA) and placed onto a magnetic stand for five min. Once the solution cleared, 22.5 µl of the supernatant was transferred into fresh wells of the Midi plate and thoroughly mixed by gently pipetting with 22.5 µl of SPB and 20 µl nuclease free water. Samples were incubated at room temperature for five min and placed back onto the magnetic stand for a further five min. Once separated, 62.5 µl of the supernatant was transferred into fresh wells, mixed with 7.5 µl of undiluted SPBs (Illumina) and incubated at room temperature for five min. Following incubation, the samples were placed back onto the magnet for a further five min. The supernatant was then discarded and the bead pellet was washed twice with 100 µl of freshly prepared 80% (v/v) ethanol for 30 s. The magnetic beads were resuspended in 17 µl of Resuspension Buffer (Illumina) and incubated at room temperature for two min. The plate was placed back on the magnet for a further two min and 15 µl of each supernatant was removed into fresh 0.2 ml PCR tubes (Thermo Fisher Scientific).

2.5.1.2 Quantification of library preparation concentrations

The concentration of each prepared library was determined using the Qubit 3.0 Fluorometer (Thermo Fisher Scientific) as per the manufacturer's instructions. Libraries with a low recovery concentration (<4 ng/µl) were excluded from further processing. Samples were normalised to a DNA concentration of 4 nM and combined into a single 1.5 ml Eppendorf tube in equal volumes (5 µl) to ensure a uniform distribution of each specimen was achieved within the library pool.

2.5.1.3 Library denaturation and MiSeq loading

Prior to MiSeq loading, 5µL of freshly prepared 0.2 N sodium hydroxide (NaOH) was added at a ratio of 1:1 to the 4 nM pooled library and incubated at room temperature for five min. The denatured pool was then diluted to a final concentration of 12 pM using prechilled HT1 hybridisation buffer (Illumina). The PhiX Control V3 library (Illumina) was used for sequencing quality assurance and was added at a concentration of 12.5 pM to the final denatured library.

2.5.1.4 Post run quality assurance and processing

Demultiplexing, adapter trimming and generation of FASTQ files from base call files (BCL) for each isolate was automatically implemented on the MiSeq upon run completion using

Illumina bcl2fastq2 Conversion Software (Version 2.20vd). The run quality and accuracy were evaluated using the on-board quality metrics, including cluster density and a Phred quality score (Q30) as per the manufacturer's guidelines. Raw cluster density thresholds of 1000-1200 K/mm2 for V2 and 1200-1400 K/mm2 for V3 kits were used to predict high data yield and quality. Base calling accuracy was assessed by quality scores, with a Q30 value of >30 representing a base call error rate of 1 in 1000 and an accuracy of 99.9%.

2.5.2 Third generation WGS

Third generation WGS was performed using the portable MinION device (Oxford Nanopore Technologies, Oxford, UK) in conjunction with the SpotON R9.4 Flow Cell (Oxford Nanopore Technologies).

2.5.2.1 Library preparation

Libraries were prepared according to the one-dimensional native barcoding genomic DNA protocol using the Ligation Sequencing Kit (SQK-LSK109) and ID native barcoding kit (EXP-NBD104) (Oxford Nanopore Technologies). It should be noted that as protocols are continuously updated on the nanopore community website (available at https://nanoporetech.com/community), the newest version was downloaded and consulted each time libraries were prepared.

2.5.2.1.1 DNA repair and end-prep

In order to repair ends and prepare for barcode ligation, high molecular weight (HMW) genomic DNA (1-10 µg) was adjusted to a final volume of 48 µl in sterile molecular-grade water and added to a master mix containing 3.5 µl NEBNext FFPE DNA Repair Buffer, 3.5 µl Ultra II End-prep reaction buffer, 3 µl Ultra II End-prep enzyme mix and 2 µl NEBNext FFPE DNA Repair Mixed (all supplied in NEBNext End repair / dA-Tailing Module reagents (New England BioLabs, Ipswich, MA, USA)). The reaction was then incubated at 20°C for 20 min, followed by 65°C for a further 20 min on a Biometra Tone thermocycler. The DNA sample was subsequently transferred to a clean 1.5 ml microfuge tube (Eppendorf), mixed with 60 µl AMPure XP beads (Beckman Coulter, California, USA) and incubated for 20 min on a Grant Bio PTR-35 360-degree vertical multi-function rotator (Grant Instruments, Cambridge, UK). Samples were then placed on a 12-tube magnetic separation rack (New England BioLabs) for one min. The resulting supernatant was removed and the bead pellet was washed twice using freshly-prepared 70% (v/v) BioUltra molecular

biology grade ethanol (Sigma Aldrich) whilst on the magnet. The beads were left to dry for one min and resuspended in 28 µl molecular grade water. The samples were then incubated at room temperature for 20 min and placed back on the magnetic rack to encourage elution. Post bead-separation, 26 µl of the supernatant was removed and retained in a fresh Eppendorf tube and quantified using the Qubit 3.0 Fluorometer (Invitrogen/Fischer Scientific) with targeted recovery of >700 ng.

2.5.2.1.2 Native barcode ligation

Following Qubit quantification, 800 ng of each end-prepped DNA sample was prepared in a final volume of 22.5 µl of sterile water. For barcode ligation, 2.5 µl Native Barcode (Oxford Nanopore Technologies) and 25 µl Blunt/TA Ligation Master Mix (New England BioLabs) were sequentially added to the end-prepped DNA and incubated at room temperature for 20 min. To purify the barcoded samples, 50 µl of the AMPure XP beads (Beckman Coulter) were added and incubated for 20 min on a vertical multi-function rotator. Samples were pelleted on the magnetic rack, washed and the eluate retained as described in Section 2.6.2.1.1. The DNA was then quantified and pooled in equimolar amounts to ensure a total concentration of >700 ng in 65 µl of sterile molecular-grade water.

2.5.2.1.3 Adapter ligation and clean-up

Adapter ligation was performed on the pooled samples by adding 5 µl Barcode Adaptor mix II (AMII, Oxford Nanopore Technologies), 20 µl 5x NebNEXT Quick Ligation Reaction Buffer and 10 µl Quick T4 DNA Ligase (New England BioLabs) followed by incubation at room temperature for 20 min. Samples were subsequently purified, again using 50 µl AMPure XP beads (Beckman Coulter), and enriched for DNA fragments of >3 kb using 250 µl Long Fragment Buffer supplied in the kit (Oxford Nanopore Technologies). The pooled sample was placed back on the magnetic rack to allow the beads to pellet and the supernatant was discarded. The beads were resuspended in 17 µl Elution Buffer (Oxford Nanopore Technologies) at 37°C for 20 min in a static incubator and subsequently placed back on the magnetic rack. Post bead separation, 15 µl of the eluate was removed and retained in a fresh Eppendorf tube and quantified using the Qubit 3.0 Fluorometer with a recovery aim of ≥ 430 ng.

2.5.2.2 Priming and loading the SpotON flow cell

The SpotON R9.4 Flow Cell (Oxford Nanopore Technologies) was primed using 800 µL of a mix containing Flush Tether (FLT) and Flush Buffer (FLB) (Oxford Nanopore Technologies) for five min. The mixture was then loaded via the priming port and caution was taken to ensure no air bubbles were introduced. The quantified library was diluted to give a final concentration between 5-50 fmol of DNA. In order to prepare for loading, 12 µl of the diluted library was mixed with 37.5 µl sequencing buffer and 25.5 µl loading beads (Oxford Nanopore Technologies). The SpotON cover was then opened and a further 200 µl of the priming mix was introduced into the flow cell via the priming port. A total volume of 75 µl of the library prepared as above was loaded in a drop-wise fashion into the SpotON sample port. Finally, all ports were closed and the run was commenced using the MinKNOW graphical user interface, with the following parameters specified: base-calling off, 72 h run time, Fast5output.

2.5.2.3 Post sequencing processing

Raw-read FAST5 files were base called and converted to FASTQ using Guppy (v6.4.6, Oxford Nanopore Technologies). Adaptor trimming and demultiplexing was then performed using Porechop (v0.2.4, https://github.com/rrwick/Porechop).

2.6 Bioinformatic Analysis

2.6.1 Second generation WGS

2.6.1.1 Data export and read trimming

Post sequencing, the MiSeq generated raw read pairs for each isolate that were imported from the Illumina BaseSpace Sequence Hub to the BioNumerics (Version 8.0v, Applied Maths, Ghent, Belgium) cloud-based bioinformatic software as FASTQ files. Prior to assembly, the default trimming algorithms (quality, structural and length) were automatically applied. Base calls and read lengths below the minimum quality and read length threshold of 10% were removed. Additionally, any low-quality read ends below the threshold of 25% of the average quality were also excluded from analysis. Raw reads were also simultaneously imported into the Seqsphere + software package (v8.5.1, Ridom GmbH, Germany) and were trimmed using FastQC v0.11.7 and Trimmomatic v0.36 under default settings. Briefly, both ends of the reads were trimmed until the average base quality was >30 in a window of 20 bases. In order to reduce the size of the output files, FASTQ reads from

each isolate were also down sampled to 180x the expected genome size of the organism being sequenced.

2.6.1.2 de novo assembly

Isolates were assembled using the incorporated SPAdes software with BayesHammer read error correction (v3.7.1) in BioNumerics. Optimal assembly parameters were identified automatically based on the read quality metrics obtained during trimming. Contigs below 1000 bp were considered unreliable and therefore excluded from further analysis. Additionally, sequence reads were also assembled using Velvet (v1.1.04), an assembly tool incorporated within the SeqSphere + software suite. This uses a '*k*-mer' data approach, which runs multiple *k*-values and uses the results from the best run to determine optimal assembly parameters.

2.6.1.3 Molecular typing

Traditional MLST STs were extracted in *silico* using WGS data in both BioNumerics and SeqSphere+. Both software packages link directly to the publicly available *E. faecium* MLST scheme, which is based on the seven house-keeping genes described by Homan *et al.* and hosted by PubMLST (https://pubmlst.org/organisms/enterococcus-faecium). Unknown or novel MLST alleles and profiles were submitted to PubMLST for ST assignment using both Seqsphere + and the automated submission tool available on the PubMLST website.

2.6.1.4 Whole-genome multi-locus sequence typing (wgMLST)

The raw FASTQ files and the FASTA contig and scaffold output files generated using the SPAdes *de novo* plugin in BioNumerics (Section 2.7.1.2) were submitted to the BioNumerics incorporated wgMLST scheme for *E. faecium*. This application consists of 5,489 stable loci present in the accessory genome and is complemented with the traditional MLST loci described previously (Section 2.7.1.3) to ensure consistency is obtained with classical and novel MLST methods. In order to obtain consensus sequences, identify alleles and assess the wgMLST profile of each isolate, two algorithms were employed using the cloud-based calculation engine. Initially, an assembly-free call method, based on a *k*-mer approach (pairwise comparison of a set of genomes based on sub-strings of length '*k*'), was used to determine the presence or absence of organism-specific loci and establish over-all allelic identity. As per the manufacturer's default settings, a *k*-mer length of 35 was utilised. Additionally, only loci with a minimum total coverage of 3x, with a minimum forward and

reverse coverage of 1x, were considered in generating the wgMLST profile. Finally, an assembly-based algorithm was employed which uses Basic Local Alignment Search Tool (BLAST)-based detection to ascertain alleles in the *de novo* assembled contigs. Default settings were utilised, including *allow gapped alignments*. A minimum similarity of 85% for an allele to be used as tentative match was applied.

2.6.1.5 Core-genome multi-locus sequence typing (cgMLST)

Gene-by-gene allele calling and complex type (CT) assignment was performed using the standardised *E. faecium* cgMLST scheme in SeqSphere+ (Ridom GmbH) based on 1,423 genes as described previously (de Been *et al.*,2015). cgMLST cluster arrangements were determined using single linkage clustering and a previously published pairwise allelic difference threshold of ≤20 (de Been *et al.*, 2015).

2.6.1.6 Genotyping

Antimicrobial-resistance and virulence-associated genes were detected *in silico* on SPAdes-assembled short-read contigs using ABRicate v.0.9.8 (https://github.com/tseemann/abricate). ABRicate is a command-line based tool which allows mass screening of FASTA contigs by querying against a variety of publicly available databases including NCBI, CARD, ARG-ANNOT, ResFinder, MEGARES, EcOH and PlasmidFinder.

2.6.1.7 Quality assurance

The quality of the raw sequence read files, *de novo* assemblies and assembly-free and assembly-based allele calls, were assessed using the in-built quality statistics window in BioNumerics. An average quality score of ≥30 and an over-all coverage of ≥50x was used as an initial raw-read cut-off to determine isolate inclusion. *De novo* assemblies were evaluated using the N50 parameter, which is defined as the sequence length of the shortest contig at 50% of the total genome length. Isolates with <95% core genome loci identified were excluded.

2.6.1.8 Phylogenetic tree analysis

Minimum spanning trees (MSTs) and neighbour-joining trees (NJT) were constructed using gene-by-gene allele calling based on the 1,423 *E. faecium* cgMLST scheme in SeqSphere+ *(R*). The MST algorithm was calculated using a modified version of Krushkal's algorithm

and the layout was generated using a force-based algorithm. NJTs were visualised using Interactive Tree of Life v6.8.1 (Letunic and Bork, 2021). A threshold of ≤20 allelic differences, as proposed by the cgMLST scheme described by De Been *et al* in 2015, was used to assign genetic relatedness between isolates and infer the likelihood of a transmission event.

2.7 Hybrid assembly

Long-read MinION and paired-end short-read MiSeq FASTQ files were combined in a hybrid assembly approach using Unicycler (v.0.4.8, https://github.com/rrwick/Unicycler) (Wick *et al.*, 2017). Assembly quality was assessed using the graph connectivity and node size metrics in Bandage v0.8.1 (https://github.com/rrwick/Bandage) (Wick *et al.*, 2015). Assembled genomes were annotated using Prokka v1.14.5 (https://github.com/tseemann/prokka) and visualised using SnapGene v.7.0.4 (https://www.snapgene.com),

2.8 Analysis of plasmid profiles

2.8.1 Plasmid profile determination

Following hybrid assembly as described in Section 2.8, bacterial genome plasmid contigs were characterised using the STAMAR pipeline (https://github.com/phac-nml/staramr). This tool queries against Resfinder, PlasmidFinder and PointFinder databases and allows determination of plasmid type and genotypic antimicrobial resistance profiles. The resulting assembled plasmids were also annotated using Prokka v1.14.5 (https://github.com/tseemann/prokka) and visualised using SnapGene v.7.0.4 (https://www.snapgene.com).

2.8.2 Genetic organisation of *vanA*-encoding regions and plasmids

The genetic organisation of *vanA*-encoding plasmids was determined followed hybrid assembly as described in Section 2.8. The resulting assembled genomes were annotated, visualised and genotypically characterised as described in Section 2.9.1. Plasmids containing *vanA* which failed to circularise using the hybrid assembly approach were investigated to rule out assembly quality issues and determine over-all topology. Contigs were initially screened for the presence of prophage sequences, replicons (i.e., the origin of replication sites and control elements) and genes encoding enzymes involved in DNA mobilisation and conjugation using the online publicly available web server tools Plasmid Finder v2.0.1

(https://cge.cbs.dtu.dk/services/PlasmidFinder/), PHAge Search Tool Enhanced Release (PHASTER) (http://phaster.ca/) and MOBscan (https://castillo.dicom.unican.es/mobscan/). Contigs were then annotated using RAST v2.0 (https://rast.nmpdr.org/), Prokka v1.14.5 (https://github.com/tseemann/prokka) and eggNOG-mapper v2.1.6 (http://eggnog-mapper.embl.de/). Coding regions encoding a putative product identified during genome annotation (excluding hypothetical protein, mobile element protein, phage related protein and related family protein) were then queried against the NCBI RefSeq Non-Redundant protein database. Sequences of linear contigs encoding *vanA* were subsequently compared with the corresponding sequences of linear plasmids pELF1 (143,416 kb), pELF2 (108,102 kb) and pELF_USZ (101,837 kb) recently described in VREfm isolates from Japan and Switzerland, respectively (Hashimoto *et al.,* 2019, 2020; Boumasmoud *et al.,* 2022). In order to determine homology, multiple alignments of the previously described linear plasmids and linear contigs identified in Irish VREfm were generated and visualised using EasyFig v2.2.2 (https://mjsull.github.io/Easyfig/). DNA sequence similarity between linear plasmids were generated using n × n matrices.

2.8.3 Pulse-Field Gel Electrophoresis

To provide further evidence of plasmid linear topology, PFGE was performed as previously described (Tickler *et al.,* 2019). Cell lysis was achieved in agarose plugs cast with lysozyme (3 mg/ml; Sigma-Aldrich, St. Louis, MO) and subsequently incubated at 37 C for 4-6 h in the presence of lysozyme and mutanolysin (1 mg/ml and 5 U/ml, respectively, Sigma-Aldrich, St. Louis, MO). To check for plasmid linearity, S1 nuclease (Promega) treatment of agarose plug slices was performed as described by Frietas *et al*. PFGE employed a Bio-Rad CHEF DRIII system (Bio-Rad, Richmond CA, USA) with 0.8% (w/v) agarose gels and switching from 1-17 s for 17 h (120-degree angle / 6 V/cm). *Sma*I-digested *Staphylococcus aureus* strain 8325 genomic DNA was used as a molecular size standard.

2.8.4 Filter mating

Conjugative transfer of plasmids encoding the vancomycin resistance gene *vanA* harboured by clinical enterococcal isolates was undertaken using the plasmid-free rifampicin- and fusidic acid-resistant recipient strains *E. faecium* 64/3 and *E. faecalis* ORG1RF as described previously (Werner *et al.*,2011). Donor isolates and recipient strains were reactivated from Microbank cryogenic storage beads on Brain Heart Infusion agar (BHIA) (Sigma-Aldrich [Merck]) and incubated for 24 h at 37°C. A single colony was then selected and inoculated into eight ml of BHIB and incubated overnight in a shaking incubator at 37°C at 200 rpm. A

50 µl aliquot of the overnight culture was used to inoculate eight ml of fresh BHIB and incubated for 2 h at 37°C in a shaking incubator at 200 rpm to encourage cells to reach mid-logarithmic growth phase. Subsequently, 50 µl of each donor and recipient culture was gently mixed in a microfuge tube and applied dropwise onto a sterile filter with a 0.45 µm pore size (Sigma-Aldrich [Merck]). Simultaneously, 50 µl of each individual donor and the recipient unmixed was utilised as a control and subject to the same protocol as described above. The filter was then placed on BHIA and incubated for 24 h at 37°C. Following incubation, the filter was transferred into a sterile 50 ml conical bottom polypropylene tube (Greiner BioOne, Kremsmünster, Austria) containing 1 ml of BHIB and gently agitated to release bacterial cells into culture. The filter was discarded and the remaining broth was centrifuged at 2000 × *g* for 5 min. The supernatant was then removed and resuspended in 500 µL of BHIB and incubated at 37°C for 1-2 h at 200 rpm. Finally, to select for transconjugants harbouring *vanA*, the culture was plated on BHIA supplemented with 5 mg/l chloramphenicol 30 mg/l rifampicin and 20 mg/l fusidic acid (Sigma-Aldrich [Merck]). The plates were then incubated at 37°C for 48 h. Presumptive transconjugant colonies growing on supplemented BHIA plates were picked and subcultured on to CBA and incubated for 24 h at 37°C. Isolates were then screened for the presence of *vanA*/*vanB* using the PCR method described in Section 2.4.2. Following confirmation, transconjugants underwent WGS as described in Section 2.6.1 and subsequently stored in Microbank cryovials at -80°C.

Chapter 3

Genomic analysis of vancomycin-resistant *Enterococcus faecium* from Irish hospitals reveals a high prevalence of ST80 and spread of similar *vanA* regions via IS*1216E* and plasmid transfer in diverse genetic lineages

3.1 Introduction

Enterococcus faecium, a highly-evolved commensal bacterium of the GIT consortium, has emerged as a globally significant, opportunistic pathogen associated with significant morbidity and mortality, particularly in immunocompromised hosts (Arias and Murray, 2012). The robust nature and considerable genomic versatility of *E. faecium* has enabled its specialised adaptation to the hospital-associated niche, resulting in a substantial increase in the clinical burden over the last two decades (García-Solache and Rice, 2019; van Hal *et al.*, 2022). Notably, the acquisition of resistance to ampicillin, gentamicin (high level), vancomycin and linezolid has significantly contributed to the clinical and public-health impact of *E. faecium* strains world-wide (Arias and Murray, 2012; Miller *et al.*, 2020; ECDC, 2023). It has been extensively reported that high intestinal colonisation pressure with MDR *E. faecium* strains, such as VREfm, is an important risk factor for the development of subsequent invasive infection such as BSIs and endocarditis, particularly in multimorbid patients (Ubeda *et al.*, 2010; Papadimitriou-Olivgeris *et al.*, 2014). For over a decade, the Republic of Ireland has reported some of the highest rates of invasive resistant enterococcal infection in Europe, ranging from 28.4%-45.8% (2006-2022), however little is known about the genomic epidemiology, population structure and transmission dynamics of *E. faecium* in Irish hospitals (ECDC, 2023).

Surveillance and bacterial typing of *E. faecium* using conventional methodologies often implemented for other nosocomial pathogens of clinical significance (e.g., MRSA), such as PFGE and MLST, has proved challenging. Previous population studies based on MLST assigned the majority of international clinical isolates to a hospital-associated lineage designated CC17 based on the identity of seven key house-keeping loci using eBURST analysis (Willems *et al.*, 2005). However, this has proven to lack discriminatory power, particularly in molecular epidemiological studies, due to high recombination rates within 5/7 of the MLST loci, the emergence of strains with a *pstS* deletion and more recently the identification of discrepancies between MLST and WGS-based data (Howden *et al.*, 2013; Pinholt *et al.*, 2015; Carter *et al.*, 2016; Raven *et al.*, 2016). Next-generation sequencing technologies have provided much needed resolution in phylogenetic analysis of *E. faecium* epidemiology and has revealed the presence of two genetically distinct groups based on BAPs modelling of MLST data, referred to as Clade A (hospital) and Clade B (commensal). The nosocomial lineage, designated Clade A, comprises isolates from humans and animals, with a further sub-division, termed clade A1, showing a predominance of isolates from hospitalised individuals, including those from previously described CC17, with a distinct evolutionary trajectory (Lebreton *et al.*, 2013; Raven *et al.*, 2017). Previous genomic studies

have highlighted the enrichment of clade A1 strains with MGE, ISs, pathogenicity islands, putative virulence determinants and most significantly resistance to antimicrobials (Lebreton *et al.,* 2013; Kim and Marco, 2014; Raven *et al.,* 2017).

Global WGS-based studies on the molecular epidemiology of clade A1 VREfm revealed a polyclonal population structure comprising a diverse array of genetically distinct clones, with evidence of endemic STs with subsequent region-specific genomic expansion resulting in co-circulation of multiple lineage-specific CT derivatives (Werner *et al.,* 2008; Howden *et al.* ,2013; Pinholt *et al.,* 2015, 2017; Raven *et al.,* 2016, 2017; Werner *et al.,* 2020; Arredondo-Alonso *et al.,* 2021; van Hal *et al.,* 2021; Saito *et al.,* 2022). Interestingly, intra- and inter- hospital spread in conjunction with the dissemination of predominant *vanA* TN*1546*-like derivatives was also recently demonstrated (Pinholt *et al.,* 2015; Egan *et al.,* 2022). A previous study of VREfm from Irish hospitals provided evidence of a unique *vanA* transposon with a truncated transposase gene in 21 isolates investigated, distinct from UK isolates (Raven *et al.,* 2016).

The objective of this part of the present study was to investigate for the first time the population structure of clade A1 VREfm from Irish hospitals using WGS and cgMLST analysis, to explore the diversity of the Tn*1546*-like *vanA* transposon in circulation and to identify potential characteristic features associated with Irish isolates in order to identify key factors that may contribute to spread. This study also sought to contextualise Irish isolates by comparison with international strains to help identify and evaluate geographical segregation of clusters and assess key differences in population biology.

3.2 Materials and Methods

3.2.1 Isolate collection

In total, 2,353 *E. faecium* isolates recovered between 1986-2023 were investigated. This comprised two distinct study populations: (i) *E. faecium* isolates recovered from seven Irish hospitals between June 2017 and December 2022 and (ii) a well-characterised collection of international comparator isolates from 30 countries representative of the Clade A1 hospital-associated *E. faecium* population. A breakdown of isolate collection is provided below.

3.2.1.1 Patient isolates

One thousand and twenty-eight *E. faecium* isolates recovered from individual patients in seven Irish hospitals were investigated (Section 3.5, Table 3.4). The majority of isolates (73%, 753/1028) were recovered in a large acute teaching hospital located in South Dublin (H1), consisting of 862 beds and a total of 26 wards (W1-W26). Hospital two (H2) isolates were recovered from a hospital in North Dublin (*N*=121), hospital three (H3) isolates were from a second hospital in North Dublin (*N*=10), hospital four (H4) isolates were from a third hospital in North Dublin (*N*=86), hospital five (H5) isolates from a hospital in the south-east of Ireland (*N*=26), hospital six (H6) isolates were from a hospital in the west of Ireland (*N*=28) and hospital seven (H7) isolates were from a hospital in the south of Ireland (*N*=4).

The isolates were recovered over distinct study periods as part of six main collection points: (a) H1 isolates including VREfm-positive screening isolates (*N*=280) collected over two-week periods each quarter for one year in all H1 wards (June 2018, October 2018, March 2019, June 2019) and all *E. faecium* BSI isolates (both VREfm and VSEfm) (*N*=72) recovered between September 2017-June 2019, (b) An additional collection of all VREfm positive screening isolates (*N*=401) recovered in the 26 H1 wards from quarter four of 2019 (September 2019-December 2019), (c) a regional collection of isolates (*N*=100) submitted to the NMRSARL from H2 and H4-H7 in quarter four of 2019 (September 2019-December 2019) comprising VREfm screening isolates (*N*=70), VREfm BSI isolates (*N*=10) and VSEfm BSI isolates (*N*=20), (d) a year-collection (February 2019-November 2019) of all positive screening VREfm isolates from H4 (*N*=86), (e) all positive VREfm isolates (*N*=79) recovered from patients on three critical care wards in H2 including one BSI, 12 urine, 49 rectal screening and 17 from 'other' clinical specimens and (f) 10 VREfm (7 rectal screening, three surgical wounds) from a critical care ward on H3 recovered as part of three outbreak investigations from June 2021, January 2022 and June 2022 (Section 3.5, Table 3.4). VREfm

isolates were stored by the diagnostic laboratories at -80°C in a Microbank cryovial (Pro-Lab Diagnostics).

3.2.1.2 International comparator reference isolates

A well-characterised, publicly available collection of clade A1 *E. faecium* isolates (*N*=1,325) from 30 countries spanning a 30-year time period (1986-2016) were included as comparators (Raven *et al.*, 2016; van Hal *et al.*, 2021) (Section 3.5, Table 3.5).

3.2.2 Phenotypic susceptibility testing

All study isolates underwent phenotypic susceptibility testing as described in Chapter 2, Section 2.3.2 Antimicrobial-resistance and virulence-associated genes were detected *in silico* on short-read WGS assemblies using ABRicate v.0.9.8 (https://github.com/tseemann/abricate).

3.2.3 Second generation Illumina short-read sequencing

3.2.3.1 Genomic DNA Extraction

All isolates underwent genomic DNA extraction for short-read sequencing as described in Chapter 2, Section 2.4.1.

3.2.3.2 Short-read sequencing

All isolates underwent short-read sequencing as described in Chapter 2, Section 2.5.1.

3.2.4 Third generation MinION long-read sequencing

3.2.4.1 Genomic DNA Extraction

Genomic DNA extraction for long-read sequencing was performed as described in Chapter 2, Section 2.4.2.

3.2.4.2 Long-read sequencing

Long-read sequencing was performed as described in Chapter 2, Section 2.5.2.

3.2.5 Bioinformatic analysis

3.2.5.1 de novo assembly

All study isolates underwent quality trimming and *de novo* assembly using Ridom SeqSphere+ v8.5.1 (Ridom GmbH) as described in Chapter 2, Sections 2.6.1.1 and 2.6.1.2.

3.2.5.2 MLST

Conventional MLST profiles were generated for all isolates using Ridom SeqSphere+ v8.5.1 (Ridom GmbH) as described in Chapter 2, Section 2.6.1.3.

3.2.5.3 wgMLST and cgMLST

Isolate genomes underwent wgMLST and cgMLST as described in Chapter 2, Sections 2.6.1.4 and 2.6.1.5.

3.2.5.4 Genotyping

Antimicrobial resistance profiling and virulence gene identification was performed *in silico* as described in Chapter 2, Section 2.6.1.6.

3.2.5.5 Phylogenetic trees

Inference of genetic relatedness, diversity, and population structure of *E. faecium* isolates in this study was carried out as described in Chapter 2, Section 2.6.1.8.

3.2.5.5.1 Neighbour joining tree

NJTs were generated using distance matrices based on cgMLST analysis using Ridom SeqSphere+ v8.5.1 (Ridom GmbH) as described in Chapter 2, Section 2.6.1.8.

3.2.6 Hybrid assembly

Hybrid assembly of paired-end short-read and long-read sequences was performed using Unicycler as described in Chapter 2, Section 2.7.

3.2.7 Plasmid analysis

3.2.7.1 Plasmid profile determination

Bacterial genome plasmid contigs were characterised as described in Chapter 2, Section 2.8.1.

3.2.7.2 Genetic organisation of vanA-encoding regions and plasmids

The genetic organization of *vanA*-encoding plasmids from Irish isolates was determined following hybrid assembly as described in Chapter 2, Section 2.8.2. A fully assembled *vanA* plasmid from VREfm screening isolate SJ11 (H1), created using the hybrid assembly approach as described in Chapter 2, Section 2.7 was chosen to act as a reference sequence for a comprehensive comparison of the *vanA* transposon across all Illumina paired-end raw reads using Burrows-Wheeler Aligner, SAMtools and BedTools (Li and Durbin, 2009; Li *et al.*, 2009; Quinlan and Hall, 2010). This strain was chosen as it had the earliest recovery date (22/08/2017) within the isolate collection that under-went hybrid assembly protocols. Briefly, Burrows-Wheeler Aligner was used to align the Illumina raw reads of all isolates against the fully assembled reference sequence. Alignment quality was assessed using Tablet. SamTools was then used to visualise alignments and sort and index reads for input into BedTools. Using the BedTools coverage command, the depth and breadth of coverage of the reference plasmid was calculated and used to determine percentage similarity between all isolates. A coverage of <70% to the reference *vanA* plasmid was used as a cut-off to identify isolates of interest, which may harbour a different genetic organisation of *van* operon genes and additional insertion sequences, to undergo third generation sequencing and hybrid assembly.

3.2.8 Filter mating

Conjugative transfer of plasmids encoding the vancomycin resistance *vanA* operon harboured by clinical enterococcal isolates was undertaken using the plasmid-free rifampicin- and fusidic acid-resistant recipient strains *E. faecium* 64/3 as described in Chapter 2, Section 2.8.4.

3.3 Results

3.3.1 Genomic epidemiology of Irish hospital *E. faecium*

In total, 1,028 *E. faecium* isolates (894 screening, 102 BSI, 12 urine and 20 'other' clinical specimens) from patients in seven Irish hospitals recovered between June 2017 and August 2022 were investigated (Section 3.5, Table 3.4). The majority (979/1028; 95.2%) were vancomycin resistant, of which 963/979 (98.3%) harboured *vanA* (vancomycin MIC>4 mg/L). A small proportion (1.5%, 15/979) of isolates harboured both a plasmid-mediated *vanA* and a chromosomally encoded *vanB*. One isolate (JH350) was found to harbour *vanB* only. The remaining 49 isolates (4.7%) (all BSI isolates) were vancomycin susceptible (vancomycin MIC≤4 mg/L). Of the isolates found to be phenotypically vancomycin susceptible, 12% (6/49) harboured a vancomycin resistance transposon remnant (three lacking *vanHAX* and three lacking *vanRS*) (Appendix 1, Table 1). The majority of isolates were from H1 (73%, 753/1028), a large Dublin hospital, whereas the remainder were from six other hospitals distributed across Ireland (H2, H3, H4, H5, H6 and H7; *N*=275).

All 1,028 isolates belonged to clade A1; the majority were identified as ST80 (743/1028; 72.3%) by conventional MLST, with the remainder belonging to ST203 (*N*=79), ST612 (*N*=44), ST787 (*N*=30), ST117 (*N*=28), ST17 (*N*=16), ST18 (*N*=14), ST2185 (*N*=14), ST789 (*N*=9), ST1395 (*N*=7), ST202 (*N*=4), ST280 (*N*=4), ST2052 (*N*=3), ST414 (*N*=3), ST2052 (*N*=3), ST192 (*N*=2), ST262 (*N*=2), ST267 (*N*=2), ST907 (*N*=2), ST1424 (*N*=2), ST1478 (*N*=2), ST1693 (*N*=2), ST78 (*N*=1), ST232 (*N*=1), ST375 (*N*=1), ST992 (*N*=1) and ST1283 (*N*=1). Eleven 'novel' isolates were submitted to pubMLST.org for ST assignment. Using cgMLST analysis based on gene-by-gene allele calling against 1,423 defined core loci and a previously recommended relatedness threshold of ≤20 allelic differences (de Been *et al.*, 2015), isolates further segregated into 65 related isolate CT groups and 60 singletons with an average cluster size of 15 (median: 5, range: 2-145) (Figure 3.1, Section 3.5, Table 3.4). The most frequent CT groups identified were CT2933 (*N*=145), CT1916 (*N*=116), CT1598 (*N*=64), CT1599 (*N*=58) and CT1511 (*N*=58), accounting for 43% (439/1028) of the total isolate population, with the three major CT groups falling within the ST80 lineage.

A high level of genomic variation was observed between isolates pairs designated within the same ST based on conventional MLST. Notably, isolates within the ST80 lineage (*N*=743) were interspersed throughout the NJT and MST and exhibited a median within-ST cgMLST allelic difference of 316 (range: 0-543) (Figure 3.1 and Figure 3.2). Both NJTs and MSTs are bioinformatic tools used to generate graphical representations of the phylogenetic and evolutionary relationship between *E. faecium* sequences based on distance matrices

generated using gene-by-gene allele calling against 1,423 defined core genes (de Been *et al.*, 2015). The MST algorithm directly connects nodes that display the shortest possible genetic distance and can therefore be utilised to infer likely transmission pathways and denote isolates as genomically related (Kruskal, 1956). Similarly, the NJT aims to minimise branch length via agglomerative clustering but does not directly connect nodes (Saitou and Nei, 1987). This finding of significant intra-ST genetic diversity is equivalent to the genomic distance observed between isolates from different ST pairs (e.g., the allelic difference observed between isolate SJ5 [ST203] and SJ26-2 [ST80] was 491) (Figure 3.2). In comparison, the pairwise median intra-CT cgMLST allelic difference for isolates within CT2933 was 5 (range: 0-25), whilst the inter-CT cgMLST allelic difference between example isolates BS258 (CT2933) and JH404 (CT1916) was 449. The majority (60/65, 92%) of cgMLST-derived clusters (≤20 allelic differences) contained isolates designated within the same ST. Five clusters contained mixtures of 2-3 STs (Figure 3.2), with the second and third ST representing a single locus variant of the predominant ST within the cluster. Interestingly, CT1424 and CT1478 contained a previously described *pstS* housekeeping gene deletion (indicated within group (b) and (d) in Figure 3.2) (Carter *et al.*, 2016). These findings suggest that whilst ST80 is the predominant endemic *E. faecium* clone in Irish hospitals, there is a more diverse and polyclonal population within the lineage that can be further discriminated into more discrete genomic clusters more accurately representative of the population structure determined using cgMLST.

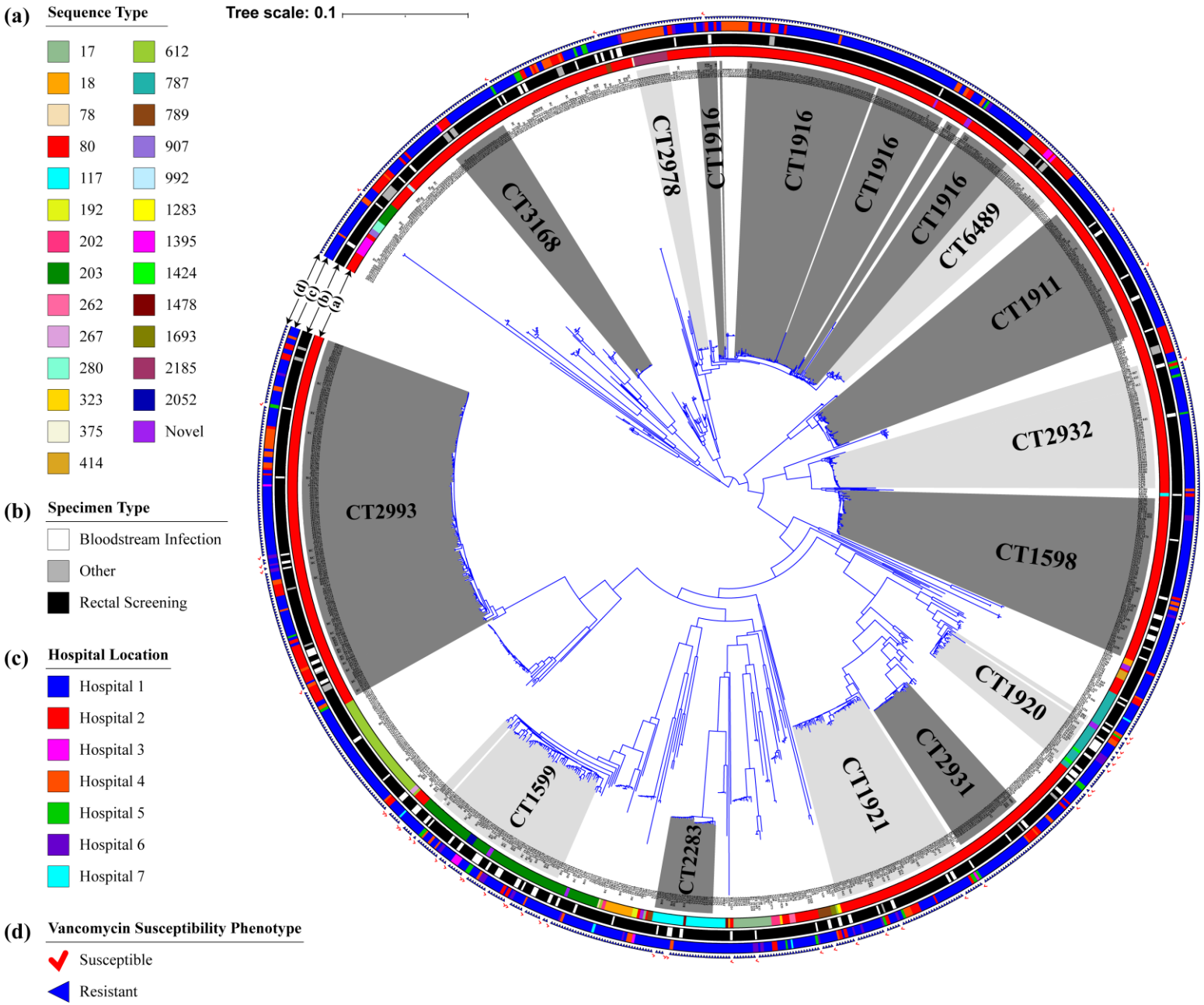
(a)
Sequence Type
17
18
78
80
117
192
202
203
262
267
280
323
375
414
612
787
789
907
992
1283
1395
1424
1478
1693
2185
2052
Novel
Tree scale: 0.1
(b)
Specimen Type
Bloodstream Infection
Other
Rectal Screening
(c)
Hospital Location
Hospital 1
Hospital 2
Hospital 3
Hospital 4
Hospital 5
Hospital 6
Hospital 7
(d)
Vancomycin Susceptibility Phenotype
Susceptible
Resistant
CT3168
CT2978
CT1916
CT1916
CT1916
CT1916
CT6489
CT1911
CT2932
CT1598
CT1920
CT2931
CT1921
CT2283
CT1599
CT2993

Figure 3.1. Neighbour-joining tree (NJT) based on cgMLST of 1,038 clade A1 *E. faecium* isolates, recovered between June 2017 and August 2022 from seven Irish hospitals. The 1,028 isolates divided into 65 clusters and 60 singletons. Major complex types (CTs) are shaded in grey and labelled accordingly. Scale bar represents the phylogenetic distance between isolates based on cgMLST. Metadata are represented encircling the NJT as denoted by the colour legends, data represented are (a) STs, (b) source of isolate, (c) origin hospital location of isolates, and (d) vancomycin phenotype.

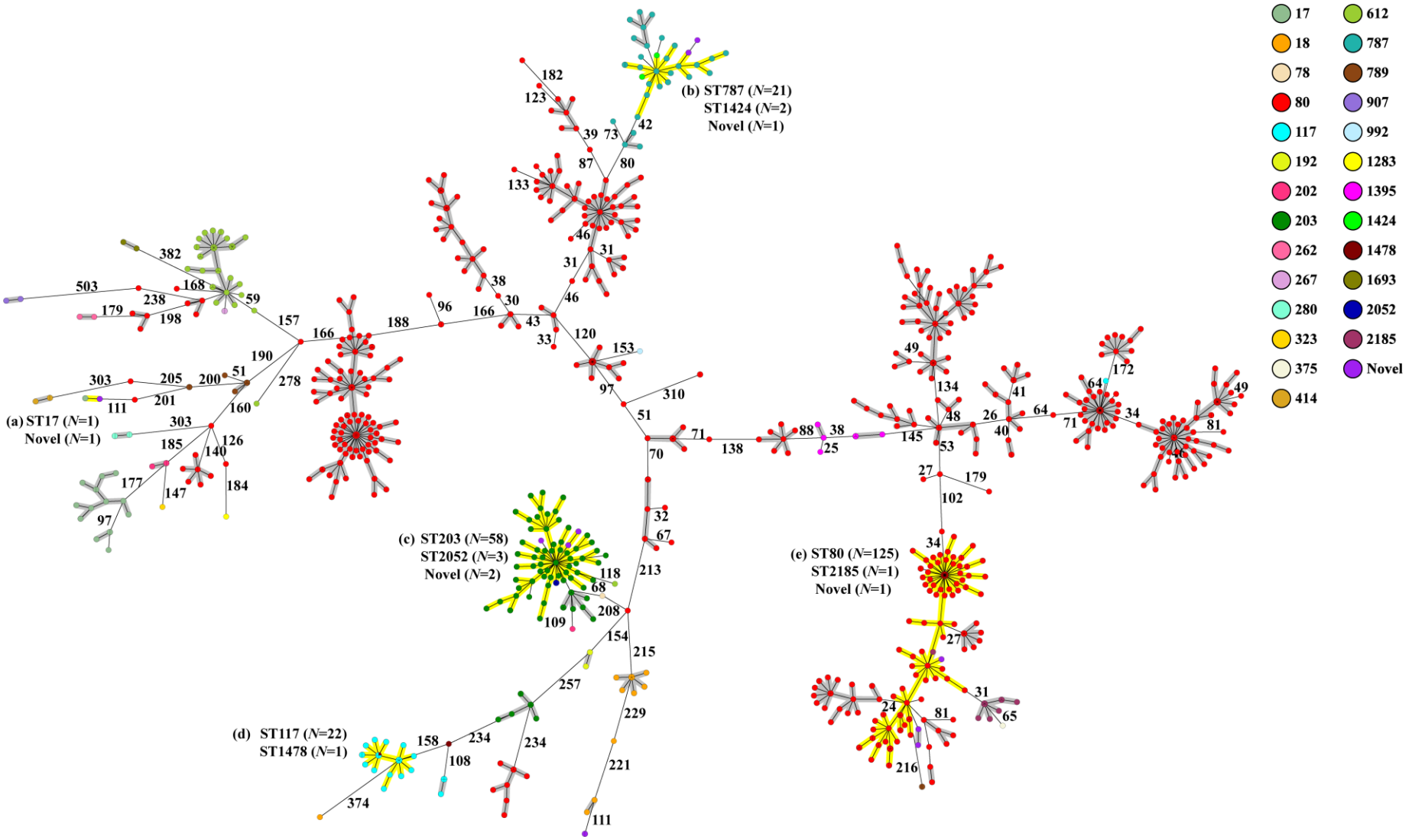

Figure 3.2. Minimum spanning tree (MST) based on core-genome multi-locus sequence typing (cgMLST) analysis of the 1,038 Clade A1 *E. faecium* isolates recovered between June 2017 and August 2022 from seven Irish hospitals. Node colours represent the sequence type (ST) as indicated in the legend. Partitions within the nodes represent the presence of ≥2 isolates. Branch numbers indicate cgMLST allelic

differences between neighbouring isolates. For clarity, allelic differences are only displayed on branches between neighbouring clusters. Twenty-six STs were identified within the isolate population. Closely related clusters of isolates (≤20 cgMLST allelic differences) are outlined by grey shading (de Been *et al.*, 2015). The majority of clusters were defined by their MLST derived ST, however five clusters contained mixtures of multiple STs which are outlined by yellow shading with (a)-(e) labelled accordingly; (a) ST17 (*N*=1) and 'novel' (*N*=1), cgMLST allelic difference = 18; (b) ST787 (*N*=21), ST1424 (*N*=2) and 'novel' (*N*=1), median cgMLST allelic difference: 10, range: 0-27; (c) ST203 (*N*=58), ST205 (*N*=3) and 'novel' (*N*=2), median cgMLST allelic difference: 18, range: 0-38; (d) ST117 (*N*=22) and ST1478 (*N*=1), median cgMLST allelic difference: 5, range: 0-13; (e) ST80 (*N*=125), ST2185 (*N*=1) and 'novel' (*N*=1), median cgMLST allelic difference: 12, range: 0-50.

After broadly grouping isolates together using conventional MLST analysis, a more comprehensive examination of isolates within the predominant ST80 lineage and the major CT clonal clusters was undertaken. Using cgMLST analysis, ST80 isolates segregated into 35 cgMLST clusters and 35 singletons, with a median cluster size of 8 (range: 2-145). Three major ST80 clusters containing closely related clonal groups were evident in an cgMLST-based NJT, comprising 45% (336/743) of the ST80 isolate population, termed CI, CII and CIII respectively (Figure 3.3).

The largest, CT2933 (termed CI hereafter), comprised rectal screening (*N*=127), BSI (*N*=11), urine (*N*=2) and 'other infection site' (*N*=5) isolates recovered over a 43-month period (October 2018-June 2022) with a median allelic difference of 5 (range: 0-25) (Figure 3.3). The majority of isolates (86/145, 59%) within CI were recovered from patients admitted to 19 H1 wards and one submitted to H1 for investigation from an external community medical practitioner. The remaining isolates were recovered from H2 (*N*=31), H3 (*N*=1), H4 (*N*=20), H5 (*N*=3) and H6 (*N*=4) (Section 3.5, Table 3.4). In total, 97% (140/145) of CI isolates were vancomycin resistant, whilst the remaining five were VSEfm and recovered from BSIs. Within this cluster, there are many examples of mixtures of closely related screening and clinical specimens, isolates from different hospitals in distinct geographical locations across Ireland and both vancomycin-susceptible and resistant phenotypes (Appendix 1, Table 1) For instance, three rectal screening isolates (BH61, RC-19-065 and RC-19-087) and four BSI (RC-19-097, RC-19-098, RC-19-100 and RC-19-103) within CI were genetically indistinguishable with a median pairwise cgMLST difference of 0 despite being recovered from seven separate patients within H2 over a 24-month period (October 2019-November 2021) (highlighted by a black box labelled (a) in Figure 3.4). Interestingly, the earliest collected isolate was a VSEfm BSI (RC-19-097) and was recovered 18 days prior to a VREfm BSI (RC-19-098) in an additional patient highlighting both the potential *de novo* emergence of vancomycin resistance from susceptible populations in the presence of selective pressures in hospital wards, as well as potential complex transmission chains. Additionally, the persistence of genetically distinct VREfm clones was evident, with 744 days observed between the earliest collected BSI VSEfm (RC-19-098) and the latest recovered carriage VREfm (BH61).

Within CI, both intra-hospital and inter-hospital transmission of genetically indistinguishable clones was evident. For example, closely related screening isolates JH164 (H1) and RC-19-026 (H5) recovered from individual patients in geographically distant hospitals (>100 km apart) over a 15-day period with an allelic difference of 3 (marked with a black box labelled (b) in Figure 3.4). Additionally, genetically indistinguishable (median

allelic difference: 2, range: 0-8) VREfm were identified from 13 H1 wards (*N*=39) and four other geographically distinct hospitals (H2 *N*=2, H4 *N*=4, H5 *N*=1 and H6 *N*=1) over 31-months (957 days; May 2019-December 2021) again suggesting widespread dissemination of a distinct VREfm clone both within the same hospital and across the Irish hospital network (marked with a black box labelled (c) in Figure 3.4).

The second largest CT cluster (termed CII) comprised 127 isolates belonging to five CT groups (CT1916 *N*=116, CT2023 *N*=1, CT2953 *N*=1, CT3175 *N*=1, CT3385 *N*=8) with a median cgMLST allelic difference of 12 (range: 0-50) (Figure 3.3 and Figure 3.5). This cluster displayed more diversity, evidenced by the greater allelic difference range and combination of multiple distinct CTs. CII consisted of a mixture of screening (*N*=122), BSI (*N*=3), urine (*N*=1) and 'other infection site' (*N*=1) VREfm isolates recovered over 47 months (December 2017-November 2021). In total, 83% (106/127) were recovered from 26 H1 wards and two isolates submitted to H1 from external community medical practitioners, with the remainder recovered from H2 (*N*=12), H4 (*N*=5), H5 (*N*=1) and H6 (*N*=3). The third CT cluster, CT1598 (termed CIII), consisted of 64 isolates (63 VREfm and 1 VSEfm) collected over 28 months (July 2017-December 2019) with a median cgMLST allelic difference of 6 (range: 0-19) (Figure 3.6, Section 3.5, Table 3.4). CIII comprised a mixture of rectal screening (*N*=55) and BSI (*N*=9) isolates recovered from 21 H1 wards (*N*=58), H2 (*N*=1), H4 (*N*=2) and H6 (*N*=3). The single VSEfm isolate within this cluster was from a BSI recovered in H1. Similar findings within CII and CIII of the emergence, dissemination, and extensive persistence of highly related ST80 variants both across multiple wards of the same hospital and throughout the Irish hospital network was evident. Additionally, the recovery of genetically indistinguishable (≤20 allelic differences) VSEfm and VREfm highlight the potential for the emergence of novel VRE clones through the continued dynamic loss/gain of the vancomycin resistance transposon.

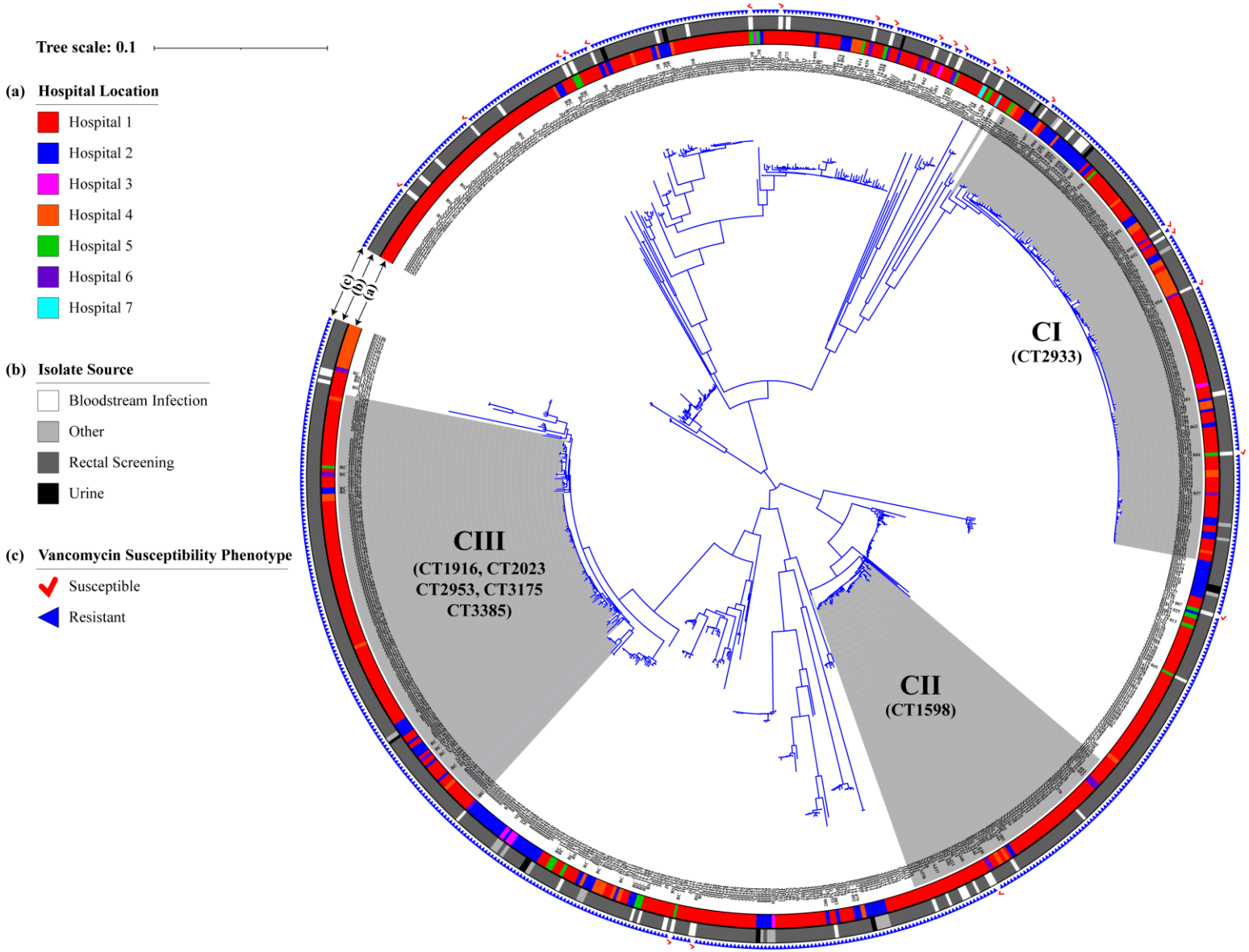
Tree scale: 0.1
(a) Hospital Location
Hospital 1
Hospital 2
Hospital 3
Hospital 4
Hospital 5
Hospital 6
Hospital 7
(b) Isolate Source
Bloodstream Infection
Other
Rectal Screening
Urine
(c) Vancomycin Susceptibility Phenotype
Susceptible
Resistant
(c)
(b)
(a)
CI
(CT2933)
CII
(CT1598)
CIII
(CT1916, CT2023
CT2953, CT3175
CT3385)

Figure 3.3. Neighbour-joining tree (NJT) based on cgMLST of 743 ST80 clade A1 *E. faecium* isolates, recovered between June 2017-August 2022 from seven Irish hospitals. The 743 isolates divided into 35 clusters and 35 singletons, with a median cluster size of 8 (range: 2-145). The three major clusters comprising 45% (336/743) of the ST80 population are shaded in grey and predominant complex types (CT) labelled accordingly. Isolates within clusters were closely related; the allelic differences between isolates in the three largest clusters were as follows: CI (CT2933 *N*=145), median: 5, range: 0-25; CII (CT1916 *N*=116, CT2023 *N*=1, CT2953 *N*=1, CT3175 *N*=1, CT3385 *N*=8), median: 12, range: 0-50; CIII (CT1598 *N*=64), median: 6, range: 0-19. Scale bar represents the phylogenetic distance between isolates based on cgMLST. Metadata is represented encircling the NJT as denoted by the colour legends, data represented is (a) origin hospital location of isolate, (b) isolate source and (c) vancomycin susceptibility phenotype.

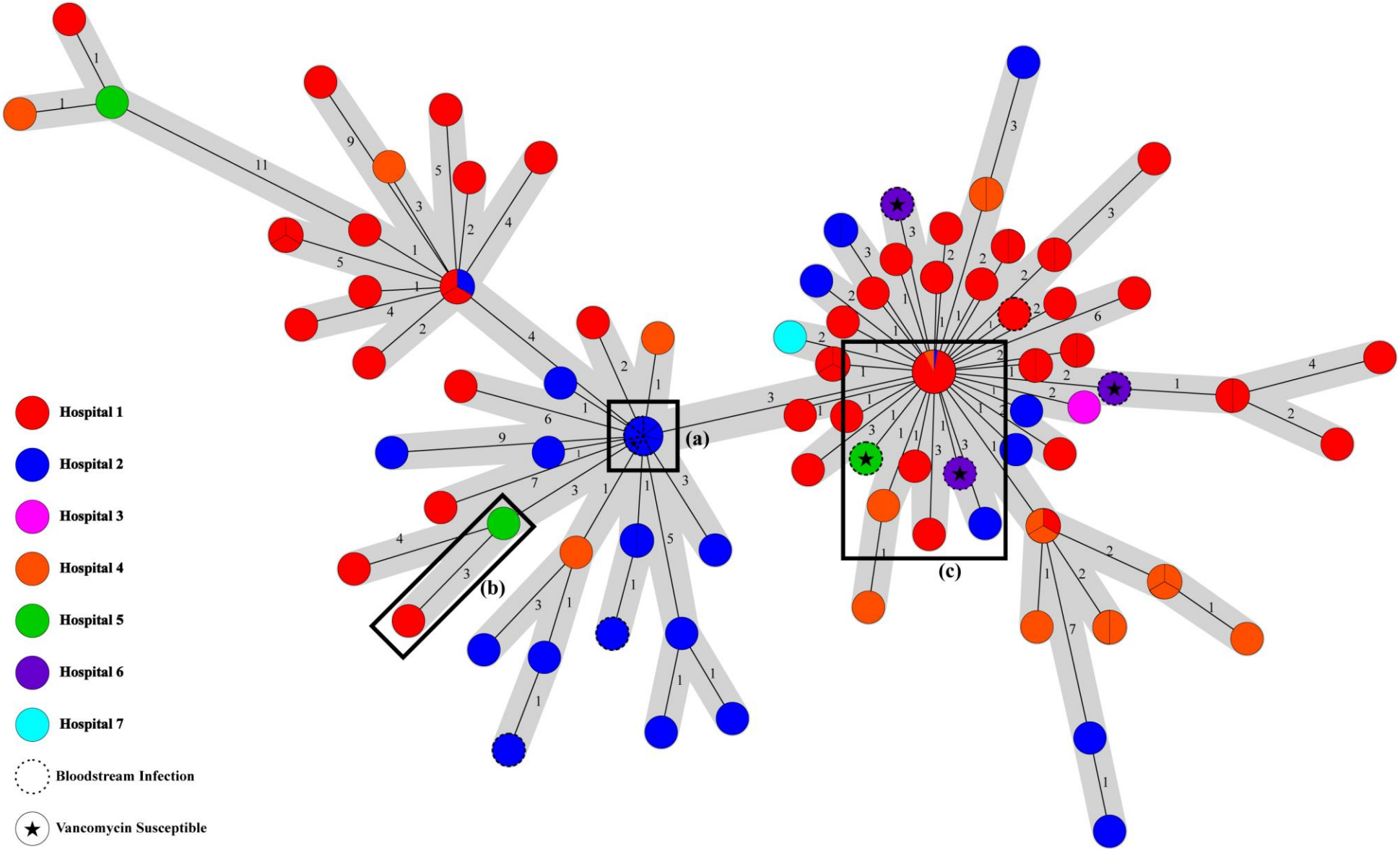
Hospital 1
Hospital 2
Hospital 3
Hospital 4
Hospital 5
Hospital 6
Hospital 7
Bloodstream Infection
Vancomycin Susceptible
(a)
(b)
(c)

Figure 3.4. Minimum spanning tree (MST) based on core-genome multi-locus sequence typing (cgMLST) analysis of 1,423 defined core loci for the 145 ST80/CT2933 isolates (referred to as CI) recovered from seven Irish hospitals over a 43-month period (October 2018-June 2022). Node colours represent the hospital (H1-H7) from which the isolate was recovered as indicated in the legend. Partitions within the nodes represent the presence of ≥2 isolates. Branch numbers indicate cgMLST allelic differences between neighbouring isolates. Isolates collected from bloodstream infections are indicated with a dashed outer node ring (*N*=11). Vancomycin susceptible isolates are indicated by the black star within the node (*N*=5). (a) Seven isolates (three rectal screening and four bloodstream infection) collected from H2 over a 24-month period (October 2019-November 2021) with a median pairwise cgMLST allelic difference of 0, (b) two rectal screening isolates recovered over a 15-day period in H1 and H5 (>100 km distance) with an allelic difference of three and (c) 45 isolates from five Irish hospitals (H1 *N*=39, H2 *N*=2, H4 *N*=4, H5 *N*=1 and H6 *N*=1) identified over 31-months (May 2019-December 2021) with a median cgMLST allelic difference of two.

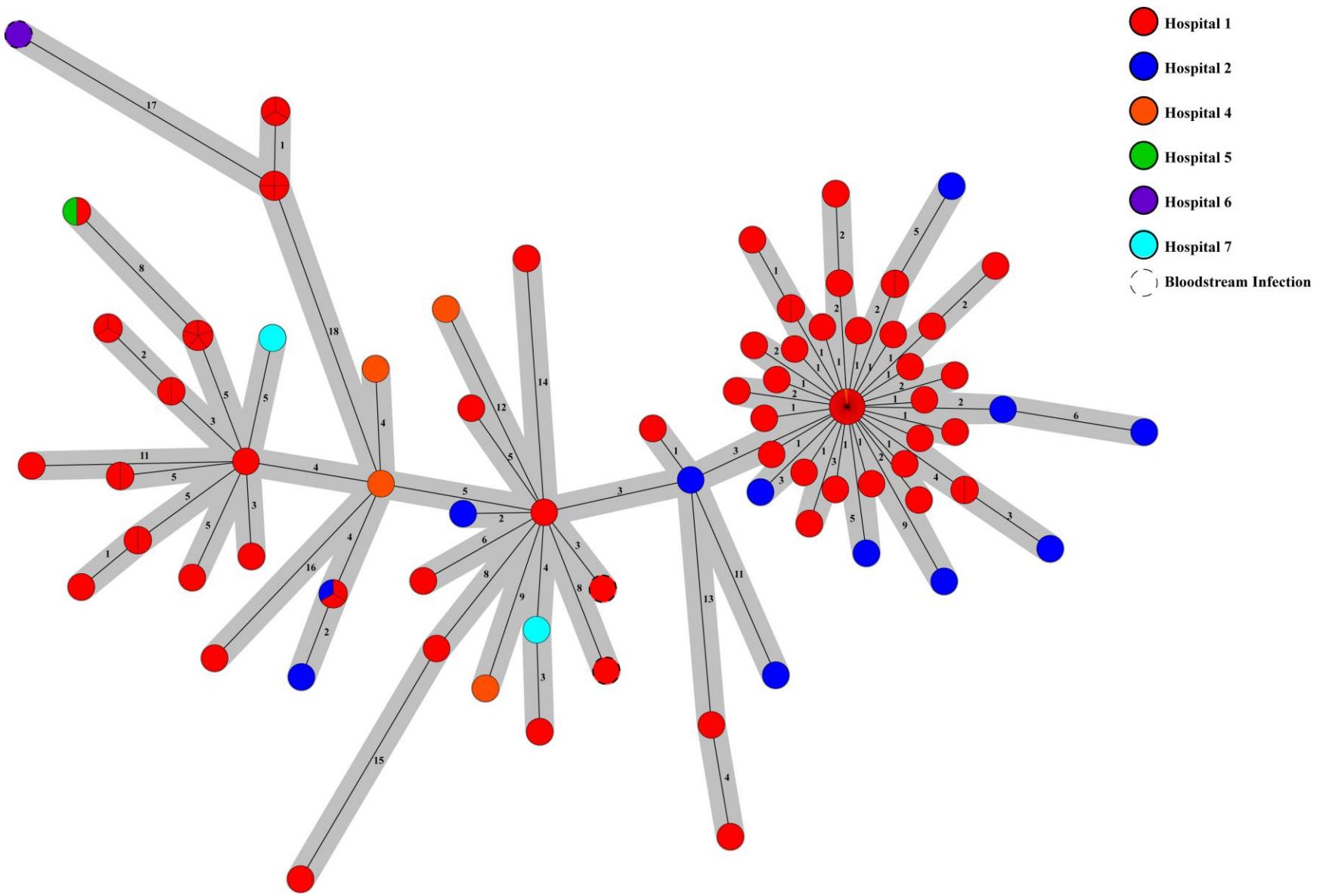
Hospital 1
Hospital 2
Hospital 4
Hospital 5
Hospital 6
Hospital 7
Bloodstream Infection

Figure 3.5. Minimum spanning tree (MST) based on core-genome multi-locus sequence typing (cgMLST) analysis of 1,423 defined core loci for the 127 ST80/CT1916/2023/2953/3175/3385 isolates (referred to as CII) recovered from six Irish hospitals over a 47-month period (December 2017-November 2021) (de Been *et al.*,2013)**.** Node colours represent the hospital (H1-H7) from which the isolate was recovered as indicated in the legend. Partitions within the nodes represent the presence of ≥2 isolates. Branch numbers indicate cgMLST allelic differences between neighbouring isolates. Isolates collected from bloodstream infections are indicated with a dashed outer node ring (*N*=2).

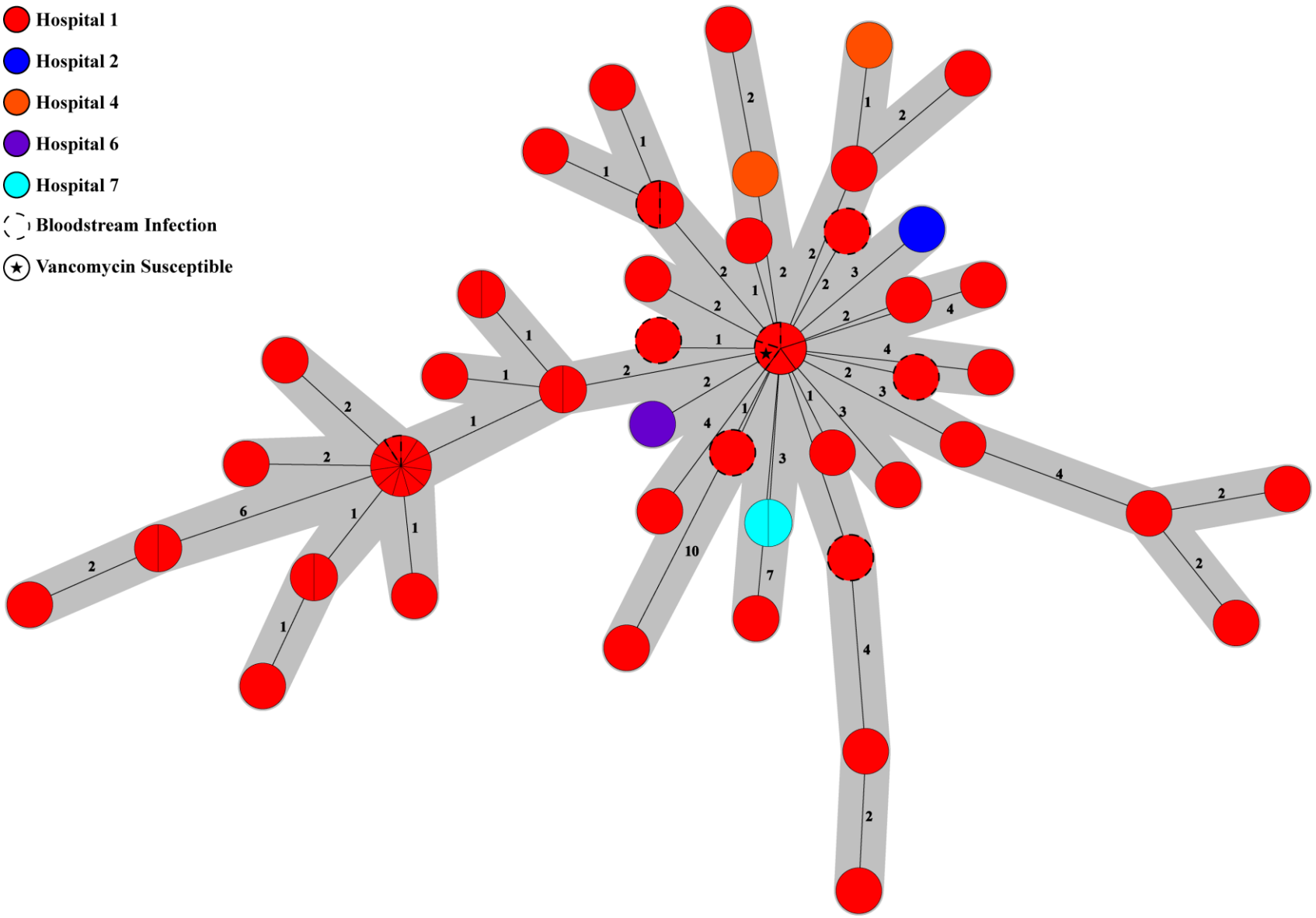
Hospital 1
Hospital 2
Hospital 4
Hospital 6
Hospital 7
Bloodstream Infection
Vancomycin Susceptible

Figure 3.6. Minimum spanning tree (MST) based on core-genome multi-locus sequence typing (cgMLST) analysis of 1,423 defined core loci for the 64 ST80/CT1598 isolates (referred to as CIII) recovered from five Irish hospitals over a 28-month period (July 2017-December 2019). Node colours represent the hospital (H1-H7) from which the isolate was recovered as indicated in the legend. Partitions within the nodes represent the presence of ≥2 isolates. Branch numbers indicate cgMLST allelic differences between neighbouring isolates. Isolates collected from bloodstream infections are indicated with a dashed outer node ring (*N*=2).

3.3.2 Irish, global and Danish *E. faecium* comparison

In order to contextualise the Irish isolates and determine if they arose from globally disseminated lineages or have emerged independently within the Irish population, the 1,028 study isolates were compared with 1,325 publicly available international *E. faecium* isolates from 30 countries (Raven *et al.,* 2016; van Hal *et al.,* 2021). These isolates were recovered across six continents (Africa *N*=2, Asia *N*=3, Australia *N*=1, Europe *N*=18, North America *N*=2 and South America *N*=4) between 1986-2016 (Appendix 1, Table 2). Phylogenetic analysis based on the 1,423 cgMLST loci revealed very little overlap between the groups of isolates, with the majority of Irish strains found clustered independently on distinct network branches within the MST (Figure 3.7) A small number of Irish isolates (15 in total) were identified in six clusters (termed cluster 1-6 hereafter) of highly-related (≤20 cgMLST allelic differences) isolates, containing mixtures of both Irish and international isolates (Figure 3.7, Table 3.1a-e).

Cluster one (C1) consisted of 24 ST203 CT20 *E. faecium* strains recovered from 2013-2019. This included eight Irish (seven VREfm and one VSEfm) and 16 global isolates originating from six countries (Australia *N*=8, Belgium *N*=1, Denmark *N*=1, Germany *N*=2, Netherlands *N*=3 and Norway *N*=1) (Table 3.1a). Isolates within this cluster exhibited a median cgMLST allelic difference of 11 (range: 0-23), with the closet neighbouring international isolate recovered from Belgium in 2012 (E1041 SRX8457586) differing by four allelic differences to three Irish rectal screening VREfm from H1. Notably, all C1 isolates harboured *vanA* exclusively with the exception of Irish BSI isolate BSI-SJ32 which was phenotypically susceptible to vancomycin and lacked *vanA*. Cluster two (C2) comprised one Irish ST17 rectal screening isolate from H2 (BH047) and 15 British ST17 isolates recovered between 2007-2021 which exhibited a median cgMLST allelic difference of 12 (0-33) (Figure 3.7, Table 3.1b). A total of three distinct CTs were identified in C2 including CT1343 (*N*=12), CT2271 (*N*=1, Irish isolate) and CT4306 (*N*=2). One isolate was not designated a CT (BSAC ec2101 ERX347456). It is important to consider that British isolates within the international collection, which were retrieved from the study of Raven *et al*, did not contain epidemiological information on their specific country of origin and were instead denoted under the umbrella term of "United Kingdom". Isolates therefore may have originated from England, Scotland, Wales, or Northern Ireland. Interestingly, the two most closely related neighbouring isolates (17 allelic differences) to BH047 within C2 were vancomycin-susceptible and isolated 10 years prior in 2010-2011. The Irish screening isolate BH047 was phenotypically vancomycin resistant and carried both a plasmid-encoded *vanA*

and a chromosomally-encoded *vanB* resistance operon. However, the *vanB* operon lacked regulatory genes (*vanBR* and *vanBS*). The remaining isolates within C2 harboured either *vanA* only (*N*=5) or were VSEfm (N=10).

Cluster three (C3) consisted of 19 isolates (one Irish H1 and 18 international) recovered between 2010-2017 which exhibited a median allelic difference of 11 (range: 0-30) (Figure 3.7) The global isolates in C3 originated from five European countries and included four Norwegian VSEfm, three German VREfm (two *vanA* and one *vanB*), five Spanish (two VREfm [*vanB*] and three VSEfm), three Danish VREfm (all *vanA*), one Belgian VREfm (*vanB*) and two Dutch VREfm (both *vanB*) (Table 3.1c). The closest global isolate to the Irish isolate in C3 was a Spanish isolate, which differed by seven allelic differences. Cluster four (C4) consisted of three isolates recovered from 2008-2019 separated by a median of 11 allelic differences (range: 0-20). This included one ST18 CT3387 VREfm from Ireland, one ST18 CT173 VREfm (*vanA*) from Slovenia and one ST18 CT173 VREfm (*vanA*) from the United Kingdom (Table 3.1d). Cluster five (C5) comprised two Irish ST262 CT3166 rectal screening isolates recovered in 2019 from H1 which exhibited 20-21 allelic differences to an ST262 CT1016 isolate recovered from Germany (Table 3.1e). The final group, cluster six (C6), contained two Irish ST80 CT3393 VREfm (*vanA*) recovered from H2 and two ST80 CT1162 VSEfm from the United Kingdom (Figure 3.7, Table 3.1e). The isolates were collected eight years apart and exhibited a median cgMLST pairwise allelic difference range of 0-23.

A sub-set of Irish *E. faecium* (*N*=640) were also compared with 989 Danish VREfm recovered from four hospitals during 2017–18. Denmark was chosen as a direct comparator due to its increase in VREfm prevalence, caused by the introduction of an ST80 clone (Pinholt *et al.*, 2019). The comparison of Irish and Danish isolates revealed 64 clusters and 69 singletons. Clusters were again predominantly country-specific, with only three containing isolates from both countries (Figure 3.8).

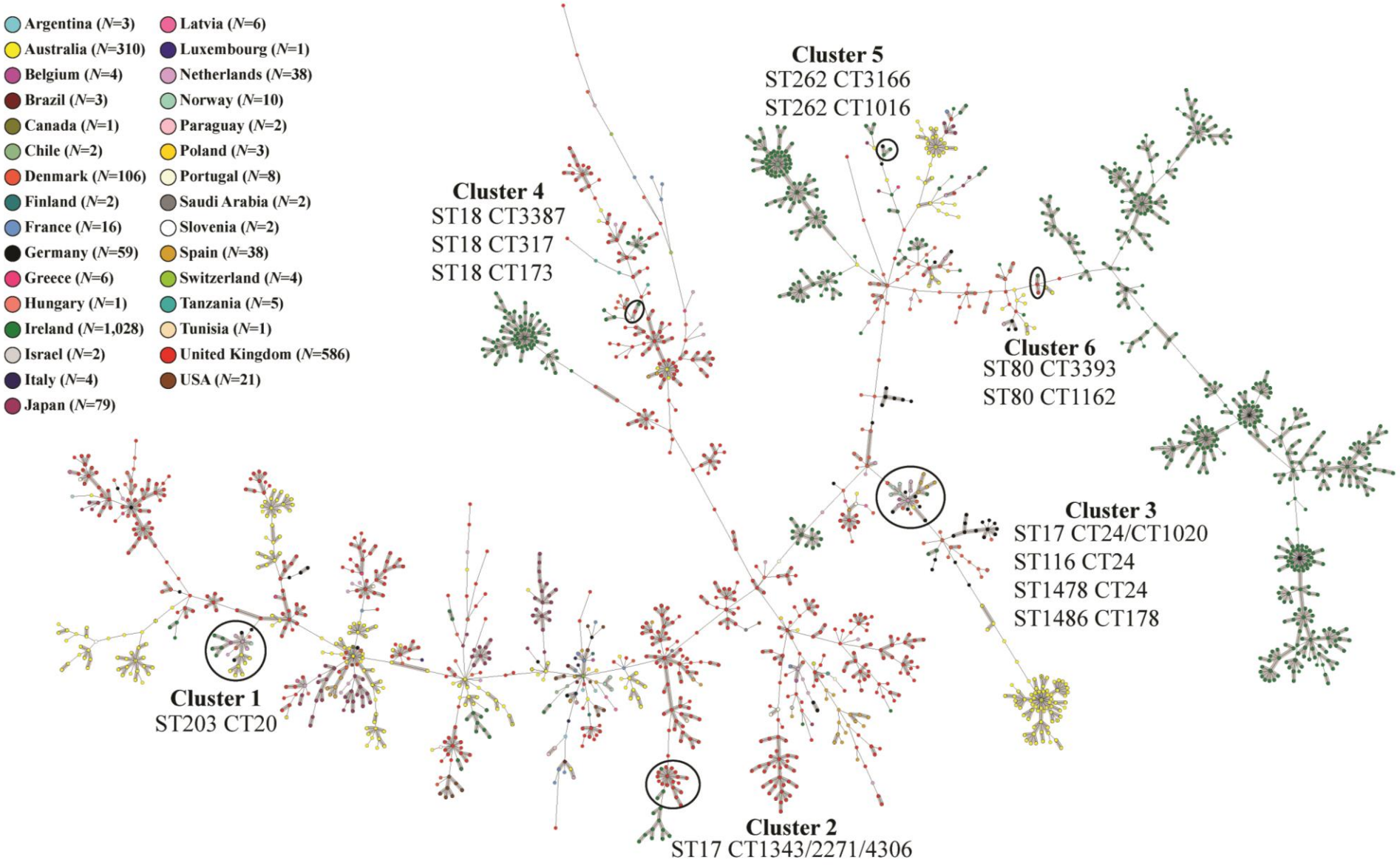
Argentina (N=3)
Australia (N=310)
Belgium (N=4)
Brazil (N=3)
Canada (N=1)
Chile (N=2)
Denmark (N=106)
Finland (N=2)
France (N=16)
Germany (N=59)
Greece (N=6)
Hungary (N=1)
Ireland (N=1,028)
Israel (N=2)
Italy (N=4)
Japan (N=79)
Latvia (N=6)
Luxembourg (N=1)
Netherlands (N=38)
Norway (N=10)
Paraguay (N=2)
Poland (N=3)
Portugal (N=8)
Saudi Arabia (N=2)
Slovenia (N=2)
Spain (N=38)
Switzerland (N=4)
Tanzania (N=5)
Tunisia (N=1)
United Kingdom (N=586)
USA (N=21)
Cluster 1
ST203 CT20
Cluster 2
ST17 CT1343/2271/4306
Cluster 3
ST17 CT24/CT1020
ST116 CT24
ST1478 CT24
ST1486 CT178
Cluster 4
ST18 CT3387
ST18 CT317
ST18 CT173
Cluster 5
ST262 CT3166
ST262 CT1016
Cluster 6
ST80 CT3393
ST80 CT1162

Figure 3.7. Minimum spanning tree of Irish Clade A1 *E. faecium* (*N*=1,028) isolated between June 2017 and August 2022 and global Clade A1 *E. faecium* (N=1,325) [786 VREfm (521 *vanA*, 265 *vanB*) and 539 VSEfm) originating from 30 countries, spanning a 30-year period (1986-2016) from the study of van Hal *et al* and Raven *et al*. Isolates are coloured by country of origin as indicated in the legend. A small number of Irish isolates (15 in total) were identified in six clusters of related isolates consisting of both Irish and international *E. faecium*. The six clusters of related isolates are encircled and numbered 1–4. The ST and CT of the isolates within the clusters are indicated. Detailed metadata and distance matrices for cluster 1-6 based on cgMLST is available in Table 3.1a-e.

Table 3.1a. Detailed metadata and distance matrices based on cgMLST analysis of global cluster 1 identified in a minimum spanning tree (MST) based on Irish Clade A1 *E. faecium* (*N*=1,028) and global Clade A1 *E. faecium* (*N*=1,325) (Figure 3.7)

Size of table exceeds page margins.

Scan and/or click QR code to access and/or download table.

Table 3.1b. Detailed metadata and distance matrices based on cgMLST analysis of global cluster 2 identified in a minimum spanning tree (MST) based on Irish Clade A1 *E. faecium* (*N*=1,028) and global Clade A1 *E. faecium* (*N*=1,325) (Figure 3.7)

Size of table exceeds page margins.

Scan and/or click QR code to access and/or download table.

Table 3.1c. Detailed metadata and distance matrices based on cgMLST analysis of global cluster 3 identified in a minimum spanning tree (MST) based on Irish Clade A1 *E. faecium* (*N*=1,028) and global Clade A1 *E. faecium* (*N*=1,325) (Figure 3.7)

Size of table exceeds page margins.

Scan and/or click QR code to access and/or download table.

Table 3.1d. Detailed metadata and distance matrices based on cgMLST analysis of global cluster 4 identified in a minimum spanning tree (MST) based on Irish Clade A1 *E. faecium* (*N*=1,028) and global Clade A1 *E. faecium* (*N*=1,325) (Figure 3.7)

Total isolate number	Isolate name	ST/CT	Country of origin	Year of isolation	Vancomycin resistance gene	cgMLST Matrix				Median pairwise cgMLST difference (range)
							JH153	**ec2744**	**E7100**	
3	JH153	18/3387	Ireland	2019	*vanA*	**JH153**				11 (0-20)
	BSAC ec2744 ERX347271	18/317	United Kingdom	2011	*vanA*	**ec2744**	11			
	E7100 ERX2790906	18/173	Slovenia	2008	*vanA*	**E7100**	20	15		

Abbreviations: Abbreviations: CT, cgMLST complex type; ST, MLST sequence type.

Table 3.1e. Detailed metadata and distance matrices based on cgMLST analysis of global cluster 5 identified in a minimum spanning tree (MST) based on Irish Clade A1 *E. faecium* (*N*=1,028) and global Clade A1 *E. faecium* (*N*=1,325) (Figure 3.7)

Total isolate number	Isolate name	ST/CT	Country of origin	Year of isolation	Vancomycin resistance gene	cgMLST Matrix				Median pairwise cgMLST difference (range)
							JH153	**ec2744**	**E7100**	
3	SJ190	262/3166	Ireland	2019	*vanA*	**JH153**				11 (0-21)
	JH121	262/3166	Ireland	2019	*vanA*	**ec2744**	2			
	E0919 SRX8457450	262/1016	Germany	2016	*vanA*	**E7100**	20	21		

Abbreviations: Abbreviations: CT, cgMLST complex type; ST, MLST sequence type.

Table 3.1f. Detailed metadata and distance matrices based on cgMLST analysis of global cluster 6 identified in a minimum spanning tree (MST) based on Irish Clade A1 *E. faecium* (*N*=1,028) and global Clade A1 *E. faecium* (*N*=1,325) (Figure 3.7)

Total isolate number	Isolate name	ST/CT	Country of origin	Year of isolation	Vancomycin resistance gene	cgMLST Matrix					Median pairwise cgMLST difference (range)
							RC-19-068	**RC-19-069**	**ec2755**	**ec2761**	
4	RC-19-068	80/3393	Ireland	2019	*vanA*	**RC-19-068**					20 (0-23)
	RC-19-069	80/3393	Ireland	2019	*vanA*	**RC-19-069**	0				
	BSAC ec2755 ERX347591	80/1162	United Kingdom	2011	Susceptible	**ec2755**	20	21			
	BSAC ec2761 ERX347593	80/1162	United Kingdom	2011	Susceptible	**ec2761**	22	23	6	0	

Abbreviations: Abbreviations: CT, cgMLST complex type; ST, MLST sequence type.

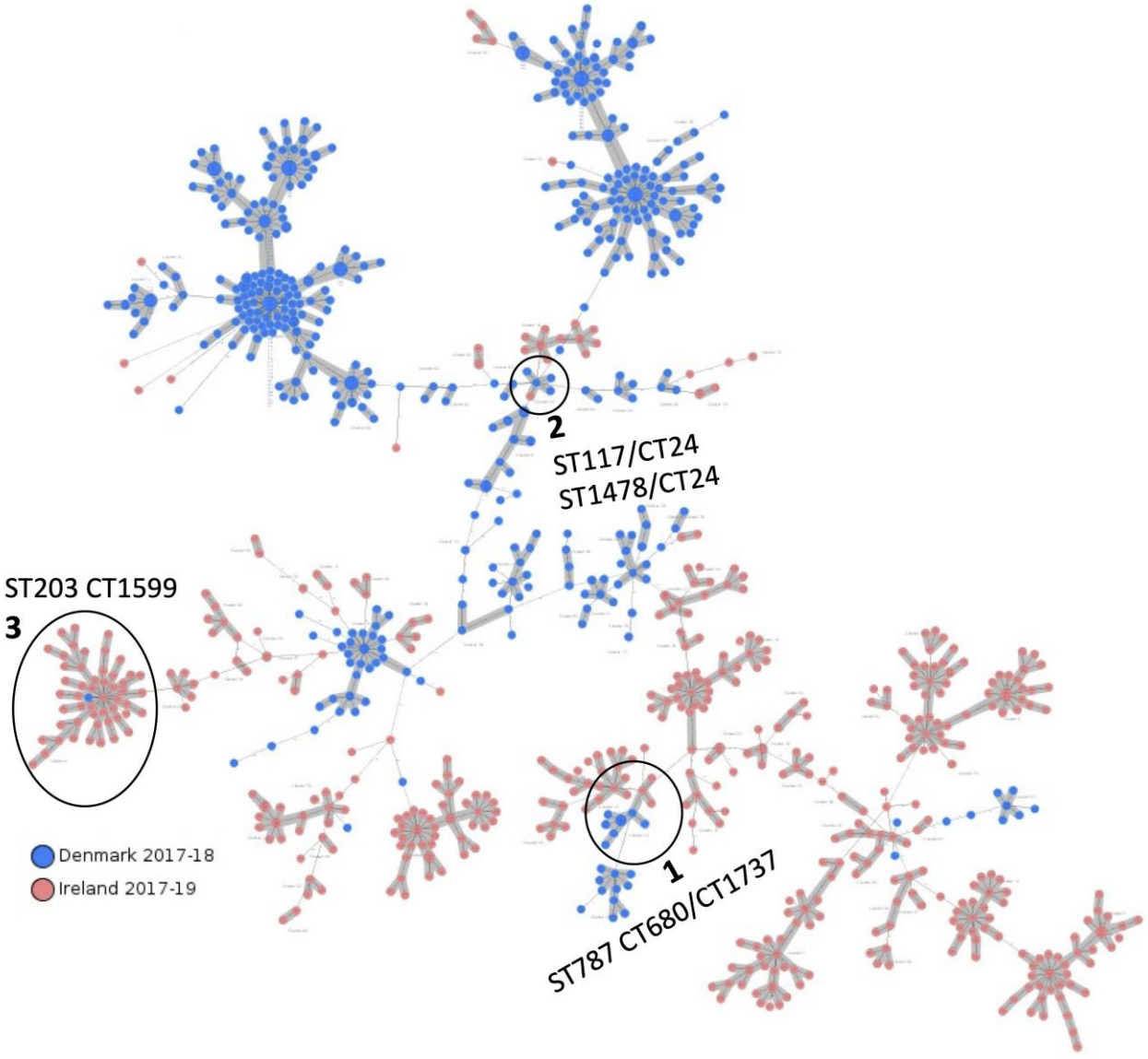
2
ST117/CT24
ST1478/CT24
ST203 CT1599
3
Denmark 2017-18
Ireland 2017-19
1
ST787 CT680/CT1737

Figure 3.8. Minimum spanning tree of Irish Clade A1 E. faecium (*N*=640) isolated between June 2017 and December 2019 and Danish VREfm (*N*=989) isolates between 2017 and 2018. Isolates are coloured by country of origin with Irish isolates coloured red and Danish isolates coloured in blue. Clusters of related isolates containing both Danish and Irish isolates are encircled and numbered 1-3. Cluster 1 consists of 18 Danish VREfm belonging to ST787 CT680/CT1737 and three Irish H1-VREfm isolated in September 2017, June 2018 and October 2019 that were separated by 12 allelic differences from the nearest Danish isolates. Cluster 2 consists of four Danish ST117 CT24 VREfm and a single Irish ST1478 CT24 (a single locus variant of ST117) VREfm, with 15 allelic differences to the nearest Danish isolate. Cluster 3 consists of a large ST203 CT1599 cluster (n=57) of Irish VREfm and VSEfm and a single Danish VREfm isolate, which exhibited six allelic differences to the nearest Irish isolate.

3.3.3 Structural organization of the *van* region in Irish VREfm

The extrachromosomal *vanA*-harbouring regions of seven VREfm representing a variety of ST and CTs (SJ10 [ST789, CT1601], SJ11 [ST1478, CT24], BSI_SJ40 [ST80, CT1598], SJ82 [ST203, CT20], SJ245 [ST117, CT2929], RC-19-039 [ST17, CT2934] and RC_19_023 [ST80, CT1916]) were fully resolved using hybrid assembly. The *vanA* regions varied in size (SJ10*vanA*, 11,022 bp; SJ11*vanA*, 13,252 bp; BSI_SJ40*vanA*, 13,269 bp; SJ82*vanA*, 10,823 bp, SJ245*vanA*, 14,168 bp, RC-19-039*vanA* RC_19_023*vanA*, 12,883 bp) and differed from the original Tn*1546 vanA* operon prototype from VREfm BM4147 (GenBank accession number: M97297) (Figure 3.9). Differences included multiple orientations of the *vanA* operon genes and in the case of SJ11*vanA*, BSI_SJ40*vanA* and RC-19_023*vanA*, a cadmium efflux accessory protein gene insertion and additional non-coding DNA sequences, such as repeat regions (Figure 3.9). RC_19_23*vanA* lacked *vanY* but remained phenotypically resistant to vancomycin and teicoplanin.

Interestingly, all seven *vanA* regions contained multiple insertions of IS*1216E* within and around the *vanA* region. When using SJ11*vanA* as a reference, 86.3% (845/979) of VREfm were found to harbour a similar *vanA* region, as demonstrated by >90% sequence identity, indicating enrichment of IS*1216E* in Irish VREfm (Figure 3.9). Six of the *vanA* regions examined harboured deletions in the *tnpA* transposase gene, mainly in the 3′ end, the extent of which varied (Figures 3.9 and 3.10). Terminal 5′ and 3′ 1000 bp sequences from the TN*1546* prototype *tnpA* transposase gene (2,967 bp) were used as references to compare the *tnpA* region across all VREfm (Arthur *et al.*, 1993). The majority (937/979; 95.7%) harboured a *tnpA* region with >99% sequence identity to the 5′ *tnpA* reference. In contrast, 81.2% (795/979) lacked the 3′ *tnpA* region with <40% sequence identity to the 3′ *tnpA* reference. These findings demonstrated the majority of VREfm harboured a *tnpA* gene with large 3′-end deletions.

(a) SJ10*vanA* ST789, CT1601 (11,210bp)

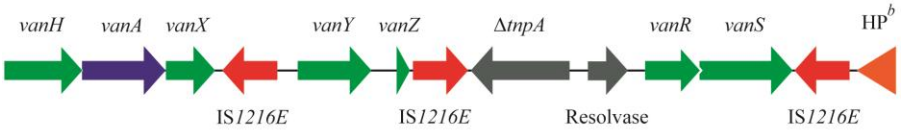

(b) SJ11*vanA* ST1478, CT24 (13,252bp)

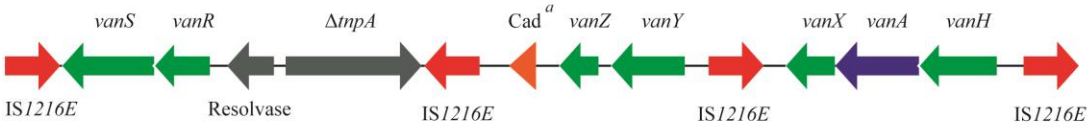

(c) BSI_SJ40*vanA* ST80, CT1598 (13,269bp)

(d) pSJ82*vanA* ST203, CT20 (10,823bp)

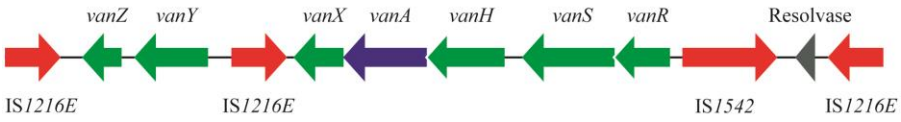

(e) pSJ245*vanA* ST117, CT2929 (14,168bp)

(f) RC-19-039*vanA* ST17, CT2934 (13,601bp)

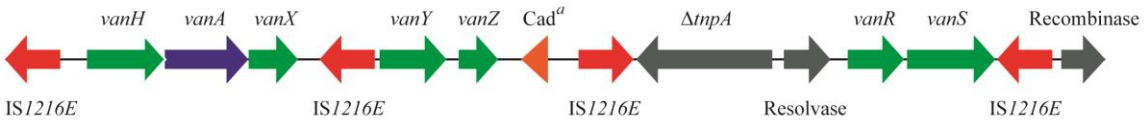

(g) RC-19-023*vanA* ST80, CT1916 (12,883bp)

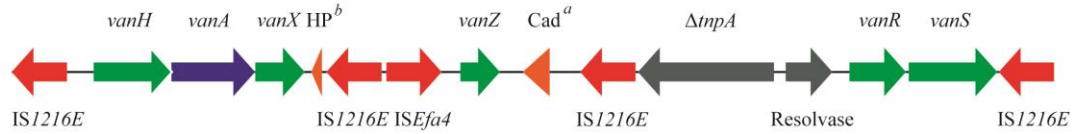

(h) Tn*1546 vanA* prototype (10,851bp)

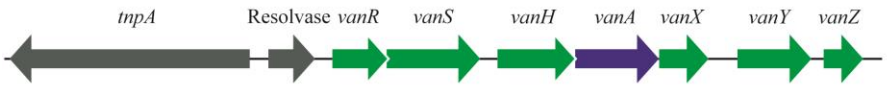

[a] Cadmium efflux system accessory protein
[b] Hypothetical Protein

1 kb

Figure 3.9. Schematic diagram showing the structural organization of *vanA* transposon regions closed by hybrid assembly from VREfm isolates from Irish hospitals. (a) SJ10 (SJ10*vanA*, 11,022 bp); (b) SJ11 (SJ11*vanA*, 13,252 bp); (c) BSI_SJ40 (BSI_SJ40*vanA*, 13269 bp); (d) SJ82 (10,823 bp *vanA* region from plasmid pSJ82*vanA*); (e) SJ245 (14,168 bp *vanA* region from plasmid pSJ245*vanA*); (f) RC_19_039 (13,601 bp *vanA* region from plasmid pRC_19_039); (g) RC_19_023 (RC_19_023*vanA*, 12,883 bp); and (h) the structural organization of the prototype *vanA* transposon Tn*1546* from VREfm BM4147 (GenBank accession number: M97297). VREfm isolates were recovered from H1 (a–e), H3 (f) and H4 (g). Genes and their orientation are denoted by directional arrows and labelled with corresponding gene names. A reference size scale bar is shown at the bottom of the diagram. The extent of the transposase *tnpA* gene sequences deleted (Δ) in the various assemblies is shown in Figure 3.10.

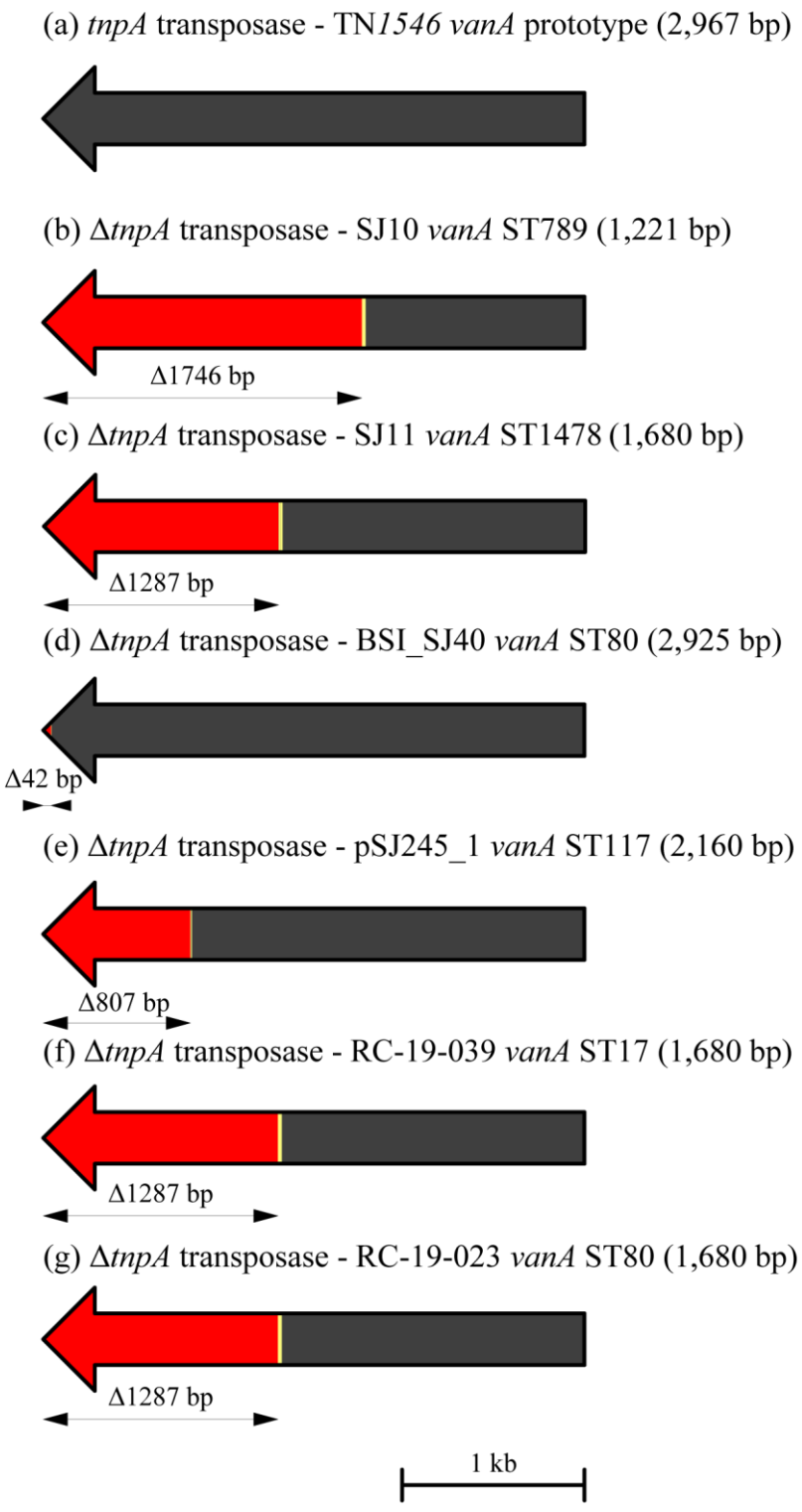

Figure 3.10. Schematic diagram showing the extent of deletions and other mutations in the *tnpA* transposase gene within the *vanA* region closed by hybrid assembly from VREfm isolates from Irish hospitals. The arrows indicate the direction of transcription. Deletions are shown in red, bp substitutions are indicated in yellow and bp insertions are

indicated in green. The extent of sequences deleted (Δ) is shown beneath each *tnpA* gene in bp and indicated by the fine arrows. (a) Wild-type *tnpA* (transposase) gene (2,967 bp) from the prototype *vanA* transposon Tn*1546* (Arthur *et al.*, 1993) (b) Δ*tnpA* gene from isolate SJ10 (SJ10*vanA*, 1,221 bp); (c) Δ*tnpA* gene from isolate SJ11 (SJ11*vanA*, 1,680 bp); (d) Δ*tnpA* gene from isolate BSI_SJ40 (BSI_SJ40*vanA*, 2,925 bp); (e) Δ*tnpA* gene from plasmid pSJ245*vanA* in isolate SJ245 (pSJ245*vanA*, 2,160 bp); (f) Δ*tnpA* gene from isolate RC_19_039 (RC_19_039*vanA*, 1,680 bp); and (g) Δ*tnpA* gene from isolate RC_19_023 (RC_19_023*vanA*, 1,680 bp). VREfm isolates were recovered from H1 (b–e), H3 (f) and H4 (g). A reference size scale bar is shown at the bottom of the diagram.

Whilst the majority of isolates harboured *vanA* exclusively, a small percentage (1.5%, 15/978) of isolates belonging to ST17 (*N*=12), ST80 (*N*=1) and ST789 (*N*=2) harboured both a plasmid-mediated *vanA* and a chromosomally encoded *vanB*. One isolate (JH350) contained *vanB* exclusively and was phenotypically susceptible to teicoplanin (Section 3.5, Table 3.4). Three representative isolates which were identified as comprising a chromosomally *vanB* through ABRicate mapping of the short-read derived FASTA contigs (RC-19-039 [see Figure 3.9 for *vanA* schematic diagram], JH022 and JH350) were chosen for hybrid assembly to provide insight into the structural organisation of the *vanB* resistance operon (Figure 3.11). The *vanB* transposon in isolate JH350 was located in the chromosome and displayed 99.69% average nucleotide identity to the Tn*1549 vanB* operon prototype from vancomycin-resistant *E. faecalis* BM4382 (GenBank accession number: AF192329.1). In VREfm screening isolates RC-19-039 and JH022, however, the chromosomally encoded *vanB* contained the *vanYW* and *vanHBX* genes, but lacked the sensor-regulator genes (*vanR* and *vanS*). Screening of the short-read derived FASTA contigs from the remaining 13 isolates harbouring both *vanA* and *vanB* using ABRicate revealed similar findings, with the absence of the *vanB*-associated regulatory genes. Interestingly, comparison of the nucleotide sequences of the regulatory genes (*vanR* and *vanS*) from the Tn*1549 vanB* operon prototype and the Tn*1546 vanA* operon prototype revealed little overlap, with only 47.65% sequence identity.

(a) Tn*1549 vanB* prototype (33,805 bp)

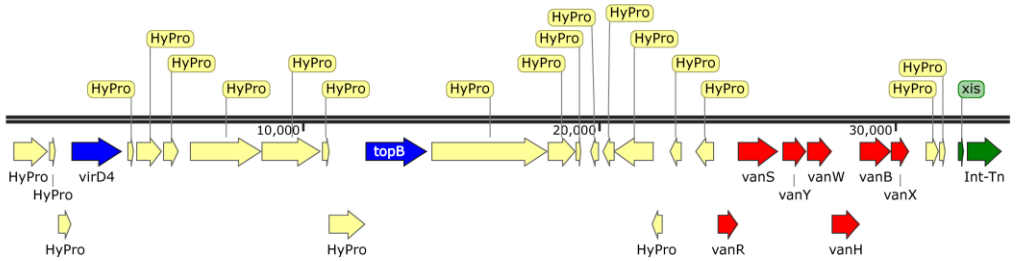

(b) JH350*vanB* (33,387 bp)

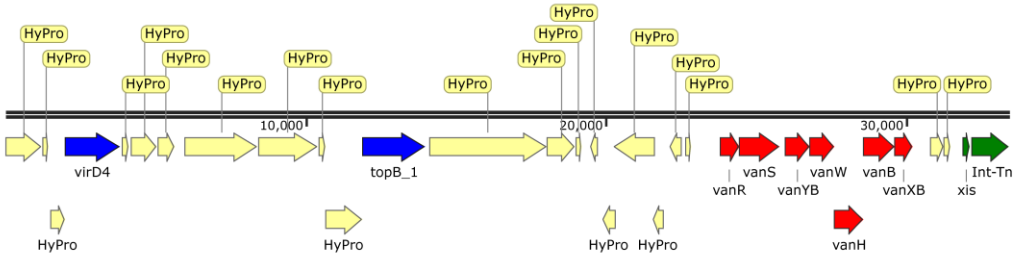

(c) JH022*vanB* (33,607 bp)

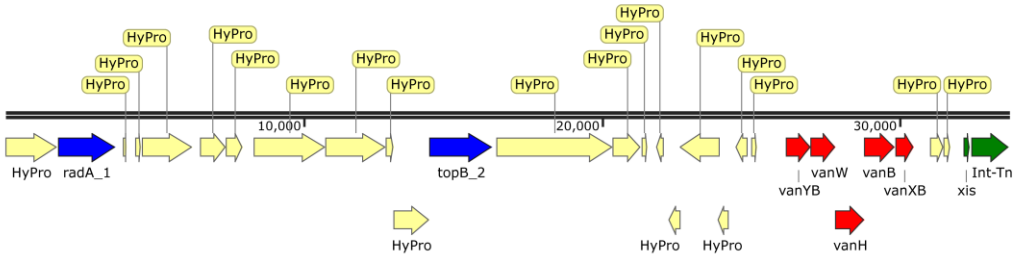

(d) RC-19-039*vanB* (31,268 bp)

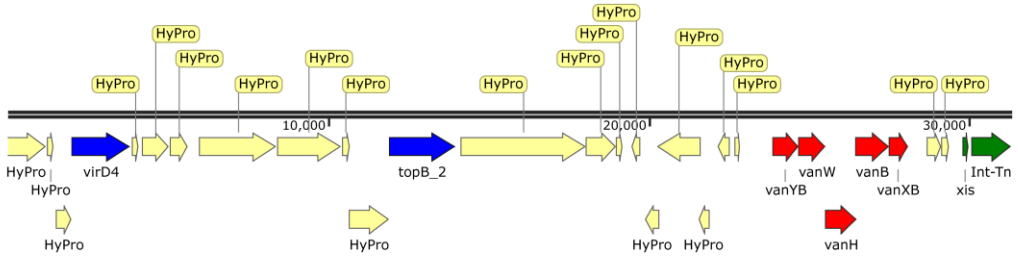

Figure 3.11. Schematic diagram showing the structural organization of *vanB* transposon regions closed by hybrid assembly from VREfm isolates from Irish hospitals. (a) the structural organization of the Tn*1549 vanB* operon prototype from vancomycin-resistant *E. faecalis* BM4382 (GenBank accession number: AF192329.1); (b) JH350 (JH350*vanB*, 33,837 bp); (c) JH022 (JH022*vanB*, 33,607 bp, lacking *vanR* and *vanS* regulatory genes) and (d) RC-19-039 (RC-19-039*vanB*, 31,268 bp, lacking *vanR* and *vanS* regulatory genes). VREfm isolates were recovered from H1 (a-b) and H6 (d). Genes and their orientation are denoted by directional arrows and labelled with corresponding gene names. A reference size scale bar is shown at the bottom of each transposon map. Abbreviations: HyPro, hypothetical protein.

3.3.4 Transmission of *vanA* via IS*1216E*-mediated transposition and circular plasmid conjugation

Four *vanA*-encoding circular plasmids were fully resolved by hybrid assembly from VREfm SJ82 (ST203), SJ245 (ST117, CT2929), JH022 (ST17, CT2934) from H1 and RC_19_039 (ST17, CT294) from H3 (Figures 3.11-3.14). Plasmids were named pSJ82*vanA* (48,934 bp), pSJ245*vanA* (40,559 bp), pJH022*vanA* (48,989 bp) and pRC_19_039*vanA* (66,751 bp), respectively. All plasmids encoded additional resistance genes, conferring resistance to streptomycin (*aadk*), aminoglycosides (*aphA*, *aacA-aphD*), macrolides (*erm*), nucleosides (*satA*) and phenicols (*cat*) (Figures 3.7-3.9). In total, 49% (137/277) of the identified coding sequences (CDS) in all four plasmids were designated as hypothetical proteins during annotation and their function could therefore not be inferred. Circular *vanA*-harbouring plasmids were subsequently characterised on the basis of associated replication genes, which revealed a total of six distinct *rep* types, including *rep1*, *rep2*, *rep7a*, *rep17* and *rep17a*, from four plasmid families (Rep_trans, Inc18, pRum and RepA_n). Interestingly, two of the plasmids exhibited extensive mosaicism and encoded up to three distinct *rep* types (SJ82; *rep7a*, *rep1* and *rep2*, RC-19-039; *rep2* and *rep17*) suggesting potential recombination between both plasmid sequences within the same strain and from diverse genetic backgrounds. Plasmids pSJ245*vanA* and pJH022*vanA* were identified as rep17a and rep17, respectively.

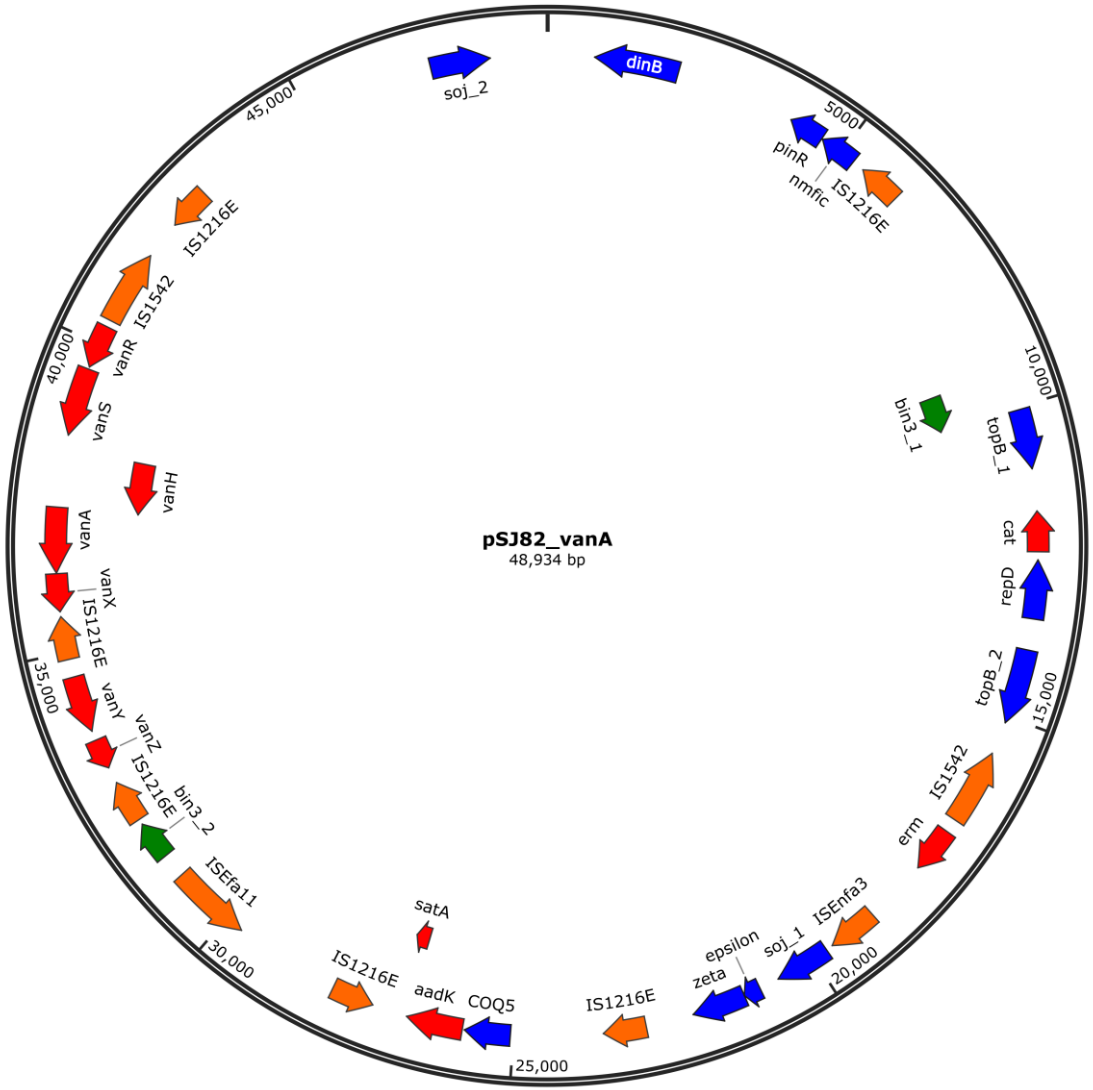
pSJ82_vanA
48,934 bp
soj_2
dinB
pinR
nmfic
IS1216E
IS1216E
IS1542
vanR
vanS
vanH
vanA
vanX
IS1216E
vanY
vanZ
IS1216E
bin3_2
ISEfa11
satA
IS1216E
aadK
COQ5
IS1216E
epsilon
zeta
soj_1
ISEnfa3
erm
IS1542
topB_2
repD
cat
topB_1
bin3_1
5000
10,000
15,000
20,000
25,000
30,000
35,000
40,000
45,000

Figure 3.12. Schematic diagram of the structural organisation of plasmid pSJ82*vanA* from the VREfm screening isolate SJ82 encoding *vanA* resolved by hybrid assembly of paired-end Illumina MiSeq short reads with Oxford Nanopore Technologies long reads. Genes of interest and their orientation are represented by arrows as follows: red indicates antibiotic resistance genes, orange indicates insertion sequences, green indicates transposase and invertase genes, blue indicates genes encoding known proteins. Due to spacing limitations, products annotated by RAST, Prokka and/or EGG-NOG Mapper as 'hypothetical protein', 'mobile element protein', 'phage protein' and 'phage-related protein' are not represented in this diagram.

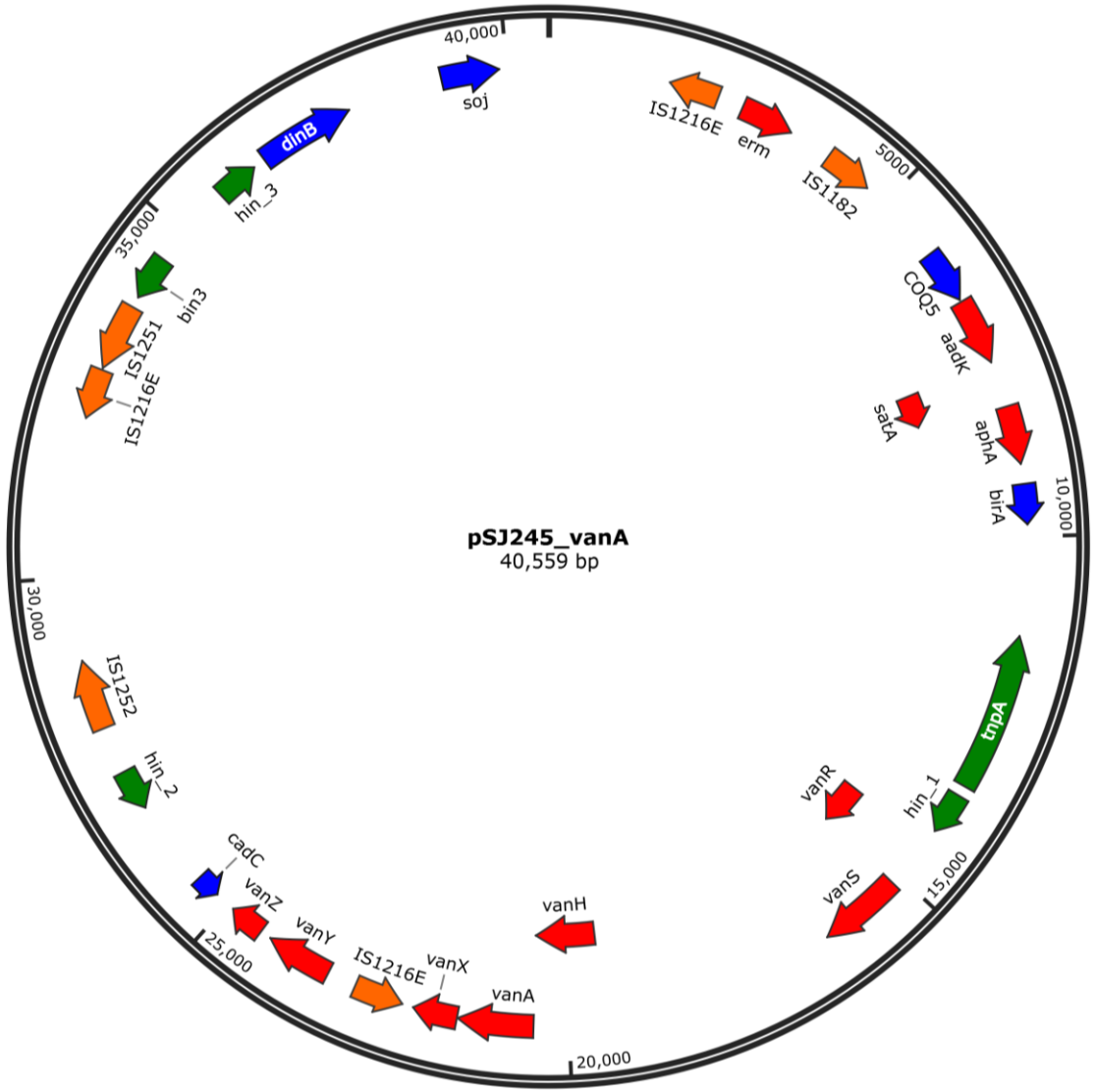
pSJ245_vanA
40,559 bp
40,000
soj
IS1216E
erm
IS1182
5000
COQ5
aadK
satA
aphA
birA
10,000
tnpA
hin_1
vanR
vanS
15,000
vanH
vanA
IS1216E
vanX
vanY
vanZ
cadC
20,000
25,000
hin_2
IS1252
30,000
IS1216E
IS1251
bin3
35,000
hin_3
dinB

Figure 3.13. Schematic diagram of the structural organisation of plasmid pSJ245*vanA* from the VREfm screening isolate SJ245 encoding *vanA* resolved by hybrid assembly of paired-end Illumina MiSeq short reads with Oxford Nanopore Technologies long reads. Genes of interest and their orientation are represented by arrows as follows: red indicates antibiotic resistance genes, orange indicates insertion sequences, green indicates transposase and invertase genes, blue indicates genes encoding known proteins. Due to spacing limitations, products annotated by RAST, Prokka and/or EGG-NOG Mapper as 'hypothetical protein', 'mobile element protein', 'phage protein' and 'phage-related protein' are not represented in this diagram.

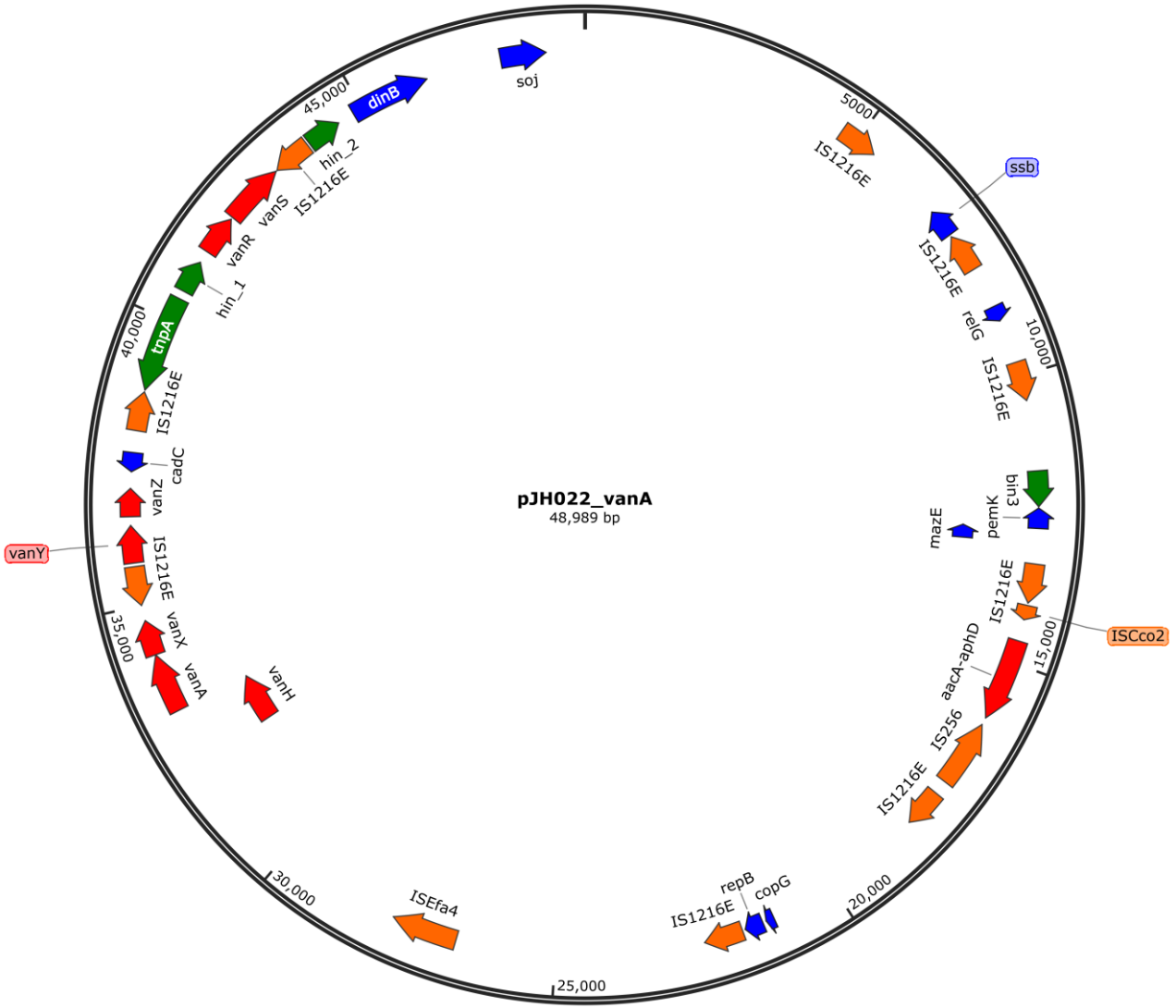
pJH022_vanA
48,989 bp
dinB
soj
IS1216E
ssb
IS1216E
relG
IS1216E
bin3
pemK
mazE
IS1216E
ISCco2
aacA-aphD
IS256
IS1216E
repB
copG
IS1216E
ISEfa4
vanH
vanA
vanX
IS1216E
vanY
vanZ
cadC
IS1216E
tnpA
hin_1
vanR
vanS
IS1216E
hin_2
5000
10,000
15,000
20,000
25,000
30,000
35,000
40,000
45,000

Figure 3.14. Schematic diagram of the structural organisation of plasmid JH022*vanA* from the VREfm screening isolate JH022 encoding *vanA* resolved by hybrid assembly of paired-end Illumina MiSeq short reads with Oxford Nanopore Technologies long reads. Genes of interest and their orientation are represented by arrows as follows: red indicates antibiotic resistance genes, orange indicates insertion sequences, green indicates transposase and invertase genes, blue indicates genes encoding known proteins. Due to spacing limitations, products annotated by RAST, Prokka and/or EGG-NOG Mapper as 'hypothetical protein', 'mobile element protein', 'phage protein' and 'phage-related protein' are not represented in this diagram.

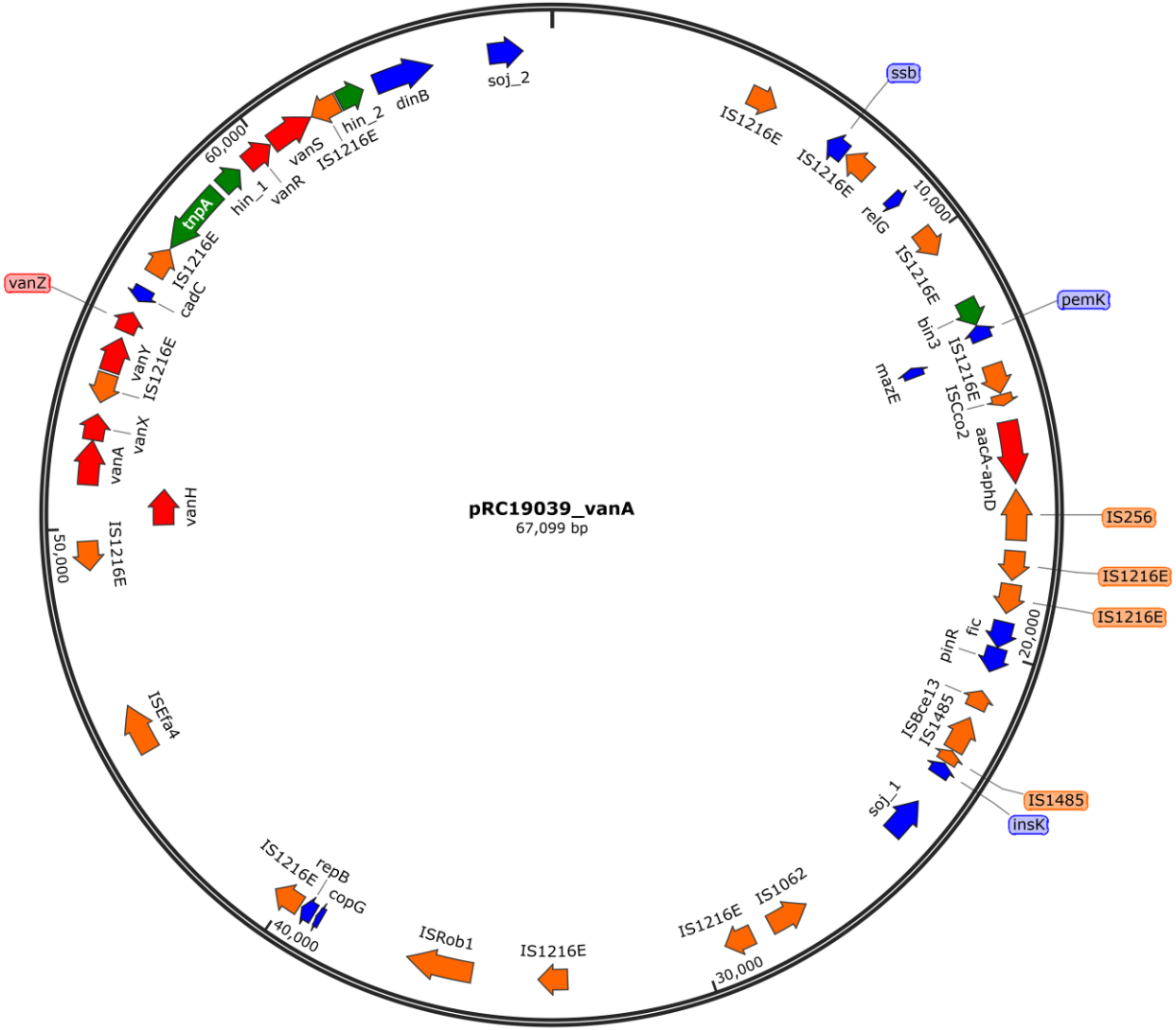
pRC19039_vanA
67,099 bp
soj_2
dinB
hin_2
vanS
IS1216E
vanR
hin_1
tnpA
IS1216E
cadC
vanZ
vanY
IS1216E
vanX
vanA
vanH
IS1216E
ISEfa4
IS1216E
repB
copG
ISRob1
IS1216E
IS1216E
IS1062
soj_1
ISBce13
IS1485
pinR
fic
IS1485
insK
IS256
IS1216E
IS1216E
aacA-aphD
ISCco2
IS1216E
bin3
pemK
mazE
IS1216E
relG
IS1216E
ssb
IS1216E
60,000
50,000
40,000
30,000
20,000
10,000

Figure 3.15. Schematic diagram of the structural organisation of plasmid pRC_19_039*vanA* from the VREfm screening isolate RC_19_039 encoding *vanA* resolved by hybrid assembly of paired-end Illumina MiSeq short reads with Oxford Nanopore Technologies long reads.
Genes of interest and their orientation are represented by arrows as follows: red indicates antibiotic resistance genes, orange indicates insertion sequences, green indicates transposase and invertase genes, blue indicates genes encoding known proteins. Due to spacing limitations, products annotated by RAST, Prokka and/or EGG-NOG Mapper as 'hypothetical protein', 'mobile element protein', 'phage protein' and 'phage-related protein' are not represented in this diagram.

Conjugation of circular plasmids encoding *vanA* from VREfm screening isolates SJ82 (ST203, CT20) and JH022 (ST17, CT293) to the plasmid-free *E. faecium* 64/3 (ST21) recipient was successful. Transconjugants derivatives were phenotypically resistant to vancomycin and teicoplanin and were denoted as SJ82_TC1 and JH022_TC1 respectively. The plasmid pJH022*vanA* (48,989 bp) from VREfm rectal screening isolated JH022 shared 99.98% average nucleotide identity with the plasmid identified in the corresponding *E. faecium* 64/3 transconjugant derivative (Figure 3.16). The *vanA* plasmid in the transconjugant SJ82_TC1, however, was much larger (175,921 bp) than plasmid pSJ82*vanA* (48,934 bp) in donor isolate SJ82 (Figure 3.12). Examination of the hybrid assembly of SJ82 revealed another large plasmid encoding two copies of the aminoglycoside resistance gene *AAC(6')-Ib*, termed pSJ82_B (232,026 bp), in addition to pSJ82*vanA*. Analysis of pSJ82*vanA*_TC1 revealed that it was composed of the *vanA* operon from pSJ82*vanA* flanked on either side by IS*1216E* (9,826 bp) inserted within a section of pSJ82_B (166,095 bp) (Figures 3.17). Mobilisation of the *vanA* region from pSJ82*vanA* into pSJ82_B was evident by the multiple alignment of the two parent plasmids with the mosaic plasmid derivative pSJ82_*vanA*_TC1, showing 99.83% and 94.70% average nucleotide identity respectively (Figure 3.18). The pSJ82*vanA vanA* region likely moved via IS*1216E*-mediated translocation to pSJ82_B and there was loss of 65,931 bp of pSJ82_B, giving rise to the hybrid plasmid pSJ82_TC (Figure 3.17). These results are in line with previous studies, which indicate that insertion sequences, such as IS*1216E*, may form putative translocatable units that can facilitate the dynamic mobilisation of antimicrobial resistance genes via replicative transposition and translocation resulting in instability in regions of enrichment (Shan *et al.*, 2020).

Other examples of IS*1216E*-mediated instability contributing to continued loss and gain of segments of genes were evident within the study population, notably in relation to the isolates displaying phenotypic susceptibly to vancomycin. For instance, VSEfm BSI isolate RC-19-036 (ST17, CT2934) recovered from H6 exhibited a vancomycin MIC of <4 mg/L. Mapping of the short-read derived FASTA contigs from this isolate using ABRicate revealed the presence of the *vanA* transposon, with the absence of the associated sensor-regulatory genes (*vanR* and *vanS*). Interestingly, hybrid-assembly of the isolate revealed the presence of a circular *vanA* encoding plasmid of 48,498 bp. The plasmid was enriched with 11 copies of IS*1216E*, with the *vanA*-remnant separated into distinct segments each flanked on either side by IS*1216E* (e.g., *vanHAX*, *vanYZ* and *tnpA*) (Figure 3.19).

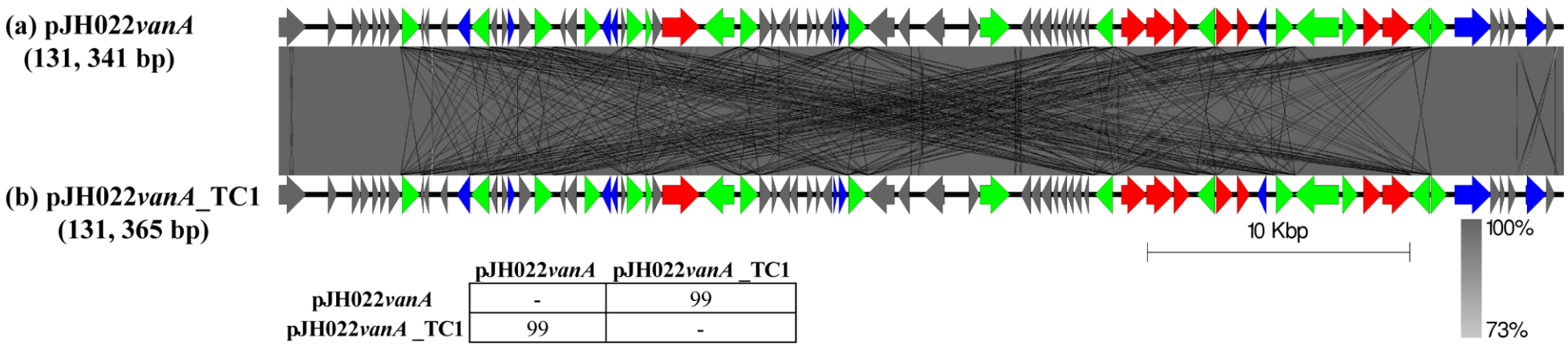

	pJH022*vanA*	pJH022*vanA* _TC1
pJH022*vanA*	-	99
pJH022*vanA* _TC1	99	-

Figure 3.16. Comparative genetic organization of circular plasmids pJH022 and pJH022_TC1. The figure shows a multiple alignment of (a) C circular plasmid from the VREfm screening isolate JH022 (131,341 bp) (b) circular plasmid from the plasmid-free rifampicin- and fusidic acid-resistant recipient strain *E. faecium* 64/3 obtained via conjugative transfer from JH022 during filter-mating experiments (131,365 bp). Coding sequences of interest and their orientation are represented by arrows as follows: red, antimicrobial resistance genes; green, transposases, insertion sequences and resolvases; blue proteins with a known coding function. Regions between alignments with shared homology are represented by grey connecting blocks and/or lines with the colour gradient indicating percentage nucleotide identity (67-100%). A scale bar is included beneath the figure. The matrix shown beneath the figure contains an n × n DNA sequence similarity between the plasmids.

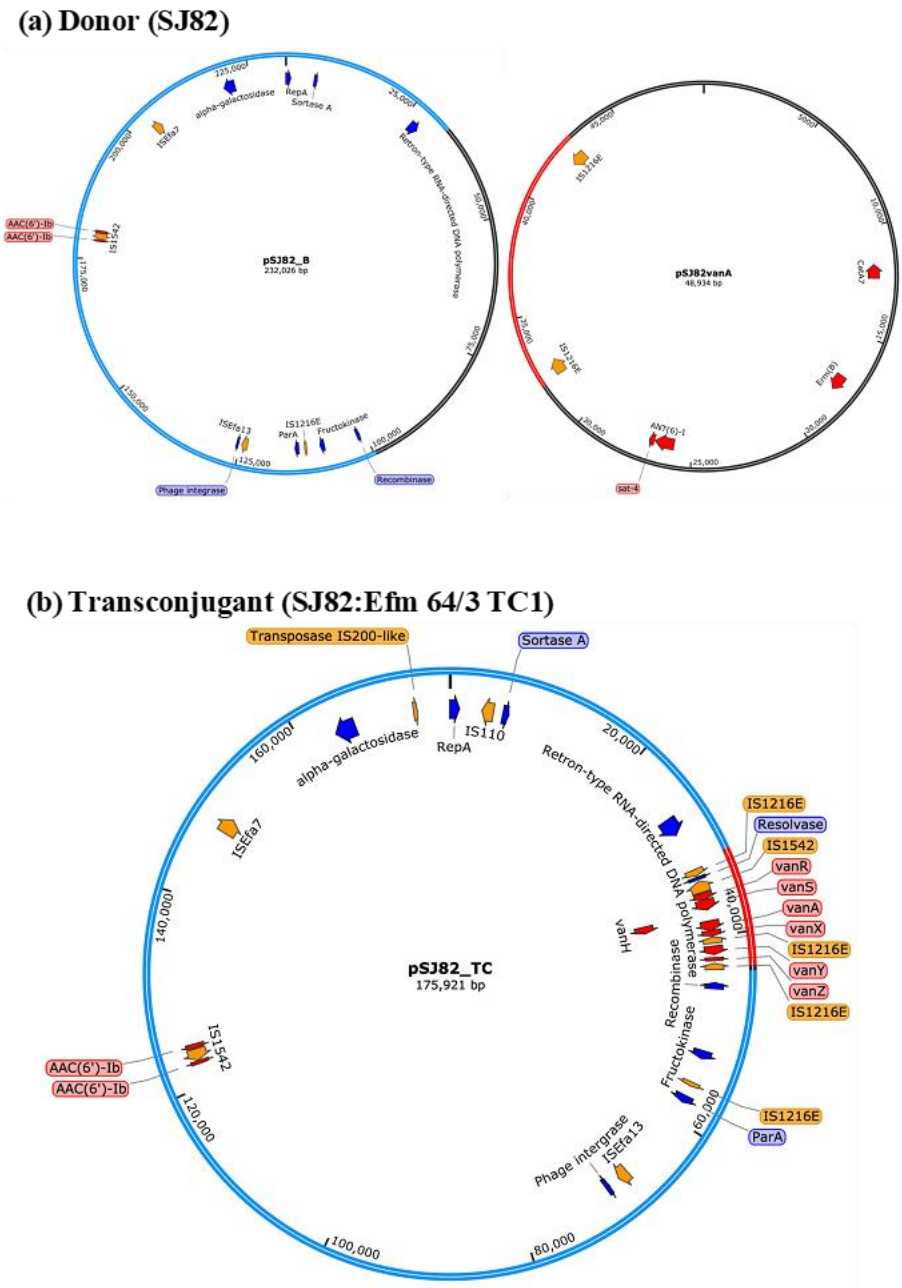

Figure 3.17: Schematic diagrams of the structural organization of (a) plasmids pSJ82_B and pSJ82*vanA* from VREfm donor strain SJ82, and (b) the vancomycin resistance plasmid pSJ82_TC from the transconjugant SJ82_TC1. Diagrams are partially annotated for clarity. Genes of interest and their orientation are represented by arrows: red indicates antibiotic resistance genes, orange indicates ISs/transposases and blue indicates genes encoding known proteins. The regions from plasmids resolved by hybrid assembly of paired-end Illumina MiSeq short reads with Oxford Nanopore Technologies long reads present in the donor isolate SJ82 (i.e., pSJ82_B and pSJ82*vanA*) that are present in the hybrid transconjugant plasmid pSJ82_TC are marked as follows: pSJ82_B region

highlighted in blue and pSJ82*vanA* region highlighted in red. Plasmid regions in pSJ82*vanA* and pSJ82_B shaded in black were not present in pSJ82_TC.

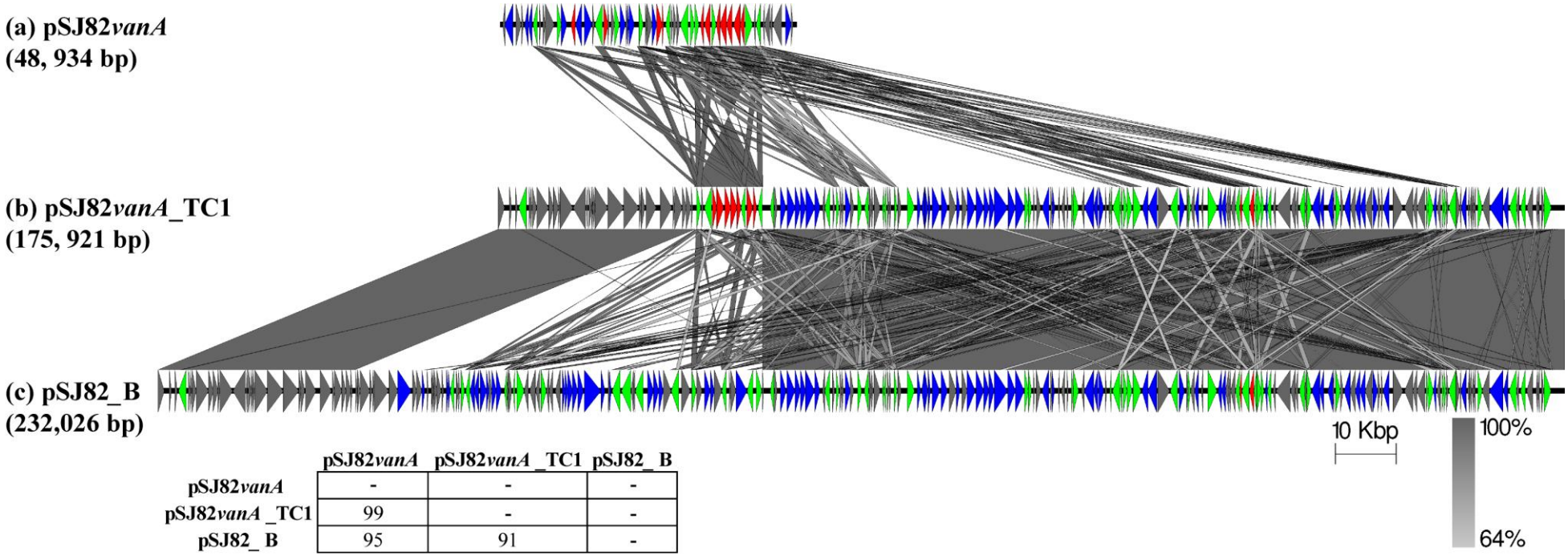

	pSJ82*vanA*	pSJ82*vanA* _TC1	pSJ82_ B
pSJ82*vanA*	-	-	-
pSJ82*vanA* _TC1	99	-	-
pSJ82_ B	95	91	-

Figure 3.18. Comparative genetic organization of circular plasmids pSJ82*vanA*, pSJ82*vanA* _TC1 and pSJ82_B. The figure shows a multiple alignment of (a) circular plasmid from the VREfm screening isolate pSJ82 harbouring *vanA* (48,934 bp) (b) circular plasmid pSJ82vanA_TC1 (175, 921 bp) from a transconjugant derivative of the plasmid-free rifampicin- and fusidic acid-resistant recipient strain *E. faecium* 64/3 obtained via conjugative transfer from SJ82 after filter-mating and (c) additional circular plasmid from the VREfm screening isolate pSJ82 (232,026 bp). Coding sequences of interest and their orientation are represented by arrows as follows: red, antimicrobial resistance genes; green, transposases, insertion sequences and resolvases; blue proteins with a known coding function. Regions between alignments with shared homology are represented by grey connecting blocks and/or lines with the colour gradient indicating percentage nucleotide identity (67-100%). A scale bar is included beneath the figure. The matrix shown beneath the figure contains an n × n DNA sequence similarity between the plasmids.

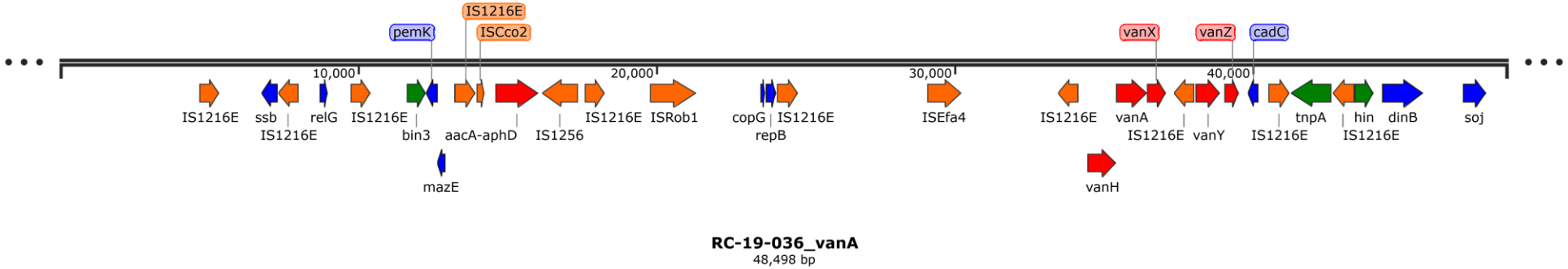

Figure 3.19. Schematic diagram of the structural organisation of plasmid pRC_19_036*vanA* from the VSEfm BSI isolate RC_19_36 encoding *vanA*-remnant resolved by hybrid assembly of paired-end Illumina MiSeq short reads with Oxford Nanopore Technologies long reads. Genes of interest and their orientation are represented by arrows as follows: red indicates antibiotic resistance genes, orange indicates insertion sequences, green indicates transposase and invertase genes, blue indicates genes encoding known proteins. Due to spacing limitations, products annotated by RAST, Prokka and/or EGG-NOG Mapper as 'hypothetical protein', 'mobile element protein', 'phage protein' and 'phage-related protein' are not represented in this diagram.

3.3.5 Identification of novel linear plasmids encoding *vanA*

Attempts to close plasmids harbouring SJ10*vanA*, SJ11*vanA*, BSI_SJ40*vanA* and RC_19_023*vanA* by hybrid assembly were unsuccessful. In each instance a single large contig harbouring *vanA* that failed to circularize was identified [89,310 bp (SJ10), 116,749 bp (SJ11), 131,341 bp (BSI_SJ40) and 109,124 bp (RC_19_023)]. As this finding appears to be a consistent phenomenon observed across a significant proportion of Irish VREfm, it was deduced that these circularised sequences were not the result of assembly errors and instead more likely to be plasmids that exhibit linear topology as reported recently in *E. faecium* isolates from Japan and Switzerland (Hashimoto *et al.*, 2019, 2020; Boumasmoud *et al.*, 2022).

To evaluate if the *vanA*-encoding contigs identified in isolates SJ11 and BSI_SJ40 by hybrid assembly were linear plasmids, the sequences of the contigs were compared with the corresponding sequences of linear plasmids pELF1 (143,316 bp), pELF2 (10,8102 bp) and pELF_USZ (101,837 bp) recently described in VREfm isolates from Japan and Switzerland, respectively (Hashimoto *et al.*, 2019, 2020; Boumasmoud *et al.*, 2022). Comparing the *vanA* contigs from SJ11 (116,749 bp) and BSI_SJ40 (131,341 bp) revealed a clear homology (Figure 3.20). Each plasmid and contig harboured genes encoding putative replication initiation proteins and proteins with a putative role in DNA partitioning and transfer. These findings strongly indicated that the *vanA*-encoding contigs identified in isolates SJ11 and BSI_SJ40 were linear plasmids, which were named pELF_SJ11 and pELF_BSI_SJ40, respectively (Figure 3.20). Details of pELF_SJ11 and pELF_BSI_JS40 genes and putative proteins encoded are provided in Tables 3.2 and 3.3. An alignment of pELF_SJ11 and pELF_BSI_SJ40 with the *vanA*-encoding contig from SJ10 is shown in Figure 3.21.

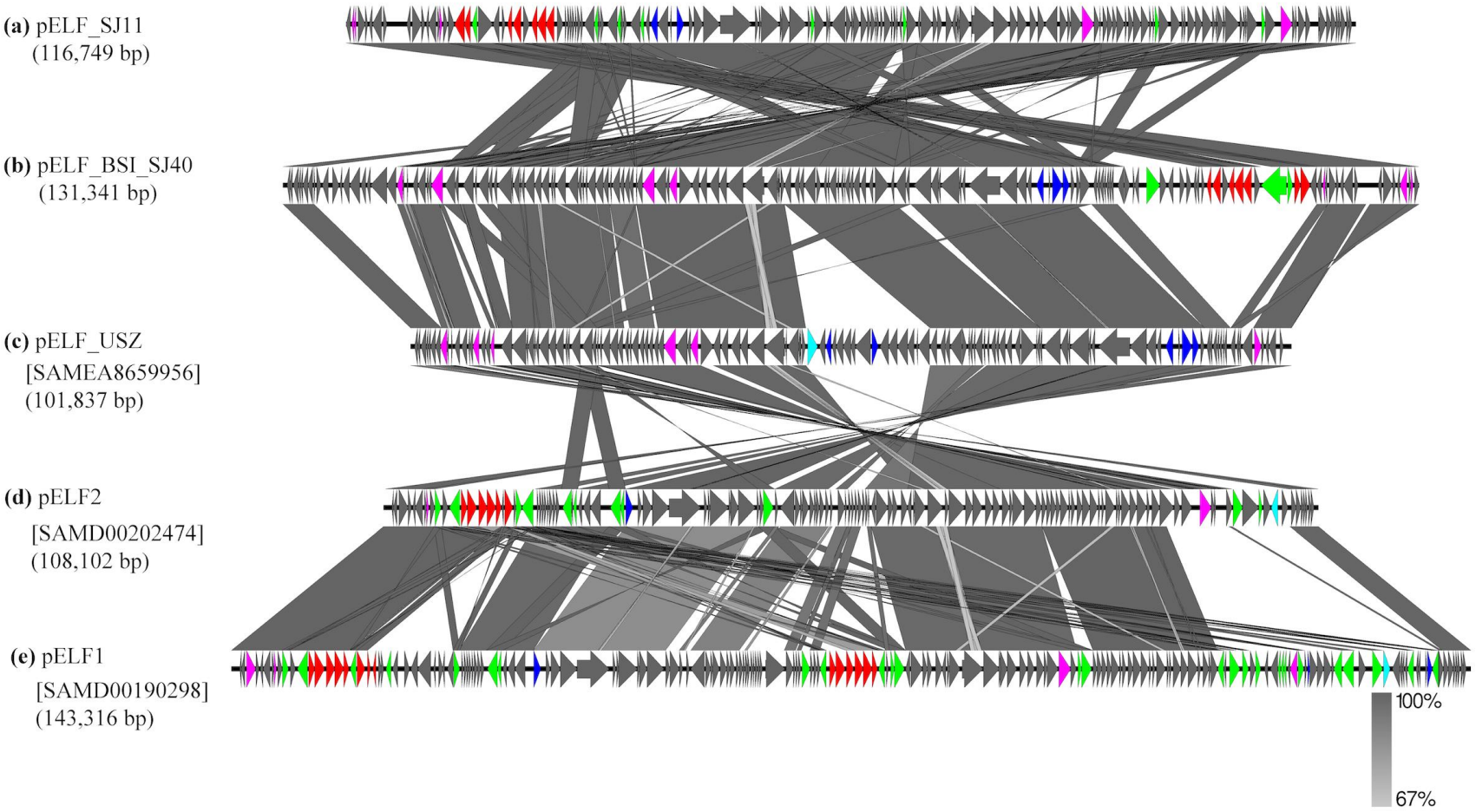

	pELF1	pELF2	pELF_BSI_SJ40	pELF_SJ11	pELF_USZ
pELF1	-	66	56	72	39
pELF2	66	-	82	82	52
pELF_BSI_SJ40	56	82	-	71	64
pELF_SJ11	72	82	71	-	60
pELF_USZ	39	52	64	60	-

Figure 3.20. Comparative genetic organization of linear plasmids pELF_SJ11 and pELF_BSI_SJ40 from Irish VREfm previously described linear plasmids from Japanese (pELF1 and pELF2) and Swiss (pELF_USZ) VREfm. The figure shows a multiple alignment of (a) pELF_SJ11, (b) pELF_BSI_SJ40, (c) pELF_USZ (Boumasmoud *et al.,* 2022) and (d) pELF2 and pELF1 (Hashimoto *et al.,* 2019, 2020) generated using EasyFig (Sullivan *et al.,* 2011). Biosample accession numbers are shown for linear plasmid sequences downloaded from the NCBI database. Coding sequences of interest and their orientation are represented by arrows as follows: red, vancomycin resistance genes; green, transposases, insertion sequences and resolvases; blue proteins with a putative role in DNA replication; cyan, additional antimicrobial resistance genes; magenta genes role in DNA partition, segregation and stabilisation. Full details of pELF_SJ11 and pELF_BSI_JS40 genes and putative proteins encoded are provided in Tables 3.2 and 3.3. Regions between alignments with shared homology are represented by grey connecting blocks and/or lines with the colour gradient indicating percentage nucleotide identity (67-100%). A scale bar is included beneath the figure. The matrix shown beneath the figure contains an n × n DNA sequence similarity between all plasmids.

Table 3.2: Coding sequences of linear plasmid pELF_BSI_SJ40 (131,341 bp) from *E. faecium* isolate BSI_SJ40 (ST80, CT1598) with putative protein products annotated with RAST, Prokka and EGGNOG mapper pipelines.

Gene	Gene location	Product description (RAST)[1]	Product description (EGGNOG-mapper)[2]	COG ID[3]	Blast - NCBI sequence comparison[4]	Max Score[4]	Percentage identity[4]	WP accession[4]
relB	798-1079	DNA-damage inducible protein	RelB antitoxin	COG3077	type II toxin-antitoxin system RelB/DinJ family antitoxin [*Enterococcus faecium*]	185	100%	WP_085802722.1
smtA	5730-6461	rRNA adenine N-6-methyltransferase	Thiopurine S-methyltransferase (TPMT)	COG0500	rRNA adenine N-6-methyltransferase [*Staphylococcus aureus*]	465	100%	ALY18984.1
-	6587-6799	Spectinomycin 9-O-adenylyltransferase	Domain of unknown function (DUF4111)	COG1708	DUF4111 domain-containing protein [*Staphylococcus aureus*]	148	100%	WP_001018931.1
radC	13,191-13,832	DNA repair protein RadC	RadC-like JAB domain	COG2003	Multispecies: DNA repair protein RadC [*Enterococcus*]	432	100%	WP_016922209.1
polYB	17,121-18,446	ImpB/MucB/SamB family protein	impB/mucB/samB family	COG0389	Y-family DNA polymerase [*Enterococcus faecium*]	859	100%	WP_002347529.1
YvpB	31,629-32,672	Sortase - Cell wall surface anchor family protein	Peptidase_C39 like family	COG4990	Multispecies: C39 family peptidase [*Enterococcus*]	711	100%	WP_002347500.1
ftsK	41,559-42,935	Cell division protein FtsK	FtsK SpoIIIE family protein	COG1674	Multispecies: cell division protein FtsK [*Enterococcus*]	874	100%	WP_002353144.1
AdaA	44,657-45,526	Streptodornase B; mitogenic factor 1	DNA/RNA non-specific endonuclease	COG2169	Multispecies: DNA/RNA non-specific endonuclease [*Enterococcus*]	557	100%	WP_002350580.1
SrtA	49,329-50,438	Sortase A, LPXTG specific	Sortase family	COG3764	Multispecies: class C sortase [*Enterococcus*]	726	100%	WP_049055866.1
SrtA	50,428-51,285	Sortase A, LPXTG specific	Sortase family	COG3764	Multispecies: class C sortase [*Enterococcus*]	424	100%	WP_002350583.1
repB	90,154-90,921	RepB	Initiator replication protein	COG5527	Multispecies: replication initiation protein [*Enterococcus*]	476	99.61%	WP_010729833.1

Table 3.2 continued overleaf

Gene	Gene location	Product description (RAST)[1]	Product description (EGGNOG-mapper)[2]	COG ID[3]	Blast - NCBI sequence comparison[4]	Max Score[4]	Percentage identity[4]	WP accession[4]
brpA	97,357-97,908	Cell envelope-associated transcriptional attenuator LytR-CpsA-Psr, subfamily F2	Cell envelope-related transcriptional attenuator domain	COG1316	Multispecies: LCP family protein [*Enterococcus*]	370	100%	WP_010730987.1
arsR	106,214-106,543	Cadmium efflux system accessory protein	Arsenical resistance operon repressor	COG0640	Multispecies: metalloregulator ArsR/SmtB family transcription factor [bacteria]	223	100%	WP_000754864.1
vanZ	106,830-107,315	Protein VanZ	PFAM VanZ like family	COG4767	Multispecies: glycopeptide resistance protein VanZ-A [Bacteria]	281	99.38%	WP_000516404.1
vanY	107,468-108,379	D-alanyl-D-alanine carboxypeptidase	D-alanyl-D-alanine carboxypeptidase	COG1876	VanY protein [*Enterococcus faecium*]	597	100%	ADO66792.1
vanX	109,375-109,983	Vancomycin B-type resistance protein VanX / D-alanyl-D-alanine dipeptidase	Catalyses hydrolysis of the D-alanyl-D-alanine dipeptide	COG2173	Multispecies: D-Ala-D-Ala dipeptidase VanX-A [Bacteria]	396	100%	WP_000402347.1
vanA	109,989-11,1020	D-alanine--D-lactate ligase vancomycin teicoplanin A-type resistance protein vanA	Belongs to the D-alanine-- ligase family	COG1181	Multispecies: D-alanine--(R)-lactate ligase VanA [bacteria]	706	100%	WP_001079845.1
vanH	111,013-111,981	Vancomycin resistance protein VanH / D-lactate dehydrogenase	D-isomer specific 2-hydroxyacid dehydrogenase- NAD binding domain	COG1052	Multispecies: D-lactate dehydrogenase VanH-A [bacteria]	670	100%	WP_001059542.1
PinE	116,165-116,740	Resolvase	Resolvase	COG1961	Resolvase [*Enterococcus faecium*]	362	100%	AKE81059.1
vanR	116,954-117,649	Vancomycin response regulator VanR	Transcriptional regulator	COG0745	Multispecies: *VanA*-type vancomycin resistance DNA-binding response regulator VanR [bacteria]	473	100%	WP_001280781.1

Table 3.2 continued overleaf

Gene	Gene location	Product description (RAST)[1]	Product description (EGGNOG-mapper)[2]	COG ID[3]	Blast - NCBI sequence comparison[4]	Max Score[4]	Percentage identity[4]	WP accession[4]
vanS	117,687-118,778	Sensor histidine kinase *VanS*	His Kinase A (phosphoacceptor) domain	COG5002	Sensor histidine kinase [*Enterococcus faecium*]	717	100%	WP_025478673.1
relE	120,230-120,496	RelE/StbE replicon stabilization toxin	ParE toxin of type II toxin-antitoxin system, parDE	COG2026	Multispecies: type II toxin-antitoxin system RelE/ParE family toxin [*Enterococcus*]	182	100%	WP_010729835.1
parA	129,136-129,954	ParA	-	-	ParA family protein [*Enterococcus faecium*]		99.63%	HAQ7433555.1
relE	130,669-130,403	RelE/StbE replicon stabilization toxin	ParE toxin of type II toxin-antitoxin system, parDE	COG2026	Multispecies : type II toxin-antitoxin system RelE/ParE family toxin [*Enterococcus*]	182	100%	WP_010729835.1

Products annotated by RAST and/or EGG-NOG Mapper as 'hypothetical protein', 'mobile element protein', 'phage protein', 'phage-related protein' and 'transposase' are not represented in this table.

[1] Putative protein product description as annotated by RAST v2.0 pipeline (http://rast.nmpdr.org/).

[2] Putative protein product description as annotated by egg-NOG mapper v2.0 pipeline (http://eggnog-mapper.embl.de/).

[3] Conserved Domain Database (CDD) Identification number.

[4] All putative protein product sequences were queried against the non-redundant protein sequence (NR) database using BLAST. The max score, percentage identity and accession. number of the best match hits are included for completeness.

Table 3.3: Coding sequences of linear plasmid pELF_SJ11 (116,749 bp) from *E. faecium* isolate SJ11 (non-typeable by conventional MLST, CT24) with putative protein products annotated with RAST, Prokka and EGGNOG mapper pipelines.

Gene	Gene location	Product description (RAST)[1]	Product description (EGGNOG-mapper)[2]	COG ID[3]	Blast - NCBI sequence comparison[4]	Max Score[4]	Percentage identity[4]	WP accession[4]
relE	666-932	RelE/StbE replicon stabilization toxin	ParE toxin of type II toxin-antitoxin system, parDE	COG2026	Multispecies: type II toxin-antitoxin system RelE/ParE family toxin [*Enterococcus*]	182	100%	WP_010729835.1
parA	9548-10,366	ParA	-	-	ParA family protein [*Enterococcus faecium*]	513	99.63%	HAQ7433555.1
relE	10,815-11,081	RelE/StbE replicon stabilization toxin	ParE toxin of type II toxin-antitoxin system, parDE	COG2026	Multispecies : type II toxin-antitoxin system RelE/ParE family toxin [*Enterococcus*]	182	100%	WP_010729835.1
vanS	12,524-13,615	Sensor histidine kinase VanS	His Kinase A (phosphoacceptor) domain	COG5002	Sensor histidine kinase [*Enterococcus faecium*]	717	100%	WP_025478673.1
vanR	13,653-14,348	Vancomycin response regulator VanR	Transcriptional regulator	COG0745	Multispecies : *VanA*-type vancomycin resistance DNA-binding response regulator VanR [bacteria]	473	100%	WP_001280781.1
PinE	14,562-15,137	Resolvase	Resolvase	COG1961	Resolvase [*Enterococcus faecium*]	362	100%	AKE81059.1
arsR	18,042-18,371	Cadmium efflux system accessory protein	Arsenical resistance operon repressor	COG0640	Multispecies : metalloregulator ArsR/SmtB family transcription factor [bacteria]	223	100%	WP_000754864.1
vanZ	18,658-19,020	Protein VanZ	PFAM VanZ like family	COG4767	Multispecies : glycopeptide resistance protein VanZ-A [bacteria]	204	100%	WP_000516404.1
vanY	19,296-20,207	D-alanyl-D-alanine carboxypeptidase	D-alanyl-D-alanine carboxypeptidase	COG1876	VanY protein [*Enterococcus faecium*]	597	100%	ADO66792.1
vanX	21,452-22,060	Vancomycin B-type resistance protein VanX / D-alanyl-D-alanine dipeptidase	Catalyses hydrolysis of the D-alanyl-D-alanine dipeptide	COG2173	Multispecies : D-Ala-D-Ala dipeptidase VanX-A [bacteria]	396	100%	WP_000402347.1

Table 3.3 continued overleaf

Gene	Gene location	Product description (RAST)[1]	Product description (EGGNOG-mapper)[2]	COG ID[3]	Blast - NCBI sequence comparison[4]	Max Score[4]	Percentage identity[4]	WP accession[4]
vanA	22,066-23,097	D-alanine--D-lactate ligase vancomycin teicoplanin A-type resistance protein *VanA*	Belongs to the D-alanine--D-alanine ligase family	COG1181	Multispecies : D-alanine--(R)-lactate ligase *VanA* [bacteria]	706	100%	WP_001079845.1
vanH	23,090-24,058	Vancomycin resistance protein VanH / D-lactate dehydrogenase	D-isomer specific 2-hydroxyacid dehydrogenase-NAD binding domain	COG1052	Multispecies : D-lactate dehydrogenase VanH-A [bacteria]	670	100%	WP_001059542.1
repB	35,237-36,004	RepB	Initiator replication protein	COG5527	Multispecies: replication initiation protein [*Enterococcus*]	476	99.61%	WP_010729833.1
YvpB	70,906-72,147	Sortase - cell wall surface anchor family protein	Peptidase_C39 like family	COG4990	Multispecies : C39 family peptidase [*Enterococcus*]	641	100%	WP_025478707.1
SrtA	76,764-77,621	Sortase A, LPXTG specific	Sortase family	COG3764	Multispecies: class C sortase [*Enterococcus*]	726	100%	WP_049055866.1
SrtA	77,611-78,720	Sortase A, LPXTG specific	Sortase family	COG3764	Multispecies : class C sortase [*Enterococcus*]	424	100%	WP_002350583.1
AdaA	82,523-83,392	Streptodornase B; mitogenic factor 1	DNA/RNA non-specific endonuclease	COG2169	Multispecies DNA/RNA non-specific endonuclease [*Enterococcus*]	557	100%	WP_002350580.1
ftsK	85,114-86,490	Cell division protein FtsK	FtsK SpoIIIE family protein	COG1674	Multispecies : cell division protein FtsK [*Enterococcus*]	874	100%	WP_002353144.1
YvpB	95,377-96,420	Sortase - Cell wall surface anchor family protein	Peptidase_C39 like family	COG3757	Multispecies : C39 family peptidase [*Enterococcus*]	711	100%	WP_002347500.1
polyYB	108,077-109,402	ImpB/MucB/SamB family protein	impB/mucB/samB family	COG0389	Y-family DNA polymerase [*Enterococcus faecium*]	859	100%	WP_002347529.1
radC	113,304-112,537	DNA repair protein RadC	RadC-like JAB domain	COG2003	Multispecies : JAB domain-containing protein [*Enterococcus*]	517	100%	WP_002320754.1

Table 3.3 continued overleaf

Gene	Gene location	Product description (RAST)[1]	Product description (EGGNOG-mapper)[2]	COG ID[3]	Blast - NCBI sequence comparison[4]	Max Score[4]	Percentage identity[4]	WP accession[4]
relB	115,671-115,952	DNA-damage inducible protein	RelB antitoxin	COG3077	Multispecies : type II toxin-antitoxin system RelB/DinJ family antitoxin [*Enterococcus*]	186	100%	WP_010733706.1

Products annotated by RAST and/or EGG-NOG Mapper as 'hypothetical protein', 'mobile element protein', 'phage protein', 'phage-related protein' and 'transposase' are not represented in this table.

[1] Putative protein product description as annotated by RAST v2.0 pipeline (http://rast.nmpdr.org/).

[2] Putative protein product description as annotated by egg-NOG mapper v2.0 pipeline (http://eggnog-mapper.embl.de/).

[3] Conserved Domain Database (CDD) Identification number.

[4] All putative protein product sequences were queried against the non-redundant protein sequence (NR) database using BLAST. The max score, percentage identity and accession number of the best match hits are included for completeness.

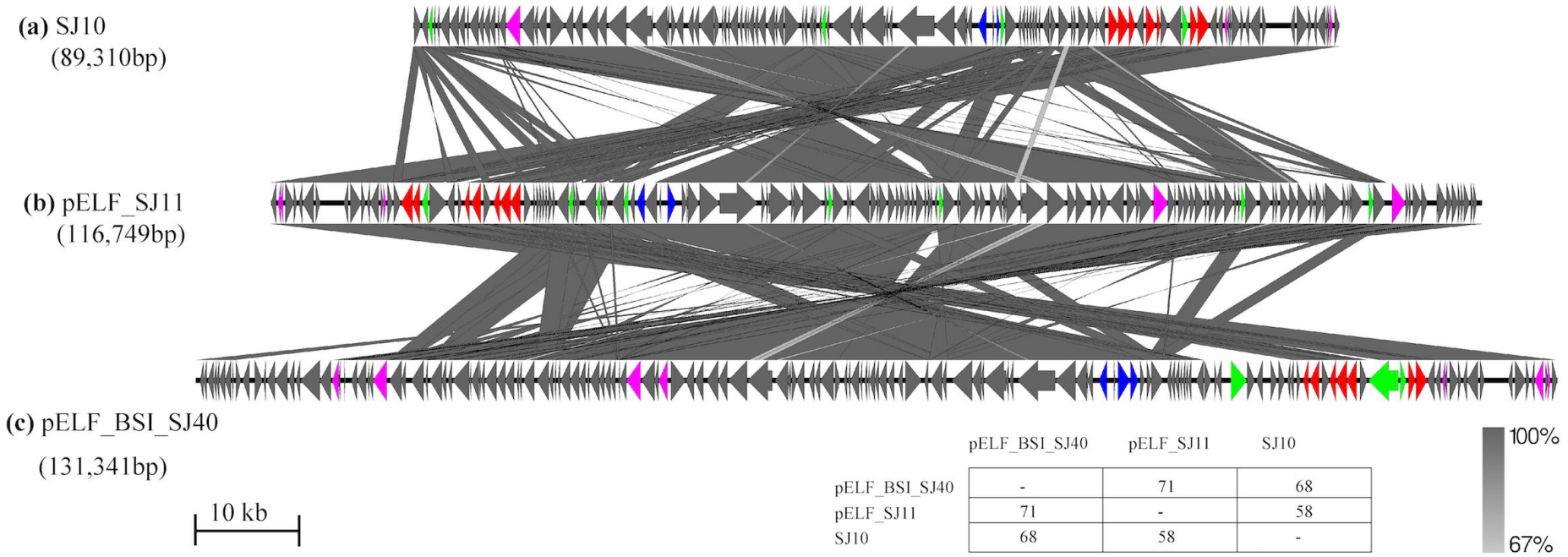

	pELF_BSI_SJ40	pELF_SJ11	SJ10
pELF_BSI_SJ40	-	71	68
pELF_SJ11	71	-	58
SJ10	68	58	-

Figure 3.21. Comparative genetic organization of linear plasmids pELF_SJ11 and pELF_BSI_SJ40 from Irish VREfm and the *vanA*-encoding contig from Irish VREfm isolate SJ10. The figure shows a multiple alignment of (a) the SJ10 *vanA*-contig, (b) pELF_SJ11 and (c) pELF_BSI_SJ40. Coding sequences of interest and their orientation are represented by arrows as follows: red, vancomycin resistance genes; green, transposases, insertion sequences and resolvases; blue proteins with a putative role in DNA replication; cyan, additional antimicrobial resistance genes; magenta genes role in DNA partition, segregation, and stabilisation. Regions between alignments with shared homology are represented by grey connecting blocks and/or lines with the colour gradient indicating percentage nucleotide identity (67-100%). A scale bar is included beneath the figure. The matrix shown beneath the figure contains an n × n DNA sequence similarity between the plasmids and SJ10 contig.

3.3.6 Conjugative ability of linear plasmids encoding *vanA*

To investigate the ability of the putative *vanA*-encoding linear plasmids to transfer into a plasmid-free and vancomycin-susceptible *E. faecium* host by conjugation, filter-mating experiments were performed under vancomycin selective pressure. The contigs encoding *vanA* were successfully transferred from SJ11 (ST1478 CT24, 116,749 bp contig) and BSI_SJ40 (ST80 CT1598, 131,341 bp contig) to recipient strain *E. faecium* 63/4 (ST 21) by conjugation, but not from SJ10 or RC_19_023*vanA*. This was demonstrated by the recovery of putative transconjugant derivatives on selective media which were phenotypically resistant to vancomycin (MIC >4 mg/L) and teicoplanin (MIC >2 mg/L). Hybrid assembly of the *E. faecium* 64/3 transconjugants derived from SJ11 (termed SJ11_TC1), BSI_SJ40 (termed BSI_SJ40_TC1) revealed the presence of two linear plasmid contigs (114,352 and 131,365 respectively) encoding *vanA* with a structural organisation similar to the donor in a genetic background matching the recipient strain (ST21) (Figure 3.22 and 3.23)

Comparative genetic analysis of the transconjugants with their respective parents revealed clear homology (Figures 3.24 and 3.25). The linear plasmid pELF_SJ11 from VREfm rectal screening isolate SJ11 shared 97.66% average nucleotide identity with the linear plasmid pELF_SJ11_TC1 found in the resulting transconjugant. Notably, there was a difference in length of 2,396 bp between the parental plasmid and the transconjugant plasmid. The diversity in the transconjugant was due to both the duplication of a 2,696 bp region encoding three hypothetical proteins and one insertion sequence (IS*Efa4*) and a loss of 5,064 bp non-coding segment at the terminal end of the *vanA*-encoding linear contig (Figure 3.22). The linear plasmid pELF_BSI_SJ40 from VREfm BSI isolate BSI_SJ40 shared 98.95% average nucleotide identity with the linear plasmid pELF_BSI_SJ40_TC1 found in the corresponding *E. faecium* 64/3 transconjugant derivative (Figure 3.26)

As the linear contigs in two of the isolates failed to transfer, an additional five VREfm isolates found to harbour *vanA* on an un-circularised contig recovered from different hospitals (JH127 [129,147 bp plasmid, H1], BS256 [111,849 bp plasmid, H4], RC-19-47 [119,364 bp, H7], RC-19-034 [114,812 bp, H6], RC-19-10 [114,103 bp, H5]) were investigated for their conjugative transferability. In all five isolates, the *vanA*-encoding linear contig was successfully transferred from the parental isolate to the recipient strain again demonstrated by the presence of transconjugants which were phenotypically resistant to vancomycin and teicoplanin. Hybrid assembly of the *E. faecium* 64/3 transconjugants derived from JH127 (termed JH127_TC1), BS256 (termed BS256_TC1), RC-19-47 (termed RC-19-47_TC1), RC-19-034 (RC-19-034_TC1) and RC-19-010 (RC-19-010_TC1)

revealed the presence of five linear plasmid contigs encoding *vanA* with comparable structural similarity of 129,158, 112,037, 119,539, 114,831 and 115,199 bp respectively (Data not shown, see Figure 3.27 for example isolate JH127_TC1).

Comparative genetic analysis of the resulting transconjugants with their respective parents revealed clear homology (Data not shown, see Figure 3.28 for example isolate JH127_TC1). Notably, the linear plasmid pELF_JH127 from VREfm screening isolate JH127 encoded both vancomycin and linezolid resistance (*poxtA*) and shared 99.98% average nucleotide identity with the linear plasmid pELF_JH127_TC1 found in the corresponding *E. faecium* 64/3 transconjugant derivative (Figure 3.28). These findings highlight the worrying phenomenon of co-selection, in which extensive antimicrobial resistance genes may be indirectly selected for under single antibiotic treatment regimens due to co-location on the same plasmid.

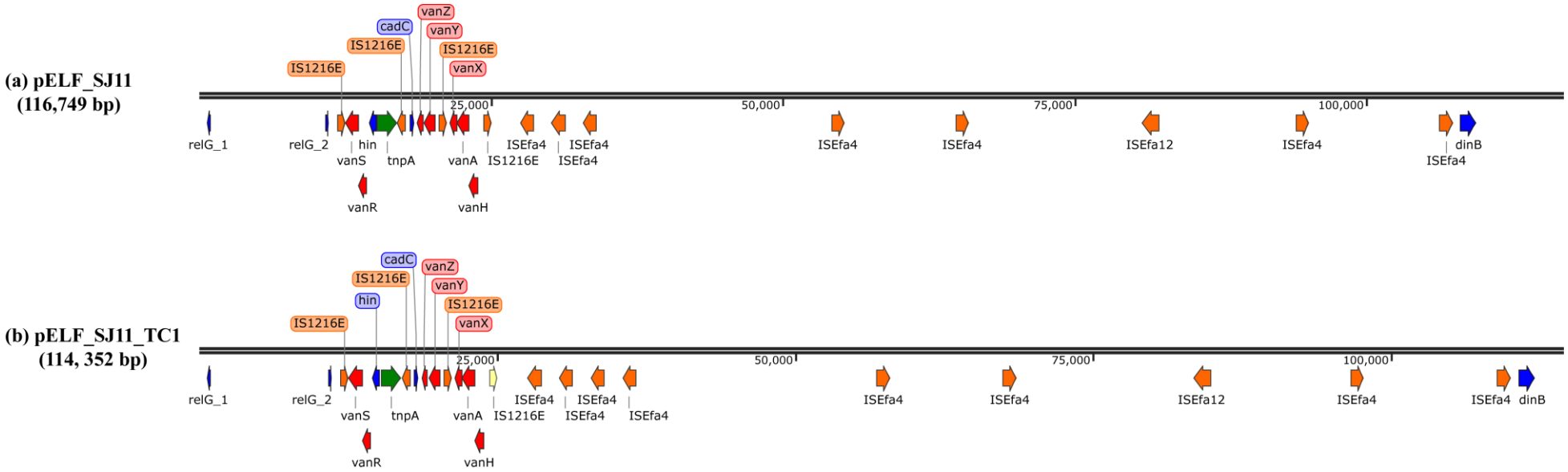

Figure 3.22. Schematic diagram showing the structural organisation of linear plasmids pELF_SJ11 and pELF_SJ11_TC1 resolved by hybrid assembly of paired-end Illumina MiSeq short reads with Oxford Nanopore Technologies long reads. (a) linear plasmid from the VREfm screening isolate SJ11 (116,749 bp) (b) linear plasmid from the corresponding *E. faecium* 64/3 transconjugant derivative obtained via conjugative transfer from SJ11 during filter-mating experiments (114,352 bp). Genes of interest and their orientation are represented by arrows as follows: red indicates antibiotic resistance genes, orange indicates insertion sequences, green indicates transposases, resolvases and invertases, blue indicates genes encoding known proteins. Due to spacing limitations, products annotated by RAST, Prokka and/or EGG-NOG Mapper as 'hypothetical protein', 'mobile element protein', 'phage protein' and 'phage-related protein' are not represented in this diagram.

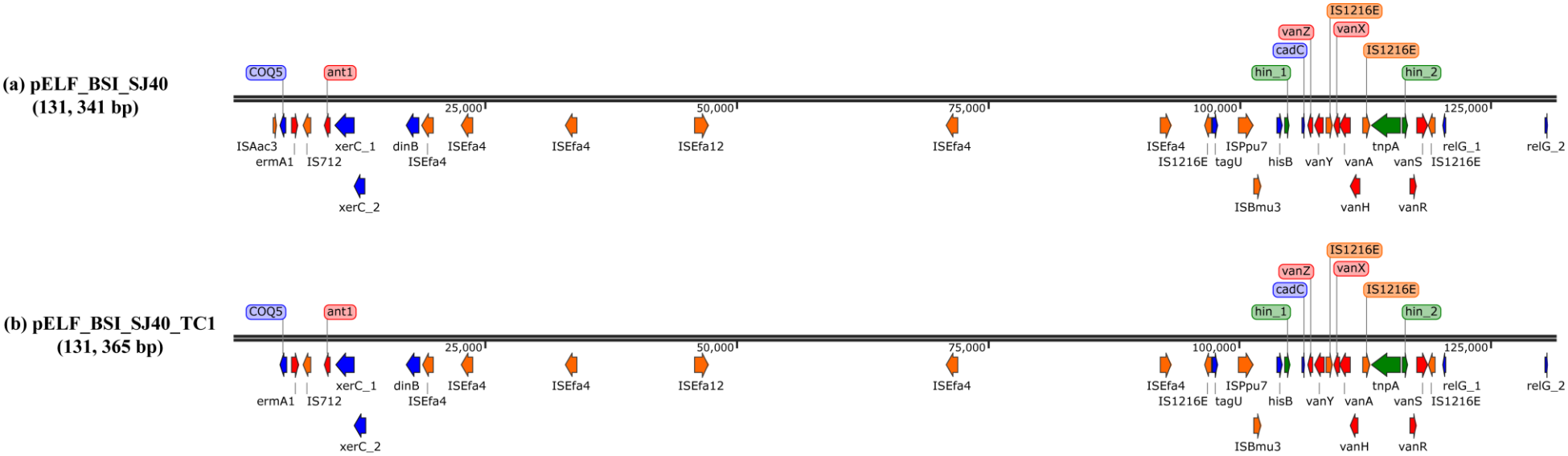

Figure 3.23. Schematic diagram of the structural organisation of linear plasmids pELF_BSI_SJ40 and pELF_BSI_SJ40_TC1 resolved by hybrid assembly of paired-end Illumina MiSeq short reads with Oxford Nanopore Technologies long reads. (a) linear plasmid from the vancomycin resistant *Enterococcus faecium* (VREfm) blood stream infection (BSI) isolate BSI_SJ40 (131,341 bp) (b) linear plasmid from the corresponding *E. faecium* 64/3 transconjugant derivative obtained via conjugative transfer from BSI_SJ40 during filter-mating experiments (131,365 bp). Genes of interest and their orientation are represented by arrows as follows: red indicates antibiotic resistance genes, orange indicates insertion sequences, green indicates transposases, resolvases and invertases, blue indicates genes encoding known proteins. Due to spacing limitations, products annotated by RAST, Prokka and/or EGG-NOG Mapper as ‘hypothetical protein’, ‘mobile element protein’, ‘phage protein’ and ‘phage-related protein’ are not represented in this diagram.

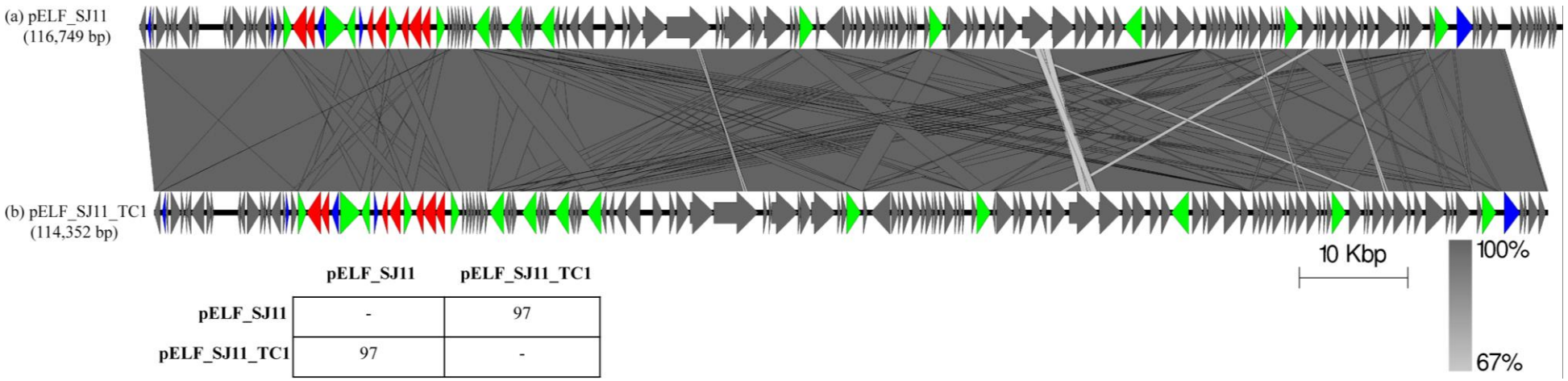

	pELF_SJ11	pELF_SJ11_TC1
pELF_SJ11	-	97
pELF_SJ11_TC1	97	-

Figure 3.24. Comparative genetic organization of linear plasmids pELF_SJ11 and pELF_SJ11_TC1. The figure shows a multiple alignment of (a) linear plasmid from the VREfm screening isolate SJ11 (116,749 bp) (b) linear plasmid from the corresponding *E. faecium* 64/3 transconjugant derivative obtained via conjugative transfer from SJ11 during filter-mating experiments (114,352 bp). Coding sequences of interest and their orientation are represented by arrows as follows: red, antimicrobial resistance genes; green, transposases, insertion sequences and resolvases; blue proteins with a known coding function. Regions between alignments with shared homology are represented by grey connecting blocks and/or lines with the colour gradient indicating percentage nucleotide identity (67-100%). A scale bar is included beneath the figure. The matrix shown beneath the figure contains an n × n DNA sequence similarity between the plasmids.

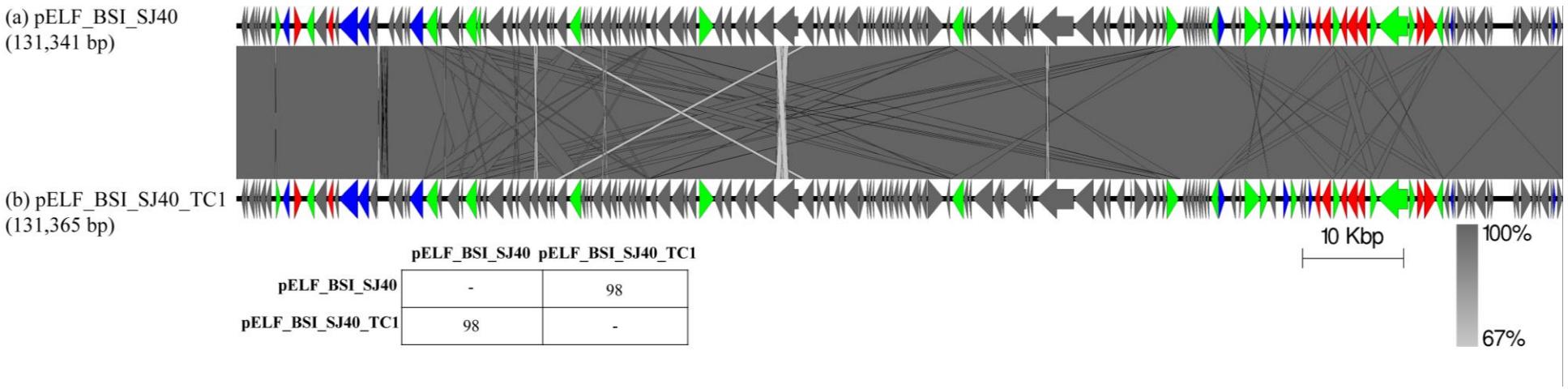

	pELF_BSI_SJ40	pELF_BSI_SJ40_TC1
pELF_BSI_SJ40	-	98
pELF_BSI_SJ40_TC1	98	-

Figure 3.25. Comparative genetic organization of linear plasmids pELF_BSI_SJ40 and pELF_BSI_SJ40_TC1. The figure shows an alignment of (a) linear plasmid from the VREfm BSI isolate BSI_SJ40 (131,341 bp) (b) linear plasmid from the corresponding *E. faecium* 64/3 transconjugant derivative obtained via conjugative transfer from BSI_SJ40 during filter-mating experiments (131,365 bp). Coding sequences of interest and their orientation are represented by arrows as follows: red, antimicrobial resistance genes; green, transposases, insertion sequences and resolvases; blue proteins with a known coding function. Regions between alignments with shared homology are represented by grey connecting blocks and/or lines with the colour gradient indicating percentage nucleotide identity (67-100%). A scale bar is included beneath the figure. The matrix shown beneath the figure contains an n × n DNA sequence similarity between the plasmids.

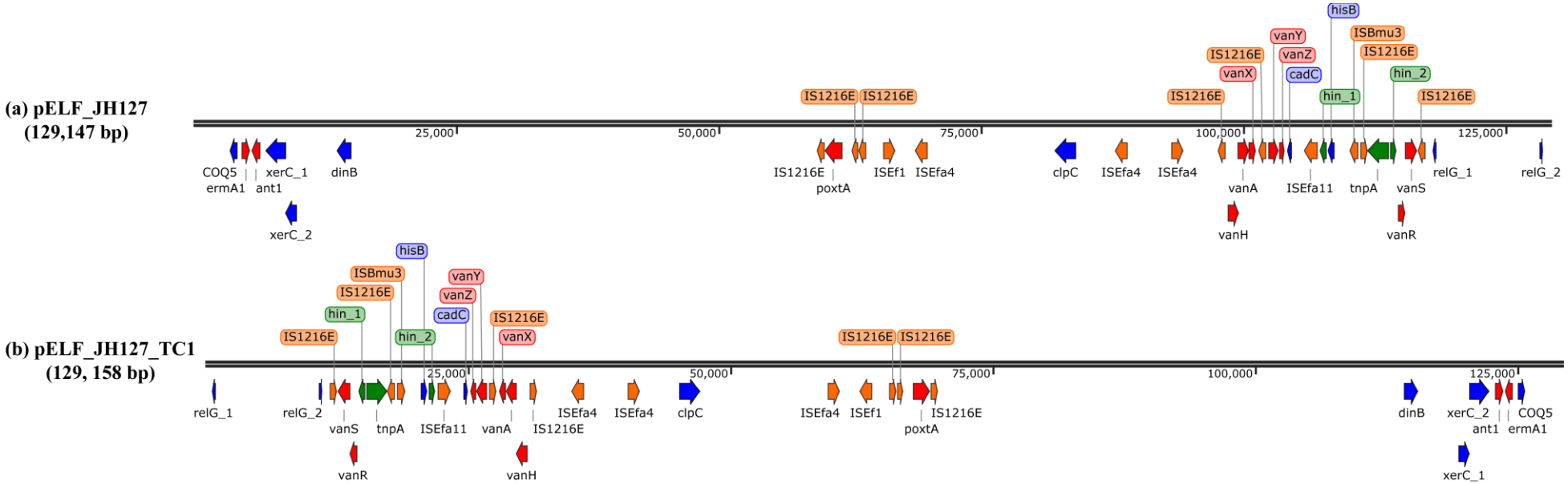

Figure 3.26. Schematic diagram of the structural organisation of linear plasmids pELF_JH127 and pELF_JH127 _TC1 resolved by hybrid assembly of paired-end Illumina MiSeq short reads with Oxford Nanopore Technologies long reads. (a) linear plasmid from the VREfm screening isolate JH127 129,147 bp) (b) linear plasmid from the corresponding *E. faecium* 64/3 transconjugant derivative obtained via conjugative transfer from JH127 during filter-mating experiments (129,158 bp). Genes of interest and their orientation are represented by arrows as follows: red indicates antibiotic resistance genes, orange indicates insertion sequences, green indicates transposases, resolvases and invertases, blue indicates genes encoding known proteins. Due to spacing limitations, products annotated by RAST, Prokka and/or EGG-NOG Mapper as 'hypothetical protein', 'mobile element protein', 'phage protein' and 'phage-related protein' are not represented in this diagram.

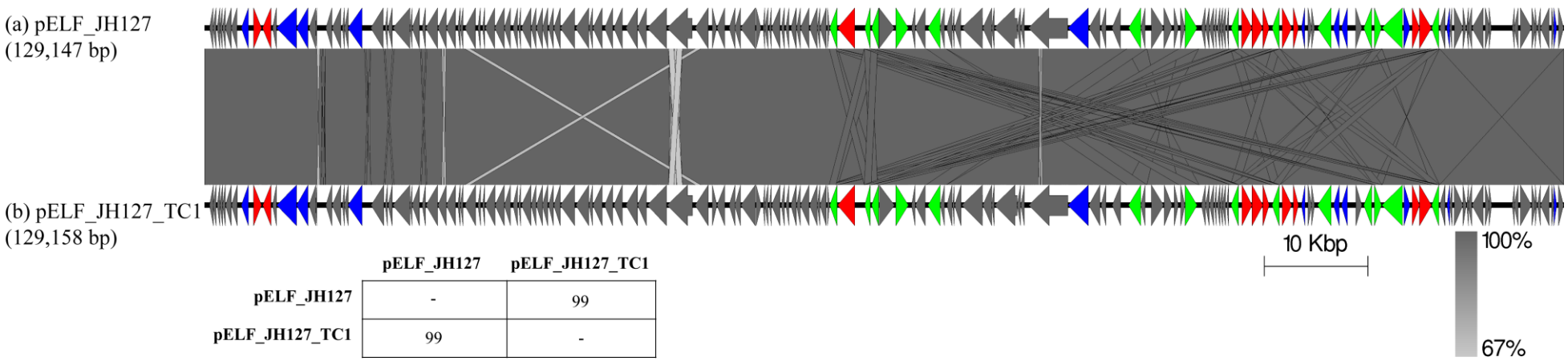

	pELF_JH127	pELF_JH127_TC1
pELF_JH127	-	99
pELF_JH127_TC1	99	-

Figure 3.27. Comparative genetic organization of linear plasmids linear plasmids pELF_JH127 and pELF_JH127 _TC1. The figure shows an alignment of (a) linear plasmid from the VREfm screening isolate JH127 129,147 bp) (b) linear plasmid from the corresponding *E. faecium* 64/3 transconjugant derivative obtained via conjugative transfer from JH127 during filter-mating experiments (129,158 bp). Coding sequences of interest and their orientation are represented by arrows as follows: red, antimicrobial resistance genes; green, transposases, insertion sequences and resolvases; blue proteins with a known coding function. Regions between alignments with shared homology are represented by grey connecting blocks and/or lines with the colour gradient indicating percentage nucleotide identity (67-100%). A scale bar is included beneath the figure. The matrix shown beneath the figure contains an n × n DNA sequence similarity between the plasmids.

3.3.7 Final confirmation of linear topology using PFGE analysis

To provide further evidence that the *vanA*-encoding linear contigs identified in Irish isolates were plasmids displaying linear topology, the total DNA of four representative isolates (SJ11, BSI_SJ40, RC-19-23 and JH127) and their *E. faecium* 64/3 transconjugant derivatives (SJ11_TC1, BSI_SJ40_TC1 and JH127_TC1) were digested with S1 nuclease and subjected to PFGE. S1 nuclease treatment functions by converting supercoiled, circularised plasmids into linear molecules (Barton *et al.,* 1995). Previous studies have shown that there is no difference in the electrophoretic mobility of linear plasmids in agarose gels following PFGE, whether undigested or digested with S1 nuclease (Cornell *et al.*,2018). The representative isolates and the transconjugants containing various plasmid sizes revealed bands at the expected size, with no difference in migration observed before and after treatment with S1 nuclease (Figure 3.28). These findings provided convincing evidence that the linear contigs identified in Irish VREfm and transconjugants were linear plasmids.

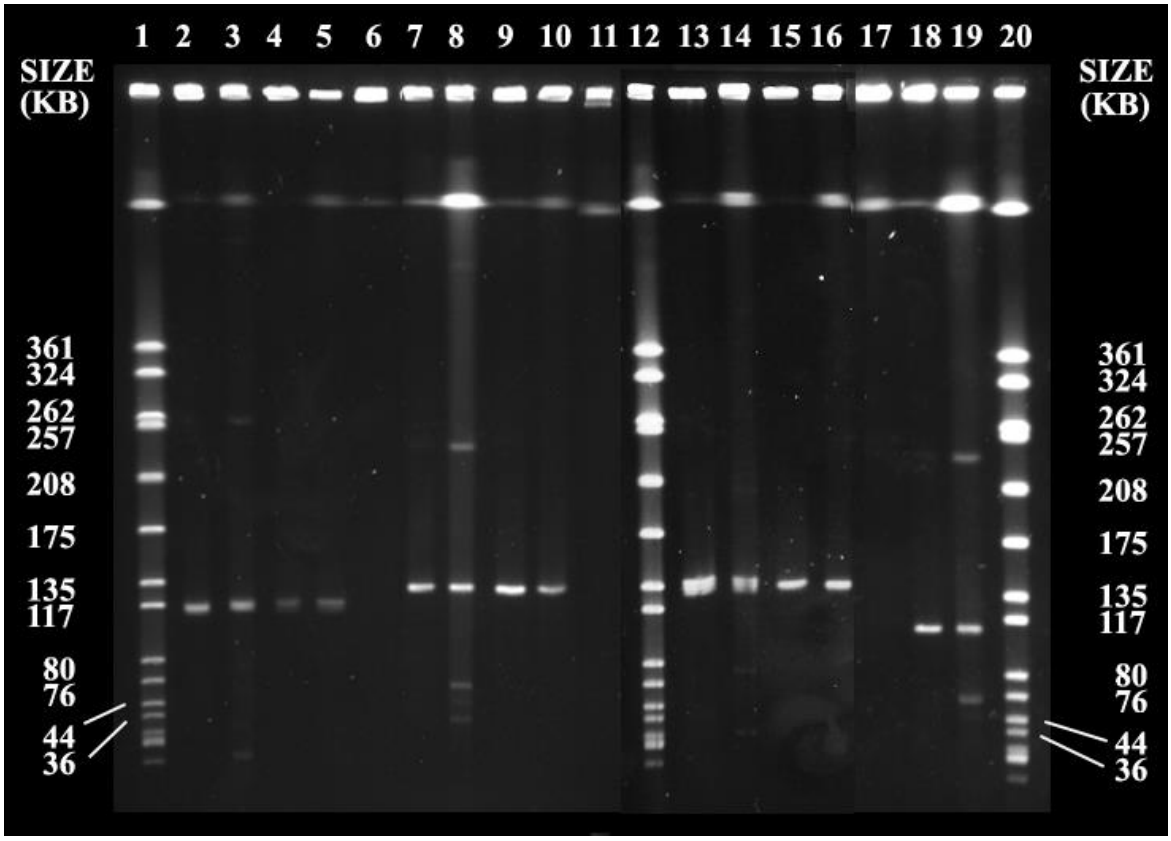

Figure 3.28. Pulse field gel electrophoresis (PFGE) analysis of undigested and S1 nuclease-treated DNA of eight representative vancomycin-resistant *Enterococcus faecium* isolates harbouring linear plasmids. Lanes are labelled 1-20 as follows: 1. *Sma*I-digested *S. aureus* molecular size standard; 2, SJ11 undigested (116,749 bp linear plasmid); 3, SJ11 S1-nuclease treated (116,749 bp linear plasmid); 4, SJ11_TC1 undigested (114,352 bp linear plasmid); 5, SJ11_TC1 S1-nuclease treated (114,352 bp linear plasmid); 6, Plasmid free *E. faecium* 64/3 recipient undigested; 7, BSI_SJ40 undigested (131,341 bp linear plasmid); 8, BSI_SJ40 S1-nuclease treated (131,341 bp linear plasmid); 9, BSI_SJ40_TC1 undigested (131,365 bp linear plasmid); 10, BSI_SJ40_TC1 S1-nuclease treated (131,365 bp linear plasmid); 11, Plasmid free *E. faecium* 64/3 recipient undigested; 12 *Sma*I-digested *S. aureus* molecular size standard; 13, JH127 undigested (129,147 bp linear plasmid); 14, JH127 S1-nuclease treated (129,147 bp linear plasmid); 15, JH127_TC1 undigested (129,158 bp linear plasmid); 16, JH127_TC1 S1-nuclease treated (129,158 bp linear plasmid); 17, Plasmid free *E. faecium* 64/3 recipient undigested; 18, RC-19-023 undigested (109,124 bp linear plasmid); 19, RC-19-023 S1-nuclease treated (109,124 bp linear plasmid) and 20, *Sma*I-digested *S. aureus* molecular size standard.

3.4 Discussion

This study provides the first comprehensive investigation of the epidemiology and population structure of clade A1 *E. faecium* recovered from hospital patients across the Republic of Ireland using a WGS-based approach. Our findings indicate that ST80 has emerged as the predominant endemic lineage of *E. faecium* in Ireland, accounting for the majority of isolates (72%) recovered across seven geographically distinct hospitals. This is in line with other WGS-based studies of clade A1 *E. faecium*, with ST80 VREfm identified as a predominant, high-risk clone causing extensive hospital outbreaks across America, Australia, and Europe (Lebreton *et al.*, 2013; Raven *et al.*, 2016; Pinholt *et al.*, 2017; Leong *et al.*, 2018; Lee *et al.*, 2018; Gorrie *et al.*, 2019; Pratama *et al.*, 2021). However, within the ST80 lineage, there is a very diverse and polyclonal population, which can be further discriminated into more discrete CT-based genomic clusters using cgMLST analysis that are more reflective of the true population structure (Figure 3.1). These findings are indicative of the continued re-introduction of a successful hospital-adapted ST80 clone in Ireland, with subsequent genomic diversification, resulting in the expansion and transmission of genetically diverse ST80-deriviatives defined by their cgMLST CT. We identified three predominant ST80 lineages (CT2933, CT1916 and CT1598) in circulation, accounting for 32% (325/1028) of the total isolate population across the entire hospital network confirming the presence of endemic-CT groups. The significant variation within the ST80 population correlates with studies from colleagues in Copenhagen, which highlighted a substantial increase in VREfm during 2011–2015 resulting from the introduction, expansion and spread of a single *vanA*-encoding ST80 clone showing significant genetic diversity (Pinholt *et al.*, 2015, 2017, 2019).

A comparison of Irish, international, and Danish isolates revealed little overlap between *E. faecium* strains from different countries (Figures 3.7 and 3.8). This finding suggests that local evolution plays a significant role in the epidemiology of VREfm, with no evidence for widespread inter-country transmission, which can occur with more clonal organisms such as hospital-acquired MRSA (ECDC, 2020). The geographic specific distribution of clones is perhaps in part attributed to the evolutionary trajectory of *E. faecium*, which is significantly influenced by both extensive horizontal acquisition of exogenous DNA segments and the highly recombinant nature of the core-genome (Crank and O'Driscoll, 2015; Guzman Prieto *et al.*, 2016). In fact, some studies have suggested that up to 44% of the core genome may be subject to homologous recombination (Leavis

et al., 2006; Howden *et al.*,2013). The high-frequency of both vertical and horizontal variation may significantly alter any apparent clonality in the global population structure of *E. faecium* clade A1 strains and contribute to the formation of country-specific endemic clonal clusters. A recent study of VREfm from 31 countries, which showed localised VREfm evolution along with evidence of localised acquisition of *van* genes, supports this suggestion (van Hal *et al.*, 2021).

A notable finding from our study was the persistence of endemic VREfm clones in both multiple wards within H1 and geographically distinct hospitals, over extended periods of time in the absence of any known epidemiological link or environmental source. Whilst it is acknowledged that the main aim of this study was to provide the first comprehensive analysis of the population structure of *E. faecium* in Ireland using highly-discriminatory methods such as WGS, it would be remiss not to address the extensive presence of widespread transmission and dissemination of major CT VREfm groups occurring both locally and at a national level. For example, ST80 CT2933 contained highly related isolates recovered from 19 H1 ward locations and six regional hospitals distributed across Ireland collected over a 43-month period (Figure 3.3). There were only ten allelic differences observed between the earliest isolate SJ55 from H1 and the latest isolate MH678 from H3 within this cluster which were recovered 1330 days apart with an approximate 5 km geographic difference. This finding may be in part explained by the movement of patients between wards and hospital networks due to the distribution of medical specialities, interdisciplinary services, and specialist staff across the healthcare consortium in Ireland. It may also reflect the sporadic sampling of external transmission networks and a possible environmental source. Nonetheless, our finding of protracted persistence of highly related isolates (≤20 allelic differences) across multiple Irish hospitals serve to highlight the need for more detailed epidemiological studies to identify the complex inter-hospital transmission networks at play and to identify unknown community reservoirs to better inform national IPC strategies and national surveillance guidelines.

Genetically indistinguishable (median allelic difference 4, range: 0-22) CT2933 VREfm were also identified from 19 H1 wards over 437 days suggesting widespread trafficking of highly related isolates throughout the same hospital. Whilst there is a significant lack of epidemiological insight into the genomic analysis in this study, with the absence of patient-movement data, this finding of widespread hospital circulation of endemic CT clones adds to the ever-growing complexity of VREfm surveillance. It has

been well established that the hospital environment plays a significant role in the acquisition and dissemination of VREfm, with high-touch near-patient surfaces, shared medical equipment and bathroom facilities contributing to spread (Drees *et al.,* 2008). A recent study conducted by McDermott and colleagues in a large north Dublin tertiary referral hospital investigated the contribution of the near-patient environment within critical care on transmission and found that 6.5% of all environmental sites tested were positive for VREfm, with 61% considered 'high-touch' in nature. This environmental persistence may be attributed to the reported tolerance of hospital-adapted *E. faecium* strains to subclinical concentrations of various disinfectants, including some alcohol preparations and chlorhexidine which allow strains to resist decontamination and cleaning (Guzmán Prieto *et al.,* 2017). Whilst this study does not address the impact of environmental persistence and the potential for unsampled staff and patient reservoirs, it is clear that current IPC strategies, cleaning regimens and surveillance protocols in Irish hospitals are inadequate to circumvent extensive transmission from occurring.

In the present study, we demonstrate the genetic structure of the *vanA* gene cluster in the Tn*1546*-like transposon from a selection of representative VREfm isolates from distinct ST and CT backgrounds (Figure 3.9). Diverse iterations of the *vanA* operon were apparent in all seven isolates, characterised by multiple insertions of an identical IS element, IS*1216E*. Previous studies have highlighted the integration of single copies of various IS elements at conserved sites in the centre of the Tn*1546* transposon, such as IS*1216V,* IS*125,* IS*Ef1*and IS*Efa* (Handwerger *et al.,* 1995; Simonsen *et al.,* 2000; Camargo *et al.,* 2004; Camargo, 2005; Werner *et al.,* 2008; Talebi *et al.,* 2008; Cha *et al.,* 2013; Pinholt *et al.,* 2017; Wardal *et al.,* 2017). To the best of our knowledge, this is the first study to demonstrate multiple insertions of IS*1216E* into Tn*1546*. Interestingly, the organisation of the Irish *vanA* transposon appears to be segmented into distinct gene clusters flanked on either side by an insertion of IS*1216E*. For example, isolate RC-19-039 shows a rearrangement in the order of the *van* genes, with *vanHAX*, *vanYZ* and *tnpA*, and *vanRS* each encoded following an insertion of IS*1216E* (Figure 3.9). Recent studies have indicated that insertion sequences, such as IS*1216E* may form translocatable units that can facilitate mobilisation of antimicrobial resistance genes by transposition and translocation (Shan *et al.,* 2020). For example, clade A1 *E. faecium* harbouring the linezolid resistance gene *poxtA* flanked by IS*1216E* have been shown to excise and form small transposable elements that cointegrate via translocation into various plasmid backbones (Shan *et al.,* 2020). Additional studies have also demonstrated the ability of

IS*1216* to form cointegrates to mobilise antimicrobial resistance genes at high frequency. This entails a copy-in mechanism, involving one IS*1216* element located on a plasmid and a target sequence. Additionally, a targeted conservative mechanism was also reported involving two copies of IS*1216*, one located on a plasmid and the second in the target sequence which occurs at a 50-fold higher frequency (Harmer and Hall, 2020). The heterogeneity of the *vanA* gene cluster observed in this study is therefore likely as a result of cointegration via the conservative route due to multiple IS*1216E* insertions. These findings indicate the introduction and continued circulation of a common Tn*1546* backbone ancestor element in Irish hospitals present across diverse genetic lineages, evidenced by 86.3% exhibiting >90% sequence identity to the SJ11*vanA* reference. Whilst the reference mapping method provides an important indication of how frequently distributed a genetic structure may be within a population, it is important to note that it does not account for the insertions of additional genetic material or the rearrangements of genes on plasmid structures. Therefore, there are likely numerous iterations and arrangements of the *vanA* region in VREfm in Ireland facilitated by the instability associated with multiple IS*1216E* insertions resulting in dynamic gain and loss of gene segments.

The consequences of the instability associated with the IS*1216E* insertions has been extensively demonstrated within this study, notably in relation to isolates displaying phenotypic susceptibility to vancomycin. For example, BSI isolate RC-19-036 harboured a *vanA*-encoding plasmid enriched with 11 copies of IS*1216E* (Figure 3.19). The *van* region of this plasmid lacked the associated sensor-regulatory genes (*vanR* and *vanS*), suggesting the RC-19-036 potentially arose from a vancomycin-resistant ancestor. This finding has important consequences for both patient management and surveillance. Enterococci are known for their remarkably malleable, open genome which can easily acquire exogenous DNA via HGT. It is therefore not surprising that gene segments that may confer a fitness cost are lost in the absence of antimicrobial selective pressure (Arias and Murray, 2012; Guzman Prieto *et al.*, 2016; Arredondo-Alonso *et al.*, 2020). However, a patient may yield an *E. faecium* BSI organism that appears to be phenotypically susceptible to vancomycin or may yield a negative VRE screen, but may harbour a vancomycin-resistant remnant as described above. It is plausible that under the selective pressure of dual antimicrobial therapy often implemented in the treatment of invasive enterococcal infections or exposure to the ward environment, an isolate may revert to vancomycin resistance via the gain of regulatory elements from an available gene pool

either *in-vivo* or within the hospital setting. This may result in unexpected treatment failures in the context of invasive infection or the transmission of resistant colonising populations from presumed VRE-negative patients missed by standard surveillance methods. This is further emphasised by the finding of genetically indistinguishable clade A1 VSEfm and VREfm isolates. For example, the earliest collected isolate in CT2933 was a VSEfm BSI which exhibited 0 allelic differences to a VREfm BSI recovered from an additional patient 18 days later. This is in line with recent studies from the United Kingdom, Australia and Sweden which indicate that VSEfm and VREfm belong to the sane clonal circulating population in hospital settings (Howden *et al.,* 2013; Sivertsen *et al.,* 2014; Brodrick *et al.,* 2016).

A key finding of this study is the conserved *tnpA* transposase gene (*orf1*) deletion, mainly in the 3'end, observed across Irish VREfm within the Tn*1546*-like *vanA* transposon (Figure 3.10). Interestingly, a previous study of VREfm from Irish hospitals provided evidence of a unique *vanA* transposon with a truncated transposase gene in 21 isolates investigated, distinct from United Kingdom isolates (Raven *et al.,* 2016). This has also been demonstrated in other studies, with the left extremity of Tn*1546* corresponding to the *orf1*gene completely deleted (Woodford *et al.,* 1998; Willems *et al.,* 1999; Hsieh *et al.,* 2010; Khan *et al.,* 2010; da Silva *et al.,* 2012; Kuo *et al.,* 2014; Pinholt *et al.,* 2017). The *tnpA* gene is associated with key transposition functions, however a study by Hsieh and colleagues reported that the Tn*1546*-like element harbouring a truncated transposase gene and a single IS*1251* copy was associated with a much higher conjugative frequency (10^{-6} vs $7x10^{-7}$) when compared with the Tn*1546* prototype. This suggests that the truncated *orf1* plus the presence of an IS*1251*-like insertion sequence may confer a functional advantage by facilitating enhanced *vanA* dissemination within the hospital environment. The high prevalence of IS*1216E* in conjunction with the absence of a functional *tnpA* transposase gene in Irish VREfm may therefore facilitate higher-frequency conjugation and widespread mobility.

Characterisation of the *vanA* encoding plasmids found in Irish hospital VREfm isolates revealed a diverse plasmidome population encompassing both circular and linear conjugative plasmids involved in vancomycin resistance gene mobilisation and spread. The circular vancomycin-resistant plasmid pool was enriched with a variety of replicon types derived from both broad and narrow host range families. This highlights the ability of the Tn*1546*-like element to successfully move via transposition to a vast array of plasmid backgrounds (Freitas *et al.,* 2016; Wardal *et al.,* 2017). This phenomenon has

been demonstrated extensively, with Heaton and colleagues highlighting the IS*1216*-mediated transfer of Tn*1546* from a non-conjugative to a conjugative plasmid within the same VREfm strain resulting in identical transposon variants in distinct plasmid backgrounds. Additionally, the identification of multi-replicon plasmids in this study provides conclusive evidence for the formation of horizontal plasmid hybrids, most likely as a result of IS*1216E* mediated-composite transposons mobilising large plasmid segments resulting in extensive diversity and mosaicism (Novais *et al.,* 2008; Sletvold *et al.,* 2010). This is supported by filter-mating experiments, with a hybrid plasmid formed under vancomycin selective pressure comprising segments from two different plasmids from the same donor isolate (Figures 3.17 and 3.18). It is clear that the diverse pool of plasmids capable of acquiring vancomycin-resistance genes in conjunction with extensive plasmid mosaicism as a result of recombination has significantly contributed towards the successful establishment, emergence and spread of *vanA* in Ireland.

Further analysis of the accessory genome of VREfm revealed the presence of plasmids carrying *vanA* that exhibited linear topology. These findings are in line with recent studies from Japan and Switzerland, which report the emergence of linear plasmids carrying *vanA*, *vanM* and functional genes involved in carbohydrate utilisation (Hashimoto *et al.,* 2019, 2020; Boumasmoud *et al.,* 2022). Comparative genomic analysis of the structure of Irish linear plasmids with those published by colleagues in Japan and Switzerland revealed some homology, suggesting the presence of a conserved lineage of pELF1-like plasmids which has diversified in different geographical contexts via the propagation of locally acquired MGEs and AMR genes (Figure 3.20) (Hashimoto *et al.,* 2020). The linear plasmids, although lacking in genes involved in plasmid-mobilisation, were conjugative in nature and successfully transferred to the *E. faecium* 64/3 plasmid-free recipient. These results mirror findings by Hashimoto and colleagues, which demonstrated a high transfer frequency of pELF1-like plasmids in both solid and liquid mediums. Additionally, enterococcal linear plasmids were not found to be associated with a significant growth or fitness cost (Hashimoto *et al.,* 2020). It is plausible, therefore, that the linear plasmids have emerged as prominent vehicles driving vancomycin resistance in Ireland, evident by the high proportion of VREfm isolates exhibiting >85% sequence identity to the pELF_SJ11*vanA* reference sequence and ready ability to transfer by conjugation.

To conclude, Irish VREfm are diverse yet harbour a characteristic *vanA* region with a truncated transposase and multiple insertions of IS*1216E* that may facilitate

spread. The *vanA* region was identified on several circular and linear conjugative plasmids. A comparison of Irish, international, and Danish VREfm/VSEfm revealing little overlap indicating that local evolution is important in the epidemiology of VREfm.

Chapter 4

Protracted transmission and persistence of ST80 vancomycin-resistant *Enterococcus faecium* clonal complex types CT2933, CT2932 and CT1916 in a large Irish hospital: a 39-month genomic study

4.1 Introduction

Enterococcus faecium has emerged as a significant, globally disseminated nosocomial pathogen associated with a wide range of infections and persistent environmental contamination (Arias and Murray, 2012). Extensive studies have highlighted both the high-level of intrinsic and acquired resistance amongst *E. faecium* hospital-adapted clones, rendering a variety of clinically important therapeutic options ineffective, most notably vancomycin and linezolid (Arias and Murray, 2012; Cheah *et al.,* 2013; Gilmore *et al.,* 2013; Miller *et al.,* 2014; Gao *et al.,* 2018; Egan *et al.,* 2020a, 2020b, 2022). Multi-drug resistant strains, such as VREfm, constitute a substantial burden of disease, particularly in immunocompromised or multi-morbid patients. At-risk groups such as critical care and haematology-oncology are disproportionately vulnerable to invasive infection, often preceding GI colonisation, with a high associated mortality rate and increased length of hospital stay (Arias and Murray, 2012; Cheah *et al.,* 2013). As a result, the World Health Organisation has listed VREfm as a high-priority pathogen for which new antimicrobial therapies are urgently required (WHO, 2017).

From an Irish perspective, the true prevalence of VREfm amongst individuals with frequent healthcare exposure is ultimately unknown, with rates of 3-40% quoted depending on the patient population (Nourse *et al.,* 2000; Morris-Downes *et al.,* 2010; Ryan *et al.,* 2015; Whelton *et al.,* 2016; McDermott *et al.,* 2018). However, as detailed in Chapter 3, Section 3.1, the Republic of Ireland has reported some of the highest rates of invasive resistant infection in Europe for over a decade, ranging from 28.4%-45.8% (2006-2022) (ECDC, 2023). The widespread success and dissemination of VREfm in Ireland is perhaps in part attributable to their ability to persist in the hospital environment for extensive periods of time despite vigorous IPC cleaning regimens, which have successfully curtailed the spread of other hospital-acquired pathogens of public health significance (Falk *et al.,* 2000; Neely and Maley, 2000; van Hal *et al.,* 2022). Previous studies have highlighted that rates of VREfm environmental contamination, particularly in communal ward areas, may reach up to 50% in hyperendemic settings similar to Ireland, which can contribute to the spread of epidemic clones via direct or indirect patient transmission (Gouliouris *et al.,* 2020). This phenomenon likely reflects the highly plastic or malleable nature of the hospital-adapted *E. faecium* pan-genome, which significantly contributes to increased fitness and survival, particularly under adverse conditions characterised by significant selective pressures such as those encountered in the hospital

environment (Baquero, 2004; van Schaik *et al.,* 2010; Howden *et al.,* 2013; Lebreton *et al.,* 2013). This is further substantiated by recent studies that reported the emergence of clade A1 VREfm strains with an increased tolerance to alcohol-based disinfectants and reduced chlorohexidine susceptibility, further promoting persistence (Guzmán Prieto *et al.,* 2017; Bhardwaj *et al.,* 2018; Pidot *et al.,* 2018).

Routine environmental sampling for *E. faecium* clones is currently not recommended by national and international guidelines, however molecular typing and genomic studies have highlighted that isolates recovered from the near-patient environment may serve as surrogate markers for colonising strains in circulation, which can further augment surveillance practices (Cassone *et al.,* 2018; Gouliouris *et al.,* 2020). Whilst the use of WGS has significantly enhanced outbreak resolution and the elucidation of possible transmission networks, its full potential and discriminatory value remains hindered by suboptimal policies for the monitoring of VRE gastrointestinal carriage in hospitalised Irish patients. Current screening practices limit surveillance to high-risk areas only and it is likely asymptomatic colonisation serves as an important unsampled reservoir of infection in the context of environmental shedding (RCPI, 2012). Rapid detection of colonisation and subsequent implementation of contact precautions and/or isolation may aid in the reduction of transmission and help to circumvent VRE-related BSI and other invasive infections, particularly in immunocompromised patients. Unfortunately, due to the low virulence of VREfm and the high colonisation pressure in Irish hospitals, outbreaks may often remain undetected until infection becomes clinically evident thus allowing substantial, uncontrolled transmission amongst hospitalised patients in the interim. This is emphasised by a previous study by Cattoir and colleagues which identified 2-10 asymptomatic carriers for each patient with clinically evident VREfm infection (Cattoir and Leclercq, 2013).

This part of the present study aimed to undertake an in-depth investigation of the transmission and persistence of VREfm clonal lineages in two critical care wards of a large Irish hospital using a genomics approach over 39-months. Patient screening and environmental *E. faecium* were investigated to identify predominant genomic clusters involved in transmission and persistence in the context of a protracted, silent outbreak. Predominant clonal lineages among isolates from six other Irish hospitals recovered over a five-year time period were also investigated.

4.2 Materials and methods

4.2.1 Isolate collection

In total, 1,297 *E. faecium* isolates recovered from seven Irish hospitals (H1-H7) between June 2017 and December 2022 were investigated retrospectively (Appendix 1, Table 1). This comprised three distinct study populations: (i) VREfm rectal screening isolates collected over a 39-month period during a retrospectively identified protracted outbreak in two wards of a large acute Dublin-based hospital (H1), (ii) limited environmental isolates recovered on the outbreak wards (iii) a well-characterised collection of national comparator isolates representative of the Irish hospital-associated VREfm population.

4.2.1.1 Patient isolates

VREfm rectal screening isolates (*N*=330) from individual patients in two wards of a large acute Dublin-based hospital (H1) between September 2019 and December 2022 were investigated (Appendix 1, Table 1). Ward A (WA) is a 15-bed cardiothoracic unit, comprising three 4-bed bays with a shared bathroom and 3 single ensuite rooms. Ward B (WB) is a 35-bed oncology unit, comprising six 4-bed bays with a shared bathroom, a 2-bed bay and 9 single ensuite rooms. Rectal screening swabs in WA and WB were taken routinely on admission with weekly universal screening thereafter as per national guidelines (RCPI, 2012). A total of 330/2885 screens from separate patients yielded VREfm following culture on chromID VRE chromogenic agar (bioMérieux, Marcy, L'Étoile, France). VREfm-positive isolates were stored by the diagnostic laboratory at -80°C in a Microbank cryovial (Pro-Lab Diagnostics). Only the first positive VREfm rectal isolate per individual patient was included for analysis in the study.

4.2.1.2 Environmental isolates

Forty-eight environmental *E. faecium* were recovered in H1 between November 2022 and December 2022 (Table 4.1). Due to COVID-19 restrictions, environmental sampling was rudimentary and limited to two 'snapshot' time-points at the end of the study period. Three single patient-occupied ensuite rooms (WA *N*=1, WB *N*=2) were chosen for surface-sampling of high-touch environmental sites (*N*=30, ten sites per room) using *Enterococcus faecium* ChromoSelect agar (Sigma-Aldrich [Merck], Ireland) contact plates (25 cm^2 area). This ensured that both VREfm and VSEfm isolates were recovered.

In total, ten environmental sites were chosen per room to encompass the patient bed space, vital-monitoring devices and ensuite bathroom facilities. The high-touch areas sampled included bedframes, both bedside tables, patient call bells, cardiac monitors, SATs probes, toilet seats and shower drains. Contact plates were incubated aerobically at 37°C for 48 h. All colonies from each sampling site that turned green, indicating the growth of *E. faecium*, were picked for subculture on CBA (Fannin Ltd.) and subjected to identification, antimicrobial susceptibility testing and WGS as described in Chapter 2, Sections 2.3.1, 2.3.2 and 2.5. All suspected *E. faecium* colonies recovered on positive-contact plates were picked for further analysis (Table 4.1, Figure 4.1).

On the second occasion, a total of 13 ward handwash basin drain outlets (WA *N=10,* WB *N=3*) were sampled using nylon-flocked eSwabs (Copan Diagnostics, California, USA). On WA, the handwash basins on three 4-bed bays, the shared bathroom facilities, two single rooms and accompanying ensuites were sampled. On WB, the handwash basin in one single room, accompanying ensuite and one shared patient bathroom were investigated. Following sampling, swabs were placed in a tube of modified Amies transport medium and plated on ChromoSelect agar and CBA (Fannin Ltd.) at 37°C for 48 h. A 100 µL aliquot was collected from each eSwab and ten-fold serial dilutions were prepared (10^{-1} -10^{-6}) in sterile phosphate buffered saline (PBS). 100uL of each dilution was subsequently spread in duplicate on *Enterococcus faecium* ChromoSelect agar and CBA agar and incubated at 37°C aerobically for 48 h. Simultaneously, an additional 100 µL was collected from each eSwab transport medium and incubated in 5 mL of Enterococcosel broth (CondaLab, Madrid, Spain) at 37°C aerobically for 48 h. Each broth was then diluted 10-fold in PBS. 100 µL of each neat and diluted sample was incubated in duplicate as described above Presumptive *E. faecium* isolates were selected based on colony colour, purified by subculture aerobically on CBA at 37°C for 24 h and subsequently identified by MALDI-TOF-MS (Figure 4.1, Table 4.1)

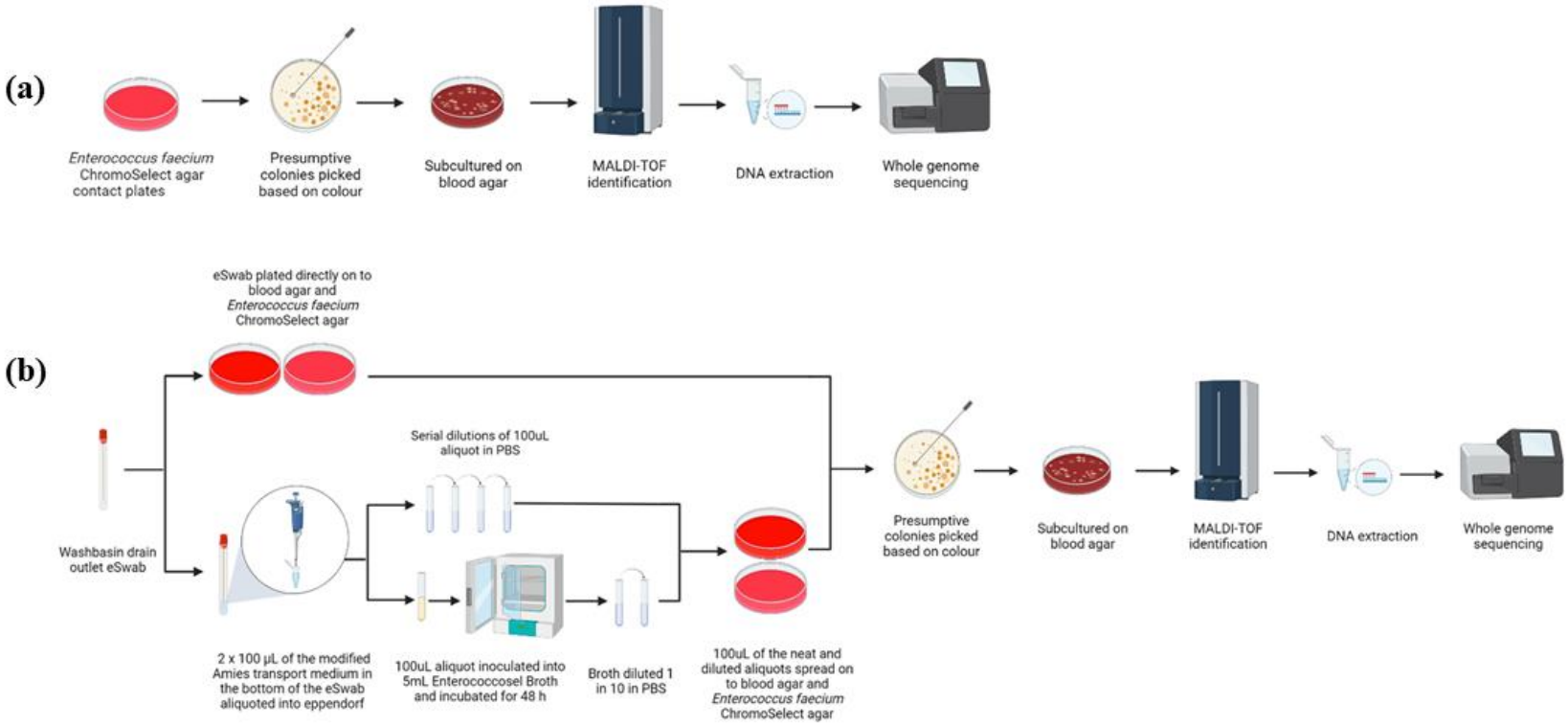

Figure 4.1. Schematic diagram pertaining to the laboratory processing of environmental isolates (*N*=48) from two critical care wards of a large Dublin acute hospital. (a) High-touch environmental sites (*N*=30) were sampled in the two wards using *Enterococcus faecium* ChromoSelect agar (Sigma-Aldrich [Merck]) contact plates (67 mm diameter, 25 cm^2 area) and incubated aerobically at 37°C for 48 h. (b) Handwash basin wastewater drain outlets (*N*=15) from both wards were sampled using nylon-flocked eSwabs (Copan Diagnostics) and then placed

in a tube of modified Amies transport medium. Swabs were directly plated on *Enterococcus faecium* ChromoSelect agar and CBA (Fannin Ltd.) and incubated aerobically at 37°C for 48 h. A 100 µL aliquot of transport medium was collected from each eSwab and serial ten-fold dilutions prepared in sterile phosphate buffered saline (PBS). 100 µL of each dilution was spread in duplicate on *Enterococcus faecium* ChromoSelect agar and CBA agar and incubated aerobically at 37°C for 48 h. Simultaneously, an additional 100 µL was collected from each eSwab transport medium and incubated aerobically in 5 mL of Enterococcus Selective Broth (CondaLab) at 37°C for 48 h. Each broth was then diluted 10-fold in PBS. A 100 µL aliquot of each neat and diluted sample was incubated in duplicate as described above. Presumptive *E. faecium* isolates (*N*=28) were selected based on colony colour, purified by subculture aerobically on CBA at 37°C for 24 h and identified by MALDI-TOF-MS (Bruker Daltonics).

Table 4.1. Detailed metadata on isolates recovered from positive environmental sites in Ward A and Ward B (*N*=48)

Surface sampling of high-touch environmental sites			
	Room 1	Room 2	Room 3
Ward Location	Ward A	Ward B	Ward B
Total Number of Positive Sites (%)[1]	2 (20%)	6 (60%)	1 (10%)
Positive Site Location (*N* of colonies recovered from positive site)	Cardiac monitor (2) Shower drain (2)	Bed Frame (1) Bedside table (9) Call bell (1) Shower drain (2) Sats probe (1)	Toilet seat (2)
Flocked eSwab sampling of handwash basin drain outlets			
	Room 2		Room 4
Ward Location	Ward A		Ward B
Total Number of Positive Drain Sites (%)[2]	2 (20%)		1 (33%)
Positive Site Location (*N* of colonies recovered from positive site)	Handwash basin in patient bedroom (9) Handwash basin in patient ensuite bathroom (10)		Handwash basin in patient bathroom (9)

[1] Percentage calculated on the basis of a total of 10 sampling sites per single patient room in both Ward A and Ward B.
[2] Percentage calculated on the basis of a total of 10 sampling drain sites in Ward A and three in Ward B.

4.2.1.3 Irish comparator reference isolates

A well-characterised in-house collection of *E. faecium* isolates (*N*=908) from seven Irish hospitals (June 2017-July 2022) were included as comparators, 648 of which were described previously (Egan *et al.,* 2022) (Appendix 1, Table 1.).

4.2.2 Infection control procedures and antimicrobial stewardship

IPC procedures were followed according to national guidelines (RCPI, 2012; HIQA, 2017). Ward-specific antimicrobial stewardship policies were developed in line with the recommendations of the Strategy for the Control of Antimicrobial Resistance in Ireland (SARI) Hospital Antibiotic Stewardship Working group (SARI, 2005). The isolation strategy for patients with clinical infection and/or colonisation with a transmissible MDR organism involved contact isolation in a single room with adjoining toilet facilities if available. Due to the limited number of ensuite rooms on WA and WB, organisms such as MRSA and CPE were prioritised in patient cohorts for isolation. As a result, patients with a clinical or screening specimen positive for VRE were not isolated and instead enteric contact precautions were observed. Additionally, a flag of 'VRE positive' was added to the patient's electronic health record. Compliance to hand hygiene on each ward was monitored using regular audits based on Health Protection Surveillance Centre (HPSC)-developed standard operating procedures for hand hygiene observation (SARI, 2005; HPSC, 2014).

4.2.3 Phenotypic susceptibility testing

All study isolates underwent phenotypic susceptibility testing as described in described in Chapter 2, Section 2.3.2 Antimicrobial-resistance and virulence-associated genes were detected *in silico* on short-read WGS assemblies using ABRicate v.0.9.8 (https://github.com/tseemann/abricate).

4.2.4 Second generation Illumina short-read sequencing

4.2.4.1 Genomic DNA Extraction

All isolates underwent genomic DNA extraction for short-read sequencing as described in Chapter 2, Section 2.4.1.

4.2.4.2 Short-read sequencing

All isolates underwent short-read sequencing as described in Chapter 2, Section 2.5.1.

4.2.5 Third generation MinION long-read sequencing

4.2.5.1 Genomic DNA Extraction

Genomic DNA extraction for long-read sequencing for reference isolates BS256, RC-19-045 and RC-19-023 was performed as described in Chapter 2, Section 2.4.2.

4.2.5.1.1 Wizard HMW DNA Extraction

For the environmental isolate (JHE024), HMW genomic DNA was extracted using the Wizard HMW DNA Extraction Kit (Promega) with a modified pre-treatment step for Gram-positive bacteria. Samples were reactivated from Microbank cryogenic storage beads on to CBA and incubated for 24 h at 37°C. A single colony was then selected and inoculated into eight ml of BHIB and incubated overnight in a shaking incubator at 37°C and 200 rpm. Following incubation, each culture was centrifuged at 2,376 × g for five min, the supernatant discarded and the pellet resuspended in 200 µl of lysis buffer A1 and transferred into a fresh tube containing lyophilised lysis enhancer A2 buffer (Inter Array). The solution was then incubated at 37°C for 2-3 h on the Eppendorf Thermomixer Comfort at 300 rpm. The remaining steps were followed as per the manufacturer's instructions. Briefly, 500 µl of HMW Lysis Buffer A (supplied with the HMW kit) was added to each sample and mixed five times using wide bore pipette tips to lyse the bacterial cells and avoid DNA shearing. The lysis solution was then incubated at 37°C for 5 min and subsequently cooled to room temperature. Following incubation, 3 µl of RNase A Solution (Promega) was added to the cell lysate and mixed by inverting seven times. The solution was then incubated at 37°C for 15 min on the Eppendorf Thermomixer Comfort.

To encourage the removal of contaminants, 20 µl of proteinase K solution was added to each sample, followed by gently inverting the tube 10 times for thorough mixing. Samples were then incubated at 56°C for 15 min and cooled to room temperature by placing on ice for one min. Protein Precipitation solution (200 µl) was added to each cell lysate and thoroughly mixed five times using wide bore pipette tips. The mixture was then centrifuged at 13,000 – 16,000 × *g* for 10 min. The supernatant was transferred to a clean 1.5 ml Eppendorf tube containing 600 µl room-temperature isopropanol. The solution was then gently mixed by inverting eight times, incubated at room temperature for one min and centrifuged at 13,000 – 16,000 × *g* for two min. The supernatant was discarded and the resulting DNA pellet was washed by adding 600 µl 70% (v/v) EtOH

and gently inverting 10 times. The EtOH was carefully discarded without disrupting the DNA pellet and allowed to air-dry for 10-15 minutes on clean absorbent paper. Purified DNA was eluted in 100 µl of sterile, prewarmed molecular-grade water in a fresh 1.5 ml Eppendorf and incubated at 65°C for one h to encourage maximum recovery.

4.2.5.2 Long-read sequencing

Long-read sequencing for reference isolates BS256, RC-19-045 and RC-19-023 was performed as described in Chapter 2, Section 2.5.2. It should be noted that during the course of the study, Oxford Nanopore Technologies discontinued the production of the SpotON R9.4 Flow Cell, Ligation Sequencing Kit (SQK-LSK109) and ID native barcoding kit (EXP-NBD104). As a result, long-read library preparation for environmental isolate JHE024 was performed using the new Native Barcoding Kit 24 v14 (SQK-NBD114.24) and sequencing was performed on the MinION platform using a R10.4.1 Flow Cell with MinKNOW software v23.04.6 (Oxford Nanopore Technologies) as described below.

4.2.5.2.1 Library preparation (Native Barcoding Kit 24 v14)

Libraries were prepared according to the Native Barcoding Kit 24 ligation sequencing genomic DNA protocol (Oxford Nanopore Technologies). It should be noted that as protocols are continuously updated on the nanopore community website (available at https://nanoporetech.com/community), the newest version was downloaded and consulted each time libraries were prepared.

(i) DNA repair and end-prep

HMW input DNA (400 ng per sample) was adjusted to a final volume of 11 µl in sterile molecular-grade water and added to a master mix containing 0.875 µl NEBNext FFPE DNA Repair Buffer, 0.875 µl Ultra II End-prep reaction buffer, 0.75 µl Ultra II End-prep enzyme mix and 0.5 µl NEBNext FFPE DNA Repair Mixed (all supplied in NEBNext End repair / dA-Tailing Module reagents (New England BioLabs)). The reaction was then incubated at 20°C for 20 min, followed by 65°C for a further 20 min on a Biometra Tone thermocycler. The DNA sample was subsequently transferred to a clean 1.5 ml microfuge tube (Eppendorf), mixed with 15 µl AMPure XP beads (Beckman Coulter) and incubated for 20 min on a Grant Bio PTR-35 360-degree vertical multi-function rotator (Grant Instruments, Cambridge, UK). Samples were then placed on a 12-tube magnetic separation rack (New England BioLabs) for one min. The resulting supernatant was removed and the bead pellet was washed twice using freshly-prepared 80% (v/v) EtOH whilst on the magnet. The beads were left to dry for one min and resuspended in 10 µl molecular grade water. The samples were then incubated at room temperature for 20 min and placed back on the magnetic rack to encourage elution. Post bead-separation, 10 µl of the supernatant was removed and retained in a fresh Eppendorf tube and quantified using the Qubit 3.0 Fluorometer (Invitrogen/Fischer Scientific). Equimolar amounts of each end-prepped DNA sample were prepared in a final volume of 7.5 µl of sterile molecular-grade water.

(ii) Native barcode ligation

For barcode ligation, 2.5 µl Native Barcode (Oxford Nanopore Technologies) and 25 µl Blunt/TA Ligation Master Mix (New England BioLabs) were sequentially added to the end-prepped DNA and incubated at room temperature for 20 min. To stop the reaction, two µl EDTA was added and the barcoded samples were then pooled in a 1.5 ml Eppendorf tube. For purification, 9 µl of AMPure XP beads (Beckman Coulter) per

sample were added and incubated for 20 min on a vertical multi-function rotator. Samples were pelleted on the magnetic rack, washed with 700 µl 80% (v/v) EtOH and resuspended in 35 µl of sterile molecular-grade water.

(i) Adapter ligation and clean-up

Adapter ligation was performed on 30 µl of the pooled samples by adding 5 µl Native Adapter (NA, Oxford Nanopore Technologies), 10 µl 5x NebNEXT Quick Ligation Reaction Buffer and 50 µl Quick T4 DNA Ligase (New England BioLabs) followed by incubation at room temperature for 20 min. Samples were subsequently purified using 20 µl AMPure XP beads (Beckman Coulter) and incubated on a vertical multi-function rotator for 20 min. The sample was subsequently pelleted on the magnetic rack and enriched for DNA fragments of >3 kb using 125 µl Long Fragment Buffer supplied in the kit (Oxford Nanopore Technologies). The pooled sample was placed back on the magnetic rack to allow the beads to pellet and the supernatant was discarded. The beads were resuspended in 15 µl Elution Buffer (Oxford Nanopore Technologies) at 37°C for 20 min in a static incubator and subsequently placed back on the magnetic rack. After bead separation, 15 µl of the eluate was removed and retained in a fresh Eppendorf tube and quantified using the Qubit 3.0 Fluorometer.

4.2.5.3 Priming and loading the SpotON flow cell

The SpotON R10.4.1 Flow Cell (Oxford Nanopore Technologies) was primed as described in Chapter 2, Section 2.5.2.2. The quantified library was diluted to give a final concentration between 35-50 fmol of DNA. Additionally, a light shield was placed on the flow cell immediately after library loading to protect the flow cell array from light resulting in optimal sequencing.

4.2.5.4 Post sequencing processing

Raw-read FAST5 files were base-called, trimmed and demultiplexed using Dorado v0.5.3 (Oxford Nanopore Technologies).

4.2.6 Bioinformatic analysis

4.2.6.1 de novo assembly

All study isolates underwent quality trimming and de novo assembly using Ridom SeqSphere+ v8.5.1 (Ridom GmbH) as described in Chapter 2, Sections 2.6.1.1 and 2.6.1.2.

4.2.6.2 MLST

Conventional MLST profiles were generated for all isolates using Ridom SeqSphere+ v8.5.1 (Ridom GmbH) as described in Chapter 2, Section 2.6.1.3.

4.2.6.3 wgMLST and cgMLST

Isolate genomes underwent wgMLST and cgMLST as described in Chapter 2, Sections 2.6.1.4 and 2.6.1.5.

4.2.6.4 Genotyping

Antimicrobial resistance profiling and virulence gene identification was performed *in silico* as described in Chapter 2, Section 2.6.1.6.

4.2.6.5 Core-genome SNP analysis

To further investigate potential diversity and discriminate isolates into more distinct genomic clusters, isolates deemed to be closely related using cgMLST (≤20 allelic differences) and assigned within the same CT group underwent cgSNP analysis. Variant annotation and sequence alignment based on cgSNPs was performed by mapping to the earliest recovered CT-specific reference genome using Snippy v4.6.0 (https://github.com/tseemann/snippy). Recombinant SNPs were removed using Gubbins v3.2.1 (https://github.com/nickjcroucher/gubbins) (Croucher *et al.*,2015). Pairwise cgSNPs-based distance matrices were generated using snp-dists v3 (https://github.com/tseemann/snp-dists).

4.2.6.6 Phylogenetic trees

Inference of genetic relatedness, diversity and population structure of *E. faecium* isolates in this study was carried out using both distance- and character-based phylogenetic methodologies. This included the use of pairwise distance matrices generated based on core-genome allelic differences and the number of substitutions per individual character site obtained based on cgSNP analysis. Additionally, a combination of epidemiological and genomic data was used to reconstruct potential transmission networks.

4.2.6.6.1 Neighbour joining tree

NJTs were generated using distance matrices based on cgMLST analysis using Ridom SeqSphere+ v8.5.1 (Ridom GmbH) as described in Chapter 2, Section 2.6.1.8.

4.2.6.6.2 Maximum likelihood tree

Maximum likelihood trees (MLTs) based on cgSNP analysis were constructed using IQ-TREE v2.2.2.6 (http://www.iqtree.org) with the extended ModelFinder (-m MFP) and 1000 ultrafast bootstrap replicates (Nguyen *et al.,* 2015). ModelFinder selection was used to identify the best-fitting model of sequence evolution by concurrently searching model and tree space using 22 substitution models for DNA, 36 for protein and 13 for flexible rate heterogeneity across sites (RHAS) (Kalyaanamoorthy *et al.,* 2017). The phylogenetic trees were visualised and annotated using Interactive Tree of Life v6.5.8 (https://itol.embl.de/) (Letunic and Bork, 2021).

4.2.6.6.3 Parsimonious transmission tree

Parsimonious transmission trees were constructed using cgSNP distance matrices and isolate collection metadata using the SeqTrack algorithm and visualised using GraphSNP (https://graphsnp.fordelab.com/graphsnp) (Jombart *et al.,* 2011; Permana *et al.,* 2023). The SeqTrack algorithm reconstructs potential transmission trees on the basis of most plausible genealogy and relies on three fundamental observations: i) in the absence of genetic recombination, each observed isolate has only one ancestry, ii) ancestors always precede their descendants in time and iii) the likelihood of the ancestry of a given isolate can be inferred from the amount of genetic difference between the isolates in the considered pool. Graph edges are weighted according to the number of SNPs between

pairs of isolates and the resulting ancestry path is chosen by the branch with the least weight (Jombart *et al.*, 2011).

4.2.7 Hybrid assembly

Hybrid assembly of paired-end short-read and long-read sequences was performed using Unicycler as described in Chapter 2, Section 2.7.

4.3 Results

4.3.1 Isolate description

In total, 378 *E. faecium* isolates recovered over 39 months from wards WA and WB of a large tertiary referral hospital in Dublin (H1) were investigated, including 330 patient rectal screening isolates (WA, 109 (33%); WB, 221 (67%)). Twenty-eight environmental isolates were recovered from 3/13 handwash basin drains (19 from two WA drains and nine from one WB drain). An additional twenty environmental isolates were recovered from surface sampling of near-patient high-touch ward sites. All patient isolates were *vanA*-encoding VREfm. The majority (43/48, 89%) of environmental isolates were VSEfm and five were *vanA*-encoding VREfm. Metadata and epidemiological information associated with the study isolates is provided in Section 4.5, Table 4.9.

4.3.2 Major cgMLST clusters of *E. faecium*

The isolates were assigned to nine STs by conventional MLST, with ST80 predominating (310/378, 82%). The remainder belonging to ST203 (*N*=32), ST612 (*N*=14), ST18 (*N*=10), ST17 (*N*=3), ST117 (*N*=3), ST787 (*N*=3), ST789 (*N*=1) and ST1395 (*N*=1) (Figure 4.2). One 'novel' isolate was submitted to pubMLST.org for ST assignment. cgMLST grouped isolates into 27 related isolate clusters and 21 singletons using the previously recommended threshold of ≤20 allelic differences with an average cluster size of 13 (median: seven; range: 2-96) (de Been *et al.,* 2015). Three major ST80 CTs comprising clonal groups were evident in an cgMLST-based NJT (CT2933, CT2932 and CT1916), comprising 55% (208/378) of the total all isolate population, termed CI, CII and CIII respectively (Figure 4.2).

The largest CT, CT2933 (termed CI hereafter), contained 96 isolates (62 screening, 34 environmental) recovered over a 39-month period (September 2019-December 2022) with an average allelic difference of eight (median: seven; range: 0-21). In total, 54% (52/96) of CI isolates were from WB, with the remainder from WA (Section 4.5, Table 4.9). Six CI environmental isolates recovered from areas including toilet seats, cardiac monitors and shower drains were VSEfm and differed from their closest neighbouring patient screening VREfm by an average of two allelic differences (range: 2-12). Twenty-eight additional CI environmental VSEfm from three washbasin drains on WA and WB differed from their closest neighbouring patient screening VREfm by an

average of eight allelic differences (range: 6-21). The majority of isolates in CT2932 (termed CII) (*N*=58) were recovered in WB (37/58; 64%) over 39 months with an average allelic difference of six (median: six, range 0-18). CII-specific environmental isolates (*N*=six) were predominantly vancomycin susceptible (4/6) and differed by an average of five allelic differences to their closest neighbouring patient screening VREfm (range: 1-17). The third CT, CT1916 (termed CIII) comprised 52 patient screening VREfm recovered over 38 months (October 2019-December 2022) with an average allelic difference of 10 (median: 11, range: 0-27). These findings indicated that isolates within CI-CIII, respectively, were closely related, suggesting potential widespread transmission.

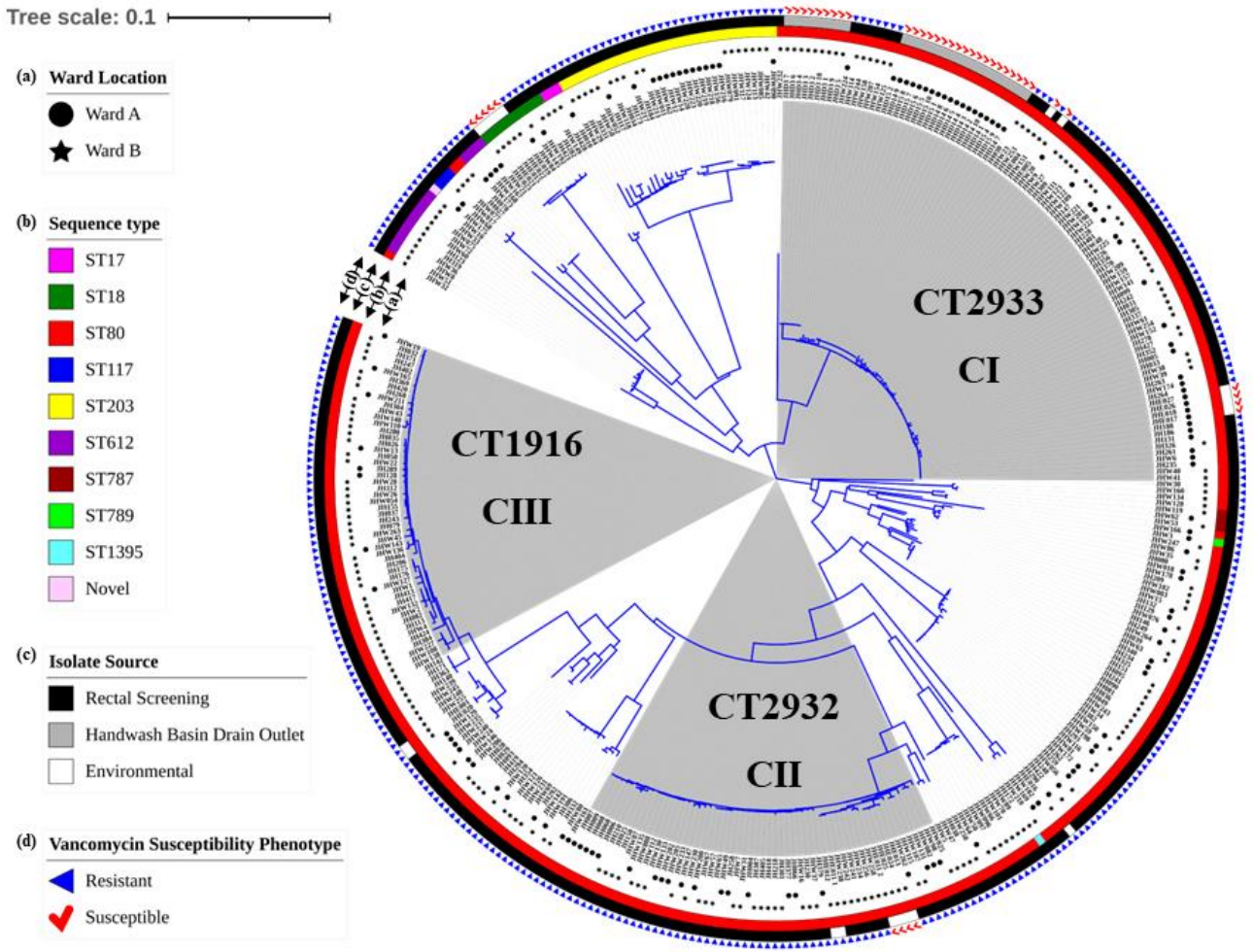

Figure 4.2: Neighbour joining tree (NJT) based on core-genome multilocus sequence type (cgMLST) analysis of 1,423 target genes for 378 clade A1 *Enterococcus faecium* isolates from two critical care wards (WA and WB) of a large Dublin acute hospital recovered between

September 2019 and December 2022. Isolates segregated into 27 clusters and 21 singletons. Three predominant clusters (CI, CII, CIII) of closely related isolates (≤20 allelic differences) were identified, which are shaded in grey with the corresponding complex type (CT) indicated; [CI] CT2933 (96 isolates): average allelic difference 7.9, range 0-21; [CII] CT2932 (58 isolates): average allelic difference 6.2, range 0-18; [CIII] CT1916 (52 isolates): average allelic difference 10.0, range 0-27. Detailed metadata pertaining to sequence type (ST), isolate source, ward location and vancomycin susceptibility phenotype are indicated in the legends. A tree scale bar is shown at the top left.

4.3.3 cgSNP analysis identifies closely related *E. faecium* subclusters

After broadly grouping isolates together using cgMLST clustering, further diversity within CI-CIII was investigated using a finer-scale analysis involving direct pairwise comparison using core genome alignment and pairwise distance calculations. To identify CT-specific subclusters, isolates were categorised into related isolate groups (RIGs) using a median pairwise cgSNP difference of ≤15 (Table 4.2). This threshold was based on reported annual *E. faecium* diversification estimates of 6-122 SNPs and the 39-month study duration (Moradigaravand *et al.,* 2017; Raven *et al.,* 2017; Bayjanov *et al.,* 2019; Dubin *et al.,* 2019). For clarity, only RIGs with ≥four isolates are described.

Table 4.2. Detailed descriptions of three major complex types (CI, CII, CIII), subclusters and their related isolate groups (RIGs) identified using cgMLST and cgSNP analysis of 378 clade A1 *Enterococcus faecium*[1] isolates from two critical care wards (W1 and W2) of a large Dublin acute hospital recovered between September 2019 and December 2022

	Clusters		
	CI	**CII**	**CIII**
ST/CT	ST80/CT2933	ST80/CT2932	ST80/CT1916
No. isolates	96	58	52
Source (*N*)	Rectal screening (62) Wash-hand basin drain outlet (28) Toilet seat (2) Cardiac monitor (2) Shower drain (2)	Rectal screening (52) Bedside table (6)	Rectal screening (52)
Median pairwise cgSNP difference (range)	25.5 (0-84)	17 (0-56)	30 (0-68)
Time period (days)	1172	1145	1174

	Sub-clusters					
	CIA	**CIB**	**CIIA**	**CIIB**	**CIIIA**	**CIIIB**
No. isolates	35	61	13	45	1	51
Source (*N*)	Rectal screening (7) Wash-hand basin drain outlet (28)	Rectal screening (55) Toilet seat (2) Cardiac monitor (2) Shower drain (2)	Rectal screening (7) Bedside table (6)	Rectal screening (45)	Rectal screening (1)	Rectal screening (51)
Median pairwise cgSNP difference (range)	26 (0-53)	14 (0-84)	15 (0-35)	9 (0-41)	-	28 (0-68)
Time period (days)	651	1146	46	779	-	1174

Table 4.2 continued overleaf

RIGs						
	No. isolates	**Isolate Source (*N*)**	**Median pairwise cgSNP difference (range)**	**Time period (days)**	**Vancomycin susceptibility phenotype (*N*)**	**Ward Distribution % (*N*)**
CIA1	9	Wash hand basin drain outlet (9)	0	0	VSEfm (9)	WB: 100% (9)
CIA2	19	Wash hand basin drain outlet (19)	0 (0-3)	0	VSEfm (19)	WA: 100% (19)
CIA3	4	Rectal screening (4)	3 (0-5)	112	VREfm (4)	WB: 100% (4)
CIB1	46	Rectal screening (40) Toilet seat (2) Cardiac monitor (2) Shower drain (2)	11 (0-19)	1143	VREfm (40) VSEfm (6)	WA: 37% (17) WB: 63% (29)
CIIA1	4	Bedside table (4)	1 (0-2)	0	VSEfm (6)	WB: 100% (4)
CIIA2	9	Rectal screening (7) Bedside table (2)	9 (0-19)	363	VREfm (9)	WB: 100% (9)
CIIB1	39	Rectal screening (39)	7 (0-24)	1144	VREfm (39)	WA: 44% (17) WB: 56% (22)
CIIIB1	4	Rectal screening (4)	3.5 (0-7)	505	VREfm (4)	WB: 100% (4)
CIIIB2	4	Rectal screening (4)	11 (0-18)	656	VREfm (4)	WB: 100% (4)
CIIIB3	27	Rectal screening (27)	8 (0-20)	687	VREfm (27)	WA: 22% (6) WB: 78% (21)

[1]All 330 rectal screening isolates were VREfm and 43/48 environmental isolates were VSEfm.

Abbreviations: ST, sequence type; CT, complex type; cgSNP, core-genome single nucleotide polymorphism; RIGs, related isolate groups; VSEfm, vancomycin susceptible *E. faecium*; VREfm, vancomycin resistant *E. faecium*; WA, Ward A; WB, Ward B.

4.3.3.1 CT Cluster CI

CI isolates exhibited a pairwise median SNP distance of 25 (average 26, range: 0-84). Two major subclusters were evident in an cgSNP MST based on 366 SNPs using the CI-specific reference JH005 (earliest CI isolate recovered), termed subcluster CIA (35 isolates (28 environmental and seven screening), median SNP difference: 26, range: 0-53) and subcluster CIB (61 isolates (six environmental and 55 screening), median SNP difference: 14, range: 0-84) (Figure 4.3). The MLT revealed further diversity within CIA and CIB; CIA segregated into three RIGs; CIA1 (nine environmental VSEfm, median SNP difference: 0), CIA2 (19 environmental VSEfm, median SNP difference: 0) and CIA3 (four screening VREfm, median SNP difference: three) (Table 4.3a-c). Subcluster CIB consisted of one major RIG, CIB1 (40 screening VREfm and six environmental VSEfm, median SNP difference: 11) and 15 intra-RIG outlier isolates (median pairwise SNP difference between isolates >15) (Figure 4.3, Table 4.3d-e).

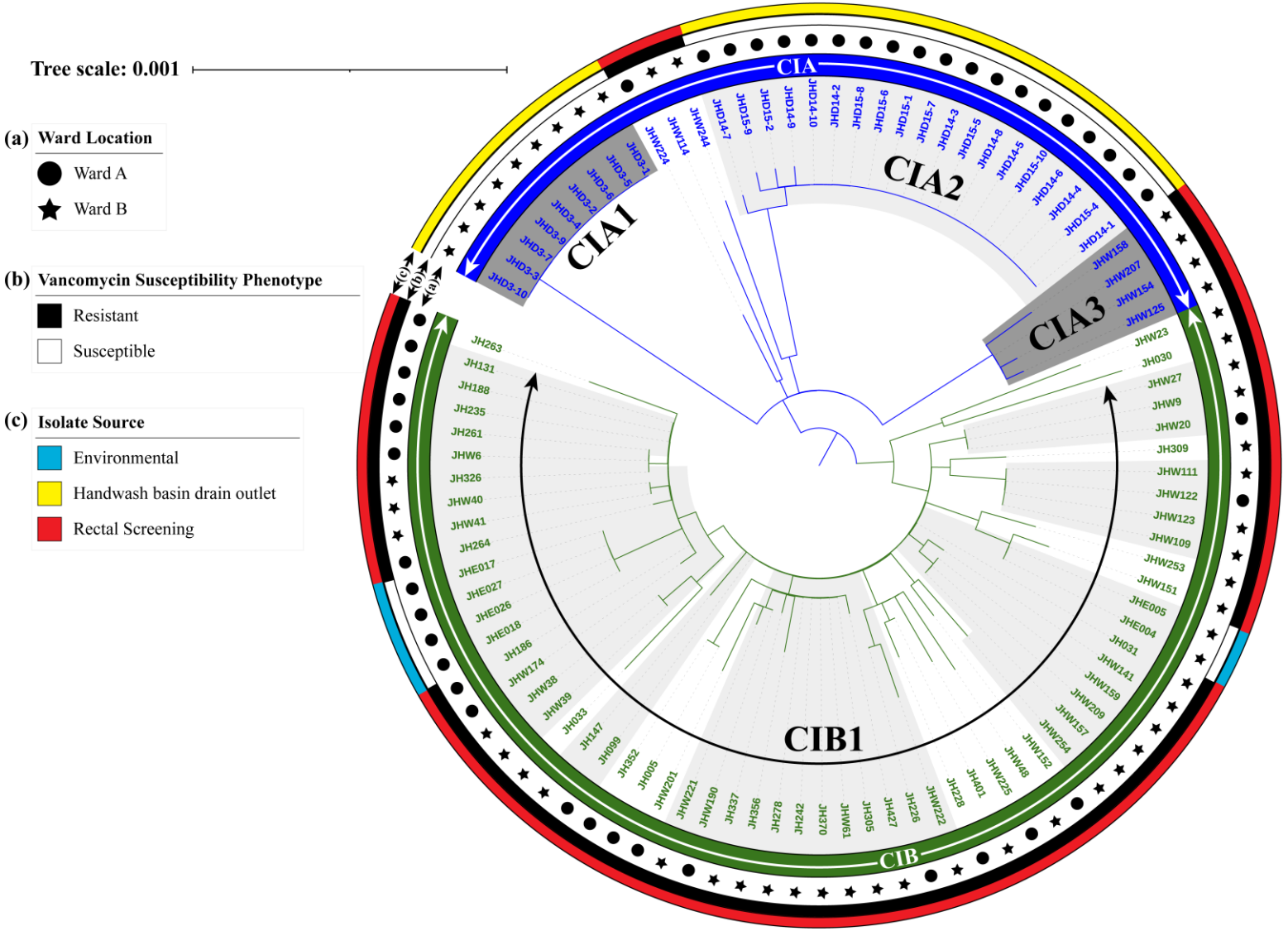
Tree scale: 0.001
(a) Ward Location
Ward A
Ward B
(b) Vancomycin Susceptibility Phenotype
Resistant
Susceptible
(c) Isolate Source
Environmental
Handwash basin drain outlet
Rectal Screening
CIA
CIA1
CIA2
CIA3
CIB
CIB1
(a)
(b)
(c)

Figure 4.3. MLT based on phylogenetic analysis of 366 core-genome single nucleotide polymorphisms (cgSNPs) for the 96 clade A1 *Enterococcus faecium* isolates belonging to CT2933 identified by cgMLST of isolates from wards WA and WA. Two major subclusters were evident within CT2933 in the MLT: sub-cluster A (CIA), represented by blue branches and inner blue ring and subcluster B (CIB), represented by green branches and inner green ring. Isolates recovered over the three-year study period that exhibited a median pairwise cgSNP difference of ≤15 were considered highly related and were further segregated into RIGs. Four distinct RIGS (≥ 4 isolates) were identified within CI (CIA1, CIA2, CIA3 and CIB1) which are shaded in dark and light grey with the corresponding labels indicated; CIA1 (9 isolates): median cgSNP distance 0, range 0, time between earliest and latest isolate 0 days; CIA2 (19 isolates) median cgSNP distance 0, range 0-3, time between earliest and latest isolate 0 days; CIA3 (4 isolates) median cgSNP distance 3, range 0-5, time between earliest and latest isolate 119 days; CIB1 (46 isolates) median cgSNP distance 11, range 0-19, time between earliest and latest isolate 1143 days. Metadata pertaining to isolate source, ward location and vancomycin susceptibility phenotype are indicated in the legend. A tree scale bar is shown at the top left. The tree is mid-point rooted. The corresponding cgSNP distance matrix for all isolates is provided in Table 4.4.

Table 4.3a. Detailed metadata and distance matrices based on pairwise cgSNP analysis of related isolate group CIA1 identified in sub-cluster CIA from CI (ST80/CT2933 lineage)

Total isolate number	Isolate name	Collection date	Source	Ward	cgSNP matrix									Median pairwise cgSNP difference (range)
					JHD3-1	**JHD3-10**	**JHD3-2**	**JHD3-3**	**JHD3-4**	**JHD3-5**	**JHD3-6**	**JHD3-7**	**JHD3-9**	
9	JHD3-1	15/12/2022	Handwash basin drain outlet	WB	**JHD3-1**									0
	JHD3-10				**JHD3-10**	0								
	JHD3-2				**JHD3-2**	0	0							
	JHD3-3				**JHD3-3**	0	0	0						
	JHD3-4				**JHD3-4**	0	0	0	0					
	JHD3-5				**JHD3-5**	0	0	0	0	0				
	JHD3-6				**JHD3-6**	0	0	0	0	0	0			
	JHD3-7				**JHD3-7**	0	0	0	0	0	0	0		
	JHD3-9				**JHD3-9**	0	0	0	0	0	0	0	0	

Abbreviations: cgSNP, Core-genome single nucleotide polymorphism; WB, Ward B.

Table 4.3b. Detailed metadata and distance matrices based on pairwise cgSNP analysis of related isolate group CIA2 identified in sub-cluster CIA from CI (ST80/CT2933 lineage)

Total isolate number	Isolate name	Collection date	Source	H1 Ward		cgSNP matrix																	Median pairwise cgSNP difference (range)
						JHD14-1	**JHD14-10**	**JHD14-2**	**JHD14-3**	**JHD14-4**	**JHD14-5**	**JHD14-6**	**JHD14-7**	**JHD14-8**	**JHD14-9**	**JHD15-1**	**JHD15-10**	**JHD15-2**	**JHD15-4**	**JHD15-5**	**JHD15-6**	**JHD15-7**	**JHD15-8**	**JHD15-9**	
19	JHD14-1	15/12/2022	Handwash basin drain outlet	WA	**JHD14-1**																			
	JHD14-10				**JHD14-10**	0																		
	JHD14-2				**JHD14-2**	0	0																	
	JHD14-3				**JHD14-3**	0	0	0																
	JHD14-4				**JHD14-4**	0	0	0	0															
	JHD14-5				**JHD14-5**	0	0	0	0	0														
	JHD14-6				**JHD14-6**	0	0	0	0	0	0													
	JHD14-7				**JHD14-7**	2	2	2	2	2	2	2													0 (0-3)
	JHD14-8				**JHD14-8**	0	0	0	0	0	0	0	2											
	JHD14-9				**JHD14-9**	1	1	1	1	1	1	1	3	1										
	JHD15-1				**JHD15-1**	0	0	0	0	0	0	0	2	0	1									
	JHD15-10				**JHD15-10**	0	0	0	0	0	0	0	2	0	1	0								
	JHD15-2				**JHD15-2**	1	1	1	1	1	1	1	3	1	2	1	1							
	JHD15-4				**JHD15-4**	0	0	0	0	0	0	0	2	0	1	0	0	1						
	JHD15-5				**JHD15-5**	0	0	0	0	0	0	0	2	0	1	0	0	1	0					
	JHD15-6				**JHD15-6**	0	0	0	0	0	0	0	2	0	1	0	0	1	0	0				
	JHD15-7				**JHD15-7**	0	0	0	0	0	0	0	2	0	1	0	0	1	0	0	0			
	JHD15-8				**JHD15-8**	0	0	0	0	0	0	0	2	0	1	0	0	1	0	0	0	0		
	JHD15-9				**JHD15-9**	1	1	1	1	1	1	1	3	1	2	1	1	2	1	1	1	1	1	

Abbreviations: cgSNP, Core-genome single nucleotide polymorphism; H1, Hospital 1; WA, Ward A.

Table 4.3c. Detailed metadata and distance matrices based on pairwise cgSNP analysis of related isolate group CIA3 identified in sub-cluster CIA from CI (ST80/CT2933 lineage)

Total isolate number	Isolate name	Collection date	Source	H1 Ward	cgSNP matrix					Median pairwise cgSNP difference (range)
						JHW125	**JHW154**	**JHW158**	**JHW207**	
	JHW125	14/04/2021			**JHW125**					
4	JHW154	04/08/2021	Rectal screening	WB	**JHW154**	2				3 (0-5)
	JHW158	11/08/2021			**JHW158**	5	5			
	JHW207	04/08/2021			**JHW207**	1	1	4		

Abbreviations: cgSNP, Core-genome single nucleotide polymorphism; H1, Hospital 1; WB, Ward B.

Table 4.3d. Detailed metadata and distance matrices based on pairwise cgSNP analysis of related isolate group CIB1 identified in sub-cluster CIA from CI (ST80/CT2933 lineage)

Size of table exceeds page margins.

Scan and/or click QR code to access and/or download table.

4.3.3.2 CT Cluster CII

CII (CT2932) isolates exhibited a pairwise median SNP distance of 17 (average: 21, range: 0-56) based on 220 SNPs. Two major subclusters were evident in a cgSNP-based MLT using the CII-specific JH004 reference (earliest CII isolate), termed sub-clusters CIIA and CIIB (Figure 4.4). Subcluster CIIA isolates (*N*=13) (seven screening VREfm, four environmental VREfm and two environmental VSEfm) exhibited a median SNP distance of 15. Subcluster CIIB isolates (45 screening VREfm) exhibited a median SNP distance of nine. Subcluster CIIA comprised two major RIGs; CIIA1 (four environmental VSEfm, median SNP distance: one) and CIIA2 (seven screening VREfm and two environmental VREfm, median SNP distance: nine) (Table 4.5a-b). Subcluster CIIB comprised one major RIG (CIIB1) (39 screening VREfm, median SNP distance: seven) (Table 4.5c-d).

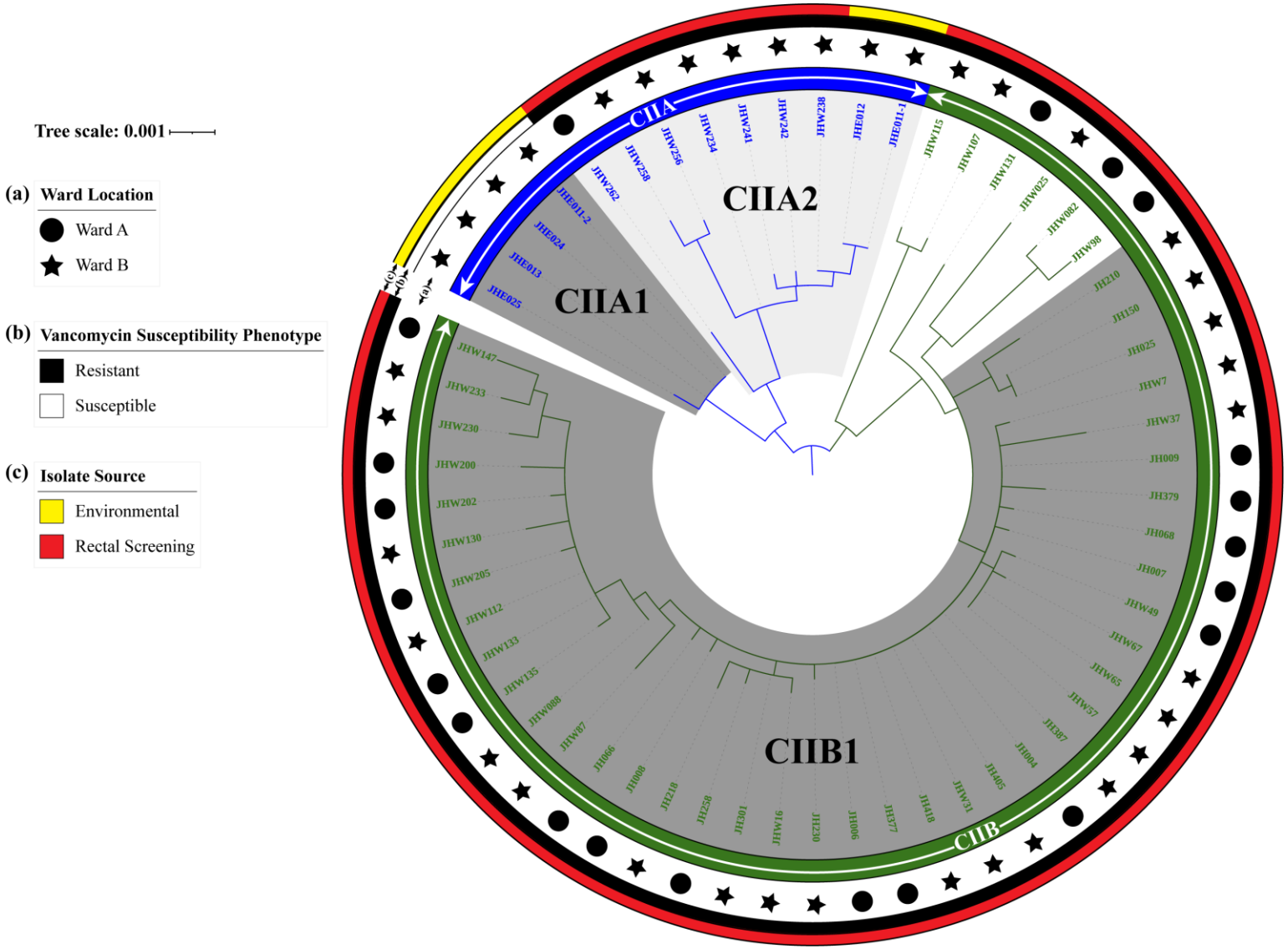
Tree scale: 0.001
(a) Ward Location
Ward A
Ward B
(b) Vancomycin Susceptibility Phenotype
Resistant
Susceptible
(c) Isolate Source
Environmental
Rectal Screening
CIIA
CIIA2
CIIA1
CIIB1
CIIB
(c)
(b)
(a)
JHE011-1
JHE012
JHW282
JHW241
JHW242
JHW234
JHW256
JHW258
JHW262
JHE011-2
JHE024
JHE013
JHE025
JHW115
JHW107
JHW131
JHW025
JHW082
JHW98
JH210
JH150
JH025
JHW7
JHW37
JH009
JH379
JH068
JH007
JHW49
JHW67
JHW65
JHW57
JH387
JH004
JH405
JHW31
JH418
JH377
JH006
JH230
JHW16
JH303
JH258
JH218
JH008
JH066
JHW87
JHW088
JHW135
JHW133
JHW112
JHW205
JHW130
JHW202
JHW200
JHW230
JHW233
JHW147

Figure 4.4. MLT based on phylogenetic analysis of 220 cgSNPs for the 58 clade A1 *Enterococcus faecium* isolates from clonal complex CT12932 (referred to as CII) identified by cgMLST of isolates from two wards of a large Dublin acute hospital between September 2019 and December 2022. Two major subclusters were evident within CII in the MLT: subcluster A (CIIA), represented by blue branches and inner blue ring and subcluster B (CIIB), represented by green branches and inner green ring. Isolates recovered over the three-year study period which exhibited a median pairwise cgSNP difference of ≤15 were considered closely related and were further segregated into related isolate groups (RIGs). Three distinct RIGS (≥ 4 isolates) were identified within CII (CIIA1, CIIA2 and CIIB1) which are shaded in dark and light grey with the corresponding labels indicated accordingly; CIIB (4 isolates): median cgSNP distance 1, range 0-2, time between earliest and latest isolate 0 days; CIIA2 (9 isolates) median cgSNP distance 9, range 0-19, time between earliest and latest isolate 363 days; CIIB1 (39 isolates) median cgSNP distance 8, range 0-24, time between earliest and latest isolate 779 days. Detailed metadata pertaining to isolate source, ward location and vancomycin susceptibility phenotype are indicated in the legend. A tree scale bar is shown at the top left. The tree is mid-point rooted.

Table 4.4a Detailed metadata and distance matrices based on cgSNP analysis of related isolate group CIIA1 identified in sub-cluster CIIA from CII (ST80/CT2932 lineage)

Total isolate number	Isolate name	Collection date	Source	H1 Ward	cgSNP matrix					Median pairwise cgSNP difference (range)
						JHE011-2	**JHE013**	**JHE024**	**JHE025**	
4	JHE011-2 JHE013 JHE024 JHE025	18/11/2022	Bedside table	WB	**JHE011-2** **JHE013** **JHE024** **JHE025**	0 0 2	0 2	2		1 (0-2)

Abbreviations: cgSNP, Core-genome single nucleotide polymorphism; H1, Hospital 1; WB, Ward B.

Table 4.4b Detailed metadata and distance matrices based on cgSNP analysis of related isolate group CIIA2 identified in sub-cluster CIIA from CII (ST80/CT2932 lineage)

Total isolate number	Isolate name	Collection date	Source (N)	H1 Ward		cgSNP matrix									Median pairwise cgSNP difference (range)
						JHE011-1	**JHE012**	**JHW234**	**JHW238**	**JHW241**	**JHW242**	**JHW256**	**JHW258**	**JHW262**	
9	JHE011-1	18/11/2022	Bedside table	WB	**JHE011-1**										9 (0-19)
	JHE012	18/11/2022	Bedside table	WB	**JHE012**	0									
	JHW234	24/11/2021	Rectal screening	WB	**JHW234**	4	4								
	JHW238	12/01/2022	Rectal screening	WB	**JHW238**	2	2	2							
	JHW241	20/01/2022	Rectal screening	WB	**JHW241**	4	4	2	2						
	JHW242	02/02/2022	Rectal screening	WB	**JHW242**	4	4	2	2	2					
	JHW256	06/09/2022	Rectal screening	WB	**JHW256**	12	12	8	10	10	10				
	JHW258	07/09/2022	Rectal screening	WB	**JHW258**	12	12	8	10	10	10	4			
	JHW262	22/11/2022	Rectal screening	WA	**JHW262**	15	15	11	13	13	13	19	19		

Abbreviations: cgSNP, Core-genome single nucleotide polymorphism; H1, Hospital 1; WA, Ward A; WB, Ward B.

Table 4.4c. Detailed metadata and distance matrices based on cgSNP analysis of related isolate group CIIB1 identified in sub-cluster CIIA from CII (ST80/CT2932 lineage)

Size of table exceeds page margins.

Scan and/or click QR code to access and/or download table.

4.3.3.3 CT Cluster CIII

CIII (CT1916) isolates (*N*=52) exhibited a pairwise median SNP distance of 30 (range 0-68), using the CIII-specific JH026 reference (earliest CIII isolate) based on 341 SNPs. CIII isolates were more clonal, with isolate JH424 forming an out-group (CIIA) and the rest forming one major subcluster (CIIIB) (median SNP distance: 28) (Figure 4.4). CIIIB comprised three RIGS; CIIIB1 (four screening VREfm, median SNP difference: 3.5), CIIIB2 (four screening VREfm, median SNP difference: 11) and CIIIB3 (27 screening VREfm, median SNP difference: eight) (Tables 4.4a-c). CIIIB3 comprised over 52% (27/52) of CIII isolates and contained six intra-RIG outliers (median SNP difference >15).

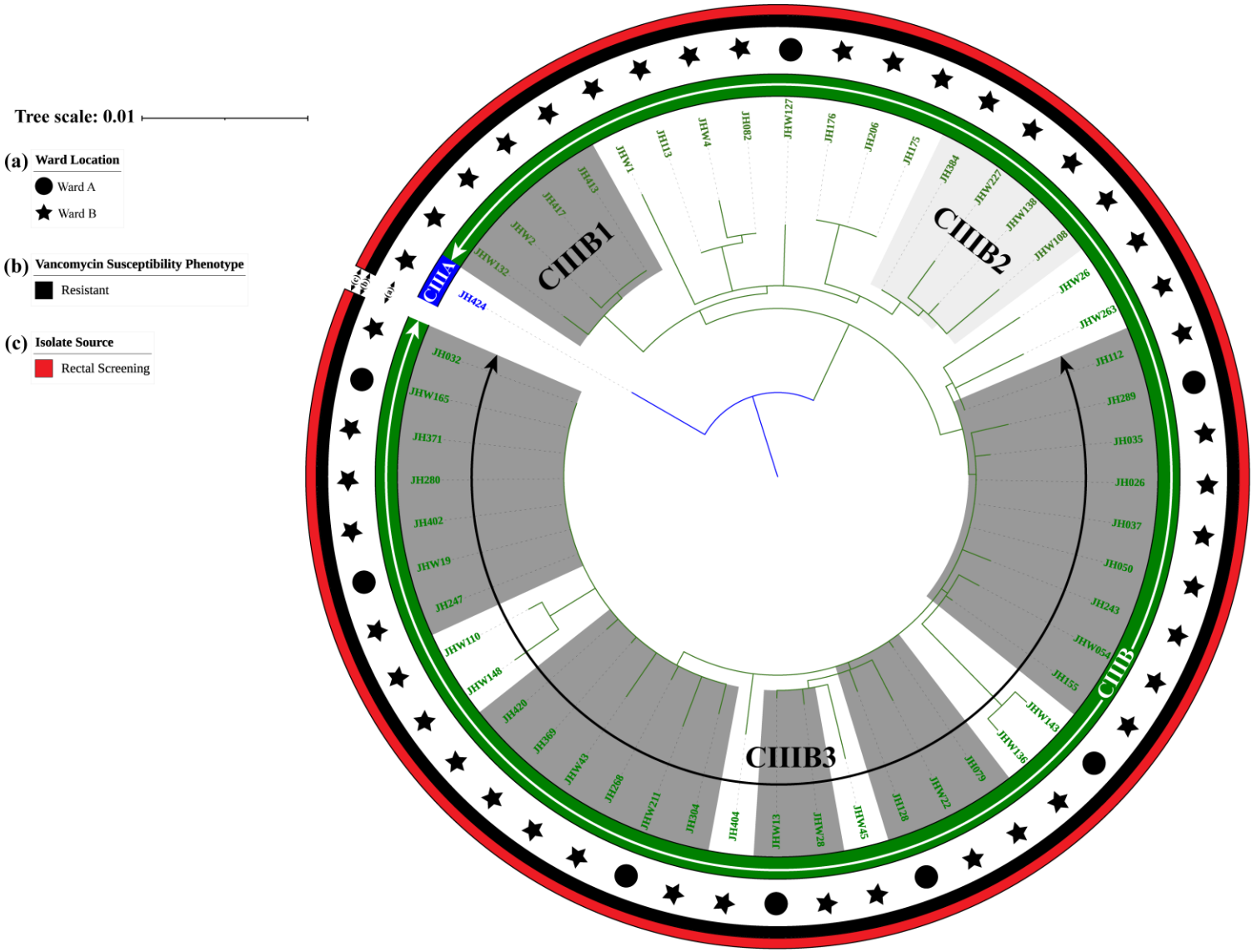
Tree scale: 0.01
(a) Ward Location
Ward A
Ward B
(b) Vancomycin Susceptibility Phenotype
Resistant
(c) Isolate Source
Rectal Screening
CIIIA
CIIIB1
CIIIB2
CIIIB3
CIIIB
JH424
JHW132
JH413
JH417
JHW2
JHW1
JH113
JHW4
JH282
JHW127
JH176
JH206
JH175
JH384
JHW227
JHW138
JHW108
JHW26
JHW263
JH112
JH289
JH035
JH026
JH037
JH050
JH243
JHW054
JH155
JHW143
JHW136
JH079
JHW22
JH128
JHW45
JHW28
JHW13
JH404
JH384
JHW211
JH268
JHW43
JH369
JH420
JHW148
JHW110
JH247
JHW19
JH402
JH280
JH371
JHW165
JH032

Figure 4.5. MLT based on phylogenetic analysis of 341 cgSNPs for the 52 clade A1 *Enterococcus faecium* isolates from clonal complex CT1916 (referred to as CTIII) identified by cgMLST of isolates from two wards of a large Dublin acute hospital between September 2019 and December 2022. One isolate formed an out-group (JH424) termed CIIA and is represented by the blue branch and inner blue ring labelled CIIIA. The remaining isolates belonged to one major subcluster termed CIIIB, represented by green branches and the inner green ring labelled CIIIB. Isolates recovered over the three-year study period that exhibited a median pairwise cgSNP difference of ≤15 were considered closely related and were further segregated into related isolate groups (RIGs). Three distinct RIGS (≥ 4 isolates) were identified within CIII (CIIIB1, CIIIB2 and CIIIB3) which are shaded in dark and light grey with the corresponding labels indicated accordingly; CIIIB1 (4 isolates): median cgSNP distance 3.5, range 0-7, time between earliest and latest isolate 505 days; CIIIB2 (4 isolates) median cgSNP distance 11, range 0-18, time between earliest and latest isolate 656 days; CIIIB3 (27 isolates) median cgSNP distance 8, range 0-20, time between earliest and latest isolate 687 days. Isolates within CIIIB3 (N=6) which are not shaded in grey and exhibited a median pairwise cgSNP of >15 were excluded from the RIG and considered to be intra-RIG outliers. Detailed metadata pertaining to isolate source, ward location and vancomycin susceptibility phenotype are indicated in the legend. A tree scale bar is shown at the top left. The tree is mid-point rooted.

Table 4.5a. Detailed metadata and distance matrices based on cgSNP analysis of related isolate group CIIIB1 identified in sub-cluster CIIIB from CIII (ST80/CT1916 lineage)

Total isolate number	Isolate name	Collection date	Source	H1 Ward		cgSNP matrix				Median pairwise cgSNP difference (range)
						JH413	**JH417**	**JHW132**	**JHW2**	
	JH413	24/12/2019			**JH413**					
4	JH417	25/12/2019	Rectal screening	WB	**JH417**	0				3.5 (0-7)
	JHW132	12/05/2021			**JHW132**	5	5			
	JHW2	01/01/2020			**JHW2**	2	2	7		

Abbreviations: cgSNP, Core-genome single nucleotide polymorphism; H1, Hospital 1; WB, Ward B.

Table 4.5b. Detailed metadata and distance matrices based on cgSNP analysis of related isolate group CIIIB2 identified in sub-cluster CIIIB from CIII (ST80/CT1916 lineage)

Total isolate number	Isolate name	Collection date	Source	H1 Ward		cgSNP matrix				Median pairwise cgSNP difference (range)
						JH384	**JHW108**	**JHW138**	**JHW227**	
4	JH384	13/12/2019	Rectal screening	WB	**JH384**					11 (0-18)
	JHW108	17/02/2021			**JHW108**	11				
	JHW138	04/06/2021			**JHW138**	5	15			
	JHW227	29/09/2021			**JHW227**	8	18	11		

Abbreviations: cgSNP, Core-genome single nucleotide polymorphism; H1, Hospital 1; WB, Ward B.

Table 4.5c. Detailed metadata and distance matrices based on cgSNP analysis of related isolate group CIIIB2 identified in sub-cluster CIIIB from CIII (ST80/CT1916 lineage)

Size of table exceeds page margins.

Scan and/or click QR code to access and/or download table.

4.3.4 VRE transmission and persistence

To investigate isolate transmission, a more stringent cgSNP threshold of ≤10 SNPs was adopted to define closely related isolates based on previous surveillance studies, mutational rates, and intra-patient isolate diversity (Pinholt *et al.,* 2015; Raven *et al.,* 2017; Gouliouris *et al.,* 2020; Higgs *et al.,* 2022). Isolates attributed to the same cgSNP sub-clusters and RIGs were investigated according to their likely epidemiological linkage based on recovery date and ward. The mean patient length of stay during the study was 11.3 days for WA and 12.3 days for WB. During the study period, the mean glycopeptide use per quarter in defined daily doses (DDDs)/100 bed days was 7.35 for WA and 5.38 for WB. Isolates recovered on the wards within ≤30 days were deemed to be epidemiologically linked, whereas isolates recovered >30 days were deemed to have no evident epidemiological linkage.

4.3.4.1 CI

CI (*N=96*) comprised 4,608 potential isolate pairs with 667 exhibiting ≤10 cgSNPs. To gain insights into the directionality of potential transmissions, a parsimonious transmission tree based on the SeqTrack algorithm was constructed (Figure 4.6), which determines the most plausible genealogy for isolate sets based on recovery date and ward location (Jombart *et al.,* 2011; Permana *et al.,* 2023). Forty-six percent (29/62) of CI patient isolates were likely involved in 23 transmissions with epidemiological support (blue branches in Figure 4.6), whilst the remaining CI-specific environmental isolates (*N*=34) could not be linked to any patient isolate within the 30-day timeframe.

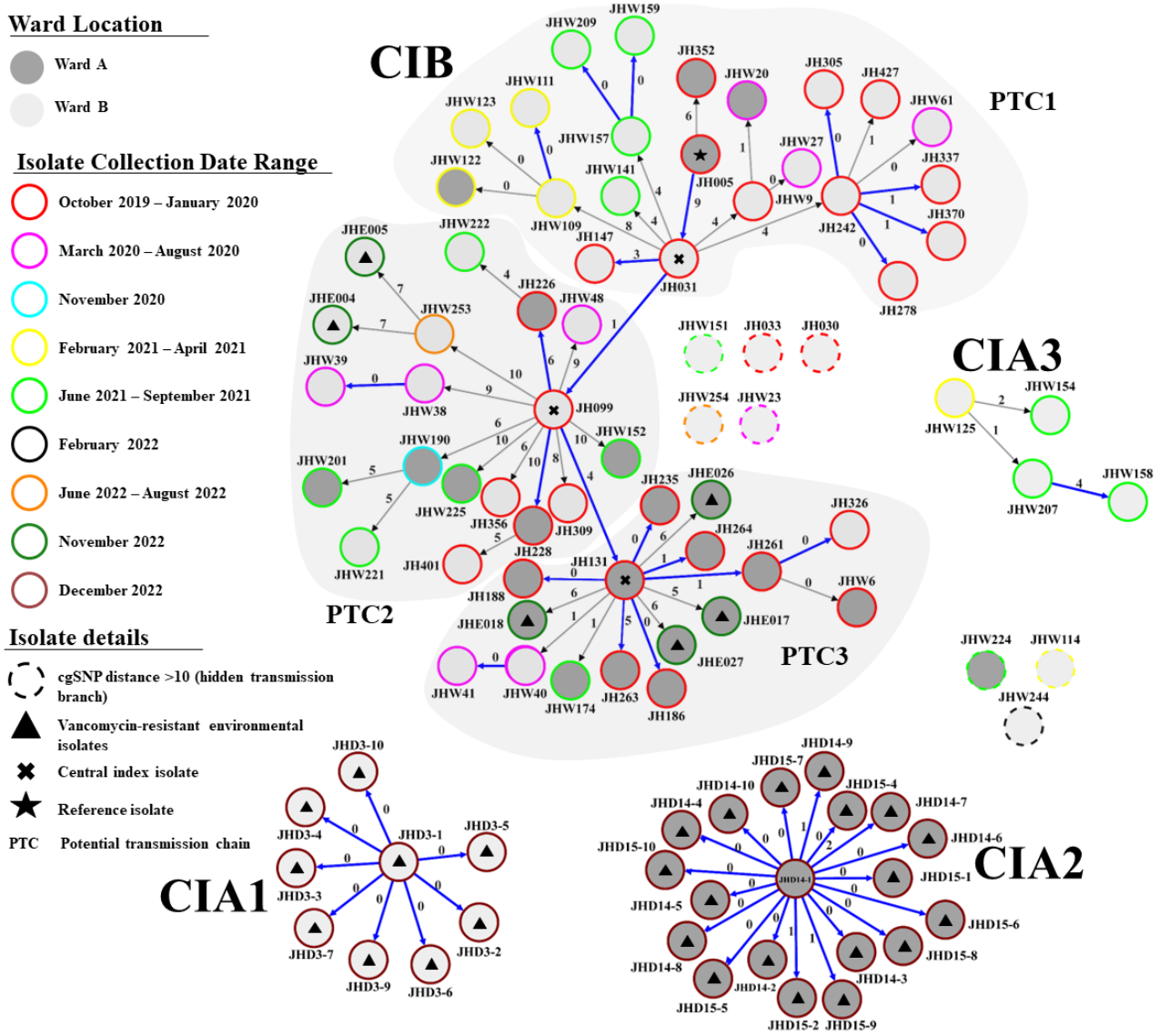
Ward Location
Ward A
Ward B
Isolate Collection Date Range
October 2019 – January 2020
March 2020 – August 2020
November 2020
February 2021 – April 2021
June 2021 – September 2021
February 2022
June 2022 – August 2022
November 2022
December 2022
Isolate details
cgSNP distance >10 (hidden transmission branch)
Vancomycin-resistant environmental isolates
Central index isolate
Reference isolate
PTC Potential transmission chain
CIB
PTC1
PTC2
PTC3
CIA1
CIA2
CIA3

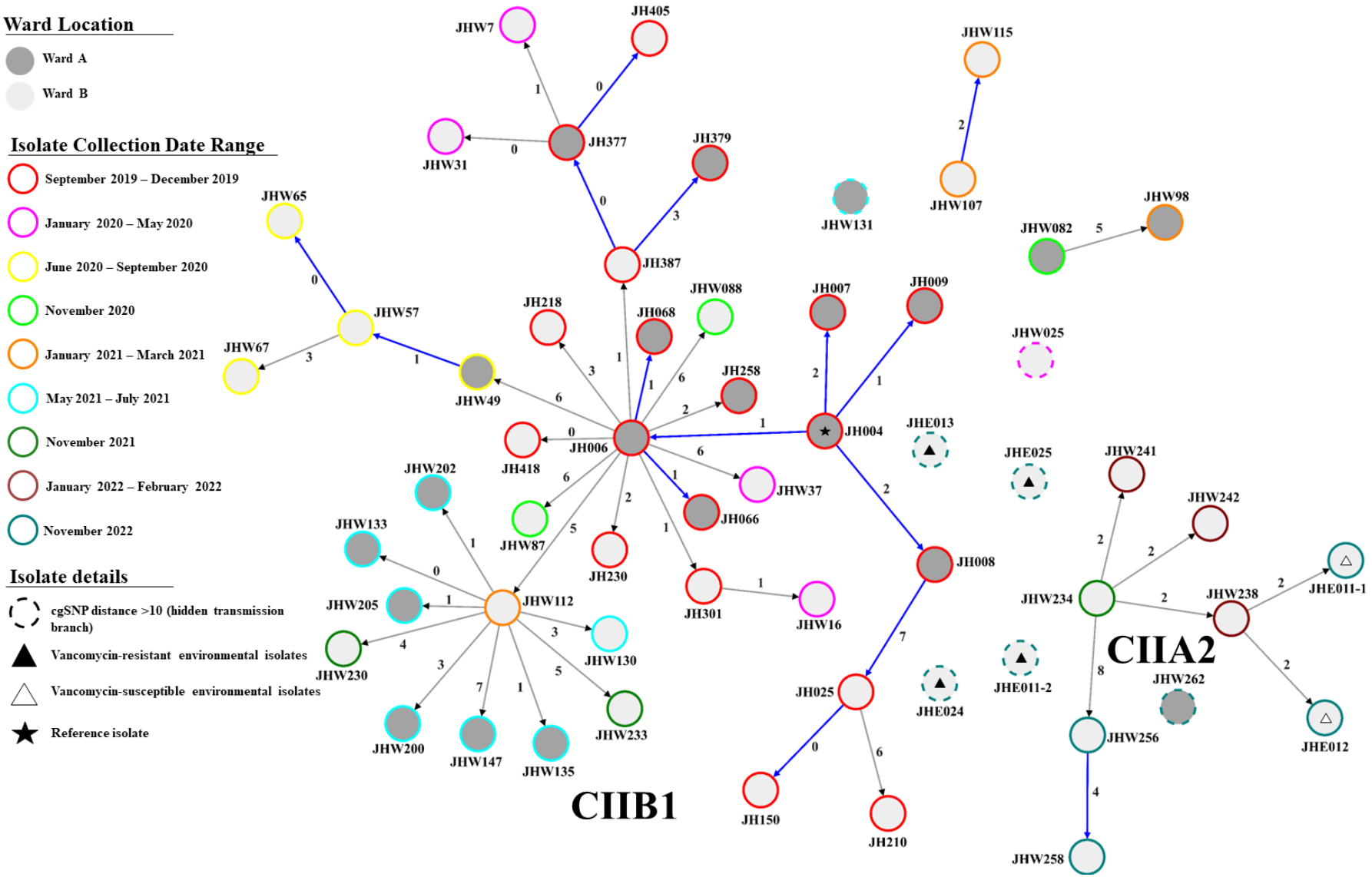
Ward Location
Ward A
Ward B
Isolate Collection Date Range
September 2019 – December 2019
January 2020 – May 2020
June 2020 – September 2020
November 2020
January 2021 – March 2021
May 2021 – July 2021
November 2021
January 2022 – February 2022
November 2022
Isolate details
cgSNP distance >10 (hidden transmission branch)
Vancomycin-resistant environmental isolates
Vancomycin-susceptible environmental isolates
Reference isolate
JHW7
JH405
JHW31
JH377
JH379
JH387
JHW115
JHW107
JHW131
JHW65
JHW57
JHW67
JHW49
JH218
JH068
JHW088
JH258
JH006
JH418
JHW202
JHW87
JHW37
JH066
JH230
JH301
JHW16
JHW133
JHW205
JHW112
JHW230
JHW130
JHW200
JHW147
JHW135
JHW233
CIIB1
JH007
JH009
JH004
JHW082
JHW98
JHW025
JHE013
JHE025
JHW241
JHW242
JH008
JHW234
JHW238
JHE011-1
JHE011-2
JHW262
JHE024
JH025
JHW256
JHE012
JH150
JH210
JHW258
CIIA2

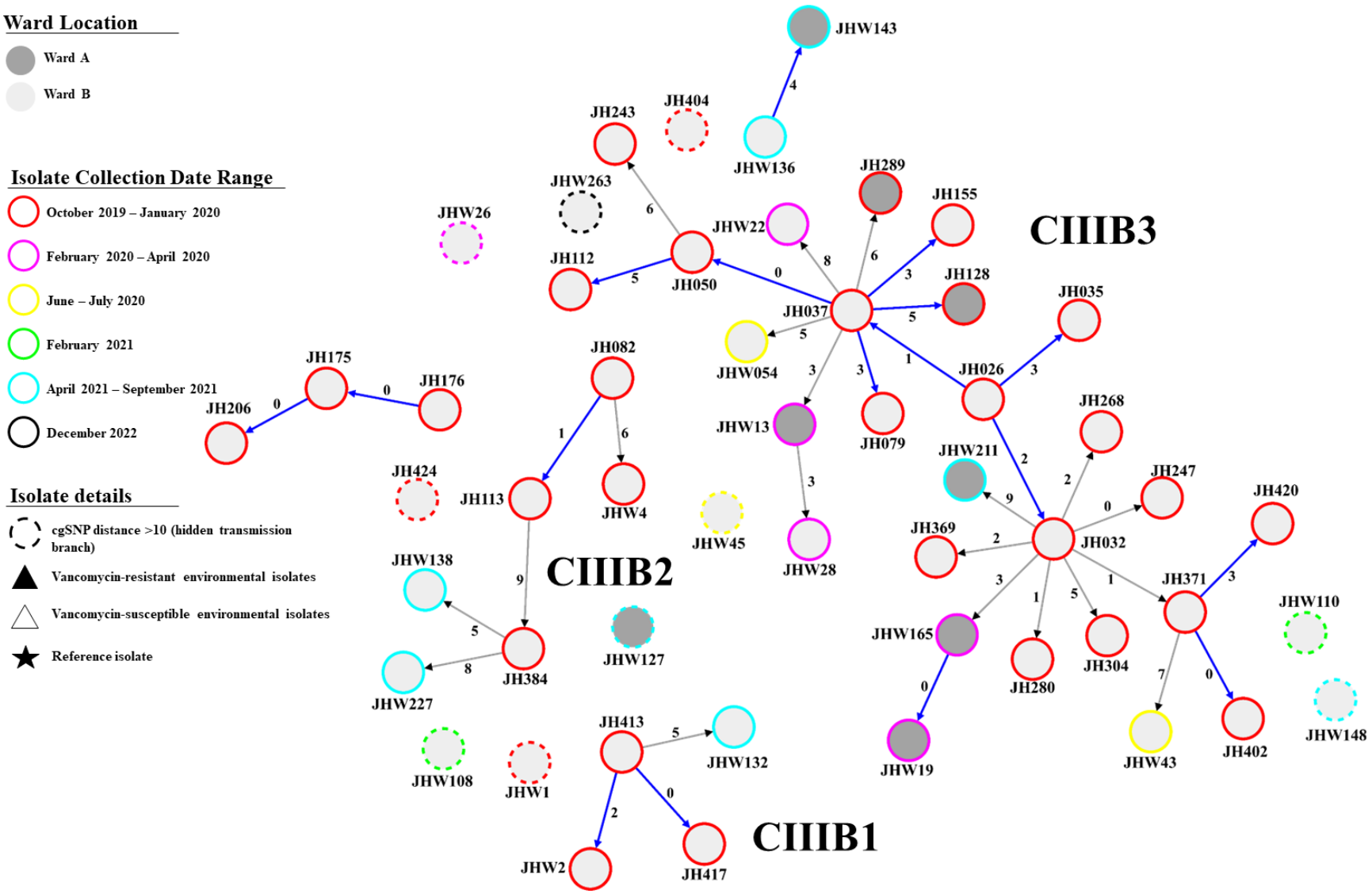
Ward Location
Ward A
Ward B
Isolate Collection Date Range
October 2019 – January 2020
February 2020 – April 2020
June – July 2020
February 2021
April 2021 – September 2021
December 2022
Isolate details
cgSNP distance >10 (hidden transmission branch)
Vancomycin-resistant environmental isolates
Vancomycin-susceptible environmental isolates
Reference isolate
JHW143
JH243
JH404
JHW136
JHW263
JH289
JH155
JHW26
JHW22
JH112
JH050
JH128
JH035
JH037
JHW054
JH082
JH175
JH176
JH206
JH026
JH268
JHW13
JH079
JHW211
JH247
JH424
JH113
JHW4
JH420
JHW45
JHW28
JH369
JH032
JHW138
JHW127
JH371
JHW110
JHW165
JH384
JH280
JH304
JHW227
JHW108
JHW1
JH413
JHW132
JHW19
JHW43
JH402
JHW148
JHW2
JH417
CIIIB3
CIIIB2
CIIIB1

Figure 4.6. Parsimonious transmission tree based on cgSNP distance and collection date of 96 clade A1 *Enterococcus faecium* isolates from the ST80/CT2933 lineage (referred to as CI) recovered from wards WA and WB between September 2019 and December 2022. The tree was generated using the SeqTrack algorithm with GraphSNP which determines the most plausible genealogy for isolate sets based on recovery date and ward location (Jombart *et al.,* 2011; Permana *et al.,* 2023). Isolates are represented by shaded circular nodes with inner node shading indicating ward location as shown in the legend. Node outer ring colour refers to isolate recovery date range as shown in the legend. Isolate names are shown outside the nodes. Isolate nodes connected by blue network branches share over-lapping recovery dates of ≤30 days. Transmission links for isolates with a cgSNP distance of >10 are hidden and are indicated with a dashed outer node ring. Numbers on the network branches show cgSNP distances. The earliest CI isolate (JH005) used as a reference for cgSNP analysis is indicated by the black star within the node. Three central presumptive index isolates (JH031, JH099 and JH0131) within CIB (indicated by a × symbol within the nodes) with epidemiological links recovered from one WA patient and two WB patients over 20 days (median cgSNP difference: 4, range: 0-10), were likely involved in three potential transmission chains (PTCs), which are highlighted by background shading. A significant proportion of likely isolate transmissions with epidemiological support was evident within all three PTCs. Vancomycin-susceptible environmental isolates are indicated by a black triangle within the nodes. Branches not to scale. An MLT based on phylogenetic analysis of 341 cgSNPs for the 96 CI isolates is shown in Figure 4.3.

CI RIGs CIA1 and CIA2 (Figure 4.6, Table 4.4a-b) contained 28 VSEfm from three washbasin drain outlets on WA and WB and differed from their closest neighbouring patient isolate by 24 cgSNPs (range: 24-79). This indicates that the sampled handwash basin drain outlets were not involved in likely transmission events. Additionally, the close relatedness of isolates within CIA1 and CIA2 reflect multiple colony picks from individual drain outlets (*N*=3) and represents within-drain diversity. CI RIG CIA3 contained four WB patient VREfm with a median pairwise SNP difference of three (range: 0-5). The earliest isolate, JHW125, was recovered 112 days prior to the other three with no evident epidemiological linkage. However, these three isolates were recovered on over-lapping dates (≤7) days suggesting potential direct transmission (Figure 4.5, Table 4.4c).

Subcluster CIB was more complex and comprised 61 isolates from 19 WA patients, four WA environmental sources, 36 WB patients and two WB environmental sources over 37 months (October 2019-November 2022; 1143 day) with an average pairwise cgSNP difference of 14 (range 0-84). Of the 1,861 potential CIB isolate pairs, 454 exhibited a pairwise cgSNP difference of ≤10. Three presumptive index VREfm were identified (JH031, JH099 and JH0131; marked with an × in Figure 4.4) with epidemiological links recovered from one WA patient and two WB patients over 20 days (median cgSNP difference: 4, range: 0-10), which were likely involved in three potential transmission chains (PTCs).

PTC1-PTC3 comprised 22, 21 and 16 isolates, respectively. A significant proportion of likely transmissions with epidemiological support across both wards within all three PTCs could be attributed to the index isolates (i.e., 11/24 (46%) patient isolates connected to index isolates by immediate network branches). However, intermediary isolates (e.g., PTC1 isolates JHW157, JHW159 and JHW209; median SNP difference: 0) also provide evidence of spread between patients on the same wards on coinciding dates. The first chain, termed PTC1, comprised 22 isolates (including JH031) within CIB recovered from four WA patients and 18 WB patients collected over 683 days (October 2019-August 2021) which exhibited a median pairwise cgSNP difference of seven (range: 0-18). The earliest collected isolate (JH005; marked with a star in Figure 4.6) recovered on WA, could be epidemiologically linked to the first presumptive index isolate (JH031) recovered from a WB patient two days later. However, there was no evident epidemiological links between the presumptive index isolate (JH031) and any other isolate within this transmission chain. The closest isolate (three cgSNPs, JH147) to the

presumptive index isolates was recovered on WB 34 days later. Four patient WB isolates with later, non-overlapping collection dates (i.e., >30 days) with the index isolate JH031 (JH242, JHW9, JHW157 and JH109) appear to be linked with the remaining suspected transmission events. This is indicative of a long-term ward-specific outbreak and suggests both direct transmission between patients that were present on the same ward on coinciding dates (e.g., patient JHW157, JHW159 and JHW209, median SNP difference: 0) and indirect transmission between patients occupying the same ward months apart (e.g., patient JHW242 and JHW61, SNP difference: 0). These findings also provide evidence of hospital dissemination from a potential common source(s), with very closely related isolates recovered on different wards with no apparent epidemiological link (e.g., patient JHW9 and JHW20, SNP difference: 1, time between isolates: 40 days) (Figure 4.4).

Simultaneously, the WB VRE PTC1 index isolate JH031 was epidemiologically linked to WB isolate JH099 recovered 12 days later. JH099 formed the presumptive index isolate for PTC2 (marked with an × in Figure 4.6). Fifteen rectal isolates within PTC2 (WA: *N*=5, WB: *N*=11) spanning 36 months (1124 days) exhibited ≤10 cgSNPs from JH099. Two VRE WA isolates (JH226 and JH228) shared over-lapping recovery dates (i.e., <30 days) with JH099, with a median pairwise cgSNP distance of eight (range: 6-10) suggesting direct transmission. There was no evident epidemiological links between the remaining isolates (all recovered >30 days of JH099) within the PTC2 transmission chain and JH099, once again suggesting indirect transfer from a potential common source(s). This is further emphasised by the recovery of two WA environmental VSE (JHE004, JHE005) from a toilet seat 37 months later (1144 days) which exhibited median pairwise cgSNP differences of 8.5 and 9.5, respectively, from the PTC1 and PTC2 presumptive index isolates JH031 and JH099.

The third presumptive transmission chain involving CIB isolates, PTC3, included eight WA patient (including the presumed index isolate JH131), four WA environmental isolates and three WB patient isolates recovered over a 36-month period (October 2019-November 2022; 1120 days) with a pairwise median cgSNP difference of 6 (range: 0-11). Six WA patient isolates within this chain (JH186, JH188, JH235, JH261, JH263 and JH264) shared overlapping collection dates (≤30 days, October 2019-November 2019) with the presumptive index isolate (JH131) suggesting direct transmission. There was also evidence of indirect transmission, with two WB patient isolates (JHW40 and JHW41) recovered 208 and 215 days after the PTC3 index WA isolate JH131, with a

median pairwise cgSNP difference of 1. Interestingly, four environmental VSE isolated from a cardiac monitor and shower drain outlets on W1 recovered 29 months (905 days) after the index case (JH131) with a median pairwise cgSNP difference of six suggesting environmental persistence. These findings also suggest that multiple simultaneous outbreaks of genomically distinct isolates within the same CT may be on-going both within and across multiple wards within the same hospital.

4.3.4.2 CII and CIII

The next two largest CT isolate groups, CII (*N*=58) and CIII (*N*=52) comprised a total of 1,682 and 1,352 potential isolate pairs, respectively, with 1,318 and 662 exhibiting ≤10 cgSNPs (Table 4.4a-c and Table 4.5a-c). Similar findings of likely patient-to-patient transmission with apparent epidemiological links and indirect transfer from an unsampled carrier and/or communal source were observed with CII and CIII isolates (Figure 4.7 and 4.8), with 15 and 17 transmissions with epidemiological support evident, respectively.

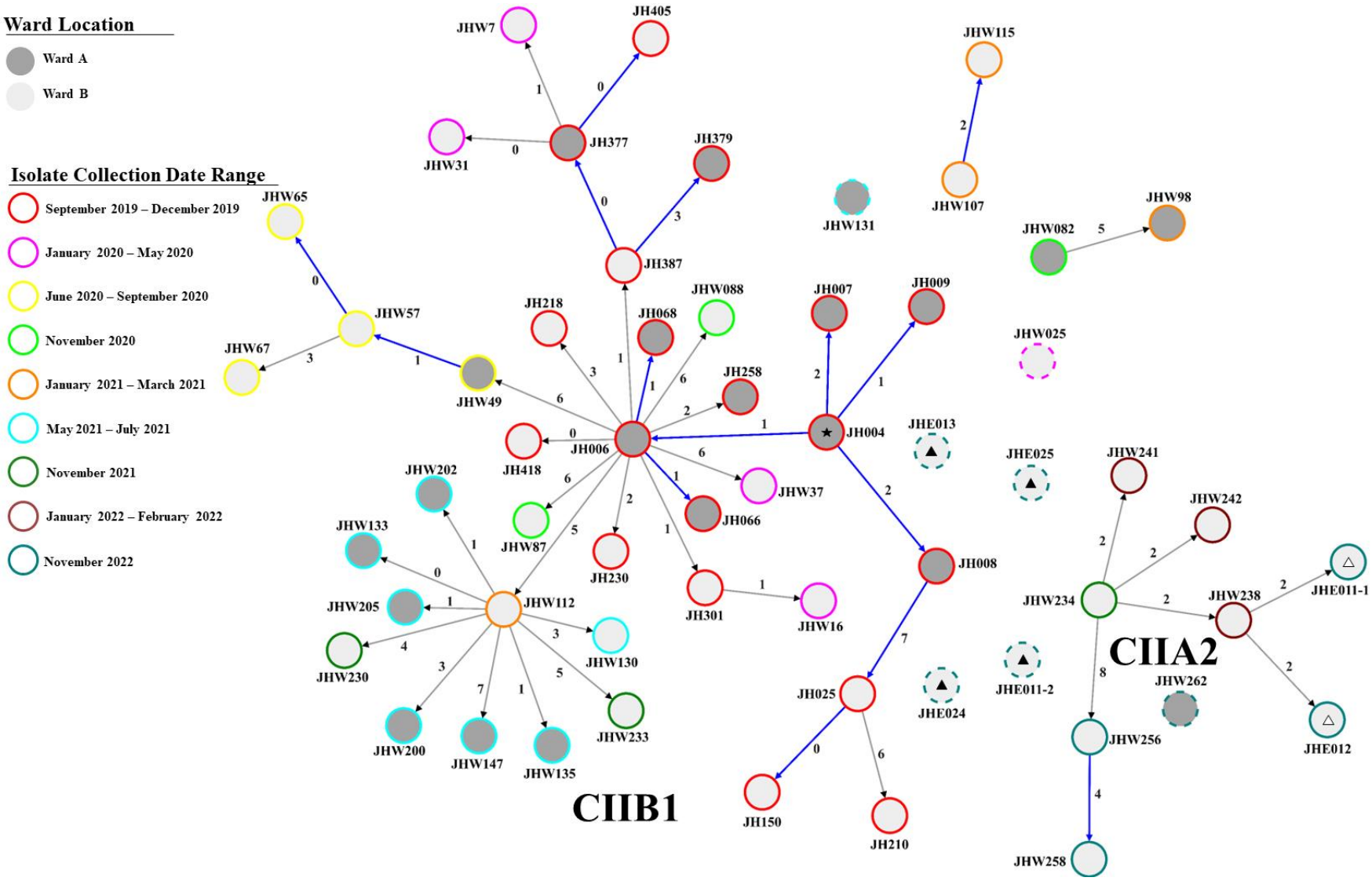
Ward Location
Ward A
Ward B
Isolate Collection Date Range
September 2019 – December 2019
January 2020 – May 2020
June 2020 – September 2020
November 2020
January 2021 – March 2021
May 2021 – July 2021
November 2021
January 2022 – February 2022
November 2022
JHW7
JH405
JHW31
JH377
JH379
JHW65
JH387
JHW57
JHW67
JHW49
JH218
JH068
JHW088
JH258
JH006
JH418
JHW202
JHW87
JHW37
JH066
JHW133
JH230
JHW205
JHW112
JH301
JHW16
JHW230
JHW130
JHW200
JHW147
JHW135
JHW233
CIIB1
JH150
JH210
JH025
JHE024
JH008
JH004
JH007
JH009
JHW131
JHW107
JHW115
JHW082
JHW98
JHW025
JHE013
JHE025
JHW241
JHW242
JHW234
JHW238
JHE011-1
JHE011-2
JHW262
JHW256
JHE012
JHW258
CIIA2

Figure 4.7. Parsimonious transmission tree based on cgSNP distance and collection time of 58 clade A1 *Enterococcus faecium* isolates from the ST80/CT2932 lineage (referred to as CII) recovered from Wards A and B between September 2019 and December 2022. The tree was generated using the SeqTrack algorithm with GraphSNP which determines the most plausible genealogy for isolate sets based on recovery date and ward location (Jombart *et al.,* 2011; Permana *et al.,* 2023). Isolates are represented by shaded circular nodes with inner node shading indicating ward location as shown in the legend. Node outer ring colour refers to isolate recovery date range as shown in the legend. Isolate names are shown outside the nodes. Isolates connected by blue network branches share over-lapping recovery dates of ≤30 days. Transmission links for isolates with a cgSNP distance of >10 are hidden and are indicated with a dashed outer ring. Numbers on the network branches show cgSNP distances. The earliest CII isolate (JH004) used as a reference for cgSNP analysis is indicated by the black star within the node. Environmental isolates (*N*=6) are indicated by a triangle within the node: black triangle, vancomycin susceptible isolate; white triangle, vancomycin resistant isolate. An MLT based on phylogenetic analysis of 220 cgSNPs for the 58 CII isolates is shown in Figure 4.4.

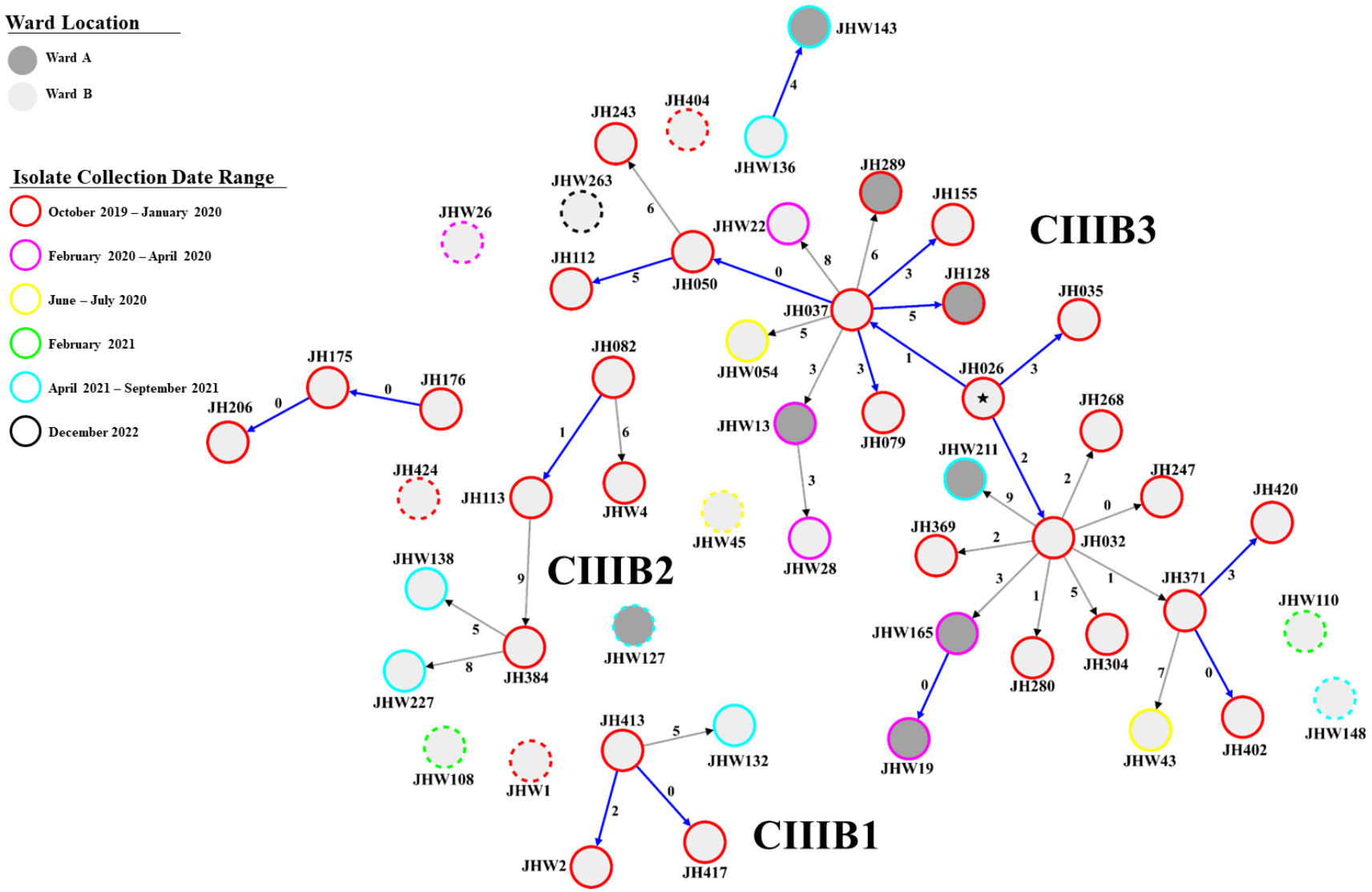
Ward Location
Ward A
Ward B
Isolate Collection Date Range
October 2019 – January 2020
February 2020 – April 2020
June – July 2020
February 2021
April 2021 – September 2021
December 2022
CIIIB3
CIIIB2
CIIIB1
JHW143
JH404
JH243
JHW136
JHW263
JH289
JH155
JHW26
JHW22
JH112
JH050
JH128
JH035
JH037
JHW054
JH082
JH175
JH176
JH206
JH026
JH268
JHW13
JH079
JHW211
JH247
JH424
JH113
JHW4
JHW45
JH420
JH369
JHW28
JH032
JHW138
JH371
JHW110
JHW165
JH384
JHW127
JH280
JH304
JHW227
JHW108
JHW1
JH413
JHW132
JHW19
JHW43
JH402
JHW148
JHW2
JH417

Figure 4.8. Parsimonious transmission tree based on cgSNP distance and collection time of 52 clade A1 *Enterococcus faecium* isolates from the ST80/CT1916 lineage (referred to as CIII) recovered from Wards A & B between September 2019 and December 2022. The tree was generated using the SeqTrack algorithm with GraphSNP which determines the most plausible genealogy for isolate sets based on recovery date and ward location (Jombart *et al.,* 2011; Permana *et al.,* 2023). Isolates are represented by shaded circular nodes with inner node shading indicating ward location as shown in the legend. Node outer ring colour refers to isolate recovery date range as shown in the legend. Isolate names are shown outside the nodes. Isolates connected by blue network branches share over-lapping recovery dates of ≤30 days. Transmission links for isolates with a cgSNP distance of >10 are hidden and are indicated with a dashed outer ring. Numbers on the network branches show cgSNP distances. The earliest CIII isolate (JH026) used as a reference for cgSNP analysis is indicated by the black star within the node. An MLT based on phylogenetic analysis of 341 cgSNPs for the 52 CIII isolates is shown in Supplemental Figure 4.5.

4.3.5 Inter-hospital VRE transmission

We previously investigated the population structure of *E. faecium* (*N*=648) from five Irish hospitals including H1, with ST80 predominance and most isolates assigned to CT1916, CT2933 and CT1598 (Egan *et al.*, 2022; Chapter 3). To investigate the impact of additional isolates on the predominant CTs on a national level, all previously described isolates, an additional 260 well-characterised isolates from seven Irish hospitals (June 2017-July 2022), and WA and WB isolates were investigated by cgMLST (Figure 4.9) (*N*=1,286). Conventional MLST assigned isolates to 32 STs with ST80 predominating (944/1286, 73%). Isolates segregated into 71 cgMLST clusters with an average size of 17 (median: 4; range: 2-215) and 67 singletons. The three major CT clusters (CI-CIII) identified in WA and WB (Figure 4.2) accounted for over 34% (440/1,286) of the larger collection consisting of 215, 88 and 137 isolates, respectively.

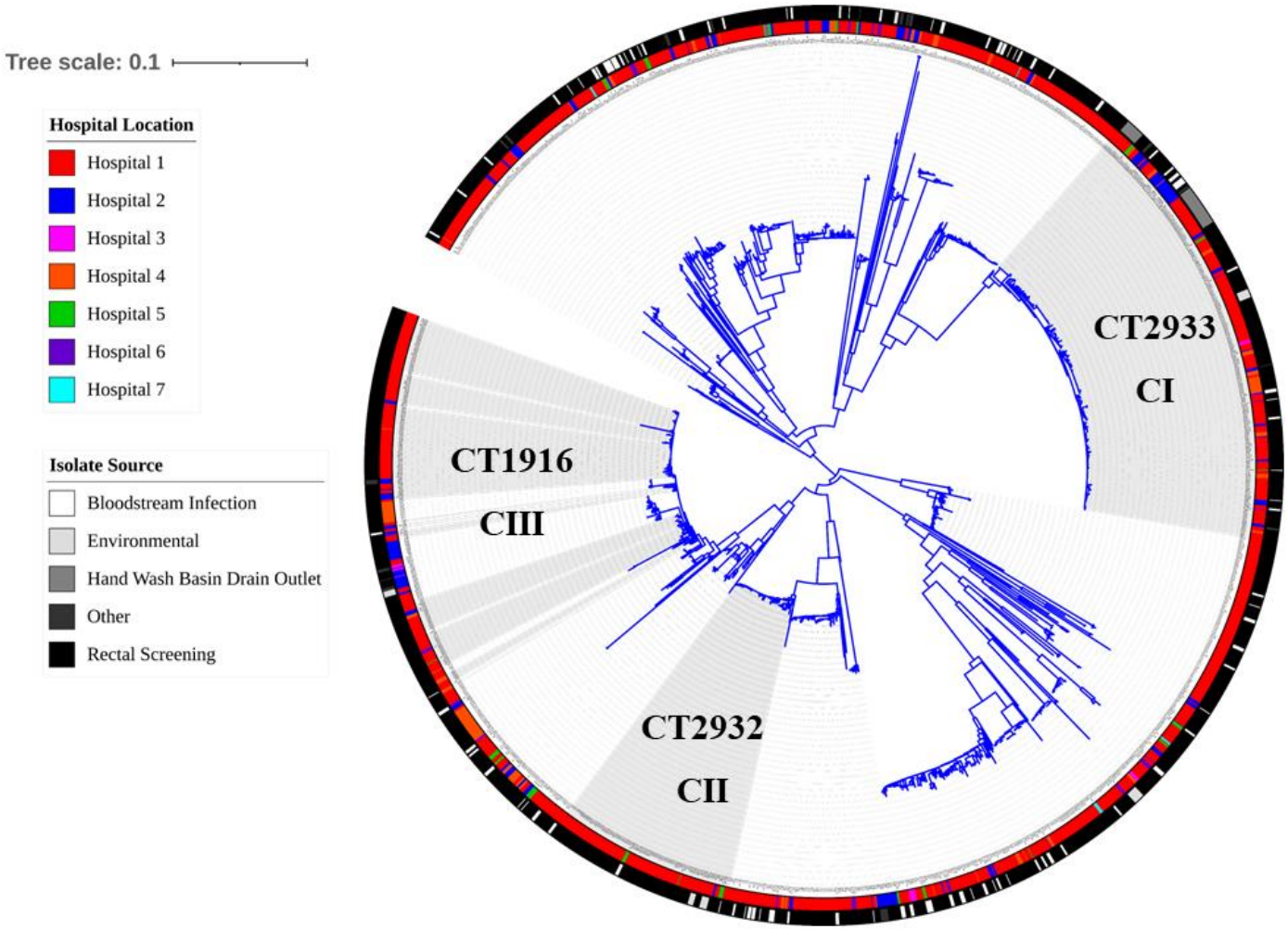

Figure 4.9. Neighbour joining tree (NJT) based on core-genome multi locus sequence type (cgMLST) analysis of 1,423 target genes for 1,286 clade A1 *Enterococcus faecium* isolates recovered from seven Irish hospitals between June 2017 and December 2022. The NJT

comprises 648 isolates from five Irish hospitals including H1 reported in a previous study from this laboratory (Egan *et al.*,2022), an additional 260 well-characterised isolates recovered from seven Irish hospitals (June 2017-July 2022), and WA and WB isolates from this study (*N*=378). Isolates segregated into 71 clusters and 67 singletons. Three distinct clusters (CI, CII, CIII) of closely related isolates (≤20 allelic differences) are highlighted, which are shaded in grey with the corresponding complex type (CT) indicated as follows: [CI] CT2933 (215 isolates): average allelic difference 7, range 0-28; [CII] CT2932 (88 isolates): average allelic difference 5, range 0-26; [CIII] CT1916 (137 isolates): average allelic difference 9, range 0-28. Metadata pertaining to hospitals and isolate source are indicated in the legends. A tree scale bar is shown at the top left.

An additional 119 ST80 CT2933 (CI) isolates were identified in the national collection from multiple H1 wards and from five other Irish hospitals (H2-H6) in distinct geographical locations between October 2018-December 2022. An MLT based on cgSNP analysis of 215 CI isolates (WA and WB N=96, national N=119) based on 731 cgSNPs identified 4,698 closely related isolate pairs (≤10 SNPs) from four Dublin (H1-H4) and two regional hospitals (H5 and H6) (Figure 4.10). The corresponding cgSNP matrices for all CI RIGs identified within the national collection (*N*=1,286 isolates) are available in Table 4.6a-f. In the larger isolate collection, RIG CIB1 comprised 114 isolates from six hospitals (H1 N=87, H2 N=6, H3 N=1, H4 N=16, H5 N=1 and H6 N=3) recovered over 45 months with a median pairwise cgSNP difference of nine (range: 0-23) (Table 4.6f). Within CIB1, many examples of closely related isolates (≤10 SNPs) recovered in geographically distant hospitals within ≤7 days were evident (e.g., isolates JH239 from H1 and RC-19-037 from H6, SNP difference: nine, recovered on the same day, >100 km distance; isolates BS307 from H4 and RC-19-044 from H5, SNP difference: 5, recovered within 2 days, >100 km distance) (Figure 4.10, Table 4.6f). Additionally, closely related VREfm were identified from 39 H1 wards providing further evidence for widespread dissemination of highly related isolate groups that may reflect potential communal or environmental sources with no evident epidemiological links. For instance, RIG CIA5 comprised eight screening VREfm from seven H1 wards and one ward within H4 over a 16-month period with a median cgSNP difference of 10.5 (range: 0-22) (Table 4.6e). Similar findings were evident within CII and CIII (Figure 4.11, Figure 4.12, Table 4.7a-d and Table 4.8a-e).

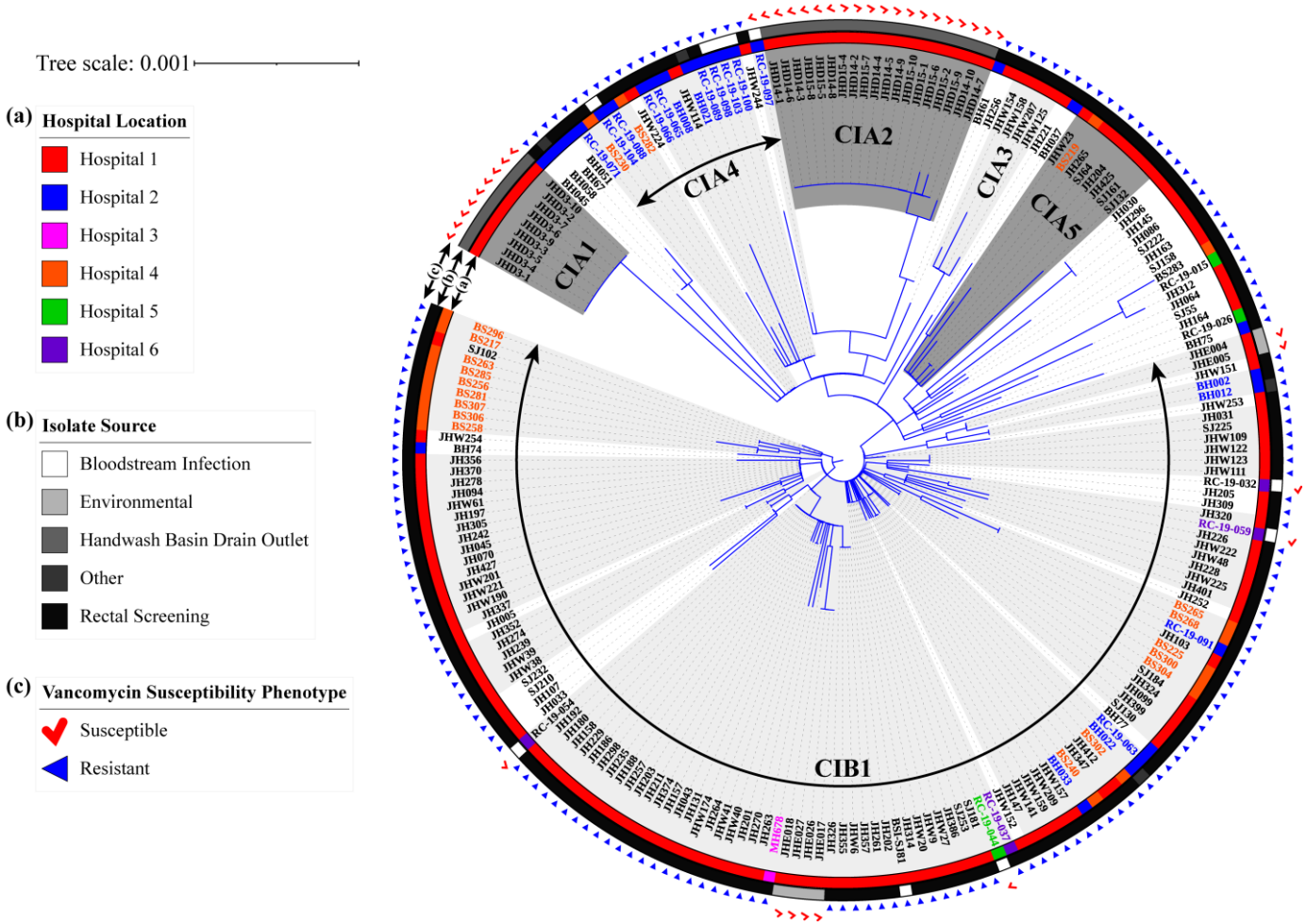

Figure 4.10. MLT based on phylogenetic analysis of 731 cgSNPs for 215 clade A1 *Enterococcus faecium* belonging to CT2933 (referred to as CI) identified by cgMLST of isolates from six Irish hospitals between October 2018 and December 2022. Isolates recovered over the four-

year period which exhibited a median pairwise cgSNP difference of ≤15 were considered highly related and were further segregated into RIGs. Six distinct RIGS (≥ 4 isolates) were identified within CI (CIA1, CIA2, CIA3, CIA4, CIA5 and CIB1) which are shaded in dark and light grey with the corresponding labels indicated accordingly; CIA1 (9 isolates): median cgSNP distance 0, time between earliest and latest isolate 0 days; CIA2 (19 isolates) median cgSNP distance 0, range 0-3, time between earliest and latest isolate 363 days; CIA3 (4 isolates) median cgSNP distance 3, range 0-5, time between earliest and latest isolate 112 days; CIA4 (15 isolates) median cgSNP distance 9, range 0-18, time between earliest and latest isolate 537 days; CIA3 (4 isolates) median cgSNP distance 3, range 0-5, time between earliest and latest isolate 112 days; CIA5 (8 isolates) median cgSNP distance 10.5, range 0-22, time between earliest and latest isolate 433 days; CIB1 (114 isolates) median cgSNP distance: 9, range 0-23, time between earliest and latest isolate 1381 days. Isolates within CIA4 (N=2) and CIB1 (N=15) which are not shaded in grey and exhibited a median pairwise cgSNP of >15 were excluded from the RIG and are considered intra-RIG outliers. Metadata pertaining to isolate source, ward location and vancomycin susceptibility phenotype are indicated in the legends. A tree scale bar is shown at the top left. The tree is mid-point rooted.

Table 4.6a. Detailed metadata and distance matrices based on pairwise cgSNP analysis of RIG CIA1 identified in sub-cluster CIA from CI (ST80/CT2933 lineage) with additional isolates from database[1]

Total isolate number	Isolate name	Collection date	Source	Hospital	cgSNP matrix									Median pairwise cgSNP difference (range)
					JHD3-1	**JHD3-10**	**JHD3-2**	**JHD3-3**	**JHD3-4**	**JHD3-5**	**JHD3-6**	**JHD3-7**	**JHD3-9**	
9	JHD3-1	15/12/2022	Handwash basin drain outlet	H1	**JHD3-1**									0
	JHD3-10				**JHD3-10**	0								
	JHD3-2				**JHD3-2**	0	0							
	JHD3-3				**JHD3-3**	0	0	0						
	JHD3-4				**JHD3-4**	0	0	0	0					
	JHD3-5				**JHD3-5**	0	0	0	0	0				
	JHD3-6				**JHD3-6**	0	0	0	0	0	0			
	JHD3-7				**JHD3-7**	0	0	0	0	0	0	0		
	JHD3-9				**JHD3-9**	0	0	0	0	0	0	0	0	

[1]The larger collection of isolates (*N*=1,286) consisted of *E. faecium* isolates from the present study (*N*=378), previously published isolates from this laboratory from five Irish hospitals (*N*=648) recovered between June 2017 and December 2019 and additional well-characterised isolates recovered from seven Irish hospitals (*N*=260) between June 2017 and July 2022.
Abbreviations: cgSNP, Core-genome single nucleotide polymorphism; H1, hospital 1.

Table 4.6b. Detailed metadata and distance matrices based on pairwise cgSNP analysis of RIG CIA2 identified in sub-cluster CIA from CI (ST80/CT2933 lineage) with additional isolates from database[1]

Total isolate number	Isolate name	Collection date	Source	Hospital		cgSNP matrix																		Median pairwise cgSNP difference (range)
						JHD14-1	**JHD14-10**	**JHD14-2**	**JHD14-3**	**JHD14-4**	**JHD14-5**	**JHD14-6**	**JHD14-7**	**JHD14-8**	**JHD14-9**	**JHD15-1**	**JHD15-10**	**JHD15-2**	**JHD15-4**	**JHD15-5**	**JHD15-6**	**JHD15-7**	**JHD15-8**	**JHD15-9**	
19	JHD14-1	15/12/2022	Handwash basin drain outlet	H1	**JHD14-1**																			0 (0-3)
	JHD14-10				**JHD14-10**	0																		
	JHD14-2				**JHD14-2**	0	0																	
	JHD14-3				**JHD14-3**	0	0	0																
	JHD14-4				**JHD14-4**	0	0	0	0															
	JHD14-5				**JHD14-5**	0	0	0	0	0														
	JHD14-6				**JHD14-6**	0	0	0	0	0	0													
	JHD14-7				**JHD14-7**	2	2	2	2	2	2	2												
	JHD14-8				**JHD14-8**	0	0	0	0	0	0	0	2											
	JHD14-9				**JHD14-9**	1	1	1	1	1	1	1	3	1										
	JHD15-1				**JHD15-1**	0	0	0	0	0	0	0	2	0	1									
	JHD15-10				**JHD15-10**	0	0	0	0	0	0	0	2	0	1	0								
	JHD15-2				**JHD15-2**	1	1	1	1	1	1	1	3	1	2	1	1							
	JHD15-4				**JHD15-4**	0	0	0	0	0	0	0	2	0	1	0	0	1						
	JHD15-5				**JHD15-5**	0	0	0	0	0	0	0	2	0	1	0	0	1	0					
	JHD15-6				**JHD15-6**	0	0	0	0	0	0	0	2	0	1	0	0	1	0	0				
	JHD15-7				**JHD15-7**	0	0	0	0	0	0	0	2	0	1	0	0	1	0	0	0			
	JHD15-8				**JHD15-8**	0	0	0	0	0	0	0	2	0	1	0	0	1	0	0	0	0		
	JHD15-9				**JHD15-9**	1	1	1	1	1	1	1	3	1	2	1	1	2	1	1	1	1	1	

[1]The larger collection of isolates (*N*=1,286) consisted of *E. faecium* isolates from the present study (*N*=378), previously published isolates from this laboratory from five Irish hospitals (*N*=648) recovered between June 2017 and December 2019 and additional well-characterised isolates recovered from seven Irish hospitals (*N*=260) between June 2017 and July 2022.
Abbreviations: cgSNP, Core-genome single nucleotide polymorphism; H1, hospital 1.

Table 4.6c. Detailed metadata and distance matrices based on pairwise cgSNP analysis of RIG CIA3 identified in sub-cluster CIA from CI (ST80/CT2933 lineage) with additional isolates from database[1]

Total isolate number	Isolate name	Collection date	Source	Hospital	cgSNP matrix					Median pairwise cgSNP difference (range)
						JHW125	**JHW154**	**JHW158**	**JHW207**	
	JHW125	14/04/2021			**JHW125**					
4	JHW154	04/08/2021	Rectal screening	H1	**JHW154**	2				3 (0-5)
	JHW158	11/08/2021			**JHW158**	5	5			
	JHW207	04/08/2021			**JHW207**	1	1	4		

[1]The larger collection of isolates (*N*=1,286) consisted of *E. faecium* isolates from the present study (*N*=378), previously published isolates from this laboratory from five Irish hospitals (*N*=648) recovered between June 2017 and December 2019 and additional well-characterised isolates recovered from seven Irish hospitals (*N*=260) between June 2017 and July 2022.
Abbreviations: cgSNP, Core-genome single nucleotide polymorphism; H1, hospital 1.

Table 4.6d. Detailed metadata and distance matrices based on pairwise cgSNP analysis of RIG CIA4 identified in sub-cluster CIA from CI (ST80/CT2933 lineage) with additional isolates from database[1]

Total isolate number	Isolate name	Collection date	Source (N)	Hospital		cgSNP matrix															Median pairwise cgSNP difference (range)
						BH008	**BH021**	**BS230**	**BS282**	**JHW114**	**RC-19-065**	**RC-19-066**	**RC-19-071**	**RC-19-088**	**RC-19-089**	**RC-19-097**	**RC-19-098**	**RC-19-100**	**RC-19-103**	**RC-19-104**	
	BH008	17/02/2021	Abdominal Drain	H2	**BH008**																
	BH021	01/05/2021	Urine	H2	**BH021**	10															
	BS230	24/06/2019	Rectal screening	H4	**BS230**	11	11														
	BS282	20/11/2019	Rectal screening	H4	**BS282**	15	13	15													
	JHW114	05/03/2021	Rectal screening	H1	**JHW114**	15	14	12	18												
15	RC-19-065	11/11/2019	Rectal screening	H2	**RC-19-065**	5	7	9	9	13											9 (0-18)
	RC-19-066	11/11/2019	Rectal screening	H2	**RC-19-066**	9	8	10	10	14	3										
	RC-19-071	12/11/2019	Rectal screening	H2	**RC-19-071**	8	6	1	9	10	2	3									
	RC-19-088	18/11/2019	Rectal screening	H2	**RC-19-088**	13	12	3	13	13	10	11	0								
	RC-19-089	19/11/2019	Rectal screening	H2	**RC-19-089**	5	8	10	10	14	0	4	3	11							
	RC-19-097	21/10/2019	Blood culture	H2	**RC-19-097**	10	6	5	9	12	5	6	3	6	6						
	RC-19-098	08/11/2019	Blood culture	H2	**RC-19-098**	8	8	3	12	9	6	7	1	4	7	4					
	RC-19-100	19/11/2019	Blood culture	H2	**RC-19-100**	5	10	12	12	14	0	4	5	13	0	6	9				
	RC-19-103	03/12/2019	Blood culture	H2	**RC-19-103**	9	9	7	13	12	8	9	3	8	9	5	4	11			
	RC-19-104	28/12/2019	Blood culture	H2	**RC-19-104**	12	12	3	15	13	10	11	1	2	11	6	4	13	8		

[1]The larger collection of isolates (*N*=1,286) consisted of *E. faecium* isolates from the present study (*N*=378), previously published isolates from this laboratory from five Irish hospitals (*N*=648) recovered between June 2017 and December 2019 and additional well-characterised isolates recovered from seven Irish hospitals (*N*=260) between June 2017 and July 2022.
Abbreviations: cgSNP, Core-genome single nucleotide polymorphism; H1, hospital 1.

Table 4.6e. Detailed metadata and distance matrices based on pairwise cgSNP analysis of RIG CIA5 identified in sub-cluster CIA from CI (ST80/CT2933 lineage) with additional isolates from database[1]

Total isolate number	Isolate name	Collection date	Source	Hospital		cgSNP matrix								Median pairwise cgSNP difference (range)
						BS219	**JH204**	**JH265**	**JH425**	**JHW23**	**SJ132**	**SJ161**	**SJ64**	
	BS219	09/05/2019		H4	**BS219**									
	JH204	05/11/2019		H1	**JH204**	12								
	JH265	18/11/2019		H1	**JH265**	16	10							
8	JH425	26/12/2019	Rectal screening	H1	**JH425**	10	2	8						10.5 (0-22)
	JHW23	18/03/2020		H1	**JHW23**	17	19	18	13					
	SJ132	07/03/2019		H1	**SJ132**	19	13	16	11	22				
	SJ161	14/03/2019		H1	**SJ161**	12	6	6	4	15	13			
	SJ64	19/10/2018		H1	**SJ64**	8	3	5	1	7	10	1		

[1]The larger collection of isolates (*N*=1,286) consisted of *E. faecium* isolates from the present study (*N*=378), previously published isolates from this laboratory from five Irish hospitals (*N*=648) recovered between June 2017 and December 2019 and additional well-characterised isolates recovered from seven Irish hospitals (*N*=260) between June 2017 and July 2022.
Abbreviations: cgSNP, Core-genome single nucleotide polymorphism; H1, hospital 1.

Table 4.6f. Detailed metadata and distance matrices based on pairwise cgSNP analysis of RIG CIB1 identified in sub-cluster CIB from CI (ST80/CT2933 lineage) with additional isolates from database[1]

Size of table exceeds page margins.

Scan and/or click QR code to access and/or download table.

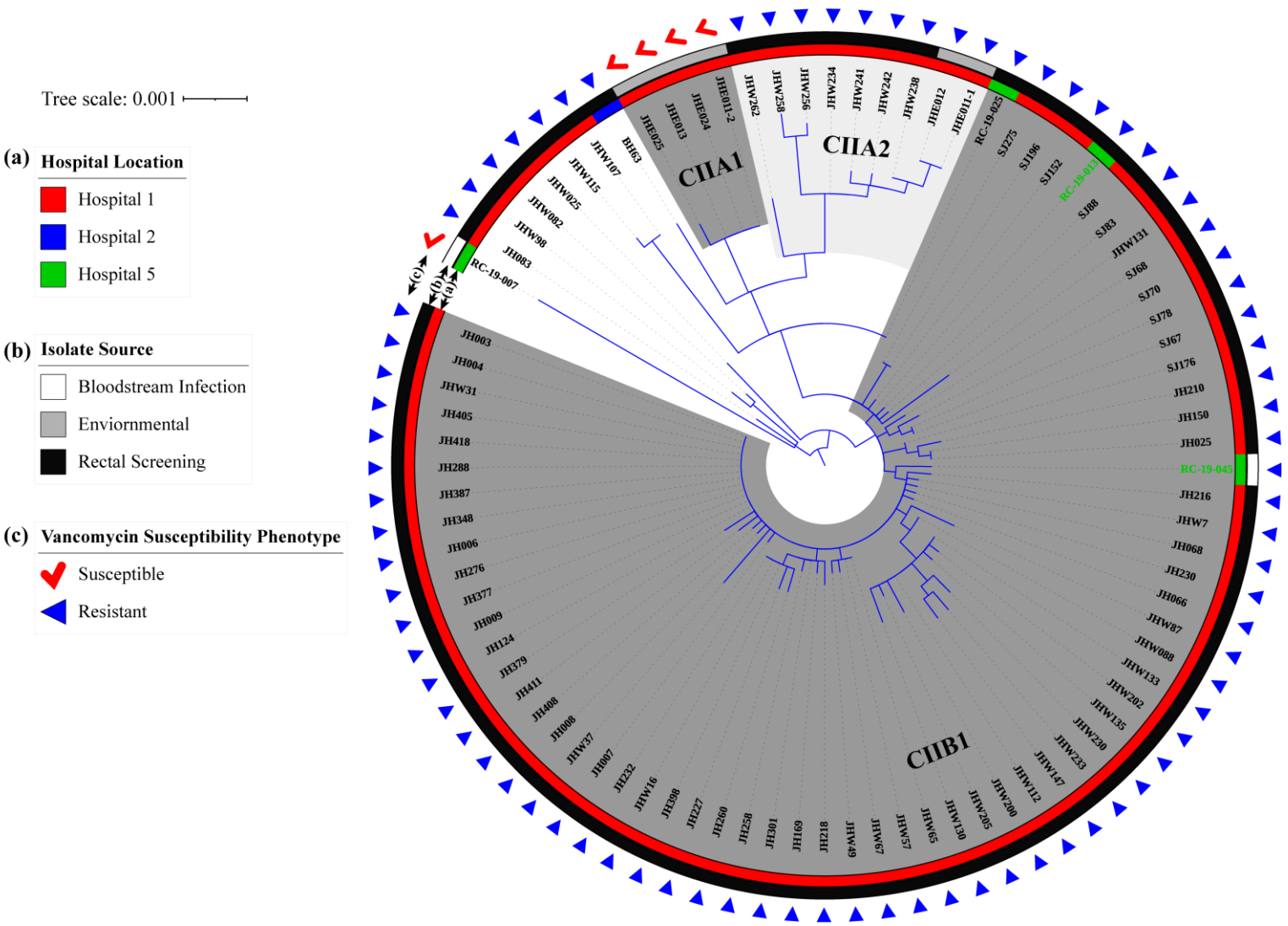
Tree scale: 0.001
(a) Hospital Location
Hospital 1
Hospital 2
Hospital 5
(b) Isolate Source
Bloodstream Infection
Enviornmental
Rectal Screening
(c) Vancomycin Susceptibility Phenotype
Susceptible
Resistant
CIIA1
CIIA2
CIIB1
(a)
(b)
(c)
RC-19-007
RC-19-025
RC-19-029
RC-19-045

Figure 4.11. MLT based on phylogenetic analysis of 315 cgSNPs for the 88 clade A1 *Enterococcus faecium* isolates CT2932 (referred to as CII) identified by cgMLST of isolates from three Irish hospitals between October 2018 and December 2022. Isolates recovered over the four-year period which exhibited a median pairwise cgSNP difference of ≤15 were considered highly related and were further segregated into RIGs. Three distinct RIGS (≥ 4 isolates) were identified within CII (CIIA1, CIIA2 and CIIB1) which are shaded in dark and light grey with the corresponding labels indicated accordingly; CIIA1 (4 isolates): median cg SNP distance 1, range 0-2, time between earliest and latest isolate 0 days; CIIA2 (9 isolates) median cgSNP distance 9, range 0-19, time between earliest and latest isolate 363 days; CIIB1 (114 isolates) median cgSNP distance 8, range 0-24, time between earliest and latest isolate 1125 days. Metadata pertaining to isolate source, ward location and vancomycin susceptibility phenotype are indicated in the legends. A tree scale bar is shown at the top left. The tree is mid-point rooted.

Table 4.7a. Detailed metadata and distance matrices based on pairwise cgSNP analysis of RIG CIIA1 identified in sub-cluster CIIA from CII (ST80/CT2932 lineage) with additional isolates from database[1]

Total isolate number	Isolate name	Collection date	Source	Hospital	cgSNP matrix					Median pairwise cgSNP difference (range)
						JHE011-2	**JHE013**	**JHE024**	**JHE025**	
4	JHE011-2	18/11/2022	Bedside Table	H1	**JHE011-2**					1 (0-2)
	JHE013		Bedside Table		**JHE013**	0				
	JHE024		Bedside Table		**JHE024**	0	0			
	JHE025		Bedside Table		**JHE025**	2	2	2		

[1]The larger collection of isolates (*N*=1,286) consisted of *E. faecium* isolates from the present study (*N*=378), previously published isolates from this laboratory from five Irish hospitals (*N*=648) recovered between June 2017 and December 2019 and additional well-characterised isolates recovered from seven Irish hospitals (*N*=260) between June 2017 and July 2022.
Abbreviations: cgSNP, Core-genome single nucleotide polymorphism; H1, Hospital 1.

Table 4.7b. Detailed metadata and distance matrices based on pairwise cgSNP analysis of RIG CIIA2 identified in sub-cluster CIIA from CII (ST80/CT2932 lineage) with additional isolates from database[1]

Total isolate number	Isolate name	Collection date	Source	Hospital		cgSNP matrix									Median pairwise cgSNP difference (range)
						JHE011-1	**JHE012**	**JHW234**	**JHW238**	**JHW241**	**JHW242**	**JHW256**	**JHW258**	**JHW262**	
	JHE011-1	18/11/2022	Bedside table		**JHE011-1**										
	JHE012	18/11/2022	Bedside table		**JHE012**	0									
9	JHW234	24/11/2021	Rectal screening	H1	**JHW234**	4	4								9 (0-19)
	JHW238	12/01/2022	Rectal screening		**JHW238**	2	2	2							
	JHW241	20/01/2022	Rectal screening		**JHW241**	4	4	2	2						
	JHW242	02/02/2022	Rectal screening		**JHW242**	4	4	2	2	2					
	JHW256	06/09/2022	Rectal screening		**JHW256**	12	12	8	10	10	10				
	JHW258	07/09/2022	Rectal screening		**JHW258**	12	12	8	10	10	10	4			
	JHW262	22/11/2022	Rectal screening		**JHW262**	15	15	11	13	13	13	19	19		

[1]The larger collection of isolates (*N*=1,286) consisted of *E. faecium* isolates from the present study (*N*=378), previously published isolates from this laboratory from five Irish hospitals (*N*=648) recovered between June 2017 and December 2019 and additional well-characterised isolates recovered from seven Irish hospitals (*N*=260) between June 2017 and July 2022.
Abbreviations: cgSNP, Core-genome single nucleotide polymorphism; H1, Hospital 1.

Table 4.7c. Detailed metadata and distance matrices based on pairwise cgSNP analysis of RIG CIIA3 identified in sub-cluster CIIA from CII (ST80/CT2932 lineage) with additional isolates from database[1]

Total isolate number	Isolate name	Collection date	Source (N)	Hospital		cgSNP matrix									Median pairwise cgSNP difference (range)
						JH144	**JHW131**	**RC-19-013**	**RC-19-025**	**SJ152**	**SJ196**	**SJ275**	**SJ83**	**SJ88**	
9	JH144	24/10/2019	Rectal screening	H1	**JH144**	0									7 (0-19)
	JHW131	07/05/2021	Rectal screening	H1	**JHW131**	19									
	RC-19-013	15/11/2019	Rectal screening	H5	**RC-19-013**	11	7								
	RC-19-025	13/11/2019	Rectal screening	H5	**RC-19-025**	14	13	7							
	SJ152	12/03/2019	Rectal screening	H1	**SJ152**	13	8	2	7						
	SJ196	18/06/2019	Rectal screening	H1	**SJ196**	17	12	6	11	6					
	SJ275	26/06/2019	Rectal screening	H1	**SJ275**	15	12	6	11	6	0				
	SJ83	26/10/2018	Rectal screening	H1	**SJ83**	13	8	2	7	2	6	6			
	SJ88	26/10/2018	Rectal screening	H1	**SJ88**	13	8	2	7	2	6	6	2		

[1]The larger collection of isolates (*N*=1,286) consisted of *E. faecium* isolates from the present study (*N*=378), previously published isolates from this laboratory from five Irish hospitals (*N*=648) recovered between June 2017 and December 2019 and additional well-characterised isolates recovered from seven Irish hospitals (*N*=260) between June 2017 and July 2022.
Abbreviations: cgSNP, Core-genome single nucleotide polymorphism; H1, Hospital 1; H5, Hospital 5.

Table 4.7d. Detailed metadata and distance matrices based on pairwise cgSNP analysis of RIG CIIB1 identified in sub-cluster CIIB from CII (ST80/CT2932 lineage) with additional isolates from database[1]

Size of table exceeds page margins.

Scan and/or click QR code to access and/or download table.

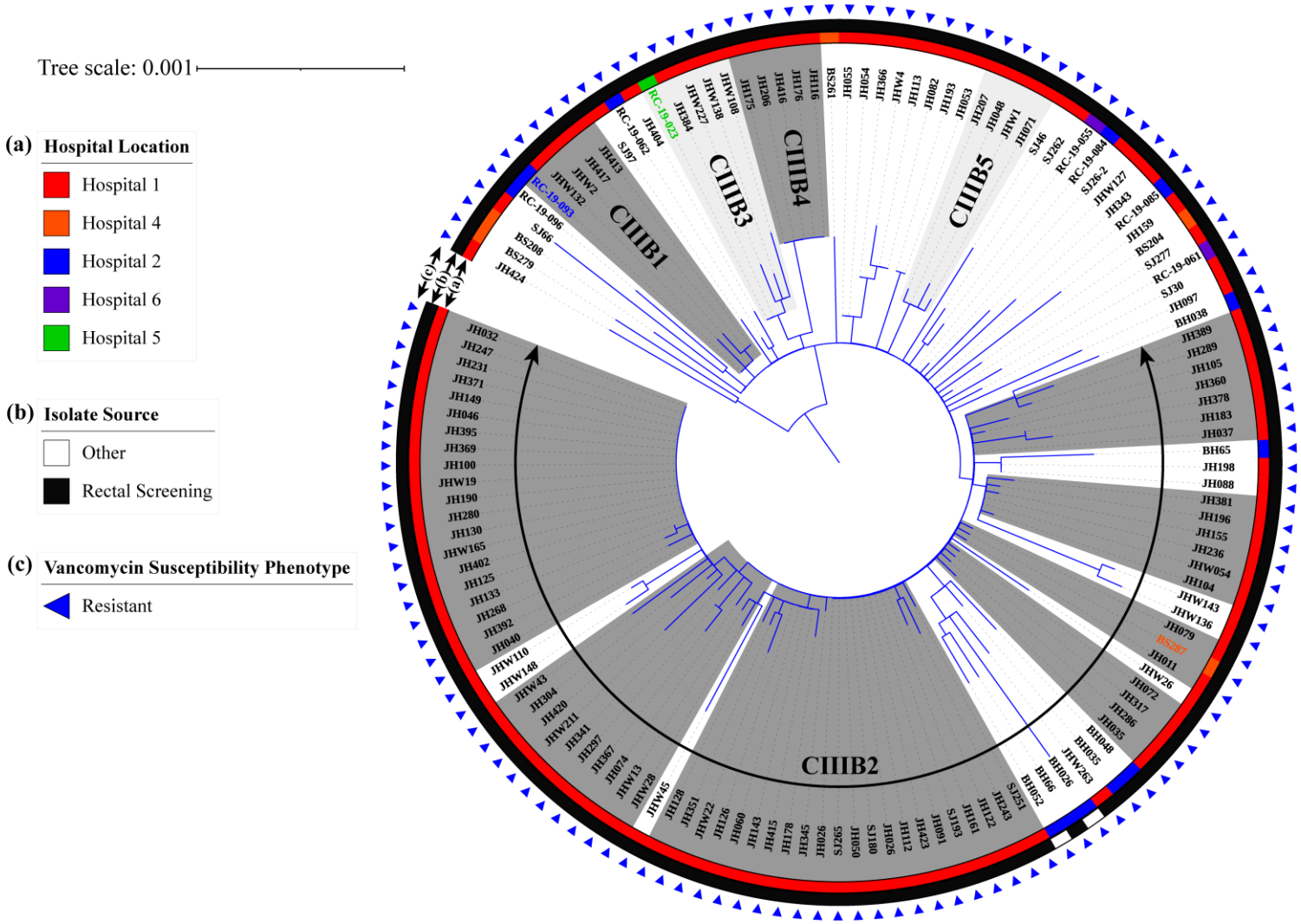
Tree scale: 0.001
(a) Hospital Location
Hospital 1
Hospital 4
Hospital 2
Hospital 6
Hospital 5
(b) Isolate Source
Other
Rectal Screening
(c) Vancomycin Susceptibility Phenotype
Resistant
CIIIB1
CIIIB2
CIIIB3
CIIIB4
CIIIB5

Figure 4.12 MLT based on phylogenetic analysis of 728 cgSNPs for the 137 clade A1 *Enterococcus faecium* isolates CT1916 (referred to as CIII) identified by cgMLST of isolates from five Irish hospitals between June 2018 and December 2022. Isolates recovered over the four-year period which exhibited a median pairwise cgSNP difference of ≤15 were considered highly related and were further segregated into RIGs. Five distinct RIGS (≥ 4 isolates) were identified within CIII (CIIB1, CIIIB2, CIIIB3, CIIIB4 and CIIIB5) which are shaded in dark and light grey with the corresponding labels indicated accordingly; CIIIB1 (5 isolates): median cgSNP distance 2, range 0-7, time between earliest and latest isolate 540 days; CIIIB2 (72 isolates) median cgSNP distance 6, range 0-24, time between earliest and latest isolate 800 days; CIIIB3 (5 isolates) median cgSNP distance 9.5, range 0-18, time between earliest and latest isolate 657 days; CIIIB4 (5 isolates) median cgSNP distance 1, range 0-2, time between earliest and latest isolate 69 days; CIIIB5 (4 isolates) median cgSNP distance 5.5 range 0-9, time between earliest and latest isolate 91 days. Isolates within CIIIB2 (*N*=14) which are not shaded in grey and exhibited a median pairwise cgSNP of >15 were excluded from the RIG and are considered intra-RIG outliers. Detailed metadata pertaining to isolate source, ward location and vancomycin susceptibility phenotype are indicated in the legends. A tree bar is shown at the top left. A tree scale bar is shown at the top left. The tree is mid-point rooted.

Table 4.8a. Detailed metadata and distance matrices based on pairwise cgSNP analysis of RIG CIIIB1 identified in sub-cluster CIIIB from CIII (ST80/CT1916 lineage) with additional isolates from database[1]

Total isolate number	Isolate name	Collection date	Source	Hospital		cgSNP matrix					Median pairwise cgSNP difference (range)
						JH413	**JH417**	**JHW132**	**JHW2**	**RC-19-023**	
4	JH413	24/12/2019	Rectal screening	H1	**JH413**						2 (0-7)
	JH417	25/12/2019		H1	**JH417**	0					
	JHW132	12/05/2021		H1	**JHW132**	5	5				
	JHW2	01/01/2020		H1	**JHW2**	2	2	7	0		
	RC-19-093	20/11/2019		H2	**RC-19-093**	2	2	5	4		

[1]The larger collection of isolates (*N*=1,286) consisted of *E. faecium* isolates from the present study (*N*=378), previously published isolates from this laboratory from five Irish hospitals (*N*=648) recovered between June 2017 and December 2019 and additional well-characterised isolates recovered from seven Irish hospitals (*N*=260) between June 2017 and July 2022.
Abbreviations: cgSNP, Core-genome single nucleotide polymorphism; H1, Hospital 1; H2, Hospital 2.

Table 4.8b. Detailed metadata and distance matrices based on pairwise cgSNP analysis of RIG CIIIB2 identified in sub-cluster CIIIB from CIII (ST80/CT1916 lineage) with additional isolates from database[1]

Size of table exceeds page margins.

Scan and/or click QR code to access and/or download table.

Table 4.8c. Detailed metadata and distance matrices based on pairwise cgSNP analysis of RIG CIIIB3 identified in sub-cluster CIIIB from CIII (ST80/CT1916 lineage) with additional isolates from database[1]

Total isolate number	Isolate name	Collection date	Source	Hospital		cgSNP matrix					Median pairwise cgSNP difference (range)
						JH384	**JHW108**	**JHW138**	**JHW227**	**RC-19-023**	
5	JH384	13/12/2019	Rectal screening	H1	**JH384**						9.5 (0-18)
	JHW108	17/02/2021		H1	**JHW108**	11					
	JHW138	04/06/2021		H1	**JHW138**	5	15				
	JHW227	29/09/2021		H1	**JHW227**	8	18	11			
	RC-19-023	20/11/2019		H5	**RC-19-023**	0	12	5	8		

[1]The larger collection of isolates (*N*=1,286) consisted of *E. faecium* isolates from the present study (*N*=378), previously published isolates from this laboratory from five Irish hospitals (*N*=648) recovered between June 2017 and December 2019 and additional well-characterised isolates recovered from seven Irish hospitals (*N*=260) between June 2017 and July 2022.
Abbreviations: cgSNP, Core-genome single nucleotide polymorphism; H1, Hospital 1; H5, Hospital 5.

Table 4.8d. Detailed metadata and distance matrices based on pairwise cgSNP analysis of RIG CIIIB4 identified in sub-cluster CIIIB from CIII (ST80/CT1916 lineage) with additional isolates from database[1]

Total isolate number	Isolate name	Collection date	Source	Hospital		cgSNP matrix					Median pairwise cgSNP difference (range)
						JH116	**JH175**	**JH176**	**JH206**	**JH416**	
5	JH116	17/10/2019	Rectal screening	H1	**JH116**						1 (0-2)
	JH175	31/10/2019		H1	**JH175**	1					
	JH176	30/10/2019		H1	**JH176**	1	0				
	JH206	06/11/2019		H1	**JH206**	1	0	0			
	JH416	24/12/2019		H1	**JH416**	2	1	1	1		

[1]The larger collection of isolates (*N*=1,286) consisted of *E. faecium* isolates from the present study (*N*=378), previously published isolates from this laboratory from five Irish hospitals (*N*=648) recovered between June 2017 and December 2019 and additional well-characterised isolates recovered from seven Irish hospitals (*N*=260) between June 2017 and July 2022.
Abbreviations: cgSNP, Core-genome single nucleotide polymorphism; H1, Hospital 1.

Table 4.8e. Detailed metadata and distance matrices based on pairwise cgSNP analysis of RIG CIIIB5 identified in sub-cluster CIIIB from CIII (ST80/CT1916 lineage) with additional isolates from database[1]

Total isolate number	Isolate name	Collection date	Source	Hospital	cgSNP matrix					Median pairwise cgSNP difference (range)
						JH048	**JH071**	**JH207**	**JHW1**	
4	JH048	03/10/2019	Rectal screening	H1	**JH048**					5.5 (0-9)
	JH071	08/10/2019			**JH071**	2				
	JH207	07/11/2019			**JH207**	4	4			
	JHW1	01/01/2020			**JHW1**	7	7	9		

[1]The larger collection of isolates (*N*=1,286) consisted of *E. faecium* isolates from the present study (*N*=378), previously published isolates from this laboratory from five Irish hospitals (*N*=648) recovered between June 2017 and December 2019 and additional well-characterised isolates recovered from seven Irish hospitals (*N*=260) between June 2017 and July 2022.
Abbreviations: cgSNP, Core-genome single nucleotide polymorphism; H1, Hospital 1.

4.3.6 VSEfm harbouring van remnants

In silico analysis of VSEfm identified four sub cluster CIIA1 environmental isolates harbouring *van* operon remnants. These isolates harboured the *vanZ* and *vanY* genes, but lacked the *vanHAX* and *vanRS* genes. One isolate (JHE024) was fully closed by hybrid assembly, which identified the *vanZ* and *vanY* genes on an 88,110 bp circular plasmid. The organization of the *van* remnant and adjacent sequences were similar to *vanA* operon regions on plasmids in Irish clinical VREfm (Figure 4.13).

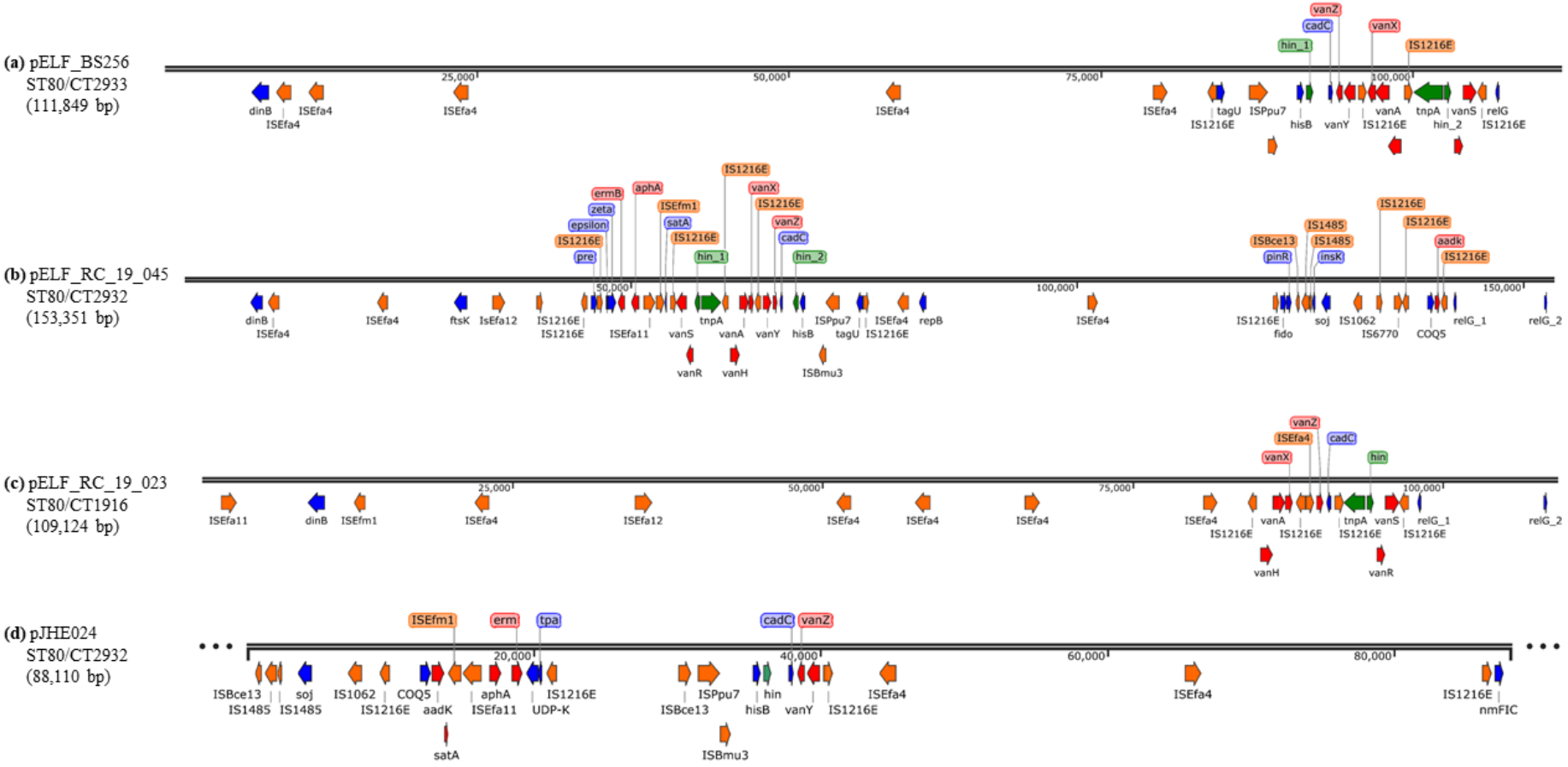
(a) pELF_BS256
ST80/CT2933
(111,849 bp)
(b) pELF_RC_19_045
ST80/CT2932
(153,351 bp)
(c) pELF_RC_19_023
ST80/CT1916
(109,124 bp)
(d) pJHE024
ST80/CT2932
(88,110 bp)

Figure 4.13. Schematic diagram showing the comparative structural organisation of *vanA*- and *van* remnant-encoding plasmids closed by hybrid assembly from clinical and environmental *Enterococcus faecium* isolates from Irish hospitals. (a) pELF_BS256 (ST80/CT2933 111,849 bp linear plasmid from VREfm rectal screen); (b) pELF_RC_19_045 (ST80/CT2932, 153,351 bp linear plasmid from VREfm bloodstream infection); (c) pELF_RC_19_023 (ST80/CT1916, 109,124 bp linear plasmid from VREfm rectal screen); (d) pJHE024 (ST80/CT2932, 88,110 bp circular plasmid from VSEfm isolate recovered from patient bedside table). Isolates were recovered from H4 (a), H5 (b-c) and H1 (d). Genes and their orientation are denoted by directional arrows and labelled with corresponding gene names. A reference size scale bar is shown above each plasmid map. Genes encoding hypothetical proteins are hidden. The plasmid map shown in (c) encoding an intact *vanA* operon was previously described by Egan *et al*. Plasmid pJHE024 (d) was identified in VSEfm environmental isolate JHE024 from the present study and harbours a *van* remnant encoding the *vanY* and *vanZ* genes

4.4 Discussion

This study provides a comprehensive, retrospective analysis using a WGS-based approach to establish high-resolution insights into the associated epidemiology, transmission dynamics and potential environmental persistence of VREfm within two critical care wards of a major acute Irish hospital. Our findings identified three predominant ST80 lineages (CT2933, CT2932 and CT1916) involved in extensive direct and indirect patient-to-patient transmission. Isolates within the major CT groups appeared highly clonal and were considered indistinguishable (≤20 allelic differences) using the conventional, published *E. faecium* cgMLST typing scheme (de Been *et al.,* 2015). However, a more diverse picture was elucidated using cgSNP analysis indicative of multiple hospital introductory events and subsequent genomic specialisation resulting in successfully established major endemic CTs. This phenomenon, termed 'genetic capitalism', has been extensively reported in clade A1 *E. faecium*, in which multi-drug resistance hospital-adapted sub-populations emerge, evolve, and eventually outcompete/predominate via the acquisition and accumulation of adaptive genes and horizontally acquired elements (Baquero, 2004; Freitas *et al.,* 2021).

Our findings further contribute to the growing knowledge base surrounding the superiority and higher resolution of SNP-based approaches in the detailed elucidation of complex VREfm transmission networks, particularly during outbreak scenarios in hyperendemic regions (Higgs *et al.,* 2022; Maechler *et al.,* 2023). Whilst cgMLST may be used to broadly identify genetically related isolate groups and provides a good indication of over-all population structure, it was not possible to infer detailed transmission chains, epidemiological links or discriminate between isolate groups on the basis of cgMLST alone and instead resulted in an over-estimation of the degree of isolate relatedness. In line with other studies, the application of additional approaches such as cgSNP analysis are required for precise outbreak elucidation and resolution, by further discriminating data into more distinct genomic transmission clusters (Gorrie *et al.,* 2019; Maechler *et al.,* 2023). However, we do acknowledge the significant computational and time requirements associated with both selecting and generating reference genomes for each cluster when using cgSNP-based methodologies which may preclude its implementation in routine hospital-based surveillance outside retrospective academic research. Higgs and colleagues recently demonstrated the value of target free pairwise genome comparisons using SKA which can provide the higher discriminatory power of

SNP-based approaches in the context of outbreak analysis and is more amenable to automated surveillance pipelines due to its ease-of-use, shorter turn-around times, and the decreased requirement of extensive bioinformatic expertise.

The complexity and prolonged nature of the transmission networks described in this study suggest the presence of multiple, intricate mechanisms at play with potential unknown reservoirs contributing to over-all dissemination. The highly dynamic pattern of two-way spread between the patient and the hospital environment is well documented, with admission to a room previously occupied by a VRE-colonised patient serving as an independent risk-factor and predictor for acquisition (Drees *et al.,* 2008). As evidenced by this study, many high-touch areas may become contaminated with endemic VREfm clones such as near-patient furniture, shared medical devices, toilet seats and even shower drains which may persist for extensive periods of time. This is mirrored in the finding of genetically indistinguishable environmental isolates from cardiac monitors and shower drains on the same ward 29-months post-recovery of a patient screening isolate with a median cgSNP difference of six (Figure 4.3 and 4.6, Table 4.3d). A study from the UK, the closest geographical neighbour of Ireland, recently reported that 48% of environmental swabs taken in two haematology wards over a six-month period were positive for VREfm and 20% of bedroom/bathroom areas remained positive following routine cleaning after patient discharge (Gouliouris *et al.,* 2020). However, frequent hospital admission amongst comorbid patients (e.g., oncology and cardiothoracic cohorts) is common and current laboratory-based methods dictate that only the first VREfm positive screen is stored on a patient. Therefore, this environmental persistence likely reflects a combination of both the ability of the organism to persist and resist decontamination, as well as the potential continued reintroduction of endemic clones from patients with frequent health-care exposure. It also emphasises the importance of interpretation of transmission chains with the inclusion of data such as historical admission records and length of bacterial colonisation.

Interestingly, the majority of environmental-specific isolates (89%, 43/48) in this study were VSE and 12% (4/48) harboured *vanA* remnant (*vanY* and *vanZ*), suggesting they potentially arose from a vancomycin-resistant ancestor. The versatility of VREfm and its ability to easily acquire antimicrobial resistance genes via horizontal gene is well documented and the loss of segments of DNA in the absence of selective pressure is to be expected (Arias and Murray, 2012; Guzman Prieto *et al.,* 2016; Arredondo-Alonso *et al.,* 2020). Additionally, the high prevalence of IS*1216E* in Irish VREfm in the absence

of a functional *vanA* transposase gene may facilitate the dynamic gain/loss of segments of, or the entirety of the *vanA* transposon in an environmental setting (Egan *et al.,* 2022). These findings suggest the importance of the consideration of VSE in surveillance practices, however further studies are required on both the role of VSE within the patient's gut consortium and their contribution to both environmental contamination, colonisation, and preceding infection with multi-drug resistant strains.

To the best of our knowledge, no studies to-date have investigated the handwash basin drains outlets and U-bends as potential reservoirs for VREfm acquisition. It has been previously reported that carbapenmase-producing bacteria have a propensity to survive within the Irish hospital drain network, which is further exacerbated by the inappropriate disposal of nutritional and enteral feed down the sink (Kearney *et al.,* 2023). The recovery of genetically identical VSE from washbasin drain outlets in patient bathrooms in two separate rooms on WA indicates potential isolate trafficking through-out the drain network. However, the closest neighbouring patient isolate differed by 24 cgSNPs and therefore any reasonable deduction about potential reservoirs or transmission cannot be made. It is of note to again emphasise that the length of colonisation of the drain is unknown and often non-clinical handwash basins lacking splash-reducing measures may be present at the patient's bedside on hospital wards resulting in increased droplet-mediated dispersal of resistant bacteria. It remains to be seen if the hospital drain network is a reservoir for *E. faecium* in hospitals and a potential hidden highway for *E. faecium* transmission.

In addition to direct patient transmission and potential environmental persistence, this study also highlights that multiple simultaneous outbreaks of genomically distinct isolates belonging to the same CT may be ongoing both within and across multiple wards within the same hospital. It is important to note that inferred epidemiological links based on parsimonious trees using the SeqTrack algorithm do not consider patient movement data, spatial location, and other key epidemiological factors that may further complicate transmission inference (Permana *et al.,* 2023). Instead, it determines the most likely genealogy and therefore transmission directionality was estimated on recovery date and ward location alone. On this basis, we do acknowledge that the inferred transmission routes may be biased by the collection dates of the isolates, as with a lot of retrospective surveillance studies, and may reflect sequential sampling rather than true transmission routes and therefore conclusions should be interpreted with that in mind. Nonetheless, this study still provides a comprehensive snapshot of the extensive potential transmission

occurring within the critical care wards in H1, even in the presence of IPC interventions and serve to highlight the on-going complexity of VREfm surveillance.

Expanding our analysis to include isolates spanning seven geographically distinct Irish hospitals over five years highlight that certain common ancestors, such as ST80 CT2933, have likely been in circulation in individuals with frequent health-care exposure within the Republic of Ireland for long periods of time in the absence of any known specific source or epidemiological link. The complexities unveiled by the finding of cross-institutional CT-specific dominance with little genetic diversity (<10 SNPs in cases), which is a phenomenon also observed by colleges across Europe (Pinholt *et al.,* 2015; Raven *et al.,* 2017; Higgs *et al.,* 2022; Maechler *et al.,* 2023), gives rise to a series of unresolved questions and again highlights the urgent requirement for extensive, genomic-wide studies in the context of a one-health consortium. It is likely that this finding in-part can be attributed to both patient and staff moment across hospital networks due to speciality referrals. However, the extensive level of inter-hospital dissemination seen on a global level begs the question, is this simply reflective of the colonisation of common VSE clonal lineages carried by the general hospital-going population that may acquire multi-drug resistance or is there a potential unidentified communal source(s)? Unfortunately, data regarding community prevalence of VREfm amongst asymptomatic healthy individuals within Ireland is limited, with ranges of 0.98%-3% quoted within the literature (Nourse *et al.,* 2000; Ryan *et al.,* 2015; Whelton *et al.,* 2016; Croughan *et al.,* 2022). This suggests that VREfm is predominantly acquired in a hospital-based setting in Ireland and we potentially lack the community reservoir seen historically throughout Europe (Klare *et al.,* 1995; van der Auwera *et al.,* 1996; Guerin *et al.,* 1998; Gambarotto *et al.,* 2000; Mascini and Bonten, 2005; Gouliouris *et al.,* 2019). For example, studies in France highlighted a community prevalence rate of 11.8%, whilst additional studies from Germany and The Netherlands reporting VRE colonisation rates of 6-12% in the community (Klare *et al.,* 1995; Endtz *et al.,* 1997; Gambarotto *et al.,* 2000; Mascini and Bonten, 2005). However, it is noteworthy that the majority of studies conducted on the prevalence of VREfm in the healthy population in Europe span from 1995-2005, which coincides with the use of avoparcin, a vancomycin analogue utilised as a growth promotor in animal husbandry. Whilst avoparcin use was banned within the EU in 1997, few up-to-date studies are available within the literature assessing the impact on community prevalence rates in healthy human populations within Europe. It is yet to be determined

if this predominance of CT2933, CT2932 and CT1916 is reflected in the normal gut microbiome of healthy individuals within Ireland.

This study had some limitations. The impact of HGT on the predominant CT sub-populations was not ascertained. Environmental screening was extremely rudimentary due to the COVID-19 pandemic limiting access and sampling strategies across the entire study-duration. Full transmission network determination relies on the inclusion of robust and highly detailed patient movement and spatial-dynamics data, which was not readily available. Therefore, potential genomic putative transmissions without epidemiological basis may possibly be explained by missing data and unsampled patients. Healthcare workers were also not sampled, which again may explain why some isolate pairs with highly related organisms lacked any reasonable epidemiological links. This may also under-estimate the true level of transmission. As with any retrospective analysis, there is potential isolate bias and we cannot be certain that all confounding variables have been identified. Another limitation is that we did not determine intra-patient isolate diversity or annual mutation rates within our own cohort due to lack of follow-up isolates and instead relied on published cgSNP data thresholds to inform putative transmission events. It is important to note however that conservative criteria were used for inferring potential transmissions (i.e. epidemiologically linked isolates recovered on the wards within ≤30 days that exhibited <10 cgSNPs).

Nonetheless, our findings are still informative for Irish hospital IPC strategies and highlight the need to potentially revisit current guidelines. For example, this study identified the inter-hospital dissemination of highly related isolates from endemic CTs across multiple wards (*N*=39) over extended time periods, which included 'non' high-risk areas which are not subject to routine VRE screening. Therefore, the scope of surveillance and screening practices are currently limited and may require extension to admission-based screening to identify non-high-risk areas serving as hidden reservoirs to help curtail widespread hospital transmission. Additionally, our findings indicate the need to consider the implementation of routine environmental screening in conjunction with the consideration of the impact of VSE carriage in IPC measures. This is particularly significant in the context of the potential for repeated gain/loss of the *vanA* operon in predominant VSE lineages via horizontal gene transfer.

Chapter 5

Multi-strain gastrointestinal carriage of genetically diverse vancomycin-resistant Clade A1 *Enterococcus faecium* amongst Irish patients with frequent health-care exposure – one pick to represent them all!

5.1 Introduction

The increasing accessibility and diminishing costs of high-throughput WGS technologies have revolutionised acute healthcare surveillance and bacterial phylogenetics by providing high-resolution insights into the emergence, adaptation, and transmission of major nosocomial pathogens such as *E. faecium*. The acquisition and subsequent intestinal colonisation of multidrug resistant strains, such as VREfm, has been well established as an important cofounder for subsequent clinical infection, both within the colonised individual and for other patients via faecal shedding into the immediate ward environment (Arias and Murray, 2012; Cattoir and Leclercq, 2013). Current approaches in sampling, characterising and tracing clinically important bacterial populations within healthcare settings rely on the assumption of single-strain carriage and/or monostrain infection which is reinforced by the selection of a single bacterial colony from a culture plate for subsequent sequencing (Croucher and Didelot, 2015). However, whilst single-isolate sequencing is a globally implemented, convenient sampling strategy, the presence of a heterogenous colonising or infecting population could significantly hinder the resolution of bacterial network inference, grossly underestimate complex transmission routes at play and diminish evolutionary dynamics (Worby *et al.,* 2014; Paterson *et al.,* 2015; Hall *et al.,* 2019).

Many studies have continually highlighted the highly recombinogenic nature of Clade A1 *E. faecium,* with the possibility of new clones continually emerging *in situ* as a result of both recombination and HGT. The highly dynamic environment of the gut consortium, together with the significant antibiotic selective pressure burden associated with a hospital environment, may potentially promote multi-strain and subspecies colonisation of VREfm in patients with frequent healthcare exposure (Baquero, 2004; van Schaik *et al.,* 2010; Howden *et al.,* 2013; Lebreton *et al.,* 2013). Additionally, as highlighted in Chapter 4, asymptomatically colonised patients can disseminate viable VREfm strains into the near-patient environment, creating a persistent reservoir of infection. This may contribute to sub-species diversity within the GIT and result in novel acquisition events for previously colonised patients. However, despite extensive global WGS-based studies on the molecular epidemiology of clade A1 VREfm, only a small number have characterised the genomic properties and frequency of multi-strain *E. faecium* GIT carriage (Moradigaravand *et al.,* 2017; Raven *et al.,* 2018; Bayjanov *et al.,* 2019; Dubin *et al.,* 2019; Both *et al.,* 2022; McHugh *et al.,* 2024).

The aim of this study was to systematically investigate the population dynamics, intra-host genetic diversity and plasmidome characteristics of clade A1 VREfm amongst asymptomatic carriers in a large Irish acute hospital.

5.2 Materials and Methods

5.2.1 Isolate collection

5.2.1.1 Patient isolates

Routine rectal screening swabs from 10 individual patients (P1-P10) in a large acute Dublin hospital (H1) were inoculated on CHROMID® VRE agar and incubated aerobically for 48 h at 37°C. Fifteen presumptive VREfm colonies recovered on CHROMID® VRE agar for each swab (*N*=150) were randomly selected and subcultured on CBA. Isolates were definitively identified as *E. faecium* by MALDI-TOF-MS and investigated by WGS. Fifteen VREfm colonies per rectal swab were chosen for investigation on the basis of practicality, reagent costs, and previous studies that investigated within patient heterogeneity (Moradigaravand *et al.*, 2017; Raven *et al.*, 2018; Bayjanov *et al.*, 2019; Dubin *et al.*, 2019; Both *et al.*, 2022; McHugh *et al.*, 2024). Rectal screens were collected as part of routine hospital admission surveillance.

Four of the VREfm-positive rectal screening swabs (P1, P3, P5 and P8) were randomly selected to provide a rudimentary snap-shot of the carriage of VSEfm in the patient cohort. The rectal swabs were initially inoculated on *Enterococcus faecium* ChromoSelect agar and incubated aerobically for 48 h at 37°C. Multiple, separate green colonies from each plate, indicative of *E. faecium*, were subcultured onto both *Enterococcus faecium* ChromoSelect agar and CHROMID® VRE agar. Only *E. faecium* colonies that did not grow on VRE agar were subjected to identification by MALDI-TOF-MS, susceptibility testing and WGS.

5.2.2 Phenotypic susceptibility testing

All study isolates underwent phenotypic susceptibility testing as described in described in Chapter 2, Section 2.3.2 Antimicrobial-resistance and virulence-associated genes were detected *in silico* on short-read WGS assemblies using ABRicate v.0.9.8 (https://github.com/tseemann/abricate).

5.2.3 Second generation Illumina short-read sequencing

5.2.3.1 Genomic DNA Extraction

All isolates underwent genomic DNA extraction for short-read sequencing as described in Chapter 2, Section 2.4.1.

5.2.3.2 Short-read sequencing

All isolates underwent short-read sequencing as described in Chapter 2, Section 2.5.1.

5.2.4 Third generation MinION long-read sequencing

Genomic DNA extraction and long-read sequencing in this chapter was undertaken commercially by MicrobesNG (https://microbesng.com/). Library preparation was performed using the Native Barcoding Kit 24 v14 (SQK-NBD114.24) and sequencing was performed on the GridION platform using a R10.4.1 Flow Cell with MinKNOW software v23.04.6.

5.2.5 Bioinformatic analysis

5.2.5.1 de novo assembly

All study isolates underwent quality trimming and *de novo* assembly using Ridom SeqSphere+ v8.5.1 (Ridom GmbH) as described in Chapter 2, Sections 2.6.1.1 and 2.6.1.2.

5.2.5.2 MLST

Conventional MLST profiles were generated for all isolates using Ridom SeqSphere+ v8.5.1 (Ridom GmbH) as described in Chapter 2, Section 2.6.1.3.

5.2.5.3 wgMLST and cgMLST

Isolate genomes underwent wgMLST and cgMLST as described in Chapter 2, Sections 2.6.1.4 and 2.6.1.5.

5.2.5.4 Genotyping

Antimicrobial resistance profiling and virulence gene identification was performed *in silico* as described in Chapter 2, Section 2.6.1.6.

5.2.5.5 Split k-mer analysis

Target free pairwise whole-genome comparison was conducted using the SKA package v1.0 (https://github.com/simonrharris/SKA) (Harris, 2018). The fastq command was used under default settings to generate *k*-mer files (*k*=15) for each isolate from the short-read WGS data. Pairwise distances and single-linkage clustering was performed using SKA distance with an identity cutoff of ≥0.9 using a relatedness threshold of seven SNPs based on recent studies (Higgs *et al.*, 2022). Reference free alignment of split *k*-mer files was carried out using the SKA align command under default settings.

5.2.5.6 Phylogenetic trees

Inference of genetic relatedness, diversity, and population structure of *E. faecium* isolates in this study was carried out as described in Chapter 2, Section 2.6.1.8 and Chapter 4, Section 4.2.6.5.

5.2.5.6.1 Neighbour joining tree

NJTs were generated using distance matrices based on cgMLST analysis using Ridom SeqSphere+ v8.5.1 (Ridom GmbH) as described in Chapter 2, Section 2.6.1.8.

4.2.5.6.2 Maximum likelihood tree

MLTs based on SKA-SNPs were constructed using IQ-TREE v2.2.2.6 (http://www.iqtree.org) as described in Chapter 4, Section 4.2.6.5.2.

5.2.6 Hybrid assembly

Hybrid assembly of paired-end short-read and long-read sequences was performed using Unicycler as described in Chapter 2, Section 2.7.

5.2.7 Plasmid analysis

5.2.7.1 Plasmid profile determination

Bacterial genome plasmid contigs were characterised as described in Chapter 2, Section 2.8.1. MOB Subfamilies were assigned using the MOB-Typer tool as part of the MOB-suite (https://github.com/phac-nml/mob-suite) (Robertson and Nash, 2018). Pairwise plasmid genomic distance estimation was calculated using Mash v2.3 (https://github.com/marbl/Mash) using default *k*-mer and sketch sizes (Ondov *et al.*, 2016).

Clustering was performed by the complete linkage method based on the Mash-calculated distance matrix using the hclust command in RStudio v2024.04.01 (RStudio Team, 2021) with a threshold of 0.06 (Robertson *et al.*, 2020). The ggplot2 package (Wickham, 2016) in in RStudio v2024.04.01 (RStudio Team, 2021) was used for dendrogram construction and plasmid data visualisation.

5.2.8 Filter mating

Conjugative transfer of plasmids encoding the vancomycin resistance *vanA* operon harboured by clinical enterococcal isolates was undertaken using the plasmid-free rifampicin- and fusidic acid-resistant recipient strains *E. faecium* 64/3 as described in Chapter 2, Section 2.8.4.

5.2.9 PFGE

PFGE was performed as described in Chapter 2, Section 2.8.3.

5.3 Results

5.3.1 Isolate description

In order to characterise the prevalence and diversity of mixed-strain gastrointestinal carriage of VREfm in Irish patients with frequent healthcare exposure, a total of 150 VREfm colonies were sequenced from rectal screening swabs taken from 10 individual patients (15 isolates per patient) on seven wards (W1 *N*=1, W2 *N*=1, W3 *N*=4, W9 *N*=1, W18 *N*=1, W20 *N*=1, WE *N*=1) of a Dublin hospital (H1). All VREfm harboured *vanA* exclusively. Thirty VSEfm isolates were identified from a total of 80 colonies selected at random on *E. faecium* selective agar following plating of four of the patient rectal screening swabs (20 colonies per rectal swab) (VSEfm: P1 *N*=7, P3 *N*=5, P5 *N*=13 and P8 *N*=5).

5.3.2 Heterogeneity of within-patient VREfm colonisation

The majority of isolates (147/150, 98%) were assigned to ST80 by conventional *in silico* MLST. Three 'novel' isolates, which were double locus variants of ST80, were submitted to pubMLT.org for ST assignment. Recent studies investigating within-patient VREfm heterogeneity have primarily utilised MLST analysis and ST groupings to define the presence of different strain types within a colonising population (Brodrick *et al.,* 2016; Moradigaravand *et al.,* 2017; Gouliouris *et al.,* 2020; Both *et al.,* 2022; McHugh *et al.,* 2024). Previous research from this laboratory demonstrated that Irish VREfm exhibit a polyclonal population structure, with a predominance of ST80 encompassing very diverse CT groups clearly differentiated by significant genomic variation and long network branches (Chapter 3) (Egan *et al.,* 2022; Kavanagh *et al.,* 2024). As a result, MLST analysis alone was insufficient in the present study to accurately capture and resolve within-patient diversity. Consequently, VREfm isolates from individual patients belonging to distinct CTs were deemed to be separate strains.

Using cgMLST analysis and a previously recommended threshold of ≤20 allelic differences to define isolate relatedness (de Been *et al.,* 2015), VREfm isolates grouped into nine distinct genomic clusters and 2 singletons with an average cluster size of 16 (median: 11; range: 2-48) (Figure 5.1). A core-genome based MST comprising study (*N*=150), national (*N*=1,286) and global (*N*=1,325) *E. faecium* isolates confirmed the assignment of the within-patient diversity isolates to the hospital-adapted clade A1 (Figure 5.2). The majority (70%, 7/10) of patients harboured a diverse colonising population, consisting of two (N=4), three (N=2) or four (N=1) unique VREfm CTs. The remaining three patients yielded isolates belonging to one CT only (Figure 5.1, Table 5.1).

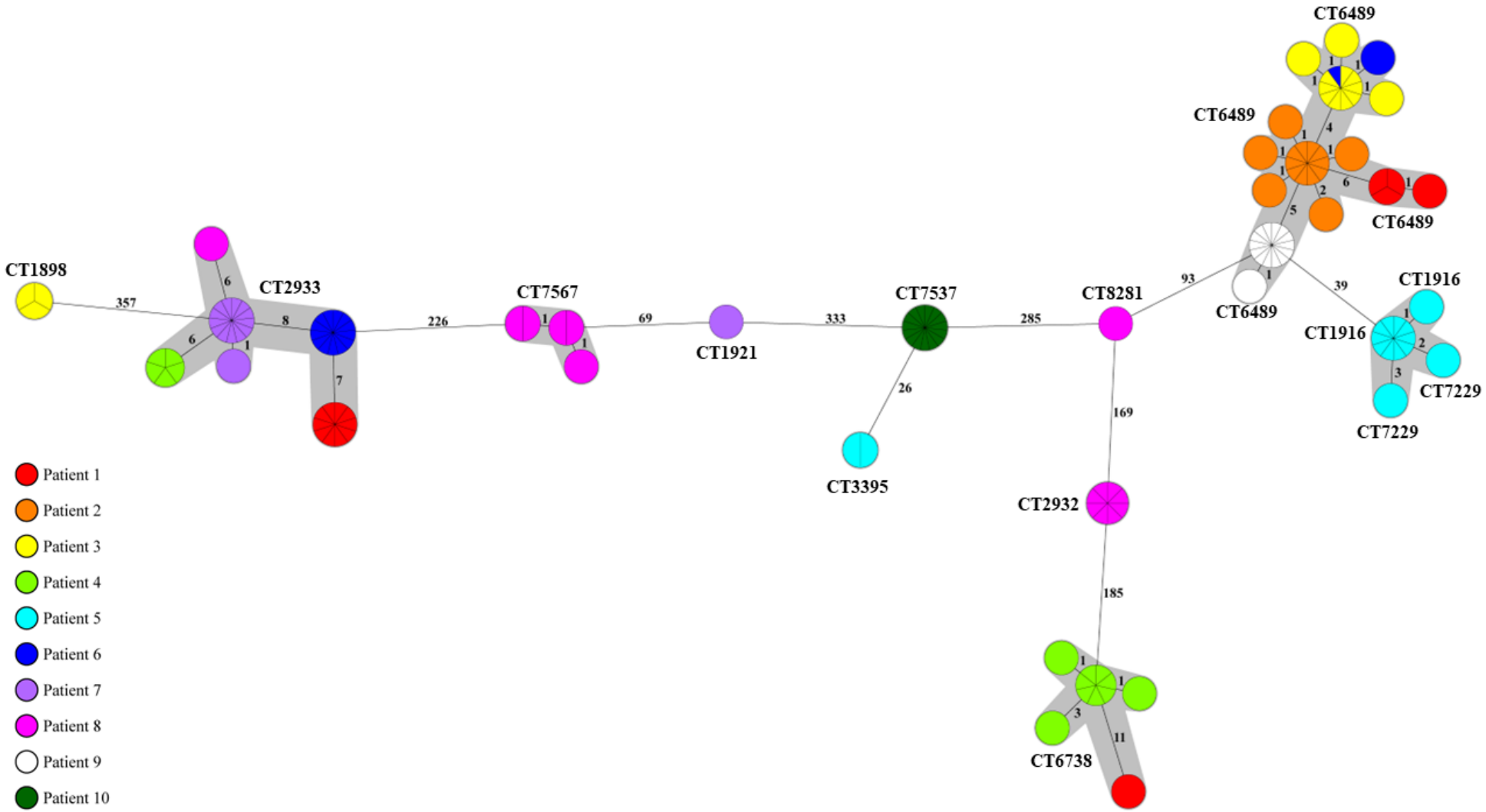
CT1898
CT2933
CT7567
CT1921
CT7537
CT8281
CT6489
CT6489
CT6489
CT1916
CT1916
CT7229
CT7229
CT3395
CT2932
CT6738
357
226
69
333
285
93
39
26
169
185
Patient 1
Patient 2
Patient 3
Patient 4
Patient 5
Patient 6
Patient 7
Patient 8
Patient 9
Patient 10

Figure 5.1. Minimum spanning tree (MST) based on core genome multi-locus sequence typing (cgMLST) analysis of 1,423 loci for 150 clade A1 VREfm isolates recovered from a single rectal screening swab from each of 10 separate patients. Node colours represent the patient number (1-10) from which the isolate was recovered as indicated in the legend. Partitions within the nodes represent the presence of ≥2 isolates. Branch numbers indicate cgMLST allelic differences between neighbouring isolates. cgMLST segregated isolates into 9 clusters and one singleton using the previously recommended relatedness threshold of ≤20 allelic differences (de Been *et al.*, 2015).

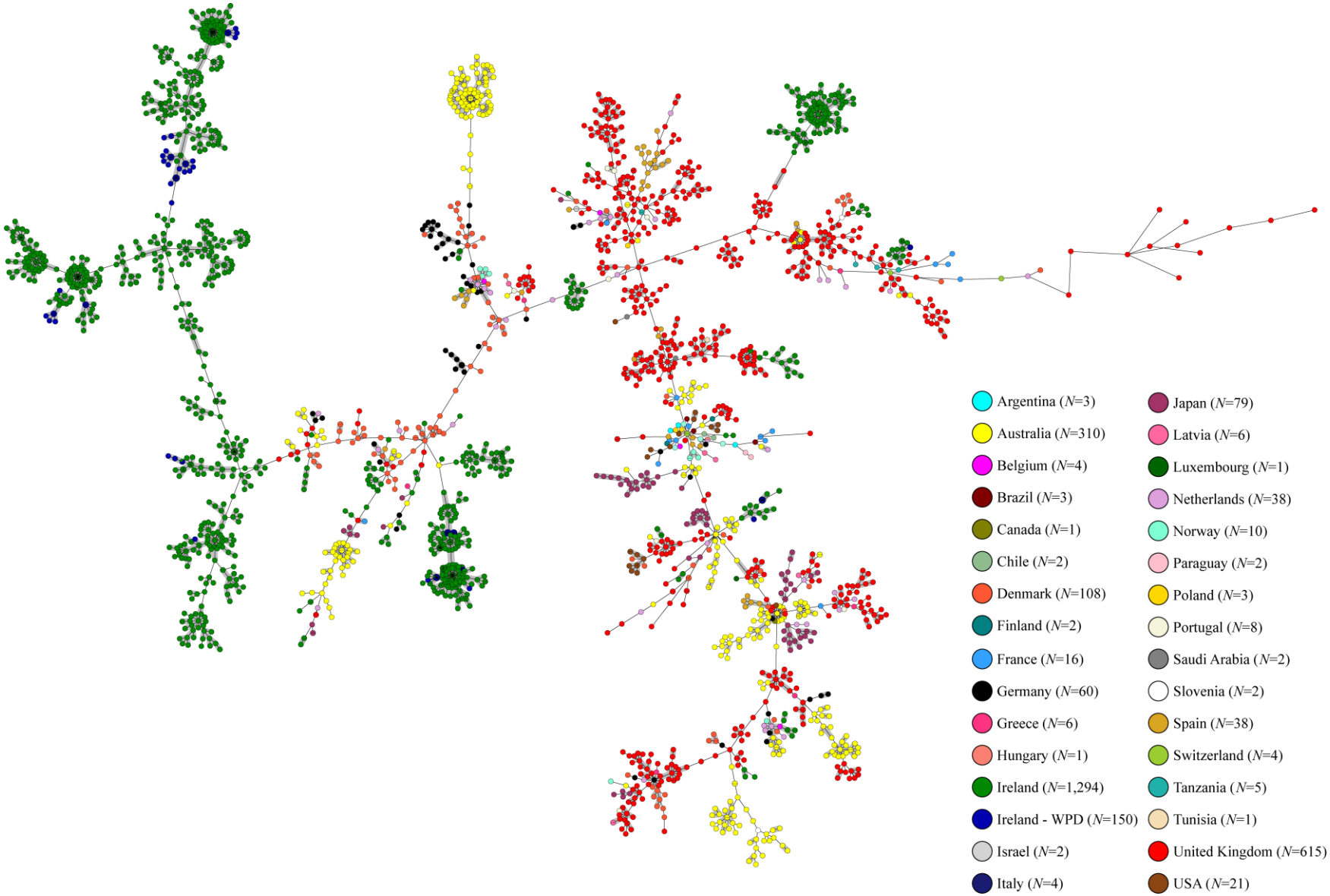
Argentina (N=3)
Australia (N=310)
Belgium (N=4)
Brazil (N=3)
Canada (N=1)
Chile (N=2)
Denmark (N=108)
Finland (N=2)
France (N=16)
Germany (N=60)
Greece (N=6)
Hungary (N=1)
Ireland (N=1,294)
Ireland - WPD (N=150)
Israel (N=2)
Italy (N=4)
Japan (N=79)
Latvia (N=6)
Luxembourg (N=1)
Netherlands (N=38)
Norway (N=10)
Paraguay (N=2)
Poland (N=3)
Portugal (N=8)
Saudi Arabia (N=2)
Slovenia (N=2)
Spain (N=38)
Switzerland (N=4)
Tanzania (N=5)
Tunisia (N=1)
United Kingdom (N=615)
USA (N=21)

Figure 5.2. Minimum spanning tree (MST) based on core genome multi-locus sequencing typing (cgMLST) analysis of 1,4234 loci of Irish Clade A1 *E. faecium* (*N*=1,444) isolated between June 2017 and December 2022 and global Clade A1 *E. faecium* (*N*=1,356) from 30 countries, spanning a 30-year time period (1986-2016) from the study of van Hal *et al.*, 2021 and Raven *et al.*, 2016. Isolates are coloured by country of origin as indicated in the legend. Irish within-patient diversity (WPD) isolates are coloured dark blue (*N*=150), whilst Irish isolates described in previous studies from this laboratory (*N*=1,294) are coloured green (Chapter 3 and Chapter 4) (Egan *et al.*, 2022; Kavanagh *et al.*, 2024).

Table 5.1. Detailed metadata and distribution of complex types (CT)s for 150 Clade A1 VREfm isolates recovered from a single rectal screening swab from each of 10 separate patients

Patient	Total number of sub-types	Isolate name	CT[1]	Frequency (N, %)[2]	Median intra-CT cgMLST allelic difference (range)	Median intra-CT pairwise SKA-SNP difference (range)	Median inter-CT cgMLST allelic differences (range)	Median inter-CT pairwise SKA-SNP difference (range)	Median pairwise cgMLST allelic difference of total patient population (range)	Median pairwise SKA-SNP difference of total patient population (range)
Patient 1	3	JHM1-3 JHM1-4 JHM1-5 JHM1-6 JHM1-7 JHM1-8 JHM1-10 JHM1-13 JHM1-14 JHM1-15	2933	Dominant (10, 66.67%)	0	0	437 (311-437)	2818 (2692-3405)	1 (0-427)	2693 (0-3405)
		JHM1-1 JHM1-2 JHM1-9 JHM1-12	6489	Moderate (4, 26.67%)	0 (0-1)	1.5 (0-3)				
		JHM1-11	6738	Minor (1, 6.6%)	-	-				
Patient 2	1	JHM2-1 JHM2-2 JHM2-3 JHM2-4 JHM2-5 JHM2-6 JHM2-7 JHM2-8 JHM2-9 JHM2-10 JHM2-11 JHM2-12 JHM2-13 JHM2-14 JHM2-15	6489	Dominant (15, 100%)	-	-	-	-	1 (0-3)	2 (0-8)

Table 5.1 continued overleaf

Patient	Total number of sub-types	Isolate name	CT[1]	Frequency (N, %)[2]	Median intra-CT cgMLST allelic difference (range)	Median intra-CT pairwise SKA-SNP difference (range)	Median inter-CT cgMLST allelic differences (range)	Median inter-CT pairwise SKA-SNP difference (range)	Median pairwise cgMLST allelic difference of total patient population (range)	Median pairwise SKA-SNP difference of total patient population (range)
Patient 3	2	JHM3-1 JHM3-4 JHM3-9	1898	Moderate (3, 20%)	0	0	484 (469-485)	3691 (3686-3700)	1 (0-485)	2 (0-3700)
		JHM3-2 JHM3-3 JHM3-5 JHM3-6 JHM3-7 JHM3-8 JHM3-10 JHM3-11 JHM3-12 JHM3-13 JHM3-14 JHM3-15	6489	Dominant (12, 80%)	0 (0-2)	2 (0-6)				
Patient 4	2	JHM4-1 JHM4-2 JHM4-12 JHM4-13 JHM4-15	2933	Moderate (5, 33.33%)	0	0	407 (404-410)	3039 (3031-3071)	3 (0-410)	30 (0-3071)
		JHM4-3 JHM4-4 JHM4-5 JHM4-6 JHM4-7 JHM4-8 JHM4-9 JHM4-10 JHM4-11 JHM4-14	6738	Dominant (10, 66.67%)	0 (0-4)	3 (0-34)				

Table 5.1 continued overleaf

Patient	Total number of sub-types	Isolate name	CT[1]	Frequency (N, %)[2]	Median intra-CT cgMLST allelic difference (range)	Median intra-CT pairwise SKA-SNP difference (range)	Median inter-CT cgMLST allelic differences (range)	Median inter-CT pairwise SKA-SNP difference (range)	Median pairwise cgMLST allelic difference of total patient population (range)	Median pairwise SKA-SNP difference of total patient population (range)
Patient 5	3	JHM5-1 JHM5-2 JHM5-3 JHM5-4 JHM5-5 JHM5-6 JHM5-7 JHM5-8 JHM5-9 JHM5-10 JHM5-14	1916	Dominant (11, 73.33%)	0 (0-1)	0 (0-2)	376 (371-378)	2502 (2496-2506)	1 (0-378)	1 (0-2506)
		JHM5-13 JHM5-11	3395	Minor (2, 13.33%)	0	0				
		JHM5-12 JHM5-15	7229	Minor (2, 13.33%)	2 (0-4)	4 (0-8)				
Patient 6	2	JHM6-1 JHM6-2 JHM6-3 JHM6-4 JHM6-5 JHM6-6 JHM6-8 JHM6-10 JHM6-11 JHM6-12 JHM6-13 JHM6-14 JHM6-15	2933	Dominant (13, 86.67%)	0 (0-1)	1 (0-10)	435 (435-436)	2948 (2946-2951)	0 (0-436)	1 (0-2951)
		JHM6-7 JHM6-9	6489	Minor (2, 13.33%)	0.5 (0-1)	2 (0-4)				

Table 5.1 continued overleaf

Patient	Total number of sub-types	Isolate name	CT[1]	Frequency (N, %)[2]	Median intra-CT cgMLST allelic difference (range)	Median intra-CT pairwise SKA-SNP difference (range)	Median inter-CT cgMLST allelic differences (range)	Median inter-CT pairwise SKA-SNP difference (range)	Median pairwise cgMLST allelic difference of total patient population (range)	Median pairwise SKA-SNP difference of total patient population (range)
Patient 7	2	JHM7-2	1921	Minor (1, 6.6%)	-	-	246 (246-247)	216 (95-217)	0 (0-247)	0 (0-217)
		JHM7-1 JHM7-3 JHM7-4 JHM7-5 JHM7-6 JHM7-7 JHM7-8 JHM7-9 JHM7-10 JHM7-11 JHM7-12 JHM7-13 JHM7-14 JHM7-15	2933	Dominant (14, 93.33%)	0 (0-1)	0 (0-4)				
Patient 8	4	JHM8-1 JHM8-3 JHM8-5 JHM8-7 JHM8-8 JHM8-11-1 JHM8-12 JHM8-13	2932	Dominant (8, 53.33%)	0	0 (0-1)	428 (169-429)	2933 (1497-3232)	229 (0-429)	2469 (0-3232)
		JHM8-4	2933	Minor (1, 6.6%)	-	-				
		JHM8-2 JHM8-6 JHM8-9-1 JHM8-10 JHM8-15	7567	Moderate (5, 33.33%)	1 (0-2)	1 (0-1)				
		JHM8-14-1	8281	Minor (1, 6.6%)	-	-				

Table 5.1 continued overleaf

Patient	Total number of sub-types	Isolate name	CT[1]	Frequency (N, %)[2]	Median intra-CT cgMLST allelic difference (range)	Median intra-CT pairwise SKA-SNP difference (range)	Median inter-CT cgMLST allelic differences (range)	Median inter-CT pairwise SKA-SNP difference (range)	Median pairwise cgMLST allelic difference of total patient population (range)	Median pairwise SKA-SNP difference of total patient population (range)
Patient 9	1	JHM9-1 JHM9-10 JHM9-11 JHM9-12 JHM9-13 JHM9-14 JHM9-15 JHM9-2 JHM9-3 JHM9-4 JHM9-5 JHM9-6 JHM9-7 JHM9-8 JHM9-9	6489	Dominant (15, 100%)	-	-	-	-	0 (0-1)	0 (0-4)
Patient 10	1	JHM10-1 JHM10-10 JHM10-11 JHM10-12 JHM10-13 JHM10-14 JHM10-15 JHM10-2 JHM10-3 JHM10-4 JHM10-5 JHM10-6-1 JHM10-7-1 JHM10-8 JHM10-9	7537	Dominant (15, 100%)	-	-	-	-	0	0

Abbreviations: CT, complex type; -, not applicable; SKA SNP, single nucleotide polymorphism split *k*-mer analysis.

[1] Genotypic information including cgMLST complex type (CT) were extracted *in silico* from whole genome data using Ridom SeqSphere+ v8.5.1 (Ridom GmbH, Münster, Germany). The cgMLST CT was determined according to the publicly available cgMLST scheme based on 1,423 loci (de Been *et al.*, 2015).

[2] Strain type frequency was classified as follows: dominant (representing >50% of sampled population), moderate (representing <35%) and minor (representing <15%). % Frequency was calculated by dividing the number of colonies of a specific CT type by the total number of sampled colonies within a sample (i.e. N/15 x 100%).

Strain types were recovered at varying frequencies; in all seven patients with multi-strain carriage, a 'dominant' VREfm CT was identified which represented 53-93% of all 15 sampled colonies from the patients concerned (≥8/15 colonies picked, range: 8-14). In 43% (3/7) of the multi-strain colonised patients, the predominant CT was CT2933, with the remainder belonging to CT2932 (*N*=1), CT1916 (*N*=1), CT6489 (*N*=1) and CT6738 (*N*=1). Moderate frequency CTs, which consisted of isolates that represented <35% (3-5 colonies) of the total sampled population from each rectal swab, were identified in four patients (4/7, 56%) (Figure 5.1, Table 5.1) Minor frequency CTs (<15%, ≤2 of the 15 colonies investigated) were identified in five patients (Table 5.1). In the three patients found to harbour only one distinct strain (i.e., patients P2, P9, P10), CT6849 was the predominant variant identified (2/3 patients, 66.66%).

A high level of genomic variation was observed between isolate pairs from different CTs within the same patients (Table 5.1, Tables 5.2a-j). For clarity and ease of reading, Table 5.2a is shown within the results section and the remaining Tables 5.2b-j are available in in the appendix at the end of this chapter (Section 5.5). For example, patient P8 yielded four distinct CTs with a median inter-CT (i.e., between strains) pairwise cgMLST allelic difference of 427 (range: 169-429) (Figure 5.1, Table 5.1). This level of diversity was also mirrored by whole-genome comparisons, with a median pairwise difference of 2933 SKA SNPs (range: 1497-3232) observed between isolate pairs recovered from P8 belonging to different CTs (Figure 5.3, Tables 5.1 and 5.2h). Similar findings of significant inter-CT genetic variation were observed for the remaining six patients harbouring multiple VREfm CTs (Tables 5.2a-j). This finding is indicative of distinct acquisition events of genetically diverse VREfm rather than *in vivo* evolution, with previous studies reporting annual within-patient diversification rates of 6-122 cgSNPs (Moradigaravand *et al.*,2017; Raven *et al.*,2017; Bayjanov *et al.*,2019; Dubin *et al.*,2019). Genetic diversity was minimal when isolate pairs of the same CT from the same patient were compared, with a median pairwise cgMLST allelic difference and SKA-SNP difference of 0 (range: 0-4) and 0 (range: 0-34), respectively, (Tables 5.1 and 5.2a-j). For the three patients that yielded VREfm belonging to only one CT, the median pairwise SKA SNP difference was 0 (average: 1, range 0-8). The finding of multiple genetically diverse VREfm strains (≥2 CTs) in 70% of patients with frequent healthcare exposure is higher than previously reported (Brodrick *et al.,* 2016; Moradigaravand *et al.,* 2017; Gouliouris *et al.,* 2020; Both *et al.,* 2022; McHugh *et al.,* 2024).

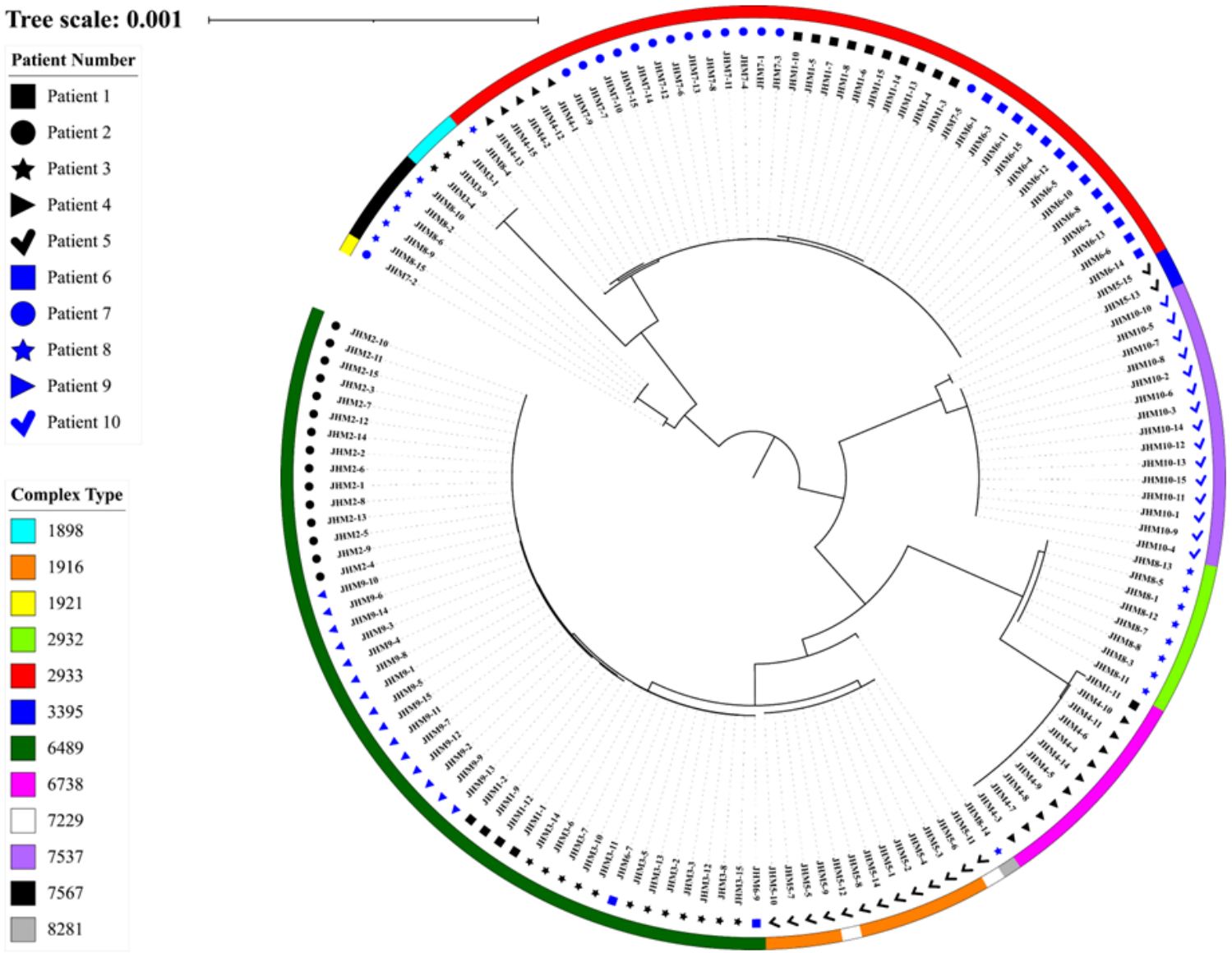
Tree scale: 0.001
Patient Number
Patient 1
Patient 2
Patient 3
Patient 4
Patient 5
Patient 6
Patient 7
Patient 8
Patient 9
Patient 10
Complex Type
1898
1916
1921
2932
2933
3395
6489
6738
7229
7537
7567
8281

Figure 5.3. Maximum likelihood tree (MLT) based on phylogenetic analysis of 150 Clade A1 vancomycin-resistant *Enterococcus faecium* (VREfm) isolates recovered from a single rectal screening swab from each of 10 separate patients. Detailed metadata pertaining to patient number and core-genome complex type (CT) are indicated in the legend. A tree scale bar is shown at the top left. The tree is mid-point rooted. The corresponding pairwise indices and distances for all isolates is provided in Tables 5.2a-j (See Section 5.5 Appendix for Table 5.2b-j).

Table 5.2a. Pairwise single nucleotide polymorphism (SNP) distance matrix based on split *k*-mer analysis (SKA) of 15 isolates recovered from patient P1

No. isolates	Isolate name	Ward	ST/CT		SKA SNP matrix														Median pairwise SKA-SNP difference (range)
					JHM1-1	**JHM1-2**	**JHM1-3**	**JHM1-4**	**JHM1-5**	**JHM1-6**	**JHM1-7**	**JHM1-8**	**JHM1-9**	**JHM1-10**	**JHM1-11**	**JHM1-12**	**JHM1-13**	**JHM1-14**	**JHM1-15**	
15	JHM1-1	W3	ST80/CT6489	**JHM1-1**																2693 (0-3405)
	JHM1-2	W3	ST80/CT6489	**JHM1-2**	3															
	JHM1-3	W3	ST80/CT2933	**JHM1-3**	2821	2818														
	JHM1-4	W3	ST80/CT2933	**JHM1-4**	2821	2818	0													
	JHM1-5	W3	ST80/CT2933	**JHM1-5**	2822	2819	0	0												
	JHM1-6	W3	ST80/CT2933	**JHM1-6**	2821	2818	0	0	0											
	JHM1-7	W3	ST80/CT2933	**JHM1-7**	2822	2819	0	0	0	0										
	JHM1-8	W3	ST80/CT2933	**JHM1-8**	2821	2818	0	0	0	0	0									
	JHM1-9	W3	ST80/CT6489	**JHM1-9**	3	0	2817	2817	2818	2817	2818	2817								
	JHM1-10	W3	ST80/CT2933	**JHM1-10**	2820	2817	0	0	0	0	0	0	2816							
	JHM1-11	W3	ST80/CT6738	**JHM1-11**	2692	2695	3403	3404	3405	3403	3404	3404	2693	3401						
	JHM1-12	W3	ST80/CT6489	**JHM1-12**	3	0	2818	2818	2819	2818	2819	2818	0	2817	2695					
	JHM1-13	W3	ST80/CT2933	**JHM1-13**	2821	2818	0	0	0	0	0	0	2817	0	3403	2818				
	JHM1-14	W3	ST80/CT2933	**JHM1-14**	2821	2818	0	0	0	0	0	0	2817	0	3403	2818	0			
	JHM1-15	W3	ST80/CT2933	**JHM1-15**	2822	2819	0	0	0	0	0	0	2818	0	3403	2819	0	0		

Abbreviations: CT, cgMLST complex type; ST, MLST sequence type, SKA SNP, single nucleotide polymorphism split *k*-mer analysis.

5.3.3 Whole-genome comparisons reveal potential transmission of minor frequency strains

The cgMLST-based MST revealed three distinct CTs (CT2933, CT6489 and CT6738) each consisting of closely related (<20 allelic differences) VREfm isolates from multiple patients (Figure 5.1) recovered between October 2022-Janurary 2023 (105 days) suggesting possible direct and/or indirect transmission. The largest of these CT clusters, CT6489, comprised 48 isolates from five patients (P1 *N*=4, P2 *N*=15, P3 *N*=12, P6 *N*=2 and P9 *N*=15) with a median pairwise allelic difference of 5 (range: 0-11). For three of the five patients (P2, P3 and P9), CT6489 was the dominant VREfm CT recovered (Table 5.1). In the remaining two patients, CT6489 was considered a moderate or minor frequency CT. However, isolates deemed to be closely related by cgMLST demonstrated greater diversity following SKA SNP analysis (Tables 5.3a-h). For clarity and ease of reading, Table 5.3a is shown within the results section and the remaining Tables 5.3b-h are available in in the appendix at the end of this chapter (Section 5.5). Pairwise whole-genome comparisons of CT6489 isolates revealed a median pairwise SNP difference of 66 (range: 0-140) (Table 5.3e). Previous studies recommended a relatedness threshold of ≤7 SKA SNPs to identify recent putative transmission events (Higgs *et al.*,2022). Based on this criterion, P3 and P6 which were present on W3 harboured very closely related VREfm CT6489 strains (median pairwise SNP difference: 3, range: 1-6) with no apparent epidemiological link (recovery date difference of 101 days) suggestive of potential transmission or acquisition from a common source. Notably, in P6, CT6489 was found at low abundance, representing only 13% (2/15) of the sampled colonies indicating a minor frequency strain that may be overlooked in the context of plate sampling strategies for outbreak resolution.

Table 5.3a. Pairwise single nucleotide polymorphism (SNP) distance matrix based on split *k*-mer analysis (SKA) of VREfm belonging to complex type (CT) 1898 identified using core-genome multi-locus sequence type (cgMLST) analysis of 150 Clade A1 VREfm isolates recovered from a single rectal screening swab from each of 10 separate patients (Figure 5.1)

No. isolates	Isolate name	Patient	Collection date	Ward	SKA SNP matrix				Median pairwise SKA-SNP difference (range)
						JHM3-1	**JHM3-4**	**JHM3-9**	
3	JHM3-1 JHM3-4 JHM3-0	3	11/10/2022	W3	**JHM3-1** **JHM3-4** **JHM3-9**	0 0	0		0

Abbreviations: CT, cgMLST complex type; ST, MLST sequence type; SKA SNP, single nucleotide polymorphism split *k*-mer analysis.

5.3.4 Heterogeneity of VREfm colonisation: do minor frequency strains represent an unsampled 'hidden highway' of transmission?

The isolates from the present study (*N*=150) were placed in a wider genomic context with the genomes of an additional 622 previously described Clade A1 clinical and screening *E. faecium* isolates (recovered between June 2017-December 2022) from individual patients and environmental sites in H1 (VREfm *N*=579, VSEfm *N*=43) from the same seven wards (W1 *N*=107, W2 *N*=156, W3 *N*=327, W9 *N*=7, W18 *N*=22 and W20 *N*=3) (Appendix 1, Table 1, Chapter 3 and 4) (Egan *et al.,* 2022; Kavanagh *et al.,* 2024). The aim of this five-year ward comparison was to highlight the frequency at which *E. faecium* subtypes, particularly moderate and minor frequency strains, were shared between patients and their environment, to provide insight into the implications of VREfm within-patient heterogeneity on *E. faecium* population biology and surveillance practices. As noted in Section 5.3.3, previous studies employing whole-genome comparisons in VREfm outbreak analysis have utilised a variety of thresholds (7-10 SNPs) to infer transmission pathways and determine genetic relatedness between isolate cohorts within specific study periods (Higgs *et al.,* 2022; Maechler *et al.,* 2023). However, as the comparison was not intended to determine recent transmission or infer epidemiological links, but instead to identify discrete genomic clusters and elucidate strain distribution, a less stringent threshold of ≤15 SKA SNP differences was adopted here to deem isolates as closely related. This was determined on the basis of a previous study which delineated the population structure of clade A1 and highlighted that isolates within groups that exhibited ≤20 SNPs displayed limited recombination and were therefore deemed as the same sub-type descending from a common ancestor (Gouliouris *et al.,* 2020). The of ≤15 SKA SNP threshold was established from a combination of the previously reported annual *E. faecium* diversification estimates, the five-year isolate recovery duration and previously defined thresholds describing subtypes (Moradigaravand *et al.,* 2017; Raven *et al.,* 2017; Bayjanov *et al.,* 2019; Dubin *et al.,* 2019)

cgMLST segregated isolates into 44 clusters and 38 singletons with 48% (368/772) belonging to CT2933, CT2932, CT1916 and CT6489 (Figure 5.4). In the larger H1 isolate collection comparison, evidence for the circulation and persistence of highly-related minority subpopulations across multiple H1 wards was supported by a small number of examples (Table 5.4a-i). For clarity and ease of reading, Table 5.4a is shown within the results section and the remaining Tables 5.4b-i are available in in the appendix at the end of this chapter (Section 5.5). For instance, CT7567 comprised six genetically indistinguishable VREfm isolates from two wards (W2 *N*=1, W3 *N*=5) recovered between December 2022-

Janurary 2023 (27 days) which exhibited a median pairwise SKA-SNP difference of 0 (range: 0-1) (Table 5.4i). Notably, 5/6 isolates were recovered from patient P8 (W3) and represented a moderate frequency strain (33.33%, 5/15 sample colonies). Low frequency *E. faecium* sub-types were also associated with long-term ward-specific persistence; CT1898 comprised 9 isolates, including a moderate frequency strain from patient P3 (20%, 3/15 sample colonies, JHM3-1, JHM3-4 and JHM3-9), recovered from two wards (W2 *N*=2, W3 *N*=7) over 39 months (June 2019-October 2022) (Table 5.4f). Interestingly, the closest two neighbouring isolates (SJ178 and SJ267) to the P3 moderate frequency strains were collected 1,217 days prior and exhibited median pairwise SNP differences of 15 and 13, respectively, (Table 5.4f). These findings, however, should be interpreted with caution as comparator H1 ward isolates were recovered by selecting a single bacterial colony from each sample. Consequently, a more detailed analysis is required to accurately determine the true inter and intra-ward distribution of strains and highlight the impact of low frequency strain transmission.

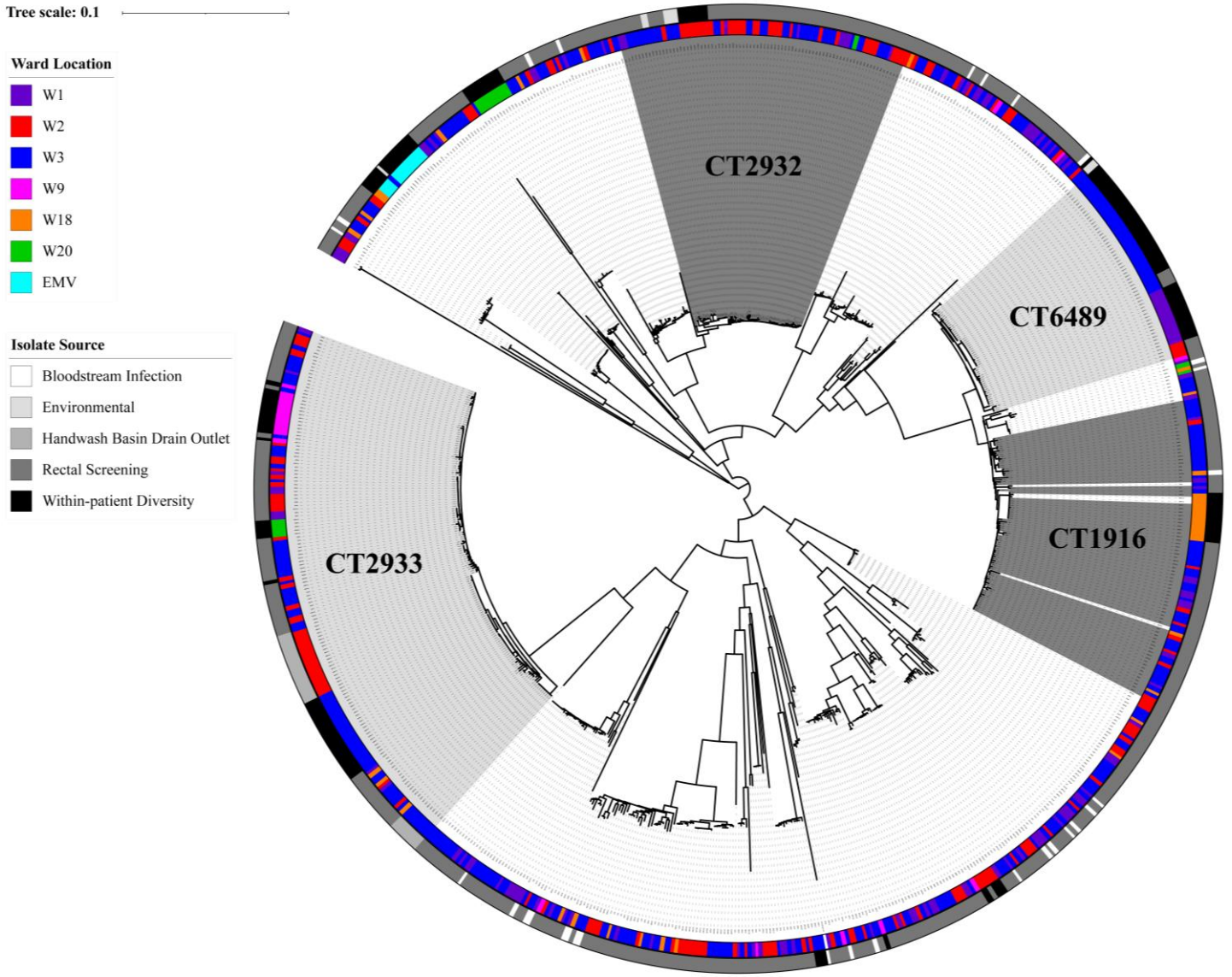
Tree scale: 0.1
Ward Location
W1
W2
W3
W9
W18
W20
EMV
Isolate Source
Bloodstream Infection
Environmental
Handwash Basin Drain Outlet
Rectal Screening
Within-patient Diversity
CT2932
CT6489
CT1916
CT2933

Figure 5.4. Neighbour joining tree (NJT) based on core-genome multi locus sequence type (cgMLST) analysis of 1,423 target genes for 772 Clade A1 *E. faecium* isolates recovered from W1, W2, W3, W9, W18, W20 and WE in Hospital 1 between June 2017 and December 2022. The NJT comprises 622 isolates from H1 reported in previous studies from this laboratory (Egan *et al.,* 2022; Kavanagh *et al.,* 2024) and within-patient diversity isolates from this study (*N*=150). Isolates segregated into 44 clusters and 38 singletons. Four distinct clusters of closely related isolates (≤20 allelic differences) are highlighted, which are shaded in grey with the corresponding complex type (CT) indicated as follows: CT2933 (151 isolates): average allelic difference: 8, range: 0-22; CT2932 (80 isolates): average allelic difference: 6, range: 0-18; CT1916 (81 isolates): average allelic difference 11, range 0-28; CT6489 (56 isolates): average allelic difference: 6 range: 0-20. Metadata pertaining to ward location, isolate source and vancomycin susceptibility phenotype are indicated in the legends. A tree scale bar is shown at the top left.

Table 5.4a. Pairwise single nucleotide polymorphism (SNP) distance matrix based on split *k*-mer analysis (SKA) of *E. faecium* isolates (*N*=151) belonging to complex type (CT) 2933 identified using core-genome multi-locus sequence type (cgMLST) analysis of 43 Clade A1 VREfm recovered from patients P1 (*N*=10), P4 (*N*=5), P6 (*N*=13), P7 (*N*=14) and P7 (*N*=1) with additional isolates from database (*N*=108) (Figure 5.4)

Size of table exceeds page margins.

Scan and/or click QR code to access and/or download table.

5.3.5 Exploring the complex plasmidome dynamics of VREfm strains from patients co-colonised with multiple strains

It has been well established that mobile genetic elements including plasmids have shaped the emergence of hospital-adapted lineages of *E. faecium* (Arredondo-Alonso *et al.*,2020). To investigate the impact of multi-strain carriage on the plasmid pool present in VREfm in individual patients, the plasmid sequences from a representative subset of 39 isolates recovered from the 10 patient rectal screening swabs (P1 *N*=6, P2 *N*=2, P3 *N*=3, P4 *N*=4, P5 *N*=5, P6 *N*=4, P7 *N*=4, P8 *N*=7, P9 *N*=2 and P10 *N*=2) were fully resolved by hybrid assembly of short-read and long-read WGS sequences (Table 5.5) The 39 isolates were selected to provide representative examples of the CT types in each patient.

A total of 193 fully resolved plasmid sequences were identified in the 39 VREfm isolates, ranging in length from 2,947 to 289,861 bp. An additional 10 plasmids, distributed amongst multiple contigs, were excluded from further analysis. In line with previous studies on hospital adapted clones, VREfm isolates harboured a median of 5 plasmids (range: 3-8) with an average size of 74,214 bp (Rosvoll *et al.*, 2010; Arredondo-Alonso *et al.*, 2020). Plasmids were subsequently grouped on the basis of associated replication genes, revealing a total of nine distinct REP types with *rep11a* (*N*=28) and *repUS15* (*N*=39) predominating (Table 5.5). A total of 12% (23/193) of plasmids were considered multi-replicon, encoding up to three distinct REP types indicating extensive mosaicism. Interestingly, the majority of plasmids (82/193, 42%) were not assigned a REP. The predicted conjugative transferability of plasmids was determined using *Mob* and mate-pair formation (MPF) protein typing (Robertson and Nash, 2018). In total, 56.5% (109/193) of plasmids were characterised as non-mobilisable, 30% (58/193) as mobilisable and 13.5% as conjugative (26/193). The majority of plasmids characterised as 'transferable' (i.e., mobilisable, and conjugative) (81/84) contained MOBP relaxase gene family types (Table 5.5). The average size of predicted transferable plasmids was larger than non-mobilisable plasmids (83,585 and 66,992 bp, respectively) which may reflect the carriage of additional gene clusters which confer a functional advantage in the hospital environment.

Table 5.5. Plasmid profiles and antimicrobial resistance gene repertoire of VREfm isolates closed by hybrid assembly (*N*=39)

Pt	Isolate	ST/CT[1]	TPN	Plasmid ID	Size (bp)	Depth	Topology	Replicon type[2]	Plasmid family type[2]	Relaxase type[3]	MPF type[3]	Predicted mobility[3]	Antimicrobial resistance genes[2]
1	JHM1-1	ST80 CT6489	4	pJHM1-1_a	208,813	1.04x	Circular	*repUS15*	RepA_N	-	-	Non-mobilisable	*aac(6')-aph(2''), ant(6)-I, lnu(B), lsa(E)*
				pELF_JHM1-1	108,997	1.49x	Linear	-	-	-	-	Non-mobilisable	*vanHAX*
				pJHM1-1b	4,461	32.6x	Circular	-	-	-	-	Non-mobilisable	-
				pJHM1-1c	2,947	75.0x	Circular	-	-	-	-	Non-mobilisable	-
	JHM1-2	ST80 CT6489	7	pJHM1-2_a	242,555	1.27x	Circular	*repUS15*	RepA_N	-	-	Non-mobilisable	*aac(6')-aph(2'')*
				pELF_JHM1-2	108,982	1.73x	Linear	-	-	-	-	Non-mobilisable	*vanHAX*
				pJHM1-2_b[4]	2 contigs TL: 33,311	5.47x (MD)	NFC	NFC	NFC	NFC	NFC	NFC	-
				pJHM1-2_c	60,113	4.87x	Circular	*repUS7*	Inc18	MOBP	MPF_T	Conjugative	-
				pJHM1-2_d	42,901	4.29x	Circular	*rep2, repUS12*	Multi-replicon (Inc18 and Rep1)	MOBP	MPF_T	Conjugative	-
				pJHM1-2_e	6,173	10.0x	Circular	*rep11a*	Rep3	MOBP	-	Mobilisable	-
				pJHM1-2_f	4,466	7.38x	Circular	-	-	-	-	Non-mobilisable	-
	JHM1-5	ST80 CT2933	4	pJHM1-5_a[4]	9 contigs TL: 101,880	1.53x (MD)	NFC	NFC	NFC	NFC	-	NFC	*vanHAX*
				pJHM1-5_b	208,813	1.0x	Circular	*repUS15*	RepA_N	-	-	Non-mobilisable	*aac(6')-aph(2''), ant(6)-Ia, lnu(B), lsa(E)*
				pJHM1-5_c	4,461	36.0x	Circular	-	-	-	-	Non-mobilisable	-
				pJHM1-5_d	2,947	83.2x	Circular	-	-	-	-	Non-mobilisable	-
	JHM1-9	ST80 CT6489	7	pJHM1-9_a[4]	25 contigs TL: 140,825	2.77x	NFC	NFC	NFC	NFC	-	NFC	*vanHAX*
				pJHM1-9_b	235,976	1.33x	Circular	*repUS15*	RepA_N	-	-	Non-mobilisable	*aac(6')-aph(2'')*
				pJHM1-9_c	92,606	1.03x	Circular	-	-	-	-	Non-mobilisable	-
				pJHM1-9_d	60,113	6.04x	Circular	*repUS7*	Inc18	MOBP	MPF_T	Conjugative	-
				pJHM1-9_e	42,901	5.11x	Circular	*rep2, repUS12*	Multi-replicon (Inc18 and Rep1)	MOBP	MPF_T	Conjugative	-
				pJHM1-9_f	4,466	9.35x	Circular	-	-	-	-	Non-mobilisable	-
				pJHM1-9_g	6,173	11.4x	Circular	*rep11a*	Rep3	MOBP	-	Mobilisable	-
	JHM1-11	ST80 CT6738	5	pJHM1-11_a[4]	8 contigs TL: 122,603	1.97x (MD)	NFC	NFC	NFC	NFC	NFC	NFC	*vanHAX*
				pJHM1-11_b	166,547	1.45x	Circular	*repUS15*	RepA_N	-	-	Non-mobilisable	*aac(6')-aph(2'')*
				pJHM1-11_c	54,148	2.66x	Circular	-	-	MOBP	MPF_T	Conjugative	-
				pJHM1-11_d	20,174	2.40x	Circular	*rep2*	Inc18	MOBP	-	Mobilisable	-
				pJHM1-11_e	5,212	10.9x	Circular	*rep18b*	Rep3	-	-	Non-mobilisable	-

Table 5.5 continued overleaf

Pt	Isolate	ST/CT[1]	TPN	Plasmid ID	Size (bp)	Depth	Topology	Replicon type[2]	Plasmid family type[2]	Relaxase type[3]	MPF type[3]	Predicted mobility[3]	Antimicrobial resistance genes[2]
1	JHM1-15	ST80 CT2933	4	pJHM1-15_a	208,813	1.12x	Circular	*repUS15*	RepA_N	-	-	Non-mobilisable	*aac(6')-aph(2''), ant(6)-Ia, lnu(B), lsa(E)*
				pELF_JHM1-15	109,014	1.74x	Linear	-	-	-	-	Non-mobilisable	*vanHAX*
				pJHM1-15_b	4,461	28.3x	Circular	-	-	-	-	Non-mobilisable	-
				pJHM1-15_c	2,947	63.7x	Circular	-	-	-	-	Non-mobilisable	-
2	JHM2-1	ST80 CT6489	7	pJHM2-1_a[4]	10 contigs TL: 186,915	1.91x (MD)	NFC	NFC	NFC	NFC	NFC	NFC	*vanHAX*
				pJHM2-1_b	243,493	1.41x	Circular	*repUS15*	RepA_N	MOBP	-	Mobilisable	*aac(6')-aph(2'')*
				pJHM2-1_c	52,079	3.27x	Circular	-	-	MOBP	MPF_T	Conjugative	-
				pJHM2-1_d	6,173	6.56x	Circular	*rep11a*	Rep3	MOBP	-	Mobilisable	-
				pJHM2-1_e	5,088	8.05x	Circular	*rep18b*	Rep3	-	-	Non-mobilisable	-
				pJHM2-1_f	4,466	4.86x	Circular	-	-	-	-	Non-mobilisable	-
				pJHM2-1_g	2,947	35.6x	Circular	-	-	-	-	Non-mobilisable	-
	JHM2-15	ST80 CT6489	8	pJHM2-15_a	289,861	1.77x	Circular	-	-	-	-	Non-mobilisable	*aac(6')-Ii*
				pELF_JHM2-15	186,911	1.79x	Linear	*rep2, repUS12*	Multi-replicon (Inc18 and Rep1)	MOBP	MPF_T	Conjugative	*vanHAX*
				pJHM2-15_b	243,493	1.25x	Circular	*repUS15*	RepA_N	MOBP	-	Mobilisable	*aac(6')-aph(2'')*
				pJHM2-15_c	52,079	2.50x	Circular	-	-	MOBP	MPF_T	Conjugative	-
				pJHM2-15_d	6,173	7.72x	Circular	*rep11a*	Rep3	MOBP	-	Mobilisable	-
				pJHM2-15_e	5,088	9.31x	Circular	*rep18b*	Rep3	-	-	Non-mobilisable	-
				pJHM2-15_f	4,466	6.30x	Circular	-	-	-	-	Non-mobilisable	-
				pJHM2-15_g	2,947	64.3x	Circular	-	-	-	-	Non-mobilisable	-
3	JHM3-2	ST80 CT6489	6	pJHM3-2_a	246,609	1.18x	Circular	*repUS15*	RepA_N	MOBP	-	Mobilisable	*aac(6')-aph(2'')*
				pELF_JHM3-2	116,719	1.95x	Linear	-	-	-	-	Non-mobilisable	*vanHAX*
				pJHM3-2_b	94,092	1.03x	Circular	-	-	-	-	Non-mobilisable	-
				pJHM3-2_c	69,935	1.71x	Circular	*rep2, repUS12, rep17*	Multi-replicon (Inc18, Rep1 and RepA_N)	MOBP	MPF_T	Conjugative	-
				pJHM3-2_d	4,466	5.60x	Circular	-	-	-	-	Non-mobilisable	-
				pJHM3-2_e	6,173	6.63x	Circular	*rep11a*	Rep3	MOBP	-	Mobilisable	-
	JHM3-9	Novel CT1898	4	pJHM3-9_a[4]	8 contigs TL: 121,752	1.70x (MD)	NFC	NFC	NFC	NFC	-	NFC	*vanHAX*
				pJHM3-9_b	274,157	0.948x	Circular	*repUS15*	RepA_N	MOBP	MPF_T	Conjugative	*aac(6')-aph(2''), ant(6)-Ia*
				pJHM3-9_c	13,529	3.84x	Circular	*rep18a*	Rep3	MOBP	-	Mobilisable	-
				pJHM3-9_d	4,461	6.66x	Circular	-	-	-	-	Non-mobilisable	-

Table 5.5 continued overleaf

Pt	Isolate	ST/CT[1]	TPN	Plasmid ID	Size (bp)	Depth	Topology	Replicon type[2]	Plasmid family type[2]	Relaxase type[3]	MPF type[3]	Predicted mobility[3]	Antimicrobial resistance genes[2]
3	JHM3-14	ST80 CT6489	5	pJHM3-14_a	248,083	1.22x	Circular	*repUS15*	RepA_N	MOBP	-	Mobilisable	*aac(6')-aph(2")*
				pELF_JHM3-14_a	110,743	2.00x	Linear	-	-	-	-	Non-mobilisable	*vanHAX*
				pELF_JHM3-14_b	65,737	2.04x	Linear	*rep2*, *repUS12*, *rep17*	Multi-replicon (Inc18, Rep1 and RepA_N)	MOBP	MPF_T	Conjugative	-
				pJHM3-14_b	6,173	7.26x	Circular	*rep11a*	Rep3	MOBP	-	Mobilisable	-
				pJHM3-14_c	4,466	5.90x	Circular	-	-	-	-	Non-mobilisable	-
4	JHM4-2	ST80 CT2933	5	pJHM4-2_a	185,389	1.02x	Circular	*repUS15*	RepA_N	-	-	Non-mobilisable	*aac(6')-aph(2"), ant(6)-Ia, lnu(B), lsa(E)*
				pELF_JHM4-2	120,782	2.36x	Linear	-	-	-	-	Non-mobilisable	*vanHAX*
				pJHM4-2_b	6,173	8.57x	Circular	*rep11a*	Rep3	MOBP	-	Mobilisable	-
				pJHM4-2_c	4,461	7.96x	Circular	-	-	-	-	Non-mobilisable	-
				pJHM4-2_d	2,947	89.6x	Circular	-	-	-	-	Non-mobilisable	-
	JHM4-4	ST80 CT6738	5	pJHM4-4_a	169,232	1.52x	Circular	*repUS15*	RepA_N	-	-	Non-mobilisable	*aac(6')-aph(2")*
				pELF_JHM4-4	119,306	2.37x	Linear	-	-	-	-	Non-mobilisable	*vanHAX*
				pJHM4-4_b	20,167	1.09x	Circular	*rep2*	Inc18	MOBP	-	Mobilisable	-
				pJHM4-4_c	14,851	1.29x	Circular	*rep17*	RepA_N	-	-	Non-mobilisable	-
				pJHM4-4_d	5,212	8.42x	Circular	*rep18b*	Rep3	-	-	Non-mobilisable	-
	JHM4-14	ST80 CT6738	5	pJHM4-14_a[4]	8 contigs TL: 20,174	2.34x (MD)	NFC	NFC	NFC	NFC	NFC	NFC	-
				pJHM4-14_b	168,232	1.23x	Circular	*repUS15*	RepA_N	-	-	Non-mobilisable	*aac(6')-aph(2")*
				pELF_JHM4-14	113,355	2.20x	Linear	-	-	-	-	Non-mobilisable	*vanHAX*
				pJHM4-14_c	14,859	2.04x	Circular	*rep17*	RepA_N	-	-	Non-mobilisable	-
				pJHM4-14_d	5,212	7.40x	Circular	*rep18b*	Rep3	-	-	Non-mobilisable	-
	JHM4-15	ST80 CT2933	5	pJHM4-15_a	168,232	1.88x	Circular	*repUS15*	RepA_N	-	-	Non-mobilisable	*aac(6')-aph(2")*
				pELF_JHM4-15	119,306	2.16x	Linear	-	-	-	-	Non-mobilisable	*vanHAX*
				pJHM4-15_b	20,174	3.08x	Circular	*rep2*	Inc18	MOBP	-	Mobilisable	-
				pJHM4-15_c	14,861	2.92x	Circular	r*ep17*	RepA_N	-	-	Non-mobilisable	-
				pJHM4-15_d	5,212	6.71x	Circular	*rep18b*	Rep3	-	-	Non-mobilisable	-
5	JHM5-6	ST80 CT1916	7	pJHM5-6_a	229,372	1.16x	Circular	*repUS15*	RepA_N	MOBP	-	Mobilisable	*aac(6')-aph(2")*
				pELF_JHM5-6	130,084	2.25x	Linear	*rep2*, *repUS12*	Multi-replicon (Inc18 and Rep1)	-	-	Non-mobilisable	*vanHAX*
				pJHM5-6_b	72,762	2.02x	Circular	*rep17*	RepA_N	MOBP	MPF_T	Conjugative	-
				pJHM5-6_c	6,303	7.82x	Circular	-	-	MOBP	-	Mobilisable	-
				pJHM5-6_d	6,173	6.92x	Circular	*rep11a*	Rep3	MOBP	-	Mobilisable	-
				pJHM5-6_e	5,569	7.71x	Circular	*rep18b*	Rep3	-	-	Non-mobilisable	-
				pJHM5-6_f	4,466	5.63x	Circular	-	-	-	-	Non-mobilisable	-

Table 5.5 continued overleaf

Pt	Isolate	ST/CT[1]	TPN	Plasmid ID	Size (bp)	Depth	Topology	Replicon type[2]	Plasmid family type[2]	Relaxase type[3]	MPF type[3]	Predicted mobility[3]	Antimicrobial resistance genes[2]
5	JHM5-9	ST80 CT1916	7	pJHM5-9_a	230,617	1.18x	Circular	*repUS15*	RepA_N	MOBP	-	Mobilisable	*aac(6')-aph(2")*
				pELF_JHM5-9	130,077	2.19x	Linear	*rep2, repUS12*	Multi-replicon (Inc18 and Rep1)	-	-	Non-mobilisable	*vanHAX*
				pJHM5-9_b	72,762	1.86x	Circular	*rep17*	RepA_N	MOBP	MPF_T	Conjugative	-
				pJHM5-9_c	6,303	7.59x	Circular	-	-	MOBP	-	Mobilisable	-
				pJHM5-9_d	6,173	6.35x	Circular	*rep11a*	Rep3	MOBP	-	Mobilisable	-
				pJHM5-9_e	5,569	7.31x	Circular	*rep18b*	Rep3	-	-	Non-mobilisable	-
				pJHM5-9_f	4,466	5.72x	Circular	-	-	-	-	Non-mobilisable	-
	JHM5-11	ST80 CT7229	7	pJHM5-11_a	230,617	1.29	Circular	*repUS15*	RepA_N	MOBP	-	Mobilisable	*aac(6')-aph(2")*
				pELF_JHM5-11	130,079	2.25x	Linear	*rep2, repUS12*	Multi-replicon (Inc18 and Rep1)	-	-	Non-mobilisable	*vanHAX*
				pJHM5-11_b	72,762	2.25x	Circular	*rep17*	RepA_N	MOBP	MPF_T	Conjugative	-
				pJHM5-11_c	6,303	8.16x	Circular	-	-	MOBP	-	Mobilisable	-
				pJHM5-11_d	6,173	7.35x	Circular	*rep11a*	Rep3	MOBP	-	Mobilisable	-
				pJHM5-11_e	5,569	7.74x	Circular	*rep18b*	Rep3	-	-	Non-mobilisable	-
				pJHM5-11_f	4,466	6.02x	Circular	-	-	-	-	Non-mobilisable	-
	JHM5-13	ST80 CT3395	5	pJHM5-13_a	248,585	1.36x	Circular	*repUS15*	RepA_N	MOBP	MPF_T	Conjugative	*aac(6')-aph(2")*
				pELF_JHM5-13	105,602	2.13x	Linear	-	-	-	-	Non-mobilisable	*vanHAX*
				pJHM5-13_b	36,791	5.45x	Circular	*rep2, repUS12, rep14a*	Multi-replicon (Inc18, Rep1 and Rep_trans)	-	-	Non-mobilisable	*ant(6)-Ia, aph(3')-III, erm(B)*
				pJHM5-13_c	6,303	10.4x	Circular	-	-	MOBP	-	Mobilisable	-
				pJHM5-13_d	6,173	9.81x	Circular	*rep11a*	Rep3	MOBP	-	Mobilisable	-
	JHM5-15	ST80 CT3395	5	pJHM5-15_a	248,585	1.41x	Circular	*repUS15*	RepA_N	MOBP	MPF_T	Conjugative	*aac(6')-aph(2")*
				pJHM5-15_b[4]	2 contigs TL: 105,609	2.13x	NFC	NFC	NFC	NFC	NFC	NFC	*vanHAX*
				pJHM5-15_c	36,791	4.78x	Circular	*rep2, repUS12, rep14a*	Multi-replicon (Inc18, Rep1 and Rep_trans)	-	-	Non-mobilisable	*ant(6)-Ia, aph(3')-III, erm(B)*
				pJHM5-15_d	6,303	9.39x	Circular	-	-	MOBP	-	Mobilisable	-
				pJHM5-15_e	6,173	8.96x	Circular	*rep11a*	Rep3	MOBP	-	Mobilisable	-
6	JHM6-4	ST80 CT2933	4	pJHM6-4_a	212,484	1.15x	Circular	*repUS15*	RepA_N	-	-	Non-mobilisable	*aac(6')-aph(2"), ant(6)-Ia, lnu(B), lsa(E)*
				pELF_JHM6-4	107,839	1.80x	Linear	-	-	MOBP	-	Mobilisable	*vanHAX*
				pJHM6-4_b	4,461	8.96x	Circular	-	-	-	-	Non-mobilisable	-
				pJHM6-4_c	2,947	68.4x	Circular	-	-	-	-	Non-mobilisable	-

Table 5.5 continued overleaf

Pt	Isolate	ST/CT[1]	TPN	Plasmid ID	Size (bp)	Depth	Topology	Replicon type[2]	Plasmid family type[2]	Relaxase type[3]	MPF type[3]	Predicted mobility[3]	Antimicrobial resistance genes[2]
6	JHM6-7	ST80 CT6489	4	pJHM6-7_a	246,386	1.19x	Circular	*repUS15*	RepA_N	MOBP	-	Mobilisable	*aac(6')-aph(2")*
				pELF_JHM6-7	122,006	1.79x	Linear	-	-	-	-	Non-mobilisable	*vanHAX*
				pJHM6-7_b	70,658	2.33x	Circular	*rep2, repUS12, rep17*	Multi-replicon (Inc18, Rep1 and RepA_N)	MOBP	MPF_T	Conjugative	-
				pJHM6-7_c	6,173	7.07x	Circular	*rep11a*	Rep3	MOBP	-	Mobilisable	-
	JHM6-9	ST80 CT6489	5	pJHM6-9_a	246,609	1.13x	Circular	*repUS15*	RepA_N	MOBP	-	Mobilisable	*aac(6')-aph(2")*
				pELF_JHM6-9	116,713	1.88x	Linear	-	-	-	-	Non-mobilisable	vanHAX
				pJHM6-9_b	70,658	1.41x	Circular	*rep2, repUS12, rep17*	Multi-replicon (Inc18, Rep1 and RepA_N)	MOBP	MPF_T	Conjugative	-
				pJHM6-9_c	6,173	6.91x	Circular	*rep11a*	Rep3	MOBP	-	Mobilisable	-
				pJHM6-9_d	4,466	5.75x	Circular	-	-	-	-	Non-mobilisable	-
	JHM6-12	ST80 CT2933	4	pJHM6-12_a	211,138	1.31x	Circular	*repUS15*	RepA_N	-	-	Non-mobilisable	*aac(6')-aph(2"), ant(6)-Ia, lnu(B), lsa(E)*
				pELF_JHM6-12	107,837	3.01x	Linear	-	-	MOBP	-	Mobilisable	*vanHAX*
				pJHM6-12_b	4,461	5.57x	Circular	-	-	-	-	Non-mobilisable	-
				pJHM6-12_c	2,947	57.8x	Circular	-	-	-	-	Non-mobilisable	-
7	JHM7-1	ST80 CT2933	7	pJHM7-1_a[4]	8 contigs TL: 116,675	1.86x	NFC	NFC	NFC	NFC	NFC	NFC	*vanHAX*
				pJHM7-1_b	208,781	1.22x	Circular	*repUS15*	RepA_N	-	-	Non-mobilisable	*aac(6')-aph(2"), ant(6)-Ia, lnu(B), lsa(E)*
				pJHM7-1_c	6,173	6.36x	Circular	*rep11a*	Rep3	MOBP	-	Mobilisable	-
				pJHM7-1_d	5,850	7.53x	Circular	-	-	-	-	Non-mobilisable	-
				pJHM7-1_e	4,461	4.95x	Circular	-	-	-	-	Non-mobilisable	-
				pJHM7-1_f	3,199	30.9x	Circular	-	-	-	-	Non-mobilisable	-
				pJHM7-1_g	2,947	35.6x	Circular	-	-	-	-	Non-mobilisable	-
	JHM7-2	ST80 CT1921	3	pJHM7-2_a	189,164	1.80x	Circular	*repUS15*	RepA_N	MOBP	MPF_T	Conjugative	-
				pELF_JHM7-2	116,676	2.38x	Linear	-	-	-	-	Non-mobilisable	*vanHAX*
				pJHM7-2_b	27,387	4.20x	Circular	*rep2, rep17*	Multi-replicon (Inc18 and RepA_N)	-	-	Non-mobilisable	*erm(B)*

Table 5.5 continued overleaf

Pt	Isolate	ST/CT[1]	TPN	Plasmid ID	Size (bp)	Depth	Topology	Replicon type[2]	Plasmid family type[2]	Relaxase type[3]	MPF type[3]	Predicted mobility[3]	Antimicrobial resistance genes[2]
7	JHM7-7	ST80 CT2933	7	pJHM7-7_a	207,412	1.16x	Circular	*repUS15*	RepA_N	-	-	Non-mobilisable	*aac(6')-aph(2''), ant(6)-Ia, lnu(B), lsa(E)*
				pELF_JHM7-7	116,675	2.23x	Linear	-	-	-	-	Non-mobilisable	*vanHAX*
				pJHM7-7_b	6,173	8.98x	Circular	*rep11a*	Rep3	MOBP	-	Mobilisable	-
				pJHM7-7_c	5,850	10.7x	Circular	-	-	-	-	Non-mobilisable	-
				pJHM7-7_d	4,461	8.67x	Circular	-	-	-	-	Non-mobilisable	-
				pJHM7-7_e	3,199	55.4x	Circular	-	-	-	-	Non-mobilisable	-
				pJHM7-7_f	2,947	59.0x	Circular	-	-	-	-	Non-mobilisable	-
	JHM7-11	ST80 CT2933	7	pJHM7-11_a	207,412	1.27x	Circular	*repUS15*	RepA_N	-	-	Non-mobilisable	*aac(6')-aph(2''), ant(6)-Ia, lnu(B), lsa(E)*
				pELF_JHM7-11	116,674	2.13x	Linear	-	-	-	-	Non-mobilisable	*vanHAX*
				pJHM7-11_b	6,173	8.32x	Circular	*rep11a*	Rep3	MOBP	-	Mobilisable	-
				pJHM7-11_c	5,850	9.76x	Circular	-	-	-	-	Non-mobilisable	-
				pJHM7-11_d	4,461	7.21x	Circular	-	-	-	-	Non-mobilisable	-
				pJHM7-11_e	3,199	44.7x	Circular	-	-	-	-	Non-mobilisable	-
				pJHM7-11_f	2,947	48.0x	Circular	-	-	-	-	Non-mobilisable	-
8	JHM8-1	ST80 CT2932	4	pJHM8-1_a	211,153	1.09x	Circular	*repUS15*	RepA_N	MOBP	-	Mobilisable	*aac(6')-aph(2'')*
				pELF_JHM8-1	146,603	2.35x	Linear	*rep2, repUS12*	Multi-replicon (Inc18 and Rep1)	-	-	Non-mobilisable	*vanHAX, ant(6)-Ia, aph(3')-III, erm(B)*
				pJHM8-1_b	6,173	6.39x	Circular	*rep11a*	Rep3	MOBP	-	Mobilisable	-
				pJHM8-1_c	4,466	5.72x	Circular	-	-	-	-	Non-mobilisable	-
	JHM8-2	ST80 CT7567	4	pJHM8-2_a	194,497	1.40x	Circular	*repUS15*	RepA_N	MOBP	MPF_T	Conjugative	*aac(6')-aph(2'')*
				pJHM8-2_b	40,922	2.37x	Circular	*rep2, rep17*	Multi-replicon (Inc18 and RepA_N)	-	-	Non-mobilisable	*vanHAX, erm(B)*
				pJHM8-2_c	6,173	6.12x	Circular	*rep11a*	Rep3	MOBP	-	Mobilisable	-
				pJHM8-2_d	4,374	11.8x	Circular	-	-	MOBV	-	Mobilisable	-
	JHM8-3	ST80 CT2932	4	pJHM8-3_a	211,153	1.15x	Circular	*repUS15*	RepA_N	MOBP	-	Mobilisable	*aac(6')-aph(2'')*
				pELF_JHM8-3	146,604	2.38x	Linear	*rep2, repUS12*	Multi-replicon (Inc18 and Rep1)	-	-	Non-mobilisable	*vanHAX, ant(6)-Ia, aph(3')-III, erm(B)*
				pJHM8-3_b	6,173	6.80x	Circular	*rep11a*	Rep3	MOBP	-	Mobilisable	-
				pJHM8-3_c	4,466	6.66x	Circular	-	-	-	-	Non-mobilisable	-
	JHM8-4	ST80 CT2933	5	pJHM8-4_a	167,557	1.53x	Circular	*repUS15*	RepA_N	-	-	Non-mobilisable	*aac(6')-aph(2'')*
				pELF_JHM8-4	110,419	1.74x	Linear	-	-	0	-	Non-mobilisable	*vanHAX*
				pJHM8-4_b	6,173	4.73x	Circular	*rep11a*	Rep3	MOBP	-	Mobilisable	-
				pJHM8-4_c	4,461	3.58x	Circular	-	-	-	-	Non-mobilisable	-
				pJHM8-4_d	2,947	3.63x	Circular	-	-	-	-	Non-mobilisable	-

Table 5.5 continued overleaf

Pt	Isolate	ST/CT[1]	TPN	Plasmid ID	Size (bp)	Depth	Topology	Replicon type[2]	Plasmid family type[2]	Relaxase type[3]	MPF type[3]	Predicted mobility[3]	Antimicrobial resistance genes[2]
8	JHM8-10	ST80 CT7567	4	pJHM8-10_a	194,526	1.67X	Circular	*repUS15*	RepA_N	MOBP	MPF_T	Conjugative	*aac(6')-aph(2")*
				pJHM8-10_b	40,922	2.81x	Circular	*rep2, rep17*	Multi-replicon (Inc18 and RepA_N)	-	-	Non-mobilisable	*vanHAX, erm(B)*
				pJHM8-10_c	6,173	5.35x	Circular	*rep11a*	Rep3	MOBP	-	Mobilisable	-
				pJHM8-10_d	4,374	3.40x	Circular	-	-	MOBV	-	Mobilisable	-
	JHM8-12	ST80 CT2932	4	pJHM8-12_a	211,159	1.15x	Circular	*repUS15*	RepA_N	MOBP	-	Mobilisable	*aac(6')-aph(2")*
				pELF_JHM8-12	140,779	2.73x	Linear	*rep2, repUS12*	Multi-replicon (Inc18 and Rep1)	-	-	Non-mobilisable	*vanHAX, ant(6)-Ia, aph(3')-III, erm(B)*
				pJHM8-12_b	6,173	5.42x	Circular	*rep11a*	Rep3	MOBP	-	Mobilisable	-
				pJHM8-12_c	4,466	4.73	Circular	-	-	-	-	Non-mobilisable	-
	JHM8-15	ST80 CT7567	4	pJHM8-15_a	194,497	1.46x	Circular	*repUS15*	RepA_N	MOBP	MPF_T	Conjugative	*aac(6')-aph(2")*
				pJHM8-15_b	40,922	3.57x	Circular	*rep2, rep17*	Multi-replicon (Inc18 and RepA_N)	-	-	Non-mobilisable	*vanHAX, erm(B)*
				pJHM8-15_c	6,173	7.44x	Circular	*rep11a*	Rep3	MOBP	-	Mobilisable	-
				pJHM8-15_d	4,374	14.9x	Circular	-	-	MOBV	-	Mobilisable	-
9	JHM9-1	ST80 CT6489	5	pJHM9-1_a[4]	25 contigs TL: 94,436	1.82x	NFC	NFC	NFC	NFC	NFC	NFC	*vanHAX*
				pJHM9-1_b	243,741	0.821x	Circular	*repUS15*	RepA_N	MOBP	-	Mobilisable	*aac(6')-aph(2")*
				pJHM9-1_c	69,920	1.63x	Circular	*rep2, repUS12, rep17*	Multi-replicon (Inc18, Rep1 and RepA_N)	MOBP	MPF_T	Conjugative	-
				pJHM9-1_d	6,173	9.31x	Circular	*rep11a*	Rep3	MOBP	-	Mobilisable	-
				pJHM9-1_e	4,466	7.84x	Circular	-	-	-	-	Non-mobilisable	-
	JHM9-15	ST80 CT6489	6	pJHM9-15_a	243,741	0.797x	Circular	*repUS15*	RepA_N	MOBP	-	Mobilisable	*aac(6')-aph(2")*
				pELF_JHM9-15	108,808	1.77x	Linear	-	-	-	-	Non-mobilisable	*vanHAX*
				pJHM9-15_b	92,194	1.10x	Circular	-	-	-	-	Non-mobilisable	-
				pJHM9-15_c	69,920	1.69x	Circular	*rep2, repUS12, rep17*	Multi-replicon (Inc18, Rep1 and RepA_N)	MOBP	MPF_T	Conjugative	-
				pJHM9-15_d	6,173	8.72x	Circular	*rep11a*	Rep3	MOBP	-	Mobilisable	-
				pJHM9-15_e	4,466	7.49x	Circular	-	-	-	-	Non-mobilisable	-

Table 5.5 continued overleaf

Pt	Isolate	ST/CT[1]	TPN	Plasmid ID	Size (bp)	Depth	Topology	Replicon type[2]	Plasmid family type[2]	Relaxase type[3]	MPF type[3]	Predicted mobility[3]	Antimicrobial resistance genes[2]
10	JHM10-1	ST80 CT7537	5	pJHM10-1_a	242,368	1.16x	Circular	*repUS15*	RepA_N	MOBP	MPF_T	Conjugative	*aac(6')-aph(2")*
				pELF_JHM10-1	143,742	2.16x	Linear	*rep2, repUS12*	Multi-replicon (Inc18 and Rep1)	-	-	Non-mobilisable	*vanHAX, ant(6)-Ia, aph(3')-III, erm(B)*
				pJHM10-1_b	6,303	9.61x	Circular	-	-	MOBP	-	Mobilisable	-
				pJHM10-1_c	6,173	8.88x	Circular	*rep11a*	Rep3	MOBP	-	Mobilisable	-
				pJHM10-1_d	4,461	7.73x	Circular	-	-	-	-	Non-mobilisable	-
	JHM10-15	ST80 CT7537	5	pJHM10-15_a	242,368	1.19x	Circular	*repUS15*	RepA_N	MOBP	MPF_T	Conjugative	*aac(6')-aph(2")*
				pELF_JHM10-15	143,742	2.10x	Linear	*rep2, repUS12*	Multi-replicon (Inc18 and Rep1)	-	-	Non-mobilisable	*vanHAX, ant(6)-Ia, aph(3')-III, erm(B)*
				pJHM10-15_b	6,303	7.58x	Circular	-	-	MOBP	-	Mobilisable	-
				pJHM10-15_c	6,173	6.86x	Circular	*rep11a*	Rep3	MOBP	-	Mobilisable	-
				pJHM10-15_d	4,461	5.69x	Circular	-	-	-	-	Non-mobilisable	-

Abbreviations: ST, sequence type; Pt, patient, ST, sequence type; CT, complex type; TPN, total number of plasmids; MPF, mating pair formation; NFC, not fully closed; -, not found; TL, total length; MD, mean depth.

[1] Genotypic information including MLST sequence type (ST) and cgMLST complex type (CT) were extracted *in silico* from whole genome data using Ridom SeqSphere+ v8.5.1 (Ridom GmbH, Münster, Germany). The CT was determined according to the publically available cgMLST scheme based on 1,423 loci (de Been *et al.*, 2015).

[2] Bacterial genome contigs were characterised using the STAMAR pipeline (https://github.com/phac-nml/staramr). This tool queries against Resfinder, PlasmidFinder and PointFinder databases and allows determination of plasmid type and genotypic antimicrobial resistance profiles.

[3] Bacterial plasmid sequences were characterised using the MOB-Typer tool as part of the MOB-suite (https://github.com/phac-nml/mob-suite). This provides *in silico* predictions of the relaxase type, mate-pair formation type and predicted transferability of the plasmid.

[4] This plasmid was not fully closed by hybrid assembly (i.e., the plasmid is not on one full contig, but is instead spread over multiple smaller contigs joined together).

5.3.6 Pairwise Mash distance-based clustering of plasmids

Pairwise plasmid genetic relatedness (*N*=193) was assessed using a reference-free approach based on Mash distances (Ondov *et al.,* 2016). A pairwise Mash distance of one indicates that no common *k*-mers are shared in sketch space between the plasmids under comparison, which implies that they are genetically unrelated. Conversely, a Mash distance of 0 indicates that the plasmids share identical *k*-mers in sketch space and are thus genetically indistinguishable. Using a previously recommended Mash threshold of 0.06 (Robertson *et al.,* 2020), plasmids grouped into 16 distinct clusters (C1-C16) and 2 singletons with an average cluster size of 12 (median: 8, range: 2-39) (Figure 5.5). The majority (68.75%, 11/16) of plasmid clusters were not CT specific and were therefore characterised as 'generalist' groups associated with Clade A1 *E. faecium,* irrespective of clonal background (Tables 5.6a-p). For clarity and ease of reading, Table 5.6a is shown within the results section and the remaining Tables 5.6b-p are available in in the appendix associated with this chapter (Section 5.5). Plasmid groups were predominantly restricted to single replicon types, with only 3/16 clusters displaying variations associated with combinations (presence or absence) of multiple plasmid family types (Tables 5.6a, d and e).

Previous studies have utilised a Mash distance threshold of ≤0.025, approximately ≥98.5% average nucleotide identity, to subdivide sequences into nested secondary clusters and identity 'near duplicate' plasmids (Robertson *et al.,* 2020; Arredondo-Alonso *et al.,* 2021). However, applying this threshold classified 1,602 plasmid pairs as 'near duplicate' which was deemed non-discriminatory and provided limited resolution in plasmidome analysis in this context. A recently described Mash threshold of ≤0.0001 (Matlock *et al.,* 2023), equivalent to ≥99.5% average nucleotide identity, was therefore adopted, despite its stringent and conservative nature. As a result, near-identical plasmids, defined as a Mash distance of ≤0.0001 (Matlock *et al.,* 2023), were observed in genetically divergent *E. faecium* subtypes indicative of multiple HGT events (Tables 5.6a-p). For example, the largest cluster, termed cluster C3, comprised 39 'mega-plasmids' of replicon type *repUS15* ranging in size from 116,547 to 274,157 bp distributed across ten diverse CTs (Table 5.6c). These plasmids carried four distinct antimicrobial resistance genes conferring resistance to antibiotic classes including aminoglycosides and lincosamides. The median number of antimicrobial resistance genes per *repUS15* plasmid was one (range: 1-4) (Table 5.6c).

Within P1, all six fully resolved VREfm isolates from a total of three different CT backgrounds (6489, 2933 and 6738) comprised a *repUS15* plasmid (Table 5.5, Table 5.6c). Interestingly, isolate JHM1-1 (ST80/CT6489) and JHM1-15 (ST80/CT2933) harboured

genetically identical (median Mash plasmid distance=0.0000) mega-plasmids, despite the isolates exhibiting a pairwise median SKA-SNP difference of 2822 (Tables 5.2a and 5.6c). Further investigation into the entire plasmidome landscape of these isolates revealed a total of four distinct plasmids in each isolate which were near-identical (Figure 5.5, Tables 5.6c, d, f, and l). Notably, none of the four plasmid types contained known relaxase or mate-pair formation type genes involved in mobilisation and were deemed 'non-conjugative' by mob-suite tools.

Near-identical plasmids in diverse genetic backgrounds recovered from multiple patients were also evident. For instance, the second largest cluster, referred to as cluster C10, contained 28 small, mobilisable plasmids (~6 kb) of replicon *rep11a* type (Figure 5.5). Isolates JHM3-14 (ST80/CT6489) from patient P3 and JHM8-1 (ST80/CT2932) from patient P8 harboured genetically identical *rep11a* plasmids (mash difference of 0.0000) despite the isolates belonging to different CTs (Table 5.6j). These findings indicate that there is potentially a common pool of plasmid backbones in circulation within Irish ST80 that are readily circulating and disseminated across diverse genetic backgrounds.

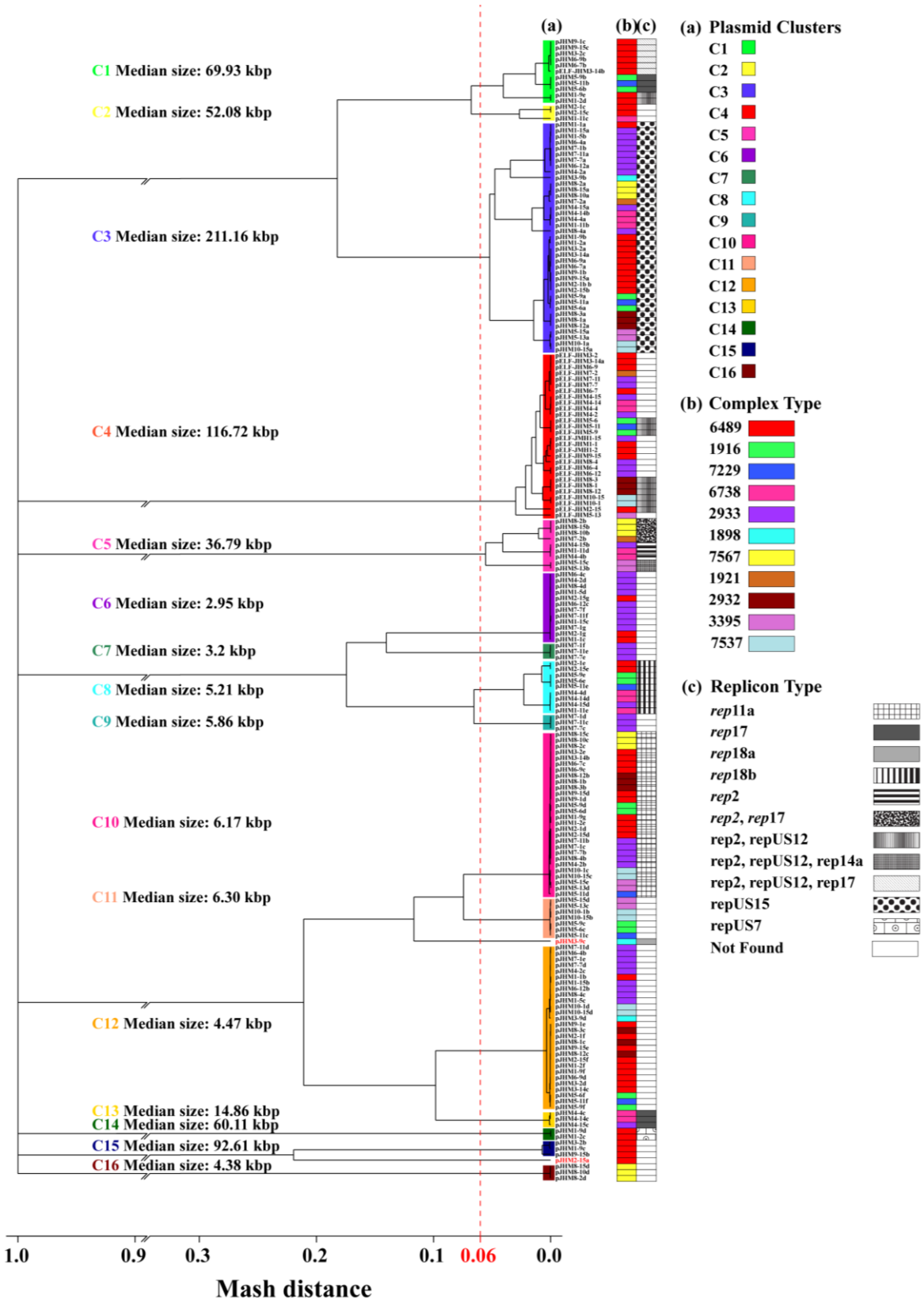

Figure 5.5. Pairwise Mash distance-based clustering of plasmids (N=193) from 39 representative VREfm investigated from 10 patient rectal screening samples. Plasmids segregated into 16 distinct clusters (C1-C16) and 2 singletons with an average cluster size of 12 (median: 8, range: 2-39) using a Mash distance of 0.06 (Robertson *et al.*, 2020). Metadata pertaining to the plasmid cluster, complex type (CT) of the isolate harbouring the

plasmid and replicon type are indicated in the legends. The median plasmid size of each cluster is indicated on the branches. The two singleton plasmid labels are coloured red.

Figure 5.5. Plasmid Mash Dendrogram (TIFF version).

Scan and/or click QR code to access and/or download high resolution image.

Table 5.6a. Detailed metadata and pairwise distance matrices based on MASH distance estimation of plasmid cluster C1

Size of table exceeds page margins.

Scan and/or click QR code to access and/or download table.

5.3.7 Linear plasmids as key vehicles of *vanA* dissemination

Among the 39 within-patient VREfm isolates investigated in detail from 10 individual patients, 72% (28/39) harboured *vanA* on a linear plasmid residing within a discrete genomic cluster identified in the mash-based dendrogram, termed C4, which exhibited a median total pairwise Mash distance of 0.00797 (range: 0-0.02980) (Figure 5.5, Tables 5.5 and 5.6d). Of the remaining 11 VREfm, three ST80/CT7567 isolates (all from patient P8) harboured *vanA* on a 40,922 bp circular plasmid and the remaining eight were found on plasmids with multiple contigs (not fully closed with hybrid assembly). The observed frequency of strains harbouring linear plasmids within this study is significantly higher than previously reported (Hashimoto *et al.*, 2019, 2020; Boumasmoud *et al.*, 2022). The median size of the linear plasmids within this cluster was 116,716 bp (range: 105,602-186,911 bp) and 19/28 were considered non-typable by standard replicon-based methodologies (Figure 5.5, Table 5.6d). To further confirm the linearity of the plasmids, PFGE analysis was performed with S1 nuclease on four representative isolates (JHM1-15, JHM2-15, JHM5-6, JHM8-1) harbouring *vanA*-encoding linear plasmids as described in Chapter 2, Section 2.8.3 and Chapter 3, Section 3.3.7. These four isolates were selected to represent a variety of CT types (CT2933, CT6489, CT7229 and CT2932) and linear plasmid sizes (109,014 bp, 186,911 bp, 130,079 bp and 146,604 bp respectively). For all four isolates, the mobility of the linear plasmids did not change following S1 nuclease treatment, with plasmids of the same size observed for each strain, respectively, in both undigested and S1 nuclease digested total DNA, indicative of linear plasmid topology (Figure 5.6)

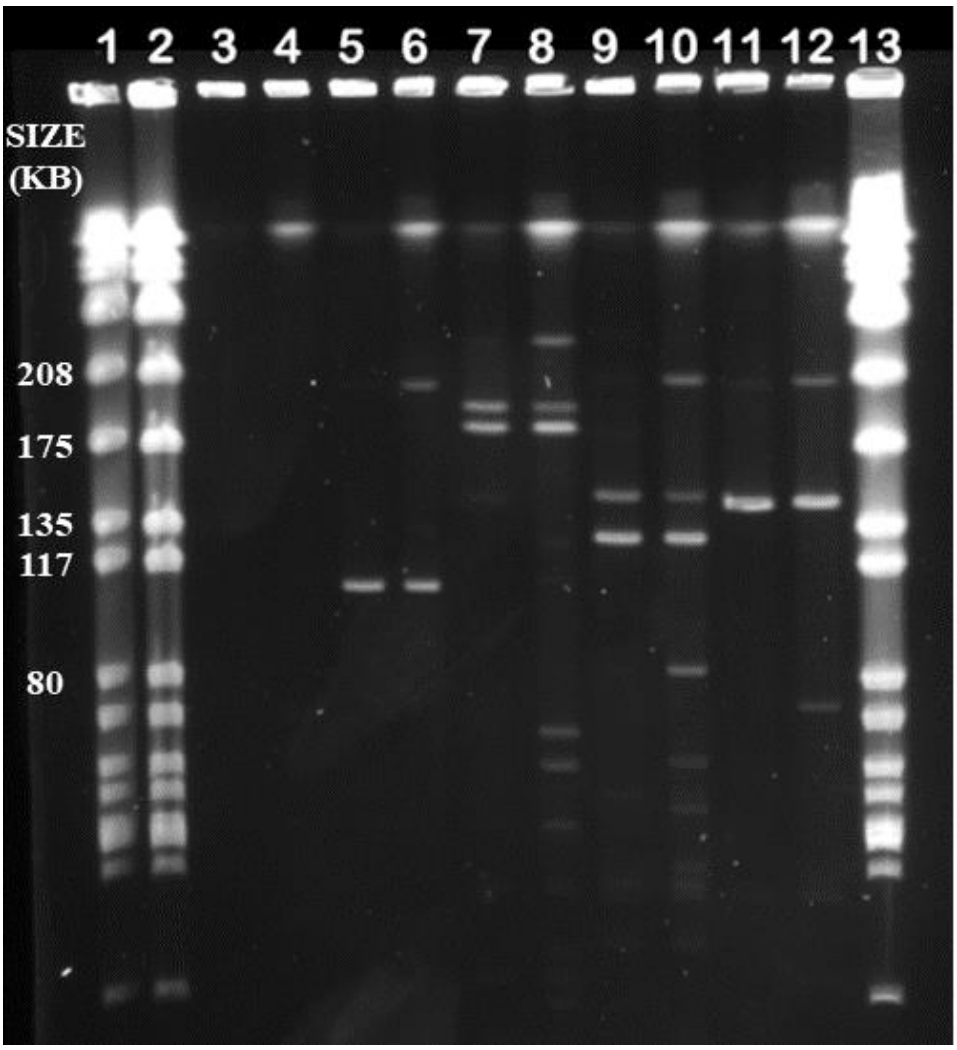

Figure 5.6. Pulse field gel electrophoresis (PFGE) analysis of undigested and S1 nuclease-treated DNA of four representative vancomycin-resistant *Enterococcus faecium* isolates harbouring *vanA*-encoding linear plasmids. Lanes are labelled 1-13 as follows: 1 and 2, *Sma*I-digested *S. aureus* size standard; 3, S1-nuclease treated plasmid free *E. faecium* strain Efm 64/3; 4, plasmid free *E. faecium* strain Efm 64/3; 5, undigested JHM1-15 (109,014 bp linear plasmid); 6, S1 nuclease-treated JHM1-15 (109,014 bp linear plasmid); 7, undigested JHM2-15 (186,811 bp linear plasmid); 8, S1 nuclease-treated JHM2-15 (186,811 bp linear plasmid); 9, undigested JHM5-6 (130,084 bp linear plasmid); 10, S1 nuclease-treated JHM5-6 (130,084 bp linear plasmid); 11, undigested JHM8-1 (146,603 bp linear plasmid); 12, S1 nuclease-treated JHM8-1 (146,603 bp linear plasmid); 13, *Sma*I-digested *S. aureus* size standard.

The majority of linear plasmids (82%, 23/28) encoded only one antimicrobial resistance determinant (*vanA* vancomycin resistance operon). The remaining five plasmids harboured the *vanHAX* transposon and three additional genes (*ant(6)-Ia, aph(3')-III, erm(B)*) conferring resistance to aminoglycoside and macrolide antibiotic classes. A core gene analysis, defined as genes present in ≥95% of the 28 linear plasmids investigated, was performed using Roary v13.3.0 (Page *et al.*,2015) with a 95% BLASTP sequence identity threshold. This revealed the presence of 87 coding sequences (CDSs), of which 86% (77/87) were denoted as hypothetical proteins and their functions were not inferred. Interestingly, this analysis identified a toxin-antitoxin (TA) systems denoted as a core gene (e.g., relG_1) involved in the stabilisation of large plasmid sequences. Seven of the designated core genes with a known coding function were components of the *vanA* operon, including *vanHAX*, *vanRS*, *tnpA* and *hin_2*, suggesting the acquisition of the vancomycin resistance operon is an important factor driving the evolution of linear plasmids in Irish VREfm.

One linear plasmid (pELF_JHM2-15 from a ST80/CT6489 VREfm recovered from patient P2) was predicted as conjugative on the basis of the presence of known relaxase and mate-pair formation markers (MOBP and MPF_T respectively, Table 5.6d) (Robertson and Nash, 2018), whilst the remainder were designated as mobilisable (*N*=2) and non-mobilisiable (*N*=25). Further plasmid sequence analysis revealed the presence of genes involved in replication initiation (*dinB* in 22 plasmids and *repN* in 1 plasmid) and DNA partitioning and transfer (*soj* in 10 plasmids). Two VREfm isolates (JHM5-6 and JHM5-13) harbouring linear plasmids of 130,077 and 105,602 bp, respectively, which were characterised as non-mobilisable due to the absence of a known relaxase and oriT were chosen for filter-mating experiments under vancomycin selection (Table 5.6d). Conjugation of the linear plasmids encoding *vanA* from donor isolates JHM5-6 and JHM5-13 to the plasmid-free *E. faecium* 64/3 (ST21) recipient was successful in both cases. Transconjugants derivatives were phenotypically resistant to vancomycin and teicoplanin exhibiting an MIC of >4 mg/L and >2 mg/L respectively. Hybrid assembly of a *E. faecium* 64/3 transconjugants derived from JHM5-6 (termed JHM5-6_TC1) and JHM5-13 (termed JHM5-13_TC1) revealed the presence of two linear plasmid contigs (131,552 bp and 105,612 bp, respectively) encoding *vanA* with a structural organisation similar to the linear plasmids in the parental isolates in a genetic background matching the recipient strain (ST21) (Figure 5.8). Additionally, comparative genetic analysis of the linear plasmids in the transconjugants with their respective parents revealed clear homology, with 99.98% and 99.99% average nucleotide identity.

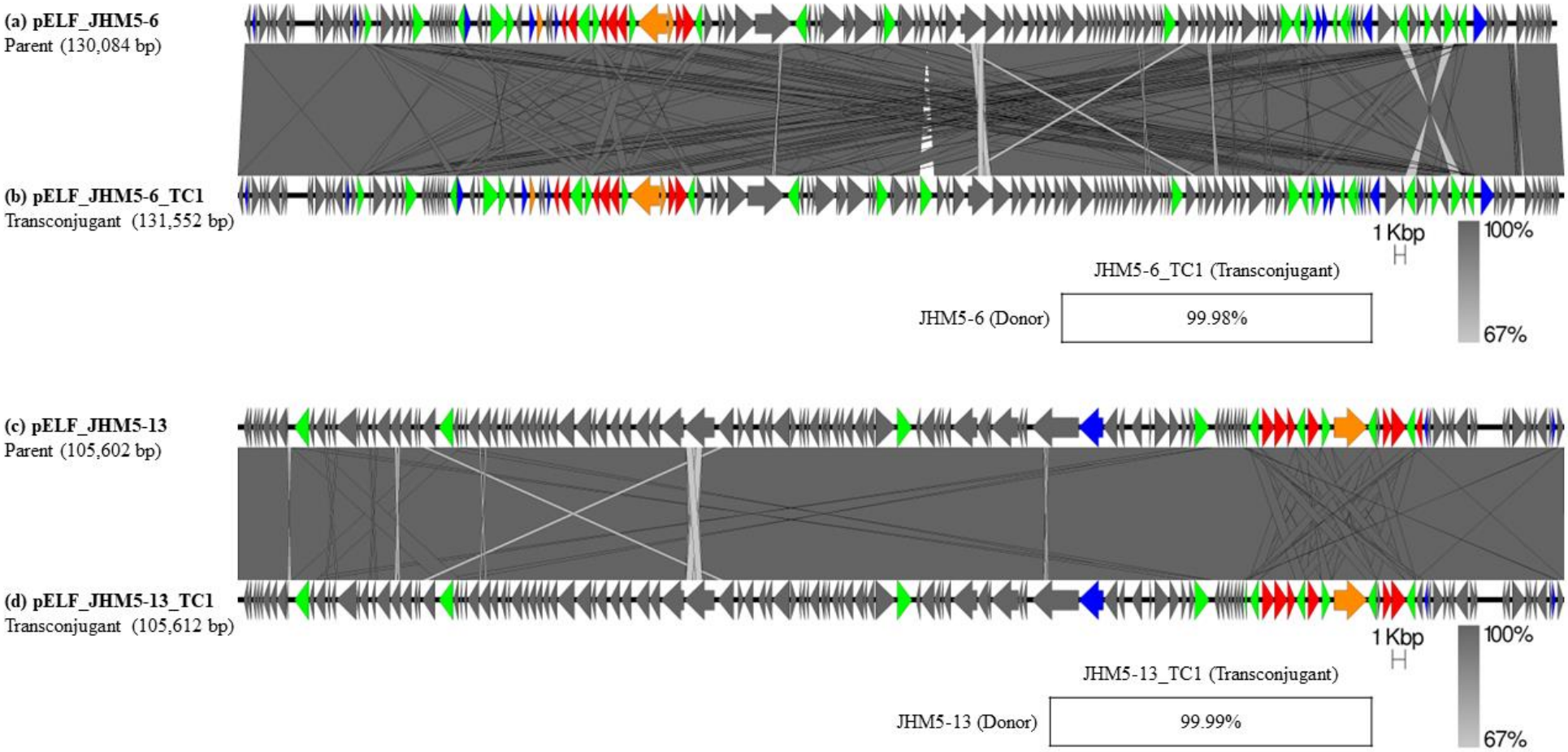

Figure 5.7. Comparative genetic organization of linear plasmids pELF_JHM5-6, pELF_JHM5-6_TC1, pELF_JHM5-13 and pELF_JHM5-13 from parental Irish vancomycin-resistant *Enterococcus faecium* (VREfm) and transconjugants derivatives of *E. faecium* 64/3 obtained following

filter-mating experiments. The figure shows a multiple alignment of (a) pELF_JHM5-6 (plasmid donor), (b) pELF_JHM5-6_TC1 (*E. faecium* 64/3 derivative – transconjugant), (c) pELF_JHM5-13 (plasmid donor) and (d) pELF_JHM5-13_TC1 (*E. faecium* 64/3 derivative – transconjugant). Coding sequences of interest and their orientation are represented by arrows as follows: red, vancomycin resistance genes; green, insertion sequences and resolvases; orange: transposases and resolvases; blue proteins with a known coding function. Regions between alignments with shared homology are represented by grey connecting blocks and/or lines with the colour gradient indicating percentage nucleotide identity (67-100%). A scale bar is included beneath the figure. The matrix shown beneath the figure contains an n × n average nucleotide identity between the plasmids.

More detailed analysis of the discrete genomic cluster comprising the 28 linear plasmids investigated, termed cluster C4, revealed the presence of near-identical (threshold of ≤0.0001) linear plasmid backbones distributed across various lineages of clade A1 *E. faecium* (Figure 5.5, Table 5.6d). For example, patient P7 harboured three VREfm isolates (CT2933 *N*=2 and CT1921 *N*=1) harbouring *vanA*-encoding linear plasmids which exhibited a median pairwise Mash distance of 0.00002 from a linear plasmid in VREfm from patients P6 and P3 (both CT6489). These findings indicate that linear plasmids are widely circulating, well dispersed horizontal vehicles essential for intra and inter-patient *vanA* dissemination within a wide variety of Clade A1 Irish VREfm lineages.

5.3.8 Analysis of the impact of within-patient VREfm diversity on the Tn*1546*-like *vanA* transposon

After determining the high-frequency of intestinal co-colonisation with multiple genetically distinct VREfm subtypes, we sought to establish the impact of multi-strain carriage on the Tn*154*6-like *vanA* transposon in circulation both within the same patient and across CT types among various patients. The extrachromosomal Tn*1546*-like *vanA* regions from 39 isolates, recovered from patients P1-10, were fully resolved using hybrid assembly (Table 5.5, Figures 5.8-5.17). For clarity and ease of reading, Figure 5.8 is shown within the results section and the remaining Figures 5.9-5.17 are available in in the appendix associated with this chapter (Section 5.5). The structural analysis of the *van* operon from multiple isolates within the same patient revealed the presence of identical *vanA* regions (≥99.9% average nucleotide identity) carried by clonally divergent CTs within the same host (e.g., patients P1, P4 and P7, Figures 5.8, 5.11 and 5.14). For example, patient P1 harboured three CT6489 and one CT2933 subtypes, all encoding a *vanA* region of 11,916 bp with an identical structural organisation of the *van* genes, four copies of IS*1216E* and a *tnpA* transposase gene harbouring a 1,287 bp deletion in the 3' terminal (Figure 5.8). Despite the identical Tn*1546*-like variants, the four VREfm isolates harboured diverse genetic backgrounds and exhibited a median pairwise SKA-SNP distance of 1410.5 (range: 0-2818) (Table 5.2a). Notably, three of the patient isolates (JHM1-1 CT6489, JHM1-2 CT6489 and JHM1-15 CT2933) harboured *vanA* on a near-identical linear plasmid (median Mash distance of 0.00017) of approximately 109,000 bp suggesting within-patient HGT events (Table 5.6d). An identical *vanA* derivative (average nucleotide identity of 99.99%) was also identified in P1 isolate JHM1-9 (CT6489), however the plasmid topology could not be determined as it was not fully resolved during hybrid assembly and instead distributed across 9 contigs of total length 101,880 bp. These results suggest patient acquisition of one distinct, predominant VREfm sub-type from either an environmental or hospital source and subsequent *in-vivo* gastrointestinal dissemination of the linear *vanA*-encoding plasmid to VSEfm sub-populations also carried in the patient's GIT under selective pressure.

There were also many examples of distinct iterations of the *van* transposon carried by multiple diverse CTs within the same patient (e.g., patients P5, P6 and P8, Figures 5.12, 5.13 and 5.15). For instance, seven isolates from three distinct clonal backgrounds were recovered from patient P8 (CT2932 *N*=3, CT2933 *N*=1 and CT7567 *N*=3) which exhibited a median pairwise SKA-SNP difference of 2881 (range: 0-3227) (Table 5.2h, Figure 5.15). Limited structural variability was seen when comparing *vanA* regions from the same CT within the same patient; the three CT2932 isolates (JHM8-1, JHM8-3, and JHM8-12) from

patient P8 all comprised a Tn*1546*-like transposon of 18,973 bp encoding the *van* genes in an identical orientation, three copies of IS*1216E*, one copy of IS*Ppu7* and IS*Bmu3* and a *tnpA* gene with a 645 bp 3' terminal deletion (Figure 5.15). This Tn*1536*-like subtype was encoded on three near-identical linear plasmids in the three separate CT2932 isolates belonging to patient P8 (median pairwise Mash distance of 0.00005) of approximately 140,000 bp which also harboured *ant(6)-Ia, aph(3')-III* and *erm(B*) antimicrobial resistance genes (Table 5.6d). Three CT7567 patient P8 isolates (JHM8-2, JHM8-10 and JHM8-15) harboured *vanA* (11,317 bp) on a 40,922 bp circular, multi-replicon plasmid that was characterised as non-mobilisiable (Figure 5.15, Table 5.6e). The CT7567 *vanA* region (*N*=3) shared an average nucleotide identity of 98.11 with CT2932 (*N*=3) within P8. Key differences in CT7567 P8 *vanA* transposons included a reverse orientation of the *van* regulatory genes (*vanRS*), absence of the *tnpA* and *hin* genes and an insertion of IS*1251* upstream of the *vanHAX* gene operon. The presence of distinct *vanA* iterations on both circular and linear plasmids in different clonal backgrounds is suggestive of multiple distinct acquisition events and expansion of several VREfm variants harbouring unique *vanA* transposons rather than *in vivo* HGT events between VREfm and VSEfm. This is further emphasised by the finding of a CT2933 VREfm colonising strain in P8 (JHM8-4) which harboured an additional *vanA* sub-type on a linear plasmid of 110,419 bp with a distinct genetic back-bone (Median pairwise Mash distance of 0.01061 to the CT2932 linear plasmids) (Table 5.6d, Figure 5.15). Interestingly, the *vanA* region of isolate JHM8-4 exhibited an average nucleotide identity of 99.31% and 97.26% with CT2932 and CT7567 isolates respectively. Detailed examination of the structural organisation of the transposon revealed different orientations of the *vanA* operon genes and a *tnpA* gene with a 1,287 bp deletion in the 3' terminal region (Figure 5.15). These findings serve to highlight the promiscuous nature of the Tn*1546*-like *vanA* transposon and its ability to utilise a variety of plasmid types to facilitate dissemination. Additionally, they provide evidence of the extensive dynamic recombination occurring within Irish VREfm *vanA* transposon regions, likely mediated by instability associated with IS*1216E* insertions as described in Chapter 3.

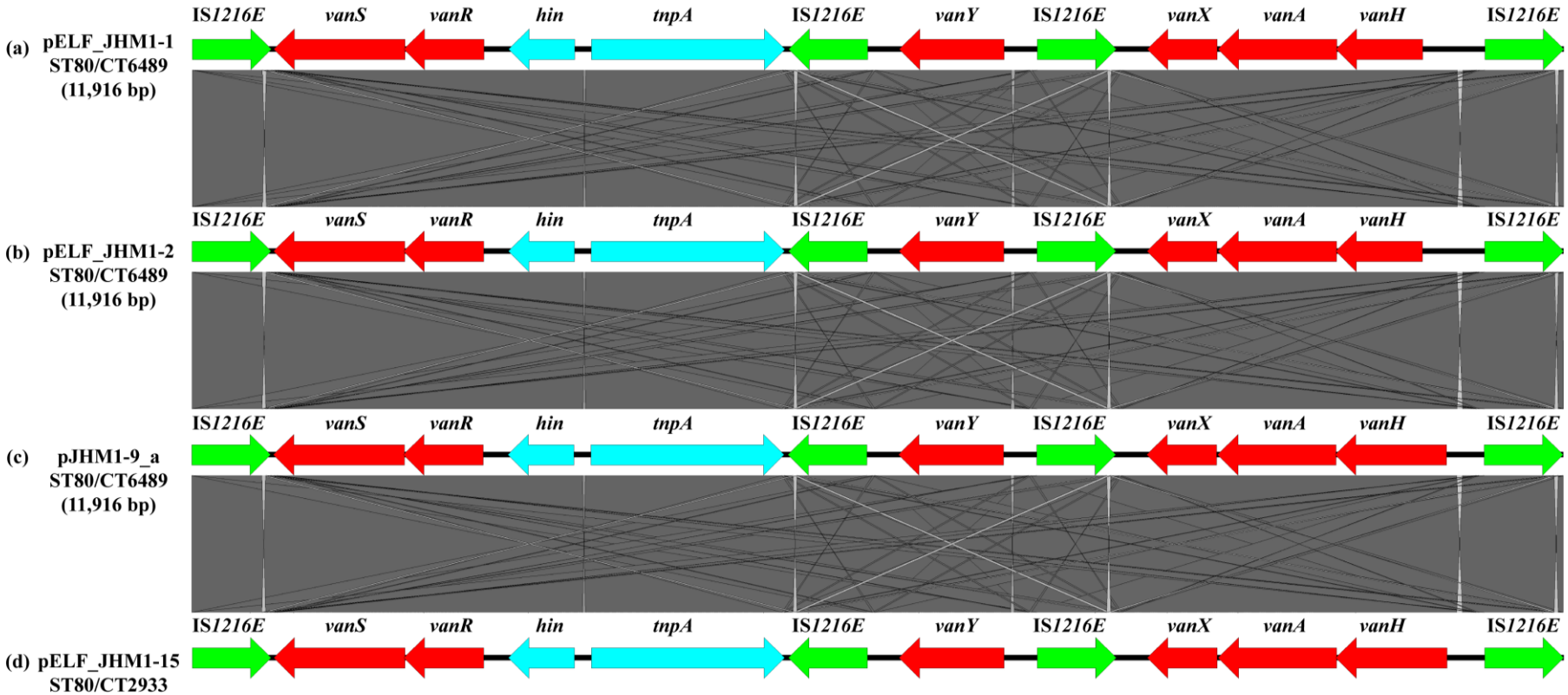

Average Nucleotide Identity (*vanA* transposon)

	pELF_JHM1-1	pELF_JHM1-2	pJHM1-9_a	pELF_JHM1-15
pELF_JHM1-1				
pELF_JHM1-2	100			
pJHM1-9_a	99.99	99.99		
pELF_JHM1-15	99.99	99.99	100	

Figure 5.8. Comparative genetic organisation of *vanA* transposon regions closed by hybrid assembly of VREfm isolates belonging to two complex types (CTs) from patient one. The figure shows an alignment of the *vanA* region encoded by four plasmids from two VREfm isolate CTs as follows: (a) pELF_JHM1-1 (ST80/CT6489, 11,916 bp), (b) pELF_JHM1-2 (ST80/CT6489, 11,916 bp), (c) pJHM1-9_a (ST80/CT6489, 11,916 bp) and (d) pELF_JHM1-15 (ST80/CT2933, 11,916 bp) generated using Easyfig (Sullivan *et al.*, 2011). Coding sequences of interest and their orientation are represented by arrows as follows: red, vancomycin resistance genes; green, insertion sequences; blue, proteins with a known coding function; cyan, transposase and invertase genes; grey, hypothetical proteins. Full details of plasmid profiles and SKA-SNP matrices are provided in Tables 5.4-5.6. Regions between alignments with shared homology are represented by grey connecting blocks and/or lines with the colour gradient indicating percentage nucleotide identity (82-100%). A scale bar is included beneath the figure.

5.3.9 Analysis of Tn*1546*-like *vanA* regions within diverse *E. faecium* clonal lineages reveals no association between transposon iterations and complex type

After investigating the influence of multi-strain VREfm carriage on *vanA* diversity, the next step was to analyse the structural organisation of the resolved extrachromosomal *vanA* harbouring regions from patients P1-10 within specific CT groups to determine if there was an association between transposon iterations and specific CTs. The two largest CTs, 2933 and 6489, comprising a total of 46% (18/39) of the within-patient diversity isolates that were fully closed by hybrid assembly were investigated (Figures 5.18 and 5.19). This analysis revealed the presence of five unique iterations of the *vanA* transposon within CT2933 isolates from five patients. The key differences included multiple insertions of different IS elements such as IS*1216E*, IS*Ef1*, IS*Ppu7* and IS*Bmu3* throughout the operon, additional gene insertions such as cadmium efflux accessory proteins, rearrangement of the *van* operon genes and various deletions in the 3'-terminal end of the *tnpA* gene (range: 645-1,287 bp) (Figure 5.18). Similar findings of multiple diverse variations of *vanA* transposon structures were observed in CT6489 isolates from five distinct patients (Figure 5.19). Interestingly, as detailed in Section 5.3.3, patients P3 and P6 harboured very closely related VREfm CT6489 strains (median pairwise SNP difference: 3, range: 1-6) suggestive of potential transmission. Comparison of the structural organisation of the *vanA* regions within these isolates revealed Tn*1546 vanA* diversity (Figure 5.19, labelled f-i) highlighting that during transmission of clonally indistinguishable variants between patients structural variation can occur at both a transposon and plasmid level with the gain/loss of segments of the operon.

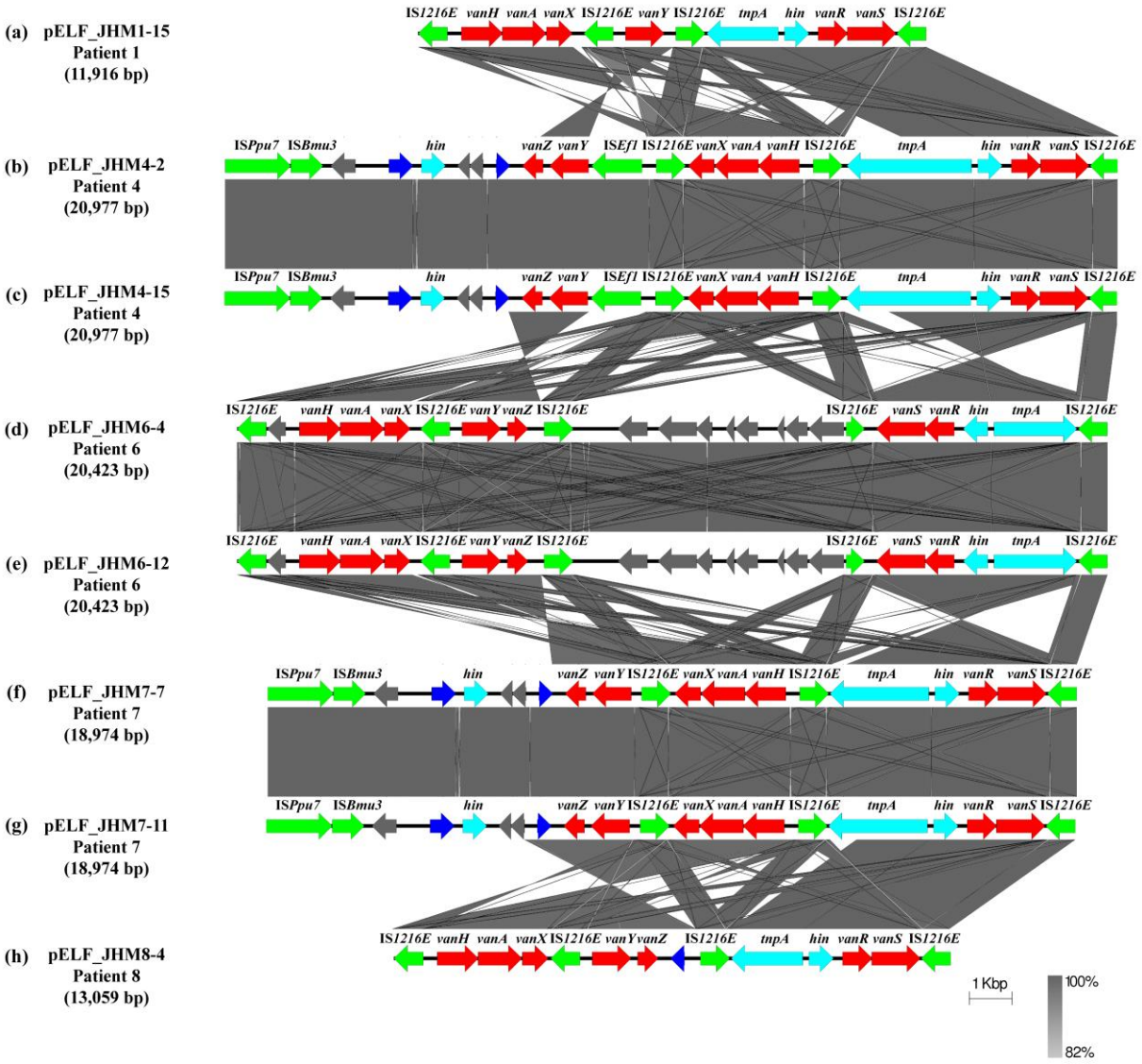
(a) pELF_JHM1-15
Patient 1
(11,916 bp)
IS1216E vanH vanA vanX IS1216E vanY IS1216E tnpA hin vanR vanS IS1216E
(b) pELF_JHM4-2
Patient 4
(20,977 bp)
ISPpu7 ISBmu3 hin vanZ vanY ISEfl IS1216E vanX vanA vanH IS1216E tnpA hin vanR vanS IS1216E
(c) pELF_JHM4-15
Patient 4
(20,977 bp)
ISPpu7 ISBmu3 hin vanZ vanY ISEfl IS1216E vanX vanA vanH IS1216E tnpA hin vanR vanS IS1216E
(d) pELF_JHM6-4
Patient 6
(20,423 bp)
IS1216E vanH vanA vanX IS1216E vanY vanZ IS1216E IS1216E vanS vanR hin tnpA IS1216E
(e) pELF_JHM6-12
Patient 6
(20,423 bp)
IS1216E vanH vanA vanX IS1216E vanY vanZ IS1216E IS1216E vanS vanR hin tnpA IS1216E
(f) pELF_JHM7-7
Patient 7
(18,974 bp)
ISPpu7 ISBmu3 hin vanZ vanY IS1216E vanX vanA vanH IS1216E tnpA hin vanR vanS IS1216E
(g) pELF_JHM7-11
Patient 7
(18,974 bp)
ISPpu7 ISBmu3 hin vanZ vanY IS1216E vanX vanA vanH IS1216E tnpA hin vanR vanS IS1216E
(h) pELF_JHM8-4
Patient 8
(13,059 bp)
IS1216E vanH vanA vanX IS1216E vanY vanZ IS1216E tnpA hin vanR vanS IS1216E
1 Kbp
100%
82%

Figure 5.18. Comparative genetic organisation of *vanA* transposon regions closed by hybrid assembly of VREfm isolates belonging to complex type (CT) 2933 from five patients. The figure shows an alignment of the *vanA* region encoded by eight plasmids from CT2933 as follows: (a) pELF_JHM1-15 (ST80/CT2933, 11,916 bp), (b) pELF_JHM4-2 (ST80/CT2933, 20,977 bp), (c) pELF_JHM4-15 (ST80/CT2933, 20,977 bp), (d) pELF_JHM6-4 (ST80/CT2933, 20,423 bp), (e) pELF_JHM6-12 (ST80/CT2933, 20,423 bp), (f) pELF_JHM7-7 (ST80/CT2933, 18,974 bp), (g) pELF_JHM7-11 (ST80/CT2933, 18,974 bp) and (h) pELF_JHM8-4 (ST80/CT2933, 13,059 bp), generated using Easyfig (Sullivan *et al.*, 2011). Coding sequences of interest and their orientation are represented by arrows as follows: red, vancomycin resistance genes; green, insertion sequences; blue, proteins with a known coding function; cyan, transposase and invertase genes; grey, hypothetical proteins. Full details of plasmid profiles and SKA-SNP matrices are provided in Tables 5.4-5.6. Regions between alignments with shared homology are represented by grey connecting blocks and/or lines with the colour gradient indicating percentage nucleotide identity (82-100%). A scale bar is included beneath the figure.

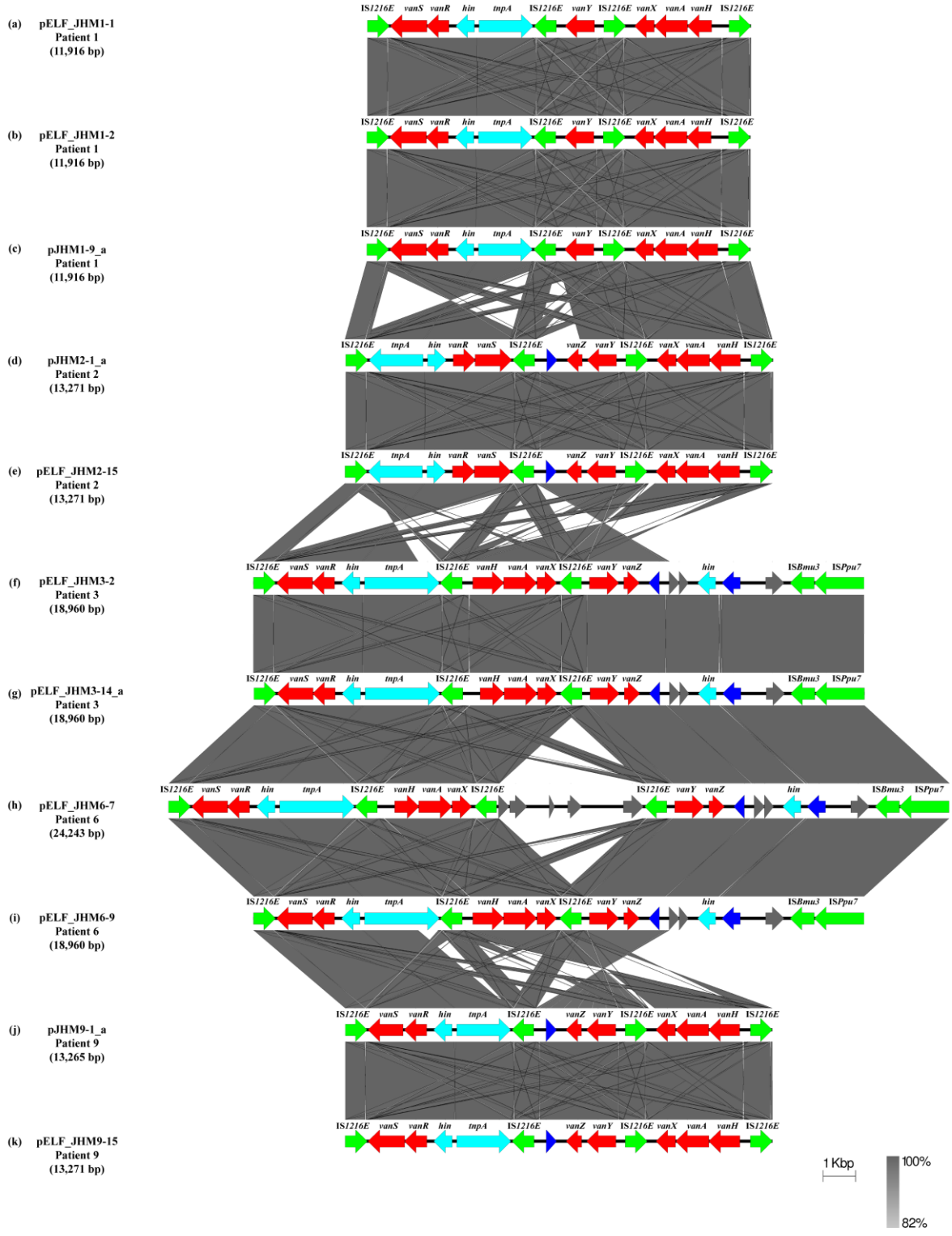

Figure 5.19. Comparative genetic organisation of *vanA* transposon regions closed by hybrid assembly of VREfm isolates belonging to complex type (CT) 6489 from five patients. The figure shows an alignment of the *vanA* region encoded by eleven plasmids from CT6489 as follows: (a) pELF_JHM1-1 (ST80/CT6489, 11,916 bp), (b) pELF_JHM1-2 (ST80/CT6489, 11,916 bp), (c) pJHM1-9_a (ST80/CT6489, 11,916 bp), (d) pJHM2-1_a (ST80/CT6489, 13,271 bp), (e) pELF_JHM2-15 (ST80/CT6489, 13,271 bp), (f)

pELF_JHM3-2 (ST80/CT6489, 18,960 bp), (g) pELF_JHM3-14_a (ST80/CT6489, 18,960 bp), (h) pELF_JHM6-7 (ST80/CT6489, 24,247 bp), (i) pELF_JHM6-9 (ST80/CT6489, 18,960 bp), (j) pJHM9-1_a (ST80/CT6489, 13,265 bp) and (k) pELF_JHM9-15 (ST80/CT6489, 13,271 bp) generated using Easyfig (Sullivan *et al.*, 2011). Coding sequences of interest and their orientation are represented by arrows as follows: red, vancomycin resistance genes; green, insertion sequences; blue, proteins with a known coding function; cyan, transposase and invertase genes; grey, hypothetical proteins. Full details of plasmid profiles and SKA-SNP matrices are provided in Tables 5.4-5.6. Regions between alignments with shared homology are represented by grey connecting blocks and/or lines with the colour gradient indicating percentage nucleotide identity (82-100%). A scale bar is included beneath the figure.

5.3.10 A snap-shot of VSEfm carriage

As demonstrated in Chapter 3 and 4, vancomycin-susceptible isolates harbouring remnants of the vancomycin resistance transposon were involved in clinical infections and can be readily recovered from the near-patient environment. These findings provide evidence that VSE populations should be considered in surveillance protocols. On this basis, four of the VREfm-positive rectal screening swabs (from patients P1, P3, P5 and P8) were randomly selected to provide a rudimentary snap-shot of the carriage of VSEfm in the patient cohort. A total of 30 VSEfm isolates were identified from 80 colonies screened from the four patient rectal screening swabs by selective plating on *E. faecium* ChromoSelect and subsequent screening for vancomycin susceptible isolates on VREfm chromogenic agar. Notably, all 30 VSEfm isolates belonged to Clade A1. The majority were identified as ST80 (25/30; 83.3%) by conventional MLST, with the remainder belonging to ST203 (*N*=5). VSEfm strains were deemed to be present at lower abundance in comparison to VREfm in the rectal screening swabs from three out of the four patients tested (Table 5.7). For example, in patient P3, five out of 20 colonies picked from the rectal screening swab were vancomycin-susceptible, evidenced by their inability to grow on vancomycin-selective agar. This represents a relative recovery rate of approximately 25%.

Phylogenetic analysis based on the 1,423 cgMLST loci revealed five distinct CT groups including CT2932 (*N*=7), CT2950 (*N*=5), CT2940 (*N*=12), CT3395 (*N*=1) and CT2933 (*N*=5) (Table 5.7). An MST based on cgMLST analysis of the study VREfm (*N*=150) and the VSEfm (*N*=30) using the previously recommended relatedness threshold of ≤20 allelic differences (de Been *et al.*,2015) revealed 11 clusters and two singletons with an average cluster size of 16 (median: 12, range: 3-48) (Figure 5.20). Two main CT clusters (≤20 allelic differences) were identified comprising mixtures of vancomycin susceptible and vancomycin resistant isolates collected from the same individual patient (Figure 5.20, Table 5.7). The largest cluster, CT2933, comprised 48 *E. faecium* isolates (five VSEfm and 43 VREfm) collected from five individual patients (P1 *N*=10, P4 *N*=5, P6 *N*=13, P7 *N*=14 and P8 *N*=5) with a median cgMLST allelic difference of eight (range: 0-11). Interestingly, within CT2933 VSEfm and VREfm isolates from patient P8 exhibited a median allelic difference of 1, indicating they were potentially genetically identical. Whole-genome comparisons based on SKA-SNP analysis further supported this finding, with a median pairwise SNP difference of one (range: 1-2). Hybrid assembly of a representative VSEfm isolate from this cluster (JHMS8-4) revealed the presence of five distinct plasmids ranging in size from 167,561-2,947 bp. Comparison of the plasmidome landscape of the VSEfm isolate (JHMS8-4) with a genetically indistinguishable VREfm isolate (JHM8-4) revealed

Table 5.7. Detailed metadata and distribution of complex types (CT)s for 30 Clade A1 VSEfm isolates recovered from a single rectal screening swab from each of four separate patients

Patient	Isolate	ST[1]	CT[2]	Total Number of Sub-Types	Median cgMLST allelic difference (range)	Median pairwise SKA-SNP difference (range)	Relative abundance of VSEfm
Patient 1	JHMS1-1 JHMS1-2 JHMS1-3 JHMS1-4 JHMS1-5 JHMS1-6 JHMS1-7	80	2932	1	0 (0-3)	1 (0-3)	7/20 colonies picked
Patient 3	JHMS3-2 JHMS3-3 JHMS3-4 JHMS3-7 JHMS3-8	203	2950	1	0	0	5/20 colonies picked
Patient 5	JHMS5-1 JHMS5-4 JHMS5-5 JHMS5-6 JHMS5-7 JHMS5-8 JHMS5-9 JHMS5-10 JHMS5-11 JHMS5-12 JHMS5-13 JHMS5-15	80	2940	2	0 (0-323)	0 (0-2363)	13/20 colonies picked
	JHMS5-3		3395				
Patient 8	JHMS8-1 JHMS8-3 JHMS8-4 JHMS8-5 JHMS8-6	80	2933	1	0	1 (0-1)	5/20 colonies picked

Abbreviations: ST, sequence type; CT, complex type; VSEfm, vancomycin-susceptible *Enterococcus faecium.*

[1] Genotypic information including MLST sequence type (ST) and cgMLST complex type (CT) were extracted *in silico* from whole genome data using Ridom SeqSphere+ v8.5.1 (Ridom GmbH, Münster, Germany). The cgMLST CT was determined according to the publicly available cgMLST scheme based on 1,423 loci (de Been *et al.,* 2015).

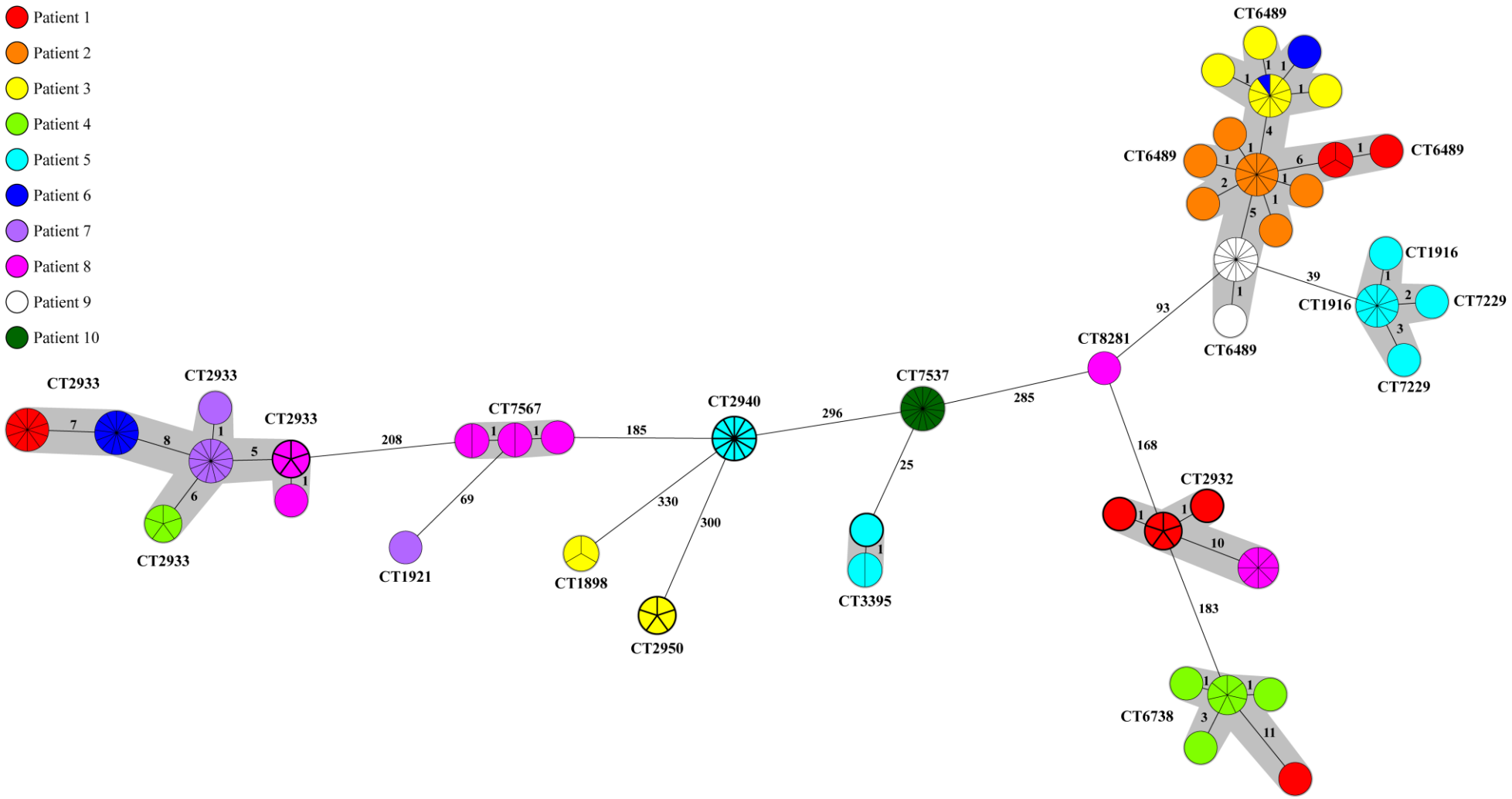

Figure 5.20. Minimum spanning tree (MST) based on core genome multi-locus sequence typing (cgMLST) analysis of 1,423 loci for 150 clade A1 VREfm isolates recovered from a single rectal screening swab from each of 10 separate patients and 30 VSEfm isolates recovered from a

single rectal swab from each of four separate patients. Node colours represent the patient number (1-10) from which the isolate was recovered as indicated in the legend. Partitions within the nodes represent the presence of ≥2 isolates. Branch numbers indicate cgMLST allelic differences between neighbouring isolates. cgMLST segregated isolates into 11 clusters and two singletons using the previously recommended threshold of ≤20 allelic differences (de Been *et al.*, 2015). VSEfm isolates collected from rectal screens are indicated with a thick black outer node ring (*N*=30).

the presence of four near-identical plasmids (average nucleotide identity ≥99.99%) (Figure 5.21). There were also some key differences. For example, VSEfm isolate JHMS8-4 lacked a linear plasmid and instead encoded a circular plasmid of 40,337 bp. Interestingly, no *van* remnants were identified in the susceptible isolate. Screening of the short-read derived FASTA contigs from the remaining four P8 CT2933 VSEfm isolates using ABRicate revealed similar findings, with the absence of any *vanA*-associated operon genes.

CT2932 comprised 15 isolates (eight VREfm from patient P8 and seven VSEfm from patient P1) with a median allelic difference of 2 (range: 0-11). However, SKA SNP methodologies revealed more diversity within this cluster, with P8 and P1 isolates exhibiting a median SNP pairwise difference of 138 (range: 134-149). A representative VSEfm isolate within CT2932 (JHMS1-1) was fully resolved using hybrid assembly to provide an insight into the accessory genome. This revealed the presence of six distinct plasmids, ranging in size from 213,737-6,357 bp encoding antimicrobial resistance genes such as *ant(6)-Ia*, *aph(3')-III* and *erm(B).* However, no vancomycin resistance genes or remnants were found. Comparison of the structural organisation of the accessory genome of the VSEfm isolate (JHMS1-1) with a CT2932 within-cluster isolate (JMH8-1) revealed the presence of some similarities (Figure 5.22). Notably, JHMS1-1 contained a linear plasmid which exhibited 99.88% average nucleotide identity to the *vanA*-encoding linear plasmid from VREfm isolate JHM8-1. Screening of the short-read derived FASTA contigs from the remaining six patient P1 CT2932 VSEfm isolates using ABRicate revealed similar findings, with the absence of any *vanA*-associated operon genes.

Two representative isolates from the remaining two CT groups comprising only VSEfm isolates (CT2940 and CT2950) were investigated using hybrid assembly (Figure 5.23). CT2950 isolate JHMS3-5 contained seven distinct plasmids, including one which displayed linear topology, ranging in size from 192,687-4,466 bp. Mapping of the short-read derived FASTA contigs from this isolate using ABRicate revealed the presence of the vanA associated sensor-regulatory genes (*vanR* and *vanS*). Interestingly, hybrid-assembly of the isolate revealed a linear plasmid of 115,993 bp encoding a *vanA* remnant. The plasmid was enriched with four copies of IS*1216E*, with the *vanA*-remnant separated into a distinct segment flanked on either side by IS*1216E* (e.g., *vanRS*, *tnpA* and *hin_2*) (Figure 5.24). Screening of the short-read derived FASTA contigs from the remaining P5 CT2950 VSEfm isolates using ABRicate did not identify any *vanA*-associated operon genes. CT2940 isolate JHMS5-15 contained four distinct plasmids ranging in size from 197,142-6,173 bp. Plasmids in this isolate encoded antimicrobial resistance genes such as *ant(6)-Ia*, *aph(3')-III* and *erm(B)*, however no vancomycin resistance remnants or genes were identified.

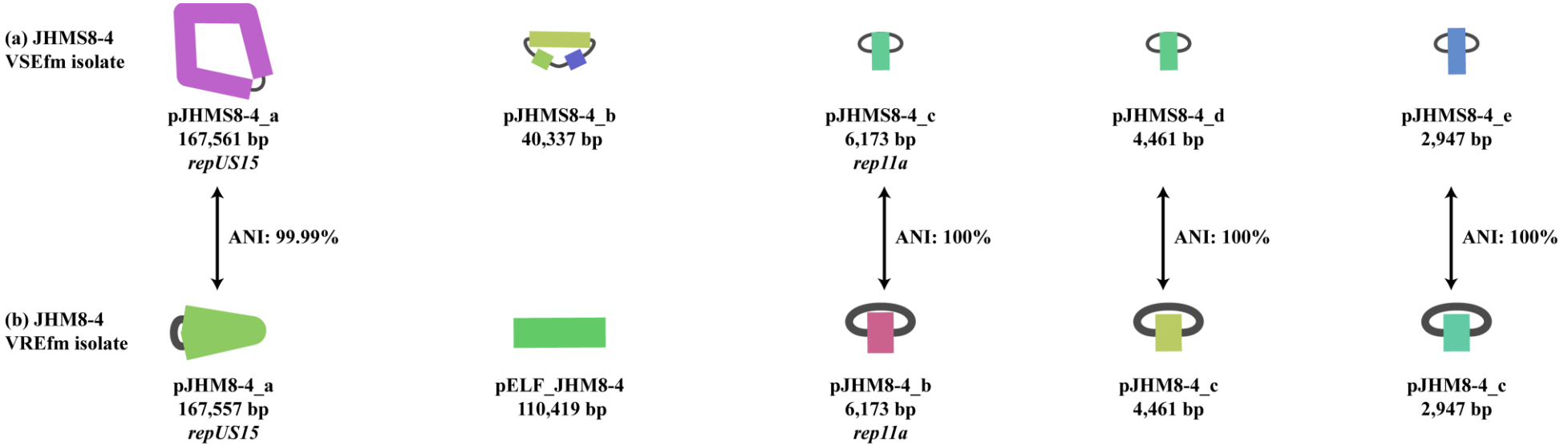

Figure 5.21. Visual representation of the complete plasmidome assembly of VSEfm isolate JHMS8-4 and VREfm isolate JHM8-4 from complex type (CT) 2933 generated using Bandage. (a) VSEfm isolate JHMS8-4 recovered from a rectal screening swab from patient P8 harbouring five distinct plasmids ranging in size from 167,561-2,947 bp and (b) VREfm isolate JHM8-4 recovered from a rectal screening swab from patient P8 harbouring five distinct plasmids ranging in size from 167,557-2,947 bp. Plasmids are represented as individual circular or linear nodes depending on topology. Plasmid names, length and associated replicon type are indicated. The average nucleotide identity (ANI) between equivalent plasmids is indicated by a percentage beside the arrows.

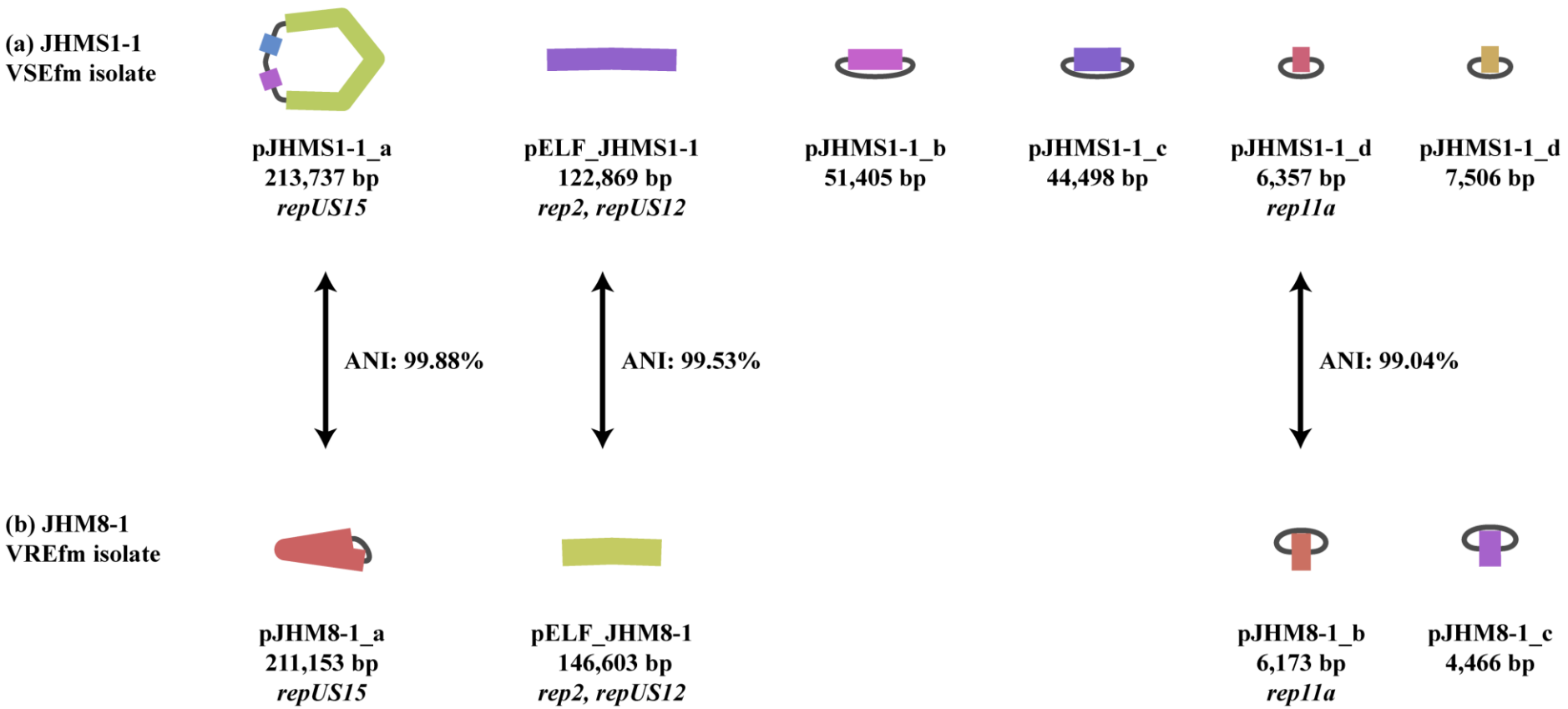

Figure 5.22. Visual representation of the complete plasmidome assembly of VSEfm isolate JHMS1-1 and VREfm isolate JHM8-1 from complex type (CT) 2932 generated using Bandage. (a) VSEfm isolate JHMS1-4 recovered from a rectal screening swab from patient P1 harbouring six distinct plasmids ranging in size from 213,737-6,357 bp and (b) VREfm isolate JHM8-1 recovered from a rectal screening swab from patient P8 harbouring four distinct plasmids ranging in size from 211,153-4,466 bp. Plasmids are represented as individual circular or linear nodes depending on topology. Plasmid names, length and associated replicon type are indicated. The average nucleotide identity (ANI) between equivalent plasmids is indicated by a percentage beside the arrows.

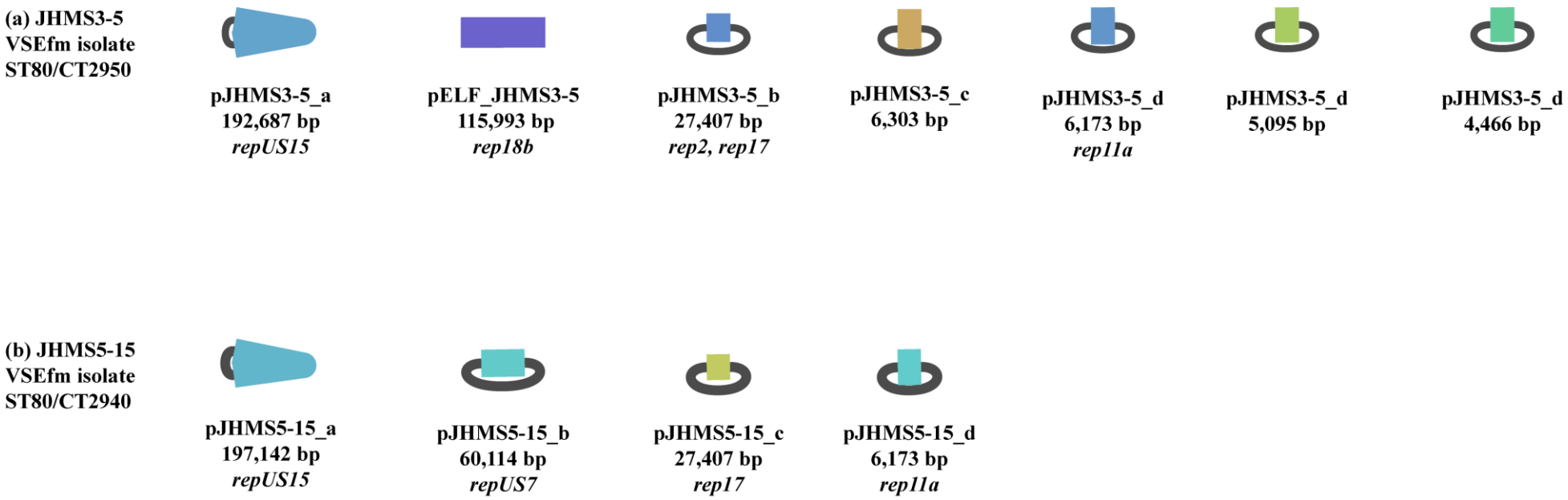

Figure 5.23. Visual representation of the complete plasmidome assembly of VSEfm isolates JHMS3-4 (CT2950) and JHMS5-15 (CT2940) generated using Bandage. (a) VSEfm isolate JHMS3-5 (ST80/CT2950) recovered from a rectal screening swab from patient three harbouring seven distinct plasmids ranging in size from 192,687-4,466 bp and (b) VSEfm isolate JHM8-1 (ST80/CT2940) recovered from a rectal screening swab from patient five harbouring four distinct plasmids ranging in size from 197,142-6,173 bp. Plasmids are represented as individual circular or linear nodes depending on topology. Plasmid names, length and associated replicon type are indicated.

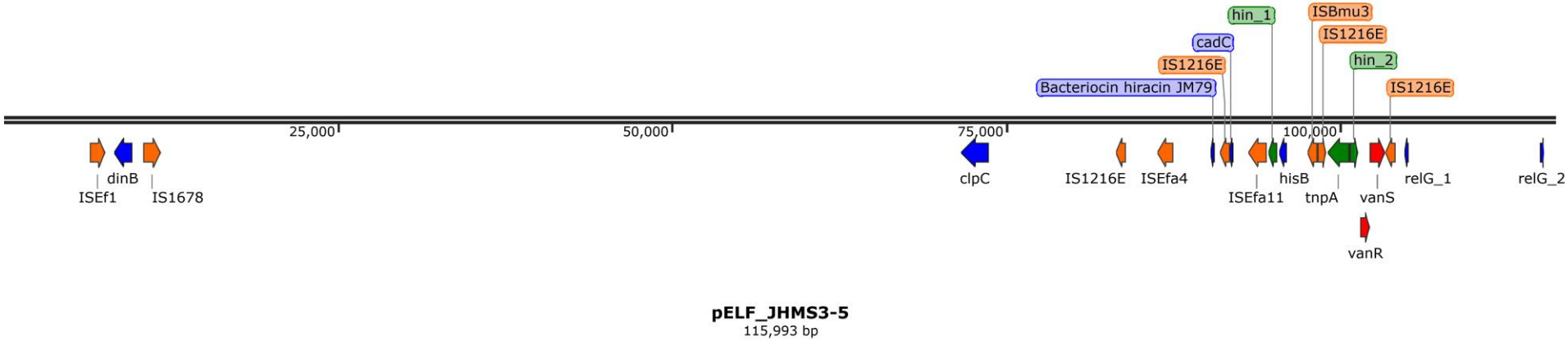

Figure 5.24. Schematic diagram of the structural organisation of plasmid pELF_JHMS3-5 from the VSEfm rectal isolate JHMS3-5 (ST80/CT2950) from patient P3 encoding a *vanA*-remnant resolved by hybrid assembly of paired-end Illumina MiSeq short reads with Oxford Nanopore Technologies long reads. Genes of interest and their orientation are represented by arrows as follows: red indicates antibiotic resistance genes, orange indicates insertion sequences, green indicates transposase and invertase genes, blue indicates genes encoding known proteins. Due to spacing limitations, products annotated by RAST, Prokka and/or EGG-NOG Mapper as 'hypothetical protein', 'mobile element protein', 'phage protein' and 'phage-related protein' are not represented in this diagram.

5.4 Discussion

This study provides a detailed insight into the population dynamics, intra-host genetic diversity and plasmidome landscape of clade A1 VREfm in asymptomatic carriers within a large Irish acute hospital. Our findings indicate that patients can harbour a heterogeneous VREfm colonising population, consisting of multiple genetically distinct sub-populations (≥2 CTs) with diverse accessory genomes. Notably, co-colonisation with highly divergent VREfm strains in 70% of the 10 patients investigated is significantly higher than previously reported. Recent studies have demonstrated that 27-51% of patients carry 2-4 VREfm variants and diversity may significantly vary over time (Brodrick *et al.,* 2016; Moradigaravand *et al.,* 2017; Gouliouris *et al.,* 2020; Both *et al.,* 2022; McHugh *et al.,* 2024). Discrepancies between reported rates perhaps reflect differences in bacterial colony picking protocols, with some studies analysing only five colonies per rectal specimen whilst others selected up to 14 for further analysis. For example, a study by Gouliouris and colleagues examined the frequency of multi-strain carriage in 185 faecal samples collected from 109 patients by analysing a median of five (range: 3-5, total: 865) colonies per primary culture plate. This revealed that 51% of patients carried multiple *E. faecium* sub-populations. The sampling strategy of 15 bacterial colonies per individual rectal swab utilised in this study was chosen on the basis of recently published work which determined the optimal number of colonies to accurately identify variants accounting for 20% of the population at a confidence level of 95% (McHugh *et al.,* 2024). Based on this criterion, the choice of five colonies by Gouliouris *et al* would have identified 50% of the population and therefore it is likely that the number of patients exhibiting VREfm colonisation heterogeneity was actually higher than reported.

Interestingly, McHugh and colleagues, whose sampling strategy formed the basis of this work, identified multiple STs within three patients (27% of samples) when utilising a similar 14-colony picking protocol. However, in our study 98% of within-patient isolates were assigned to ST80 and MLST alone was insufficient to accurately capture the cloud of diversity with respect to multi-strain carriage. These findings, in conjunction with the results of our study, serve to further highlight the emergence, genomic diversification, and clonal expansion of ST80 derivatives within the Irish population. As detailed in Chapter 3, the high-frequency of both vertical and horizontal transmission seen with Clade A1 *E. faecium* may significantly contribute to the formation of country-specific endemic clonal clusters. As a result, perhaps true comparisons of the frequency of multi-strain carriage of VREfm between countries are not truly appropriate nor informative, particularly when considering the unique

and independent evolutionary trajectory of Irish VREfm (Egan *et al.,* 2022). Additionally, it is important to note a vast number of external factors may also contribute to country-specific variations such as differences in antibiotic prescription guidelines, ward structure, patient demographics, surveillance strategies, IPC control measures and the overall burden of VREfm carriage. When considering the hyperendemicity of VREfm in Ireland, in conjunction with the extensive intra- and inter-hospital dissemination and environmental persistence as described in Chapter 4, it is unsurprising that that a high proportion of patient cohorts with frequent healthcare exposure carry a diverse array of VREfm strains.

As detailed in Section 5.3.2, a high-level of genomic variation was observed between isolate pairs from different CTs within the same patient. For example, pairwise cgMLST allelic and SKA SNP differences of 427 and 2933, respectively, were demonstrated between sub-populations within the same patient (Figure 5.1, Table 5.1). In fact, in some instances co-existing variants within the same patient were more closely related to strains present in other patients than to each other (Tables 5.3a-h). This level of diversity is therefore likely due to repeated independent strain acquisition and/or a single transmission event of a mixed population. Longitudinal studies on the genetic changes observed between VREfm isolates collected sequentially from patients over time support this conclusion, with annual within-patient mutation rates of 6-122 SNPS/genome/year reported in the literature (Moradigaravand *et al.,* 2017; Raven *et al.,* 2017; Bayjanov *et al.,* 2019; Dubin *et al.,* 2019). Interestingly, there is also evidence of intra-CT variation due to genomic diversification, perhaps reflective of a highly competitive gastrointestinal environment with extensive selective pressures as a result of multiple colonising strains. For example, 13 colonies from patient P6 were designated as CT2933 based on cgMLST and exhibited a median pairwise SNP difference of one. However, the range of SNPs varied between isolates within this cohort, with a range of 0-10, highlighting micro-diversity following acquisition. It is reasonable to suggest that genetic exchange within the GIT between divergent VREfm lineages may accelerate adaptation and increase levels of intra-strain variation.

Whilst the primary aim of this this study was to provide a comprehensive insight into the frequency and distribution of multi-strain *E. faecium* carriage in hospital-going populations, the potential implications for surveillance and outbreak resolution cannot be overlooked. Unfortunately, current conventional sequencing methodologies are systematically biased against the detection of pathogen diversity. Given the extent of heterogeneity observed amongst colonising VREfm populations identified in this chapter, this issue is extremely concerning and adds to the ever-growing complexity of VREfm in Irish hospitals. Whilst this study lacks epidemiological context due to the absence of patient

movement data, there are examples of potential acquisition and/or transmission of low abundance strains across the hospital study wards, which may be overlooked in single-colony sequencing protocols. For example, Patients P3 and P6 harboured very closely related VREfm CT6489 strains (≤6 SNPs) recovered within 101 days on W3 (Table 5.3e). In patient P6, CT6489 represented a minor frequency population which could potentially be missed in the context of conventional genomic surveillance using WGS technologies. This oversight could result in the incorrect exclusion of a patient during outbreak resolution and may significantly hinder the ability to accurately elucidate transmission networks and implement effective IPC measures. We also utilised a comparator dataset (Chapter 3 and 4 study isolates) to identify if the divergent colonising lineages identified here, particularly in relation to minor and moderate frequency strains, were commonly circulating within the study wards. This comparison revealed that low abundance strains can persist for extensive periods of time (>40 months) both within and between H1 wards and could potentially be acquired or transmitted amongst patients through direct patient-to-patient spread or unidentified reservoirs. It is important to note that comparator isolates were recovered by selecting a single bacterial colony from each patient sample and therefore the true distribution of minor frequency strains and their impact on transmission and/or acquisition is likely to be underestimated and poorly understood. Nonetheless, this study does provide evidence that within-patient VREfm co-colonisation and heterogeneous low abundance strains may represent a significant and extremely important unsampled reservoir contributing to complex transmission networks within the Irish hospital network. It is clear that further epidemiological studies using detailed patient metadata are required to fully discern the impact of the high frequency of multi-strain VREfm carriage within the Irish population.

The routine implementation of sequencing multiple *E. faecium* colonies per sample in the overall surveillance infrastructure would entail significant cost implications, ancillary storage requirements, more complex bioinformatic analysis and even increase turn-around-time. Identifying an optimal number of colonies for sequencing is crucial to accurately reflect within-patient diversity whilst remaining justifiable within the context of hospital financial constraints. For example, McHugh and colleagues demonstrated that analysing <14 colonies per sample produced fewer transmission links and lower phylogenetic network clustering scores. The authors concluded, however, that single-colony picks are suitable in many settings, particularly in the case of the Scottish VREfm population with 73% of cases showing limited within-patient diversity (McHugh *et al.,* 2024). However, it is evident that within the Irish hospital network, due to a hyper-endemic VREfm population with frequent

(up to 70%) multi-strain carriage, picking multiple bacterial colonies in surveillance would only serve to significantly improve the resolving power of WGS in outbreak investigations. However, the cost of processing, analysing, and storing library preparations would, unsurprisingly, scale exponentially with the number of independent colonies sampled. Given the current hesitancy in implementing admission screening and environmental surveillance for VREfm within Irish diagnostics, it seems unrealistic to expect that multiple colony sequencing will be a viable strategy within surveillance in the next number of years. The use of a 'one plus pool' analysis approach may provide a potential solution to this problem, which involves sequencing a single, pure bacterial colony from a specimen to represent the 'dominant' variant in conjunction with pooling and sequencing all remaining colonies on the plate to accurately ascertain the presence of within-patient diversity (Raghuram *et al.,* 2023). This may potentially mitigate the disadvantages associated with sequencing multiple bacterial colonies per specimen and allow samples to be identified and selected which may require further colony-sequencing. Other potential methodologies involve strain-specific 'plate sweep' metagenomics, in which a mixture of colonies are harvested from enrichment cultures, sequenced and subsequent bioinformatic pipelines are utilised to classify the presence of individual strains (Mu *et al.,* 2019; Anyansi *et al.,* 2020; Mäklin *et al.,* 2021). The practicality of this approach however remains to be seen as delineating highly similar strains utilising metagenomic tools is complex and many require the use of reference databases, which may prevent the identification of novel or newly emerging derivatives (Anyansi *et al.,* 2020). It is clear that extensive work is required before recommendations can be made to further augment IPC and surveillance strategies in regard to co-colonisation and outbreak resolution. It does, however, provide clear evidence that the absence of genetic links between bacterial strains utilising single-colony sequencing does not necessarily rule out patient transmission and instead may represent more complex, low abundance strain dissemination.

In conjunction with the clonal diversity of within-patient carriage, we also sought to examine the implications of mixed-strain colonisation on the *E. faecium* plasmidome pool. Our findings demonstrate that the majority of plasmid types identified (179/193, 93%) were not CT-restricted and were instead distributed across a variety of strains within diverse genetic backgrounds (Tables 5.6a-p). These results indicate that there is potentially a common pool of plasmid backbones in circulation within ST80 derivatives that can be readily transmitted both vertically and horizontally. This is in line with previous studies, which revealed that Clade A1 *E. faecium* plasmids are rapidly disseminated within healthcare networks and are transmitted between strains irrespective of their genetic lineage

(Arredondo-Alonso *et al.,* 2020; McHugh *et al.,* 2024). This is further emphasised by our finding of near-identical plasmid backgrounds (four distinct plasmids exhibiting ≤0.0001 Mash distances) in two genetically diverse VREfm isolates (CT6489 and CT2933, median SNP difference of 2822) recovered from patient P1 (Figure 5.5, Tables 5.6c, d, f and l). It is likely that the high-frequency of within-patient VREfm heterogeneity drives the horizontal exchange of near-identical plasmids between diverse clonal backgrounds within the gut consortium which can subsequently become disseminated through direct patient transfer or indirectly via contamination of the ward environment. Notably, the four plasmid types identified here were deemed 'non-mobilisable' by mob-suite tools due to the absence of relaxase and mate-pair formation type genes involved in plasmid transfer. It seems unlikely that four near-identical plasmids would transfer directly between strains utilising transformation, transduction or even as a result of natural competence. These findings are more in accordance with conjugative horizontal transfer of plasmids in conjunction with co-mobilisation of smaller plasmid types. This highlights the limitations of bioinformatic tools, in that current databases do not provide an exhaustive list of all mobilisation genes and the presence of novel genes encoding unidentified 'hypothetical proteins' may in-fact represent new, undescribed relaxase and mate-pair formation type genes. This is emphasised by our finding of a high proportion of 'unknown' coding sequences assigned on enterococcal plasmids during annotation. For example, we demonstrated the conjugative transfer of large, linear plasmids under selective pressure in the absence of any known relaxase or mate-pair formation genes.

In line with previous studies on hospital adapted clones, VREfm isolates harboured a median of five plasmids (range: 3-8) with an average size of 74,214 bp and were frequently associated with antimicrobial resistance genes (39%, 73/193) (Rosvoll *et al.,* 2010; Arredondo-Alonso *et al.,* 2020). Interestingly, the majority of plasmid-encoded antimicrobial resistance genes were co-localised on a single plasmid type which provides conducive evidence for the importance of antimicrobial stewardship to prevent co-selection in the hospital population (Tables 5.6c-e). Interestingly, a recent study assessing within-host diversity of *Pseudomonas aeruginosa* suggested that mixed strain pathogen populations significantly accelerate the evolution of antibiotic resistance in patients (Diaz Caballero *et al.,*2023). It is not unreasonable, therefore, to speculate that the high proportion of within-patient diversity demonstrated here may in part explain the widespread emergence, dissemination and success of VREfm within the Irish healthcare network. The most prominent finding of this study's accessory genome analysis is the predominance of plasmids displaying linear topology as vehicles of vancomycin resistance dissemination

(72%, 28/39 isolates investigated). This observed frequency is significantly higher than previously reported in the literature (Hashimoto *et al.,* 2019, 2020; Boumasmoud *et al.,* 2022). For example, pELF1-like linear plasmids were observed in 0.9% of enterococcal strains (16/1,769) investigated in a Japanese study, all of which were *E. faecium*, and only three harboured vancomycin resistance genes (all *vanA*). Additionally the authors analysed 14 linear plasmids available on the NCBI database from international *E. faecium* isolates (Denmark, Norway, China, the United States, Switzerland, India, and the Netherlands) and reported that 35% (5/14) encoded vancomycin resistance genes (Hashimoto *et al.,* 2023). Core-gene analysis of linear plasmids in this study (*N*=28) revealed that 8% (7/87) of conserved, core CDS (present in ≥95% of isolates) were directly attributed to the vancomycin resistance operon genes. This provides convincing evidence that Tn*1546*-like *vanA* acquisition is a significant driver of linear plasmid evolution in Irish isolates and is potentially responsible for their high prevalence. It is also worth noting that linear plasmids within our study were enriched with IS*1216E* elements, potentially contributing to the propagation and movement of *vanA* resistance genes to this plasmid type. As described in Chapter 3, IS*1216E*-mediated instability is a contributory factor in the success of Tn*1546*-like *vanA* within Ireland. Therefore, IS-mediated transfer of the *vanA* transposon to linear plasmid families within *E. faecium*, followed by subsequent adaptation and high-level retention, likely reflects highly efficient plasmid characteristics, such as low fitness cost combined with high stability and conjugative transferability making linear plasmids the most effective vehicle for HGT.

As previous chapters have highlighted the interspersal of VREfm and VSEfm in transmission clusters, this chapter aimed to provide a rudimentary snapshot of the potential diversity associated with VSEfm carriage. Interestingly, all 30 VSEfm recovered from multiple-colony picks from four individual patients (P1, P3, P5 and P8) were assigned to CC17 and consequently Clade A1 (Table 5.7). This finding is in line with recent studies which demonstrate that in a hospital setting, commensal Clade B VSEfm strains are readily displaced by nosocomial Clade A1 isolates due to the selective advantage associated with high-levels of antimicrobial resistance genes and the ability to suppress growth via bacteriocin production and other unknown mechanisms (Montealegre *et al.,* 2016; Singh *et al.,* 2022; Wagner *et al.,* 2024). Multi-strain carriage of VSEfm does not appear to be as frequently encountered as VREfm: for example, only one patient harboured multiple VSEfm CTs (patient P5, Table 5.7). Highly similar plasmidome backgrounds were evident within VSEfm isolates, which is to be expected considering that a high proportion were identified as ST80 (25/30, 83%) based on conventional MLST. Interestingly, however, there are

instances of genetically identical VSEfm and VREfm recovered from the same patient with plasmidome differences. For example, patient P8 harboured six CT2933 isolates (five VSEfm and one VREfm) which exhibited a median SKA SNP difference of one (Figure 5.20). Comparison of the accessory genomes of a representative VSEfm and VREfm from this cluster revealed the presence of near-identical plasmidomes (four plasmids present in both isolates sharing ≥99.99% nucleotide identity). A notable difference, however, was the absence of a linear plasmid in the VSEfm isolate, with a circular plasmid of 40,337 bp in lieu (Figure 5.21). When considering the previously discussed significance of linear plasmids in the dissemination of *vanA*, it begs the question – what came first: the Clade A1 VSEfm or VREfm? Perhaps in this instance, the VSEfm isolate represented a minor frequency susceptible colonising strain which potentially gained the linear plasmid via HGT in the GIT of patient P8 from an additionally acquired heterogeneous VREfm strain and/or it could additionally represent the dynamic loss of the *vanA* transposon. This is merely speculation, however, and any observations could not be fully substantiated due to the absence of *van* remnants in the VSEfm isolates in this patient. However, it is interesting to note that other VREfm isolates from patient P8 (e.g., JHM8-2, JHM8-10 and JHM8-15) harboured a *rep2, rep17* circular plasmid of approximately 40,922 bp encoding *vanA* which exhibited 47.28% to the circular plasmid identified in VSEfm isolate JHMS8-4 (Figure 5.15). As stated in Chapter 4, the dynamic gain and loss of gene segments under selective pressures it to be expected in a highly recombinant and plastic organism such as *E. faecium*, particularly in conjunction with the instability associated with IS*1216E* enrichment in Irish isolates. This is further emphasised by the finding of a *vanA* remnant (*vanY* and *vanZ*) in VSEfm isolate JHMS3-5, suggesting it potentially arose from a vancomycin-resistant ancestor. These findings serve to further emphasise the importance of considering VSE populations in surveillance practices.

To conclude, the VREfm population within Irish hospitals exhibit significant intra-host genetic diversity and co-colonisation is frequent, with 70% of patients harbouring multiple, genetically distinct strains. Our findings emphasise the limitations of current WGS sequencing protocols in the detection of pathogen diversity and highlight the urgent need for further studies to optimise sampling strategies to facilitate the reconstruction of accurate and representative transmission pathways. Near-identical plasmid backbones facilitate HGT across diverse genetic lineages, with linear plasmids constituting an essential vehicle for *vanA* dissemination. Additionally, this study further highlights the importance of consideration of VSE carriage in surveillance and IPC measures. Collectively, these results

raise more questions than they answer and serve to underscore the urgent need for further detailed genomic studies to unravel the complexity of *E. faecium* in Irish hospital networks.

5.5 Appendix

Table 5.2b. Pairwise single nucleotide polymorphism (SNP) distance matrix based on split *k*-mer analysis (SKA) of 15 isolates recovered from patient two (P2)

No. isolates	Isolate name	Ward	ST/CT		SKA SNP matrix														Median pairwise SKA-SNP difference (range)
					JHM2-1	**JHM2-2**	**JHM2-3**	**JHM2-4**	**JHM2-5**	**JHM2-6**	**JHM2-7**	**JHM2-8**	**JHM2-9**	**JHM2-10**	**JHM2-11**	**JHM2-12**	**JHM2-13**	**JHM2-14**	**JHM2-15**	
	JHM2-1	W1	ST80/CT6489	**JHM2-1**																
	JHM2-2	W1	ST80/CT6489	**JHM2-2**	3															
	JHM2-3	W1	ST80/CT6489	**JHM2-3**	2	1														
	JHM2-4	W1	ST80/CT6489	**JHM2-4**	3	2	1													
	JHM2-5	W1	ST80/CT6489	**JHM2-5**	3	2	1	2												
15	JHM2-6	W1	ST80/CT6489	**JHM2-6**	3	2	1	2	2											2 (0-8)
	JHM2-7	W1	ST80/CT6489	**JHM2-7**	2	1	0	1	1	1										
	JHM2-8	W1	ST80/CT6489	**JHM2-8**	2	1	0	1	1	1	0									
	JHM2-9	W1	ST80/CT6489	**JHM2-9**	2	1	0	1	1	1	0	0								
	JHM2-10	W1	ST80/CT6489	**JHM2-10**	7	6	5	6	6	6	5	5	5							
	JHM2-11	W1	ST80/CT6489	**JHM2-11**	3	2	1	2	2	2	1	1	1	6						
	JHM2-12	W1	ST80/CT6489	**JHM2-12**	5	4	3	4	4	4	3	3	3	8	4					
	JHM2-13	W1	ST80/CT6489	**JHM2-13**	5	4	3	4	4	4	3	3	3	8	4	6				
	JHM2-14	W1	ST80/CT6489	**JHM2-14**	3	2	1	2	2	2	1	1	1	6	2	2	4			
	JHM2-15	W1	ST80/CT6489	**JHM2-15**	3	2	1	3	2	3	1	1	2	6	2	4	4	2		

Abbreviations: CT, cgMLST complex type; ST, MLST sequence type, SKA SNP, single nucleotide polymorphism split *k*-mer analysis.

Table 5.2c. Pairwise single nucleotide polymorphism (SNP) distance matrix based on split *k*-mer analysis (SKA) of 15 isolates recovered from patient three (P3)

No. isolates	Isolate name	Ward	ST/CT		SKA SNP matrix															Median pairwise SKA-SNP difference (range)
					JHM3-1	**JHM3-2**	**JHM3-3**	**JHM3-4**	**JHM3-5**	**JHM3-6**	**JHM3-7**	**JHM3-8**	**JHM3-9**	**JHM3-10**	**JHM3-11**	**JHM3-12**	**JHM3-13**	**JHM3-14**	**JHM3-15**	
15	JHM3-1	W3	Novel/CT1898	**JHM3-1**																2 (0-3700)
	JHM3-2	W3	ST80/CT6489	**JHM3-2**	3686															
	JHM3-3	W3	ST80/CT6489	**JHM3-3**	3690	0														
	JHM3-4	W3	Novel/CT1898	**JHM3-4**	0	3686	3689													
	JHM3-5	W3	ST80/CT6489	**JHM3-5**	3691	1	1	3691												
	JHM3-6	W3	ST80/CT6489	**JHM3-6**	3694	2	2	3694	3											
	JHM3-7	W3	ST80/CT6489	**JHM3-7**	3688	3	3	3688	4	3										
	JHM3-8	W3	ST80/CT6489	**JHM3-8**	3690	0	0	3690	1	2	3									
	JHM3-9	W3	Novel/CT1898	**JHM3-9**	0	3689	3692	0	3694	3697	3691	3693								
	JHM3-10	W3	ST80/CT6489	**JHM3-10**	3697	1	1	3697	2	3	4	1	3700							
	JHM3-11	W3	ST80/CT6489	**JHM3-11**	3692	0	0	3692	1	2	3	0	3695	1						
	JHM3-12	W3	ST80/CT6489	**JHM3-12**	3689	1	1	3689	2	3	4	1	3692	2	1					
	JHM3-13	W3	ST80/CT6489	**JHM3-13**	3690	0	0	3689	1	2	3	0	3692	1	0	1				
	JHM3-14	W3	ST80/CT6489	**JHM3-14**	3691	1	1	3691	2	1	2	1	3694	2	1	2	1			
	JHM3-15	W3	ST80/CT6489	**JHM3-15**	3691	1	2	3691	2	3	4	1	3694	2	1	2	2	2		

Abbreviations: CT, cgMLST complex type; ST, MLST sequence type, SKA SNP, single nucleotide polymorphism split *k*-mer analysis.

Table 5.2d. Pairwise single nucleotide polymorphism (SNP) distance matrix based on split *k*-mer analysis (SKA) of 15 isolates recovered from patient four (P4)

No. isolates	Isolate name	Ward	ST/CT		SKA SNP matrix														Median pairwise SKA-SNP difference (range)
					JHM4-1	**JHM4-2**	**JHM4-3**	**JHM4-4**	**JHM4-5**	**JHM4-6**	**JHM4-7**	**JHM4-8**	**JHM4-9**	**JHM4-10**	**JHM4-11**	**JHM4-12**	**JHM4-13**	**JHM4-14**	**JHM4-15**	
15	JHM4-1	W20	ST80/CT2933	**JHM4-1**																30 (0-3071)
	JHM4-2	W20	ST80/CT2933	**JHM4-2**	0															
	JHM4-3	W20	ST80/CT6738	**JHM4-3**	3039	3039														
	JHM4-4	W20	ST80/CT6738	**JHM4-4**	3040	3040	5													
	JHM4-5	W20	ST80/CT6738	**JHM4-5**	3031	3031	4	3												
	JHM4-6	W20	ST80/CT6738	**JHM4-6**	3038	3038	4	1	2											
	JHM4-7	W20	ST80/CT6738	**JHM4-7**	3039	3039	3	2	1	1										
	JHM4-8	W20	ST80/CT6738	**JHM4-8**	3036	3036	3	2	1	1	0									
	JHM4-9	W20	ST80/CT6738	**JHM4-9**	3036	3036	3	2	1	1	0	0								
	JHM4-10	W20	ST80/CT6738	**JHM4-10**	3068	3067	34	29	31	30	27	28	29							
	JHM4-11	W20	ST80/CT6738	**JHM4-11**	3041	3041	5	4	3	3	2	2	2	29						
	JHM4-12	W20	ST80/CT2933	**JHM4-12**	0	0	3037	3039	3031	3037	3038	3035	3035	3066	3040					
	JHM4-13	W20	ST80/CT2933	**JHM4-13**	0	0	3042	3043	3034	3041	3042	3039	3039	3071	3044	0				
	JHM4-14	W20	ST80/CT6738	**JHM4-14**	3043	3043	5	4	3	3	2	2	2	30	4	3042	3046			
	JHM4-15	W20	ST80/CT2933	**JHM4-15**	0	0	3039	3040	3031	3038	3039	3036	3036	3067	3041	0	0	3043		

Abbreviations: CT, cgMLST complex type; ST, MLST sequence type, SKA SNP, single nucleotide polymorphism split *k*-mer analysis.

Table 5.2e. Pairwise single nucleotide polymorphism (SNP) distance matrix based on split k-mer analysis (SKA) of 15 isolates recovered from patient five (P5)

No. isolates	Isolate name	Ward	ST/CT		SKA SNP matrix														Median pairwise SKA-SNP difference (range)
					JHM5-1	**JHM5-2**	**JHM5-3**	**JHM5-4**	**JHM5-5**	**JHM5-6**	**JHM5-7**	**JHM5-8**	**JHM5-9**	**JHM5-10**	**JHM5-11**	**JHM5-12**	**JHM5-13**	**JHM5-14**	**JHM5-15**	
15	JHM5-1	W18	ST80/CT1916	**JHM5-1**																1 (0-2506)
	JHM5-2	W18	ST80/CT1916	**JHM5-2**	1															
	JHM5-3	W18	ST80/CT1916	**JHM5-3**	0	1														
	JHM5-4	W18	ST80/CT1916	**JHM5-4**	0	1	0													
	JHM5-5	W18	ST80/CT1916	**JHM5-5**	1	2	1	1												
	JHM5-6	W18	ST80/CT1916	**JHM5-6**	0	1	0	0	1											
	JHM5-7	W18	ST80/CT1916	**JHM5-7**	0	1	0	0	1	0										
	JHM5-8	W18	ST80/CT1916	**JHM5-8**	0	1	0	1	2	0	0									
	JHM5-9	W18	ST80/CT1916	**JHM5-9**	0	1	0	0	1	0	0	0								
	JHM5-10	W18	ST80/CT1916	**JHM5-10**	0	1	0	0	1	0	0	0	0							
	JHM5-11	W18	ST80/CT7229	**JHM5-11**	4	5	4	4	5	4	4	4	4	4						
	JHM5-12	W18	ST80/CT7229	**JHM5-12**	4	5	4	4	5	4	4	4	4	4	8					
	JHM5-13	W18	ST80/CT3395	**JHM5-13**	2496	2503	2502	2501	2503	2502	2502	2502	2502	2502	2506	2506				
	JHM5-14	W18	ST80/CT1916	**JHM5-14**	0	1	0	0	1	1	0	0	0	0	4	4	2502			
	JHM5-15	W18	ST80/CT3395	**JHM5-15**	2496	2503	2502	2501	2503	2502	2502	2502	2502	2502	2506	2506	0	2502		

Abbreviations: CT, cgMLST complex type; ST, MLST sequence type, SKA SNP, single nucleotide polymorphism split *k*-mer analysis.

Table 5.2f. Pairwise single nucleotide polymorphism (SNP) distance matrix based on split *k*-mer analysis (SKA) of 15 isolates recovered from patient six (P6)

No. isolates	Isolate name	Ward	ST/CT		SKA SNP matrix															Median pairwise SKA-SNP difference (range)
					JHM6-1	**JHM6-2**	**JHM6-3**	**JHM6-4**	**JHM6-5**	**JHM6-6**	**JHM6-7**	**JHM6-8**	**JHM6-9**	**JHM6-10**	**JHM6-11**	**JHM6-12**	**JHM6-13**	**JHM6-14**	**JHM6-15**	
15	JHM6-1	W3	ST80/CT2933	**JHM6-1**																1 (0-2951)
	JHM6-2	W3	ST80/CT2933	**JHM6-2**	1															
	JHM6-3	W3	ST80/CT2933	**JHM6-3**	1	0														
	JHM6-4	W3	ST80/CT2933	**JHM6-4**	2	1	1													
	JHM6-5	W3	ST80/CT2933	**JHM6-5**	1	0	0	1												
	JHM6-6	W3	ST80/CT2933	**JHM6-6**	1	0	0	1	0											
	JHM6-7	W3	ST80/CT6489	**JHM6-7**	2947	2948	2948	2947	2948	2946										
	JHM6-8	W3	ST80/CT2933	**JHM6-8**	1	0	0	1	0	0	2947									
	JHM6-9	W3	ST80/CT6489	**JHM6-9**	2949	2950	2950	2949	2950	2948	4	2949								
	JHM6-10	W3	ST80/CT2933	**JHM6-10**	2	5	9	10	9	6	2949	0	2951							
	JHM6-11	W3	ST80/CT2933	**JHM6-11**	2	1	1	2	1	1	2946	1	2948	1						
	JHM6-12	W3	ST80/CT2933	**JHM6-12**	2	1	1	0	1	1	2946	1	2949	1	2					
	JHM6-13	W3	ST80/CT2933	**JHM6-13**	1	0	0	1	0	0	2947	0	2950	0	1	1				
	JHM6-14	W3	ST80/CT2933	**JHM6-14**	1	0	0	1	0	0	2946	0	2948	0	1	1	0			
	JHM6-15	W3	ST80/CT2933	**JHM6-15**	1	0	0	1	0	0	2946	0	2948	0	1	1	0	0		

Abbreviations: CT, cgMLST complex type; ST, MLST sequence type, SKA SNP, single nucleotide polymorphism split *k*-mer analysis.

Table 5.2g. Pairwise single nucleotide polymorphism (SNP) distance matrix based on split *k*-mer analysis (SKA) of 15 isolates recovered from patient seven (P7)

No. isolates	Isolate name	Ward	ST/CT		SKA SNP matrix														Median pairwise SKA-SNP difference (range)
					JHM7-1	**JHM7-2**	**JHM7-3**	**JHM7-4**	**JHM7-5**	**JHM7-6**	**JHM7-7**	**JHM7-8**	**JHM7-9**	**JHM7-10**	**JHM7-11**	**JHM7-12**	**JHM7-13**	**JHM7-14**	**JHM7-15**	
15	JHM7-1	W9	ST80/CT2933	**JHM7-1**																0 (0-1940)
	JHM7-2	W9	ST80/CT1921	**JHM7-2**	1940															
	JHM7-3	W9	ST80/CT2933	**JHM7-3**	0	1939														
	JHM7-4	W9	ST80/CT2933	**JHM7-4**	0	1939	0													
	JHM7-5	W9	ST80/CT2933	**JHM7-5**	0	1912	0	0												
	JHM7-6	W9	ST80/CT2933	**JHM7-6**	0	1940	0	0	0											
	JHM7-7	W9	ST80/CT2933	**JHM7-7**	0	1939	0	0	0	0										
	JHM7-8	W9	ST80/CT2933	**JHM7-8**	0	1940	0	0	0	0	0									
	JHM7-9	W9	ST80/CT2933	**JHM7-9**	0	1939	0	0	0	0	0	0								
	JHM7-10	W9	ST80/CT2933	**JHM7-10**	1	1940	1	1	1	1	1	1	1							
	JHM7-11	W9	ST80/CT2933	**JHM7-11**	0	1939	0	0	0	0	0	0	0	1						
	JHM7-12	W9	ST80/CT2933	**JHM7-12**	0	1939	0	0	0	0	0	0	0	1	0					
	JHM7-13	W9	ST80/CT2933	**JHM7-13**	0	1939	0	0	0	0	0	0	0	1	0	0				
	JHM7-14	W9	ST80/CT2933	**JHM7-14**	0	1939	0	0	0	0	0	0	0	1	0	0	0			
	JHM7-15	W9	ST80/CT2933	**JHM7-15**	0	1938	0	0	0	0	0	0	0	1	0	0	0	0		

Abbreviations: CT, cgMLST complex type; ST, MLST sequence type, SKA SNP, single nucleotide polymorphism split *k*-mer analysis.

Table 5.2h. Pairwise single nucleotide polymorphism (SNP) distance matrix based on split *k*-mer analysis (SKA) of 15 isolates recovered from patient eight (P8)

No. isolates	Isolate name	Ward	ST/CT		SKA SNP matrix														Median pairwise SKA-SNP difference (range)
					JHM8-1	**JHM8-2**	**JHM8-3**	**JHM8-4**	**JHM8-5**	**JHM8-6**	**JHM8-7**	**JHM8-8**	**JHM8-9**	**JHM8-10**	**JHM8-11**	**JHM8-12**	**JHM8-13**	**JHM8-14**	**JHM8-15**	
15	JHM8-1	W2	ST80/CT2932	**JHM8-1**																2469 (0-3232)
	JHM8-2	W2	ST80/CT7567	**JHM8-2**	2967															
	JHM8-3	W2	ST80/CT2932	**JHM8-3**	0	2968														
	JHM8-4	W2	ST80/CT2933	**JHM8-4**	3226	1810	3227													
	JHM8-5	W2	ST80/CT2932	**JHM8-5**	1	2968	1	3228												
	JHM8-6	W2	ST80/CT7567	**JHM8-6**	2932	1	2933	1819	2933											
	JHM8-7	W2	ST80/CT2932	**JHM8-7**	0	2968	0	3228	1	2933										
	JHM8-8	W2	ST80/CT2932	**JHM8-8**	0	2968	0	3227	1	2933	0									
	JHM8-9	W2	ST80/CT7567	**JHM8-9**	2933	1	2934	1819	2934	0	2934	2934								
	JHM8-10	W2	ST80/CT7567	**JHM8-10**	2967	0	2968	1810	2968	1	2968	2968	1							
	JHM8-11	W2	ST80/CT2932	**JHM8-11**	0	2969	0	3232	1	2934	0	0	2935	2969						
	JHM8-12	W2	ST80/CT2932	**JHM8-12**	0	2969	0	3229	1	2934	0	0	2935	2969	0					
	JHM8-13	W2	ST80/CT2932	**JHM8-13**	0	2967	0	3227	1	2932	0	0	2933	2967	0	0				
	JHM8-14	W2	ST80/CT8281	**JHM8-14**	1498	1497	2594	1497	2484	1498	1497	2484	2484	2469	1503	1499	1497			
	JHM8-15	W2	ST80/CT7567	**JHM8-15**	2880	0	2881	1570	2881	1	2881	2881	1	0	2882	2882	2880	2428		

Abbreviations: CT, cgMLST complex type; ST, MLST sequence type, SKA SNP, single nucleotide polymorphism split *k*-mer analysis.

Table 5.2i. Pairwise single nucleotide polymorphism (SNP) distance matrix based on split *k*-mer analysis (SKA) of 15 isolates recovered from patient nine (P9)

No. isolates	Isolate name	Ward	ST/CT		SKA SNP matrix															Median pairwise SKA-SNP difference (range)
					JHM9-1	**JHM9-2**	**JHM9-3**	**JHM9-4**	**JHM9-5**	**JHM9-6**	**JHM9-7**	**JHM9-8**	**JHM9-9**	**JHM9-10**	**JHM9-11**	**JHM9-12**	**JHM9-13**	**JHM9-14**	**JHM9-15**	
15	JHM9-1	W3	ST80/CT6489	**JHM9-1**																0 (0-4)
	JHM9-2	W3	ST80/CT6489	**JHM9-2**	0															
	JHM9-3	W3	ST80/CT6489	**JHM9-3**	1	0														
	JHM9-4	W3	ST80/CT6489	**JHM9-4**	0	0	1													
	JHM9-5	W3	ST80/CT6489	**JHM9-5**	0	0	0	0												
	JHM9-6	W3	ST80/CT6489	**JHM9-6**	0	0	0	0	0											
	JHM9-7	W3	ST80/CT6489	**JHM9-7**	0	0	0	0	0	0										
	JHM9-8	W3	ST80/CT6489	**JHM9-8**	0	0	0	0	0	0	0									
	JHM9-9	W3	ST80/CT6489	**JHM9-9**	0	0	0	0	0	0	0	0								
	JHM9-10	W3	ST80/CT6489	**JHM9-10**	1	1	1	2	1	1	1	1	1							
	JHM9-11	W3	ST80/CT6489	**JHM9-11**	0	0	0	0	0	0	0	0	0	1						
	JHM9-12	W3	ST80/CT6489	**JHM9-12**	0	0	0	1	0	0	0	0	0	1	0					
	JHM9-13	W3	ST80/CT6489	**JHM9-13**	4	4	4	4	4	4	4	4	4	5	4	4				
	JHM9-14	W3	ST80/CT6489	**JHM9-14**	0	0	0	0	0	0	0	0	0	1	0	0	4			
	JHM9-15	W3	ST80/CT6489	**JHM9-15**	0	0	0	0	0	0	0	0	0	1	0	0	4	0		

Abbreviations: CT, cgMLST complex type; ST, MLST sequence type, SKA SNP, single nucleotide polymorphism split *k*-mer analysis.

Table 5.2j. Pairwise single nucleotide polymorphism (SNP) distance matrix based on split *k*-mer analysis (SKA) of 15 isolates recovered from patient ten (P10)

No. isolates	Isolate name	Ward	ST/CT		SKA SNP matrix														Median pairwise SKA-SNP difference (range)
					JHM10-1	**JHM10-2**	**JHM10-3**	**JHM10-4**	**JHM10-5**	**JHM10-6**	**JHM10-7**	**JHM10-8**	**JHM10-9**	**JHM10-10**	**JHM10-11**	**JHM10-12**	**JHM10-13**	**JHM10-14**	**JHM10-15**	
	JHM10-1	EMV	ST80/CT7537	**JHM10-1**																
	JHM10-2	EMV	ST80/CT7537	**JHM10-2**	0															
	JHM10-3	EMV	ST80/CT7537	**JHM10-3**	0	0														
	JHM10-4	EMV	ST80/CT7537	**JHM10-4**	0	0	0													
	JHM10-5	EMV	ST80/CT7537	**JHM10-5**	0	0	0	0												
15	JHM10-6	EMV	ST80/CT7537	**JHM10-6**	0	0	0	0	0											0
	JHM10-7	EMV	ST80/CT7537	**JHM10-7**	0	0	0	0	0	0										
	JHM10-8	EMV	ST80/CT7537	**JHM10-8**	0	0	0	0	0	0	0									
	JHM10-9	EMV	ST80/CT7537	**JHM10-9**	0	0	0	0	0	0	0	0								
	JHM10-10	EMV	ST80/CT7537	**JHM10-10**	0	0	0	0	0	0	0	0	0							
	JHM10-11	EMV	ST80/CT7537	**JHM10-11**	0	0	0	0	0	0	0	0	0	0						
	JHM10-12	EMV	ST80/CT7537	**JHM10-12**	0	0	0	0	0	0	0	0	0	0	0					
	JHM10-13	EMV	ST80/CT7537	**JHM10-13**	0	0	0	0	0	0	0	0	0	0	0	0				
	JHM10-14	EMV	ST80/CT7537	**JHM10-14**	0	0	0	0	0	0	0	0	0	0	0	0	0			
	JHM10-15	EMV	ST80/CT7537	**JHM10-15**	0	0	0	0	0	0	0	0	0	0	0	0	0	0		

Abbreviations: CT, cgMLST complex type; ST, MLST sequence type, SKA SNP, single nucleotide polymorphism split *k*-mer analysis.

Table 5.3b. Pairwise single nucleotide polymorphism (SNP) distance matrix based on split *k*-mer analysis (SKA) of eleven VREfm belonging to complex type (CT) 1916 identified using core-genome multi-locus sequence type (cgMLST) analysis of 150 Clade A1 VREfm isolates recovered from a single rectal screening swab from each of 10 separate patients (Figure 5.1)

No. isolates	Isolate name	Patient	Collection date	Ward	SKA SNP matrix											Median pairwise SKA-SNP difference (range)
					JHM5-1	**JHM5-2**	**JHM5-3**	**JHM5-4**	**JHM5-5**	**JHM5-6**	**JHM5-7**	**JHM5-8**	**JHM5-9**	**JHM5-10**	**JHM5-14**	
11	JHM5-1	5	14/10/2022	W18	**JHM5-1**											0 (0-2)
	JHM5-2				**JHM5-2**	1										
	JHM5-3				**JHM5-3**	0	1									
	JHM5-4				**JHM5-4**	0	1	0								
	JHM5-5				**JHM5-5**	1	2	1	1							
	JHM5-6				**JHM5-6**	0	1	0	0	1						
	JHM5-7				**JHM5-7**	0	1	0	0	1	0					
	JHM5-8				**JHM5-8**	0	1	0	1	2	0	0				
	JHM5-9				**JHM5-9**	0	1	0	0	1	0	0	0			
	JHM5-10				**JHM5-10**	0	1	0	0	1	0	0	0	0		
	JHM5-14				**JHM5-14**	0	1	0	0	1	1	0	0	0	0	

Abbreviations: CT, cgMLST complex type; ST, MLST sequence type; SKA SNP, single nucleotide polymorphism split *k*-mer analysis.

Table 5.3c. Pairwise single nucleotide polymorphism (SNP) distance matrix based on split *k*-mer analysis (SKA) of eight VREfm belonging to complex type (CT) 2932 identified using core-genome multi-locus sequence type (cgMLST) analysis of 150 clade A1 VREfm isolates recovered from a single rectal screening swab from each of 10 separate patients (Figure 5.1)

No. isolates	Isolate name	Patient	Collection date	Ward	SKA SNP matrix								Median pairwise SKA-SNP difference (range)
					JHM8-1	**JHM8-3**	**JHM8-5**	**JHM8-7**	**JHM8-8**	**JHM8-11**	**JHM8-12**	**JHM8-13**	
8	JHM8-1	8	24/01/2023	W2	**JHM8-1**								0 (0-1)
	JHM8-3				**JHM8-3**	0							
	JHM8-5				**JHM8-5**	1	0						
	JHM8-7				**JHM8-7**	0	0	1					
	JHM8-8				**JHM8-8**	0	0	1	0				
	JHM8-11				**JHM8-11**	0	0	1	0	0			
	JHM8-12				**JHM8-12**	0	0	1	0	0	0		
	JHM8-13				**JHM8-13**	0	0	1	0	0	0		

Abbreviations: CT, cgMLST complex type; ST, MLST sequence type; SKA SNP, single nucleotide polymorphism split *k*-mer analysis.

Table 5.3d. Pairwise single nucleotide polymorphism (SNP) distance matrix based on split *k*-mer analysis (SKA) of 43 VREfm belonging to complex type (CT) 2933 identified using core-genome multi-locus sequence type (cgMLST) analysis of 150 clade A1 VREfm isolates recovered from a single rectal screening swab from each of 10 separate patients (Figure 5.1)

Size of table exceeds page margins.

Scan and/or click QR code to access and/or download table.

Table 5.3e. Pairwise single nucleotide polymorphism (SNP) distance matrix based on split *k*-mer analysis (SKA) of 48 VREfm belonging to complex type (CT) 6489 identified using core-genome multi-locus sequence type (cgMLST) analysis of 150 clade A1 VREfm isolates recovered from a single rectal screening swab from each of 10 separate patients (Figure 5.1)

Size of table exceeds page margins.

Scan and/or click QR code to access and/or download table.

Table 5.3f. Pairwise single nucleotide polymorphism (SNP) distance matrix based on split *k*-mer analysis (SKA) of 11 VREfm belonging to complex type (CT) 6738 identified using core-genome multi-locus sequence type (cgMLST) analysis of 150 clade A1 VREfm isolates recovered from a single rectal screening swab from each of 10 separate patients (Figure 5.1)

No. isolates	Isolate name	Patient	Collection date	H1 ward	SKA SNP matrix										Median pairwise SKA-SNP difference (range)
					JHM1-11	**JHM4-3**	**JHM4-4**	**JHM4-5**	**JHM4-6**	**JHM4-7**	**JHM4-8**	**JHM4-9**	**JHM4-10**	**JHM4-11**	**JHM4-14**	
11	JHM1-11	1	12/10/2022	W3	**JHM1-11**											3 (0-217)
	JHM4-3	4	12/10/2022	W20	**JHM4-3**	194										
	JHM4-4				**JHM4-4**	192	5									
	JHM4-5				**JHM4-5**	168	4	3								
	JHM4-6				**JHM4-6**	192	4	1	2							
	JHM4-7				**JHM4-7**	191	3	2	1	1						
	JHM4-8				**JHM4-8**	191	3	2	1	1	0					
	JHM4-9				**JHM4-9**	191	3	2	1	1	0	0				
	JHM4-10				**JHM4-10**	217	34	29	31	30	27	28	29			
	JHM4-11				**JHM4-11**	193	5	4	3	3	2	2	2	29		
	JHM4-14				**JHM4-14**	192	5	4	3	3	2	2	2	30	4	

Abbreviations: CT, cgMLST complex type; ST, MLST sequence type; H1, hospital one; W1, ward one; W20, ward 20; SKA SNP, single nucleotide polymorphism split *k*-mer analysis.

Table 5.3g. Pairwise single nucleotide polymorphism (SNP) distance matrix based on split *k*-mer analysis (SKA) of 15 VREfm belonging to complex type (CT) 7537 identified using core-genome multi-locus sequence type (cgMLST) analysis of 150 clade A1 VREfm isolates recovered from a single rectal screening swab from each of 10 separate patients (Figure 5.1)

No. isolates	Isolate name	Patient	Collection date	Ward	SKA SNP matrix														Median pairwise SKA-SNP difference (range)
					JHM10-1	**JHM10-2**	**JHM10-3**	**JHM10-4**	**JHM10-5**	**JHM10-6**	**JHM10-7**	**JHM10-8**	**JHM10-9**	**JHM10-10**	**JHM10-11**	**JHM10-12**	**JHM10-13**	**JHM10-14**	**JHM10-15**	
15	JHM10-1	10	24/01/2023	WE	**JHM10-1**															0
	JHM10-2				**JHM10-2**	0														
	JHM10-3				**JHM10-3**	0	0													
	JHM10-4				**JHM10-4**	0	0	0												
	JHM10-5				**JHM10-5**	0	0	0	0											
	JHM10-6				**JHM10-6**	0	0	0	0	0										
	JHM10-7				**JHM10-7**	0	0	0	0	0	0									
	JHM10-8				**JHM10-8**	0	0	0	0	0	0	0								
	JHM10-9				**JHM10-9**	0	0	0	0	0	0	0	0							
	JHM10-10				**JHM10-10**	0	0	0	0	0	0	0	0	0						
	JHM10-11				**JHM10-11**	0	0	0	0	0	0	0	0	0	0					
	JHM10-12				**JHM10-12**	0	0	0	0	0	0	0	0	0	0	0				
	JHM10-13				**JHM10-13**	0	0	0	0	0	0	0	0	0	0	0	0			
	JHM10-14				**JHM10-14**	0	0	0	0	0	0	0	0	0	0	0	0	0		
	JHM10-15				**JHM10-15**	0	0	0	0	0	0	0	0	0	0	0	0	0	0	

Abbreviations: CT, cgMLST complex type; ST, MLST sequence type; H1, hospital one; WE, ward E; SKA SNP, single nucleotide polymorphism split *k*-mer analysis.

Table 5.3h. Pairwise single nucleotide polymorphism (SNP) distance matrix based on split k-mer analysis (SKA) of five VREfm belonging to complex type (CT) 7567 identified using core-genome multi-locus sequence type (cgMLST) analysis of 150 clade A1 VREfm isolates recovered from a single rectal screening swab from each of 10 separate patients (Figure 5.1)

No. isolates	Isolate name	Patient	Collection date	Ward	SKA SNP matrix						Median pairwise SKA-SNP difference (range)
						JHM8-2	**JHM8-6**	**JHM8-9**	**JHM8-10**	**JHM8-15**	
5	JHM8-2	8	24/01/2023	W3	**JHM8-2**						1 (0-1)
	JHM8-6				**JHM8-6**	1					
	JHM8-9				**JHM8-9**	1	0				
	JHM8-10				**JHM8-10**	0	1	1			
	JHM8-15				**JHM8-15**	0	1	1	0		

Abbreviations: CT, cgMLST complex type; ST, MLST sequence type; SKA SNP, single nucleotide polymorphism split *k*-mer analysis.

Table 5.4b. Pairwise single nucleotide polymorphism (SNP) distance matrix based on split *k*-mer analysis (SKA) of *E. faecium* isolates (*N*=80) belonging to complex type (CT) 2932 identified using core-genome multi-locus sequence type (cgMLST) analysis of eight Clade A1 VREfm recovered from patient P8 with additional isolates from database (*N*=72) (Figure 5.4)

Size of table exceeds page margins.

Scan and/or click QR code to access and/or download table.

Table 5.4c. Pairwise single nucleotide polymorphism (SNP) distance matrix based on split *k*-mer analysis (SKA) of *E. faecium* isolates (*N*=81) belonging to complex type (CT) 1916 identified using core-genome multi-locus sequence type (cgMLST) analysis of 11 Clade A1 VREfm recovered from patient P5 with additional isolates from database (*N*=70) (Figure 5.4)

Size of table exceeds page margins.

Scan and/or click QR code to access and/or download table.

Table 5.4d. Pairwise single nucleotide polymorphism (SNP) distance matrix based on split *k*-mer analysis (SKA) of *E. faecium* isolates (*N*=56) belonging to complex type (CT) 6489 identified using core-genome multi-locus sequence type (cgMLST) analysis of 48 Clade A1 VREfm recovered from patient P1 (*N*=5), P2 (*N*=14), P3 (*N*=12), P6 (*N*=2) and P9 (*N*=15) with additional isolates from database (*N*=8) (Figure 5.4)

Size of table exceeds page margins.

Scan and/or click QR code to access and/or download table.

Table 5.4e. Pairwise single nucleotide polymorphism (SNP) distance matrix based on split *k*-mer analysis (SKA) of *E. faecium* isolates belonging to complex type (CT) 6738 identified using core-genome multi-locus sequence type (cgMLST) analysis of eleven Clade A1 VREfm recovered from patient P1 (*N*=1) and P4 (*N*=10) (Figure 5.4)[1]

No. isolates	Isolate name	Collection Date	Ward		SKA SNP matrix											Median pairwise SKA-SNP difference (range)
					JHM1-11	**JHM4-10**	**JHM4-11**	**JHM4-14**	**JHM4-3-1**	**JHM4-4**	**JHM4-5**	**JHM4-6**	**JHM4-7**	**JHM4-8**	**JHM4-9**	
	JHM1-11	12/10/2022	W3	**JHM1-11**												
	JHM4-10	12/10/2022	W20	**JHM4-10**	217											
	JHM4-11	12/10/2022	W20	**JHM4-11**	193	29										
	JHM4-14	12/10/2022	W20	**JHM4-14**	192	30	4									3 (0-217)
	JHM4-3-1	12/10/2022	W20	**JHM4-3-1**	194	34	5	5								
11	JHM4-4	12/10/2022	W20	**JHM4-4**	192	29	4	4	5							
	JHM4-5	12/10/2022	W20	**JHM4-5**	168	31	3	3	4	3						
	JHM4-6	12/10/2022	W20	**JHM4-6**	192	30	3	3	4	1	2					
	JHM4-7	12/10/2022	W20	**JHM4-7**	191	27	2	2	3	2	1	1				
	JHM4-8	12/10/2022	W20	**JHM4-8**	191	28	2	2	3	2	1	1	0			
	JHM4-9	12/10/2022	W20	**JHM4-9**	191	29	2	2	3	2	1	1	0	0		

Abbreviations: SKA-SNP, single nucleotide polymorphism split *k*-mer analysis.
[1]Isolates from patient P1 and P4 are highlighted in green font.

Table 5.4f. Pairwise single nucleotide polymorphism (SNP) distance matrix based on split *k*-mer analysis (SKA) of *E. faecium* (*N*=9) isolates belonging to complex type (CT) 1898 identified using core-genome multi-locus sequence type (cgMLST) analysis of three clade A1 VREfm recovered from patient P3 with additional isolates from database[1] (*N*=6) (Figure 5.4)[2]

No. isolates	Isolate name	Collection Date	Ward	SKA SNP matrix									Median pairwise SKA-SNP difference (range)
				JH421	**JHM3-1**	**JHM3-4**	**JHM3-9**	**JHW145**	**JHW192**	**JHW84**	**SJ178**	**SJ267**	14 (0-216)
9	JH421	25/12/2019	W3	**JH421**									
	JHM3-1	11/10/2022	W3	**JHM3-1**	216								
	JHM3-4	11/10/2022	W3	**JHM3-4**	216	0							
	JHM3-9	11/10/2022	W3	**JHM3-9**	216	0	0						
	JHW145	01/07/2021	W3	**JHW145**	136	97	97	97					
	JHW192	29/11/2020	W2	**JHW192**	212	17	17	17	94				
	JHW84	09/11/2020	W2	**JHW84**	121	112	112	112	156	110			
	SJ178	12/06/2019	W3	**SJ178**	209	15	15	15	92	8	108		
	SJ267	26/06/2019	W3	**SJ267**	206	13	13	14	90	6	106	2	

Abbreviations: SKA-SNP, single nucleotide polymorphism split *k*-mer analysis; W2, ward two; W3, ward three.

[1] The larger collection of isolates (*N*=772) consisted of *E. faecium* isolates from the present study (*N*=150) and previously published, well-characterised isolates from this laboratory from H1 wards W1, W2, W3, W9, W18, W20 and WE (*N*=622) recovered between October 2018 and December 2022.

[2]Isolates from P3 are highlighted in green font, whilst isolates from the database are coloured in black font.

Table 5.4g. Pairwise single nucleotide polymorphism (SNP) distance matrix based on split *k*-mer analysis (SKA) of *E. faecium* isolates (*N*=4) belonging to complex type (CT) 3395 identified using core-genome multi-locus sequence type (cgMLST) analysis of two clade A1 VREfm recovered from patient P5 with additional isolates from database[1] (*N*=2) (Figure 5.4)[2]

No. isolates	Isolate name	Collection Date	Ward	SKA SNP matrix					Median pairwise SKA-SNP difference (range)
					JHM5-13	**JHM5-15**	**JHW169**	**JHW182**	
4	JHM5-13	14/10/2022	W18	**JHM5-13**					
	JHM5-15	14/10/2022	W18	**JHM5-15**	0				
	JHW169	29/02/2020	W2	**JHW169**	138	138			
	JHW182	08/09/2020	W2	**JHW182**	69	69	107		

Abbreviations: SKA-SNP, single nucleotide polymorphism split *k*-mer analysis; W2, ward two; W18, ward 18.
[1]The larger collection of isolates (*N*=772) consisted of *E. faecium* isolates from the present study (*N*=150) and previously published, well-characterised isolates from this laboratory from H1 wards W1, W2, W3, W9, W18, W20 and WE (*N*=622) recovered between October 2018 and December 2022.
[2]Isolates from P5 are highlighted in green font, whilst isolates from the database are coloured in black font.

Table 5.4h. Pairwise single nucleotide polymorphism (SNP) distance matrix based on split *k*-mer analysis (SKA) of *E. faecium* isolates (*N*=18) belonging to complex type (CT) 1921 identified using core-genome multi-locus sequence type (cgMLST) analysis of one Clade A1 VREfm recovered from patient P7 with additional isolates from database (*N*=17) (Figure 5.4)

Size of table exceeds page margins.

Scan and/or click QR code to access and/or download table.

Table 5.4i. Pairwise single nucleotide polymorphism (SNP) distance matrix based on split *k*-mer analysis (SKA) of *E. faecium* isolates (*N*=6) belonging to complex type (CT) 7567 identified using core-genome multi-locus sequence type (cgMLST) analysis of five clade A1 VREfm recovered from patient P8 with additional isolates from database[1] (*N*=1) (Figure 5.4)[2]

No. isolates	Isolate name	Collection Date	Ward	SKA SNP matrix							Median pairwise SKA-SNP difference (range)
					JHM8-10	**JHM8-15**	**JHM8-2**	**JHM8-6**	**JHM8-9-1**	**JHW264**	
6	JHM8-10	24/01/2023	W3	**JHM8-10**							0 (0-1)
	JHM8-15	24/01/2023	W3	**JHM8-15**	0						
	JHM8-2	24/01/2023	W3	**JHM8-2**	0	0					
	JHM8-6	24/01/2023	W3	**JHM8-6**	1	1	1				
	JHM8-9-1	24/01/2023	W3	**JHM8-9-1**	1	1	1	0			
	JHW264	28/12/2022	W2	**JHW264**	0	0	0	1	1		

Abbreviations: SKA-SNP, single nucleotide polymorphism split *k*-mer analysis; W2, ward two; W3, ward three.
[1]The larger collection of isolates (*N*=772) consisted of *E. faecium* isolates from the present study (*N*=150) and previously published, well-characterised isolates from this laboratory from H1 wards W1, W2, W3, W9, W18, W20 and WE (*N*=622) recovered between October 2018 and December 2022.
[2]Isolates from P8 are highlighted in green font, whilst isolates from the database are coloured in black font.

Table 5.6b. Detailed metadata and pairwise distance matrices based on MASH distance estimation of plasmid cluster C2

Plasmid name	Patient	Complex type[1]	Size (kbp)	Replicon type[2]	Plasmid family[2]	Relaxase type[3]	Mate-pair formation type[3]	Antimicrobial resistance genes[2]	Mash distance matrix		
										pJHM2-1_c	**pJHM2-15_c**
pJHM2-1_c	Patient 2	6489	52.079	NF	NF	MOBP	MPF_T	NF	**pJHM2-1_c**		
pJHM2-15_c		6489	52.079	NF	NF	MOBP	MPF_T	NF	**pJHM2-15_c**	0.00000	

Abbreviations: NF, not found.

[1] Genotypic information including cgMLST complex type (CT) were extracted *in silico* from whole genome data using Ridom SeqSphere+ v8.5.1 (Ridom GmbH, Münster, Germany). The CT was determined according to the publically available cgMLST scheme based on 1,423 loci (Been M, *et al.*,2015).

[2] Bacterial genome contigs were characterised using the STAMAR pipeline (https://github.com/phac-nml/staramr). This tool queries against Resfinder, PlasmidFinder and PointFinder databases and allows determination of plasmid type and genotypic antimicrobial resistance profiles.

[3] Bacterial plasmid sequences were characterised using the MOB-Typer tool as part of the MOB-suite (https://github.com/phac-nml/mob-suite). This provides *in silico* predictions of the relaxase type, mate-pair formation type and predicted transferability of the plasmid.

Table 5.6c. Detailed metadata and pairwise distance matrices based on MASH distance estimation of plasmid cluster C3

Size of table exceeds page margins.

Scan and/or click QR code to access and/or download table.

Table 5.6d Detailed metadata and pairwise distance matrices based on MASH distance estimation of plasmid cluster C4

Size of table exceeds page margins.

Scan and/or click QR code to access and/or download table.

Table 5.6e Detailed metadata and pairwise distance matrices based on MASH distance estimation of plasmid cluster C5

Plasmid name	Patient	CT[1]	Size (kbp)	Replicon type[2]	Plasmid family[2]	Relaxase type[3]	MPF type[3]	AMR genes[2]		Mash distance matrix								
										pJHM1-11_d	**pJHM4-15_b**	**pJHM4-4_b**	**pJHM5-13_b**	**pJHM5-15_c**	**pJHM7-2_b**	**pJHM8-10_b**	**pJHM8-15_b**	**pJHM8-2_b**
pJHM1-11_d	Patient 1	6738	20.174	*rep2*	Inc18	MOBP	NF	NF	**pJHM1-11_d**									
pJHM4-15_b	Patient 4	2933	20.174	*rep2*	Inc18	MOBP	NF	NF	**pJHM4-15_b**	0.00007								
pJHM4-4_b		6738	20.167	*rep2*	Inc18	MOBP	NF	NF	**pJHM4-4_b**	0.00014	0.00012							
pJHM5-13_b	Patient 5	3395	36.791	*rep2*, *repUS12*, *rep14a*	Multi-replicon (Inc18, Rep1 and Rep_trans)	NF	NF	*ant(6)-Ia*, *aph(3')-III*, *erm(B)*	**pJHM5-13_b**	0.04503	0.04519	0.04503						
pJHM5-15_c		3395	36.791	*rep2*, *repUS12*, *rep14a*	Multi-replicon (Inc18, Rep1 and Rep_trans)	NF	NF	*ant(6)-Ia*, *aph(3')-III*, *erm(B)*	**pJHM5-15_c**	0.04503	0.04519	0.04503	0.00000					
pJHM7-2_b	Patient 7	1921	27.387	*rep2*, *rep17*	Multi-replicon (Inc18 and RepA_N)	NF	NF	*erm(B)*	**pJHM7-2_b**	0.03078	0.03097	0.03088	0.04667	0.04667				
pJHM8-10_b	Patient 8	7567	40.922	*rep2*, *rep17*	Multi-replicon (Inc18 and RepA_N)	NF	NF	*vanHAX*, *erm(B)*	**pJHM8-10_b**	0.04059	0.04086	0.04072	0.05543	0.05543	0.01023			
pJHM8-15_b		7567	40.922	*rep2*, *rep17*	Multi-replicon (Inc18 and RepA_N)	NF	NF	*vanHAX*, *erm(B)*	**pJHM8-15_b**	0.04059	0.04086	0.04072	0.05543	0.05543	0.01019	0.00002		
pJHM8-2_b		7567	40.922	*rep2*, *rep17*	Multi-replicon (Inc18 and RepA_N)	NF	NF	*vanHAX*, *erm(B)*	**pJHM8-2_b**	0.04059	0.04086	0.04072	0.05543	0.05543	0.01019	0.00002	0.00000	

Abbreviations: CT, complex type; MPF Type, mate-pair formation type; AMR, antimicrobial resistance genes; NF, not found.

[1] Genotypic information including cgMLST complex type (CT) were extracted *in silico* from whole genome data using Ridom SeqSphere+ v8.5.1 (Ridom GmbH, Münster, Germany). The CT was determined according to the publically available cgMLST scheme based on 1,423 loci (de Been *et al.*, 2015).

[2] Bacterial genome contigs were characterised using the STAMAR pipeline (https://github.com/phac-nml/staramr). This tool queries against Resfinder, PlasmidFinder and PointFinder databases and allows determination of plasmid type and genotypic antimicrobial resistance profiles.

[3] Bacterial plasmid sequences were characterised using the MOB-Typer tool as part of the MOB-suite (https://github.com/phac-nml/mob-suite). This provides *in silico* predictions of the relaxase type, mate-pair formation type and predicted transferability of the plasmid.

Table 5.6f Detailed metadata and pairwise distance matrices based on MASH distance estimation of plasmid cluster C6

Size of table exceeds page margins.

Scan and/or click QR code to access and/or download table.

Table 5.6g Detailed metadata and pairwise distance matrices based on MASH distance estimation of plasmid cluster C7

Plasmid name	Patient	Complex type[1]	Size (kbp)	Replicon type[2]	Plasmid family[2]	Relaxase type[3]	Mate-pair formation Type[3]	Antimicrobial resistance genes[2]	Mash distance matrix			
										pJHM7-1_f	**pJHM7-11_e**	**pJHM7-7_e**
pJHM7-1_f		2933	3.199	NF	NF	NF	NF	NF	**pJHM7-1_f**			
pJHM7-11_e	Patient 7	2933	3.199	NF	NF	NF	NF	NF	**pJHM7-11_e**	0.00019		
pJHM7-7_e		2933	3.199	NF	NF	NF	NF	NF	**pJHM7-7_e**	0.00029	0.00024	

Abbreviations: NF, not found.

[1] Genotypic information including cgMLST complex type (CT) were extracted *in silico* from whole genome data using Ridom SeqSphere+ v8.5.1 (Ridom GmbH, Münster, Germany). The CT was determined according to the publically available cgMLST scheme based on 1,423 loci (de Been *et al.*, 2015).

[2] Bacterial genome contigs were characterised using the STAMAR pipeline (https://github.com/phac-nml/staramr). This tool queries against Resfinder, PlasmidFinder and PointFinder databases and allows determination of plasmid type and genotypic antimicrobial resistance profiles.

[3] Bacterial plasmid sequences were characterised using the MOB-Typer tool as part of the MOB-suite (https://github.com/phac-nml/mob-suite). This provides *in silico* predictions of the relaxase type, mate-pair formation type and predicted transferability of the plasmid.

Table 5.6h. Detailed metadata and pairwise distance matrices based on MASH distance estimation of plasmid cluster C8

Plasmid name	Patient	CT[1]	Size (kbp)	Replicon type[2]	Plasmid family[2]	Relaxase type[3]	MPF type[3]	AMR genes[2]		Mash distance matrix								
										pJHM1-11_e	**pJHM2-1_e**	**pJHM2-15_e**	**pJHM4-14_d**	**pJHM4-15_d**	**pJHM4-4_d**	**pJHM5-11_e**	**pJHM5-6_e**	**pJHM5-9_e**
pJHM1-11_e	Patient 1	6738	5.212	*rep18b*	Rep3	NF	NF	NF	**pJHM1-11_e**									
pJHM2-1_e	Patient 2	6489	5.088	*rep18b*	Rep3	NF	NF	NF	**pJHM2-1_e**	0.02235								
pJHM2-15_e		6489	5.088	*rep18b*	Rep3	NF	NF	NF	**pJHM2-15_e**	0.02221	0.00014							
pJHM4-14_d	Patient 4	6738	5.212	*rep18b*	Rep3	NF	NF	NF	**pJHM4-14_d**	0.00046	0.02286	0.02257						
pJHM4-15_d		2933	5.212	*rep18b*	Rep3	NF	NF	NF	**pJHM4-15_d**	0.00048	0.02278	0.02249	0.00026					
pJHM4-4_d		6738	5.212	*rep18b*	Rep3	NF	NF	NF	**pJHM4-4_d**	0.00036	0.02249	0.02221	0.00017	0.00019				
pJHM5-11_e	Patient 5	7229	5.569	*rep18b*	Rep3	NF	NF	NF	**pJHM5-11_e**	0.01589	0.00752	0.00745	0.01583	0.01578	0.01556			
pJHM5-6_e		1916	5.569	*rep18b*	Rep3	NF	NF	NF	**pJHM5-6_e**	0.01572	0.00749	0.00741	0.01562	0.01556	0.01535	0.00012		
pJHM5-9_e		1916	5.569	*rep18b*	Rep3	NF	NF	NF	**pJHM5-9_e**	0.01572	0.00745	0.00738	0.01567	0.01562	0.01540	0.00012	0.00010	

Abbreviations: CT, complex type; MPF Type, mate-pair formation type; AMR, antimicrobial resistance genes; NF, not found.

[1] Genotypic information including cgMLST complex type (CT) were extracted *in silico* from whole genome data using Ridom SeqSphere+ v8.5.1 (Ridom GmbH, Münster, Germany). The CT was determined according to the publically available cgMLST scheme based on 1,423 loci (de Been *et al.*, 2015).

[2] Bacterial genome contigs were characterised using the STAMAR pipeline (https://github.com/phac-nml/staramr). This tool queries against Resfinder, PlasmidFinder and PointFinder databases and allows determination of plasmid type and genotypic antimicrobial resistance profiles.

[3] Bacterial plasmid sequences were characterised using the MOB-Typer tool as part of the MOB-suite (https://github.com/phac-nml/mob-suite). This provides *in silico* predictions of the relaxase type, mate-pair formation type and predicted transferability of the plasmid.

Table 5.6i. Detailed metadata and pairwise distance matrices based on MASH distance estimation of plasmid cluster C9

Plasmid name	Patient	Complex type[1]	Size (kbp)	Replicon type[2]	Plasmid family[2]	Relaxase type[3]	Mate-pair formation Type[3]	Antimicrobial resistance genes[2]	Mash distance matrix			
										pJHM7-1_d	**pJHM7-11_c**	**pJHM7-7_c**
pJHM7-1_d		2933	5.85	NF	NF	NF	NF	NF	**pJHM7-1_d**			
pJHM7-11_c	Patient 7	2933	5.85	NF	NF	NF	NF	NF	**pJHM7-11_c**	0.00000		
pJHM7-7_c		2933	5.85	NF	NF	NF	NF	NF	**pJHM7-7_c**	0.00012	0.00012	

Abbreviations: NF, not found.

[1] Genotypic information including cgMLST complex type (CT) were extracted *in silico* from whole genome data using Ridom SeqSphere+ v8.5.1 (Ridom GmbH, Münster, Germany). The CT was determined according to the publically available cgMLST scheme based on 1,423 loci (de Been *et al.*, 2015).

[2] Bacterial genome contigs were characterised using the STAMAR pipeline (https://github.com/phac-nml/staramr). This tool queries against Resfinder, PlasmidFinder and PointFinder databases and allows determination of plasmid type and genotypic antimicrobial resistance profiles.

[3] Bacterial plasmid sequences were characterised using the MOB-Typer tool as part of the MOB-suite (https://github.com/phac-nml/mob-suite). This provides *in silico* predictions of the relaxase type, mate-pair formation type and predicted transferability of the plasmid.

Table 5.6j Detailed metadata and pairwise distance matrices based on MASH distance estimation of plasmid cluster C10

Size of table exceeds page margins.

Scan and/or click QR code to access and/or download table.

Table 5.6k. Detailed metadata and pairwise distance matrices based on MASH distance estimation of plasmid cluster C11

Plasmid name	Patient	Complex type[1]	Size (kbp)	Replicon type[2]	Plasmid family[2]	Relaxase type[3]	Mate-pair formation Type[3]	Antimicrobial resistance genes[2]	Mash distance matrix						
										pJHM10-1_b	**pJHM10-15_b**	**pJHM5-11_c**	**pJHM5-13_c**	**pJHM5-15_d**	**pJHM5-6_c**	**pJHM5-9_c**
pJHM10-1_b	Patient 10	7537	6.303	NF	NF	MOBP	NF	NF	**pJHM10-1_b**							
pJHM10-15_b		7537	6.303	NF	NF	MOBP	NF	NF	**pJHM10-15_b**	0.00000						
pJHM5-11_c		7229	6.303	NF	NF	MOBP	NF	NF	**pJHM5-11_c**	0.00051	0.00051					
pJHM5-13_c		3395	6.303	NF	NF	MOBP	NF	NF	**pJHM5-13_c**	0.00012	0.00012	0.00039				
pJHM5-15_d	Patient 5	3395	6.303	NF	NF	MOBP	NF	NF	**pJHM5-15_d**	0.00022	0.00022	0.00048	0.00010			
pJHM5-6_c		1916	6.303	NF	NF	MOBP	NF	NF	**pJHM5-6_c**	0.00053	0.00053	0.00017	0.00041	0.00031		
pJHM5-9_c		1916	6.303	NF	NF	MOBP	NF	NF	**pJHM5-9_c**	0.00053	0.00053	0.00017	0.00041	0.00031	0.00000	

Abbreviations: NF, not found.

[1] Genotypic information including cgMLST complex type (CT) were extracted *in silico* from whole genome data using Ridom SeqSphere+ v8.5.1 (Ridom GmbH, Münster, Germany). The CT was determined according to the publically available cgMLST scheme based on 1,423 loci (de Been *et al.*, 2015).

[2] Bacterial genome contigs were characterised using the STAMAR pipeline (https://github.com/phac-nml/staramr). This tool queries against Resfinder, PlasmidFinder and PointFinder databases and allows determination of plasmid type and genotypic antimicrobial resistance profiles.

[3] Bacterial plasmid sequences were characterised using the MOB-Typer tool as part of the MOB-suite (https://github.com/phac-nml/mob-suite). This provides *in silico* predictions of the relaxase type, mate-pair formation type and predicted transferability of the plasmid.

Table 5.6l Detailed metadata and pairwise distance matrices based on MASH distance estimation of plasmid cluster C12

Size of table exceeds page margins.

Scan and/or click QR code to access and/or download table.

Table 5.6m. Detailed metadata and pairwise distance matrices based on MASH distance estimation of plasmid cluster C13

Plasmid name	Patient	Complex type[1]	Size (kbp)	Replicon type[2]	Plasmid family[2]	Relaxase type[3]	Mate-pair formation Type[3]	Antimicrobial resistance genes[2]	Mash distance matrix			
										pJHM4-4_c	**pJHM4-14_c**	**pJHM4-15_c**
pJHM4-4_c		6738	14.851	*rep17*	RepA_N	NF	NF	NF	**pJHM4-4_c**			
pJHM4-14_c	Patient 4	6738	14.859	*rep17*	RepA_N	NF	NF	NF	**pJHM4-14_c**	0.00034		
pJHM4-15_c		2933	14.861	*rep17*	RepA_N	NF	NF	NF	**pJHM4-15_c**	0.00093	0.00068	

Abbreviations: NF, not found.

[1] Genotypic information including cgMLST complex type (CT) were extracted *in silico* from whole genome data using Ridom SeqSphere+ v8.5.1 (Ridom GmbH, Münster, Germany). The CT was determined according to the publically available cgMLST scheme based on 1,423 loci (de Been *et al.*, 2015).

[2] Bacterial genome contigs were characterised using the STAMAR pipeline (https://github.com/phac-nml/staramr). This tool queries against Resfinder, PlasmidFinder and PointFinder databases and allows determination of plasmid type and genotypic antimicrobial resistance profiles.

[3] Bacterial plasmid sequences were characterised using the MOB-Typer tool as part of the MOB-suite (https://github.com/phac-nml/mob-suite). This provides *in silico* predictions of the relaxase type, mate-pair formation type and predicted transferability of the plasmid.

Table 5.6n. Detailed metadata and pairwise distance matrices based on MASH distance estimation of plasmid cluster C14

Plasmid name	Patient	Complex type[1]	Size (kbp)	Replicon type[2]	Plasmid family[2]	Relaxase type[3]	Mate-pair formation type[3]	Antimicrobial resistance genes[2]	Mash distance matrix		
										pJHM1-2_c	**pJHM1-9_d**
pJHM1-2_c	Patient 1	6489	60.113	*repUS7*	Inc18	MOBP	MPF_T	NF	**pJHM1-2_c**		
pJHM1-9_d		6489	60.113	*repUS7*	Inc18	MOBP	MPF_T	NF	**pJHM1-9_d**	0.00000	

Abbreviations: NF, not found.

[1] Genotypic information including cgMLST complex type (CT) were extracted *in silico* from whole genome data using Ridom SeqSphere+ v8.5.1 (Ridom GmbH, Münster, Germany). The CT was determined according to the publically available cgMLST scheme based on 1,423 loci (de Been *et al.,* 2015).

[2] Bacterial genome contigs were characterised using the STAMAR pipeline (https://github.com/phac-nml/staramr). This tool queries against Resfinder, PlasmidFinder and PointFinder databases and allows determination of plasmid type and genotypic antimicrobial resistance profiles.

[3] Bacterial plasmid sequences were characterised using the MOB-Typer tool as part of the MOB-suite (https://github.com/phac-nml/mob-suite). This provides *in silico* predictions of the relaxase type, mate-pair formation type and predicted transferability of the plasmid.

Table 5.6o. Detailed metadata and pairwise distance matrices based on MASH distance estimation of plasmid cluster C15

Plasmid name	Patient	Complex type[1]	Size (kbp)	Replicon type[2]	Plasmid family[2]	Relaxase type[3]	Mate-pair formation type[3]	Antimicrobial resistance genes[2]	Mash distance matrix			
										pJHM1-9_c	**pJHM3-2_b**	**pJHM9-15_b**
pJHM1-9_c	Patient 1	6489	92.606	NF	NF	NF	NF	NF	**pJHM1-9_c**			
pJHM3-2_b	Patient 3	6489	94.092	NF	NF	NF	NF	NF	**pJHM3-2_b**	0.00091		
pJHM9-15_b	Patient 9	6489	92.194	NF	NF	NF	NF	NF	**pJHM9-15_b**	0.00611	0.00720	

Abbreviations: NF, not found.

[1] Genotypic information including cgMLST complex type (CT) were extracted *in silico* from whole genome data using Ridom SeqSphere+ v8.5.1 (Ridom GmbH, Münster, Germany). The CT was determined according to the publically available cgMLST scheme based on 1,423 loci (de Been *et al.*, 2015).

[2] Bacterial genome contigs were characterised using the STAMAR pipeline (https://github.com/phac-nml/staramr). This tool queries against Resfinder, PlasmidFinder and PointFinder databases and allows determination of plasmid type and genotypic antimicrobial resistance profiles.

[3] Bacterial plasmid sequences were characterised using the MOB-Typer tool as part of the MOB-suite (https://github.com/phac-nml/mob-suite). This provides *in silico* predictions of the relaxase type, mate-pair formation type and predicted transferability of the plasmid.

Table 5.6p. Detailed metadata and pairwise distance matrices based on MASH distance estimation of plasmid cluster C16

Plasmid name	Patient	Complex type[1]	Size (kbp)	Replicon type[2]	Plasmid family[2]	Relaxase type[3]	Mate-pair formation type[3]	Antimicrobial resistance genes[2]	Mash distance matrix		
									pJHM8-15_d	**pJHM8-10_d**	**pJHM8-2_d**
pJHM8-15_d		7567	4.374	NF	NF	MOBV	NF	NF	**pJHM8-15_d**		
pJHM8-10_d	Patient 8	7567	4.374	NF	NF	MOBV	NF	NF	**pJHM8-10_d**	0.00022	
pJHM8-2_d		7567	4.374	NF	NF	MOBV	NF	NF	**pJHM8-2_d**	0.00026	0.00024

Abbreviations: NF, not found.

[1] Genotypic information including cgMLST complex type (CT) were extracted *in silico* from whole genome data using Ridom SeqSphere+ v8.5.1 (Ridom GmbH, Münster, Germany). The CT was determined according to the publically available cgMLST scheme based on 1,423 loci (de Been *et al.*, 2015).

[2] Bacterial genome contigs were characterised using the STAMAR pipeline (https://github.com/phac-nml/staramr). This tool queries against Resfinder, PlasmidFinder and PointFinder databases and allows determination of plasmid type and genotypic antimicrobial resistance profiles.

[3] Bacterial plasmid sequences were characterised using the MOB-Typer tool as part of the MOB-suite (https://github.com/phac-nml/mob-suite). This provides *in silico* predictions of the relaxase type, mate-pair formation type and predicted transferability of the plasmid

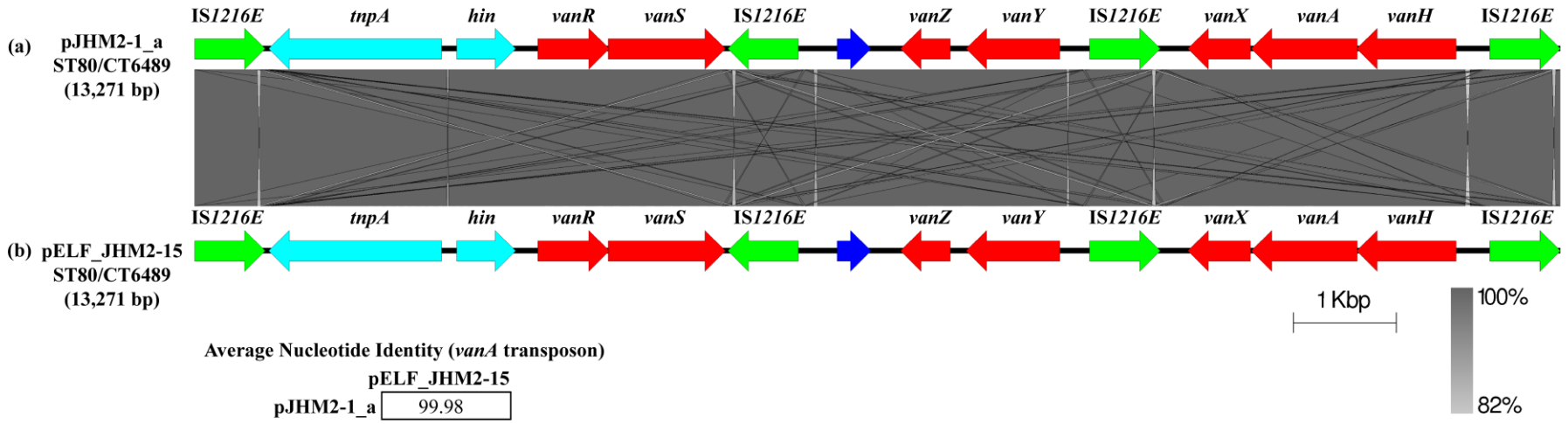

Figure 5.9. Comparative genetic organisation of *vanA* transposon regions closed by hybrid assembly of VREfm isolates belonging to one complex type (CT) from patient P2. The figure shows an alignment of the *vanA* region encoded by indistinguishable plasmids from two VREfm ST80/CT6489 isolates as follows: (a) pJHM2-1_a (ST80/CT6489, 13,271 bp) and (b) pELF_JHM2-15 (ST80/CT6489, 13,271 bp) generated using Easyfig (Sullivan *et al.*,2011). Coding sequences of interest and their orientation are represented by arrows as follows: red, vancomycin resistance genes; green, insertion sequences; blue, proteins with a known coding function; cyan, transposase and invertase genes; grey, hypothetical proteins. Full details of plasmid profiles and SKA-SNP matrices are provided in Tables 5.4-5.6. Regions between alignments with shared homology are represented by grey connecting blocks and/or lines with the colour gradient indicating percentage nucleotide identity (82-100%). A scale bar is included beneath the figure.

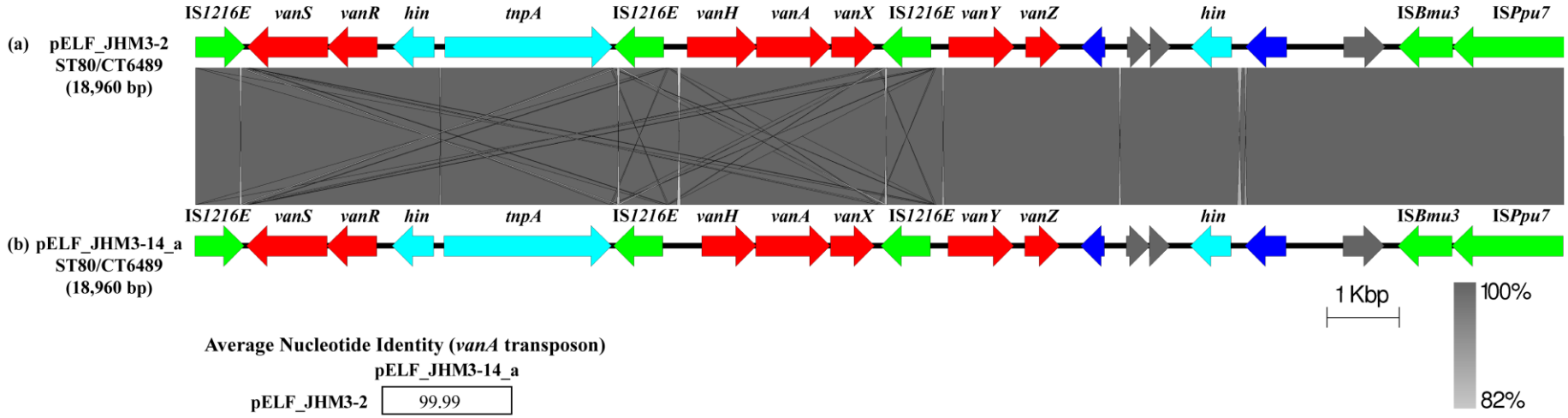

Figure 5.10. Comparative genetic organisation of *vanA* transposon regions closed by hybrid assembly of VREfm isolates belonging to one complex type (CT) from patient P3. The figure shows an alignment of the *vanA* region encoded by indistinguishable plasmids from two VREfm ST80/CT6489 isolates as follows: (a) pELF_JHM3-2 (ST80/CT6489, 18,960 bp) and (b) pELF_JHM3-14_A (ST80/CT6489, 18,960 bp) generated using Easyfig (Sullivan *et al.*, 2011). Coding sequences of interest and their orientation are represented by arrows as follows: red, vancomycin resistance genes; green, insertion sequences; blue, proteins with a known coding function; cyan, transposase and invertase genes; grey, hypothetical proteins. Full details of plasmid profiles and SKA-SNP matrices are provided in Tables 5.4-5.6. Regions between alignments with shared homology are represented by grey connecting blocks and/or lines with the colour gradient indicating percentage nucleotide identity (82-100%). A scale bar is included beneath the figure.

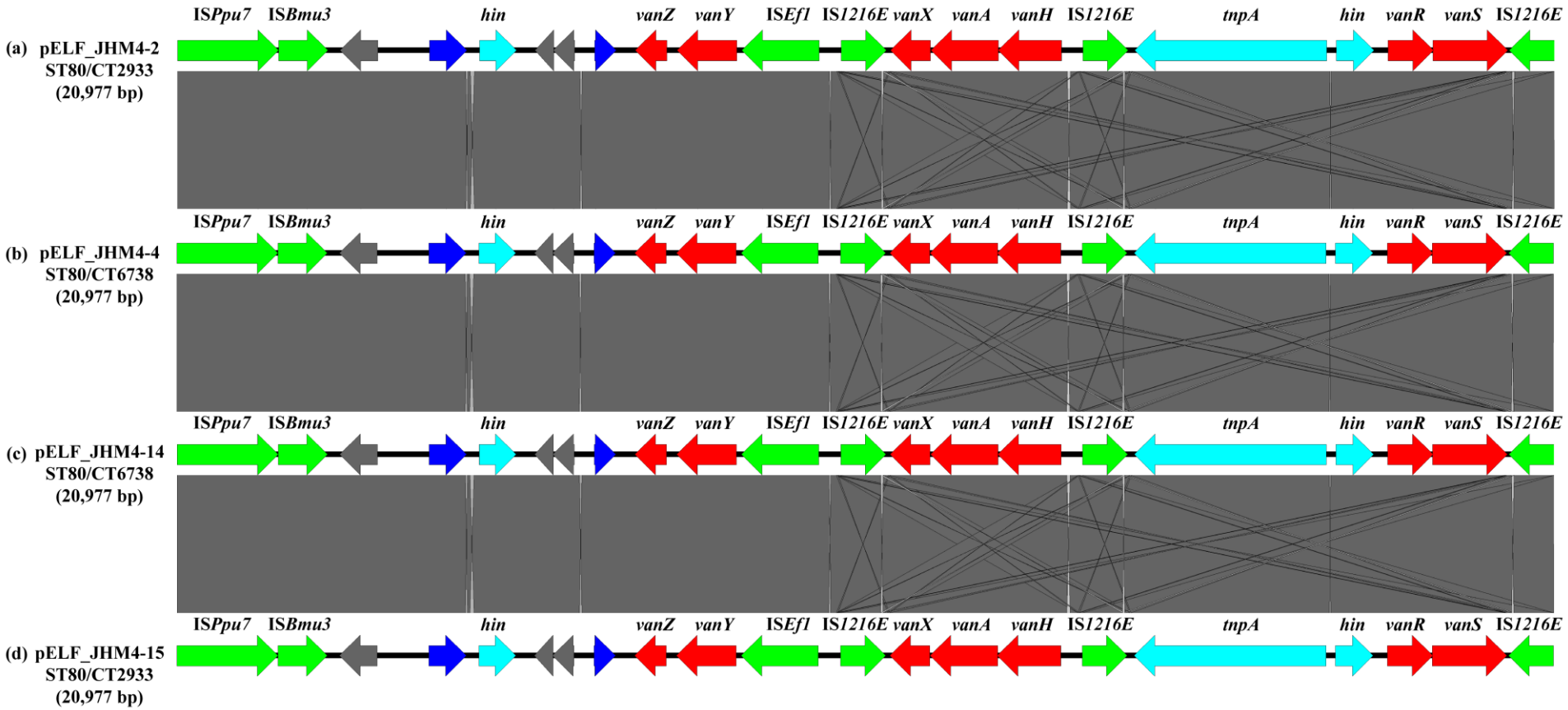

Average Nucleotide Identity (*vanA* transposon)

	pELF_JHM4-2	pELF_JHM4-4	pELF_JHM4-14	pELF_JHM4-15
pELF_JHM4-2				
pELF_JHM4-4	99.99			
pELF_JHM4-14	100	99.99		
pELF_JHM4-15	99.99	100	99.99	

Figure 5.11. Comparative genetic organisation of *vanA* transposon regions closed by hybrid assembly of four VREfm isolates belonging to two complex types (CTs) from patient P4. The figure shows an alignment of the *vanA* region encoded by four plasmids from separate VREfm isolates belonging to two CTs as follows: (a) pELF_JHM4-2 (ST80/CT2933, 20,977 bp), (b) pELF_JHM4-4 (ST80/CT6738, 20,977 bp), (c) pELF_JHM4-14 (ST80/CT6738, 20,977 bp) and (d) pELF_JHM4-15 (ST80/CT2933, 20,977 bp) generated using Easyfig (Sullivan *et al.*, 2011). Coding sequences of interest and their orientation are represented by arrows as follows: red, vancomycin resistance genes; green, insertion sequences; blue, proteins with a known coding function; cyan, transposase and invertase genes; grey, hypothetical proteins. Full details of plasmid profiles and SKA-SNP matrices are provided in Tables 5.4-5.6. Regions between alignments with shared homology are represented by grey connecting blocks and/or lines with the colour gradient indicating percentage nucleotide identity (82-100%). A scale bar is included beneath the figure.

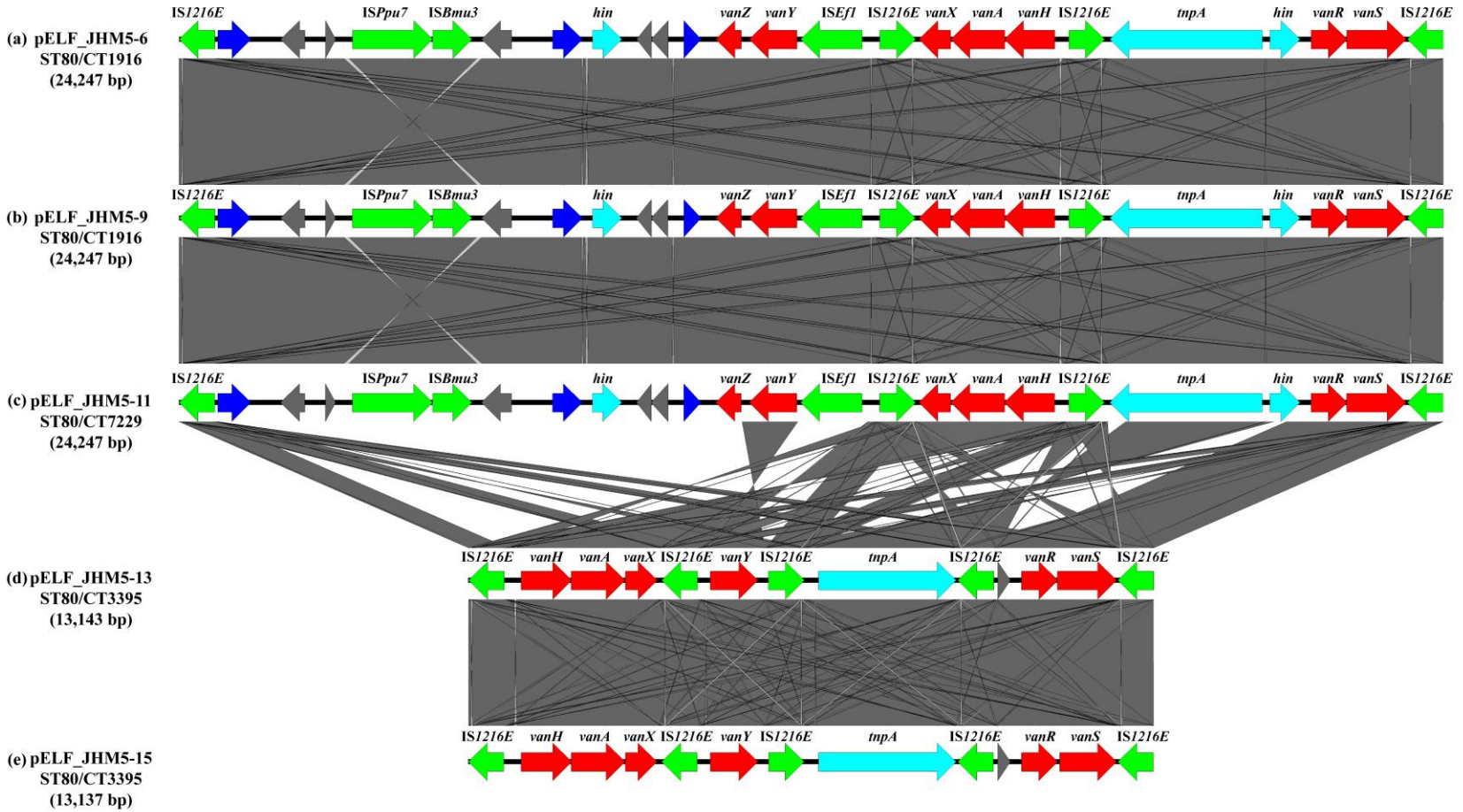

Average Nucleotide Identity (*vanA* transposon)

	pELF_JHM5-6	pELF_JHM5-9	pELF_JHM5-11	pELF_JHM5-13	pELF_JHM5-15
pELF_JHM5-6					
pELF_JHM5-9	99.99				
pELF_JHM5-11	99.99	99.99			
pELF_JHM5-13	98.27	98.18	98.27		
pELF_JHM5-15	98.27	98.18	98.27	100	

Figure 5.12. Comparative genetic organisation of *vanA* transposon regions closed by hybrid assembly of five VREfm isolates belonging to three complex types (CTs) from patient P5. The figure shows an alignment of the *vanA* region encoded by five plasmids from separate VREfm isolates belonging to three CTs as follows: (a) pELF_JHM5-6 (ST80/CT1916, 24,247 bp), (b) pELF_JHM5-9 (ST80/CT1916, 24,247 bp), (c) pELF_JHM5-11 (ST80/CT7229, 24,247 bp), (d) pELF_JHM5-13 (ST80/CT3395, 13,143 bp) and (e) pELF_JHM5-13 (ST80/CT3395, 13,137 bp) generated using Easyfig (Sullivan *et al.*, 2011). Coding sequences of interest and their orientation are represented by arrows as follows: red, vancomycin resistance genes; green, insertion sequences; blue, proteins with a known coding function; cyan, transposase and invertase genes; grey, hypothetical proteins. Full details of plasmid profiles and SKA-SNP matrices are provided in Tables 5.4-5.6. Regions between alignments with shared homology are represented by grey connecting blocks and/or lines with the colour gradient indicating percentage nucleotide identity (82-100%). A scale bar is included beneath the figure.

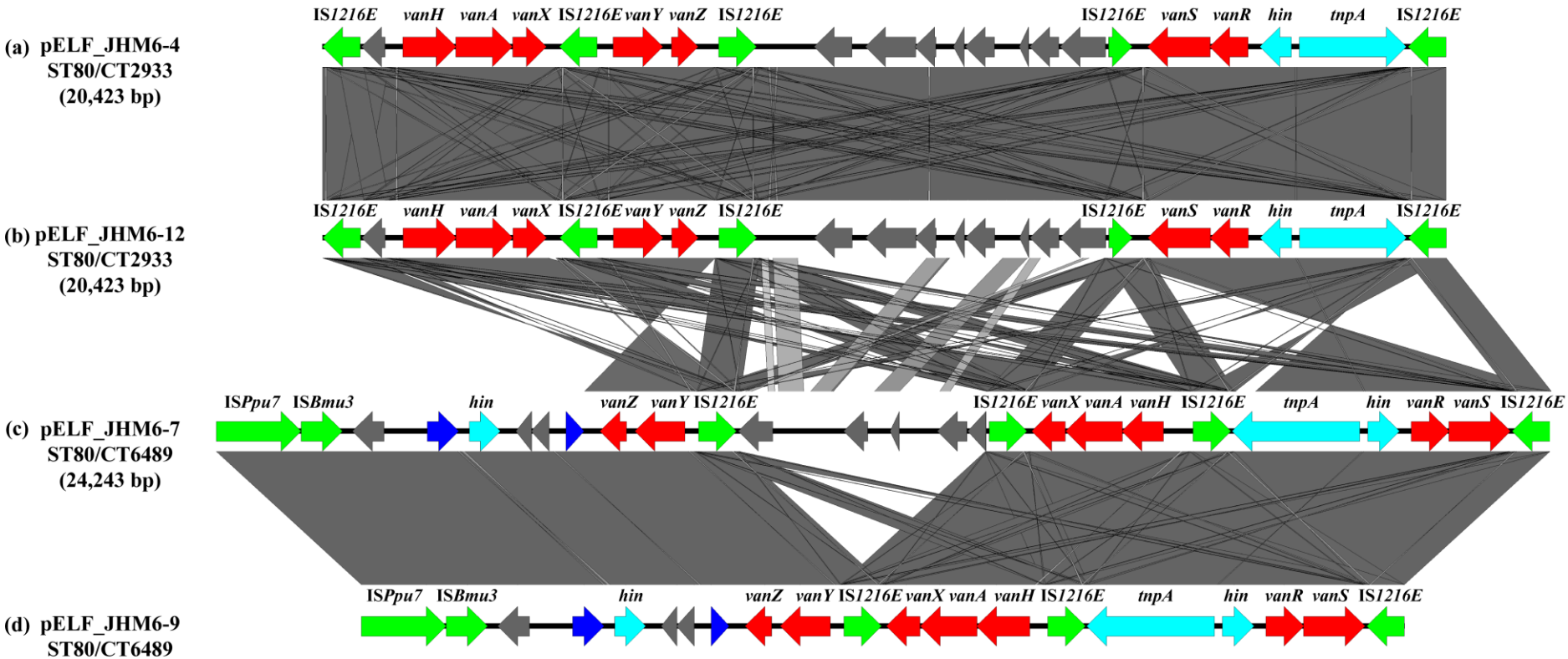

Average Nucleotide Identity (*vanA* transposon)

	pELF_JHM6-4	pELF_JHM6-12	pELF_JHM6-7	pELF_JHM6-9
pELF_JHM6-4				
pELF_JHM6-12	99.96			
pELF_JHM6-7	97.27	97.31		
pELF_JHM6-9	99.04	99.04	99.99	

Figure 5.13. Comparative genetic organisation of *vanA* transposon regions closed by hybrid assembly of four VREfm isolates belonging to two complex types (CTs) from patient P6. The figure shows an alignment of the *vanA* region encoded by four plasmids from separate VREfm isolates belonging to two CTs as follows: (a) pELF_JHM6-4 (ST80/CT2933, 20,423 bp), (b) pELF_JHM6-12 (ST80/CT2933, 20,423 bp), (c) pELF_JHM6-7 (ST80/CT6489, 24,247 bp) and (d) pELF_JHM6-9 (ST80/CT6489, 18,960 bp) generated using Easyfig (Sullivan *et al.,* 2011). Coding sequences of interest and their orientation are represented by arrows as follows: red, vancomycin resistance genes; green, insertion sequences; blue, proteins with a known coding function; cyan, transposase and invertase genes; grey, hypothetical proteins. Full details of plasmid profiles and SKA-SNP matrices are provided in Tables 5.4-5.6. Regions between alignments with shared homology are represented by grey connecting blocks and/or lines with the colour gradient indicating percentage nucleotide identity (82-100%). A scale bar is included beneath the figure.

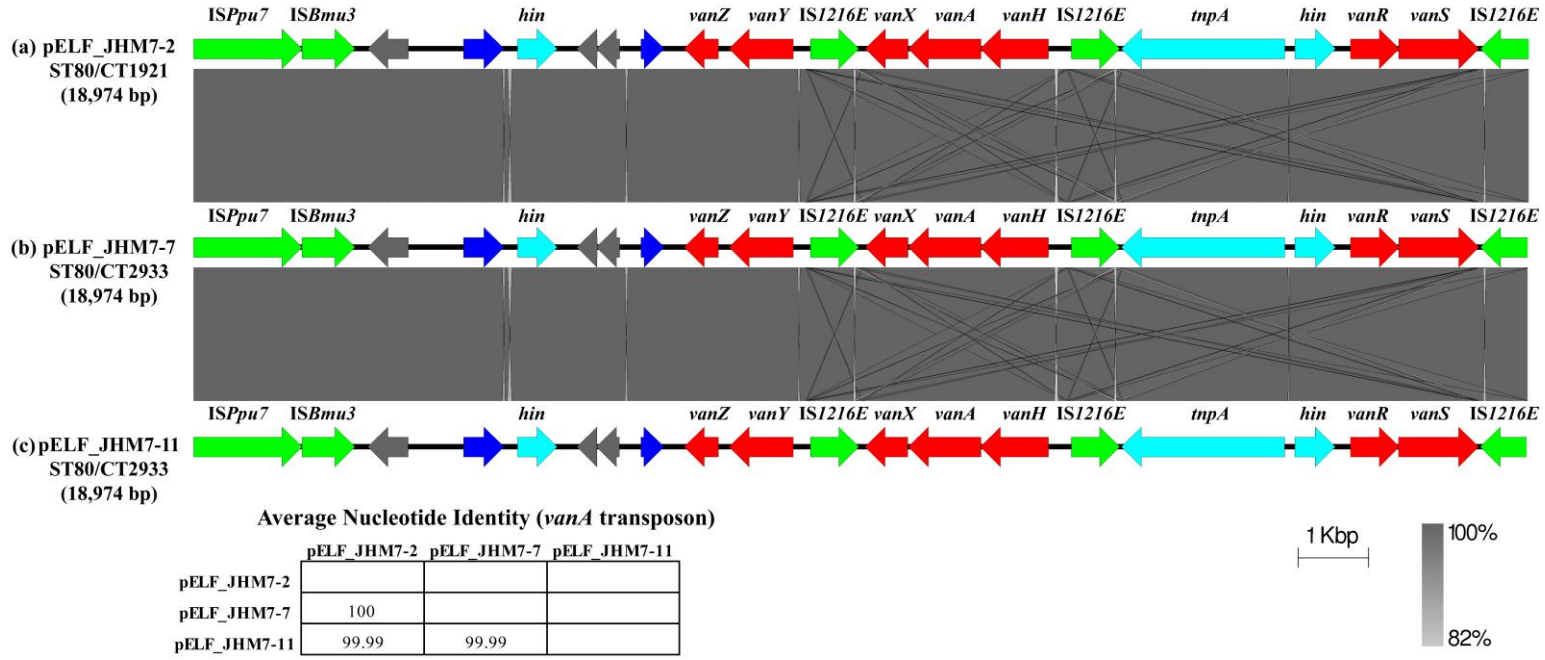

Figure 5.14. Comparative genetic organisation of *vanA* transposon regions closed by hybrid assembly of three VREfm isolates belonging to two complex types (CTs) from patient P7. The figure shows an alignment of the *vanA* region encoded by three plasmids from separate VREfm isolates belonging to two CTs as follows: (a) pELF_JHM7-2 (ST80/CT1921, 18,974 bp), (b) pELF_JHM7-7 (ST80/CT2933, 18,974 bp) and (c) pELF_JHM7-11 (ST80/CT2933, 18,974 bp) generated using Easyfig (Sullivan *et al.*, 2011). Coding sequences of interest and their orientation are represented by arrows as follows: red, vancomycin resistance genes; green, insertion sequences; blue, proteins with a known coding function; cyan, transposase and invertase genes; grey, hypothetical proteins. Full details of plasmid profiles and SKA-SNP matrices are provided in Tables 5.4-5.6. Regions between alignments with shared homology are represented by grey connecting blocks and/or lines with the colour gradient indicating percentage nucleotide identity (82-100%). A scale bar is included beneath the figure.

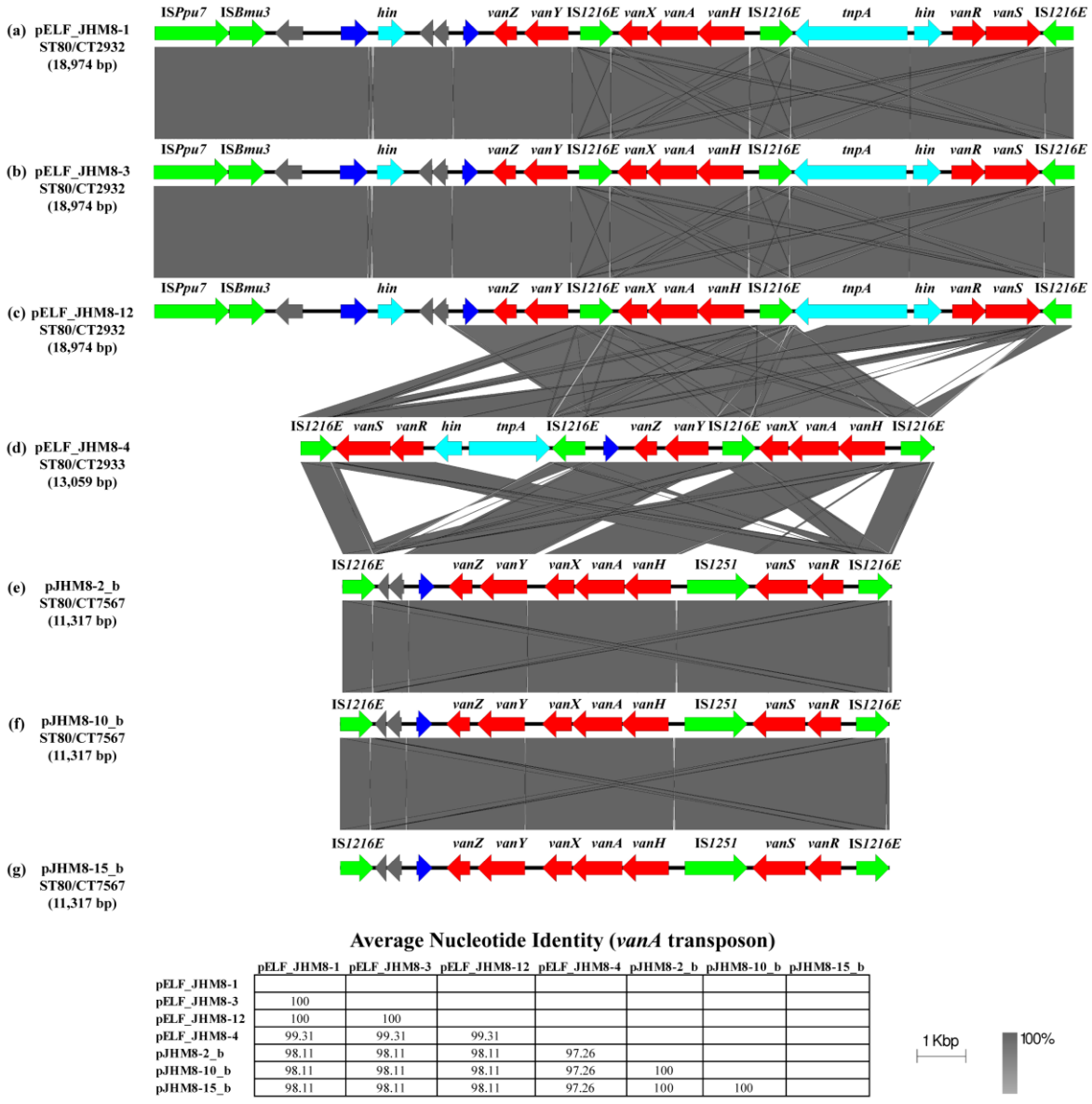

Figure 5.15. Comparative genetic organisation of *vanA* transposon regions closed by hybrid assembly of seven VREfm isolates belonging to three complex types (CTs) from patient P8. The figure shows an alignment of the *vanA* region encoded by seven plasmids from separate VREfm isolates belonging to three CTs as follows: (a) pELF_JHM8-1 (ST80/CT2932, 18,974 bp), (b) pELF_JHM8-3 (ST80/CT2932, 18,974 bp), (c) pELF_JHM8-12 (ST80/CT2932, 18,974 bp), (d) pELF_JHM8-4 (ST80/CT2933, 13,059 bp), (e) pJHM8-2 (ST80/CT7567, 11,317 bp), (f) pJHM8-10 (ST80/CT7567, 11,317 bp) and (g) pJHM8-15 (ST80/CT7576, 11,317 bp) generated using Easyfig (Sullivan *et al.*, 2011). Coding sequences of interest and their orientation are represented by arrows as follows: red, vancomycin resistance genes; green, insertion sequences; blue, proteins with a known coding function; cyan, transposase and invertase genes; grey, hypothetical proteins. Full details of

plasmid profiles and SKA-SNP matrices are provided in Tables 5.4-5.6. Regions between alignments with shared homology are represented by grey connecting blocks and/or lines with the colour gradient indicating percentage nucleotide identity (82-100%). A scale bar is included beneath the figure.

Figure 5.15. Comparative genetic organisation of *vanA* transposon regions closed by hybrid assembly of VREfm isolates belonging to three complex types (CTs) from patient eight (TIFF version).

Scan and/or click QR code to access and/or download high resolution image.

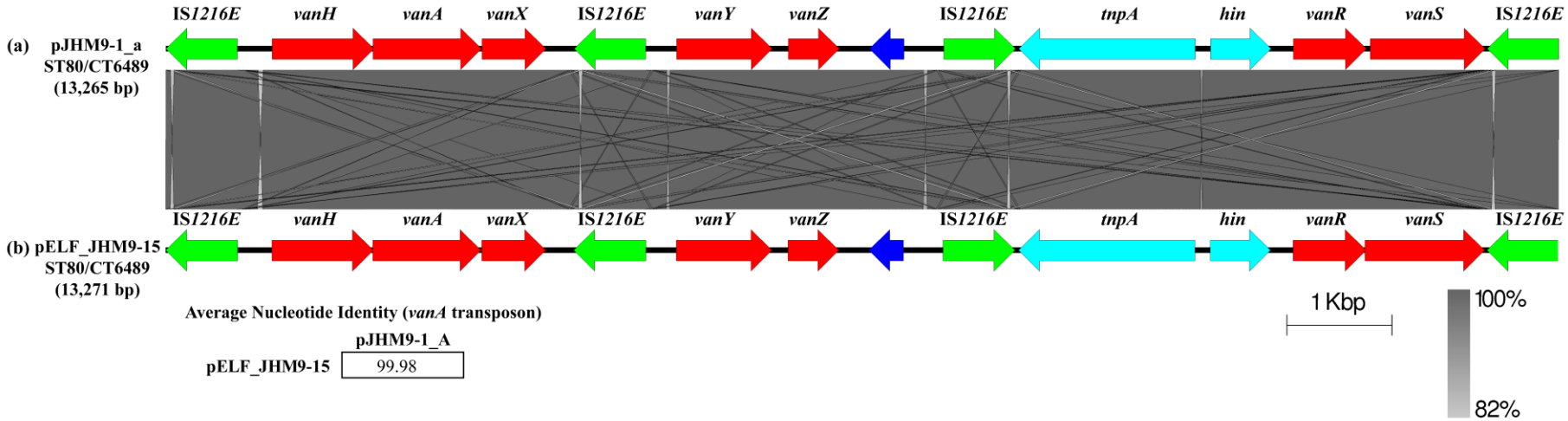

Figure 5.16. Comparative genetic organisation of *vanA* transposon regions closed by hybrid assembly of two VREfm isolates belonging to one complex type (CT) from patient P9. The figure shows an alignment of the *vanA* region encoded by two plasmids from two separate VREfm isolates belonging to one CT as follows: (a) pJHM9-1_a (ST80/CT6489, 13,265 bp) and (b) pELF_JHM9-15 (ST80/CT6489, 13,271 bp) generated using Easyfig (Sullivan *et al.*, 2011). Coding sequences of interest and their orientation are represented by arrows as follows: red, vancomycin resistance genes; green, insertion sequences; blue, proteins with a known coding function; cyan, transposase and invertase genes; grey, hypothetical proteins. Full details of plasmid profiles and SKA-SNP matrices are provided in Tables 5.4-5.6. Regions between alignments with shared homology are represented by grey connecting blocks and/or lines with the colour gradient indicating percentage nucleotide identity (82-100%). A scale bar is included beneath the figure.

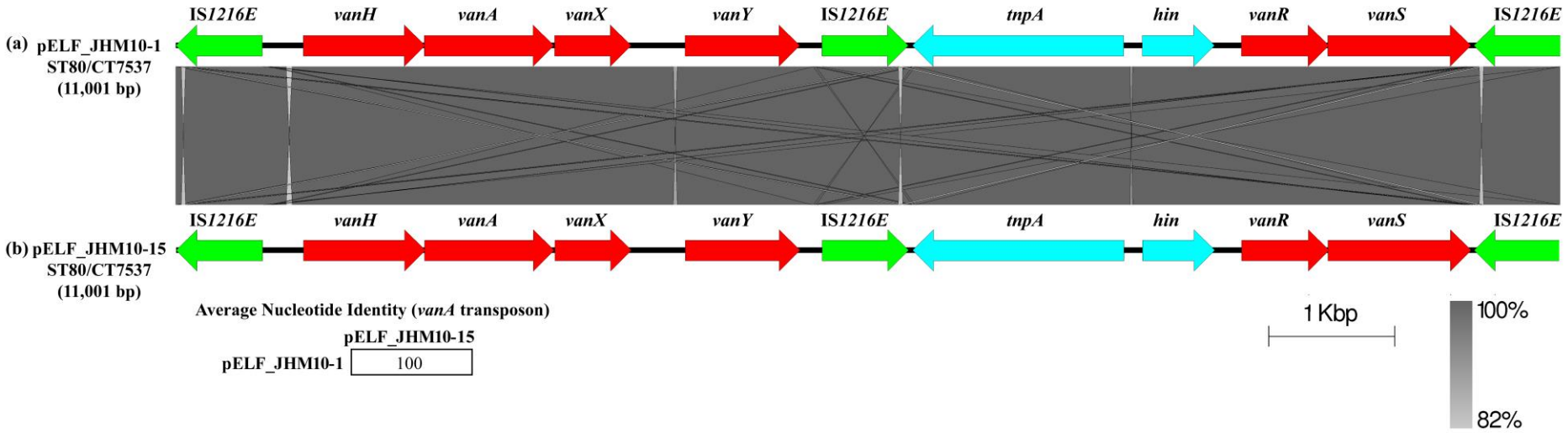

Figure 5.17. Comparative genetic organisation of *vanA* transposon regions closed by hybrid assembly of two VREfm isolates belonging to one complex type (CT) from patient P10. The figure shows an alignment of the *vanA* region encoded by two plasmids from two separate VREfm isolates belonging to one CT as follows: (a) pELF_JHM10-1 (ST80/CT7537, 11,001 bp) and (b) pELF_JHM10-15 (ST80/CT7537, 11,001 bp) generated using Easyfig (Sullivan *et al.*, 2011). Coding sequences of interest and their orientation are represented by arrows as follows: red, vancomycin resistance genes; green, insertion sequences; blue, proteins with a known coding function; cyan, transposase and invertase genes; grey, hypothetical proteins. Full details of plasmid profiles and SKA-SNP matrices are provided in Tables 5.4-5.6. Regions between alignments with shared homology are represented by grey connecting blocks and/or lines with the colour gradient indicating percentage nucleotide identity (82-100%). A scale bar is included beneath the figure.

Chapter 6

General Discussion

6.1 VREfm in Ireland: a game of clones

For well-over a decade, the burden of disease caused by multi-drug resistance enterococci, notably VREfm, both on the hospital-going population and the healthcare system in Ireland has been substantial. As detailed in Chapter 1 Sections 1.6 and 1.7, this is highlighted by the high proportion of resistant, invasive enterococcal infections reported annually to EARS-Net (ranging from 28.4-55.8% between 2006-2022) (ECDC, 2020, 2023). Additionally, in 2021 alone, VREfm accounted for a total number of attributable DALYs of 25.70 per 100,000 population with an estimated economic burden of €3,070,201 due to both VREfm and VREfs (HIQA, 2017). Despite rigorous IPC and antimicrobial stewardship campaigns that have successfully mitigated other clinically important MDR bacteria such as MRSA, there has been little to no indication of a decline in the impact of enterococci (RCPI, 2014). Despite the hyperendemicity of VREfm in Ireland, in conjunction with the increasing reports of the rapidly deteriorating efficacy of last line antimicrobials such as linezolid, it is concerning to see a significant lack of up-to-date epidemiological and genomic-based studies in the literature that may potentially inform surveillance policies to curtail the further rise of VREfm (Egan *et al.,* 2020a, 2020b). To the best of our knowledge, the findings presented in this thesis represent the first detailed, systematic analysis of the population structure, epidemiology, and transmission dynamics of Clade A1 *E. faecium* in hospitals in the Republic of Ireland using high-resolution WGS technologies.

Chapter 3 sought to comprehensively investigate the population biology and diversity of VREfm across Irish hospital networks using a combination of short- and long read sequencing, focusing on the diversity of the Tn*1546*-like *vanA* transposon in circulation and comparing Irish isolates with international strains to explore geographical variations. This work identified that ST80 has emerged as the predominant endemic lineage in Ireland, accounting for 72% of isolates recovered across seven geographically distinct hospitals. Within this high-risk clonal group, there is a very diverse and polyclonal population that can be further discriminated into more discrete CT groups using cgMLST. Notably, three main ST80 lineages, CT2933, CT1916 and CT1598, have succeeded in the game of clones and are the predominant strains in circulation, accounting for 32% of the total investigated isolate population. Whilst the emergence and subsequent expansion of ST80 is comparable to the findings of WGS-based studies of clade A1 *E. faecium* across America, Australia and Europe, Irish strains appear to have a unique evolutionary trajectory with little to no inter-country transmission evident (Lebreton *et al.,* 2013; Raven *et al.,* 2016; Pinholt *et al.,* 2017; Lee *et al.,* 2018; Leong *et al.,* 2018; Gorrie *et al.,* 2019; Pratama *et al.,* 2021). Chapter 4 builds on these findings to examine the transmission dynamics and persistence of VREfm

clonal lineages in two critical care wards of a large Irish hospital over 39 months in the context of a protracted, silent outbreak, whilst additionally assessing the interplay between environmental contamination and subsequent patient acquisition. The findings presented in Chapter 4 further substantiate the emergence of predominant ST80 clonal lineages (CT2933, CT2923 and CT1916) responsible for concurrent, extensive patient-to-patient transmission with epidemiological support. The work described in this chapter underscores the superiority and higher resolution provided by SNP-based approaches, with cgMLST providing an over-estimation of isolate relatedness, which is line with recent studies that benchmark approaches for identifying *E. faecium* in healthcare settings (Higgs *et al.*, 2022). The most notable finding, however, was the two-way dynamic relationship between patients and the hospital environment, with genetically indistinguishable *E. faecium* isolates recovered from near-patient, high-touch areas such as bed-rails, medical devices and sharded bathroom facilities. Additionally, the majority of environmental isolates were VSEfm, some with remnants of vancomycin resistance genes, indicating the importance of considering VSEfm isolates in surveillance procedures.

Finally, Chapter 5 investigates the diversity of VREfm and VSEfm within the GIT of individual patients, systematically analysing the plasmidome of co-colonising strains to better understand the impact on transmission networks and the extensive pool of Tn*1546*-like *vanA* transposons identified in Chapter 3. The findings reveal that patients often harbour multiple genetically distinct VREfm strains, with 70% of the patients investigated showing co-colonisation by divergent strains. The chapter also highlights the limitations of current sequencing methodologies in detecting pathogen diversity and emphasises the importance of optimised sampling strategies. The frequent HGT, particularly involving linear plasmids carrying vancomycin resistance genes, underscores the complexity of VREfm transmission and the need for enhanced surveillance and IPC measures. In line with the findings in Chapters 3 and 4, VSEfm play an overlooked role in this dynamic, suggesting that further detailed genomic studies are required to provide evidence-based recommendations for surveillance practices. Collectively, the findings of this thesis indicate that further detailed genomic based studies are required to better understand and manage the spread of *E. faecium* in the Irish hospital network.

6.2 Out of sight, not out of existence: is it time to rethink VRE surveillance?

At the outset of this research project, a crucial consideration was whether the existing surveillance guidelines for the management of VRE in the Irish healthcare setting are still appropriate and fit for intended purpose. Current national guidelines for the control of MDR bacteria in healthcare settings, as published by the Health Protection Surveillance Centre (HPSC) in 2014, recommends the screening of patients in high-risk areas only. In short, patients falling within the following cohorts are actively screened: oncology or haematology patients, those within critical care such as the ICU or high dependency unit (HDU), patients known to be previously VRE-positive on re-admission and patients transferred from any other external referral hospitals (RCPI, 2014).

When evaluating the suitability of screening guidelines, it is crucial to consider surveillance practices in the context of the frequency of VREfm carriage within the general hospital population. Previous studies investigating rates of colonisation in Irish hospitals vary in their inclusion criteria and specimen type. For example, a study by McDermott and colleagues in 2018 found that 19% (30/157) of patients screened for VRE within the ICU were colonised. A further surveillance study conducted in an Irish tertiary referral hospital in 2010 identified a VRE carriage rate of ~40% among 200 determined from in-patient stool specimens (RCPI, 2014). In contrast, an additional Irish study anonymously screened 100 faecal samples from patients attending the emergency department of an Irish hospital and reported a prevalence rate of 1%, compared to 38% with hospital inpatients (Ryan *et al.,* 2015). More recently, a study in a large academic teaching hospital demonstrated a colonisation rate of 31.4% (61/194) amongst the general hospital population and 22.2% (6/27) from specimens recovered from patients from other hospitals (Whelton *et al.,* 2016). These findings are mirrored by an investigation into the prevalence of VRE in a variety of clinical specimens in Mercy University Hospital Cork, which demonstrated a prevalence of 24.7% (21/85) (Casey, 2021). Collectively, this data highlights that VRE is hyperendemic in the Irish hospital setting, with the national guidelines indicating that 10-20 times more patients are colonised with VRE compared to actively infected, which may provide a significant reservoir of infection (RCPI, 2014).

On this basis, a large proportion of patients who do not fall within the 'high-risk' category may be potentially colonised with VREfm and remain unidentified, resulting in a substantial 'silent' VREfm reservoir contributing to significant transmission and environmental contamination within the Irish hospital network. Whilst prevalence rates were not addressed in this study, the inclusion of rectal screening specimens in Chapter 3 from all 26 H1 wards provided important evidence for the persistence and transmission of highly-

related, endemic VREfm clones (≤20 cgMLST allelic differences) across both high risk and non-high risk ward areas. Further analysis using more discriminatory SNP-based methods in Chapter 4 supported these findings, with closely related VREfm colonising strains (≤10 SNPs) identified in all 26 H1 wards indicative of widespread and extensive intra-hospital dissemination. These results are in line with a point-prevalence survey carried out in a large United Kingdom based hospital intended to gain understanding into carriage of CPE in the general adult population (excluding the emergency department, day care wards and paediatric wards). An incidental finding of this study was a high proportion of VRE carriage (24.1%, 130/540 samples tested) across 39/42 wards investigated

When considering that patients admitted to a variety of H1 wards with diverse medical needs may attend communal clinical and non-clinical areas, such as diagnostic radiology or even the hospital shop, this finding is perhaps unsurprising. Additionally, the movement of staff throughout hospital ward networks, such as specialist medical teams, physical and occupational therapists, hospital pharmacists, dieticians and porters is likely a contributing factor. The findings in this research project provide convincing evidence that the current scope of surveillance and IPC practices are inadequate and urgent evidence-based recommendations are required, including an extension of practice to include a more comprehensive selection of screening cohorts. The optimal approach to active VRE surveillance is subject to much debate and remains controversial. Implementing universal patient screening (i.e., screening all patients on admission to hospital) is often suggested as an alternative strategy to current guidelines. In theory, this would potentially mitigate transmission and subsequent acquisition by proactively identifying colonised patients and allowing immediate implementation of appropriate contact precautions or isolation. The feasibility of this, however, remains to be seen and should be considered with regard to clinical benefits, resource requirements, cost implications and hospital infrastructure which will be discussed below.

6.2.1 Cost-benefit ratio

Limited patient outcome studies currently exist within the literature investigating the cost-benefit ratio of implementing more intensive screening protocols, such as admission testing, for the control of VRE in healthcare settings. Various studies have shown that active surveillance of at-risk groups significantly reduces VRE burden and lowers the incidence of subsequent infection in immunocompromised individuals (Montecalvo *et al.,* 2001; Ostrowsky *et al.,* 2001; Edmond, 2003; Shadel *et al.,* 2006; Huskins *et al.,* 2011; Matsushima *et al.,* 2012; Bodily *et al.,* 2013; Fisher *et al.,* 2016). It is well established that a high density

of VRE colonisation in high-risk, multimorbid patients is an independent risk factor for subsequent invasive infection. Some studies suggest an approximate 24- to 42-fold risk of endogenously acquired BSI in VRE colonised cohorts compared to non-colonised patients (Hendrix *et al.*, 2001; Alevizakos *et al.*, 2017). The findings of Chapter 3 supports this, with many examples of genetically indistinguishable isolates recovered from BSIs and rectal screening. A study investigating an outbreak of VRE BSI in a haematology unit reported a reduction of eightfold in invasive infection with the implementation of stool surveillance (Hachem *et al.*, 2004). Additionally, Perencevich *et al.* utilised a mathematical model to attempt to determine potential benefits of active surveillance and predicted a 65% reduction in VRE colonisation events in an ICU setting.

Given that VRE acquisition and colonisation is a critical risk factor in this patient cohort, the optimal approach to preventing the significant morbidity and mortality associated with clinical infection involves implementing control bundles to prevent colonisation. Whilst these findings highlight the well-established benefits of active surveillance in high-risk areas, which is in line with current guidelines, there is a notable lack of studies investigating the frequency of subsequent clinical infection in immunocompetent patients colonised with VRE. Previous research suggest that 10-20 times more patients are colonised than infected, implying a low infection rate in non-high-risk populations (Armeanu and Bonten, 2005; Zirakzadeh and Patel, 2006). Therefore, in a hyperendemic region such as Ireland, where a high proportion of hospital patients likely encounter or are colonised with VRE, the implementation of universal admission screening would likely have to be justified in its efficacy in preventing cross-ward colonising events and subsequent invasive infection in immunocompromised patients. Given the complex transmission networks identified in Chapter 4, in conjunction with the extensive intra-ward dissemination of highly-related VREfm endemic clones, identification of silent patient reservoirs and subsequent implementation of IPC bundles could potentially decrease colonisation density and as a result reduce invasive infection rates. However, it is acknowledged that there is currently insufficient evidence in the literature to support this assertion and this merely remains an observation which warrants further research and discussion. Hand hygiene remains the most crucial IPC intervention for the prevention of healthcare associated infections and safeguarding of vulnerable immunocompromised patients (Irish Department of Health, 2023). Extensive studies have highlighted that improvements in hand hygiene practices can reduce rates of acquisition and colonisation of VREfm by decreasing transient contamination of the hands of healthcare workers thereby reducing environmental contamination and direct staff-to-patient transmission. However, recent surveys have demonstrated that national

compliance to hand hygiene guidelines are sub-optimal (HIQA, 2017; Irish Department of Health, 2023). For example, a direct observational audit carried out in 45 Irish hospitals in 2023 revealed a national compliance of 92.5%. The HSE target is for 90% compliance measured against five key hand hygiene moments, including before touching a patient, a clean or aseptic procedure, after body fluid exposure, after touching a patient and after touching a patient's environment (SARI, 2005). However, some hospitals reported lower rates of compliance such as 87.1% in Tallaght University hospital, 86.7% in the Mater Misericordiaie University hospital and 89.5% in Wexford General hospital. Key lapses in hand hygiene practices were seen among medical staff, with average rates of 81.% compliance compared with 94.8% of nurses and 91.4% of auxiliary support staff such as porters. Compliance on average was highest after touching a patient (94.6%) in comparison with only 88.6% after touching a patient's surroundings (HPSC, 2023). These findings indicate that fundamental failures in basic IPC interventions occur at high frequency in Irish hospitals and likely contribute to VREfm hyperendemicity.

In conjunction with patient outcome, implementing universal admission screening must be financially justified against the savings associated with prevention of VRE colonisation and BSI. This is routinely analysed through key metrics such as length of hospital stay, antimicrobial usage, and the incremental cost-effective ratio (ICER) expressed in monetary value (such as Euro) per quality-adjusted life years (QALYs) gained (Montecalvo *et al.*, 2001; Edmond, 2003; Shadel *et al.*, 2006; Morgan *et al.*, 2010; Mac *et al.*, 2019). One study utilised a microsimulation model to investigate the cost-effectiveness of implementing VRE screening and subsequent patient isolation in a general medical ward. This demonstrated that screening and isolation prevented six health-care associated colonisations per 1000 admissions and accrued 0.0152 incremental QALYS at a cost of $112, resulting in an ICER of $7850 per QALY. This is considered cost-effective at a threshold of $50,000/QALY per year (Mac *et al.*, 2019). An additional study analysed the costs and savings associated with an intensive 15-component IPC programme in an adult oncology unit with VRE endemicity and found that whilst the cost of enhanced IPC strategies, including surveillance, was $116,515, the savings associated with fewer VRE BSI/colonisation events ($123,081 and $2,755, respectively) and reductions in antimicrobial use ($179,997) resulted in an over-all financial saving of $189,318 over a one-year period. The authors suggested that these enhanced strategies would be cost-beneficial in wards where the number of patients with VRE BSI is from six to nine per year (Montecalvo *et al.*, 2001).

It is important to note that again these studies either provide modelling-based estimates of cost savings or are limited to high-risk areas only and therefore do not provide evidence on the cost-benefit ratio of admission screening. However, they serve to highlight the importance of screening practices in mitigating the significant financial burden of VRE on hospital networks. It is not hard to deduce that admission screening and subsequent IPC measures may contribute to overall hospital cost reductions by potentially decreasing rates of invasive infection, lengths of stay and resulting in less complex antimicrobial therapies. However, again, it is important to note that this is an observation and requires further studies to substantiate. Additionally the cost of universal screening could be substantial and may not be financially justifiable nor viable in the context of over-all hospital infrastructures. However, when considering that HIQA estimated that the median economic burden of antimicrobial resistance due to VREfm and VREfs was approximately €3,070,201 in Ireland in 2019, it is clear that urgent changes to surveillance and IPC strategies are required (HIQA, 2021). Given the uncontrolled level of transmission occurring in the background of VRE hyperendemicity, as demonstrated in both Chapter 3 and 4, it is likely that this burden will only increase. Therefore, the implementation of admission screening, which may be more expensive and labour-intensive, may again be rationalised if it could potentially contribute to the over-all cost-saving measurements within the hospital whilst also providing a higher standard of patient care associated with improved outcomes.

Realistically, however, estimating the efficacy, cost-benefits and actively implementing universal admission screening would be extremely difficult given that true prevalence rates within the majority of Irish hospitals are ultimately unknown. This would have to be established to gain detailed insights into hidden reservoirs of infection and provide evidence-based recommendations to improve current surveillance methodologies. Perhaps a more pragmatic approach would involve utilising point-prevalence surveys to increase the scope of surveillance and to identify wards with a significant VRE colonisation burden which may benefit from active surveillance protocols thereby potentially preventing cross-ward-dissemination. This research project provides convincing, highly discriminatory evidence using WGS that inter and intra-hospital transmission of VREfm in Ireland is a significant and worrisome public health concern. This finding hopefully serves to initiate and prompt much-needed conversations amongst healthcare professionals surrounding the appropriateness of current IPC and screening protocols. Whilst it is acknowledged that admission screening may not be the most appropriate or beneficial measure in this instance, the guidelines should be subjected to thorough and robust review to better define evidence-based recommendations to curtail transmission.

6.2.2 Resource requirements

A more comprehensive surveillance policy, such as admission screening or increased targeted screening, would have significant implications on resource requirements within the Irish hospital infrastructure, particularly in regard to both specimen collection and diagnostic microbiology laboratories. Currently, the majority of clinical laboratories within the Republic of Ireland rely on standardised, selective plating of rectal specimens on chromogenic agar to identify presumptive VRE colonies despite the existence of less-labour intensive and more automated molecular-based methodologies (Humphreys, 2014). Many studies have indicated a high sensitivity and specificity of chromogenic media in the detection of VRE, with some suggesting rates of 99.1% and 94.8% respectively (Stamper *et al.,* 2010). Interestingly, more recently diagnostic laboratories have implemented culture-independent methods, such as detection of nucleic acids, for the direct identification of CPE from rectal screening specimens (HSE AMRIC, 2022). When considering that current screening guidelines for the control of CPE recommend universal admission screening, there is perhaps latent capacity for utilising specimens collected in this regard to conduct VREfm prevalence studies and also potentially to implement multiplex, molecular based assays to detect MDR rectal-based colonising bacteria, including VREfm, if surveillance policies are updated. For example, *vanA* and *vanB* can currently be detected using a variety of commercially available assays on the LightCycler platform (Roche, Mannheim, Germany), Xpert Xpress (Cepheid, California, United States) and the BD Max (BD, Berkshire, United Kingdom). Additionally, more recently high-throughput, fully automated systems such as the FlowFlex solution (extraction: MagnaPure96, PCR setup: Hamilton and PCR: LightCycler) and Cobas 5800/6800/8800 PCR systems (Roche, Basel, Switzerland) have been validated for VRE screening (Giersch *et al.,* 2024). However, molecular platforms currently lack specificity for *vanB* due to the presence of anaerobic bacteria such as *Clostridium* and *Ruminococcuss spp*. that harbour *vanB* within the GIT (Ballard *et al.,* 2005; Mak *et al.,* 2009). The impact of this disparate specificity and high positive predictive value on the detection of *vanB*-harbouring VREfm from colonising populations remains to be seen, as *vanA* currently predominates as the primary genetic variant responsible for vancomycin resistance in Ireland as demonstrated in Chapters 3, 4 and 5.

An extension of scope to include admission or increased targeted screening, even in the presence of high-throughput walk-away technologies, would likely have substantial implications on the microbiology laboratory workload. Approximate figures obtained from a large Irish tertiary referral hospital indicate that on average 29,746 CPE screens were processed annually, in comparison to an average of 3,389 VRE screens (2022-2023)

(McFadden 2024, personal communication, 26 July 2024). This would result in an approximate 9-fold increase in the workload associated with VRE screening for the microbiology laboratory on the basis that CPE figures represent real-time estimates of the volume of pre-admission screens. It is important to note that the CPE figures discussed above may be biased by a variety of factors including initiation of enhanced ward surveillance due to outbreak investigation or duplicate specimens. Nonetheless, they still provide an important indication of the impact of implementing admission screening on laboratory resource management. When considering the current shortages in the medical scientist profession and as a result the suboptimal staffing levels in some laboratories, it is perhaps impractical to suggest or expect that VREfm admission screening would be a viable strategy or become nationally adopted in surveillance in the next decade. However, perhaps a more pragmatic approach, as mentioned above, may be to identify key non-high-risk wards with a high colonisation burden serving as the main silent reservoirs of infection in transmission to high-risk areas. As demonstrated in Chapter 4, however, the transmission networks involved in VREfm spread are extremely complex and often multi-factorial. Before key recommendations can be made in regard to the management of enteric MDR bacteria such as VRE, it is essential to conduct more extensive genomic studies comprising comprehensive staff, patient, and environmental sampling in conjunction with epidemiological data to better understand complex networks at play. Additionally, targeted educational campaigns to promote the importance of staff compliance, particularly amongst medics, with IPC bundles such as hand hygiene, are crucial in curtailing the high levels of VREfm transmission.

6.2.3 Suboptimal infrastructure

An important consideration in enhancing or changing national policies on the management of patients with MDR enteric pathogens is the suboptimal infrastructure of Irish hospitals. Current guidelines recommend that best-practice is to isolate patients who are colonised or infected with VRE in a single room with ensuite facilitates and initiate enteric contact precautions (RCPI, 2014). The ability to effectively manage VRE-positive patients and facilitate adherence to recommended isolation guidelines in Ireland is restricted due to the low availability of single-bed rooms which are often prioritised for the identification of patient cohorts colonised with MDR organisms of higher infection control consequence such as CPE. An expert report by the SARI in 2009 concluded that new hospital inpatient facilities should consist predominantly of single-patient rooms that existing multi-bed wards should comprise no more than three beds, however little progress has been made in this regard. A point prevalence survey conducted in 2023 across Europe identified that the median

proportion of single rooms per country was 24.3%, with a median capacity of 2.2 beds per room. Ireland reported a median of 31.4% of beds in single rooms across 64 hospitals. This finding is supported by a report conducted on 60 Irish acute hospitals in May 2017, with the proportion of single-bed rooms in public hospitals ranging from 15%-19%, with 52% in private hospitals (HPSC, 2017).

It is likely that identifying a substantially higher proportion of asymptomatic VRE carriers through enhanced surveillance protocols would have significant implications for resource management in terms of the ability to effectively isolate and initiate IPC protocols. Whilst the optimal approach is to isolate, one could argue that identifying non-high-risk patients who are VRE colonised may be effectively managed by initiation of contact precautions as preceding infection rate in this population is generally low and the objective is simply to prevent cross-ward-transmission to immunocompromised patients (Armeanu and Bonten, 2005). Additionally it would serve as a means to promote staff awareness of the importance of compliance to hand hygiene. Unfortunately, conflicting data is currently available in the literature on the benefits of contact precautions, with some studies reporting an increase in the incidence of invasive enterococcal infections upon discontinuation and others disputing their efficacy (Edmond *et al.,* 2015; Martin *et al.,* 2016; Morgan *et al.,* 2017; Johnstone *et al.,* 2020). However, it is acknowledged that contact precautions are often implemented as part of a multi-faceted IPC regimen and remain of limited clinical benefit as a stand-alone intervention. Some studies have highlighted the use of rigorous patient cohorting in the management of VRE in endemic settings or in high-transmission areas where isolating VRE-positive patients in single-rooms is not feasible (Popiel and Miller, 2014). Similar to methods utilised in the control of the COVID-19 pandemic in Ireland, this would involve the creation of a VRE cohort unit to which all VRE-positive patients would be transferred as soon as they were detected, except in the case of patients needing specialised or intensive care. One study reported that a VRE-specific ward, with dedicated staff and a security guard to enforce adherence to hand hygiene and personal protective equipment, faced challenges including adverse physical and emotional outcomes such as anxiety and depression, and reduced patient satisfaction with treatment (Popiel and Miller, 2014). However, the practicality and clinical benefit of this in Ireland remains uncertain. In the absence of intensive control methods, such as isolating patients in single rooms with ensuite facilities, VREfm has become endemic in Irish hospitals, driven by multi-clonal direct and indirect patient-to-patient transmission, as extensively discussed in Chapter 4.

6.2.4 Environmental screening

A key finding of this research project is the highly dynamic pattern of two-way spread between the patient and the hospital environment. For example, in Chapter 4, many high-touch patient areas and shared bathroom facilities were found to be contaminated with endemic VREfm clones closely related to patient isolates. Previous Irish studies have indicated that such communal areas are generally heavily contaminated, exceeding proposed microbial thresholds for cleanliness of the hospital environment. For example, one study demonstrated that toilet door handles of shared bathroom facilities were the most heavily contaminated surface of all sites investigated, with a significant microbial burden. Whist the presence indicator organisms, such as VREfm, were not assessed in this study, it nonetheless provides significant evidence that the hospital environment is a significant reservoir of bacteria and enhanced cleaning regimens are urgently required (Claro *et al.,* 2015). This is further supported by the findings in Chapter 3, which highlighted genetically indistinguishable ST80 VREfm clones present in patients over 60-months in H1, indicative of a potential environmental or staff source. It is evident that the ability of VREfm to persist in the Irish hospital environment and resist decontamination in conjunction with the limited availability of isolation rooms due to suboptimal infrastructure has underpinned its successful emergence and widespread dissemination. This is mirrored in the finding of genetically indistinguishable environmental isolates in Chapter 4 from cardiac monitors and shower drains on the same ward 29-months post-recovery of a patient screening isolate with a median cgSNP difference of six. Therefore, the exposure of patients to VREfm in the ward environment represents an important, under-investigated source of acquisition, contributing to significant colonisation pressure and promoting the on-going cycle of transmission in Irish wards (Chemaly *et al.,* 2014; Cassone *et al.,* 2018; Suleyman *et al.,* 2018; Zhou *et al.,* 2019; Blane *et al.,* 2023). The national IPC guidelines are currently limited and recommend the use of environmental VRE screening in an outbreak setting only (RCPI, 2014). Additionally, to the best of our knowledge, the use of routine environmental monitoring for MDR enteric organisms within Irish hospitals is limited to CPE only. However, our study provides important evidence that current hospital cleaning strategies are ineffective and environmental screening is urgently required to identify clinical areas that require enhanced interventions such as routine terminal cleaning programmes using hydrogen peroxide vapour fogging, ultraviolet light and/or bleach (Grabsch *et al.,* 2012; Passaretti *et al.,* 2013; Anderson *et al.,* 2017; Mitchell *et al.,* 2019). Environmental monitoring and cleaning interventions should also be applied to 'non-clinal' ward areas such as nurse's stations, treatment preparation rooms, staff canteens and even equipment storage rooms. Whilst we

did not investigate the role of healthcare workers in the environmental contamination and transmission of VREfm, a previous study from this laboratory investigating a linezolid-resistant VREfm outbreak in an acute Irish hospital suggested that the hands of staff members were the main source of contamination of environmental sites, with isolates identified in 'clean areas' such as treatment rooms (Egan *et al.*, 2020a)

A potential improvement to current national guidelines could therefore involve incorporating environmental screening protocols in high-risk wards to identify areas which require enhanced cleaning regimens and additionally monitor compliance to IPC protocols. Given that improvements in suboptimal hospital infrastructure are unlikely in the next decade, a promising intervention could involve allocating additional resources towards improved cleaning regimens and decontamination protocols, supported by monthly environmental monitoring. Additionally, as stated in Chapter 4, Section 4.1 isolates recovered from the near-patient environment may even serve as proxies for colonising strains in circulation, which can only serve to further augment surveillance (Cassone *et al.*, 2018; Gouliouris *et al.*, 2020).

6.2.5 VSEfm surveillance

To the best of our knowledge, this represents the first Irish study to investigate the frequency and population structure of VSEfm within the GIT of patients with frequent healthcare exposure. Although the study is limited by its sample size (a total of 30 VSEfm from four patients identified from 80 colonies investigated) and is considered a rudimentary snapshot, it nonetheless provides and valuable insights into the dynamic colonising population of *E. faecium* and highlights the displacement of commensal Clade B VSEfm strains by Clade A1 upon hospital exposure. These findings underscore the need for further genomic studies to comprehensively understand the epidemiology, population structure and contribution of VSEfm to transmission dynamics in Ireland. Currently, there is significant disparity in the proportion of studies investigating VSEfm populations compared to VREfm. Susceptible isolates are often overlooked in screening practices and are dismissed as commensal organisms in diagnostic laboratories, unless isolated from critical specimens such as BSIs. This oversight persists despite evidence of the dynamic loss/gain cycle of the TN*1546*-like *vanA* transposon in *E. faecium*. Chapters 3, 4 and 5 demonstrate extensively that VSEfm isolates recovered from BSIs, rectal swabs, and near-patient environments harbour *van* remnants, suggesting such strains originated from vancomycin-resistant ancestors. Additionally, it was highlighted in Chapter 5 that VSEfm strains, in some instances, comprise a near-identical plasmidome landscape to VREfm isolates from both the same

clonal background and genetically divergent lineages. These findings are further supported by the interspersal of closely related VSEfm and VREfm throughout Chapter 3, 4 and 5. Whilst there is future scope to enhance the management of *E. faecium* in healthcare settings by integrating VSEfm screening with traditional surveillance methodologies, additional research is needed to assess the clinical utility and value of this. Furthermore, it is essential to provide robust, highly discriminatory evidence on the interaction and evolutionary relationship between Clade A1 VSEfm and VREfm to fully elucidate transmission dynamics and inform IPC strategies.

6.3 Implications of unprecedented VREfm transmission: enterococcal plasmids, here and there, or absolutely everywhere?

A key finding of this research is the dual pattern of VREfm dissemination in Irish hospitals, previously described as 'bimodal', through both the clonal spread of resistant strains backgrounds and the horizontal transfer of vancomycin resistance gene determinants (Almyroudis *et al.*, 2011; Popiel and Miller, 2014). Whilst patient-to-patient transmission of resistant clones can be effectively mitigated by IPC measures, such as contact precautions and targeted environmental cleaning, the horizontal spread of highly promiscuous plasmids and resistance elements, such as the TN*1546 vanA* transposon, amongst diverse *E. faecium* lineage poses a significant challenge. The HGT of resistant determinants between VREfm and VSEfm lineages within the GIT of co-colonised patients, as demonstrated in Chapter 5, results in the continual emergence of new high-risk clones, significantly complicating efforts to control VREfm in healthcare settings. This is emphasised by findings of clonally diverse VREfm isolates exhibiting significant SNP variability with identical plasmidome landscapes and transposon structure Additionally, the high frequency of transposon heterogeneity revealed by the work described in Chapter 3 and Chapter 5, facilitated by instability associated with IS*1216E* enrichment, likely contributes to VREfm endemicity within Ireland. Selective pressure is likely a contributing factor to this wide-spread HGT of AMR-harbouring enterococcal plasmids. Therefore, antimicrobial stewardship in conjunction with increased staff awareness through educational campaigns may be an important approach to mitigate risk. A survey conducted in 2023 by the HPSC determined the median glycopeptide consumption rate in 42 acute hospitals in Ireland was 8.4 DDD per 100 patient bed days. In fact, in 2021 the ECDC reported that Ireland is the 5th highest consumer of glycopeptides in Europe.

An additional important consideration, highlighted across Chapters 3, 4 and 5 is the worrisome phenomenon of co-selection in VREfm. In some instances, the vancomycin

resistance transposon was co-localised with other AMR genes such as *ant(6)-Ia, aph(3')-III, erm(B)* and even *poxtA* conferring resistance to aminoglycoside, macrolides and oxazolidinones. On this basis, plasmids harbouring vancomycin and/or linezolid resistance genes could be indirectly selected for by the usage of other antimicrobial agents. Fortunately, a decreasing trend in the use of macrolides, lincosamides, streptogramins and aminoglycosides have been observed over the last five years in acute Irish hospitals, with rates of 8.1 (macrolides, lincosamides, streptogramins) and 2.8 (aminoglycosides) DDD per 100 patient bed days, respectively (HPSC, 2023b). These findings highlights the urgent need for continued prudent antimicrobial usage not only within hospital sectors, but also in agricultural and veterinary settings. The concept of a One Health approach, which involves a multisectoral, trans-disciplinary collaborative effort between human healthcare, farming, wildlife, the environment, and wastewater sectors, is key in combatting antimicrobial resistance (Walsh, 2018). Antimicrobial use in animal husbandry is a significant risk factor for the dissemination of MDR bacteria and resistant determinants from animals to humans, via both the consumption of produce and direct contact with treated animals and their environment. Additionally, many of the antimicrobials utilised in the treatment of farm and domestic animals mirror those prescribed for human consumption. For example, Ireland ranked 17/30 in EU member states for antimicrobial usage in animals (mg/kg biomass) in 2016, with 66.6% formulated as premixes predominantly used as in-feed or in-water medication for the pig and poultry sectors (Irish Department of Health, 2018). The most commonly used antimicrobial for animal husbandry in Ireland is tetracycline, representing 39.9% of total veterinary sales. Interestingly, macrolides and aminoglycoside classes represent 6.9% and 6.2%, respectively, (Irish Department of Health, 2018). The implementation of EU legislation which prevents the use of routine prophylactic antimicrobials in animal husbandry has significantly decreased the overall antibiotic use in the agricultural sector (EPC, 2019). In fact, antibiotic use in veterinary medicine across Europe has fallen an average of 53% between 2011-2022 (Animal Health Europe, 2022).

6.3.1 Better the devil you know than the devil you don't – interspecies dissemination of vancomycin resistance and pan-resistant *E. faecium*

Glycopeptide antibiotics, such as vancomycin and teicoplanin, are typically considered the treatment of choice for the management of patients with invasive infections caused by MDR pathogens such MRSA, penicillin resistant *S. pneumoniae* and *C. difficle*. Whilst enterococci are typically considered of low virulence and limited pathogenic potential, a substantial concern linked to the uncontrolled and extensive transmission of VREfm, in a background

of hyperendemicity, is the potential inter-species transfer of resistance determinants to bacteria of higher clinical consequence, such as *S. aureus*. Initially, HGT between *Enterococcus spp*. and *S. aureus* was demonstrated in *in vitro* studies only, however the simultaneous emergence of two vancomycin-resistant *S. aureus* (VRSA) isolates was subsequently described in 2002 in the USA (Noble, 1992; Chang *et al.,* 2003; de Niederhäusern *et al.,* 2011). To the best of our knowledge, a total of 52 VRSA strains harbouring horizontally-acquired *van* genes have been described in the literature to date in a variety of countries, across multiple continents (USA *N*=14, India *N*=16, Iran *N*=11, Pakistan *N*=9, Brazil *N*=1 and Portugal *N*=1) (Tiwari and Sen, 2006; Weigel *et al.,* 2007; Aligholi *et al.,* 2008; Saha *et al.,* 2008; Gaddad *et al.,* 2011; Mirani and Jamil, 2011; Azimian *et al.,* 2012; Askari *et al.,* 2013; Melo-Cristino *et al.,* 2013; Rossi *et al.,* 2014; Panesso *et al.,* 2015; Azhar *et al.,* 2017). In 13/52 described cases, vancomycin resistant *Enterococcus spp*. were co-isolated with VRSA (Cong *et al.,* 2020). Fortunately, the incidence of VRSA currently remains relatively rare suggesting *in vivo* transfer occurs at a low frequency. However, VRSA remains a significant public health concern and as a result, IPC and antimicrobial stewardship programmes that aim to prevent colonisation and/or infection of both VRE and MRSA may minimise co-infection and reduce the probability of inter-species vancomycin resistance. More recently, reports of acquired linezolid resistance genes such as *cfr*, *optrA* and *poxtA* in clinical MRSA strains have been emerging, potentially originating from VREfm (Fan *et al.,* 2016; Antonelli *et al.,* 2018). It is likely that given the high burden of VRE in Irish hospitals, co-colonisation of patients with both MRSA and VREfm may occur at a much higher frequency potentially promoting the increased inter-species transfer of vancomycin and linezolid resistance genes.

Reports of resistance to last-line antimicrobials, such as linezolid, tigecycline and daptomycin, are increasing in *Enterococcus spp*. across Europe (Kamboj *et al.,* 2011; Bender *et al.,* 2016, 2018; Brenciani *et al.,* 2019; Sassi *et al.,* 2019; Egan *et al.,* 2020a, 2020b). In fact, Ireland has reported the highest levels of linezolid resistant enterococci (22.7%) in Europe to date as a result of acquired resistance genes such as *optrA* and *poxtA* (Egan *et al.,* 2020b). Additionally, our laboratory was the first globally to report an outbreak of linezolid-resistant VREfm due to the acquisition, clonal expansion, and dissemination of an *optrA*-encoding plasmid (*Egan et al.,* 2020a). It is clear that without effective IPC interventions, enhanced surveillance protocols and appropriate patient management, VREfm will continue to constitute a significant burden on the Irish healthcare system with uncontrolled transmission potentially resulting in the emergence of pan-resistant *E. faecium* with no appropriate antimicrobial therapy options.

6.4 The application of WGS-based typing methods in *E. faecium*

The current study demonstrates the high-resolution and superior discriminatory value of both short and long-read WGS-based methods in the surveillance and typing of VREfm. In Chapters 3, 4 and 5, a variety of WGS-based methodologies were utilised in combination with epidemiological data to (i) investigate population structure and diversity of VREfm across both Irish hospital networks and internationally, (ii) retrospectively analyse outbreaks within critical care wards and describe transmission networks and (iii) elucidate the frequency and population structure of within-patient VREfm diversity.

In Chapter 3, cgMLST analysis was utilised to investigate the epidemiology of VREfm in Ireland. This identified the presence of predominant circulating lineages confirming the emergence of endemic, high-risk clones. Additionally, international comparisons were utilised to place Irish *E. faecium* in a global context to determine country-specific evolutionary traits. This was previously unfeasible in the context of more traditional typing methods such as PFGE. However, the increasing availability of both WGS-based studies and publicly available high-quality genomes in repositories such as the NCBI sequence read archive (SRA) have facilitated both the national and international comparison of strains. Additionally, the publication of typing schemes, such as cgMLST in *E. faecium*, readily facilitates the intra- and inter-laboratory comparison of strains from published studies. Overall cgMLST in this chapter was more informative of VREfm population structure, with classical MLST typing schemes providing an over-estimation of isolate relatedness. For example, the majority of isolates were identified as ST80 utilising classical MLST, however a more polyclonal population with substantial diversity was evident utilising cgMLST analysis. Additionally, the use of a combination of short- and long-read WGS technologies in Chapter 3 enabled the generation of complete bacterial and plasmid genomes allowing the first descriptions of highly promiscuous and unstable Tn*1546*-like *vanA* transposons in VREfm from Irish hospitals. This serves to highlight the limitations of current short-read WGS technologies in *E. faecium* surveillance. Due to the presence of a high proportion of highly repetitive regions within the enterococcal genome, locating and resolving the position of short-read derived contigs in the bacterial genome during assembly is often challenging. As a result, long-read technologies can be utilised to bridge this gap and polish short-reads to provide a more comprehensive and fully closed bacterial genome.

In Chapter 4, cgMLST was utilised to identify clusters representing recent transmission. However, more discriminatory techniques such as cgSNP analysis were employed to provide a more accurate phylogenetic picture. The findings of this study highlight that cgMLST alone provides a significant over-estimation of genetic relatedness in

VREfm and should therefore be utilised as the first step within an analysis pipeline to broadly group related isolates together. This allows the identification of clusters that require further discrimination through character-based phylogenies such as SNP. These findings highlight the value of trialling a variety of bioinformatic techniques before selecting the most appropriate methodologies for detailed data interpretation. The application of SNP-based techniques, however, limit the ability to easily compare strains across national and international laboratories due to the requirement for both study and cluster-specific reference genomes to provide the most discriminatory results. This requires significant bioinformatic expertise and computational resources, which may not be readily available in routine microbiology laboratories. Additionally, cgSNP methodologies often involve the removal of highly-recombinant regions, such as the accessory genome, which have been shown both in this research and other studies to be extremely important in the evolution of VREfm in the hospital setting (Higgs *et al.*, 2022).

In Chapter 5, the application of SKA SNP analysis permitted the whole-genome nucleotide-level comparison of a variety of closely and distantly related isolates, without the need for a reference genome. This is a promising potential alternative to cgMLST and cgSNP analysis in the sequencing algorithm for VREfm surveillance. The findings of this chapter also demonstrate the substantial influence of pre-analytical factors, such as single vs multi-colony picks, on the results obtained downstream. This highlights the need to optimise sampling strategies before implementing routine surveillance practices. Finally, the identification of near-identical plasmid landscapes in clonally divergent VREfm suggestive of HGT was facilitated by the use of hybrid assembly approaches with short- and long-read sequencing. This demonstrates that whilst short-read sequencing technologies may provide a good indication of transmission events in isolates deemed closely related, horizontal transmission between diverse VREfm genetic backgrounds cannot be ruled out on the basis of short-read technologies alone.

6.5 Future work

The ability to effectively manage and ultimately curtail the widespread inter and intra-hospital transmission of VREfm in Irish hospitals is of vital public-health and IPC importance. It is clear that further work is required to expand on the findings of this thesis and provide insights into the role of VSEfm in hospital transmission dynamics. Investigating the genomic evolution and population biology of VSEfm in both hospital and community populations could potentially provide crucial insights into the complex and multifactorial transmission networks at play both on a local and national level. It may also highlight the

contribution of commensal strain displacement on VREfm burden, particularly in hyperendemic settings such as Ireland, and provide direct evidence for the inclusion of screening for VSEfm carriage in surveillance protocols for high-risk patients. Additionally, large-scale genomic studies are necessary to assess the interplay between within-patient VSEfm and VREfm, particularly in the context of HGT. This could provide crucial insights into the emergence of novel clones and highlight potential evidence-based recommendations to comprehensively improve the efficacy of national surveillance and IPC guidelines. The expansion of genomic studies to include environmental reservoirs of VREfm and VSEfm both within the community and hospital setting in the context of a one-health perspective could also inform control measures and offer new insights to manage *E. faecium* colonisation and reduce the spread of antimicrobial resistance.

6.6 Concluding remarks

The emergence, expansion, and persistence of VREfm in Irish hospitals constitutes a substantial clinical, public health and financial burden, particularly in immunocompromised patients. Despite extensive evidence over the last decade highlighting the significant morbidity and mortality associated with the prominent levels of resistant invasive enterococcal infection reported in Ireland, this issue remains largely unaddressed. The complex diversity of high-risk *E. faecium* clones in circulation, coupled with widespread intra and inter-hospital dissemination via direct patient contact, environmental reservoirs and other unidentified mechanisms, highlight the emergence of VREfm as a major nosocomial pathogen of significant public health concern in Ireland. There is an urgent requirement for more comprehensive approaches to VREfm surveillance, including both systematic reviews and reassessment of the adequacy of national IPC guidelines. Furthermore, adopting more comprehensive WGS-based surveillance in routine epidemiological investigations and implementing monthly environmental monitoring are crucial steps required in addressing the evolving challenges posed by both VREfm and VSEfm. The high frequency of within-patient diversity of VREfm carriage highlighted in this study underscore the necessity for developing polyclonal screening tests capable of robustly identifying patients who may be co-colonised with genetically diverse clones that should be subject to enhanced colony sampling protocols during outbreak surveillance. The implementation of advanced surveillance methodologies, potentially through automated systems, could significantly enhance the accuracy and efficiency of detecting, monitoring, and resolving complex transmission networks in diverse VREfm populations. This approach would provide a more

comprehensive understanding of infection transmission dynamics and provide the evidence to inform more effective IPC approaches.

Bibliography

Ahmed, M.O. and Baptiste, K.E. (2018). Vancomycin-resistant enterococci: a review of antimicrobial resistance mechanisms and perspectives of human and animal health. *Microbial Drug Resistance*, 24(5), pp. 590-606. Available at: https://doi.org/10.1089/mdr.2017.0147.

Alam, M.M., Kobayashi, N., Ishino, M., Sumi, A., Kobayashi, K.I., Uehara, N. and Watanabe, N. (2005). Detection of a novel *aph(2")* allele (*aph[2"]-Ie*) conferring high-level gentamicin resistance and a spectinomycin resistance gene *ant(9)-Ia* (*aad9*) in clinical isolates of enterococci. *Microbial Drug Resistance*, 11(3), pp. 239-247. Available at: https://doi.org/10.1089/mdr.2005.11.239.

Alevizakos, M., Gaitanidis, A., Nasioudis, D., Tori, K., Flokas, M.E. and Mylonakis, E. (2017). Colonization with vancomycin-resistant enterococci and risk for bloodstream infection among patients with malignancy: a systematic review and meta-analysis. *Open Forum Infectious Diseases*, 4(1). Available at: https://doi.org/10.1093/ofid/ofw246.

Aligholi, M., Emaneini, M., Jabalameli, F., Shahsavan, S., Dabiri, H. and Sedaght, H. (2008). Emergence of high-level vancomycin-resistant *Staphylococcus aureus* in the Imam Khomeini Hospital in Tehran. *Medical Principles and Practice*, 17(5), pp. 432–434. Available at: https://doi.org/10.1159/000141513.

Almyroudis, N.G., Lesse, A.J., Hahn, T., Samonis, G., Hazamy, P.A., Wongkittiroch, K., Wang, E.S., McCarthy, P.L., Wetzler, M. and Segal, B.H. (2011). Molecular epidemiology and risk factors for colonization by vancomycin-resistant *Enterococcus* in patients with hematologic malignancies. *Infection Control & Hospital Epidemiology*, 32(5), pp. 490–496. Available at: https://doi.org/10.1086/659408.

Anderson, D.J., Chen, L.F., Weber, D.J., Moehring, R.W., Lewis, S.S., Triplett, P.F., Blocker, M., Becherer, P., Schwab, J.C., Knelson, L.P., Lokhnygina, Y., Rutala, W.A., Kanamori, H., Gergen, M.F. and Sexton, D.J. (2017). Enhanced terminal room disinfection and acquisition and infection caused by multidrug-resistant organisms and *Clostridium difficile* (the benefits of enhanced terminal room disinfection study): a cluster-randomised, multicentre, crossover study. *The Lancet*, 389(10071), pp. 805–814. Available at: https://doi.org/10.1016/S0140-6736(16)31588-4.

Animal Health Europe (2022). Trends in Animal Antibiotic Use Europe. Available at: https://www.bvl.bund.de/SharedDocs/Pressemitteilungen/05_tierarzneimittel/2023/2023_PM_Abgabemengen_Antibiotika_Tiermedizin.html [Accessed 25 July 2024].

Antonelli, A., D'Andrea, M.M., Brenciani, A., Galeotti, C.L., Morroni, G., Pollini, S., Varaldo, P.E. and Rossolini, G.M. (2018). Characterization of *poxtA*, a novel phenicol–oxazolidinone–tetracycline resistance gene from an MRSA of clinical origin. *Journal of Antimicrobial Chemotherapy*, 73(7), pp. 1763–1769. Available at: https://doi.org/10.1093/jac/dky088.

Anyansi, C., Straub, T.J., Manson, A.L., Earl, A.M. and Abeel, T. (2020). Computational methods for strain-level microbial detection in colony and metagenome sequencing data. *Frontiers in Microbiology*, 2020(11), p. 1925. eCollection 2020. Available at: https://doi.org/10.3389/fmicb.2020.01925.

Archambaud, C., Derré-Bobillot, A., Lapaque, N., Rigottier-Gois, L. and Serror, P. (2019). Intestinal translocation of enterococci requires a threshold level of enterococcal overgrowth in the lumen. *Scientific Reports*, 9(1), p. 8926. Available at: https://doi.org/10.1038/s41598-019-45441-3.

Arias, C.A., Contreras, G.A. and Murray, B.E. (2010). Management of multidrug-resistant enterococcal infections. *Clinical Microbiology and Infection*, 16(6), pp. 555-562. Available at: https://doi.org/10.1111/j.1469-0691.2010.03214.x.

Arias, C.A. and Murray, B.E. (2012). The rise of the enterococcus: beyond vancomycin resistance. *Nature Reviews Microbiology*, 10(4), pp. 266–278. Available at: https://doi.org/10.1038/nrmicro2761.

Armeanu, E. and Bonten, M.J.M. (2005). Control of vancomycin-resistant enterococci: one size fits all?. *Clinical Infectious Diseases*, 41(2), pp. 210–216. Available at: https://doi.org/10.1086/431206.

Arredondo-Alonso, S., Top, J., Corander, J., Willems, R.J.L. and Schürch, A.C. (2021). Mode and dynamics of *vanA*-type vancomycin resistance dissemination in Dutch hospitals. *Genome Medicine*, 13(1), p. 9. Available at: https://doi.org/10.1186/s13073-020-00825-3.

Arredondo-Alonso, S., Top, J., McNally, A., Puranen, S., Pesonen, M., Pensar, J., Marttinen, P., Braat, J.C., Rogers, M.R.C., van Schaik, W., Kaski, S., Willems, R.J.L., Corander, J. and Schürch, A.C. (2020). Plasmids shaped the recent emergence of the major nosocomial pathogen *Enterococcus faecium*. *mBio*, 11(1), pp. e03284-19. Available at: https://doi.org/10.1128/mBio.03284-19.

Arthur, M. and Courvalin, P. (1993). Genetics and mechanisms of glycopeptide resistance in enterococci. *Antimicrobial Agents and Chemotherapy*, 37(8): pp. 1563-1571. Available at: https://doi.org/10.1128/AAC.37.8.1563.

Arthur, M., Molinas, C., Depardieu, F. and Courvalin, P. (1993). Characterization of Tn*1546*, a Tn*3*-related transposon conferring glycopeptide resistance by synthesis of depsipeptide peptidoglycan precursors in *Enterococcus faecium* BM4147. *Journal of Bacteriology*, 175(1), pp. 117–127. Available at: https://doi.org/10.1128/jb.175.1.117-127.1993.

Askari, E., Tabatabai, S.M., Arianpoor, A. and Nasab, M.N. (2013). *vanA*-positive vancomycin–resistant *Staphylococcus aureus. Infectious Diseases in Clinical Practice*, 21(2), pp. 91–93. Available at: https://doi.org/10.1097/IPC.0b013e31826e8199.

Aslangul, E., Massias, L., Meulemans, A., Chau, F., Andremont, A., Courvalin, P., Fantin, B. and Ruimy, R. (2006). Acquired gentamicin resistance by permeability impairment in *Enterococcus faecalis*. *Antimicrobial Agents and Chemotherapy*, 50(11), pp. 3615-3621. Available at: https://doi.org/10.1128/AAC.00390-06.

Azhar, A., Rasool, S., Haque, Asma, Shan, S., Saeed, M., Ehsan, B. and Haque, A. (2017). Detection of high levels of resistance to linezolid and vancomycin in *Staphylococcus aureus*. *Journal of Medical Microbiology*. 66(9), pp. 1328–1331. Available at: https://doi.org/10.1099/jmm.0.000566.

Azimian, A., Havaei, S.A., Fazeli, H., Naderi, M., Ghazvini, K., Samiee, S.M., Soleimani, M. and Peerayeh, S.N. (2012). Genetic characterization of a vancomycin-resistant *Staphylococcus aureus* isolate from the respiratory tract of a patient in a university hospital in northeastern Iran. *Journal of Clinical Microbiology*. 50(11), pp. 3581–3585. Available at: https://doi.org/10.1128/JCM.01727-12.

Ballard, S.A., Grabsch, E.A., Johnson, P.D.R. and Grayson, M.L. (2005). Comparison of three PCR primer sets for identification of *vanB* gene carriage in feces and correlation with carriage of vancomycin-resistant enterococci: interference by *vanB* -containing anaerobic bacilli. *Antimicrobial Agents and Chemotherapy*, 49(1), pp. 77–81. Available at: https://doi.org/10.1128/AAC.49.1.77-81.2005.

Baquero, F. (2004). From pieces to patterns: evolutionary engineering in bacterial pathogens. *Nature Reviews Microbiology*, 2(6), pp. 510–518. Available at: https://doi.org/10.1038/nrmicro909.

Barton, B.M., Harding, G.P. and Zuccarelli, A.J. (1995). A general method for detecting and sizing large plasmids. *Analytical Biochemistry*, 226(2), pp. 235–240. Available at: https://doi.org/10.1006/abio.1995.1220.

Bayjanov, J.R., Baan, J., Rogers, M.R.C., Troelstra, A., Willems, R.J.L. and van Schaik, W. (2019). *Enterococcus faecium* genome dynamics during long-term asymptomatic

patient gut colonization. *Microbial Genomics*, 5(7), p. e000277. Available at: https://doi.org/10.1099/mgen.0.000277.

Bennett, P.M. (2004). Genome plasticity: insertion sequence elements, transposons and integrons, and DNA rearrangement. *Methods in Molecular Biology*, 266, pp. 71–113. Available at: https://doi.org/10.1385/1-59259-763-7:071.

Besser, J., Carleton, H.A., Gerner-Smidt, P., Lindsey, R.L. and Trees, E. (2018). Next-generation sequencing technologies and their application to the study and control of bacterial infections. *Clinical Microbiology and Infection*, 24(4), pp. 335-341. Available at: https://doi.org/10.1016/j.cmi.2017.10.013.

Bhardwaj, P., Hans, A., Ruikar, K., Guan, Z. and Palmer, K.L. (2018). Reduced chlorhexidine and daptomycin susceptibility in vancomycin-resistant *Enterococcus faecium* after serial chlorhexidine exposure. *Antimicrobial Agents and Chemotherapy*, 62(1), pp. e01235-17. Available at: https://doi.org/10.1128/AAC.01235-17.

Bi, R., Qin, T., Fan, W., Ma, P. and Gu, B. (2018). The emerging problem of linezolid-resistant enterococci. *Journal of Global Antimicrobial Resistance*, 13, pp. 11-19. Available at: https://doi.org/10.1016/j.jgar.2017.10.018.

Bialvaei, A.Z., Rahbar, M., Yousefi, M., Asgharzadeh, M. and Kafil, H.S. (2017). Linezolid: a promising option in the treatment of Gram-positives. *Journal of Antimicrobial Chemotherapy*, 72(2), pp. 354-364. Available at: https://doi.org/10.1093/jac/dkw450.

Blane, B., Coll, F., Raven, K., Allen, O., Kappeler, A.R.M., Pai, S., Floto, R.A., Peacock, S.J. and Gouliouris, T. (2023). Impact of a new hospital with close to 100% single-occupancy rooms on environmental contamination and incidence of vancomycin-resistant *Enterococcus faecium* colonization or infection: a genomic surveillance study. *Journal of Hospital Infection*, 139, pp. 192–200. Available at: https://doi.org/10.1016/j.jhin.2023.06.025.

Bodily, M., McMullen, K.M., Russo, A.J., Kittur, N.D., Hoppe-Bauer, J. and Warren, D.K. (2013). Discontinuation of reflex testing of stool samples for vancomycin-resistant enterococci resulted in increased prevalence. *Infection Control & Hospital Epidemiology*, 34(8), pp. 838–840. Available at: https://doi.org/10.1086/671276.

Bonten, M.J., Willems, R. and Weinstein, R.A. (2001). Vancomycin-resistant enterococci: why are they here, and where do they come from? *Lancet Infectious Diseases*, 1(5), pp. 314-325. Available at: https://doi.org/10.1016/S1473-3099(01)00145-1.

Both, A., Kruse, F., Mirwald, N., Franke, G., Christner, M., Huang, J., Hansen, J.L., Kröger, N., Berneking, L., Lellek, H., Aepfelbacher, M. and Rohde, H. (2022). Population dynamics in colonizing vancomycin-resistant *Enterococcus faecium* isolated from immunosuppressed patients. *Journal of Global Antimicrobial Resistance*, 28, pp. 267–273. Available at: https://doi.org/10.1016/j.jgar.2022.01.027.

Boumasmoud, M., Dengler Haunreiter, V., Schweizer, T.A., Meyer, L., Chakrakodi, B., Schreiber, P.W., Seidl, K., Kühnert, D., Kouyos, R.D. and Zinkernagel, A.S. (2022). Genomic surveillance of vancomycin-resistant *Enterococcus faecium* reveals spread of a linear plasmid conferring a nutrient utilization advantage. *mBio*, 13(2), p. e0377121. Available at: https://doi.org/10.1128/mbio.03771-21.

Brandl, K., Plitas, G., Mihu, C.N., Ubeda, C., Jia, T., Fleisher, M., Schnabl, B., DeMatteo, R.P. and Pamer, E.G. (2008). Vancomycin-resistant enterococci exploit antibiotic-induced innate immune deficits. *Nature*, 455(7214), pp. 804–807. Available at: https://doi.org/10.1038/nature07250.

Brodrick, H.J., Raven, K.E., Harrison, E.M., Blane, B., Reuter, S., Török, M.E., Parkhill, J. and Peacock, S.J. (2016). Whole-genome sequencing reveals transmission of vancomycin-resistant *Enterococcus faecium* in a healthcare network. *Genome Medicine*, 8(1), p. 4. Available at: https://doi.org/10.1186/s13073-015-0259-7.

Bruniera, F.R., Ferreira, F.M., Saviolli, L.R.M., Bacci, M.R., Feder, D., Pedreira, M.D.L.G., Peterlini, M.A.S., Azzalis, L.A., Junqueira, V.B.C. and Fonseca, F.L.A. (2015). The use of vancomycin with its therapeutic and adverse effects: a review. *European Review for Medical and Pharmacological Sciences*, 19(4), pp. 694-700.

Bush, S.J., Foster, D., Eyre, D.W., Clark, E.L., De Maio, N., Shaw, L.P., Stoesser, N., Peto, T.E.A., Crook, D.W. and Walker, A.S. (2020). Genomic diversity affects the accuracy of bacterial single-nucleotide polymorphism–calling pipelines. *GigaScience*, 9(2). Available at: https://doi.org/10.1093/gigascience/giaa007.

Butler, A.M., Olsen, M.A., Merz, L.R., Guth, R.M., Woeltje, K.F., Camins, B.C. and Fraser, V.J. (2010). Attributable costs of enterococcal bloodstream infections in a nonsurgical hospital cohort. *Infection Control & Hospital Epidemiology*, 31(1), pp. 28-35. Available at: https://doi.org/10.1086/649020.

Byappanahalli, M.N., Nevers, M.B., Korajkic, A., Staley, Z.R. and Harwood, V.J. (2012). Enterococci in the environment. *Microbiology and Molecular Biology Reviews*, 76(4), pp. 685-706. Available at: https://doi.org/10.1128/mmbr.00023-12.

Camargo, I. (2005). Occurrence of insertion sequences within the genomes and Tn*1546*-like elements of glycopeptide-resistant enterococci isolated in Brazil, and identification

of a novel element, IS*Efa*5. *International Journal of Medical Microbiology*, 294(8), pp. 513–519. Available at: https://doi.org/10.1016/j.ijmm.2004.11.003.

Camargo, I.L.B.C., Del Peloso, P.F., Da Costa Leite, C.F., Goldman, G.H. and Darini, A.L.C. (2004). Identification of an unusual *vanA* element in glycopeptide-resistant *Enterococcus faecium* in Brazil following international transfer of a bone marrow transplant patient. *Canadian Journal of Microbiology*, 50(9), pp. 767–770. Available at: https://doi.org/10.1139/w04-054.

Carias, L.L., Rudin, S.D., Donskey, C.J. and Rice, L.B. (1998). Genetic linkage and cotransfer of a novel, *vanB*-containing transposon (Tn*5382*) and a low-affinity penicillin-binding protein 5 gene in a clinical vancomycin-resistant *Enterococcus faecium* isolate. *Journal of Bacteriology*, 180(17), pp. 4426-4434. Available at: https://doi.org/10.1128/jb.180.17.4426-4434.1998.

Carmeli, Y., Eliopoulos, G., Mozaffari, E. and Samore, M. (2002). Health and economic outcomes of vancomycin-resistant enterococci. *Archives of Internal Medicine*, 162(19), pp. 2223-2228. Available at: https://doi.org/10.1001/archinte.162.19.2223.

Carter, G.P., Buultjens, A.H., Ballard, S.A., Baines, S.L., Tomita, T., Strachan, J., Johnson, P.D.R., Ferguson, J.K., Seemann, T., Stinear, T.P. and Howden, B.P. (2016). Emergence of endemic MLST non-typeable vancomycin-resistant *Enterococcus faecium*. *Journal of Antimicrobial Chemotherapy*, 71(12), pp. 3367–3371. Available at: https://doi.org/10.1093/jac/dkw314.

Casey, D. (2021). An investigation into the prevalence of vancomycin-resistant enterococci within an Irish hospital. *International Undergraduate Journal of Health Sciences*, 1(2). Available at: https://doi.org/10.61862/2811-5937.1014.

Cassini, A., Colzani, E., Pini, A., Mangen, M.J.J., Plass, D., McDonald, S.A., Maringhini, G., van Lier, A., Haagsma, J.A., Havelaar, A.H., Kramarz, P. and Kretzschmar, M.E. (2018). Impact of infectious diseases on population health using incidence-based disability-adjusted life years (DALYs): results from the burden of communicable diseases in Europe study, European Union and European economic countries, 2009 to 2013. *Eurosurveillance*, 23(16), pp. 17-00454. Available at: https://doi.org/10.2807/1560-7917.ES.2018.23.16.17-00454.

Cassini, A., Högberg, L.D., Plachouras, D., Quattrocchi, A., Hoxha, A., Simonsen, G.S., Colomb-Cotinat, M., Kretzschmar, M.E., Devleesschauwer, B., Cecchini, M., Ouakrim, D.A., Oliveira, T.C., Struelens, M.J., Suetens, C., Monnet, D.L., Strauss, R., Mertens, K., Struyf, T., Catry, B., Latour, K., Ivanov, I.N., Dobreva, E.G., Tambic Andraševic, A., Soprek, S., Budimir, A., Paphitou, N., Žemlicková, H.,

Schytte Olsen, S., Wolff Sönksen, U., Märtin, P., Ivanova, M., Lyytikäinen, O., Jalava, J., Coignard, B., Eckmanns, T., Abu Sin, M., Haller, S., Daikos, G.L., Gikas, A., Tsiodras, S., Kontopidou, F., Tóth, Á., Hajdu, Á., Guólaugsson, Ó., Kristinsson, K.G., Murchan, S., Burns, K., Pezzotti, P., Gagliotti, C., Dumpis, U., Liuimiene, A., Perrin, M., Borg, M.A., de Greeff, S.C., Monen, J.C., Koek, M.B., Elstrøm, P., Zabicka, D., Deptula, A., Hryniewicz, W., Caniça, M., Nogueira, P.J., Fernandes, P.A., Manageiro, V., Popescu, G.A., Serban, R.I., Schréterová, E., Litvová, S., Štefkovicová, M., Kolman, J., Klavs, I., Korošec, A., Aracil, B., Asensio, A., Pérez-Vázquez, M., Billström, H., Larsson, S., Reilly, J.S., Johnson, A. and Hopkins, S. (2019). Attributable deaths and disability-adjusted life-years caused by infections with antibiotic-resistant bacteria in the EU and the European Economic Area in 2015: a population-level modelling analysis. *The Lancet Infectious Diseases*, 19(1), pp. 56-66. Available at: https://doi.org/10.1016/S1473-3099(18)30605-4.

Cassone, M., Mantey, J., Perri, M.B., Gibson, K., Lansing, B., McNamara, S., Patel, P.K., Cheng, V.C.C., Walters, M.S., Stone, N.D., Zervos, M.J. and Mody, L. (2018). Environmental panels as a proxy for nursing facility patients with methicillin-resistant *Staphylococcus aureus* and vancomycin-resistant *Enterococcus* colonization. *Clinical Infectious Diseases*, 67(6), pp. 861–868. Available at: https://doi.org/10.1093/cid/ciy115.

Cattoir, V. and Leclercq, R. (2013). Twenty-five years of shared life with vancomycin-resistant enterococci: is it time to divorce? *Journal of Antimicrobial Chemotherapy*, 68(4), pp. 731–742. Available at: https://doi.org/10.1093/jac/dks469.

Cha, J.O., Yoo, J.I., Kim, H.K., Kim, H.S., Yoo, J.S., Lee, Y.S. and Jung, Y.H. (2013). Diversity of Tn*1546* in *vanA* positive *Enterococcus faecium* clinical isolates with *vanA*, *vanB*, and *vanD* phenotypes and susceptibility to vancomycin. *Journal of Applied Microbiology*, 115(4), pp. 969–976. Available at: https://doi.org/10.1111/jam.12300.

Chang, S., Sievert, D.M., Hageman, J.C., Boulton, M.L., Tenover, F.C., Downes, F.P., Shah, S., Rudrik, J.T., Pupp, G.R., Brown, W.J., Cardo, D. and Fridkin, S.K. (2003). Infection with vancomycin-resistant *Staphylococcus aureus* containing the *vanA* resistance gene. *New England Journal of Medicine*, 348(14), pp. 1342–1347. Available at: https://doi.org/10.1056/NEJMoa025025.

Cheah, A.A.Y., Spelman, T., Liew, D., Peel, T., Howden, B.P., Spelman, D., Grayson, M.L., Nation, R.L. and Kong, D.D.M. (2013). Enterococcal bacteraemia: factors influencing mortality, length of stay and costs of hospitalization. *Clinical*

Microbiology and Infection, 19(4), pp. e181–189. Available at: https://doi.org/10.1111/1469-0691.12132.

Chemaly, R.F., Simmons, S., Dale, C., Ghantoji, S.S., Rodriguez, M., Gubb, J., Stachowiak, J. and Stibich, M. (2014). The role of the healthcare environment in the spread of multidrug-resistant organisms: update on current best practices for containment. *Therapeutic Advances in Infectious Disease*, 2(3–4), pp. 79–90. Available at: https://doi.org/10.1177/2049936114543287.

Chen, Z., Erickson, D.L. and Meng, J. (2020). Benchmarking hybrid assembly approaches for genomic analyses of bacterial pathogens using Illumina and Oxford Nanopore sequencing. *BMC Genomics*, 21(1), p. 631. Available at: https://doi.org/10.1186/s12864-020-07041-8.

Chow, J.W. (2000). Aminoglycoside resistance in enterococci. *Clinical Infectious Diseases*, 31(2), pp. 586-589. Available at: https://doi.org/10.1086/313949.

Chow, J.W., Zervos, M.J., Lerner, S.A., Thal, L.A., Donabedian, S.M., Jaworski, D.D., Tsai, S., Shaw, K.J. and Clewell, D.B. (1997). A novel gentamicin resistance gene in *Enterococcus*. *Antimicrobial Agents and Chemotherapy*, 41(3), pp. 511-514. Available at: https://doi.org/10.1128/aac.41.3.511.

Claro, T., O'Reilly, M., Daniels, S. and Humphreys, H. (2015). Surface microbial contamination in hospitals: a pilot study on methods of sampling and the use of proposed microbiologic standards. *American Journal of Infection Control*, 43(9), pp. 1000–1002. Available at: https://doi.org/10.1016/j.ajic.2015.05.009.

Coll, F. (2021). Key variables affecting genetic distance calculations in genomic epidemiology. *The Lancet Microbe*, 2(10), pp. e486–487. Available at: https://doi.org/10.1016/S2666-5247(21)00183-X.

Cong, Y., Yang, S. and Rao, X. (2020). Vancomycin resistant *Staphylococcus aureus* infections: a review of case updating and clinical features. *Journal of Advanced Research*, 21, pp. 169–176. Available at: https://doi.org/10.1016/j.jare.2019.10.005.

Conlan, S., Park, M., Deming, C., Thomas, P.J., Young, A.C., Coleman, H., Sison, C., Weingarten, R.A., Lau, A.F., Dekker, J.P., Palmore, T.N., Frank, K.M. and Segre, J.A. (2016). Plasmid dynamics in KPC-positive *Klebsiella pneumoniae* during long-term patient colonization. *mBio*, 7(3), pp. e00742-16. Available at: https://doi.org/10.1128/mBio.00742-16.

Conlan, S., Thomas, P.J., Deming, C., Park, M., Lau, A.F., Dekker, J.P., Snitkin, E.S., Clark, T.A., Luong, K., Song, Y., Tsai, Y.C., Boitano, M., Dayal, J., Brooks, S.Y., Schmidt, B., Young, A.C., Thomas, J.W., Bouffard, G.G., Blakesley, R.W., Mullikin, J.C.,

Korlach, J., Henderson, D.K., Frank, K.M., Palmore, T.N. and Segre, J.A. (2014). Single-molecule sequencing to track plasmid diversity of hospital-associated carbapenemase-producing *Enterobacteriaceae*. *Science Translational Medicine*, 6(254). Available at: https://doi.org/10.1126/scitranslmed.3009845.

Coombs, G.W., Pearson, J.C., Daley, D.A., Le, T., Robinson, O.J., Gottlie, T., Howden, B.P., Johnson, P.D.R., Bennett, C.M., Stinear, T.P. and Turnidge, J.D. (2014). Molecular epidemiology of enterococcal bacteremia in Australia. *Journal of Clinical Microbiology*, 52(3), pp. 897-905. Available at: https://doi.org/10.1128/JCM.03286-13.

Coque, T.M. (2002). High occurrence of *esp* among ampicillin-resistant and vancomycin-susceptible *Enterococcus faecium* clones from hospitalized patients. *Journal of Antimicrobial Chemotherapy*, 50(6), pp. 1035–1038. Available at: https://doi.org/10.1093/jac/dkf229.

Costa, Y., Galimand, M., Leclercq, R., Duval, J. and Courvalin, P. (1993). Characterization of the chromosomal *aac(6')-Ii* gene specific for *Enterococcus faecium*. *Antimicrobial Agents and Chemotherapy*, 37(9), pp. 1896-1903. Available at: https://doi.org/10.1128/AAC.37.9.1896.

Courvalin, P. (2006). Vancomycin resistance in Gram-positive cocci. *Clinical Infectious Diseases*, 42(1), pp. 25-34. Available at: https://doi.org/10.1086/491711.

Courvalin, P., Carlier, C. and Collatz, E. (1980). Plasmid-mediated resistance to aminocyclitol antibiotics in group D streptococci. *Journal of Bacteriology*, 143(2), pp. 541-551. Available at: https://doi.org/10.1128/jb.143.2.541-551.1980.

Crank, C. and O'Driscoll, T. (2015). Vancomycin-resistant enterococcal infections: epidemiology, clinical manifestations, and optimal management. *Infection and Drug Resistance*, 8, p. 217. Available at: https://doi.org/10.2147/IDR.S54125.

Croucher, N.J. and Didelot, X. (2015). The application of genomics to tracing bacterial pathogen transmission. *Current Opinion in Microbiology*, 23, pp. 62–67. Available at: https://doi.org/10.1016/j.mib.2014.11.004.

Croucher, N.J., Page, A.J., Connor, T.R., Delaney, A.J., Keane, J.A., Bentley, S.D., Parkhill, J. and Harris, S.R. (2015). Rapid phylogenetic analysis of large samples of recombinant bacterial whole genome sequences using Gubbins. *Nucleic Acids Research*, 43(3), pp. e15–15. Available at: https://doi.org/10.1093/nar/gku1196.

Croughan, S., O'Cronin, D., O'Brien, D., Roberts, F., Underwood, S., O'Connell, J., Jackson, A., McCarthy, J. and Fahey, S. (2022). Vancomycin-resistant enterococci

in patients attending for colonoscopy: an estimate of community prevalence. *Irish Medical Journal*, 115(8), p. 649.

Dahl, K.H., Lundblad, E.W., Røkenes, T.P., Olsvik, Ø. and Sundsfjord, A. (2000). Genetic linkage of the *vanB2* gene cluster to Tn*5382* in vancomycin-resistant enterococci and characterization of two novel insertion sequences. *Microbiology*, 146(6), pp. 1469-1479. Available at: https://doi.org/10.1099/00221287-146-6-1469.

de Been, M., Pinholt, M., Top, J., Bletz, S., Mellmann, A., van Schaik, W., Brouwer, E., Rogers, M., Kraat, Y., Bonten, M., Corander, J., Westh, H., Harmsen, D. and Willems, R.J.L. (2015). Core genome multilocus sequence typing scheme for high-resolution typing of *Enterococcus faecium*. *Journal of Clinical Microbiology*, 53(12), pp. 3788–3797. Available at: https://doi.org/10.1128/JCM.01946-15.

de Been, M., van Schaik, W., Cheng, L., Corander, J. and Willems, R.J. (2013). Recent recombination events in the core genome are associated with adaptive evolution in *Enterococcus faecium*. *Genome Biology and Evolution*, 5(8), pp. 1524–1535. Available at: https://doi.org/10.1093/gbe/evt111.

Diaz Caballero, J., Wheatley, R.M., Kapel, N., López-Causapé, C., Van der Schalk, T., Quinn, A., Shaw, L.P., Ogunlana, L., Recanatini, C., Xavier, B.B., Timbermont, L., Kluytmans, J., Ruzin, A., Esser, M., Malhotra-Kumar, S., Oliver, A. and MacLean, R.C. (2023). Mixed strain pathogen populations accelerate the evolution of antibiotic resistance in patients. *Nature Communications*, 14(1), p. 4083. Available at: https://doi.org/10.1038/s41467-023-39416-2.

Drees, M., Snydman, D.R., Schmid, C.H., Barefoot, L., Hansjosten, K., Vue, P.M., Cronin, M., Nasraway, S.A. and Golan, Y. (2008). Prior environmental contamination increases the risk of acquisition of vancomycin-resistant enterococci. *Clinical Infectious Diseases*, 46(5), pp. 678–685. Available at: https://doi.org/10.1086/527394.

Dubin, K.A., Mathur, D., McKenney, P.T., Taylor, B.P., Littmann, E.R., Peled, J.U., van den Brink, M.R.M., Taur, Y., Pamer, E.G. and Xavier, J.B. (2019). Diversification and evolution of vancomycin-resistant *Enterococcus faecium* during intestinal domination. *Infection and Immunity*, 87(7), pp. e00102-19. Available at: https://doi.org/10.1128/IAI.00102-19.

Dubin, K.A. and Palmer, E.G. (2014). Enterococci and their Interactions with the intestinal microbiome. *Microbiology Spectrum*, 5(6). Available at: https://doi.org/10.1128/microbiolspec.bad-0014-2016.

ECDC (2020). Antimicrobial resistance in the EU/EEA (EARS-Net), Annual Epidemiological Report 2019. Available at: https://www.ecdc.europa.eu/en/publications-data/surveillance-antimicrobial-resistance-europe-2019 [Accessed 15 April 2024].

ECDC (2023). Antimicrobial resistance in the EU/EEA (EARS-Net) - Annual epidemiological report for 2022. Available at: https://www.ecdc.europa.eu/en/publications-data/surveillance-antimicrobial-resistance-europe-2022 [Accessed 15 April 2024].

ECDC (2024). Point prevalence survey of healthcare-associated infections and antimicrobial use in European acute care hospitals 2022-2023. Stockholm. Available at: https://doi.org/10.2900/88011.

Edmond, M. (2003). Cost-effectiveness of perirectal surveillance cultures for controlling vancomycin-resistant *Enterococcus*. *Infection Control & Hospital Epidemiology*, 24(5), pp. 309–310. Available at: https://doi.org/10.1086/503479.

Edmond, M.B., Masroor, N., Stevens, M.P., Ober, J. and Bearman, G. (2015). The impact of discontinuing contact precautions for VRE and MRSA on device-associated infections. *Infection Control & Hospital Epidemiology*, 36(8), pp. 978–980. Available at: https://doi.org/10.1017/ice.2015.99.

Egan, S.A., Kavanagh, N.L., Shore, A.C., Mollerup, S., Samaniego Castruita, J.A., O'Connell, B., McManus, B.A., Brennan, G.I., Pinholt, M., Westh, H. and Coleman, D.C. (2022). Genomic analysis of 600 vancomycin-resistant *Enterococcus faecium* reveals a high prevalence of ST80 and spread of similar *vanA* regions via IS*1216E* and plasmid transfer in diverse genetic lineages in Ireland. *Journal of Antimicrobial Chemotherapy*, 77(2), pp. 320–330. Available at: https://doi.org/10.1093/jac/dkab393.

Egan, S.A., Shore, A.C., O'Connell, B., Brennan, G.I. and Coleman, D.C. (2020a). Linezolid resistance in *Enterococcus faecium* and *Enterococcus faecalis* from hospitalized patients in Ireland: high prevalence of the MDR genes *optrA* and *poxtA* in isolates with diverse genetic backgrounds. *Journal of Antimicrobial Chemotherapy*, 75(7), pp. 1704–1711. Available at: https://doi.org/10.1093/jac/dkaa075.

Egan, S.A., Corcoran, S., McDermott, H., Fitzpatrick, M., Hoyne, A., McCormack, O., Cullen, A., Brennan, G.I., O'Connell, B. and Coleman, D.C (2020b). Hospital outbreak of linezolid-resistant and vancomycin-resistant ST80 *Enterococcus faecium* harbouring an *optrA*-encoding conjugative plasmid investigated by whole-genome

sequencing. *Journal of Hospital Infection*, 105(4), pp. 726-735. Available at: https://doi:10.1016/j.jhin.2020.05.013.

Endtz, H.P., van den Braak, N., van Belkum, A., Kluytmans, J.A., Koeleman, J.G., Spanjaard, L., Voss, A., Weersink, A.J., Vandenbroucke-Grauls, C.M., Buiting, A.G., van Duin, A. and Verbrugh, H.A. (1997). Fecal carriage of vancomycin-resistant enterococci in hospitalized patients and those living in the community in The Netherlands. *Journal of Clinical Microbiology*, 35(12), pp. 3026–3031. Available at: https://doi.org/10.1128/jcm.35.12.3026-3031.1997.

EPC (2019) Regulation (EU) 2019/6 of the European Parliament and of the Council of 11 December 2018 on veterinary medicinal products and repealing Directive 2001/82/EC (Text with EEA relevance), *Official Journal of the European Union*. Available at: https://eur-lex.europa.eu/eli/reg/2019/6/oj (Accessed: 29 July 2024).

EUCAST (2023). The European Committee on Antimicrobial Susceptibility Testing. Breakpoint tables for interpretation of MICs and zone diameters. Version 13.0, 2023. Available at: http://www.eucast.org/fileadmin/src/media/PDFs/EUCAST_files/Breakpoint_tables/v_5.0_Breakpoint_Table_01.pdf. [Accessed 15 April 2024].

Falk, P.S., Winnike, J., Woodmansee, C., Desai, M. and Mayhall, C.G. (2000). Outbreak of vancomycin-resistant enterococci in a burn unit. *Infection Control & Hospital Epidemiology*, 21(9), pp. 575–582. Available at: https://doi.org/10.1086/501806.

Fan, R., Li, D., Wang, Y., He, T., Feßler, A.T., Schwarz, S. and Wu, C. (2016). Presence of the *optrA* gene in methicillin-resistant *Staphylococcus sciuri* of porcine origin. *Antimicrobial Agents and Chemotherapy*, 60(12), pp. 7200–7205. Available at: https://doi.org/10.1128/AAC.01591-16.

Feil, E.J., Li, B.C., Aanensen, D.M., Hanage, W.P. and Spratt, B.G. (2004). eBURST: Inferring patterns of evolutionary descent among clusters of related bacterial genotypes from multilocus sequence typing data. *Journal of Bacteriology*, 186(5), pp. 1518-1530. Available at: https://doi.org/10.1128/JB.186.5.1518-1530.2004.

Feng, K., Costa, J. and Edwards, J.S. (2018). Next-generation sequencing library construction on a surface. *BMC Genomics*, 19(1), p. 416. Available at: https://doi.org/10.1186/s12864-018-4797-4.

Ferretti, J.J., Gilmore, K.S. and Courvalin, P. (1986). Nucleotide sequence analysis of the gene specifying the bifunctional 6'-aminoglycoside acetyltransferase 2''-aminoglycoside phosphotransferase enzyme in *Streptococcus faecalis* and identification and cloning of gene regions specifying the two activities. *Journal of*

Bacteriology, 167(2), pp. 641-638. Available at: https://doi.org/10.1128/jb.167.2.631-638.1986.

Fiore, E., Van Tyne, D. and Gilmore, M.S. (2019). Pathogenicity of enterococci. *Microbiology Spectrum*, 7(4). Available at: https://doi.org/10.1128/microbiolspec.GPP3-0053-2018.

Fisher, D., Pang, L., Salmon, S., Lin, R.T.P., Teo, C., Tambyah, P., Jureen, R., Cook, A.R. and Otter, J.A. (2016). A successful vancomycin-resistant enterococci reduction bundle at a Singapore hospital. *Infection Control & Hospital Epidemiology*, 37(1), pp. 107–109. Available at: https://doi.org/10.1017/ice.2015.251.

Flamm, R.K., Farrell, D.J., Mendes, R.E., Ross, J.E., Sader, H.S. and Jones, R.N. (2012). LEADER Surveillance program results for 2010: An activity and spectrum analysis of linezolid using 6801 clinical isolates from the United States (61 medical centers). *Diagnostic Microbiology and Infectious Disease*, 74(1), pp. 54-61. Available at: https://doi.org/10.1016/j.diagmicrobio.2012.05.012.

Freitas, A.R., Novais, C., Tedim, A.P., Francia, M.V., Baquero, F., Peixe, L. and Coque, T.M. (2013). Microevolutionary events involving narrow host plasmids influences local fixation of vancomycin-resistance in *Enterococcus* populations. *PLoS ONE*, 8(3), p. e60589. Available at: https://doi.org/10.1371/journal.pone.0060589.

Freitas, A.R., Pereira, A.P., Novais, C. and Peixe, L. (2021). Multidrug-resistant high-risk *Enterococcus faecium* clones: can we really define them? *International Journal of Antimicrobial Agents*, 57(1), p. 106227. Available at: https://doi.org/10.1016/j.ijantimicag.2020.106227.

Freitas, A.R., Tedim, A.P., Francia, M. V., Jensen, L.B., Novais, C., Peixe, L., Sánchez-Valenzuela, A., Sundsfjord, A., Hegstad, K., Werner, G., Sadowy, E., Hammerum, A.M., Garcia-Migura, L., Willems, R.J., Baquero, F. and Coque, T.M. (2016). Multilevel population genetic analysis of *vanA* and *vanB Enterococcus faecium* causing nosocomial outbreaks in 27 countries (1986–2012). *Journal of Antimicrobial Chemotherapy*, 71(12), pp. 3351–3366. Available at: https://doi.org/10.1093/jac/dkw312.

Gaddad, S., Thati, V. and Shivannavar, C. (2011). Vancomycin resistance among methicillin resistant *Staphylococcus aureus* isolates from intensive care units of tertiary care hospitals in Hyderabad. *The Indian Journal of Medical Research*, 134(5), p. 704. Available at: https://doi.org/10.4103/0971-5916.91001.

Galimand, M., Schmitt, E., Panvert, M., Desmolaize, B., Douthwaite, S., Mechulam, Y. and Courvalin, P. (2011). Intrinsic resistance to aminoglycosides in *Enterococcus*

faecium is conferred by the 16S rRNA m5C1404-specific methyltransferase *EfmM*. *RNA*, 17(2). Available at: https://doi.org/10.1261/rna.2233511.

Galloway-Peña, J., Roh, J.H., Latorre, M., Qin, X. and Murray, B.E. (2012). Genomic and SNP analyses demonstrate a distant separation of the hospital and community-associated clades of *Enterococcus faecium*. *PLoS ONE*, 7(1), p. e30187. Available at: https://doi.org/10.1371/journal.pone.0030187.

Galloway-Peña, J.R., Nallapareddy, S.R., Arias, C.A., Eliopoulos, G.M. and Murray, B.E. (2009). Analysis of clonality and antibiotic resistance among early clinical isolates of *Enterococcus faecium* in the United States. *The Journal of Infectious Diseases*, 200(10), pp. 1566–1573. Available at: https://doi.org/10.1086/644790.

Gambarotto, K., Ploy, M.C., Turlure, P., Grélaud, C., Martin, C., Bordessoule, D. and Denis, F. (2000). Prevalence of vancomycin-resistant enterococci in fecal samples from hospitalized patients and nonhospitalized controls in a cattle-rearing area of France. *Journal of Clinical Microbiology*, 38(2), pp. 620-624. Available at: https://doi.org/10.1128/jcm.38.2.620-624.2000.

Gao, W., Howden, B.P. and Stinear, T.P. (2018). Evolution of virulence in *Enterococcus faecium*, a hospital-adapted opportunistic pathogen. *Current Opinion in Microbiology*, 41, pp. 76–82. Available at: https://doi.org/10.1016/j.mib.2017.11.030.

García-Solache, M. and Rice, L.B. (2019). The *Enterococcus*: a model of adaptability to its environment. *Clinical Microbiology Reviews*, 32(2), pp. e00058-18. Available at: https://doi.org/10.1128/CMR.00058-18.

Gardner, S.N. and Hall, B.G. (2013). When whole-genome alignments just won't work: KSNP v2 software for alignment-free SNP discovery and phylogenetics of hundreds of microbial genomes. *PLoS ONE*, 8(12), pp. e81760. Available at: https://doi.org/10.1371/journal.pone.0081760.

Geraci, J.E. and Martin, W.J. (1954). Antibiotic therapy of bacterial endocarditis. VI. Subacute enterococcal endocarditis; clinical, pathologic and therapeutic consideration of 33 cases. *Circulation*, 10(2), pp. 173-194. Available at: https://doi.org/10.1161/01.CIR.10.2.173.

Giersch, K., Tanida, K., Both, A., Nörz, D., Heim, D., Rohde, H., Aepfelbacher, M. and Lütgehetmann, M. (2024). Adaptation and validation of a quantitative *vanA*/*vanB* DNA screening assay on a high-throughput PCR system. *Scientific Reports*, 14(1), p. 3523. Available at: https://doi.org/10.1038/s41598-024-54037-5.

Gilmore, M.S., Lebreton, F. and van Schaik, W. (2013). Genomic transition of enterococci from gut commensals to leading causes of multidrug-resistant hospital infection in the antibiotic era. *Current Opinion in Microbiology*, 16(1), pp. 10-16. Available at: https://doi.org/10.1016/j.mib.2013.01.006.

Goodwin, S., McPherson, J.D. and McCombie, W.R. (2016). Coming of age: Ten years of next-generation sequencing technologies. *Nature Reviews Genetics*, 17(16), pp. 333-351. Available at: https://doi.org/10.1038/nrg.2016.49.

Gorrie, C., Higgs, C., Carter, G., Stinear, T.P. and Howden, B. (2019). Genomics of vancomycin-resistant *Enterococcus faecium*. *Microbial Genomics*, 5(7), pp. e000283. Available at: https://doi.org/10.1099/mgen.0.000283.

Gorrie, C.L., Da Silva, A.G., Ingle, D.J., Higgs, C., Seemann, T., Stinear, T.P., Williamson, D.A., Kwong, J.C., Grayson, M.L., Sherry, N.L. and Howden, B.P. (2021). Key parameters for genomics-based real-time detection and tracking of multidrug-resistant bacteria: a systematic analysis. *The Lancet Microbe*, 2(11), pp. e575–583. Available at: https://doi.org/10.1016/S2666-5247(21)00149-X.

Gouliouris, T., Coll, F., Ludden, C., Blane, B., Raven, K.E., Naydenova, P., Crawley, C., Török, M.E., Enoch, D.A., Brown, N.M., Harrison, E.M., Parkhill, J. and Peacock, S.J. (2020). Quantifying acquisition and transmission of *Enterococcus faecium* using genomic surveillance. *Nature Microbiology*, 6(1), pp. 103–111. Available at: https://doi.org/10.1038/s41564-020-00806-7.

Gouliouris, T., Raven, K.E., Ludden, C., Blane, B., Corander, J., Horner, C.S., Hernandez-Garcia, J., Wood, P., Hadjirin, N.F., Radakovic, M., Holmes, M.A., de Goffau, M., Brown, N.M., Parkhill, J. and Peacock, S.J. (2018). Genomic surveillance of *Enterococcus faecium* reveals limited sharing of strains and resistance genes between livestock and humans in the United Kingdom. *mBio*, 9(6), pp. e01780-18. Available at: https://doi.org/10.1128/mBio.01780-18.

Gouliouris, T., Raven, K.E., Moradigaravand, D., Ludden, C., Coll, F., Blane, B., Naydenova, P., Horner, C., Brown, N.M., Corander, J., Limmathurotsakul, D., Parkhill, J. and Peacock, S.J. (2019). Detection of vancomycin-resistant *Enterococcus faecium* hospital-adapted lineages in municipal wastewater treatment plants indicates widespread distribution and release into the environment. *Genome Research*, 29(4), pp. 626–634. Available at: https://doi.org/10.1101/gr.232629.117.

Grabsch, E.A., Mahony, A.A., Cameron, D.R.M., Martin, R.D., Heland, M., Davey, P., Petty, M., Xie, S. and Grayson, M.L. (2012). Significant reduction in vancomycin-resistant *Enterococcus* colonization and bacteraemia after introduction of a bleach-

based cleaning–disinfection programme. *Journal of Hospital Infection*, 82(4), pp. 234–242. Available at: https://doi.org/10.1016/j.jhin.2012.08.010.

Guerin, F., Perrier-Gros-Claude, J.D., Foissaud, V., Masseron, T. and Thierry, J. (1998). Vancomycin resistant *Enterococcus* in France. High prevalence in a young ambulatory care patient population. *Presse Medicale*, 27(28), pp. 1427–1429.

Guzmán Prieto, A.M., van Schaik, W., Rogers, M.R.C., Coque, T.M., Baquero, F., Corander, J. and Willems, R.J.L. (2016). Global emergence and dissemination of enterococci as nosocomial pathogens: Attack of the clones? *Frontiers in Microbiology*, 7, p. 788. eCollection 2016. Available at: https://doi.org/10.3389/fmicb.2016.00788.

Guzmán Prieto, A.M., Wijngaarden, J., Braat, J.C., Rogers, M.R.C., Majoor, E., Brouwer, E.C., Zhang, X., Bayjanov, J.R., Bonten, M.J.M., Willems, R.J.L. and van Schaik, W. (2017). The two-component system ChtRS contributes to chlorhexidine tolerance in *Enterococcus faecium*. *Antimicrobial Agents and Chemotherapy*, 61(5), pp. e02122-02126. Available at: https://doi.org/10.1128/AAC.02122-16.

Hachem, R., Graviss, L., Hanna, H., Arbuckle, R., Dvorak, T., Hackett, B., Gonzalez, V., Perego, C., Tarrand, J. and Raad, I. (2004). Impact of surveillance for vancomycin-resistant enterococci on controlling a bloodstream outbreak among patients with hematologic malignancy. *Infection Control & Hospital Epidemiology*, 25(5), pp. 391–394. Available at: https://doi.org/10.1086/502411.

Hall, M.D., Holden, M.T., Srisomang, P., Mahavanakul, W., Wuthiekanun, V., Limmathurotsakul, D., Fountain, K., Parkhill, J., Nickerson, E.K., Peacock, S.J. and Fraser, C. (2019). Improved characterisation of MRSA transmission using within-host bacterial sequence diversity. *eLife*, 8, p. e46402. Available at: https://doi.org/10.7554/eLife.46402.

Hammerum, A.M., Baig, S., Kamel, Y., Roer, L., Pinholt, M., Gumpert, H., Holzknecht, B., Røder, B., Justesen, U.S., Samulioniené, J., Kjærsgaard, M., Østergaard, C., Holm, A., Dzajic, E., Søndergaard, T.S., Gaini, S., Edquist, P., Alm, E., Lilje, B., Westh, H., Stegger, M. and Hasman, H. (2017). Emergence of *vanA Enterococcus faecium* in Denmark, 2005-15. *Journal of Antimicrobial Chemotherapy*, 72(8), pp. 2184-2190. Available at: https://doi.org/10.1093/jac/dkx138.

Hammerum, A.M., Justesen, U.S., Pinholt, M., Roer, L., Kaya, H., Worning, P., Nygaard, S., Kemp, M., Clausen, M.E., Nielsen, K.L., Samulioniené, J., Kjærsgaard, M., Østergaard, C., Coia, J., Søndergaard, T.S., Gaini, S., Schønning, K., Westh, H., Hasman, H. and Holzknecht, B.J. (2019). Surveillance of vancomycin-resistant enterococci reveals shift in dominating clones and national spread of a vancomycin-

variable *vanA Enterococcus faecium* ST1421-CT1134 clone, Denmark, 2015 to March 2019. *Eurosurveillance*, 24(34), p. 1900503. Available at: https://doi.org/10.2807/1560-7917.ES.2019.24.34.1900503.

Handwerger, S. and Skoble, J. (1995). Identification of chromosomal mobile element conferring high-level vancomycin resistance in *Enterococcus faecium*. *Antimicrobial Agents and Chemotherapy*, 39(11), pp. 2446–2453. Available at: https://doi.org/10.1128/AAC.39.11.2446.

Handwerger, S., Skoble, J., Discotto, L.F. and Pucci, M.J. (1995). Heterogeneity of the *vanA* gene cluster in clinical isolates of enterococci from the northeastern United States. *Antimicrobial Agents and Chemotherapy*, 39(2), pp. 362–368. Available at: https://doi.org/10.1128/AAC.39.2.362.

Hanrahan, J., Hoyen, C. and Rice, L.B. (2000). Geographic distribution of a large mobile element that transfers ampicillin and vancomycin resistance between *Enterococcus faecium* strains. *Antimicrobial Agents and Chemotherapy*, 44(5), pp. 1349-1351. Available at: https://doi.org/10.1128/AAC.44.5.1349-1351.2000.

Harmer, C.J. and Hall, R.M. (2020). IS*26* family members IS*257* and IS*1216* also form cointegrates by copy-in and targeted conservative routes. *mSphere*, 5(1), pp. e00811-19. Available at: https://doi.org/10.1128/mSphere.00811-19.

Harris, S.R. (2018). SKA: Split *k*-mer analysis toolkit for bacterial genomic epidemiology. *bioRxiv*, p. 453142. Available at: https://doi.org/10.1101/453142.

Hashimoto, Y., Kita, I., Suzuki, M., Hirakawa, H., Ohtaki, H. and Tomita, H. (2020). First report of the local spread of vancomycin-resistant enterococci ascribed to the interspecies transmission of a *vanA* gene cluster-carrying linear plasmid. *mSphere*, 5(2), pp. e00102-20. Available at: https://doi.org/10.1128/mSphere.00102-20.

Hashimoto, Y., Suzuki, M., Kobayashi, S., Hirahara, Y., Kurushima, J., Hirakawa, H., Nomura, T., Tanimoto, K. and Tomita, H. (2023). Enterococcal linear plasmids adapt to *Enterococcus faecium* and spread within multidrug-resistant clades. *Antimicrobial Agents and Chemotherapy*, 67(4), pp. e0161922. Available at: https://doi.org/10.1128/aac.01619-22.

Hashimoto, Y., Taniguchi, M., Uesaka, K., Nomura, T., Hirakawa, H., Tanimoto, K., Tamai, K., Ruan, G., Zheng, B. and Tomita, H. (2019). Novel multidrug-resistant enterococcal mobile linear plasmid pELF1 encoding *vanA* and *vanM* gene clusters from a Japanese vancomycin-resistant enterococci isolate. *Frontiers in Microbiology*, 10, p. 2568. eCollection 2019. Available at: https://doi.org/10.3389/fmicb.2019.02568.

Hasman, H. and Aarestrup, F.M. (2002). *tcrB* , a gene conferring transferable copper resistance in *Enterococcus faecium*: Occurrence, transferability, and linkage to macrolide and glycopeptide resistance. *Antimicrobial Agents and Chemotherapy*, 46(5), pp. 1410–1416. Available at: https://doi.org/10.1128/AAC.46.5.1410-1416.2002.

Health Protection Surveillance Centre (2014) Hand hygiene observational standard operating procedure (Hand Hygiene Audit Tools). Available at: https://www.hpsc.ie/a-z/microbiologyantimicrobialresistance/infectioncontrolandhai/handhygiene/handhygieneaudit/handhygieneaudittools (Accessed: 15 April 2024).

Hegstad, K., Mikalsen, T., Coque, T.M., Werner, G. and Sundsfjord, A. (2010). Mobile genetic elements and their contribution to the emergence of antimicrobial resistant *Enterococcus faecalis* and *Enterococcus faecium*. *Clinical Microbiology and Infection*, 16(6), pp. 541–554. Available at: https://doi.org/10.1111/j.1469-0691.2010.03226.x.

Heikens, E., Bonten, M.J.M. and Willems, R.J.L. (2007). Enterococcal surface protein Esp is important for biofilm formation of *Enterococcus faecium* E1162. *Journal of Bacteriology*, 189(22), pp. 8233–8240. Available at: https://doi.org/10.1128/JB.01205-07.

Heikens, E., van Schaik, W., Leavis, H.L., Bonten, M.J.M. and Willems, R.J.L. (2008). Identification of a novel genomic island specific to hospital-acquired clonal complex 17 *Enterococcus faecium* isolates. *Applied and Environmental Microbiology*, 74(22), pp. 7094–7097. Available at: https://doi.org/10.1128/AEM.01378-08.

Heikens, E., Singh, K. V., Jacques-Palaz, K.D., van Luit-Asbroek, M., Oostdijk, E.A.N., Bonten, M.J.M., Murray, B.E. and Willems, R.J.L. (2011), Contribution of the enterococcal surface protein Esp to pathogenesis of *Enterococcus faecium* endocarditis. *Microbes and Infection*, 13(14–15), pp. 1185–1190. Available at: https://doi.org/10.1016/j.micinf.2011.08.006.

Hendrickx, A.P.A., Bonten, M.J.M., van Luit-Asbroek, M., Schapendonk, C.M.E., Kragten, A.H.M. and Willems, R.J.L. (2008). Expression of two distinct types of pili by a hospital-acquired *Enterococcus faecium* isolate. *Microbiology*, 154(10), pp. 3212–3223. Available at: https://doi.org/10.1099/mic.0.2008/020891-0.

Hendrickx, A.P.A., van Luit-Asbroek, M., Schapendonk, C.M.E., van Wamel, W.J.B., Braat, J.C., Wijnands, L.M., Bonten, M.J.M. and Willems, R.J.L. (2009). SgrA, a nidogen-binding LPXTG surface adhesin implicated in biofilm formation, and EcbA,

a collagen binding MSCRAMM, are two novel adhesins of hospital-acquired *Enterococcus faecium*. *Infection and Immunity*, 77(11), pp. 5097–5106. Available at: https://doi.org/10.1128/IAI.00275-09.

Hendrickx, A.P.A., van Wamel, W.J.B., Posthuma, G., Bonten, M.J.M. and Willems, R.J.L. (2007). Five genes encoding surface-exposed LPXTG proteins are enriched in hospital-adapted *Enterococcus faecium* clonal complex 17 isolates. *Journal of Bacteriology*, 189(22), pp. 8321–8332. Available at: https://doi.org/10.1128/JB.00664-07.

Hendrix, C.W., Hammond, J.M.J., Swoboda, S.M., Merz, W.G., Harrington, S.M., Perl, T.M., Dick, J.D., Borschel, D.M., Halczenko, P.W., Pelz, R.K., Rocco, L.E., Conway, J.E., Brower, R.G. and Lipsett, P.A. (2001). Surveillance strategies and impact of vancomycin-resistant enterococcal colonization and infection in critically ill patients. *Annals of Surgery*, 233(2), pp. 259–265. Available at: https://doi.org/10.1097/00000658-200102000-00016.

Higgs, C., Sherry, N.L., Seemann, T., Horan, K., Walpola, H., Kinsella, P., Bond, K., Williamson, D.A., Marshall, C., Kwong, J.C., Grayson, M.L., Stinear, T.P., Gorrie, C.L. and Howden, B.P. (2022). Optimising genomic approaches for identifying vancomycin-resistant *Enterococcus faecium* transmission in healthcare settings. *Nature Communications*, 13(1), p. 509. Available at: https://doi.org/10.1038/s41467-022-28156-4.

HIQA (2017). National Standards for the prevention and control of healthcare-associated infections in acute healthcare services. Available at: https://www.hiqa.ie/reports-and-publications/standard/2017-national-standards-prevention-and-control-healthcare (Accessed: 15 April 2024).

HIQA (2021). Economic burden of antimicrobial resistance: An analysis of additional costs associated with resistant infections. Dublin. Available at: https://www.hiqa.ie/reports-and-publications/health-technology-assessment/economic-burden-antimicrobial-resistance (Accessed: 15 April 2024).

Hodel-Christian, S.L. and Murray, B.E. (1991). Characterization of the gentamicin resistance transposon Tn*5281* from *Enterococcus faecalis* and comparison to staphylococcal transposons Tn*4001* and Tn*4031*. *Antimicrobial Agents and Chemotherapy*, 35(6), pp. 1147–1152. Available at: https://doi.org/10.1128/AAC.35.6.1147.

Hollenbeck, B.L. and Rice, L.B. (2012). Intrinsic and acquired resistance mechanisms in *Enterococcus*. *Virulence*, 3(5), pp. 421-433. Available at: https://doi.org/10.4161/viru.21282.

Hollingshead, S. and Vapnek, D. (1985). Nucleotide sequence analysis of a gene encoding a streptomycin/spectinomycin adenyltransferase. *Plasmid*, 13(1), pp. 17-30. Available at: https://doi.org/10.1016/0147-619X(85)90052-6.

Homan, W.L., Tribe, D., Poznanski, S., Li, M., Hogg, G., Spalburg, E., van Embden, J.D.A. and Willems, R.J.L. (2002). Multilocus sequence typing scheme for *Enterococcus faecium*. *Journal of Clinical Microbiology*, 40(6), pp. 1963-1971. Available at: https://doi.org/10.1128/JCM.40.6.1963-1971.2002.

Howden, B.P., Holt, K.E., Lam, M.M.C., Seemann, T., Ballard, S., Coombs, G.W., Tong, S.Y.C., Grayson, M.L., Johnson, P.D.R. and Stinear, T.P. (2013). Genomic insights to control the emergence of vancomycin-resistant enterococci. *mBio*, 4(4), pp. e00412-13. Available at: https://doi.org/10.1128/mBio.00412-13.

HPSC (2017). Point prevalence survey of hospital-acquired infections and antimicrobial use in European acute care hospitals: May 2017 - national report Ireland. Available at: www.hpsc.ie (Accessed: 28 July 2024).

HPSC (2023a). National hand hygiene compliance results from period 15 (May/June 2018) to period 26 (Oct/Dec 2023). Available at: https://www.hpsc.ie/a-z/microbiologyantimicrobialresistance/europeansurveillanceofantimicrobialconsumptionesac/PublicMicroB/HHA/Report1.html (Accessed: 29 July 2024).

HPSC (2023b.) Surveillance of antimicrobial consumption in hospital sector, 2023. Available at: https://www.hpsc.ie/a-z/microbiologyantimicrobialresistance/europeansurveillanceofantimicrobialconsumptionesac/PublicMicroB/SACHC/Report1.html (Accessed: 28 July 2024).

HSE AMRIC (2022). Management and control of carbapenemase producing *Enterobacterales* (CPE) in all healthcare settings HSE AMRIC national guidance document, Version 1.0 December 2022. Available at: https://www.hpsc.ie/a-z/microbiologyantimicrobialresistance/strategyforthecontrolofantimicrobialresistanceinirelandsari/carbapenemresistantenterobacteriaceaecre/guidanceandpublications/Management%20and%20Control%20of%20Carbapenemase%20Producing%20Enterobacterales%20(CPE)%20in%20all%20Healthcare%20Settings.pdf (Accessed: 28 July 2024).

Hsieh, Y.-C., Lee, W.-S., Ou, T.-Y. and Hsueh, P.-R. (2010). Clonal spread of CC17 vancomycin-resistant *Enterococcus faecium* with multilocus sequence type 78

(ST78) and a novel ST444 in Taiwan. *European Journal of Clinical Microbiology & Infectious Diseases*, 29(1), pp. 25–30. Available at: https://doi.org/10.1007/s10096-009-0810-9.

Huddleston, J.R. (2014). Horizontal gene transfer in the human gastrointestinal tract: potential spread of antibiotic resistance genes. *Infection and Drug Resistance*, 7, p. 167. Available at: https://doi.org/10.2147/IDR.S48820.

Humphreys, H. (2014) Controlling the spread of vancomycin-resistant enterococci. Is active screening worthwhile? *Journal of Hospital Infection*, 88(4), pp. 191–198. Available at: https://doi.org/10.1016/j.jhin.2014.09.002.

Huskins, W.C., Huckabee, C.M., O'Grady, N.P., Murray, P., Kopetskie, H., Zimmer, L., Walker, M.E., Sinkowitz-Cochran, R.L., Jernigan, J.A., Samore, M., Wallace, D. and Goldmann, D.A. (2011). Intervention to reduce transmission of resistant bacteria in intensive care. *New England Journal of Medicine*, 364(15), pp. 1407–1418. Available at: https://doi.org/10.1056/NEJMoa1000373.

Irish Department of Health (2018). Ireland's First One Health Report on Antimicrobial Use and Antimicrobial resistance. Available at: https://www.gov.ie/pdf/?file=https://assets.gov.ie/11418/66ec356a49754ee7a0b53268170b9b9c.pdf (Accessed: 28 July 2024).

Irish Department of Health (2023). Infection Prevention and Control National Clinical Guideline No. 30. Available at: https://www.hse.ie/eng/services/list/2/gp/antibiotic-prescribing/infection-prevention-and-control/ (Accessed: 15 April 2024).

Jain, M., Tyson, J.R., Loose, M., Ip, C.L.C., Eccles, D.A., O'Grady, J., Malla, S., Leggett, R.M., Wallerman, O., Jansen, H.J., Zalunin, V., Birney, E., Brown, B.L., Snutch, T.P., Olsen, H.E. and MinION Analysis and Reference Consortium (2017). MinION analysis and reference consortium: Phase 2 data release and analysis of R9.0 chemistry, *F1000Research*, 6, pp. 760. Available at: https://doi.org/10.12688/f1000research.113541.

Johnstone, J., Shing, E., Saedi, A., Adomako, K., Li, Y., Brown, K.A. and Garber, G. (2020). Discontinuing contact precautions for vancomycin-resistant *Enterococcus* (VRE) is associated with rising VRE bloodstream infection rates in Ontario hospitals, 2009–2018: A quasi-experimental study. *Clinical Infectious Diseases*, 71(7), pp. 1756–1759. Available at: https://doi.org/10.1093/cid/ciaa009.

Jombart, T., Eggo, R.M., Dodd, P.J. and Balloux, F. (2011). Reconstructing disease outbreaks from genetic data: a graph approach. *Heredity*, 106(2), pp. 383–390. Available at: https://doi.org/10.1038/hdy.2010.78.

Kalyaanamoorthy, S., Minh, B.Q., Wong, T.K.F., von Haeseler, A. and Jermiin, L.S. (2017). ModelFinder: fast model selection for accurate phylogenetic estimates. *Nature Methods*, 14(6), pp. 587–589. Available at: https://doi.org/10.1038/nmeth.4285.

Kavanagh, N.L., Kinnevey, P.M., Egan, S.A., McManus, B.A., O'Connell, B., Brennan, G.I. and Coleman, D.C. (2024). Protracted transmission and persistence of ST80 vancomycin-resistant *Enterococcus faecium* clonal complex types CT2933, CT2932 and CT1916 in a large Irish hospital: a 39-month whole-genome sequencing study. *Journal of Hospital Infection*, 151(9), pp. 11–20. Available at: https://doi.org/10.1016/j.jhin.2024.06.002.

Kaye, K.S., Engemann, J.J., Mozaffari, E. and Carmeli, Y. (2004). Reference group choice and antibiotic resistance outcomes. *Emerging Infectious Diseases*, 10(6), pp. 1125-1128. Available at: https://doi.org/10.3201/eid1006.020665.

Kchouk, M., Gibrat, J.F. and Elloumi, M. (2017). Generations of sequencing technologies: From first to next generation. *Biology and Medicine*, 09(03). Available at: https://doi.org/10.4172/0974-8369.1000395.

Kearney, A., Humphreys, H. and Fitzgerald-Hughes, D. (2023), Nutritional drinks and enteral feeds promote the growth of carbapenemase-producing Enterobacterales in conditions that simulate disposal in hospital sinks. *Journal of Hospital Infection*, 139, pp. 74–81. Available at: https://doi.org/10.1016/j.jhin.2023.05.008.

Khan, M.A., Northwood, J.B., Loor, R.G.J., Tholen, A.T.R., Riera, E., Falcón, M., Network, P.A., van Belkum, A., van Westreenen, M. and Hays, J.P. (2010). High prevalence of ST-78 infection-associated vancomycin-resistant *Enterococcus faecium* from hospitals in Asunción, Paraguay. *Clinical Microbiology and Infection*, 16(6), pp. 624–627. Available at: https://doi.org/10.1111/j.1469-0691.2009.02898.x.

Kim, E.B. and Marco, M.L. (2014). Nonclinical and clinical *Enterococcus faecium* strains, but not *Enterococcus faecalis* strains, have distinct structural and functional genomic features. *Applied and Environmental Microbiology*, 80(1), pp. 154–165. Available at: https://doi.org/10.1128/AEM.03108-13.

Klare, I., Heier, H., Claus, H., Bohme, G., Marin, S., Seltmann, G., Hakenbeck, R., Antanassova, V. and Witte, W. (1995). *Enterococcus faecium* Strains with *vanA* -mediated high-level glycopeptide resistance isolated from animal foodstuffs and fecal samples of humans in the community. *Microbial Drug Resistance*, 1(3), pp. 265–272. Available at: https://doi.org/10.1089/mdr.1995.1.265.

Klassen, J.L. and Currie, C.R. (2012). Gene fragmentation in bacterial draft genomes: Extent, consequences and mitigation. *BMC Genomics*, 13(1). Available at: https://doi.org/10.1186/1471-2164-13-14.

Kohanski, M.A., Dwyer, D.J., Hayete, B., Lawrence, C.A. and Collins, J.J. (2007). A common mechanism of cellular death induced by bactericidal antibiotics. *Cell*, 130(5), pp. 797-810. Available at: https://doi.org/10.1016/j.cell.2007.06.049.

Kramer, A., Schwebke, I. and Kampf, G. (2006). How long do nosocomial pathogens persist on inanimate surfaces? A systematic review. *BMC Infectious Diseases*, 6(1), p. 130. Available at: https://doi.org/10.1186/1471-2334-6-130.

Kruskal, J.B. (1956). On the shortest spanning subtree of a graph and the traveling salesman problem. *Proceedings of the American Mathematical Society*, 7(1), pp. 48–50. Available at: https://doi.org/10.1090/S0002-9939-1956-0078686-7.

Kuo, A.-J., Su, L.-H., Shu, J.-C., Wang, J.-T., Wang, J.-H., Fung, C.-P., Chia, J.-H., Lu, J.-J. and Wu, T.-L. (2014). National surveillance on vancomycin-resistant *Enterococcus faecium* in Taiwan: Emergence and widespread of ST414 and a Tn*1546*-like element with simultaneous insertion of IS*1251*-like and IS*1678*. *PLoS ONE*, 9(12), p. e115555. Available at: https://doi.org/10.1371/journal.pone.0115555.

Lam, M.M.C., Seemann, T., Bulach, D.M., Gladman, S.L., Chen, H., Haring, V., Moore, R.J., Ballard, S., Grayson, M.L., Johnson, P.D.R., Howden, B.P. and Stinear, T.P. (2012). Comparative analysis of the first complete *Enterococcus faecium* genome. *Journal of Bacteriology*, 194(9), pp. 2334–2341. Available at: https://doi.org/10.1128/JB.00259-12.

Launay, A., Ballard, S.A., Johnson, P.D.R., Grayson, M.L. and Lambert, T. (2006). Transfer of vancomycin resistance transposon Tn*1549* from *Clostridium symbiosum* to *Enterococcus spp*. in the gut of gnotobiotic mice. *Antimicrobial Agents and Chemotherapy*, 50(3), pp. 1054-1062. Available at: https://doi.org/10.1128/AAC.50.3.1054-1062.2006.

Leach, K.L., Swaney, S.M., Colca, J.R., McDonald, W.G., Blinn, J.R., Thomasco, L.M.M., Gadwood, R.C., Shinabarger, D., Xiong, L. and Mankin, A.S. (2007). The site of action of oxazolidinone antibiotics in living bacteria and in human mitochondria. *Molecular Cell*, 26(3), pp. 393-402. Available at: https://doi.org/10.1016/j.molcel.2007.04.005.

Leavis, H.L., Bonten, M.J. and Willems, R.J. (2006). Identification of high-risk enterococcal clonal complexes: global dispersion and antibiotic resistance. *Current Opinion in*

Microbiology, 9(5), pp. 454–460. Available at: https://doi.org/10.1016/j.mib.2006.07.001.

Leavis, H.L., Willems, R.J.L., van Wamel, W.J.B., Schuren, F.H., Caspers, M.P.M. and Bonten, M.J.M. (2007). Insertion sequence–driven diversification creates a globally dispersed emerging multi-resistant subspecies of *E. faecium*. *PLoS Pathogens*, 3(1), p. e7. Available at: https://doi.org/10.1371/journal.ppat.0030007.

Lebreton, F., Manson, A.L., Saavedra, J.T., Straub, T.J., Earl, A.M. and Gilmore, M.S. (2017). Tracing the enterococci from Paleozoic origins to the hospital. *Cell*, 169(5), pp. 849-861. Available at: https://doi.org/10.1016/j.cell.2017.04.027.

Lebreton, F., van Schaik, W., Manson McGuire, A., Godfrey, P., Griggs, A., Mazumdar, V., Corander, J., Cheng, L., Saif, S., Young, S., Zeng, Q., Wortman, J., Birren, B., Willems, R.J.L., Earl, A.M. and Gilmore, M.S. (2013). Emergence of epidemic multidrug-resistant *Enterococcus faecium* from animal and commensal strains. *mBio*, 4(4), pp. e00534-13. Available at: https://doi.org/10.1128/mBio.00534-13.

Lee, A.S., White, E., Monahan, L.G., Jensen, S.O., Chan, R. and van Hal, S.J. (2018). Defining the role of the environment in the emergence and persistence of *vanA* vancomycin-resistant *Enterococcus* (VRE) in an intensive care unit: A molecular epidemiological study. *Infection Control & Hospital Epidemiology*, 39(6), pp. 668–675. Available at: https://doi.org/10.1017/ice.2018.29.

Lee, R.S., Gonçalves da Silva, A., Baines, S.L., Strachan, J., Ballard, S., Carter, G.P., Kwong, J.C., Schultz, M.B., Bulach, D.M., Seemann, T., Stinear, T.P. and Howden, B.P. (2018). The changing landscape of vancomycin-resistant *Enterococcus faecium* in Australia: a population-level genomic study. *Journal of Antimicrobial Chemotherapy*, 73(12), pp. 3268-3278. Available at: https://doi.org/10.1093/jac/dky331.

Leendertse, M., Heikens, E., Wijnands, L.M., van Luit-Asbroek, M., Teske, G.J.D., Roelofs, J.J.T.H., Bonten, M.J.M., van der Poll, T. and Willems, R.J.L. (2009). Enterococcal surface protein transiently aggravates *Enterococcus faecium* – Induced urinary tract infection in mice. *The Journal of Infectious Diseases*, 200(7), pp. 1162–1165. Available at: https://doi.org/10.1086/605609.

Leong, K.W.C., Cooley, L.A., Anderson, T.L., Gautam, S.S., McEwan, B., Wells, A., Wilson, F., Hughson, L. and O'Toole, R.F. (2018). Emergence of vancomycin-resistant *Enterococcus faecium* at an Australian hospital: A whole genome sequencing analysis. *Scientific Reports*, 8(1), p. 6274. Available at: https://doi.org/10.1038/s41598-018-24614-6.

Letunic, I. and Bork, P. (2021). Interactive Tree Of Life (iTOL) v5: an online tool for phylogenetic tree display and annotation. *Nucleic Acids Research*, 49(W1), pp. 293-296. Available at: https://doi.org/10.1093/nar/gkab301.

Li, H. and Durbin, R. (2009). Fast and accurate short read alignment with Burrows–Wheeler transform. *Bioinformatics*, 25(14), pp. 1754–1760. Available at: https://doi.org/10.1093/bioinformatics/btp324.

Li, H., Handsaker, B., Wysoker, A., Fennell, T., Ruan, J., Homer, N., Marth, G., Abecasis, G. and Durbin, R. (2009). The sequence alignment/map format and SAMtools. *Bioinformatics*, 25(16), pp. 2078–2079. Available at: https://doi.org/10.1093/bioinformatics/btp352.

Liu, Y.Y., Wang, Y., Walsh, T.R., Yi, L.X., Zhang, R., Spencer, J., Doi, Y., Tian, G., Dong, B., Huang, X., Yu, L.F., Gu, D., Ren, H., Chen, X., Lv, L., He, D., Zhou, H., Liang, Z., Liu, J.H. and Shen, J. (2016). Emergence of plasmid-mediated colistin resistance mechanism MCR-1 in animals and human beings in China: A microbiological and molecular biological study. *The Lancet Infectious Diseases*, 16(2), pp. 161-168. Available at: https://doi.org/10.1016/S1473-3099(15)00424-7.

López, M., Hormazábal, J.C., Maldonado, A., Saavedra, G., Baquero, F., Silva, J., Torres, C. and del Campo, R. (2009). Clonal dissemination of *Enterococcus faecalis* ST201 and *Enterococcus faecium* CC17-ST64 containing Tn*5382-vanB2* among 16 hospitals in Chile. *Clinical Microbiology and Infection*, 15(6), pp. 586-588. Available at: https://doi.org/10.1111/j.1469-0691.2009.02741.x.

Mac, S., Fitzpatrick, T., Johnstone, J. and Sander, B. (2019). Vancomycin-resistant enterococci (VRE) screening and isolation in the general medicine ward: a cost-effectiveness analysis. *Antimicrobial Resistance & Infection Control*, 8(1), p. 168. Available at: https://doi.org/10.1186/s13756-019-0628-x.

Maechler, F., Weber, A., Schwengers, O., Schwab, F., Denkel, L., Behnke, M., Gastmeier, P. and Kola, A. (2023). Split *k*-mer analysis compared to cgMLST and SNP-based core genome analysis for detecting transmission of vancomycin-resistant enterococci: results from routine outbreak analyses across different hospitals and hospitals networks in Berlin, Germany. *Microbial Genomics*, 9(1), p. e000937. Available at: https://doi.org/10.1099/mgen.0.000937.

Mak, A., Miller, M.A., Chong, G. and Monczak, Y. (2009). Comparison of PCR and culture for screening of vancomycin-resistant enterococci: Highly disparate results for *vanA* and *vanB*. *Journal of Clinical Microbiology*, 47(12), pp. 4136–4137. Available at: https://doi.org/10.1128/JCM.01547-09.

Mäklin, T., Kallonen, T., David, S., Boinett, C.J., Pascoe, B., Méric, G., Aanensen, D.M., Feil, E.J., Baker, S., Parkhill, J., Sheppard, S.K., Corander, J. and Honkela, A. (2021). High-resolution sweep metagenomics using fast probabilistic inference. *Wellcome Open Research*, 5, p. 14. Available at: https://doi.org/10.12688/wellcomeopenres.15639.2.

Marshall, S.H., Donskey, C.J., Hutton-Thomas, R., Salata, R.A. and Rice, L.B. (2002). Gene dosage and linezolid resistance in *Enterococcus faecium* and *Enterococcus faecalis*. *Antimicrobial Agents and Chemotherapy*, 46(10), pp. 3334-3336. Available at: https://doi.org/10.1128/AAC.46.10.3334-3336.2002.

Martin, D.P. and Beiko, R.G. (2010). Genetic recombination and bacterial population structure. In *Bacterial Population Genetics in Infectious Disease*. (Robinson A, Fiel E.J and Falush D, Editors), Wiley-Blackwell, New Jersey, pp. 61–85. Available at: https://doi.org/10.1002/9780470600122.ch4.

Martin, E.M., Russell, D., Rubin, Z., Humphries, R., Grogan, T.R., Elashoff, D. and Uslan, D.Z. (2016). Elimination of routine contact precautions for endemic methicillin-resistant *Staphylococcus aureus* and vancomycin-resistant *Enterococcus* : A retrospective quasi-experimental study. *Infection Control & Hospital Epidemiology*, 37(11), pp. 1323–1330. Available at: https://doi.org/10.1017/ice.2016.156.

Mascini, E.M. and Bonten, M.J.M. (2005). Vancomycin-resistant enterococci: Consequences for therapy and infection control. *Clinical Microbiology and Infection*, 11(4), pp. 43-56. Available at: https://doi.org/10.1111/j.1469-0691.2005.01164.x.

Matlock, W., Lipworth, S., Chau, K.K., AbuOun, M., Barker, L., Kavanagh, J., Andersson, M., Oakley, S., Morgan, M., Crook, D.W., Read, D.S., Anjum, M., Shaw, L.P. and Stoesser, N. (2023). Enterobacterales plasmid sharing amongst human bloodstream infections, livestock, wastewater, and waterway niches in Oxfordshire, UK. *eLife*, 12, pp. e85302. Available at: https://doi.org/10.7554/eLife.85302.

Matsushima, A., Takakura, S., Yamamoto, M., Matsumura, Y., Shirano, M., Nagao, M., Ito, Y., Iinuma, Y., Shimizu, T., Fujita, N. and Ichiyama, S. (2012). Regional spread and control of vancomycin-resistant *Enterococcus faecium* and *Enterococcus faecalis* in Kyoto, Japan. *European Journal of Clinical Microbiology & Infectious Diseases*, 31(6), pp. 1095–1100. Available at: https://doi.org/10.1007/s10096-011-1412-x.

Mcdermott, H., Skally, M., O'Rourke, J., Humphreys, H. and Fitzgerald-Hughes, D. (2018). Vancomycin-resistant enterococci (VRE) in the intensive care unit in a nonoutbreak setting: Identification of potential reservoirs and epidemiological associations

between patient and environmental VRE. *Infection Control and Hospital Epidemiology*, 39(1), pp. 40-45. Available at: https://doi.org/10.1017/ice.2017.248.

McHugh, M.P., Pettigrew, K.A., Taori, S., Evans, T.J., Leanord, A., Gillespie, S.H., Templeton, K.E. and Holden, M.T.G. (2024). Consideration of within-patient diversity highlights transmission pathways and antimicrobial resistance gene variability in vancomycin-resistant *Enterococcus faecium*. *Journal of Antimicrobial Chemotherapy*, 79(3), pp. 656–668. Available at: https://doi.org/10.1093/jac/dkae023.

Meka, V.G. and Gold, H.S. (2004). Antimicrobial resistance to linezolid. *Clinical Infectious Diseases*, 39(7), pp. 1010-1015. Available at: https://doi.org/10.1086/423841.

Melo-Cristino, J., Resina, C., Manuel, V., Lito, L. and Ramirez, M. (2013). First case of infection with vancomycin-resistant *Staphylococcus aureus* in Europe. *The Lancet*, 382(9888), p. 205. Available at: https://doi.org/10.1016/S0140-6736(13)61219-2.

Mendes, R.E., Deshpande, L., Streit, J.M., Sader, H.S., Castanheira, M., Hogan, P.A. and Flamm, R.K. (2018). ZAAPS programme results for 2016: An activity and spectrum analysis of linezolid using clinical isolates from medical centres in 42 countries. *Journal of Antimicrobial Chemotherapy*, 73(7), pp. 1880-1887. Available at: https://doi.org/10.1093/jac/dky099.

Mendes, R.E., Hogan, P.A., Jones, R.N., Sader, H.S. and Flamm, R.K. (2016). Surveillance for linezolid resistance via the Zyvox annual appraisal of potency and spectrum (ZAAPS) programme (2014): Evolving resistance mechanisms with stable susceptibility rates. *Journal of Antimicrobial Chemotherapy*, 71(7), pp. 1860-1865. Available at: https://doi.org/10.1093/jac/dkw052.

Miller, W.R., Munita, J.M. and Arias, C.A. (2014). Mechanisms of antibiotic resistance in enterococci. *Expert Review of Anti-Infective Therapy*, 12(10), pp. 1221-1236. Available at: https://doi.org/10.1586/14787210.2014.956092.

Miller, W.R., Murray, B.E., Rice, L.B. and Arias, C.A. (2020). Resistance in vancomycin-resistant enterococci. *Infectious Disease Clinics of North America*, 34(4), pp. 751–771. Available at: https://doi.org/10.1016/j.idc.2020.08.004.

Mirani, Z.A. and Jamil, N. (2011). Effect of sub-lethal doses of vancomycin and oxacillin on biofilm formation by vancomycin intermediate resistant *Staphylococcus aureus*. *Journal of Basic Microbiology*, 51(2), pp. 191–195. Available at: https://doi.org/10.1002/jobm.201000221.

Mitchell, B.G., Hall, L., White, N., Barnett, A.G., Halton, K., Paterson, D.L., Riley, T. V, Gardner, A., Page, K., Farrington, A., Gericke, C.A. and Graves, N. (2019). An

environmental cleaning bundle and health-care-associated infections in hospitals (REACH): a multicentre, randomised trial. *The Lancet Infectious Diseases*, 19(4), pp. 410–418. Available at: https://doi.org/10.1016/S1473-3099(18)30714-X.

Mlaga, K.D., Garcia, V., Colson, P., Ruimy, R., Rolain, J.-M. and Diene, S.M. (2021). Extensive comparative genomic analysis of *Enterococcus faecalis* and *Enterococcus faecium* reveals a direct association between the absence of CRISPR–Cas systems, the presence of anti-endonuclease (*ardA*) and the acquisition of vancomycin resistance in *E. faecium*. *Microorganisms*, 9(6), p. 1118. Available at: https://doi.org/10.3390/microorganisms9061118.

Moellering, R.C. and Weinberg, A.N. (1971). Studies on antibiotic synergism against enterococci. II. Effect of various antibiotics on the uptake of 14 C-labeled streptomycin by enterococci. *The Journal of Clinical Investigation*, 50(12), pp. 2580-2584. Available at: https://doi.org/10.1172/JCI106758.

Montealegre, M.C., Singh, K. V. and Murray, B.E. (2016). Gastrointestinal tract colonization dynamics by different *Enterococcus faecium* clades. *Journal of Infectious Diseases*, 213(12), pp. 1914–1922. Available at: https://doi.org/10.1093/infdis/jiv597.

Montecalvo, M.A., Jarvis, W.R., Uman, J., Shay, D.K., Petrullo, C., Horowitz, H.W. and Wormser, G.P. (2001). Costs and savings associated with infection control measures that reduced transmission of vancomycin-resistant enterococci in an endemic setting. *Infection Control & Hospital Epidemiology*, 22(7), pp. 437–442. Available at: https://doi.org/10.1086/501931.

Moradigaravand, D., Gouliouris, T., Blane, B., Naydenova, P., Ludden, C., Crawley, C., Brown, N.M., Török, M.E., Parkhill, J. and Peacock, S.J. (2017). Within-host evolution of *Enterococcus faecium* during longitudinal carriage and transition to bloodstream infection in immunocompromised patients. *Genome Medicine*, 9(1), p. 119. Available at: https://doi.org/10.1186/s13073-017-0507-0.

Morgan, D.J., Day, H.R., Furuno, J.P., Young, A., Johnson, J.K., Bradham, D.D. and Perencevich, E.N. (2010). Improving efficiency in active surveillance for methicillin-resistant *Staphylococcus aureus* or vancomycin-resistant *Enterococcus* at hospital admission. *Infection Control & Hospital Epidemiology*, 31(12), pp. 1230-1235. Available at: https://doi.org/10.1086/657335.

Morgan, D.J., Wenzel, R.P. and Bearman, G. (2017). Contact precautions for endemic MRSA and VRE. *JAMA*, 318(4), p. 329. Available at: https://doi.org/10.1001/jama.2017.7419.

Morris-Downes, M., Smyth, E.G., Moore, J., Thomas, T., Fitzpatrick, F., Walsh, J., Caffrey, V., Morris, A., Foley, S. and Humphreys, H. (2010). Surveillance and endemic vancomycin-resistant enterococci: some success in control is possible. *Journal of Hospital Infection*, 75(3), pp. 228–233. Available at: https://doi.org/10.1016/j.jhin.2010.01.004.

Mu, A., Kwong, J.C., Isles, N.S., Gonçalves da Silva, A., Schultz, M.B., Ballard, S.A., Lane, C.R., Carter, G.P., Williamson, D.A., Seemann, T., Stinear, T.P. and Howden, B.P. (2019). Reconstruction of the genomes of drug-resistant pathogens for outbreak investigation through metagenomic sequencing. *mSphere*, 4(1), pp. e00529-18. Available at: https://doi.org/10.1128/mSphere.00529-18.

Mundt, J.O. (1963). Occurrence of enterococci in animals in a wild environment. *Applied microbiology*, 11, pp. 136-140. Available at: https://doi.org/10.1128/aem.11.2.136-140.1963.

Murray, B.E. (1990). The life and times of the *Enterococcus*. *Clinical Microbiology Reviews*, 3(1), pp. 46-65. Available at: https://doi.org/10.1128/CMR.3.1.46.

Neely, A.N. and Maley, M.P. (2000). Survival of enterococci and staphylococci on hospital fabrics and plastic. *Journal of Clinical Microbiology*, 38(2), pp. 724–726. Available at: https://doi.org/10.1128/JCM.38.2.724-726.2000.

Nguyen, L.-T., Schmidt, H.A., von Haeseler, A. and Minh, B.Q. (2015). IQ-TREE: A fast and effective stochastic algorithm for estimating maximum-likelihood phylogenies. *Molecular Biology and Evolution*, 32(1), pp. 268–274. Available at: https://doi.org/10.1093/molbev/msu300.

de Niederhäusern, S., Bondi, M., Messi, P., Iseppi, R., Sabia, C., Manicardi, G. and Anacarso, I. (2011). Vancomycin-resistance transferability from *vanA* enterococci to *Staphylococcus aureus*. *Current Microbiology*, 62(5), pp. 1363–1367. Available at: https://doi.org/10.1007/s00284-011-9868-6.

Noble, W. (1992). Co-transfer of vancomycin and other resistance genes from *Enterococcus faecalis* NCTC 12201 to *Staphylococcus aureus*. FEMS *Microbiology Letters*, 93(2), pp. 195–198. Available at: https://doi.org/10.1016/0378-1097(92)90528-V.

Norman, A., Hansen, L.H. and Sørensen, S.J. (2009). Conjugative plasmids: vessels of the communal gene pool. *Philosophical Transactions of the Royal Society B: Biological Sciences*, 364(1527), pp. 2275–2289. Available at: https://doi.org/10.1098/rstb.2009.0037.

Nourse, C., Byrne, C., Murphy, H., Kaufmann, M.E., Clarke, A. and Butler, K. (2000). Eradication of vancomycin resistant *Enterococcus faecium* from a paediatric

oncology unit and prevalence of colonization in hospitalized and community-based children. *Epidemiology and Infection*, 124(1), pp. 53–59. Available at: https://doi.org/10.1017/S095026889900326X.

Novais, C., Freitas, A.R., Sousa, João C., Baquero, F., Coque, T.M. and Peixe, L. V. (2008). Diversity of Tn*1546* and its role in the dissemination of vancomycin-resistant enterococci in Portugal. *Antimicrobial Agents and Chemotherapy*, 52(3), pp. 1001–1008. Available at: https://doi.org/10.1128/AAC.00999-07.

Ondov, B.D., Treangen, T.J., Melsted, P., Mallonee, A.B., Bergman, N.H., Koren, S. and Phillippy, A.M. (2016). Mash: fast genome and metagenome distance estimation using MinHash. *Genome Biology*, 17(1), p. 132. Available at: https://doi.org/10.1186/s13059-016-0997-x.

Orsi, G.B. and Ciorba, V. (2013). Vancomycin resistant enterococci healthcare associated infections. *Annali di igiene : medicina preventiva e di comunità*, 25(6), pp. 485-492. Available at: https://doi.org/10.7416/ai.2013.1948.

Ostrowsky, B.E., Trick, W.E., Sohn, A.H., Quirk, S.B., Holt, S., Carson, L.A., Hill, B.C., Arduino, M.J., Kuehnert, M.J. and Jarvis, W.R. (2001). Control of vancomycin-resistant *Enterococcus* in health care facilities in a region. *New England Journal of Medicine*, 344(19), pp. 1427–1433. Available at: https://doi.org/10.1056/NEJM200105103441903.

Page, A.J., Cummins, C.A., Hunt, M., Wong, V.K., Reuter, S., Holden, M.T.G., Fookes, M., Falush, D., Keane, J.A. and Parkhill, J. (2015). Roary: rapid large-scale prokaryote pan genome analysis. *Bioinformatics*, 31(22), pp. 3691–3693. Available at: https://doi.org/10.1093/bioinformatics/btv421.

Palmer, K.L., Godfrey, P., Griggs, A., Kos, V.N., Zucker, J., Desjardins, C., Cerqueira, G., Gevers, D., Walker, S., Wortman, J., Feldgarden, M., Haas, B., Birren, B. and Gilmore, M.S. (2012). Comparative genomics of enterococci: Variation in *Enterococcus faecalis*, clade structure in *E. faecium*, and defining characteristics of *E. gallinarum* and *E. casseliflavus*. *mBio*, 3(1), pp. e00318-11. Available at: https://doi.org/10.1128/mBio.00318-11.

Palmer, K.L., Kos, V.N. and Gilmore, M.S. (2010). Horizontal gene transfer and the genomics of enterococcal antibiotic resistance. *Current Opinion in Microbiology*, 13(5), pp. 632–639. Available at: https://doi.org/10.1016/j.mib.2010.08.004.

Panesso, D., Planet, P.J., Diaz, L., Hugonnet, J.-E., Tran, T.T., Narechania, A., Munita, J.M., Rincon, S., Carvajal, L.P., Reyes, J., Londoño, A., Smith, H., Sebra, R., Deikus, G., Weinstock, G.M., Murray, B.E., Rossi, F., Arthur, M. and Arias, C.A. (2015).

Methicillin-susceptible, vancomycin-resistant *Staphylococcus aureus*, Brazil. *Emerging Infectious Diseases*, 21(10), pp. 1844–1848. Available at: https://doi.org/10.3201/eid2110.141914.

Papadimitriou-Olivgeris, M., Drougka, E., Fligou, F., Kolonitsiou, F., Liakopoulos, A., Dodou, V., Anastassiou, E.D., Petinaki, E., Marangos, M., Filos, K.S. and Spiliopoulou, I. (2014). Risk factors for enterococcal infection and colonization by vancomycin-resistant enterococci in critically ill patients. *Infection*, 42(6), pp. 1013–1022. Available at: https://doi.org/10.1007/s15010-014-0678-1.

Parte, A.C. (2018). LPSN - List of prokaryotic names withstanding in nomenclature (Bacterio.net), 20 years on. *International Journal of Systematic and Evolutionary Microbiology*, 68(6), pp. 1825-1829. Available at: https://doi.org/10.1099/ijsem.0.002786.

Parte, A.C., Carbasse, J.S., Meier-Kolthoff, J.P., Reimer, L.C. and Göker, M. (2020). List of prokaryotic names with standing in nomenclature (LPSN) moves to the DSMZ. *International Journal of Systematic and Evolutionary Microbiology*, 70(11), pp. 5607-5612. Available at: https://doi.org/10.1099/ijsem.0.004332.

Passaretti, C.L., Otter, J.A., Reich, N.G., Myers, J., Shepard, J., Ross, T., Carroll, K.C., Lipsett, P. and Perl, T.M. (2013). An evaluation of environmental decontamination with hydrogen peroxide vapor for reducing the risk of patient acquisition of multidrug-resistant organisms. *Clinical Infectious Diseases*, 56(1), pp. 27–35. Available at: https://doi.org/10.1093/cid/cis839.

Paterson, G.K., Harrison, E.M., Murray, G.G.R., Welch, J.J., Warland, J.H., Holden, M.T.G., Morgan, F.J.E., Ba, X., Koop, G., Harris, S.R., Maskell, D.J., Peacock, S.J., Herrtage, M.E., Parkhill, J. and Holmes, M.A. (2015). Capturing the cloud of diversity reveals complexity and heterogeneity of MRSA carriage, infection and transmission. *Nature Communications*, 6(1), p. 6560. Available at: https://doi.org/10.1038/ncomms7560.

Patterson, J.E. and Kelly, C.C. (1998). Pulsed-field gel electrophoresis as an epidemiologic tool for enterococci and streptococci, In *Methods for Studying the Genetics, Molecular Biology, Physiology, and Pathogenesis of the Streptococci*. (Fives-Tayor P and LeBlanc D, Editors), Springer, Dordrecht, pp. 233-239. Available at: https://doi.org/10.1007/978-94-017-2258-2_26.

Pelz, R.K., Lipsett, P.A., Swoboda, S.M., Diener-West, M., Powe, N.R., Brower, R.G., Perl, T.M., Hammond, J.M. and Hendrix, C.W. (2002). Vancomycin-sensitive and vancomycin-resistant enterococcal infections in the ICU: Attributable costs and

outcomes. *Intensive Care Medicine*, 28(6), pp. 692-697. Available at: https://doi.org/10.1007/s00134-002-1276-8.

Permana, B., Beatson, S.A. and Forde, B.M. (2023). GraphSNP: an interactive distance viewer for investigating outbreaks and transmission networks using a graph approach. *BMC Bioinformatics*, 24(1), p. 209. Available at: https://doi.org/10.1186/s12859-023-05332-x.

Pidot, S.J., Gao, W., Buultjens, A.H., Monk, I.R., Guerillot, R., Carter, G.P., Lee, J.Y.H., Lam, M.M.C., Grayson, M.L., Ballard, S.A., Mahony, A.A., Grabsch, E.A., Kotsanas, D., Korman, T.M., Coombs, G.W., Robinson, J.O., Gonçalves da Silva, A., Seemann, T., Howden, B.P., Johnson, P.D.R. and Stinear, T.P. (2018). Increasing tolerance of hospital *Enterococcus faecium* to handwash alcohols. *Science Translational Medicine*, 10(452), p. e6115. Available at: https://doi.org/10.1126/scitranslmed.aar6115.

Pinholt, M., Bayliss, S.C., Gumpert, H., Worning, P., Jensen, V.V.S., Pedersen, M., Feil, E.J. and Westh, H. (2019). WGS of 1058 *Enterococcus faecium* from Copenhagen, Denmark, reveals rapid clonal expansion of vancomycin-resistant clone ST80 combined with widespread dissemination of a *vanA*-containing plasmid and acquisition of a heterogeneous accessory genome. *Journal of Antimicrobial Chemotherapy*, 74(7), pp. 1776–1785. Available at: https://doi.org/10.1093/jac/dkz118.

Pinholt, M., Gumpert, H., Bayliss, S., Nielsen, J.B., Vorobieva, V., Pedersen, M., Feil, E., Worning, P. and Westh, H. (2017). Genomic analysis of 495 vancomycin-resistant *Enterococcus faecium* reveals broad dissemination of a *vanA* plasmid in more than 19 clones from Copenhagen, Denmark. *Journal of Antimicrobial Chemotherapy*, 72(1), pp. 40–47. Available at: https://doi.org/10.1093/jac/dkw360.

Pinholt, M., Larner-Svensson, H., Littauer, P., Moser, C.E., Pedersen, M., Lemming, L.E., Ejlertsen, T., Søndergaard, T.S., Holzknecht, B.J., Justesen, U.S., Dzajic, E., Olsen, S.S., Nielsen, J.B., Worning, P., Hammerum, A.M., Westh, H. and Jakobsen, L. (2015). Multiple hospital outbreaks of *vanA Enterococcus faecium* in Denmark, 2012–13, investigated by WGS, MLST and PFGE. *Journal of Antimicrobial Chemotherapy*, 70(9), pp. 2474–2482. Available at: https://doi.org/10.1093/jac/dkv142.

Popiel, K.Y. and Miller, M.A. (2014). Evaluation of vancomycin-resistant enterococci (VRE)–associated morbidity following relaxation of VRE screening and isolation

precautions in a tertiary care hospital. *Infection Control & Hospital Epidemiology*, 35(7), pp. 818–825. Available at: https://doi.org/10.1086/676860.

Pratama, R., Beukers, A.G., McIver, C.J., Keighley, C.L., Taylor, P.C. and van Hal, S.J. (2021). A *vanA* vancomycin-resistant *Enterococcus faecium* ST80 outbreak resulting from a single importation event. *Journal of Antimicrobial Chemotherapy*, 77(1), pp. 31–37. Available at: https://doi.org/10.1093/jac/dkab379.

Prystowsky, J., Siddiqui, F., Chosay, J., Shinabarger, D.L., Millichap, J., Peterson, L.R. and Noskin, G.A. (2001). Resistance to linezolid: Characterization of mutations in rRNA and comparison of their occurrences in vancomycin-resistant enterococci. *Antimicrobial Agents and Chemotherapy*, 45(7), pp. 2154-2156. Available at: https://doi.org/10.1128/AAC.45.7.2154-2156.2001.

Puchter, L., Chaberny, I.F., Schwab, F., Vonberg, R.P., Bange, F.C. and Ebadi, E. (2018). Economic burden of nosocomial infections caused by vancomycin-resistant enterococci. *Antimicrobial Resistance and Infection Control*, 7(1), p. 1. Available at: https://doi.org/10.1186/s13756-017-0291-z.

Qin, X., Galloway-Peña, J.R., Sillanpaa, J., Roh, J.H., Nallapareddy, S.R., Chowdhury, S., Bourgogne, A., Choudhury, T., Muzny, D.M., Buhay, C.J., Ding, Y., Dugan-Rocha, S., Liu, W., Kovar, C., Sodergren, E., Highlander, S., Petrosino, J.F., Worley, K.C., Gibbs, R.A., Weinstock, G.M. and Murray, B.E. (2012). Complete genome sequence of *Enterococcus faecium* strain TX16 and comparative genomic analysis of *Enterococcus faecium* genomes. *BMC Microbiology*, 12(1), p. 135. Available at: https://doi.org/10.1186/1471-2180-12-135.

Quainoo, S., Coolen, J.P.M., van Hijum, S.A.F.T., Huynen, M.A., Melchers, W.J.G., van Schaik, W. and Wertheim, H.F.L. (2017). Whole-genome sequencing of bacterial pathogens: The future of nosocomial outbreak analysis. *Clinical Microbiology Reviews*, 31(1), pp. e00082-17. Available at: https://doi.org/10.1128/CMR.00016-17.

Quinlan, A.R. and Hall, I.M. (2010). BEDTools: a flexible suite of utilities for comparing genomic features. *Bioinformatics*, 26(6), pp. 841–842. Available at: https://doi.org/10.1093/bioinformatics/btq033.

Quintiliani, R. and Courvalin, P. (1996). Characterization of Tn*1547*, a composite transposon flanked by the IS*16* and IS*256*-like elements, that confers vancomycin resistance in *Enterococcus faecalis* BM4281. *Gene*, 172(1), pp. 1–8. Available at: https://doi.org/10.1016/0378-1119(96)00110-2

Raghuram, V., Gunoskey, J.J., Hofstetter, K.S., Jacko, N.F., Shumaker, M.J., Hu, Y.J., Read, T.D. and David, M.Z. (2023). Comparison of genomic diversity between single and pooled *Staphylococcus aureus* colonies isolated from human colonization cultures. *Microbial Genomics*, 9(11), p. 001111. Available at: https://doi.org/10.1099/mgen.0.001111.

Raven, K.E., Gouliouris, T., Brodrick, H., Coll, F., Brown, N.M., Reynolds, R., Reuter, S., Török, M.E., Parkhill, J. and Peacock, S.J. (2017). Complex routes of nosocomial vancomycin-resistant *Enterococcus faecium* transmission revealed by genome sequencing. *Clinical Infectious Diseases*, 64(7), pp. 886–893. Available at: https://doi.org/10.1093/cid/ciw872.

Raven, K.E., Gouliouris, T., Parkhill, J. and Peacock, S.J. (2018). Genome-based analysis of *Enterococcus faecium* bacteremia associated with recurrent and mixed-strain infection. *Journal of Clinical Microbiology*, 56(3), pp. e01520-17. Available at: https://doi.org/10.1128/JCM.01520-17.

Raven, K.E., Reuter, S., Reynolds, R., Brodrick, H.J., Russell, J.E., Török, M.E., Parkhill, J. and Peacock, S.J. (2016). A decade of genomic history for healthcare-associated *Enterococcus faecium* in the United Kingdom and Ireland. *Genome Research*, 26(10), pp. 1388–1396. Available at: https://doi.org/10.1101/gr.204024.116.

RCPI (2014). Guidelines for the Prevention and Control of Multi-drug resistant organisms (MDRO) excluding MRSA in the healthcare setting. Available at: https://www.hpsc.ie/az/microbiologyantimicrobialresistance/infectioncontrolandhai/guidelines/Guidelines%20for%20the%20Prevention%20and%20Control%20of%20MDRO_Final%20Revised_July%202014.pdf. (Accessed: 15 April 2024).

Rice, L.B. and Carias, L.L. (1998). Transfer of Tn*5385*, a composite, multiresistance chromosomal element from *Enterococcus faecalis*. *Journal of Bacteriology*, 180(3), pp. 714–721. Available at: https://doi.org/10.1128/JB.180.3.714-721.1998.

Rice, L.B., Carias, L.L. and Marshall, S.H. (1995). Tn*5384*, a composite enterococcal mobile element conferring resistance to erythromycin and gentamicin whose ends are directly repeated copies of IS*256*. *Antimicrobial Agents and Chemotherapy*, 39(5), pp. 1147–1153. Available at: https://doi.org/10.1128/AAC.39.5.1147.

Rice, L.B., Carias, L.L., Rudin, S., Laktičová, V., Wood, A. and Hutton-Thomas, R. (2005). *Enterococcus faecium* low-affinity *pbp5* is a transferable determinant. *Antimicrobial Agents and Chemotherapy*, 49(12), pp. 5007-5012. Available at: https://doi.org/10.1128/AAC.49.12.5007-5012.2005.

Rice, L.B. and Murray, B.E. (1995). Beta-lactamase-producing enterococci. *Developments in Biological Standardization*, 85, pp. 107-114.

Rios, R., Reyes, J., Carvajal, L.P., Rincon, S., Panesso, D., Echeverri, A.M., Dinh, A., Kolokotronis, S.-O., Narechania, A., Tran, T.T., Munita, J.M., Murray, B.E., Planet, P.J., Arias, C.A. and Diaz, L. (2020). Genomic epidemiology of vancomycin-resistant *Enterococcus faecium* (VREfm) in Latin America: Revisiting the global VRE population structure. *Scientific Reports*, 10(1), p. 5636. Available at: https://doi.org/10.1038/s41598-020-62371-7.

Robertson, J., Bessonov, K., Schonfeld, J. and Nash, J.H.E. (2020). Universal whole-sequence-based plasmid typing and its utility to prediction of host range and epidemiological surveillance. *Microbial Genomics*, 6(10). Available at: https://doi.org/10.1099/mgen.0.000435.

Robertson, J. and Nash, J.H.E. (2018). MOB-suite: software tools for clustering, reconstruction and typing of plasmids from draft assemblies. *Microbial Genomics*, 4(8), pp. e000206. Available at: https://doi.org/10.1099/mgen.0.000206.

Rossi, F., Diaz, L., Wollam, A., Panesso, D., Zhou, Y., Rincon, S., Narechania, A., Xing, G., Di Gioia, T.S.R., Doi, A., Tran, T.T., Reyes, J., Munita, J.M., Carvajal, L.P., Hernandez-Roldan, A., Brandão, D., van der Heijden, I.M., Murray, B.E., Planet, P.J., Weinstock, G.M. and Arias, C.A. (2014). Transferable vancomycin resistance in a community-associated MRSA lineage. *New England Journal of Medicine*, 370(16), pp. 1524–1531. Available at: https://doi.org/10.1056/NEJMoa1303359.

Rosvoll, T.C.S., Lindstad, B.L., Lunde, T.M., Hegstad, K., Aasnæs, B., Hammerum, A.M., Lester, C.H., Simonsen, G.S., Sundsfjord, A. and Pedersen, T. (2012). Increased high-level gentamicin resistance in invasive *Enterococcus faecium* is associated with *aac(6')Ie-aph(2")Ia* -encoding transferable megaplasmids hosted by major hospital-adapted lineages. *FEMS Immunology & Medical Microbiology*, 66(2), pp. 166–176. Available at: https://doi.org/10.1111/j.1574-695X.2012.00997.x.

Rosvoll, T.C.S., Pedersen, T., Sletvold, H., Johnsen, Pål.J., Sollid, J.E., Simonsen, G.S., Jensen, L.B., Nielsen, K.M. and Sundsfjord, A. (2010). PCR-based plasmid typing in *Enterococcus faecium* strains reveals widely distributed pRE25-, pRUM-, pIP501- and pHTβ-related replicons associated with glycopeptide resistance and stabilizing toxin–antitoxin systems. *FEMS Immunology & Medical Microbiology*, 58(2), pp. 254–268. Available at: https://doi.org/10.1111/j.1574-695X.2009.00633.x.

RStudio Team (2021). RStudio: Integrated Development for R, *RStudio, Inc., Boston, MA*.

Available at: https://www.r-project.org/conferences/useR-2011/abstracts/180111-allairejj.pdf.

Ryan, L., O'Mahony, E., Wrenn, C., FitzGerald, S., Fox, U., Boyle, B., Schaffer, K., Werner, G. and Klare, I. (2015). Epidemiology and molecular typing of VRE bloodstream isolates in an Irish tertiary care hospital. *Journal of Antimicrobial Chemotherapy*, 70(10), pp. 2718-2724. Available at: https://doi.org/10.1093/jac/dkv185.

Rybkine, T., Mainardi, J.L., Sougakoff, W., Collatz, E. and Gutmann, L. (1998). Penicillin-binding protein 5 sequence alterations in clinical isolates of *Enterococcus faecium* with different levels of β-lactam resistance. *Journal of Infectious Diseases*, 178(1), pp. 159-163. Available at: https://doi.org/10.1086/515605.

Sadowy, E. (2018). Linezolid resistance genes and genetic elements enhancing their dissemination in enterococci and streptococci. *Plasmid*, 99, pp. 89–98. Available at: https://doi.org/10.1016/j.plasmid.2018.09.011.

Saha, B., Singh, A.K., Ghosh, A. and Bal, M. (2008). Identification and characterization of a vancomycin-resistant *Staphylococcus aureus* isolated from Kolkata (South Asia). *Journal of Medical Microbiology*, 57(1), pp. 72–79. Available at: https://doi.org/10.1099/jmm.0.47144-0.

Saito, N., Kitazawa, J., Horiuchi, H., Yamamoto, T., Kimura, M., Inoue, F., Matsui, M., Minakawa, S., Itoga, M., Tsuchiya, J., Suzuki, S., Hisatsune, J., Gu, Y., Sugai, M. and Kayaba, H. (2022). Interhospital transmission of vancomycin-resistant *Enterococcus faecium* in Aomori, Japan. *Antimicrobial Resistance & Infection Control*, 11(1), p. 99. Available at: https://doi.org/10.1186/s13756-022-01136-5.

Saitou, N. and Nei, M. (1987). The neighbor-joining method: a new method for reconstructing phylogenetic trees. *Molecular Biology and Evolution*, 4(4), pp. 406-425. Available at: https://doi.org/10.1093/oxfordjournals.molbev.a040454.

Sanderson, H., Gray, K.L., Manuele, A., Maguire, F., Khan, A., Liu, C., Navanekere Rudrappa, C., Nash, J.H.E., Robertson, J., Bessonov, K., Oloni, M., Alcock, B.P., Raphenya, A.R., McAllister, T.A., Peacock, S.J., Raven, K.E., Gouliouris, T., McArthur, A.G., Brinkman, F.S.L., Fink, R.C., Zaheer, R. and Beiko, R.G. (2022) Exploring the mobilome and resistome of *Enterococcus faecium* in a One Health context across two continents. *Microbial Genomics*, 8(9). Available at: https://doi.org/10.1099/mgen.0.000880.

SARI Infection Control Subcommittee (2005). Guidelines for hand hygiene in Irish health care settings. Available at: https://www.hpsc.ie/a-

z/microbiologyantimicrobialresistance/strategyforthecontrolofantimicrobialresistanceinirelandsari (Accessed: 15 April 2024).

Schürch, A.C., Arredondo-Alonso, S., Willems, R.J.L. and Goering, R. v. (2018). Whole genome sequencing options for bacterial strain typing and epidemiologic analysis based on single nucleotide polymorphism versus gene-by-gene–based approaches. *Clinical Microbiology and Infection*, 24(4), pp. 350-354. Available at: https://doi.org/10.1016/j.cmi.2017.12.016.

Shadel, B.N., Puzniak, L.A., Gillespie, K.N., Lawrence, S.J., Kollef, M. and Mundy, L.M. (2006). Surveillance for vancomycin-resistant enterococci: type, rates, costs, and implications. *Infection Control & Hospital Epidemiology*, 27(10), pp. 1068–1075. Available at: https://doi.org/10.1086/507960.

Shan, X., Li, X.-S., Wang, N., Schwarz, S., Zhang, S.-M., Li, D. and Du, X.-D. (2020). Studies on the role of IS*1216E* in the formation and dissemination of *poxtA*-carrying plasmids in an *Enterococcus faecium* clade A1 isolate. *Journal of Antimicrobial Chemotherapy*, 75(11), pp. 3126–3130. Available at: https://doi.org/10.1093/jac/dkaa325.

Sheppard, A.E., Stoesser, N., Wilson, D.J., Sebra, R., Kasarskis, A., Anson, L.W., Giess, A., Pankhurst, L.J., Vaughan, A., Grim, C.J., Cox, H.L., Yeh, A.J., Sifri, C.D., Walker, A.S., Peto, T.E., Crook, D.W. and Mathers, A.J. (2016). Nested Russian doll-like genetic mobility drives rapid dissemination of the carbapenem resistance gene *bla kpc*. *Antimicrobial Agents and Chemotherapy*, 60(6), pp. 3737-3778. Available at: https://doi.org/10.1128/AAC.00464-16.

Shinabarger, D.L., Marotti, K.R., Murray, R.W., Lin, A.H., Melchior, E.P., Swaney, S.M., Dunyak, D.S., Demyan, W.F. and Buysse, J.M. (1997. Mechanism of action of oxazolidinones: Effects of linezolid and eperezolid on translation reactions. *Antimicrobial Agents and Chemotherapy*, 41(10), pp. 2132-2136. Available at: https://doi.org/10.1128/aac.41.10.2132.

da Silva, L.P.P., Pitondo-Silva, A., Martinez, R. and da Costa Darini, A.L. (2012). Genetic features and molecular epidemiology of *Enterococcus faecium* isolated in two university hospitals in Brazil. *Diagnostic Microbiology and Infectious Disease*, 74(3), pp. 267–271. Available at: https://doi.org/10.1016/j.diagmicrobio.2012.07.012.

Simonsen, G.S., Myhre, M.R.M., Dahl, K.H., Olsvik, Ø. and Sundsf Jord, A. (2000). Typeability of Tn*1546*-like elements in vancomycin-resistant enterococci using

long-range PCRs and specific analysis of polymorphic regions. *Microbial Drug Resistance*, 6(1), pp. 49–57. Available at: https://doi.org/10.1089/mdr.2000.6.49.

Singh, K. V., Montealegre, M.C. and Murray, B.E. (2022). *Enterococcus faecium* clade competition in the presence of β-Lactam antibiotics in a mouse GI tract colonization model. *Antimicrobial Agents and Chemotherapy*, 66(11), p. e0090322. Available at: https://doi.org/10.1128/aac.00903-22.

Sivertsen, A., Billström, H., Melefors, Ö., Liljequist, B.O., Wisell, K.T., Ullberg, M., Özenci, V., Sundsfjord, A. and Hegstad, K. (2014). A multicentre hospital outbreak in Sweden caused by introduction of a *vanB2* transposon into a stably maintained pRUM-plasmid in an *Enterococcus faecium* ST192 clone. *PLoS ONE*, 9(8), p. e103274. Available at: https://doi.org/10.1371/journal.pone.0103274.

Sletvold, H., Johnsen, P.J., Wikmark, O.-G., Simonsen, G.S., Sundsfjord, A. and Nielsen, K.M. (2010). Tn*1546* is part of a larger plasmid-encoded genetic unit horizontally disseminated among clonal *Enterococcus faecium* lineages. *Journal of Antimicrobial Chemotherapy*, 65(9), pp. 1894–1906. Available at: https://doi.org/10.1093/jac/dkq219.

Song, X., Srinivasan, A., Plaut, D. and Perl, T.M. (2003). Effect of nosocomial vancomycin-resistant enterococcal bacteremia on mortality, length of stay, and costs. *Infection Control & Hospital Epidemiology*, 24(4), pp. 251-256. Available at: https://doi.org/10.1086/502196.

Stamper, P.D., Shulder, S., Bekalo, P., Manandhar, D., Ross, T.L., Speser, S., Kingery, J. and Carroll, K.C. (2010). Evaluation of BBL CHROMagar VanRE for detection of vancomycin-resistant enterococci in rectal swab specimens. *Journal of Clinical Microbiology*, 48(11), pp. 4294–4297. Available at: https://doi.org/10.1128/JCM.01522-10.

Stogios, P.J. and Savchenko, A. (2020). Molecular mechanisms of vancomycin resistance. *Protein Science*, 29(3), pp. 654-669. Available at: https://doi.org/10.1002/pro.3819.

Stosor, V., Peterson, L.R., Postelnick, M. and Noskin, G.A. (1998). *Enterococcus faecium* bacteremia: Does vancomycin resistance make a difference? *Archives of Internal Medicine*, 158(5), pp. 522-527. Available at: https://doi.org/10.1001/archinte.158.5.522.

Suleyman, G., Alangaden, G. and Bardossy, A.C. (2018). The role of environmental contamination in the transmission of nosocomial pathogens and healthcare-associated infections. *Current Infectious Disease Reports*, 20(6), p. 12. Available at: https://doi.org/10.1007/s11908-018-0620-2.

Sullivan, M.J., Petty, N.K. and Beatson, S.A. (2011). Easyfig: a genome comparison visualizer. *Bioinformatics*, 27(7), pp. 1009–1010. Available at: https://doi.org/10.1093/bioinformatics/btr039.

Talebi, M., Pourshafie, M.R., Katouli, M. and Möllby, R. (2008). Molecular structure and transferability of Tn*1546*-Like Elements in *Enterococcus faecium* isolates from clinical, sewage, and surface water samples in Iran. *Applied and Environmental Microbiology*, 74(5), pp. 1350–1356. Available at: https://doi.org/10.1128/AEM.02254-07.

Thal, L.A., Chow, J.W., Clewell, D.B. and Zervos, M.J. (1994). Tn*924*, a chromosome-borne transposon encoding high-level gentamicin resistance in *Enterococcus faecalis*. *Antimicrobial Agents and Chemotherapy*, 38(5), pp. 1152–1156. Available at: https://doi.org/10.1128/AAC.38.5.1152.

Thomas, C.M. (2014). Evolution and population genetics of bacterial plasmids, In *Plasmid Biology*. (Funnell B and Philips G, Editors), Washington, DC, USA: ASM Press, pp. 507–528. Available at: https://doi.org/10.1128/9781555817732.ch25.

Tickler, I.A., Tenover, F.C., Dewell, S., Le, V.M., Blackman, R.N., Goering, R. V., Rogers, A.E., Piwonka, H., Jung-Hynes, B.D., Chen, D.J., Loeffelholz, M.J., Gnanashanmugam, D. and Baron, E.J. (2019). *Streptococcus agalactiae* strains with chromosomal deletions evade detection with molecular methods. *Journal of Clinical Microbiology*, 57(4), pp. e02040-18. Available at: https://doi.org/10.1128/JCM.02040-18.

Tiwari, H.K. and Sen, M.R. (2006). Emergence of vancomycin resistant *Staphylococcus aureus* (VRSA) from a tertiary care hospital from northern part of India. *BMC Infectious Diseases*, 6(1), p. 156. Available at: https://doi.org/10.1186/1471-2334-6-156.

Tomita, H., Pierson, C., Lim, S.K., Clewell, D.B. and Ike, Y. (2002). Possible connection between a widely disseminated conjugative gentamicin resistance (pMG1-like) plasmid and the emergence of vancomycin resistance in *Enterococcus faecium*. *Journal of Clinical Microbiology*, 40(9), pp. 3326-3333. Available at: https://doi.org/10.1128/JCM.40.9.3326-3333.2002.

Tsai, S.F., Zervos, M.J., Clewell, D.B., Donabedian, S.M., Sahm, D.F. and Chow, J.W. (1998). A new high-level gentamicin resistance gene, *aph(2'')-Id*, in *Enterococcus spp. Antimicrobial Agents and Chemotherapy*, 42(5), pp. 1229-1232. Available at: https://doi.org/10.1128/aac.42.5.1229.

Ubeda, C., Taur, Y., Jenq, R.R., Equinda, M.J., Son, T., Samstein, M., Viale, A., Socci, N.D., van den Brink, M.R.M., Kamboj, M. and Pamer, E.G. (2010). Vancomycin-resistant *Enterococcus* domination of intestinal microbiota is enabled by antibiotic treatment in mice and precedes bloodstream invasion in humans. *Journal of Clinical Investigation*, 120(12), pp. 4332–4341. Available at: https://doi.org/10.1172/JCI43918.

Uelze, L., Grützke, J., Borowiak, M., Hammerl, J.A., Juraschek, K., Deneke, C., Tausch, S.H. and Malorny, B. (2020). Typing methods based on whole genome sequencing data. *One Health Outlook*, 2(1), p. 3. Available at: https://doi.org/10.1186/s42522-020-0010-1.

van der Auwera, P., Pensart, N., Korten, V., Murray, B.E. and Leclercq, R. (1996). Influence of oral glycopeptides on the fecal flora of human volunteers: selection of highly glycopeptide-resistant enterococci. *Journal of Infectious Diseases*, 173(5), pp. 1129–1136. Available at: https://doi.org/10.1093/infdis/173.5.1129.

van Hal, S.J., Beukers, A.G., Timms, V.J., Ellem, J.A., Taylor, P., Maley, M.W., Newton, P.J., Ferguson, J.K., Lee, A., Chen, S.C.A. and Sintchenko, V. (2018). Relentless spread and adaptation of non-typeable *vanA* vancomycin-resistant *Enterococcus faecium:* A genome-wide investigation. *Journal of Antimicrobial Chemotherapy*, 73(6), pp. 1487-1491. Available at: https://doi.org/10.1093/jac/dky074.

van Hal, S.J., Willems, R.J.L., Gouliouris, T., Ballard, S.A., Coque, T.M., Hammerum, A.M., Hegstad, K., Pinholt, M., Howden, B.P., Malhotra-Kumar, S., Werner, G., Yanagihara, K., Earl, A.M., Raven, K.E., Corander, J. and Bowden, R. (2022). The interplay between community and hospital *Enterococcus faecium* clones within health-care settings: a genomic analysis. *The Lancet Microbe*, 3(2), pp. e133–e141. Available at: https://doi.org/10.1016/S2666-5247(21)00236-6.

van Hal, S.J., Willems, R.J.L., Gouliouris, T., Ballard, S.A., Coque, T.M., Hammerum, A.M., Hegstad, K., Westh, H.T., Howden, B.P., Malhotra-Kumar, S., Werner, G., Yanagihara, K., Earl, A.M., Raven, K.E., Corander, J. and Bowden, R. (2021). The global dissemination of hospital clones of *Enterococcus faecium*. *Genome Medicine*, 13(1), p. 52. Available at: https://doi.org/10.1186/s13073-021-00868-0.

van Schaik, W., Top, J., Riley, D.R., Boekhorst, J., Vrijenhoek, J.E., Schapendonk, C.M., Hendrickx, A.P., Nijman, I.J., Bonten, M.J., Tettelin, H. and Willems, R.J. (2010). Pyrosequencing-based comparative genome analysis of the nosocomial pathogen *Enterococcus faecium* and identification of a large transferable pathogenicity island.

BMC Genomics, 11(1), p. 239. Available at: https://doi.org/10.1186/1471-2164-11-239.

Wagner, T.M., Pöntinen, A.K., Fenzel, C.K., Engi, D., Janice, J., Almeida-Santos, A.C., Tedim, A.P., Freitas, A.R., Peixe, L., van Schaik, W., Johannessen, M. and Hegstad, K. (2024). Interactions between commensal *Enterococcus faecium* and *Enterococcus lactis* and clinical isolates of *Enterococcus faecium*. *FEMS Microbes*, 5. Available at: https://doi.org/10.1093/femsmc/xtae009.

Walsh, T.R. (2018). A one-health approach to antimicrobial resistance. *Nature Microbiology*, 3(8), pp. 854–855. Available at: https://doi.org/10.1038/s41564-018-0208-5.

Wang, Y., Lv, Y., Cai, J., Schwarz, S., Cui, L., Hu, Z., Zhang, R., Li, J., Zhao, Q., He, T., Wang, D., Wang, Z., Shen, Y., Li, Y., Feßler, A.T., Wu, C., Yu, H., Deng, X., Xia, X. and Shen, J. (2015). A novel gene, *optrA*, that confers transferable resistance to oxazolidinones and phenicols and its presence in *Enterococcus faecalis* and *Enterococcus faecium* of human and animal origin. *Journal of Antimicrobial Chemotherapy*, 70(8), pp. 2182-2190. Available at: https://doi.org/10.1093/jac/dkv116.

Wardal, E., Kuch, A., Gawryszewska, I., Żabicka, D., Hryniewicz, W. and Sadowy, E. (2017). Diversity of plasmids and Tn*1546*-type transposons among *vanA Enterococcus faecium* in Poland. *European Journal of Clinical Microbiology & Infectious Diseases*, 36(2), pp. 313–328. Available at: https://doi.org/10.1007/s10096-016-2804-8.

Wardal, E., Markowska, K., Zabicka, D., Wróblewska, M., Giemza, M., Mik, E., Połowniak-Pracka, H., Woźniak, A., Hryniewicz, W. and Sadowy, E. (2014). Molecular analysis of *vanA* outbreak of *Enterococcus faecium* in two Warsaw hospitals: The importance of mobile genetic elements. *BioMed Research International*, 2014. Available at: https://doi.org/10.1155/2014/575367.

Weigel, L.M., Donlan, R.M., Shin, D.H., Jensen, B., Clark, N.C., McDougal, L.K., Zhu, W., Musser, K.A., Thompson, J., Kohlerschmidt, D., Dumas, N., Limberger, R.J. and Patel, J.B. (2007). High-level vancomycin-resistant *Staphylococcus aureus* isolates associated with a polymicrobial biofilm. *Antimicrobial Agents and Chemotherapy*, 51(1), pp. 231–238. Available at: https://doi.org/10.1128/AAC.00576-06.

Werner, G. (2013). Molecular typing of enterococci/VRE. *Journal of Bacteriology & Parasitology*, 01(S5). Available at: https://doi.org/10.4172/2155-9597.s5-001.

Werner, G., Coque, T.M., Hammerum, A.M., Hope, R., Hryniewicz, W., Johnson, A., Klare, I., Kristinsson, K.G., Leclercq, R., Lester, C.H., Lillie, M., Novais, C., Olsson-Liljequist, B., Peixe, L. v., Sadowy, E., Simonsen, G.S., Top, J., Vuopio-Varkila, J., Willems, R.J., Witte, W. and Woodford, N. (2008). Emergence and spread of vancomycin resistance among enterococci in Europe. *Eurosurveillance*, 13(47), p. 19046. Available at: https://doi.org/10.2807/ese.13.47.19046-en.

Werner, G., Freitas, A.R., Coque, T.M., Sollid, J.E., Lester, C., Hammerum, A.M., Garcia-Migura, L., Jensen, L.B., Francia, M. v., Witte, W., Willems, R.J. and Sundsfjord, A. (2011). Host range of enterococcal *vanA* plasmids among Gram-positive intestinal bacteria. *Journal of Antimicrobial Chemotherapy*, 66(2), pp. 273-282. Available at: https://doi.org/10.1093/jac/dkq455.

Werner, Guido, Klare, I., Fleige, C. and Witte, W. (2008). Increasing rates of vancomycin resistance among *Enterococcus faecium* isolated from German hospitals between 2004 and 2006 are due to wide clonal dissemination of vancomycin-resistant enterococci and horizontal spread of *vanA* clusters. *International Journal of Medical Microbiology*, 298(5–6), pp. 515–527. Available at: https://doi.org/10.1016/j.ijmm.2007.05.008.

Werner, G., Neumann, B., Weber, R.E., Kresken, M., Wendt, C., Bender, J.K., Becker, K., Borgmann, S., Diefenbach, A., Hamprecht, A., Hogardt, M., Wichelhaus, T., Kemp, V., Huebner, N.-O., Kaasch, A., Geginat, G., Kohnen, W., Menzer, A., Krause, T., Miethke, T., Pranada, F., Radojn, F., Tobisch, S., Jansen, V., Regnath, T., Bührlen, U., Schneider-Brachert, W., Schwarz, R., Luemen, M., Skov, R., Thuermer, A., Baum, H. von, Weig, M., Uwe, G., Zabel, L., Wulffen, H. von and Döring, S. (2020). Thirty years of VRE in Germany – expect the unexpected: The view from the National Reference Centre for Staphylococci and Enterococci. *Drug Resistance Updates*, 53, p. 100732. Available at: https://doi.org/10.1016/j.drup.2020.100732.

Whelton, E., Lynch, C., O'Reilly, B., Corcoran, G.D., Cryan, B., Keane, S.M., Sleator, R.D. and Lucey, B. (2016). Vancomycin-resistant enterococci carriage in an acute Irish hospital. *Journal of Hospital Infection*, 93(2), pp. 175–180. Available at: https://doi.org/10.1016/j.jhin.2016.03.005.

Wick, R.R., Judd, L.M., Gorrie, C.L. and Holt, K.E. (2017). Unicycler: Resolving bacterial genome assemblies from short and long sequencing reads. *PLoS Computational Biology*, 13(6), p. e1005595. Available at: https://doi.org/10.1371/journal.pcbi.1005595.

Wick, R.R., Schultz, M.B., Zobel, J. and Holt, K.E. (2015). Bandage: interactive visualization of *de novo* genome assemblies. *Bioinformatics*, 31(20), pp. 3350–3352. Available at: https://doi.org/10.1093/bioinformatics/btv383.

Wickham, H. (2016) ggplot2. In *Elegant Graphics for Data Analysis*. Springer, New York. Available at: https://doi.org/10.1007/978-3-319-24277-4.

Willems, R.J. and van Schaik, W. (2009). Transition of *Enterococcus faecium* from commensal organism to nosocomial pathogen. *Future Microbiology*, 4(9), pp. 1125–1135. Available at: https://doi.org/10.2217/fmb.09.82.

Willems, Rob J. L., Top, J., van den Braak, N., van Belkum, A., Mevius, D.J., Hendriks, G., van Santen-Verheuvel, M. and van Embden, J.D.A. (1999). Molecular diversity and evolutionary relationships of Tn*1546*-like elements in enterococci from humans and animals. *Antimicrobial Agents and Chemotherapy*, 43(3), pp. 483–491. Available at: https://doi.org/10.1128/AAC.43.3.483.

Willems, Rob J.L., Top, J., van den Braak, N., van Belkum, A., Mevius, D.J., Hendriks, G., van Santen-Verheuvel, M. and van Embden, J.D.A. (1999). Molecular diversity and evolutionary relationships of Tn*1546*-like elements in enterococci from humans and animals. *Antimicrobial Agents and Chemotherapy*, 43(3), pp. 483-491. Available at: https://doi.org/10.1128/aac.43.3.483.

Willems, R.J.L., Top, J., van Santen, M., Robinson, D.A., Coque, T.M., Baquero, F., Grundmann, H. and Bonten, M.J.M. (2005). Global spread of vancomycin-resistant *Enterococcus faecium* from distinct nosocomial genetic complex. *Emerging Infectious Diseases*, 11(6), pp. 821–828. Available at: https://doi.org/10.3201/1106.041204.

Willems, R.J.L., Top, J., van Schaik, W., Leavis, H., Bonten, M., Sirń, J., Hanage, W.P. and Corander, J. (2012). Restricted gene flow among hospital subpopulations of *Enterococcus faecium*. *mBio*, 3(4), pp. e00151-121. Available at: https://doi.org/10.1128/mBio.00151-12.

Willems, R.J.L., Top, J., van den Braak, N., van Belkum, A., Endtz, H., Mevius, D., Stobberingh, E., van den Bogaard, A. and van Embden, J.D.A. (2000). Host specificity of vancomycin-resistant *Enterococcus faecium*. *The Journal of Infectious Diseases*, 182(3), pp. 816–823. Available at: https://doi.org/10.1086/315752.

Woodford, N., Adebiyi, A.-M.A., Palepou, M.-F.I. and Cookson, B.D. (1998). Diversity of *vanA* glycopeptide resistance elements in enterococci from humans and nonhuman sources. *Antimicrobial Agents and Chemotherapy*, 42(3), pp. 502–508. Available at: https://doi.org/10.1128/AAC.42.3.502.

Woodford, N., Johnson, A.P., Morrison, D. and Speller, D.C.E. (1995). Current perspectives on glycopeptide resistance. *Clinical Microbiology Reviews*, 8(4), pp. 585-615. Available at: https://doi.org/10.1128/cmr.8.4.585.

Worby, C.J., Lipsitch, M. and Hanage, W.P. (2014). Within-host bacterial diversity hinders accurate reconstruction of transmission networks from genomic distance data. *PLoS Computational Biology*, 10(3), p. e1003549. Available at: https://doi.org/10.1371/journal.pcbi.1003549.

Zapun, A., Contreras-Martel, C. and Vernet, T. (2008). Penicillin-binding proteins and β-lactam resistance. *FEMS Microbiology Reviews*, 32(2), pp. 361-385. Available at: https://doi.org/10.1111/j.1574-6976.2007.00095.x.

Zhou, M.J., Li, J., Salmasian, H., Zachariah, P., Yang, Y.-X. and Freedberg, D.E. (2019). The local hospital milieu and healthcare-associated vancomycin-resistant *Enterococcus* acquisition. *Journal of Hospital Infection*, 101(1), pp. 69–75. Available at: https://doi.org/10.1016/j.jhin.2018.07.018.

Zhou, X., Chlebowicz, M.A., Bathoorn, E., Rosema, S., Couto, N., Lokate, M., Arends, J.P., Friedrich, A.W. and Rossen, J.W.A. (2018). Elucidating vancomycin-resistant *Enterococcus faecium* outbreaks: The role of clonal spread and movement of mobile genetic elements, *Journal of Antimicrobial Chemotherapy*, 73(12), pp. 3259-3267. Available at: https://doi.org/10.1093/jac/dky349.

Zimin, A. (2014). MaSuRCA 2.1.0 genome assembler quick start guide, *Bioinformatics*, 29(21).

Zirakzadeh, A. and Patel, R. (2006). Vancomycin-resistant enterococci: Colonization, infection, detection, and treatment. *Mayo Clinic Proceedings*, 81(4), pp. 529–536. Available at: https://doi.org/10.4065/81.4.529.

Appendix 1

Table 1. Phenotypic and genotypic characteristics and whole-genome sequencing data analysis of 1,028 clade A1 *Enterococcus faecium* isolates recovered from Irish hospitals between June 2017-August 2022

Specimen no.	Date of sample[1]	Hospital	H1 Ward[2]	Specimen	Vanc[3]	Vanc Resistance Gene[4]	ST[5]	cgMLST CT[5]	SJ11*vanA*[6]
BH001	29/03/2022	H2	U	Screening	R	*vanA*	80	6489	99.98%
BH002	05/04/2022	H2	U	Screening	R	*vanA*	80	2933	98.90%
BH004	26/04/2022	H2	U	Screening	R	*vanA*	80	6489	99.98%
BH005	03/05/2022	H2	U	Screening	R	*vanA*	1283	7016	94.97%
BH006	26/04/2022	H2	U	Screening	R	*vanA*	80	6489	99.96%
BH007	26/04/2022	H2	U	Screening	R	*vanA*	80	6489	99.97%
BH008	17/02/2021	H2	U	Right abdominal drain	R	*vanA*	80	2933	88.35%
BH010	13/03/2021	H2	U	Fluid	R	*vanA*	80	3168	98.45%
BH011	12/03/2021	H2	U	Tip	R	*vanA*	80	3383	95.68%
BH012	20/03/2021	H2	U	Abdominal fluid	R	*vanA*	80	2933	98.63%
BH013	23/03/2021	H2	U	Abdominal fluid	R	*vanA*	80	3395	99.96%
BH014	26/03/2021	H2	U	Urine	R	*vanA*	80	6986	99.96%
BH015	22/03/2021	H2	U	Urine	R	*vanA*	80	3168	98.45%
BH016	29/03/2021	H2	U	Urine	R	*vanA*	80	6489	99.97%
BH017	07/04/2021	H2	U	Groin Tissue	R	*vanA*	80	2933	98.64%
BH018	18/04/2021	H2	U	Swab	R	*vanA*	80	3383	95.10%
BH019	17/04/2021	H2	U	Intrabdominal pus	R	*vanA*	80	3395	99.98%
BH020	22/04/2021	H2	U	Urine	R	*vanA*	80	6738	99.97%
BH021	01/05/2021	H2	U	Urine	R	*vanA*	80	2933	99.96%
BH022	01/05/2021	H2	U	Fluid chest drain	R	*vanA*	80	2933	98.65%

Table 1 continued overleaf

Specimen no.	Date of sample[1]	Hospital	H1 Ward[2]	Specimen	Vanc[3]	Vanc Resistance Gene[4]	ST[5]	cgMLST CT[5]	SJ11*vanA*[6]
BH023	16/05/2021	H2	U	Urine	R	*vanA*	80	2931	99.98%
BH024	14/05/2021	H2	U	Screening	R	*vanA*	80	1921	98.26%
BH025	17/05/2021	H2	U	Abdominal wound swab	R	*vanA*	80	3395	99.96%
BH026	29/05/2021	H2	U	Urine	R	*vanA*	80	1916	95.52%
BH027	04/06/2021	H2	U	Bile	R	*vanA*	80	3395	99.96%
BH029	14/06/2021	H2	U	Urine	R	*vanA*	80	6489	99.95%
BH030	18/06/2021	H2	U	N/A	R	*vanA*	80	6489	99.97%
BH032	24/06/2021	H2	U	Urine	R	*vanA*	80	1921	38.96%
BH033	03/08/2021	H2	U	Screening	R	*vanA*	80	2933	98.63%
BH034	29/07/2021	H2	U	Rectal Pus	R	*vanA*	80	3168	29.16%
BH035	04/08/2021	H2	U	Screening	R	*vanA*	80	1916	98.16%
BH036	03/08/2021	H2	U	Screening	R	*vanA*	80	6489	99.98%
BH037	09/08/2021	H2	U	Screening	R	*vanA*	80	2933	99.97%
BH038	20/08/2021	H2	U	Screening	R	*vanA*	80	1916	95.51%
BH039	18/08/2021	H2	U	Screening	R	*vanA*	80	6738	99.96%
BH040	15/08/2021	H2	U	Screening	R	*vanA*	80	6489	99.97%
BH041	23/08/2021	H2	U	Urine	R	*vanA*	80	6738	99.97%
BH042	23/08/2021	H2	U	Screening	R	*vanA*	80	6489	88.02%
BH043	27/08/2021	H2	U	Screening	R	*vanA*	1693	2532	88.22%
BH044	30/08/2021	H2	U	Screening	R	*vanA*	80	6489	99.98%
BH045	06/09/2021	H2	U	Screening	R	*vanA*	80	2933	99.96%
BH046	04/09/2021	H2	U	Screening	R	*vanA*	18	3164	96.11%
BH047	15/09/2021	H2	U	Screening	R	*vanA* and *vanB*	17	2271	99.22%
BH048	14/09/2021	H2	U	Screening	R	*vanA*	80	1916	95.49%
BH049	07/09/2021	H2	U	Screening	R	*vanA*	80	6738	99.96%

Table 1 continued overleaf

Specimen no.	Date of sample[1]	Hospital	H1 Ward[2]	Specimen	Vanc[3]	Vanc Resistance Gene[4]	ST[5]	cgMLST CT[5]	SJ11*vanA*[6]
BH050	21/09/2021	H2	U	Screening	R	*vanA*	80	3168	26.88%
BH051	24/09/2021	H2	U	Urine	R	*vanA*	80	2933	99.97%
BH052	23/09/2021	H2	U	Ovarian fluid	R	*vanA*	80	1916	96.20%
BH056	06/10/2021	H2	U	Screening	R	*vanA*	80	2933	98.63%
BH057	11/10/2021	H2	U	Screening	R	*vanA*	80	6738	99.97%
BH058	21/10/2021	H2	U	Abdominal swab	R	*vanA*	80	2933	99.97%
BH059	31/10/2021	H2	U	Urine	R	*vanA*	80	3395	99.95%
BH060	01/11/2021	H2	U	Screening	R	*vanA*	80	3395	99.93%
BH082	14/06/2022	H2	U	Screening	R	*vanA*	80	6988	95.50%
BH083	14/06/2022	H2	U	Screening	R	*vanA*	80	6988	95.49%
BH089	12/04/2022	H2	U	Screening	R	*vanA*	80	6489	99.97%
BH090	14/06/2022	H2	U	Screening	R	*vanA*	612	2942	98.63%
BH092	02/08/2022	H2	U	Screening	R	*vanA*	80	6738	98.63%
BH3	26/04/2022	H2	U	Screening	R	*vanA*	80	6489	99.97%
BH61	03/11/2021	H2	U	Screening	R	*vanA*	80	2933	89.63%
BH63	09/11/2021	H2	U	Screening	R	*vanA*	80	2932	98.61%
BH65	09/11/2021	H2	U	Screening	R	*vanA*	80	1916	95.64%
BH66	13/11/2021	H2	U	Screening	R	*vanA*	80	1916	97.31%
BH67	13/11/2021	H2	U	Screening	R	*vanA*	80	2933	99.97%
BH68	16/11/2021	H2	U	Screening	R	*vanA*	80	6489	99.97%
BH69	18/11/2021	H2	U	Toe tissue	R	*vanA*	80	6738	99.98%
BH70	16/11/2021	H2	U	Abdominal pus	R	*vanA*	80	6489	99.97%
BH71	16/11/2021	H2	U	Screening	R	*vanA*	80	6738	99.96%
BH72	22/11/2021	H2	U	Screening	R	*vanA*	80	6738	88.37%
BH74	30/11/2021	H2	U	Screening	R	*vanA*	80	2933	98.41%

Table 1 continued overleaf

Specimen no.	Date of sample[1]	Hospital	H1 Ward[2]	Specimen	Vanc[3]	Vanc Resistance Gene[4]	ST[5]	cgMLST CT[5]	SJ11*vanA*[6]
BH75	05/12/2021	H2	U	Screening	R	*vanA*	80	2933	98.63%
BH77	18/12/2021	H2	U	Screening	R	*vanA*	80	2933	71.48%
BH78	28/12/2021	H2	U	Screening	R	*vanA*	80	3225	88.19%
BH79	24/12/2021	H2	U	Screening	R	*vanA*	80	6738	99.97%
BH80	13/04/2021	H2	U	BSI	R	*vanA*	117	6987	98.62%
BH84	17/05/2022	H2	U	Screening	R	*vanA*	80	6489	99.98%
BH85	15/03/2022	H2	U	Screening	R	*vanA*	80	6489	99.97%
BH86	29/03/2022	H2	U	Screening	R	*vanA*	80	1921	88.20%
BH87	17/05/2022	H2	U	Screening	R	*vanA*	80	6489	99.96%
BS204	07/02/2019	H4	U	Screening	R	*vanA*	80	1916	98.71%
BS205	11/02/2019	H4	U	Screening	R	*vanA*	80	1598	98.57%
BS206	13/02/2019	H4	U	Screening	R	*vanA*	80	1185	93.26%
BS208	26/02/2019	H4	U	Screening	R	*vanA*	80	1916	99.95%
BS209	20/03/2019	H4	U	Screening	R	*vanA*	2185	2978	95.50%
BS210	05/03/2019	H4	U	Screening	R	*vanA*	1395	2284	98.61%
BS211	14/03/2019	H4	U	Screening	R	*vanA*	80	2931	99.95%
BS212	27/03/2019	H4	U	Screening	R	*vanA*	80	1185	94.43%
BS213	10/04/2019	H4	U	Screening	R	*vanA*	203	1599	93.26%
BS214	15/04/2019	H4	U	Screening	R	*vanA*	Novel	3174	99.92%
BS215	23/04/2019	H4	U	Screening	R	*vanA*	2185	2978	95.48%
BS216	27/04/2019	H4	U	Screening	R	*vanA*	787	6272	93.43%
BS217	29/04/2019	H4	U	Screening	R	*vanA*	80	2933	98.63%
BS218	08/05/2019	H4	U	Screening	R	*vanA*	612	2942	97.22%
BS219	09/05/2019	H4	U	Screening	R	*vanA*	80	2933	29.18%
BS220	13/05/2019	H4	U	Screening	R	*vanA*	80	1598	99.98%

Table 1 continued overleaf

Specimen no.	Date of sample[1]	Hospital	H1 Ward[2]	Specimen	Vanc[3]	Vanc Resistance Gene[4]	ST[5]	cgMLST CT[5]	SJ11*vanA*[6]
BS221	21/05/2019	H4	U	Screening	R	*vanA*	2185	2978	95.50%
BS222	23/05/2019	H4	U	Screening	R	*vanA*	192	6273	99.99%
BS224	30/05/2019	H4	U	Screening	R	*vanA*	80	3383	95.84%
BS225	07/06/2019	H4	U	Screening	R	*vanA*	80	2933	98.60%
BS226	10/06/2019	H4	U	Screening	R	*vanA*	203	1599	8.86%
BS227	11/06/2019	H4	U	Screening	R	*vanA*	117	2283	99.95%
BS228	11/06/2019	H4	U	Screening	R	*vanA*	2185	2978	95.50%
BS230	24/06/2019	H4	U	Screening	R	*vanA*	80	2933	99.96%
BS233	09/07/2019	H4	U	Screening	R	*vanA*	Novel	6274	95.14%
BS234	22/07/2019	H4	U	Screening	R	*vanA*	80	6275	95.17%
BS235	26/07/2019	H4	U	Screening	R	*vanA*	80	1185	93.24%
BS236	29/07/2019	H4	U	Screening	R	*vanA*	80	2977	95.33%
BS237	29/07/2019	H4	U	Screening	R	*vanA*	2185	2978	95.50%
BS238	30/07/2019	H4	U	Screening	R	*vanA*	2185	2978	95.50%
BS239	01/08/2019	H4	U	Screening	R	*vanA*	203	6276	93.23%
BS240	09/08/2019	H4	U	Screening	R	*vanA*	80	2933	98.63%
BS241	12/08/2019	H4	U	Screening	R	*vanA*	80	2931	99.98%
BS243	27/08/2019	H4	U	Screening	R	*vanA*	80	6277	98.64%
BS244	29/08/2019	H4	U	Screening	R	*vanA*	2185	2978	95.45%
BS245	02/09/2019	H4	U	Screening	R	*vanA*	2185	2978	95.50%
BS246	05/09/2019	H4	U	Screening	R	*vanA*	80	6277	99.98%
BS248	18/09/2019	H4	U	Screening	R	*vanA*	2185	2978	95.48%
BS249	18/09/2019	H4	U	Screening	R	*vanA*	375	6278	95.50%
BS251	23/09/2019	H4	U	Screening	R	*vanA*	2185	2978	95.47%
BS252	23/09/2019	H4	U	Screening	R	*vanA*	2185	2978	95.52%

Table 1 continued overleaf

Specimen no.	Date of sample[1]	Hospital	H1 Ward[2]	Specimen	Vanc[3]	Vanc Resistance Gene[4]	ST[5]	cgMLST CT[5]	SJ11*vanA*[6]
BS253	25/09/2019	H4	U	Screening	R	*vanA*	80	6277	97.99%
BS254	27/09/2019	H4	U	Screening	R	*vanA*	2185	2978	95.44%
BS255	14/10/2019	H4	U	Screening	R	*vanA*	80	6277	98.66%
BS256	17/10/2019	H4	U	Screening	R	*vanA*	80	2933	98.64%
BS257	23/10/2019	H4	U	Screening	R	*vanA*	80	6277	98.62%
BS258	23/10/2019	H4	U	Screening	R	*vanA*	80	2933	99.90%
BS259	23/10/2019	H4	U	Screening	R	*vanA*	80	1921	99.98%
BS260	23/10/2019	H4	U	Screening	R	*vanA*	2185	2978	95.59%
BS261	23/10/2019	H4	U	Screening	R	*vanA*	80	1916	95.51%
BS263	25/10/2019	H4	U	Screening	R	*vanA*	80	2933	77.70%
BS265	29/10/2019	H4	U	Screening	R	*vanA*	80	2933	98.63%
BS266	29/10/2019	H4	U	Screening	R	*vanA*	80	6277	98.64%
BS267	29/10/2019	H4	U	Screening	R	*vanA*	80	2977	95.33%
BS268	29/10/2019	H4	U	Screening	R	*vanA*	80	2933	98.60%
BS269	29/10/2019	H4	U	Screening	R	*vanA*	80	3394	93.28%
BS270	30/10/2019	H4	U	Screening	R	*vanA*	80	1921	99.96%
BS271	31/10/2019	H4	U	Screening	R	*vanA*	80	6277	98.65%
BS272	01/11/2019	H4	U	Screening	R	*vanA*	80	6277	98.63%
BS274	08/11/2019	H4	U	Screening	R	*vanA*	203	20	78.47%
BS275	11/11/2019	H4	U	Screening	R	*vanA*	80	6277	98.64%
BS277	11/11/2019	H4	U	Screening	R	*vanA*	80	3395	99.94%
BS278	12/11/2019	H4	U	Screening	R	*vanA*	80	6277	98.62%
BS279	13/11/2019	H4	U	Screening	R	*vanA*	80	1916	95.34%
BS280	18/11/2019	H4	U	Screening	R	*vanA*	80	3394	61.59%
BS281	19/11/2019	H4	U	Screening	R	*vanA*	80	2933	98.61%

Table 1 continued overleaf

Specimen no.	Date of sample[1]	Hospital	H1 Ward[2]	Specimen	Vanc[3]	Vanc Resistance Gene[4]	ST[5]	cgMLST CT[5]	SJ11*vanA*[6]
BS282	20/11/2019	H4	U	Screening	R	*vanA*	80	2933	93.21%
BS283	26/11/2019	H4	U	Screening	R	*vanA*	80	2933	99.97%
BS285	02/12/2019	H4	U	Screening	R	*vanA*	80	2933	98.54%
BS287	03/12/2019	H4	U	Screening	R	*vanA*	80	1916	95.49%
BS289	10/12/2019	H4	U	Screening	R	*vanA*	80	1921	99.97%
BS290	12/12/2019	H4	U	Screening	R	*vanA*	80	2941	98.64%
BS291	18/12/2019	H4	U	Screening	R	*vanA*	787	1920	67.61%
BS292	31/12/2019	H4	U	Screening	R	*vanA*	203	20	83.02%
BS295	03/01/2019	H4	U	Screening	R	*vanA*	1693	2532	95.61%
BS296	06/02/2019	H4	U	Screening	R	*vanA*	80	2933	99.21%
BS297	14/02/2019	H4	U	Screening	R	*vanA*	203	1599	68.02%
BS298	25/02/2019	H4	U	Screening	R	*vanA*	203	1599	95.50%
BS299	13/05/2019	H4	U	Screening	R	*vanA*	192	6273	99.97%
BS300	15/05/2019	H4	U	Screening	R	*vanA*	80	2933	98.60%
BS302	16/05/2019	H4	U	Screening	R	*vanA*	80	2933	98.63%
BS303	23/05/2019	H4	U	Screening	R	*vanA*	203	1599	99.94%
BS304	23/05/2019	H4	U	Screening	R	*vanA*	80	2933	98.55%
BS305	08/07/2019	H4	U	Screening	R	*vanA*	80	7017	98.58%
BS306	15/07/2019	H4	U	Screening	R	*vanA*	80	2933	98.64%
BS307	29/11/2019	H4	U	Screening	R	*vanA*	80	2933	98.55%
BSI_SJ10	03/11/2017	H1	W22	BSI	S	-	787	1920	23.52%
BSI_SJ11	03/11/2017	H1	W6	BSI	R	*vanA*	80	2272	99.97%
BSI_SJ12	19/11/2017	H1	W1	BSI	R	*vanA*	1424	1920	95.52%
BSI_SJ13	28/11/2017	H1	W1	BSI	S	-	203	1599	26.19%
BSI_SJ14	08/12/2017	H1	W18	BSI	R	*vanA*	Novel	1916	95.52%

Table 1 continued overleaf

Specimen no.	Date of sample[1]	Hospital	H1 Ward[2]	Specimen	Vanc[3]	Vanc Resistance Gene[4]	ST[5]	cgMLST CT[5]	SJ11*vanA*[6]
BSI_SJ15	15/12/2017	H1	W23	BSI	R	*vanA*	787	2273	88.11%
BSI_SJ16	19/12/2017	H1	W19	BSI	R	*vanA*	992	2274	88.16%
BSI_SJ17	20/12/2017	H1	W3	BSI	S	Contains *vanA* remnant, lacks *vanRS*	203	1599	64.92%
BSI_SJ18	22/12/2017	H1	W1	BSI	S	-	787	1920	23.63%
BSI_SJ2	20/09/2017	H1	W1	BSI	R	*vanA*	787	2281	98.47%
BSI_SJ20	27/12/2017	H1	W23	BSI	S	-	203	2276	26.65%
BSI_SJ21	01/01/2018	H1	W5	BSI	R	*vanA*	80	1598	98.63%
BSI_SJ22	08/02/2018	H1	W8	BSI	R	*vanA*	612	2277	98.63%
BSI_SJ23	23/02/2018	H1	W20	BSI	R	*vanA*	80	2278	87.05%
BSI_SJ24	03/03/2018	H1	W1	BSI	S	-	80	2279	24.96%
BSI_SJ25	08/03/2018	H1	W20	BSI	R	*vanA*	80	2278	99.98%
BSI_SJ27	19/03/2018	H1	W8	BSI	R	*vanA*	80	2278	87.09%
BSI_SJ28	13/04/2018	H1	W7	BSI	S	-	787	5148	25.31%
BSI_SJ29	17/04/2018	H1	W6	BSI	S	Contains *vanA* remnant, lacks *vanHAX*	203	2280	76.82%
BSI_SJ3	28/09/2017	H1	W6	BSI	R	*vanA*	787	1920	95.51%
BSI_SJ31	04/05/2018	H1	W4	BSI	R	*vanA*	787	1920	98.64%
BSI_SJ32	05/05/2018	H1	W4	BSI	S	-	203	20	31.49%
BSI_SJ33	11/05/2018	H1	W2	BSI	R	*vanA*	80	1911	88.81%
BSI_SJ34	11/05/2018	H1	W1	BSI	R	*vanA*	787	1920	98.66%
BSI_SJ35	12/05/2018	H1	W24	BSI	S	-	117	2283	30.24%
BSI_SJ36	15/05/2018	H1	W6	BSI	R	*vanA*	1395	2284	98.63%
BSI_SJ37	29/05/2018	H1	W19	BSI	R	*vanA*	80	1598	97.81%
BSI_SJ38	10/06/2018	H1	W1	BSI	R	*vanA*	80	1598	98.63%
BSI_SJ4	03/10/2017	H1	W6	BSI	R	*vanA*	80	1602	88.47%
BSI_SJ40	26/06/2018	H1	W19	BSI	R	*vanA*	80	1598	98.45%

Table 1 continued overleaf

Specimen no.	Date of sample[1]	Hospital	H1 Ward[2]	Specimen	Vanc[3]	Vanc Resistance Gene[4]	ST[5]	cgMLST CT[5]	SJ11*vanA*[6]
BSI_SJ41	29/06/2018	H1	W25	BSI	S	-	80	1697	29.13%
BSI_SJ42	02/07/2018	H1	W1	BSI	R	*vanA*	80	3153	88.14%
BSI_SJ43	08/07/2018	H1	W8	BSI	R	*vanA*	80	2931	99.96%
BSI_SJ44	15/07/2018	H1	W6	BSI	R	*vanA*	80	1598	98.62%
BSI_SJ45	26/07/2018	H1	W8	BSI	S	-	787	1920	24.66%
BSI_SJ46	27/07/2018	H1	W1	BSI	R	*vanA*	80	1598	98.63%
BSI_SJ47	21/08/2018	H1	W3	BSI	R	*vanA*	203	1599	99.97%
BSI_SJ48	14/09/2018	H1	W8	BSI	S	-	267	2951	30.06%
BSI_SJ49	16/09/2018	H1	W6	Screening	R	*vanA* and *vanB*	17	2934	98.56%
BSI_SJ5	07/10/2017	H1	W6	BSI	S	-	203	1599	23.97%
BSI_SJ50	02/11/2018	H1	W3	BSI	S	-	117	2283	46.56%
BSI_SJ52	16/11/2018	H1	W6	BSI	S	-	203	3155	49.94%
BSI_SJ53	07/12/2018	H1	W1	BSI	R	*vanA*	80	2940	99.96%
BSI_SJ54	09/12/2018	H1	W21	BSI	S	Contains *vanA* remnant, lacks *vanHAX*	80	1921	64.59%
BSI_SJ56	21/12/2018	H1	W18	BSI	R	*vanA*	203	1599	98.69%
BSI_SJ57	27/12/2018	H1	W6	BSI	R	*vanA*	2185	1916	95.49%
BSI_SJ58	03/01/2019	H1	W6	BSI	S	-	203	1599	26.78%
BSI_SJ59	05/01/2019	H1	W6	BSI	R	*vanA*	80	2939	99.96%
BSI_SJ6	09/10/2017	H1	W12	BSI	R	*vanA*	80	1598	98.64%
BSI_SJ62	08/01/2019	H1	W24	BSI	R	*vanA*	203	1599	96.75%
BSI_SJ63	09/01/2019	H1	W3	BSI	S	-	80	3157	33.09%
BSI_SJ64	13/01/2019	H1	W21	BSI	S	-	203	1599	24.46%
BSI_SJ65	17/01/2019	H1	W19	BSI	S	-	117	2283	38.74%
BSI_SJ66	22/01/2019	H1	W1	BSI	S	-	80	3158	40.87%
BSI_SJ67	04/02/2019	H1	W30	BSI	S	-	80	1911	29.32%

Table 1 continued overleaf

Specimen no.	Date of sample[1]	Hospital	H1 Ward[2]	Specimen	Vanc[3]	Vanc Resistance Gene[4]	ST[5]	cgMLST CT[5]	SJ11*vanA*[6]
BSI_SJ69	12/02/2019	H1	W28	BSI	R	*vanA*	203	1599	82.68%
BSI_SJ7	11/10/2017	H1	W3	BSI	S	-	80	2286	27.76%
BSI_SJ70	27/02/2019	H1	W16	BSI	R	*vanA*	80	1598	98.61%
BSI_SJ71	06/03/2019	H1	W21	BSI	R	*vanA*	203	2950	98.63%
BSI_SJ72	14/03/2019	H1	W6	BSI	S	-	80	1598	23.55%
BSI_SJ73	20/03/2019	H1	W1	BSI	R	*vanA*	80	1921	98.62%
BSI_SJ74	24/03/2019	H1	W1	BSI	S	-	80	3225	23.59%
BSI_SJ75	31/03/2019	H1	W8	BSI	R	*vanA*	612	2362	98.63%
BSI_SJ76	17/04/2019	H1	W3	BSI	R	*vanA*	80	1911	95.27%
BSI_SJ77	17/04/2019	H1	W1	BSI	S	-	612	3226	23.57%
BSI_SJ78	19/04/2019	H1	W1	BSI	R	*vanA*	117	2283	98.54%
BSI_SJ79	28/04/2019	H1	W6	BSI	R	*vanA*	80	3227	99.92%
BSI_SJ8	16/10/2017	H1	W26	BSI	S	Contains *vanA* remnant, lacks *vanRS*	80	1911	53.53%
BSI_SJ81	06/05/2019	H1	W31	BSI	R	*vanA*	80	2933	98.60%
BSI_SJ82	09/06/2019	H1	W28	BSI	R	*vanA*	18	1898	98.66%
BSI_SJ83	11/06/2019	H1	W1	BSI	R	*vanA*	612	2362	99.96%
BSI_SJ9	30/10/2017	H1	W3	BSI	S	-	789	1601	30.65%
JH002	29/09/2019	H1	W1	Screening	R	*vanA*	80	2931	99.98%
JH003	01/10/2019	H1	W12	Screening	R	*vanA*	80	2932	98.65%
JH004	30/09/2019	H1	W2	Screening	R	*vanA*	80	2932	98.62%
JH005	30/09/2019	H1	W2	Screening	R	*vanA*	80	2933	98.60%
JH006	30/09/2019	H1	W2	Screening	R	*vanA*	80	2932	98.61%
JH007	30/09/2019	H1	W2	Screening	R	*vanA*	80	2932	98.60%
JH008	30/09/2019	H1	W2	Screening	R	*vanA*	80	2932	98.62%
JH009	30/09/2019	H1	W2	Screening	R	*vanA*	80	2932	98.63%

Table 1 continued overleaf

Specimen no.	Date of sample[1]	Hospital	H1 Ward[2]	Specimen	Vanc[3]	Vanc Resistance Gene[4]	ST[5]	cgMLST CT[5]	SJ11*vanA*[6]
JH010	30/09/2019	H1	W2	Screening	R	*vanA* and *vanB*	17	2934	95.89%
JH011	30/09/2019	H1	W12	Screening	R	*vanA*	80	1916	95.50%
JH012	30/09/2019	H1	W24	Screening	R	*vanA*	80	1598	98.61%
JH013	30/09/2019	H1	W33	Screening	R	*vanA*	80	2935	99.98%
JH014	01/10/2019	H1	W37	Screening	R	*vanA*	80	2936	99.96%
JH017	01/10/2019	H1	W1	Screening	R	*vanA*	18	1898	98.64%
JH018	30/09/2019	H1	W6	Screening	R	*vanA*	80	1921	89.11%
JH019	30/09/2019	H1	W6	Screening	R	*vanA*	18	1898	98.57%
JH020	03/10/2019	H1	W33	Screening	R	*vanA*	117	2283	99.95%
JH021	01/10/2019	H1	W36	Screening	R	*vanA*	78	2937	91.57%
JH022	01/10/2019	H1	W6	Screening	R	*vanA* and *vanB*	17	2934	96.26%
JH023	02/10/2019	H1	W10	Screening	R	*vanA*	80	2938	99.96%
JH024	03/10/2019	H1	W27	Screening	R	*vanA*	787	680	99.18%
JH025	02/10/2019	H1	W3	Screening	R	*vanA*	80	2932	98.62%
JH026	02/10/2019	H1	W3	Screening	R	*vanA*	80	1916	95.52%
JH027	02/10/2019	H1	W3	Screening	R	*vanA*	80	2947	99.92%
JH028	02/10/2019	H1	W3	Screening	R	*vanA*	80	2939	88.17%
JH029	02/10/2019	H1	W3	Screening	R	*vanA*	80	2939	88.29%
JH030	02/10/2019	H1	W3	Screening	R	*vanA*	80	2933	98.65%
JH031	02/10/2019	H1	W3	Screening	R	*vanA*	80	2933	98.63%
JH032	02/10/2019	H1	W3	Screening	R	*vanA*	80	1916	95.51%
JH033	02/10/2019	H1	W3	Screening	R	*vanA*	80	2933	97.96%
JH034	02/10/2019	H1	W3	Screening	R	*vanA*	203	1599	98.07%
JH035	02/10/2019	H1	W3	Screening	R	*vanA*	80	1916	95.47%
JH036	02/10/2019	H1	W3	Screening	R	*vanA*	80	2940	99.94%

Table 1 continued overleaf

Specimen no.	Date of sample[1]	Hospital	H1 Ward[2]	Specimen	Vanc[3]	Vanc Resistance Gene[4]	ST[5]	cgMLST CT[5]	SJ11*vanA*[6]
JH037	02/10/2019	H1	W3	Screening	R	*vanA*	80	1916	95.51%
JH038	02/10/2019	H1	W3	Screening	R	*vanA*	80	2986	98.62%
JH039	02/10/2019	H1	W3	Screening	R	*vanA*	80	2941	98.61%
JH040	01/10/2019	H1	W1	Screening	R	*vanA*	80	1916	95.50%
JH041	01/10/2019	H1	W1	Screening	R	*vanA*	612	2362	97.00%
JH042	03/10/2019	H1	W4	Screening	R	*vanA*	612	2942	98.60%
JH043	02/10/2019	H1	W1	Screening	R	*vanA*	80	2933	96.69%
JH044	03/10/2019	H1	W1	Screening	R	*vanA*	80	2987	88.16%
JH045	01/10/2019	H1	W1	Screening	R	*vanA*	80	2933	98.55%
JH046	01/10/2019	H1	W1	Screening	R	*vanA*	80	1916	95.49%
JH047	01/10/2019	H1	W1	Screening	R	*vanA*	80	1598	98.63%
JH048	03/10/2019	H1	W7	Screening	R	*vanA*	80	1916	98.60%
JH049	04/10/2019	H1	W3	Screening	R	*vanA*	80	2940	99.98%
JH050	03/10/2019	H1	W3	Screening	R	*vanA*	80	1916	99.98%
JH051	04/10/2019	H1	W1	Screening	R	*vanA*	80	1921	88.18%
JH052	03/10/2019	H1	W6	Screening	R	*vanA*	612	2362	98.62%
JH053	04/10/2019	H1	W19	Screening	R	*vanA*	80	1916	93.93%
JH054	04/10/2019	H1	W21	Screening	R	*vanA*	80	1916	99.98%
JH055	04/10/2019	H1	W21	Screening	R	*vanA*	80	1916	99.98%
JH056	06/10/2019	H1	W37	Screening	R	*vanA*	80	2989	99.95%
JH057	04/10/2019	H1	W7	Screening	R	*vanA*	80	2931	99.97%
JH058	04/10/2019	H1	W27	Screening	R	*vanA*	80	1602	93.37%
JH059	05/10/2019	H1	W22	Screening	R	*vanA*	80	2936	89.73%
JH060	07/10/2019	H1	W7	Screening	R	*vanA*	80	1916	95.48%
JH061	06/10/2019	H1	W19	Screening	R	*vanA*	80	2938	32.21%

Table 1 continued overleaf

Specimen no.	Date of sample[1]	Hospital	H1 Ward[2]	Specimen	Vanc[3]	Vanc Resistance Gene[4]	ST[5]	cgMLST CT[5]	SJ11*vanA*[6]
JH063	06/10/2019	H1	W6	Screening	R	*vanA*	280	2990	98.46%
JH064	06/10/2019	H1	W6	Screening	R	*vanA*	80	2933	97.18%
JH065	04/10/2019	H1	W1	Screening	R	*vanA*	203	2276	99.59%
JH066	08/10/2019	H1	W2	Screening	R	*vanA*	80	2932	98.64%
JH068	08/10/2019	H1	W2	Screening	R	*vanA*	80	2932	98.61%
JH069	08/10/2019	H1	W4	Screening	R	*vanA*	80	2936	99.95%
JH070	08/10/2019	H1	W1	Screening	R	*vanA*	80	2933	98.65%
JH071	08/10/2019	H1	W1	Screening	R	*vanA*	80	1916	99.96%
JH072	07/10/2019	H1	W25	Screening	R	*vanA*	80	1916	95.47%
JH073	07/10/2019	H1	W8	Screening	R	*vanA*	203	1599	99.98%
JH074	08/10/2019	H1	W27	Screening	R	*vanA*	80	1916	95.49%
JH075	08/10/2019	H1	W29	Screening	R	*vanA*	80	1911	95.32%
JH077	09/10/2019	H1	W16	Screening	R	*vanA*	Novel	3382	91.73%
JH078	08/10/2019	H1	W19	Screening	R	*vanA*	80	2947	98.64%
JH079	09/10/2019	H1	W3	Screening	R	*vanA*	80	1916	97.10%
JH080	09/10/2019	H1	W3	Screening	R	*vanA*	80	1893	97.93%
JH081	09/10/2019	H1	W3	Screening	R	*vanA*	80	2940	99.97%
JH082	09/10/2019	H1	W3	Screening	R	*vanA*	80	1916	99.98%
JH083	10/10/2019	H1	W1	Screening	R	*vanA*	80	2932	98.56%
JH084	10/10/2019	H1	W1	Screening	R	*vanA*	80	3383	95.04%
JH085	10/10/2019	H1	W6	Screening	R	*vanA*	117	2929	99.95%
JH086	11/10/2019	H1	W18	Screening	R	*vanA*	80	2933	99.95%
JH088	10/10/2019	H1	W19	Screening	R	*vanA*	80	1916	95.49%
JH089	11/10/2019	H1	W36	Screening	R	*vanA*	203	1599	99.96%
JH090	12/10/2019	H1	W3	Screening	R	*vanA*	80	2931	99.96%

Table 1 continued overleaf

Specimen no.	Date of sample[1]	Hospital	H1 Ward[2]	Specimen	Vanc[3]	Vanc Resistance Gene[4]	ST[5]	cgMLST CT[5]	SJ11*vanA*[6]
JH091	11/10/2019	H1	W6	Screening	R	*vanA*	80	1916	99.98%
JH092	14/10/2019	H1	W22	Screening	R	*vanA*	80	1598	98.60%
JH093	13/10/2019	H1	W3	Screening	R	*vanA*	80	3383	95.13%
JH094	13/10/2019	H1	W7	Screening	R	*vanA*	80	2933	98.52%
JH095	12/10/2019	H1	W3	Screening	R	*vanA*	80	2931	99.83%
JH096	13/10/2019	H1	W8	Screening	R	*vanA*	80	2931	99.96%
JH097	14/10/2019	H1	W33	Screening	R	*vanA*	80	1916	95.33%
JH098	08/10/2019	H1	W4	Screening	R	*vanA*	Novel	1599	96.48%
JH099	14/10/2019	H1	W2	Screening	R	*vanA*	80	2933	96.26%
JH100	14/10/2019	H1	W18	Screening	R	*vanA*	80	1916	95.96%
JH101	14/10/2019	H1	W36	Screening	R	*vanA*	203	1599	99.96%
JH102	15/10/2019	H1	W33	Screening	R	*vanA*	80	3168	98.61%
JH103	14/10/2019	H1	W6	Screening	R	*vanA*	80	2933	98.57%
JH104	15/10/2019	H1	W30	Screening	R	*vanA*	80	1916	95.59%
JH105	15/10/2019	H1	W24	Screening	R	*vanA*	80	1916	95.49%
JH106	15/10/2019	H1	W5	Screening	R	*vanA*	80	1201	99.96%
JH107	15/10/2019	H1	W24	Screening	R	*vanA*	80	2933	98.65%
JH108	15/10/2019	H1	W5	Screening	R	*vanA*	80	1911	88.25%
JH109	16/10/2019	H1	W22	Screening	R	*vanA*	80	2938	99.95%
JH110	15/10/2019	H1	W37	Screening	R	*vanA*	80	3168	98.61%
JH111	15/10/2019	H1	W6	Screening	R	*vanA*	80	3384	99.16%
JH112	16/10/2019	H1	W3	Screening	R	*vanA*	80	1916	99.97%
JH113	16/10/2019	H1	W3	Screening	R	*vanA*	80	1916	99.96%
JH114	16/10/2019	H1	W7	Screening	R	*vanA*	Novel	3382	89.75%
JH115	16/10/2019	H1	W39	Screening	R	*vanA*	80	3383	95.10%

Table 1 continued overleaf

Specimen no.	Date of sample[1]	Hospital	H1 Ward[2]	Specimen	Vanc[3]	Vanc Resistance Gene[4]	ST[5]	cgMLST CT[5]	SJ11*vanA*[6]
JH116	17/10/2019	H1	W21	Screening	R	*vanA*	80	1916	98.40%
JH117	16/10/2019	H1	W2	Screening	R	*vanA*	203	1599	99.97%
JH118	18/10/2019	H1	W7	Screening	R	*vanA*	80	1598	98.64%
JH120	17/10/2019	H1	W35	Screening	R	*vanA*	612	2942	98.63%
JH121	18/10/2019	H1	W19	Screening	R	*vanA*	262	3166	98.48%
JH122	20/10/2019	H1	W25	Screening	R	*vanA*	80	1916	88.04%
JH123	18/10/2019	H1	W3	Screening	R	*vanA*	612	2942	98.61%
JH124	18/10/2019	H1	W7	Screening	R	*vanA*	80	2932	98.64%
JH125	19/10/2019	H1	W36	Screening	R	*vanA*	80	1916	95.50%
JH126	20/10/2019	H1	W25	Screening	R	*vanA*	80	1916	95.51%
JH127	20/10/2019	H1	W6	Screening	R	*vanA*	80	1921	99.97%
JH128	22/10/2019	H1	W2	Screening	R	*vanA*	80	1916	95.51%
JH129	22/10/2019	H1	W2	Screening	R	*vanA*	80	1921	88.30%
JH130	22/10/2019	H1	W4	Screening	R	*vanA*	80	1916	95.63%
JH131	22/10/2019	H1	W2	Screening	R	*vanA*	80	2933	99.97%
JH132	22/10/2019	H1	W2	Screening	R	*vanA*	80	1921	98.63%
JH133	20/10/2019	H1	W7	Screening	R	*vanA*	80	1916	95.48%
JH136	22/10/2019	H1	W35	Screening	R	*vanA*	80	1598	97.53%
JH137	23/10/2019	H1	W26	Screening	R	*vanA*	80	1921	99.32%
JH138	23/10/2019	H1	W18	Screening	R	*vanA*	80	2938	99.98%
JH140	23/10/2019	H1	W3	Screening	R	*vanA*	80	3385	99.98%
JH141	23/10/2019	H1	W33	Screening	R	*vanA*	203	2950	98.63%
JH142	23/10/2019	H1	W3	Screening	R	*vanA*	80	3385	99.96%
JH143	24/10/2019	H1	W36	Screening	R	*vanA*	80	1916	95.49%
JH144	24/10/2019	H1	W4	Screening	R	*vanA*	80	2932	98.66%

Table 1 continued overleaf

Specimen no.	Date of sample[1]	Hospital	H1 Ward[2]	Specimen	Vanc[3]	Vanc Resistance Gene[4]	ST[5]	cgMLST CT[5]	SJ11*vanA*[6]
JH145	23/10/2019	H1	W1	Screening	R	*vanA*	80	2933	98.47%
JH146	23/10/2019	H1	W2	Screening	R	*vanA*	80	1921	99.16%
JH147	25/10/2019	H1	W3	Screening	R	*vanA*	80	2933	98.63%
JH148	24/10/2019	H1	W21	Screening	R	*vanA*	80	3386	99.97%
JH149	25/10/2019	H1	W16	Screening	R	*vanA*	80	1916	95.49%
JH150	24/10/2019	H1	W3	Screening	R	*vanA*	80	2932	98.63%
JH151	24/10/2019	H1	W3	Screening	R	*vanA*	80	2931	99.97%
JH152	24/10/2019	H1	W24	Screening	R	*vanA*	80	1921	88.95%
JH153	26/10/2019	H1	W1	Screening	R	*vanA*	18	3387	83.86%
JH154	28/10/2019	H1	W1	Screening	R	*vanA*	80	3163	98.62%
JH155	29/10/2019	H1	W3	Screening	R	*vanA*	80	1916	95.51%
JH156	29/10/2019	H1	W24	Screening	R	*vanA*	80	1598	98.68%
JH157	28/10/2019	H1	W22	Screening	R	*vanA*	80	2933	95.84%
JH158	30/10/2019	H1	W8	Screening	R	*vanA*	80	2933	96.50%
JH159	29/10/2019	H1	W6	Screening	R	*vanA*	80	1916	99.96%
JH160	29/10/2019	H1	W27	Screening	R	*vanA*	80	2931	99.97%
JH161	29/10/2019	H1	W8	Screening	R	*vanA*	80	1916	95.49%
JH162	26/10/2019	H1	W7	Screening	R	*vanA*	80	2947	98.61%
JH163	29/10/2019	H1	W24	Screening	R	*vanA*	80	2933	99.97%
JH164	29/10/2019	H1	W6	Screening	R	*vanA*	80	2933	98.61%
JH165	30/10/2019	H1	W12	Screening	R	*vanA*	80	2931	99.97%
JH166	29/10/2019	H1	W1	Screening	R	*vanA*	612	2942	96.97%
JH167	29/10/2019	H1	W1	Screening	R	*vanA*	612	2942	96.98%
JH168	29/10/2019	H1	W12	Screening	R	*vanA*	17	3381	18.55%
JH169	29/10/2019	H1	W1	Screening	R	*vanA*	80	2932	98.65%

Table 1 continued overleaf

Specimen no.	Date of sample[1]	Hospital	H1 Ward[2]	Specimen	Vanc[3]	Vanc Resistance Gene[4]	ST[5]	cgMLST CT[5]	SJ11*vanA*[6]
JH170	30/10/2019	H1	W18	Screening	R	*vanA*	80	2936	98.66%
JH171	30/10/2019	H1	W3	Screening	R	*vanA*	80	3385	99.97%
JH172	30/10/2019	H1	W3	Screening	R	*vanA*	1395	3169	98.65%
JH173	30/10/2019	H1	W3	Screening	R	*vanA*	203	1599	99.96%
JH174	30/10/2019	H1	W35	Screening	R	*vanA*	203	1599	98.64%
JH175	31/10/2019	H1	W3	Screening	R	*vanA*	80	1916	98.40%
JH176	30/10/2019	H1	W3	Screening	R	*vanA*	80	1916	98.40%
JH177	31/10/2019	H1	W1	Screening	R	*vanA* and *vanB*	17	3381	99.94%
JH178	01/11/2019	H1	W7	Screening	R	*vanA*	80	1916	95.50%
JH179	03/11/2019	H1	W12	Screening	R	*vanA*	80	1598	99.96%
JH180	01/11/2019	H1	W22	Screening	R	*vanA*	80	2933	95.16%
JH181	02/11/2019	H1	W7	Screening	R	*vanA*	80	1911	98.60%
JH182	02/11/2019	H1	W37	Screening	R	*vanA*	80	2931	99.97%
JH183	04/11/2019	H1	W22	Screening	R	*vanA*	80	1916	95.51%
JH184	03/11/2019	H1	W3	Screening	R	*vanA*	203	1599	98.62%
JH185	03/11/2019	H1	W19	Screening	R	*vanA*	1395	3169	98.62%
JH186	05/11/2019	H1	W2	Screening	R	*vanA*	80	2933	95.22%
JH187	05/11/2019	H1	W1	Screening	R	*vanA*	80	3385	99.98%
JH188	04/11/2019	H1	W2	Screening	R	*vanA*	80	2933	95.13%
JH189	04/11/2019	H1	W33	Screening	R	*vanA*	80	3168	99.98%
JH190	04/11/2019	H1	W22	Screening	R	*vanA*	80	1916	95.50%
JH191	05/11/2019	H1	W18	Screening	R	*vanA*	203	2276	96.94%
JH192	04/11/2019	H1	W26	Screening	R	*vanA*	80	2933	95.19%
JH193	04/11/2019	H1	W19	Screening	R	*vanA*	80	1916	94.47%
JH194	04/11/2019	H1	W35	Screening	R	*vanA*	80	1602	88.25%

Table 1 continued overleaf

Specimen no.	Date of sample[1]	Hospital	H1 Ward[2]	Specimen	Vanc[3]	Vanc Resistance Gene[4]	ST[5]	cgMLST CT[5]	SJ11*vanA*[6]
JH195	04/11/2019	H1	W4	Screening	R	*vanA*	80	3394	99.97%
JH196	05/11/2019	H1	W5	Screening	R	*vanA*	80	1916	95.47%
JH197	05/11/2019	H1	W5	Screening	R	*vanA*	80	2933	98.64%
JH198	05/11/2019	H1	W24	Screening	R	*vanA*	80	1916	95.50%
JH199	05/11/2019	H1	W6	Screening	R	*vanA*	280	2990	99.79%
JH200	05/11/2019	H1	W5	Screening	R	*vanA*	612	5070	98.69%
JH201	05/11/2019	H1	W5	Screening	R	*vanA*	80	2933	95.18%
JH202	05/11/2019	H1	W5	Screening	R	*vanA*	80	2933	98.65%
JH203	05/11/2019	H1	W37	Screening	R	*vanA*	80	2933	95.17%
JH204	05/11/2019	H1	W5	Screening	R	*vanA*	80	2933	98.48%
JH205	05/11/2019	H1	W5	Screening	R	*vanA*	80	2933	99.96%
JH206	06/11/2019	H1	W3	Screening	R	*vanA*	80	1916	98.39%
JH207	07/11/2019	H1	W7	Screening	R	*vanA*	80	1916	98.60%
JH209	06/11/2019	H1	W3	Screening	R	*vanA*	80	3163	98.66%
JH210	06/11/2019	H1	W3	Screening	R	*vanA*	80	2932	98.65%
JH211	05/11/2019	H1	W1	Screening	R	*vanA*	80	2933	95.16%
JH212	06/11/2019	H1	W1	Screening	R	*vanA*	203	1599	98.64%
JH213	06/11/2019	H1	W1	Screening	R	*vanA*	80	3168	98.61%
JH214	05/11/2019	H1	W1	Screening	R	*vanA* and *vanB*	17	2934	96.26%
JH215	07/11/2019	H1	W24	Screening	R	*vanA*	612	2362	98.65%
JH216	07/11/2019	H1	W20	Screening	R	*vanA*	80	2932	98.63%
JH217	07/11/2019	H1	W31	Screening	R	*vanA*	80	2987	91.54%
JH218	08/11/2019	H1	W3	Screening	R	*vanA*	80	2932	98.66%
JH219	09/11/2019	H1	W7	Screening	R	*vanA* and *vanB*	17	2934	94.92%
JH220	08/11/2019	H1	W27	Screening	R	*vanA*	117	2283	99.95%

Table 1 continued overleaf

Specimen no.	Date of sample[1]	Hospital	H1 Ward[2]	Specimen	Vanc[3]	Vanc Resistance Gene[4]	ST[5]	cgMLST CT[5]	SJ11*vanA*[6]
JH221	11/11/2019	H1	W18	Screening	R	*vanA*	80	2933	98.42%
JH222	04/11/2019	H1	W16	Screening	R	*vanA*	80	1598	98.60%
JH223	11/11/2019	H1	W1	Screening	R	*vanA*	80	1201	99.98%
JH225	07/11/2019	H1	W12	Screening	R	*vanA*	80	3168	98.61%
JH226	10/11/2019	H1	W2	Screening	R	*vanA*	80	2933	98.57%
JH227	12/11/2019	H1	W1	Screening	R	*vanA*	80	2932	98.62%
JH228	08/11/2019	H1	W2	Screening	R	*vanA*	80	2933	99.90%
JH229	11/11/2019	H1	W8	Screening	R	*vanA*	80	2933	95.18%
JH230	10/11/2019	H1	W3	Screening	R	*vanA*	80	2932	98.61%
JH231	11/11/2019	H1	W8	Screening	R	*vanA*	80	1916	95.51%
JH232	11/11/2019	H1	W34	Screening	R	*vanA*	80	2932	98.64%
JH233	12/11/2019	H1	W37	Screening	R	*vanA*	80	1921	85.27%
JH234	12/11/2019	H1	W2	Screening	R	*vanA*	80	2931	100.00%
JH235	11/11/2019	H1	W2	Screening	R	*vanA*	80	2933	95.02%
JH236	12/11/2019	H1	W30	Screening	R	*vanA*	80	1916	95.47%
JH237	12/11/2019	H1	W24	Screening	R	*vanA*	80	7024	98.62%
JH239	12/11/2019	H1	W34	Screening	R	*vanA*	80	2933	98.64%
JH241	13/11/2019	H1	W3	Screening	R	*vanA*	80	2931	99.96%
JH242	13/11/2019	H1	W3	Screening	R	*vanA*	80	2933	99.70%
JH243	13/11/2019	H1	W3	Screening	R	*vanA*	80	1916	95.99%
JH244	13/11/2019	H1	W7	Screening	R	*vanA*	80	1467	98.62%
JH245	13/11/2019	H1	W8	Screening	R	*vanA*	80	1911	99.98%
JH246	12/11/2019	H1	W1	Screening	R	*vanA*	80	3385	99.98%
JH247	13/11/2019	H1	W3	Screening	R	*vanA*	80	1916	95.51%
JH248	12/11/2019	H1	W2	Screening	R	*vanA*	80	3168	99.12%

Table 1 continued overleaf

Specimen no.	Date of sample[1]	Hospital	H1 Ward[2]	Specimen	Vanc[3]	Vanc Resistance Gene[4]	ST[5]	cgMLST CT[5]	SJ11*vanA*[6]
JH251	14/11/2019	H1	W4	Screening	R	*vanA*	18	1898	98.62%
JH252	14/11/2019	H1	W7	Screening	R	*vanA*	80	2933	98.63%
JH253	14/11/2019	H1	W21	Screening	R	*vanA*	80	1598	98.64%
JH254	16/11/2019	H1	W25	Screening	R	*vanA*	80	7025	25.12%
JH255	15/11/2019	H1	W27	Screening	R	*vanA*	80	1911	88.13%
JH256	14/11/2019	H1	GP	Screening	R	*vanA*	80	2933	99.94%
JH257	16/11/2019	H1	W1	Screening	R	*vanA*	80	2933	95.19%
JH258	19/11/2019	H1	W2	Screening	R	*vanA*	80	2932	98.66%
JH259	19/11/2019	H1	W2	Screening	R	*vanA*	80	3168	98.63%
JH260	19/11/2019	H1	W1	Screening	R	*vanA*	80	2932	98.64%
JH261	18/11/2019	H1	W2	Screening	R	*vanA*	80	2933	95.19%
JH262	19/11/2019	H1	W2	Screening	R	*vanA*	80	3168	98.62%
JH263	18/11/2019	H1	W2	Screening	R	*vanA*	80	2933	95.10%
JH264	18/11/2019	H1	W2	Screening	R	*vanA*	80	2933	95.11%
JH265	18/11/2019	H1	W6	Screening	R	*vanA*	80	2933	98.45%
JH268	20/11/2019	H1	W3	Screening	R	*vanA*	80	1916	95.47%
JH269	20/11/2019	H1	W7	Screening	R	*vanA*	80	1911	90.21%
JH270	20/11/2019	H1	W37	Screening	R	*vanA*	80	2933	98.66%
JH271	20/11/2019	H1	W7	Screening	R	*vanA*	80	6281	99.83%
JH272	21/11/2019	H1	W1	Screening	R	*vanA*	80	1921	96.73%
JH273	22/11/2019	H1	W18	Screening	R	*vanA*	203	2950	98.63%
JH274	21/11/2019	H1	W7	Screening	R	*vanA*	80	2933	99.94%
JH275	21/11/2019	H1	W37	Screening	R	*vanA*	80	2947	98.62%
JH276	21/11/2019	H1	W16	Screening	R	*vanA*	80	2932	98.63%
JH277	21/11/2019	H1	W26	Screening	R	*vanA*	80	1598	95.47%

Table 1 continued overleaf

Specimen no.	Date of sample[1]	Hospital	H1 Ward[2]	Specimen	Vanc[3]	Vanc Resistance Gene[4]	ST[5]	cgMLST CT[5]	SJ11*vanA*[6]
JH278	24/11/2019	H1	W3	Screening	R	*vanA*	80	2933	93.24%
JH279	24/11/2019	H1	W25	Screening	R	*vanA* and *vanB*	17	2934	98.62%
JH280	23/11/2019	H1	W3	Screening	R	*vanA*	80	1916	99.98%
JH281	24/11/2019	H1	W25	Screening	R	*vanA*	612	2942	88.15%
JH282	22/11/2019	H1	W3	Screening	R	*vanA*	18	1898	98.68%
JH283	24/11/2019	H1	W18	Screening	R	*vanA*	80	5981	95.22%
JH285	22/11/2019	H1	W31	Screening	R	*vanA*	80	2931	98.57%
JH286	22/11/2019	H1	W31	Screening	R	*vanA*	80	1916	99.90%
JH287	22/11/2019	H1	W31	Screening	R	*vanA*	203	1599	88.30%
JH288	23/11/2019	H1	W8	Screening	R	*vanA*	80	2932	99.98%
JH289	26/11/2019	H1	W2	Screening	R	*vanA*	80	1916	98.45%
JH290	26/11/2019	H1	W2	Screening	R	*vanA*	80	3168	95.46%
JH292	26/11/2019	H1	W2	Screening	R	*vanA*	80	5981	99.95%
JH293	26/11/2019	H1	W2	Screening	R	*vanA*	80	3168	98.57%
JH294	26/11/2019	H1	W2	Screening	R	*vanA*	80	5981	99.97%
JH295	25/11/2019	H1	W38	Screening	R	*vanA*	80	1598	98.64%
JH296	25/11/2019	H1	W26	Screening	R	*vanA*	80	2933	98.45%
JH297	25/11/2019	H1	W4	Screening	R	*vanA*	80	1916	93.72%
JH298	27/11/2019	H1	W21	Screening	R	*vanA*	80	2933	95.17%
JH299	26/11/2019	H1	W37	Screening	R	*vanA*	117	2283	99.97%
JH300	26/11/2019	H1	W34	Screening	R	*vanA*	117	2283	99.97%
JH301	27/11/2019	H1	W3	Screening	R	*vanA*	80	2932	98.62%
JH302	26/11/2019	H1	W8	Screening	R	*vanA*	203	1599	99.95%
JH303	27/11/2019	H1	W30	Screening	R	*vanA*	203	1599	83.22%
JH304	27/11/2019	H1	W3	Screening	R	*vanA*	80	1916	95.50%

Table 1 continued overleaf

Specimen no.	Date of sample[1]	Hospital	H1 Ward[2]	Specimen	Vanc[3]	Vanc Resistance Gene[4]	ST[5]	cgMLST CT[5]	SJ11*vanA*[6]
JH305	27/11/2019	H1	W3	Screening	R	*vanA*	80	2933	98.63%
JH306	27/11/2019	H1	W3	Screening	R	*vanA*	80	1911	99.97%
JH309	27/11/2019	H1	W3	Screening	R	*vanA*	80	2933	99.97%
JH310	28/11/2019	H1	W37	Screening	R	*vanA*	80	6282	88.79%
JH311	27/11/2019	H1	W4	Screening	R	*vanA*	80	1911	99.96%
JH312	27/11/2019	H1	W24	Screening	R	*vanA*	80	2933	99.95%
JH313	27/11/2019	H1	W31	Screening	R	*vanA*	80	2987	89.11%
JH314	26/11/2019	H1	W12	Screening	R	*vanA*	80	2933	98.57%
JH315	27/11/2019	H1	W1	Screening	R	*vanA*	80	2931	99.96%
JH316	27/11/2019	H1	W19	Screening	R	*vanA*	80	2931	99.96%
JH317	28/11/2019	H1	W25	Screening	R	*vanA*	80	1916	99.97%
JH318	01/12/2019	H1	W37	Screening	R	*vanA*	80	2936	90.34%
JH319	29/11/2019	H1	W3	Screening	R	*vanA*	612	2942	98.63%
JH320	29/11/2019	H1	W7	Screening	R	*vanA*	80	2933	98.63%
JH321	29/11/2019	H1	W7	Screening	R	*vanA*	80	2936	89.36%
JH322	29/11/2019	H1	W4	Screening	R	*vanA*	80	3168	98.62%
JH323	03/12/2019	H1	W1	Screening	R	*vanA*	612	2942	98.88%
JH324	03/12/2019	H1	W12	Screening	R	*vanA*	80	2933	98.60%
JH325	03/12/2019	H1	W2	Screening	R	*vanA*	80	2931	99.96%
JH326	02/12/2019	H1	W3	Screening	R	*vanA*	80	2933	96.21%
JH327	02/12/2019	H1	W21	Screening	R	*vanA*	203	2950	89.94%
JH328	02/12/2019	H1	W18	Screening	R	*vanA*	80	3168	98.62%
JH329	03/12/2019	H1	GP	Screening	R	*vanA*	80	1602	95.41%
JH330	03/12/2019	H1	W25	Screening	R	*vanA*	612	2942	98.63%
JH331	04/12/2019	H1	W3	Screening	R	*vanA*	203	1599	99.96%

Table 1 continued overleaf

Specimen no.	Date of sample[1]	Hospital	H1 Ward[2]	Specimen	Vanc[3]	Vanc Resistance Gene[4]	ST[5]	cgMLST CT[5]	SJ11*vanA*[6]
JH332	04/12/2019	H1	W3	Screening	R	*vanA*	80	1911	99.96%
JH333	03/12/2019	H1	W7	Screening	R	*vanA*	80	1911	95.53%
JH334	03/12/2019	H1	W7	Screening	R	*vanA*	80	1598	98.63%
JH335	03/12/2019	H1	W37	Screening	R	*vanA*	80	1911	98.62%
JH336	04/12/2019	H1	GP	Screening	R	*vanA*	80	1911	88.29%
JH337	04/12/2019	H1	W3	Screening	R	*vanA*	80	2933	98.66%
JH338	04/12/2019	H1	W34	Screening	R	*vanA*	80	1921	99.96%
JH340	03/12/2019	H1	W2	Screening	R	*vanA*	80	2931	99.95%
JH341	05/12/2019	H1	W10	Screening	R	*vanA*	80	1916	88.18%
JH342	05/12/2019	H1	W1	Screening	R	*vanA*	80	6420	88.18%
JH343	05/12/2019	H1	GP	Screening	R	*vanA*	80	1916	98.64%
JH344	05/12/2019	H1	W5	Screening	R	*vanA*	203	1599	96.27%
JH345	05/12/2019	H1	W5	Screening	R	*vanA*	80	1916	95.50%
JH346	07/12/2019	H1	W8	Screening	R	*vanA*	80	1921	85.74%
JH347	07/12/2019	H1	W22	Screening	R	*vanA*	80	2933	98.66%
JH348	07/12/2019	H1	W34	Screening	R	*vanA*	80	2932	98.63%
JH349	07/12/2019	H1	W33	Screening	R	*vanA*	80	1921	98.64%
JH350	09/12/2019	H1	GP	Screening	R	*vanB*	18	1463	33.22%
JH351	06/12/2019	H1	W1	Screening	R	*vanA*	80	1916	95.48%
JH352	10/12/2019	H1	W2	Screening	R	*vanA*	80	2933	98.63%
JH353	08/12/2019	H1	W1	Screening	R	*vanA*	80	6421	89.24%
JH354	10/12/2019	H1	W2	Screening	R	*vanA*	80	5981	99.98%
JH355	10/12/2019	H1	W1	Screening	R	*vanA*	80	2933	95.19%
JH356	09/12/2019	H1	W3	Screening	R	*vanA*	80	2933	88.93%
JH357	09/12/2019	H1	W1	Screening	R	*vanA*	80	2933	95.20%

Table 1 continued overleaf

Specimen no.	Date of sample[1]	Hospital	H1 Ward[2]	Specimen	Vanc[3]	Vanc Resistance Gene[4]	ST[5]	cgMLST CT[5]	SJ11*vanA*[6]
JH360	10/12/2019	H1	W37	Screening	R	*vanA*	80	1916	96.19%
JH361	10/12/2019	H1	W8	Screening	R	*vanA*	80	2938	99.18%
JH362	09/12/2019	H1	W8	Screening	R	*vanA*	612	2942	98.61%
JH363	09/12/2019	H1	W3	Screening	R	*vanA*	80	3385	99.99%
JH364	12/12/2019	H1	W38	Screening	R	*vanA*	80	2947	98.61%
JH365	11/12/2019	H1	W8	Screening	R	*vanA*	Novel	6422	98.63%
JH366	12/12/2019	H1	W8	Screening	R	*vanA*	80	1916	69.67%
JH367	12/12/2019	H1	W16	Screening	R	*vanA*	80	1916	95.59%
JH368	12/12/2019	H1	W18	Screening	R	*vanA*	80	2278	84.22%
JH369	11/12/2019	H1	W3	Screening	R	*vanA*	80	1916	95.48%
JH370	11/12/2019	H1	W3	Screening	R	*vanA*	80	2933	99.97%
JH371	11/12/2019	H1	W3	Screening	R	*vanA*	80	1916	95.49%
JH372	12/12/2019	H1	W34	Screening	R	*vanA*	80	1921	99.93%
JH373	13/12/2019	H1	W18	Screening	R	*vanA*	80	3385	99.92%
JH374	14/12/2019	H1	W7	Screening	R	*vanA*	80	2933	95.16%
JH375	15/12/2019	H1	W7	Screening	R	*vanA*	80	1921	82.85%
JH376	15/12/2019	H1	W16	Screening	R	*vanA*	612	2942	98.61%
JH377	17/12/2019	H1	W2	Screening	R	*vanA*	80	2932	99.67%
JH378	17/12/2019	H1	W1	Screening	R	*vanA*	80	1916	95.50%
JH379	17/12/2019	H1	W2	Screening	R	*vanA*	80	2932	98.63%
JH381	16/12/2019	H1	W35	Screening	R	*vanA*	80	1916	95.49%
JH382	13/12/2019	H1	W3	Screening	R	*vanA*	80	2940	88.34%
JH383	15/12/2019	H1	W27	Screening	R	*vanA*	18	1898	98.62%
JH384	13/12/2019	H1	W3	Screening	R	*vanA*	80	1916	92.46%
JH385	14/12/2019	H1	W5	Screening	R	*vanA*	612	2942	98.63%

Table 1 continued overleaf

Specimen no.	Date of sample[1]	Hospital	H1 Ward[2]	Specimen	Vanc[3]	Vanc Resistance Gene[4]	ST[5]	cgMLST CT[5]	SJ11*vanA*[6]
JH386	13/12/2019	H1	W24	Screening	R	*vanA*	80	2933	98.56%
JH387	13/12/2019	H1	W3	Screening	R	*vanA*	80	2932	98.61%
JH388	17/12/2019	H1	W7	Screening	R	*vanA*	80	2931	91.21%
JH389	13/12/2019	H1	W18	Screening	R	*vanA*	80	1916	95.50%
JH390	13/12/2019	H1	W36	Screening	R	*vanA*	80	7018	95.47%
JH391	15/12/2019	H1	W8	Screening	R	*vanA*	80	2931	98.87%
JH392	17/12/2019	H1	W6	Screening	R	*vanA*	80	1916	95.49%
JH393	17/12/2019	H1	W34	Screening	R	*vanA*	80	3168	98.64%
JH395	18/12/2019	H1	W25	Screening	R	*vanA*	80	1916	95.48%
JH396	19/12/2019	H1	W16	Screening	R	*vanA*	80	6615	99.16%
JH397	19/12/2019	H1	W22	Screening	R	*vanA*	80	3225	98.64%
JH398	18/12/2019	H1	W22	Screening	R	*vanA*	80	2932	98.61%
JH399	18/12/2019	H1	W34	Screening	R	*vanA*	80	2933	98.97%
JH400	19/12/2019	H1	W1	Screening	R	*vanA*	80	1893	98.60%
JH401	19/12/2019	H1	W3	Screening	R	*vanA*	80	2933	99.92%
JH402	18/12/2019	H1	W3	Screening	R	*vanA*	80	1916	95.49%
JH403	19/12/2019	H1	W16	Screening	R	*vanA*	80	2931	99.96%
JH404	18/12/2019	H1	W3	Screening	R	*vanA*	80	1916	95.49%
JH405	18/12/2019	H1	W3	Screening	R	*vanA*	80	2932	98.63%
JH406	21/12/2019	H1	W18	Screening	R	*vanA*	80	1598	98.62%
JH407	22/12/2019	H1	W27	Screening	R	*vanA*	17	2934	96.27%
JH408	21/12/2019	H1	W27	Screening	R	*vanA* and *vanB*	80	2932	98.64%
JH409	22/12/2019	H1	W16	Screening	R	*vanA*	80	1921	83.65%
JH410	21/12/2019	H1	W8	Screening	R	*vanA*	80	7019	95.46%
JH411	23/12/2019	H1	W1	Screening	R	*vanA*	80	2932	99.37%

Table 1 continued overleaf

Specimen no.	Date of sample[1]	Hospital	H1 Ward[2]	Specimen	Vanc[3]	Vanc Resistance Gene[4]	ST[5]	cgMLST CT[5]	SJ11*vanA*[6]
JH412	23/12/2019	H1	W16	Screening	R	*vanA*	80	2933	98.63%
JH413	24/12/2019	H1	W3	Screening	R	*vanA*	80	1916	99.94%
JH414	24/12/2019	H1	W1	Screening	R	*vanA*	80	6420	89.38%
JH415	26/12/2019	H1	W1	Screening	R	*vanA*	80	1916	96.13%
JH416	24/12/2019	H1	W16	Screening	R	*vanA*	80	1916	98.40%
JH417	25/12/2019	H1	W3	Screening	R	*vanA*	80	1916	99.98%
JH418	25/12/2019	H1	W3	Screening	R	*vanA*	80	2932	98.58%
JH419	25/12/2019	H1	W3	Screening	R	*vanA*	80	6421	88.44%
JH420	25/12/2019	H1	W3	Screening	R	*vanA*	80	1916	97.59%
JH421	25/12/2019	H1	W3	Screening	R	*vanA*	18	1898	96.50%
JH422	25/12/2019	H1	W3	Screening	R	*vanA*	80	3168	98.63%
JH423	27/12/2019	H1	W27	Screening	R	*vanA*	80	1916	95.49%
JH424	26/12/2019	H1	W3	Screening	R	*vanA*	80	1916	95.62%
JH425	26/12/2019	H1	W21	Screening	R	*vanA*	80	2933	98.36%
JH426	24/12/2019	H1	W19	Screening	R	*vanA*	80	1911	88.16%
JH427	24/12/2019	H1	W3	Screening	R	*vanA*	80	2933	98.60%
JH428	28/12/2019	H1	W3	Screening	R	*vanA* and *vanB*	17	2934	95.98%
JH76	09/10/2019	H1	W16	Screening	R	*vanA* and *vanB*	17	3381	97.43%
MH204	16/06/2021	H3	U	Screening	R	*vanA*	2052	1599	99.93%
MH205	16/06/2021	H3	U	Screening	R	*vanA*	2052	1599	99.97%
MH206	16/06/2021	H3	U	Screening	R	*vanA*	2052	1599	99.98%
MH207	16/06/2021	H3	U	Screening	R	*vanA*	80	5991	90.83%
MH518	26/01/2022	H3	U	Surgical wound	R	*vanA*	80	6489	95.47%
MH519	26/01/2022	H3	U	Surgical wound	R	*vanA*	80	6489	99.96%
MH520	26/01/2022	H3	U	Surgical wound	R	*vanA*	80	3168	94.23%

Table 1 continued overleaf

Specimen no.	Date of sample[1]	Hospital	H1 Ward[2]	Specimen	Vanc[3]	Vanc Resistance Gene[4]	ST[5]	cgMLST CT[5]	SJ11*vanA*[6]
MH521	26/01/2022	H3	U	Screening	R	*vanA*	80	6510	99.97%
MH678	06/06/2022	H3	U	Screening	R	*vanA*	80	2933	98.60%
MH679	06/06/2022	H3	U	Screening	R	*vanA*	80	6489	99.96%
RC-19-001	04/10/2019	H5	U	BSI	S	-	80	3388	28.08%
RC-19-002	U	H5	U	BSI	S	-	203	1599	35.17%
RC-19-003	11/10/2019	H5	U	BSI	S	-	203	1599	26.02%
RC-19-004	12/10/2019	H5	U	BSI	S	-	787	1920	28.59%
RC-19-005	19/10/2019	H5	U	BSI	S	-	203	1599	37.56%
RC-19-006	31/10/2019	H5	U	BSI	S	-	80	1893	30.43%
RC-19-007	25/10/2019	H5	U	BSI	S	-	80	2932	37.61%
RC-19-008	28/10/2019	H5	U	BSI	R	*vanA*	80	3227	99.95%
RC-19-009	11/11/2019	H5	U	Screening	R	*vanA*	80	3227	99.95%
RC-19-011	14/11/2019	H5	U	Screening	R	*vanA*	80	1921	91.27%
RC-19-012	15/11/2019	H5	U	Screening	R	*vanA*	80	2939	88.15%
RC-19-013	15/11/2019	H5	U	Screening	R	*vanA*	80	2932	98.63%
RC-19-014	18/11/2019	H5	U	Screening	R	*vanA*	80	1921	99.96%
RC-19-015	15/11/2019	H5	U	Screening	R	*vanA*	80	2933	99.97%
RC-19-016	14/11/2019	H5	U	Screening	R	*vanA*	80	1921	98.62%
RC-19-019	19/11/2019	H5	U	Screening	R	*vanA*	80	2939	99.99%
RC-19-020	24/11/2019	H5	U	Screening	R	*vanA*	80	3384	90.68%
RC-19-021	24/11/2019	H5	U	Screening	R	*vanA*	80	2939	99.96%
RC-19-022	22/11/2019	H5	U	Screening	R	*vanA*	80	2947	89.22%
RC-19-023	20/11/2019	H5	U	Screening	R	*vanA*	80	1916	90.88%
RC-19-024	11/11/2019	H5	U	Screening	R	*vanA*	80	1893	99.96%
RC-19-025	13/11/2019	H5	U	Screening	R	*vanA*	80	2932	98.62%

Table 1 continued overleaf

Specimen no.	Date of sample[1]	Hospital	H1 Ward[2]	Specimen	Vanc[3]	Vanc Resistance Gene[4]	ST[5]	cgMLST CT[5]	SJ11*vanA*[6]
RC-19-026	13/11/2019	H5	U	Screening	R	*vanA*	80	2933	88.18%
RC-19-028	U	H6	U	BSI	S	-	80	3389	32.53%
RC-19-029	U	H6	U	BSI	S	-	80	1921	25.09%
RC-19-030	22/11/2019	H6	U	Screening	R	*vanA*	80	1598	98.66%
RC-19-031	22/11/2019	H6	U	Screening	R	*vanA*	203	1599	88.38%
RC-19-032	U	H6	U	BSI	S	-	80	2933	27.72%
RC-19-033	15/11/2019	H6	U	Screening	R	*vanA* and *vanB*	17	2934	0.00%
RC-19-034	12/11/2019	H6	U	Screening	R	*vanA*	203	3390	98.63%
RC-19-035	U	H6	U	BSI	R	*vanA*	80	3385	99.98%
RC-19-036	04/12/2019	H6	U	BSI	S	Contains *vanA*+*vanB* remnant, lacks *vanRS*	17	2934	74.80%
RC-19-037	12/11/2019	H6	U	Screening	R	*vanA*	80	2933	98.63%
RC-19-038	11/11/2019	H6	U	Screening	R	*vanA*	203	1599	99.95%
RC-19-039	12/11/2019	H6	U	Screening	R	*vanA* and *vanB*	17	2934	98.00%
RC-19-040	12/11/2019	H6	U	Screening	R	*vanA*	18	1898	99.91%
RC-19-041	15/11/2019	H6	U	Screening	R	*vanA*	787	1920	86.69%
RC-19-042	U	H6	U	BSI	S	-	80	1921	27.31%
RC-19-043	19/11/2019	H6	U	Screening	R	*vanA*	80	3391	99.95%
RC-19-044	27/11/2019	H5	U	BSI	S	-	80	2933	23.52%
RC-19-045	19/11/2019	H5	U	BSI	R	*vanA*	80	2932	98.61%
RC-19-046	U	H7	U	Screening	R	*vanA*	787	1914	99.18%
RC-19-049	U	H7	U	Screening	R	*vanA*	612	3392	99.96%
RC-19-050	U	H6	U	BSI	S	-	203	1599	23.69%
RC-19-051	U	H6	U	BSI	R	*vanA*	203	1599	99.97%
RC-19-052	10/11/2019	H6	U	Screening	R	*vanA*	80	1598	98.61%
RC-19-053	19/11/2019	H6	U	Screening	R	*vanA*	80	1598	99.25%

Table 1 continued overleaf

Specimen no.	Date of sample[1]	Hospital	H1 Ward[2]	Specimen	Vanc[3]	Vanc Resistance Gene[4]	ST[5]	cgMLST CT[5]	SJ11*vanA*[6]
RC-19-054	U	H6	U	BSI	S	Contains *vanA* remnant, lacks *vanHAX*	80	2933	79.86%
RC-19-055	11/11/2019	H6	U	Screening	R	*vanA*	80	1916	98.63%
RC-19-056	16/11/2019	H6	U	Screening	R	*vanA*	787	1920	90.39%
RC-19-057	U	H6	U	BSI	S	-	787	1920	57.19%
RC-19-058	U	H6	U	BSI	S	-	80	1921	25.16%
RC-19-059	U	H6	U	BSI	S	-	80	2933	35.66%
RC-19-060	18/11/2019	H6	U	Screening	R	*vanA*	80	1921	98.61%
RC-19-061	15/11/2019	H6	U	Screening	R	*vanA*	80	1916	99.20%
RC-19-062	08/11/2019	H2	U	Screening	R	*vanA*	80	1916	93.23%
RC-19-063	08/11/2019	H2	U	Screening	R	*vanA*	80	2933	96.91%
RC-19-064	10/11/2019	H2	U	Screening	R	*vanA*	203	1599	99.96%
RC-19-065	11/11/2019	H2	U	Screening	R	*vanA*	80	2933	95.12%
RC-19-066	11/11/2019	H2	U	Screening	R	*vanA*	80	2933	95.10%
RC-19-067	11/11/2019	H2	U	Screening	R	*vanA*	80	3383	95.13%
RC-19-068	12/11/2019	H2	U	Screening	R	*vanA*	80	3393	98.60%
RC-19-069	12/11/2019	H2	U	Screening	R	*vanA*	80	3393	98.59%
RC-19-070	12/11/2019	H2	U	Screening	R	*vanA*	80	3394	93.22%
RC-19-071	12/11/2019	H2	U	Screening	R	*vanA*	80	2933	99.98%
RC-19-072	12/11/2019	H2	U	Screening	R	*vanA*	203	1599	98.62%
RC-19-073	12/11/2019	H2	U	Screening	R	*vanA*	202	1912	99.98%
RC-19-074	12/11/2019	H2	U	Screening	R	*vanA*	80	1921	88.34%
RC-19-075	12/11/2019	H2	U	Screening	R	*vanA*	80	2933	99.92%
RC-19-076	12/11/2019	H2	U	Screening	R	*vanA*	612	2362	96.35%
RC-19-077	13/11/2019	H2	U	Screening	R	*vanA*	80	3394	94.96%
RC-19-078	13/11/2019	H2	U	Screening	R	*vanA*	Novel	1920	95.21%

Table 1 continued overleaf

Specimen no.	Date of sample[1]	Hospital	H1 Ward[2]	Specimen	Vanc[3]	Vanc Resistance Gene[4]	ST[5]	cgMLST CT[5]	SJ11*vanA*[6]
RC-19-079	14/11/2019	H2	U	Screening	R	*vanA*	80	3395	99.95%
RC-19-080	14/11/2019	H2	U	Screening	R	*vanA*	80	2931	95.47%
RC-19-081	15/11/2019	H2	U	Screening	R	*vanA*	80	1598	99.96%
RC-19-082	16/11/2019	H2	U	Screening	R	*vanA*	80	2940	99.95%
RC-19-083	17/11/2019	H2	U	Screening	R	*vanA*	80	2940	99.95%
RC-19-084	18/11/2019	H2	U	Screening	R	*vanA*	80	1916	99.97%
RC-19-085	18/11/2019	H2	U	Screening	R	*vanA*	80	1916	99.96%
RC-19-086	18/11/2019	H2	U	Screening	R	*vanA*	80	3383	95.01%
RC-19-087	18/11/2019	H2	U	Screening	R	*vanA*	80	3394	93.40%
RC-19-088	18/11/2019	H2	U	Screening	R	*vanA*	80	2933	99.96%
RC-19-089	19/11/2019	H2	U	Screening	R	*vanA*	80	2933	95.06%
RC-19-090	18/11/2019	H2	U	Screening	R	*vanA*	80	2931	99.95%
RC-19-091	19/11/2019	H2	U	Screening	R	*vanA*	80	2933	98.63%
RC-19-092	20/11/2019	H2	U	Screening	R	*vanA*	80	3395	99.96%
RC-19-093	20/11/2019	H2	U	Screening	R	*vanA*	80	1916	99.97%
RC-19-094	21/11/2019	H2	U	Screening	R	*vanA*	80	1921	89.87%
RC-19-095	21/11/2019	H2	U	Screening	R	*vanA*	80	1921	98.63%
RC-19-096	23/11/2019	H2	U	Screening	R	*vanA*	80	1916	80.11%
RC-19-097	21/10/2019	H2	U	BSI	S	-	80	2933	30.36%
RC-19-098	08/11/2019	H2	U	BSI	R	*vanA*	80	2933	100.00%
RC-19-10	19/10/2019	H5	U	BSI	S		80	6990	98.63%
RC-19-100	19/11/2019	H2	U	BSI	R	*vanA*	80	2933	96.19%
RC-19-101	21/12/2019	H2	U	BSI	R	*vanA*	80	2933	99.92%
RC-19-102	03/12/2019	H2	U	BSI	R	*vanA*	80	2931	99.97%
RC-19-103	03/12/2019	H2	U	BSI	R	*vanA*	80	2933	93.91%

Table 1 continued overleaf

Specimen no.	Date of sample[1]	Hospital	H1 Ward[2]	Specimen	Vanc[3]	Vanc Resistance Gene[4]	ST[5]	cgMLST CT[5]	SJ11*vanA*[6]
RC-19-104	28/12/2019	H2	U	BSI	R	*vanA*	80	2933	99.95%
RC-19-47	U	H7	U	Screening	R	*vanA*	80	1467	98.64%
RC-19-48	U	H7	U	Screening	R	*vanA*	80	3384	90.78%
SJ1	05/09/2017	H1	W2	Screening	R	*vanA*	80	1598	98.66%
SJ10	30/08/2017	H1	W3	Screening	R	*vanA*	789	1601	87.80%
SJ100	04/03/2019	H1	W9	Screening	R	*vanA*	Novel	1919	95.49%
SJ101	04/03/2019	H1	W12	Screening	R	*vanA*	117	2283	98.42%
SJ102	04/03/2019	H1	W6	Screening	R	*vanA*	80	2933	98.66%
SJ103	05/03/2019	H1	W2	Screening	R	*vanA*	202	2945	95.21%
SJ104	05/03/2019	H1	W2	Screening	R	*vanA*	80	1598	98.63%
SJ105	05/03/2019	H1	W1	Screening	R	*vanA*	612	2362	98.63%
SJ106	05/03/2019	H1	W4	Screening	R	*vanA*	80	2947	87.60%
SJ107	05/03/2019	H1	W1	Screening	R	*vanA*	907	2948	99.16%
SJ108	05/03/2019	H1	W2	Screening	R	*vanA*	80	1598	98.60%
SJ109	05/03/2019	H1	W1	Screening	R	*vanA*	80	1921	71.39%
SJ11	22/08/2017	H1	W10	Screening	R	*vanA*	1478	24	99.98%
SJ110	05/03/2019	H1	W23	Screening	R	*vanA*	80	2931	99.92%
SJ111	05/03/2019	H1	W7	Screening	R	*vanA*	612	2942	98.64%
SJ112	06/03/2019	H1	W12	Screening	R	*vanA*	80	1911	88.20%
SJ113	06/03/2019	H1	W3	Screening	R	*vanA*	117	2283	95.12%
SJ114	06/03/2019	H1	W3	Screening	R	*vanA*	80	1598	98.48%
SJ115	06/03/2019	H1	W3	Screening	R	*vanA*	80	2936	95.36%
SJ116	06/03/2019	H1	W23	Screening	R	*vanA*	787	1914	99.97%
SJ117	06/03/2019	H1	W3	Screening	R	*vanA*	80	1921	82.70%
SJ118	06/03/2019	H1	W2	Screening	R	*vanA*	80	1911	88.30%

Table 1 continued overleaf

Specimen no.	Date of sample[1]	Hospital	H1 Ward[2]	Specimen	Vanc[3]	Vanc Resistance Gene[4]	ST[5]	cgMLST CT[5]	SJ11*vanA*[6]
SJ119	06/03/2019	H1	W3	Screening	R	*vanA*	203	2950	98.63%
SJ12	14/08/2017	H1	W11	Screening	R	*vanA*	203	20	78.49%
SJ120	06/03/2019	H1	W3	Screening	R	*vanA*	203	1599	85.57%
SJ121	06/03/2019	H1	W3	Screening	R	*vanA*	80	1598	96.09%
SJ122	06/03/2019	H1	W3	Screening	R	*vanA*	80	1911	95.38%
SJ123	06/03/2019	H1	W3	Screening	R	*vanA*	80	1598	98.63%
SJ124	06/03/2019	H1	W3	Screening	R	*vanA*	612	2942	98.63%
SJ125	06/03/2019	H1	W3	Screening	R	*vanA*	80	1911	88.15%
SJ126	06/03/2019	H1	W6	Screening	R	*vanA*	203	1599	95.85%
SJ127	06/03/2019	H1	W3	Screening	R	*vanA*	80	1598	98.60%
SJ128	06/03/2019	H1	W3	Screening	R	*vanA*	80	1598	98.63%
SJ129	06/03/2019	H1	W22	Screening	R	*vanA*	80	1911	88.16%
SJ13	29/08/2017	H1	W3	Screening	R	*vanA*	789	1601	87.03%
SJ130	06/03/2019	H1	W2	Screening	R	*vanA*	80	2933	98.55%
SJ131	06/03/2019	H1	W3	Screening	R	*vanA*	203	2950	95.47%
SJ132	07/03/2019	H1	W18	Screening	R	*vanA*	80	2933	98.42%
SJ133	07/03/2019	H1	W3	Screening	R	*vanA*	787	1920	96.41%
SJ134	08/03/2019	H1	W9	Screening	R	*vanA*	80	1911	90.68%
SJ135	08/03/2019	H1	W23	Screening	R	*vanA*	80	1598	98.63%
SJ136	08/03/2019	H1	W7	Screening	R	*vanA*	80	1921	94.49%
SJ137	08/03/2019	H1	W7	Screening	R	*vanA*	203	2950	98.62%
SJ138	09/03/2019	H1	W3	Screening	R	*vanA*	80	1598	98.65%
SJ139	10/03/2019	H1	W1	Screening	R	*vanA*	80	1911	96.97%
SJ14	05/09/2017	H1	W2	Screening	R	*vanA*	80	1598	98.63%
SJ140	10/03/2019	H1	W18	Screening	R	*vanA*	117	2283	95.17%

Table 1 continued overleaf

Specimen no.	Date of sample[1]	Hospital	H1 Ward[2]	Specimen	Vanc[3]	Vanc Resistance Gene[4]	ST[5]	cgMLST CT[5]	SJ11*vanA*[6]
SJ141	10/03/2019	H1	W18	Screening	R	*vanA*	80	1598	98.61%
SJ142	10/03/2019	H1	W3	Screening	R	*vanA*	80	1598	98.61%
SJ143	11/03/2019	H1	W25	Screening	R	*vanA*	80	1598	98.61%
SJ144	11/03/2019	H1	GP	Screening	R	*vanA*	203	1599	98.48%
SJ145	12/03/2019	H1	W1	Screening	R	*vanA*	80	1911	95.35%
SJ147	12/03/2019	H1	W25	Screening	R	*vanA*	80	1921	98.61%
SJ148	12/03/2019	H1	W2	Screening	R	*vanA*	80	1911	88.25%
SJ149	12/03/2019	H1	W1	Screening	R	*vanA*	907	2948	98.61%
SJ15	04/09/2017	H1	W9	Screening	R	*vanA*	80	1602	88.28%
SJ150	12/03/2019	H1	W12	Screening	R	*vanA* and *vanB*	789	3159	98.63%
SJ151	12/03/2019	H1	W3	Screening	R	*vanA*	80	1598	98.59%
SJ152	12/03/2019	H1	W5	Screening	R	*vanA*	80	2932	98.61%
SJ153	12/03/2019	H1	W9	Screening	R	*vanA*	80	2931	99.95%
SJ154	12/03/2019	H1	W2	Screening	R	*vanA*	80	3160	99.96%
SJ155	12/03/2019	H1	W32	Screening	R	*vanA*	612	2362	98.63%
SJ156	12/03/2019	H1	W23	Screening	R	*vanA*	203	1599	99.95%
SJ158	13/03/2019	H1	W3	Screening	R	*vanA*	80	2933	98.60%
SJ159	13/03/2019	H1	W3	Screening	R	*vanA*	80	1598	98.63%
SJ16	12/06/2018	H1	W1	Screening	R	*vanA*	17	1919	98.63%
SJ160	13/03/2019	H1	W12	Screening	R	*vanA* and *vanB*	789	3159	98.62%
SJ161	14/03/2019	H1	W8	Screening	R	*vanA*	80	2933	98.45%
SJ162	14/03/2019	H1	W3	Screening	R	*vanA*	80	1598	98.60%
SJ164	14/03/2019	H1	W8	Screening	R	*vanA*	80	1598	98.62%
SJ165	15/03/2019	H1	W8	Screening	R	*vanA*	80	1598	98.63%
SJ167	15/03/2019	H1	W6	Screening	R	*vanA*	203	1599	95.44%

Table 1 continued overleaf

Specimen no.	Date of sample[1]	Hospital	H1 Ward[2]	Specimen	Vanc[3]	Vanc Resistance Gene[4]	ST[5]	cgMLST CT[5]	SJ11*vanA*[6]
SJ168	09/06/2019	H1	W3	Screening	R	*vanA*	1478	2283	99.95%
SJ169	11/06/2019	H1	W2	Screening	R	*vanA*	80	3161	99.17%
SJ17	13/06/2018	H1	W3	Screening	R	*vanA*	80	1911	88.22%
SJ17.2	16/06/2018	H1	W3	Screening	R	*vanA*	80	1911	88.21%
SJ170	07/06/2019	H1	W1	Screening	R	*vanA*	789	3162	98.65%
SJ171	11/06/2019	H1	W5	Screening	R	*vanA*	117	2283	99.90%
SJ172	11/06/2019	H1	W7	Screening	R	*vanA*	80	1911	88.31%
SJ173	11/06/2019	H1	W3	Screening	R	*vanA*	787	1920	98.63%
SJ174	12/06/2019	H1	W6	Screening	R	*vanA*	80	1911	95.32%
SJ175	12/06/2019	H1	W3	Screening	R	*vanA*	612	2942	98.63%
SJ176	12/06/2019	H1	W3	Screening	R	*vanA*	80	2932	98.60%
SJ177	12/06/2019	H1	W7	Screening	R	*vanA*	80	1911	96.82%
SJ178	12/06/2019	H1	W3	Screening	R	*vanA*	18	1898	98.62%
SJ179	12/06/2019	H1	W3	Screening	R	*vanA*	80	3163	98.61%
SJ18	11/06/2018	H1	W12	Screening	R	*vanA*	202	1912	99.98%
SJ180	12/06/2019	H1	W1	Screening	R	*vanA*	80	1916	95.47%
SJ181	12/06/2019	H1	W12	Screening	R	*vanA*	80	2933	98.57%
SJ182	11/06/2019	H1	W1	Screening	R	*vanA*	80	1911	88.27%
SJ183	13/06/2019	H1	W1	Screening	R	*vanA*	80	2941	98.64%
SJ184	14/06/2019	H1	W27	Screening	R	*vanA*	80	2933	98.64%
SJ185	09/06/2019	H1	W6	Screening	R	*vanA*	18	3164	96.27%
SJ186	16/06/2019	H1	W6	Screening	R	*vanA*	612	2362	98.63%
SJ187	17/06/2019	H1	W6	Screening	R	*vanA*	80	1893	99.96%
SJ188	15/06/2019	H1	W21	Screening	R	*vanA*	612	2362	98.58%
SJ189	15/06/2019	H1	W23	Screening	R	*vanA*	80	3165	98.62%

Table 1 continued overleaf

Specimen no.	Date of sample[1]	Hospital	H1 Ward[2]	Specimen	Vanc[3]	Vanc Resistance Gene[4]	ST[5]	cgMLST CT[5]	SJ11*vanA*[6]
SJ19	12/06/2018	H1	W5	Screening	R	*vanA*	80	1913	88.14%
SJ190	17/06/2019	H1	W7	Screening	R	*vanA*	262	3166	99.77%
SJ192	15/06/2019	H1	W22	Screening	R	*vanA*	80	1921	88.13%
SJ193	18/06/2019	H1	W1	Screening	R	*vanA*	80	1916	95.48%
SJ194	18/06/2019	H1	W1	Screening	R	*vanA*	80	1911	88.31%
SJ195	18/06/2019	H1	W1	Screening	R	*vanA*	323	561	98.66%
SJ196	18/06/2019	H1	W1	Screening	R	*vanA*	80	2932	98.61%
SJ197	14/06/2019	H1	W1	Screening	R	*vanA*	612	2362	98.58%
SJ198	18/06/2019	H1	W2	Screening	R	*vanA*	80	3167	98.59%
SJ199	18/06/2019	H1	W1	Screening	R	*vanA*	80	1598	98.61%
SJ2	06/06/2017	H1	W2	Screening	R	*vanA*	789	1596	86.93%
SJ20	12/06/2018	H1	W1	Screening	R	*vanA*	787	1914	98.67%
SJ200	17/06/2019	H1	W7	Screening	R	*vanA*	612	2362	98.61%
SJ201	18/06/2019	H1	W6	Screening	R	*vanA*	203	1599	98.62%
SJ202	18/06/2019	H1	W6	Screening	R	*vanA*	80	1911	89.74%
SJ203	19/06/2019	H1	W3	Screening	R	*vanA*	612	2942	98.60%
SJ204	19/06/2019	H1	W3	Screening	R	*vanA*	80	3163	98.62%
SJ205	19/06/2019	H1	W3	Screening	R	*vanA*	612	2942	98.61%
SJ206	18/06/2019	H1	W2	Screening	R	*vanA*	80	3168	98.59%
SJ207	18/06/2019	H1	W4	Screening	R	*vanA*	80	1911	88.30%
SJ208	19/06/2019	H1	W3	Screening	R	*vanA*	80	1598	98.63%
SJ209	19/06/2019	H1	W3	Screening	R	*vanA*	612	2942	98.63%
SJ21	15/06/2018	H1	W6	Screening	R	*vanA*	80	1915	99.96%
SJ210	19/06/2019	H1	W3	Screening	R	*vanA*	80	2933	98.62%
SJ211	19/06/2019	H1	W3	Screening	R	*vanA*	612	2362	98.61%

Table 1 continued overleaf

Specimen no.	Date of sample[1]	Hospital	H1 Ward[2]	Specimen	Vanc[3]	Vanc Resistance Gene[4]	ST[5]	cgMLST CT[5]	SJ11*vanA*[6]
SJ212	19/06/2019	H1	W24	Screening	R	*vanA*	80	1598	98.63%
SJ213	20/06/2019	H1	W3	Screening	R	*vanA*	80	1911	88.24%
SJ214	18/06/2019	H1	W1	Screening	R	*vanA*	80	1185	96.91%
SJ215	18/06/2019	H1	W1	Screening	R	*vanA*	787	1914	99.98%
SJ216	18/06/2019	H1	W12	Screening	R	*vanA*	80	1185	93.25%
SJ217	18/06/2019	H1	W12	Screening	R	*vanA*	80	1921	90.43%
SJ218	18/06/2019	H1	W12	Screening	R	*vanA*	117	2283	99.96%
SJ219	19/06/2019	H1	W1	Screening	R	*vanA*	612	2362	98.60%
SJ22	14/06/2018	H1	W7	Screening	R	*vanA*	787	1914	88.30%
SJ220	20/06/2019	H1	W2	Screening	R	*vanA*	117	2929	99.95%
SJ221	18/06/2019	H1	W6	Screening	R	*vanA*	1395	3169	98.56%
SJ222	20/06/2019	H1	W1	Screening	R	*vanA*	80	2933	98.60%
SJ223	19/06/2019	H1	W3	Screening	R	*vanA*	80	1921	98.62%
SJ224	19/06/2019	H1	W3	Screening	R	*vanA*	80	3168	98.63%
SJ225	19/06/2019	H1	W3	Screening	R	*vanA*	80	2933	99.19%
SJ226	19/06/2019	H1	W23	Screening	R	*vanA*	789	3162	98.63%
SJ227	20/06/2019	H1	W27	Screening	R	*vanA*	80	3170	99.95%
SJ228	18/06/2019	H1	W2	Screening	R	*vanA*	80	3168	98.60%
SJ229	19/06/2019	H1	W2	Screening	R	*vanA*	787	1920	94.51%
SJ23	12/06/2018	H1	W13	Screening	R	*vanA*	80	1598	98.61%
SJ230	20/06/2019	H1	W1	Screening	R	*vanA*	117	2283	99.90%
SJ231	20/06/2019	H1	W23	Screening	R	*vanA*	80	1598	98.63%
SJ232	19/06/2019	H1	W3	Screening	R	*vanA*	80	2933	97.10%
SJ233	20/06/2019	H1	W25	Screening	R	*vanA*	80	1911	88.13%
SJ234	20/06/2019	H1	W23	Screening	R	*vanA*	80	3171	88.94%

Table 1 continued overleaf

Specimen no.	Date of sample[1]	Hospital	H1 Ward[2]	Specimen	Vanc[3]	Vanc Resistance Gene[4]	ST[5]	cgMLST CT[5]	SJ11*vanA*[6]
SJ235	20/06/2019	H1	W14	Screening	R	*vanA*	203	1599	98.62%
SJ236	20/06/2019	H1	W3	Screening	R	*vanA*	80	1921	98.61%
SJ237	21/06/2019	H1	W3	Screening	R	*vanA*	80	3168	98.62%
SJ238	21/06/2019	H1	W7	Screening	R	*vanA*	80	3172	99.96%
SJ239	23/06/2019	H1	W6	Screening	R	*vanA*	117	2283	99.96%
SJ24	11/06/2018	H1	W6	Screening	R	*vanA*	787	1914	88.22%
SJ240	21/06/2019	H1	W3	Screening	R	*vanA*	80	1911	99.92%
SJ241	22/06/2019	H1	W3	Screening	R	*vanA*	80	1598	98.62%
SJ242	23/06/2019	H1	W7	Screening	R	*vanA*	612	2362	98.63%
SJ243	23/06/2019	H1	W16	Screening	R	*vanA*	80	3163	95.65%
SJ244	24/06/2019	H1	W6	Screening	R	*vanA*	414	2952	95.89%
SJ245	22/06/2019	H1	W2	Screening	R	*vanA*	117	2929	99.93%
SJ246	25/06/2019	H1	W4	Screening	R	*vanA*	80	1911	88.26%
SJ247	25/06/2019	H1	W4	Screening	R	*vanA*	117	2283	88.16%
SJ248	25/06/2019	H1	W1	Screening	R	*vanA*	80	2938	99.97%
SJ249	25/06/2019	H1	W1	Screening	R	*vanA*	612	2362	98.67%
SJ25	10/06/2018	H1	W6	Screening	R	*vanA*	80	1911	88.17%
SJ250	25/06/2019	H1	W1	Screening	R	*vanA*	80	2941	98.62%
SJ251	20/06/2019	H1	W1	Screening	R	*vanA*	80	1916	95.47%
SJ252	24/06/2019	H1	W18	Screening	R	*vanA*	203	1599	95.24%
SJ253	24/06/2019	H1	W6	Screening	R	*vanA*	80	2933	98.57%
SJ254	24/06/2019	H1	W6	Screening	R	*vanA*	80	1911	89.79%
SJ255	24/06/2019	H1	W6	Screening	R	*vanA*	80	1893	99.96%
SJ256	23/06/2019	H1	W3	Screening	R	*vanA*	612	2942	98.64%
SJ257	23/06/2019	H1	W1	Screening	R	*vanA*	80	1911	88.13%

Table 1 continued overleaf

Specimen no.	Date of sample[1]	Hospital	H1 Ward[2]	Specimen	Vanc[3]	Vanc Resistance Gene[4]	ST[5]	cgMLST CT[5]	SJ11*vanA*[6]
SJ258	24/06/2019	H1	W23	Screening	R	*vanA*	80	3173	99.97%
SJ259	22/06/2019	H1	W2	Screening	R	*vanA*	80	1598	98.57%
SJ26.2	15/06/2018	H1	W3	Screening	R	*vanA*	80	1916	100.00%
SJ260	24/06/2019	H1	W26	Screening	R	*vanA*	Novel	3174	89.30%
SJ261	25/06/2019	H1	W6	Screening	R	*vanA*	280	2990	98.43%
SJ262	24/06/2019	H1	GP	Screening	R	*vanA*	80	1916	95.51%
SJ263	25/06/2019	H1	W27	Screening	R	*vanA*	117	2283	99.92%
SJ264	26/06/2019	H1	W3	Screening	R	*vanA*	612	2942	98.61%
SJ265	26/06/2019	H1	W3	Screening	R	*vanA*	80	1916	95.43%
SJ266	26/06/2019	H1	W3	Screening	R	*vanA*	80	3175	95.47%
SJ267	26/06/2019	H1	W3	Screening	R	*vanA*	18	1898	98.64%
SJ270	26/06/2019	H1	W3	Screening	R	*vanA*	80	1921	98.60%
SJ271	26/06/2019	H1	W3	Screening	R	*vanA*	612	2942	98.63%
SJ272	27/06/2019	H1	W1	Screening	R	*vanA*	80	2938	99.92%
SJ273	27/06/2019	H1	W7	Screening	R	*vanA*	117	2929	99.91%
SJ274	25/06/2019	H1	W2	Screening	R	*vanA*	117	2929	99.94%
SJ275	26/06/2019	H1	W1	Screening	R	*vanA*	80	2932	98.62%
SJ276	25/06/2019	H1	W12	Screening	R	*vanA*	80	1598	98.63%
SJ277	25/06/2019	H1	W1	Screening	R	*vanA*	80	1916	95.47%
SJ278	25/06/2019	H1	W12	Screening	R	*vanA*	80	1185	93.24%
SJ279	27/06/2019	H1	W3	Screening	R	*vanA*	612	2942	98.62%
SJ28	11/06/2018	H1	W3	Screening	R	*vanA*	787	1920	99.92%
SJ280	27/06/2019	H1	W27	Screening	R	*vanA*	80	1911	99.98%
SJ281	26/06/2019	H1	W3	Screening	R	*vanA*	80	1911	88.15%
SJ282	29/06/2019	H1	W18	Screening	R	*vanA*	117	2283	98.68%

Table 1 continued overleaf

Specimen no.	Date of sample[1]	Hospital	H1 Ward[2]	Specimen	Vanc[3]	Vanc Resistance Gene[4]	ST[5]	cgMLST CT[5]	SJ11*vanA*[6]
SJ283	29/06/2019	H1	W18	Screening	R	*vanA*	203	2950	95.22%
SJ284	30/06/2019	H1	W3	Screening	R	*vanA*	80	2938	99.97%
SJ285	28/06/2019	H1	W7	Screening	R	*vanA*	80	2941	98.57%
SJ286	28/06/2019	H1	W3	Screening	R	*vanA*	80	2938	99.90%
SJ287	30/06/2019	H1	W3	Screening	R	*vanA*	80	1911	88.30%
SJ288	30/06/2019	H1	W3	Screening	R	*vanA*	117	2283	99.98%
SJ289	30/06/2019	H1	W6	Screening	R	*vanA*	280	2990	98.45%
SJ29	10/06/2018	H1	W8	Screening	R	*vanA*	203	1599	99.13%
SJ290	01/07/2019	H1	W6	Screening	R	*vanA*	414	2952	95.46%
SJ291	28/06/2019	H1	W12	Screening	R	*vanA*	80	1598	99.44%
SJ3	04/09/2017	H1	W7	Screening	R	*vanA*	203	20	100.00%
SJ30	12/06/2018	H1	W14	Screening	R	*vanA*	80	1916	99.97%
SJ31	12/06/2018	H1	W3	Screening	R	*vanA*	1424	1920	83.43%
SJ32	13/06/2018	H1	W15	Screening	R	*vanA*	80	1911	88.16%
SJ33	12/06/2018	H1	W16	Screening	R	*vanA*	80	1921	85.55%
SJ34	17/06/2018	H1	W17	Screening	R	*vanA*	80	1598	98.63%
SJ35	17/06/2018	H1	W15	Screening	R	*vanA*	80	1911	88.16%
SJ36	18/06/2018	H1	W3	Screening	R	*vanA*	80	1911	88.31%
SJ37	19/06/2018	H1	W6	Screening	R	*vanA*	80	1921	88.31%
SJ38	18/06/2018	H1	W1	Screening	R	*vanA*	787	1920	96.54%
SJ39	18/06/2018	H1	W6	Screening	R	*vanA*	787	680	99.13%
SJ4	30/08/2017	H1	W9	Screening	R	*vanA*	789	1601	87.27%
SJ40	19/06/2018	H1	W12	Screening	R	*vanA*	202	1912	99.98%
SJ41	19/06/2018	H1	W18	Screening	R	*vanA*	203	1599	99.98%
SJ42	19/06/2018	H1	W13	Screening	R	*vanA*	80	1598	98.61%

Table 1 continued overleaf

Specimen no.	Date of sample[1]	Hospital	H1 Ward[2]	Specimen	Vanc[3]	Vanc Resistance Gene[4]	ST[5]	cgMLST CT[5]	SJ11*vanA*[6]
SJ43	19/06/2018	H1	W16	Screening	R	*vanA*	80	1921	86.53%
SJ44	20/06/2018	H1	W3	Screening	R	*vanA*	203	1599	100.00%
SJ45	20/06/2018	H1	W3	Screening	R	*vanA*	80	1921	83.03%
SJ46	20/06/2018	H1	W3	Screening	R	*vanA*	80	1916	100.00%
SJ47	20/06/2018	H1	W1	Screening	R	*vanA*	80	2023	95.50%
SJ48	20/06/2018	H1	W3	Screening	R	*vanA*	80	1598	98.63%
SJ49	20/06/2018	H1	W3	Screening	R	*vanA*	787	1920	99.98%
SJ5	08/08/2017	H1	W8	Screening	R	*vanA*	203	1599	100.00%
SJ50	20/06/2018	H1	W3	Screening	R	*vanA*	203	1599	97.93%
SJ51	19/10/2018	H1	W1	Screening	R	*vanA*	80	1911	88.15%
SJ52	16/10/2018	H1	W1	Screening	R	*vanA*	80	3155	99.98%
SJ53	15/10/2018	H1	W1	Screening	R	*vanA*	80	1911	88.10%
SJ54	15/10/2018	H1	W4	Screening	R	*vanA*	80	2939	99.98%
SJ55	15/10/2018	H1	W2	Screening	R	*vanA*	80	2933	88.08%
SJ56	15/10/2018	H1	W1	Screening	R	*vanA*	80	1911	88.10%
SJ58	16/10/2018	H1	W3	Screening	R	*vanA*	203	2950	99.96%
SJ59	16/10/2018	H1	W1	Screening	R	*vanA*	203	2939	99.97%
SJ6	24/07/2017	H1	W2	Screening	R	*vanA*	80	1598	98.65%
SJ60	16/10/2018	H1	GP	Screening	R	*vanA*	80	1921	98.66%
SJ61	17/10/2018	H1	W1	Screening	R	*vanA*	203	1599	99.98%
SJ62	18/10/2018	H1	W3	Screening	R	*vanA*	80	1911	88.26%
SJ64	19/10/2018	H1	W10	Screening	R	*vanA*	80	2933	23.52%
SJ65	19/10/2018	H1	W1	Screening	R	*vanA*	80	1602	88.07%
SJ66	19/10/2018	H1	W1	Screening	R	*vanA*	80	1916	95.49%
SJ67	22/10/2018	H1	W2	Screening	R	*vanA*	80	2932	98.60%

Table 1 continued overleaf

Specimen no.	Date of sample[1]	Hospital	H1 Ward[2]	Specimen	Vanc[3]	Vanc Resistance Gene[4]	ST[5]	cgMLST CT[5]	SJ11*vanA*[6]
SJ68	19/10/2018	H1	W2	Screening	R	*vanA*	80	2932	98.61%
SJ69	19/10/2018	H1	W2	Screening	R	*vanA*	203	1599	86.36%
SJ7	03/09/2017	H1	W9	Screening	R	*vanA*	203	1599	99.98%
SJ70	19/10/2018	H1	W2	Screening	R	*vanA*	80	2932	98.60%
SJ71	19/10/2018	H1	W4	Screening	R	*vanA*	203	20	78.15%
SJ72	22/10/2018	H1	W7	Screening	R	*vanA*	80	1201	99.98%
SJ73	23/10/2018	H1	W3	Screening	R	*vanA*	203	2950	99.97%
SJ74	23/10/2018	H1	W3	Screening	R	*vanA*	80	1598	98.65%
SJ75	23/10/2018	H1	W3	Screening	R	*vanA*	80	1921	82.63%
SJ76	23/10/2018	H1	W3	Screening	R	*vanA*	80	1921	99.95%
SJ77	23/10/2018	H1	W6	Screening	R	*vanA*	203	20	78.49%
SJ78	23/10/2018	H1	W2	Screening	R	*vanA*	80	2932	98.61%
SJ79	23/10/2018	H1	W1	Screening	R	*vanA*	1395	3227	98.62%
SJ8	20/08/2017	H1	W1	Screening	R	*vanA*	787	1600	55.73%
SJ80	26/10/2018	H1	W2	Screening	R	*vanA*	80	1911	91.04%
SJ81	26/10/2018	H1	W4	Screening	R	*vanA*	117	2283	99.97%
SJ82	26/10/2018	H1	W1	Screening	R	*vanA*	203	20	79.87%
SJ83	26/10/2018	H1	W1	Screening	R	*vanA*	80	2932	99.70%
SJ85	26/10/2018	H1	W5	Screening	R	*vanA*	80	1911	90.06%
SJ86	26/10/2018	H1	W5	Screening	R	*vanA*	80	1911	95.69%
SJ87	26/10/2018	H1	W5	Screening	R	*vanA*	80	1911	99.96%
SJ88	26/10/2018	H1	W5	Screening	R	*vanA*	80	2932	98.62%
SJ89	03/03/2019	H1	W23	Screening	R	*vanA*	80	1921	99.96%
SJ9	25/07/2017	H1	W1	Screening	R	*vanA*	1395	1597	98.66%
SJ90	03/03/2019	H1	W3	Screening	R	*vanA*	80	1598	98.45%

Table 1 continued overleaf

Specimen no.	Date of sample[1]	Hospital	H1 Ward[2]	Specimen	Vanc[3]	Vanc Resistance Gene[4]	ST[5]	cgMLST CT[5]	SJ11*vanA*[6]
SJ91	03/03/2019	H1	W3	Screening	R	*vanA*	80	1598	98.62%
SJ92	03/03/2019	H1	W3	Screening	R	*vanA*	267	2951	95.49%
SJ93	03/03/2019	H1	W3	Screening	R	*vanA*	Novel	1599	95.23%
SJ94	03/03/2019	H1	W3	Screening	R	*vanA*	80	1598	96.10%
SJ95	03/03/2019	H1	W3	Screening	R	*vanA*	117	2283	95.18%
SJ97	04/03/2019	H1	W3	Screening	R	*vanA*	80	1916	99.96%
SJ98	04/03/2019	H1	W6	Screening	R	*vanA*	414	2952	95.18%
SJ99	04/03/2019	H1	W9	Screening	R	*vanA*	80	2953	95.47%

Abbreviations: Van, vancomycin; ST, sequence type; CT, complex type; BSI, bloodstream infection; R, resistant; S, susceptible; H, hospital; W, ward; N/A, not assigned; NT, not typeable; U, unavailable, GP, community medical practitioner.

[1] Exact date of sample not available for all isolates, in these cases isolates were collected during October-December 2019.

[2] Eight vancomycin-resistant *E. faecium* isolates from H1 were recovered from rectal screening samples submitted by community medical practitioners.

[3] Interpreted using clinical breakpoints taken from the European Committee on Antimicrobial Susceptibility Testing guidelines (EUCAST, 2024).

[4] Vancomycin resistance genotypes were extracted in silico from short-read whole genome data using ABRicate (https://github.com/tseemann/abricate).

[5]Genotypic information including MLST sequence type (ST) and cgMLST complex type (CT) were extracted *in silico* from whole genome data using Ridom SeqSphere+ v8.5.1 (Ridom GmbH, Münster, Germany). The CT was determined according to the publicly available cgMLST scheme based on 1,423 loci (de Been *et al*., 2015).

[6] Coverage (%) of isolates against the transposon region from SJ11*vanA* resolved by hybrid assembly.

Table 2. Details of the publicly available short-read sequencing data of global Clade A1 *Enterococcus faecium* isolates (*N*=1,325) from NCBI used to contextualise Irish *E. faecium*

Sample ID	Sample Accession	Study Accession	Collection Date	Country of Isolation	Predicted vancomycin susceptibility[1]
ERX347716	SAMEA1967440	PRJEB4345	2009	United Kingdom	Susceptible
ERX349893	SAMEA1969240	PRJEB4345	2007	United Kingdom	Susceptible
ERX347759	SAMEA1969798	PRJEB4345	2010	United Kingdom	Susceptible
ERX347850	SAMEA1972111	PRJEB4345	2007	United Kingdom	Resistant (*vanA*)
ERX347829	SAMEA2142474	PRJEB4345	2009	United Kingdom	Resistant (*vanA*)
ERX347891	SAMEA2143077	PRJEB4345	2011	United Kingdom	Susceptible
ERX347707	SAMEA2143510	PRJEB4345	2009	United Kingdom	Resistant (*vanA*)
ERX347862	SAMEA2143765	PRJEB4345	2006	United Kingdom	Susceptible
ERX347835	SAMEA2144371	PRJEB4345	2007	United Kingdom	Resistant (*vanA*)
ERX342673	SAMEA2144485	PRJEB4345	2007	United Kingdom	Susceptible
ERX342674	SAMEA2144849	PRJEB4345	2009	United Kingdom	Resistant (*vanA*)
ERX347933	SAMEA2144936	PRJEB4345	2012	United Kingdom	Susceptible
ERX347820	SAMEA2145117	PRJEB4345	2009	United Kingdom	Susceptible
ERX347766	SAMEA2145390	PRJEB4345	2011	United Kingdom	Susceptible
2701STDY5569115 ERX342701	SAMEA2145396	PRJEB4345	2012	United Kingdom	Resistant (*vanA*)
ERX347710	SAMEA2145560	PRJEB4345	2006	United Kingdom	Susceptible
ERX349823	SAMEA2145669	PRJEB4345	2012	United Kingdom	Susceptible
ERX347753	SAMEA2145781	PRJEB4345	2009	United Kingdom	Susceptible
ERX342728	SAMEA2146127	PRJEB4345	2010	United Kingdom	Susceptible
ERX347705	SAMEA2146589	PRJEB4345	2008	United Kingdom	Resistant (*vanA*)
ERX349820	SAMEA2146613	PRJEB4345	2011	United Kingdom	Resistant (*vanA*)

Table 2 continued overleaf

Sample ID	Sample Accession	Study Accession	Collection Date	Country of Isolation	Predicted vancomycin susceptibility[1]
ERX360945	SAMEA2146840	PRJEB4345	2008	United Kingdom	Resistant (*vanA*)
ERX347825	SAMEA2146844	PRJEB4345	2010	United Kingdom	Susceptible
ERX349807	SAMEA2146884	PRJEB4345	2010	United Kingdom	Resistant (*vanA*)
ERX349874	SAMEA2146967	PRJEB4345	2011	United Kingdom	Resistant (*vanA*)
ERX347773	SAMEA2147347	PRJEB4345	2007	United Kingdom	Resistant (*vanA*)
ERX347706	SAMEA2147386	PRJEB4345	2009	United Kingdom	Resistant (*vanA*)
ERX347921	SAMEA2147574	PRJEB4345	2009	United Kingdom	Resistant (*vanA*)
ERX349850	SAMEA2147837	PRJEB4345	2007	United Kingdom	Resistant (*vanA*)
ERX342721	SAMEA2147944	PRJEB4345	2012	United Kingdom	Susceptible
ERX342649	SAMEA2148075	PRJEB4345	2009	United Kingdom	Susceptible
ERX347681	SAMEA2148195	PRJEB4345	2012	United Kingdom	Susceptible
ERX349814	SAMEA2148286	PRJEB4345	2012	United Kingdom	Susceptible
ERX347720	SAMEA2148477	PRJEB4345	2010	United Kingdom	Susceptible
2701STDY5569435 ERX347757	SAMEA2148590	PRJEB4345	2012	United Kingdom	Resistant (*vanA*)
ERX347811	SAMEA2148623	PRJEB4345	2006	United Kingdom	Resistant (*vanA*)
ERX347818	SAMEA2148636	PRJEB4345	2009	United Kingdom	Resistant (*vanA*)
ERX347789	SAMEA2148769	PRJEB4345	2010	United Kingdom	Susceptible
ERX347918	SAMEA2149130	PRJEB4345	2007	United Kingdom	Susceptible
ERX347727	SAMEA2149301	PRJEB4345	2010	United Kingdom	Resistant (*vanA*)
ERX342712	SAMEA2149661	PRJEB4345	2010	United Kingdom	Resistant (*vanA*)
ERX349873	SAMEA2149979	PRJEB4345	2010	United Kingdom	Susceptible
ERX347881	SAMEA2149996	PRJEB4345	2008	United Kingdom	Susceptible
ERX342713	SAMEA2150716	PRJEB4345	2008	United Kingdom	Resistant (*vanA*)

Table 2 continued overleaf

Sample ID	Sample Accession	Study Accession	Collection Date	Country of Isolation	Predicted vancomycin susceptibility[1]
ERX347685	SAMEA2150825	PRJEB4345	2008	United Kingdom	Susceptible
ERX360931	SAMEA2150875	PRJEB4345	2011	United Kingdom	Resistant (*vanA*)
ERX347802	SAMEA2151254	PRJEB4345	2006	United Kingdom	Resistant (*vanA*)
ERX342648	SAMEA2151512	PRJEB4345	2007	United Kingdom	Susceptible
ERX347928	SAMEA2151753	PRJEB4345	2012	United Kingdom	Susceptible
ERX360930	SAMEA2151772	PRJEB4345	2009	United Kingdom	Resistant (*vanA*)
ERX342741	SAMEA2152475	PRJEB4345	2008	United Kingdom	Susceptible
ERX347934	SAMEA2152523	PRJEB4345	2011	United Kingdom	Resistant (*vanA*)
ERX349824	SAMEA2152547	PRJEB4345	2007	United Kingdom	Resistant (*vanA*)
ERX349813	SAMEA2152856	PRJEB4345	2011	United Kingdom	Susceptible
ERX342678	SAMEA2152857	PRJEB4345	2007	United Kingdom	Resistant (*vanA*)
ERX347861	SAMEA2153215	PRJEB4345	2008	United Kingdom	Susceptible
ERX347860	SAMEA2153388	PRJEB4345	2008	United Kingdom	Resistant (*vanA*)
ERX347823	SAMEA2153486	PRJEB4345	2008	United Kingdom	Resistant (*vanA*)
ERX342689	SAMEA2153652	PRJEB4345	2010	United Kingdom	Resistant (*vanA*)
ERX347679	SAMEA2154026	PRJEB4345	2008	United Kingdom	Susceptible
ERX347893	SAMEA2154297	PRJEB4345	2011	United Kingdom	Susceptible
ERX342716	SAMEA2154328	PRJEB4345	2007	United Kingdom	Resistant (*vanA*)
ERX349878	SAMEA2154441	PRJEB4345	2012	United Kingdom	Susceptible
2701STDY5568921 ERX347858	SAMEA2154532	PRJEB4345	2012	United Kingdom	Resistant (*vanA*)
ERX347875	SAMEA2154569	PRJEB4345	2011	United Kingdom	Resistant (*vanA*)
ERX349821	SAMEA2154647	PRJEB4345	2008	United Kingdom	Resistant (*vanA*)
ERX347874	SAMEA2154769	PRJEB4345	2007	United Kingdom	Resistant (*vanB*)

Table 2 continued overleaf

Sample ID	Sample Accession	Study Accession	Collection Date	Country of Isolation	Predicted vancomycin susceptibility[1]
ERX342667	SAMEA2155053	PRJEB4345	2007	United Kingdom	Resistant (*vanA*)
2701STDY5569081 ERX347688	SAMEA2155069	PRJEB4345	2012	United Kingdom	Resistant (*vanA*)
ERX347667	SAMEA2155160	PRJEB4345	2008	United Kingdom	Resistant (*vanA*)
ERX347817	SAMEA2155441	PRJEB4345	2010	United Kingdom	Resistant (*vanA*)
ERX347896	SAMEA2155476	PRJEB4345	2008	United Kingdom	Susceptible
ERX347690	SAMEA2155593	PRJEB4345	2009	United Kingdom	Resistant (*vanA*)
ERX349817	SAMEA2155647	PRJEB4345	2010	United Kingdom	Resistant (*vanA*)
ERX342664	SAMEA2156170	PRJEB4345	2012	United Kingdom	Susceptible
ERX347804	SAMEA2156302	PRJEB4345	2011	United Kingdom	Resistant (*vanA*)
ERX349858	SAMEA2156326	PRJEB4345	2008	United Kingdom	Susceptible
ERX347883	SAMEA2157045	PRJEB4345	2009	United Kingdom	Susceptible
ERX347781	SAMEA2157054	PRJEB4345	2011	United Kingdom	Resistant (*vanA*)
ERX347925	SAMEA2157371	PRJEB4345	2009	United Kingdom	Resistant (*vanA*)
ERX347808	SAMEA2158364	PRJEB4345	2010	United Kingdom	Resistant (*vanA*)
ERX347700	SAMEA2158563	PRJEB4345	2010	United Kingdom	Susceptible
ERX347876	SAMEA2158662	PRJEB4345	2007	United Kingdom	Susceptible
ERX342732	SAMEA2158947	PRJEB4345	2012	United Kingdom	Susceptible
ERX349871	SAMEA2159244	PRJEB4345	2011	United Kingdom	Susceptible
2701STDY5569083 ERX347843	SAMEA2159966	PRJEB4345	2012	United Kingdom	Resistant (*vanA*)
2701STDY5569110 ERX347740	SAMEA2160311	PRJEB4345	2012	United Kingdom	Resistant (*vanB*)
ERX342691	SAMEA2160445	PRJEB4345	2007	United Kingdom	Resistant (*vanA*)
ERX342666	SAMEA2160738	PRJEB4345	2010	United Kingdom	Susceptible
ERX347725	SAMEA2160746	PRJEB4345	2009	United Kingdom	Resistant (*vanA*)

Table 2 continued overleaf

Sample ID	Sample Accession	Study Accession	Collection Date	Country of Isolation	Predicted vancomycin susceptibility[1]
ERX360932	SAMEA2161933	PRJEB4345	2010	United Kingdom	Resistant (*vanA*)
ERX342707	SAMEA2161968	PRJEB4345	2009	United Kingdom	Susceptible
ERX347691	SAMEA2162288	PRJEB4345	2007	United Kingdom	Resistant (*vanA*)
ERX347783	SAMEA2162516	PRJEB4345	2011	United Kingdom	Resistant (*vanA*)
ERX342722	SAMEA2162849	PRJEB4345	2006	United Kingdom	Resistant (*vanA*)
ERX347786	SAMEA2163343	PRJEB4345	2011	United Kingdom	Susceptible
ERX347771	SAMEA2163506	PRJEB4345	2009	United Kingdom	Resistant (*vanA*)
ERX349860	SAMEA2163546	PRJEB4345	2012	United Kingdom	Susceptible
wtchgD00002028	SAMEA3388987	PRJEB8624	2003	Australia	Susceptible
wtchgD00002029	SAMEA3388988	PRJEB8624	2012	Australia	Susceptible
wtchgD00002030	SAMEA3388989	PRJEB8624	2004	Australia	Susceptible
wtchgD00002031	SAMEA3388990	PRJEB8624	2012	Australia	Resistant (*vanB*)
wtchgD00002032	SAMEA3388991	PRJEB8624	2006	Australia	Susceptible
wtchgD00002033	SAMEA3388992	PRJEB8624	2012	Australia	Susceptible
wtchgD00002034	SAMEA3388993	PRJEB8624	2007	Australia	Resistant (*vanB*)
wtchgD00002035	SAMEA3388994	PRJEB8624	2013	Australia	Susceptible
wtchgD00002036	SAMEA3388995	PRJEB8624	2011	Australia	Resistant (*vanB*)
wtchgD00002038	SAMEA3388997	PRJEB8624	2011	Australia	Resistant (*vanB*)
wtchgD00002039	SAMEA3388998	PRJEB8624	2012	Australia	Resistant (*vanB*)
wtchgD00002040 ERX962672	SAMEA3388999	PRJEB8624	2011	Australia	Susceptible
wtchgD00002042 ERX962674	SAMEA3389001	PRJEB8624	2012	Australia	Susceptible
wtchgD00002043	SAMEA3389002	PRJEB8624	2012	Australia	Resistant (*vanB*)
wtchgD00002044	SAMEA3389003	PRJEB8624	2004	Australia	Susceptible

Table 2 continued overleaf

Sample ID	Sample Accession	Study Accession	Collection Date	Country of Isolation	Predicted vancomycin susceptibility[1]
wtchgD00002045 ERX962677	SAMEA3389004	PRJEB8624	2012	Australia	Susceptible
wtchgD00002047	SAMEA3389005	PRJEB8624	2012	Australia	Resistant (*vanB*)
wtchgD00002048	SAMEA3389006	PRJEB8624	2006	Australia	Susceptible
wtchgD00002049 ERX962680	SAMEA3389007	PRJEB8624	2012	Australia	Resistant (*vanB*)
wtchgD00002050	SAMEA3389008	PRJEB8624	2007	Australia	Susceptible
wtchgD00002051	SAMEA3389009	PRJEB8624	2013	Australia	Susceptible
wtchgD00002053	SAMEA3389011	PRJEB8624	2012	Australia	Resistant (*vanA*)
wtchgD00002054	SAMEA3389012	PRJEB8624	2011	Australia	Susceptible
wtchgD00002055	SAMEA3389013	PRJEB8624	2013	Australia	Resistant (*vanA*)
wtchgD00002056	SAMEA3389014	PRJEB8624	2011	Australia	Resistant (*vanB*)
wtchgD00002057	SAMEA3389015	PRJEB8624	2012	Australia	Susceptible
wtchgD00002058	SAMEA3389016	PRJEB8624	2012	Australia	Resistant (*vanB*)
wtchgD00002060	SAMEA3389017	PRJEB8624	2012	Australia	Susceptible
wtchgD00002061	SAMEA3389018	PRJEB8624	2005	Australia	Susceptible
wtchgD00002062	SAMEA3389019	PRJEB8624	2012	Australia	Susceptible
wtchgD00002063	SAMEA3389020	PRJEB8624	2006	Australia	Susceptible
wtchgD00002064	SAMEA3389021	PRJEB8624	2012	Australia	Susceptible
wtchgD00002066	SAMEA3389022	PRJEB8624	2013	Australia	Susceptible
wtchgD00002067	SAMEA3389023	PRJEB8624	2011	Australia	Susceptible
wtchgD00002068	SAMEA3389024	PRJEB8624	2013	Australia	Susceptible
wtchgD00002069 ERX962698	SAMEA3389025	PRJEB8624	2011	Australia	Resistant (*vanB*)
wtchgD00002070	SAMEA3389026	PRJEB8624	2012	Australia	Susceptible
wtchgD00002071	SAMEA3389027	PRJEB8624	2011	Australia	Susceptible

Table 2 continued overleaf

Sample ID	Sample Accession	Study Accession	Collection Date	Country of Isolation	Predicted vancomycin susceptibility[1]
wtchgD00002072	SAMEA3389028	PRJEB8624	2012	Australia	Resistant (*vanB*)
wtchgD00002073	SAMEA3389029	PRJEB8624	2012	Australia	Resistant (*vanB*)
wtchgD00002075	SAMEA3389030	PRJEB8624	2004	Australia	Susceptible
wtchgD00002076	SAMEA3389031	PRJEB8624	2012	Australia	Susceptible
wtchgD00002077	SAMEA3389032	PRJEB8624	2007	Australia	Susceptible
wtchgD00002078	SAMEA3389033	PRJEB8624	2012	Australia	Susceptible
wtchgD00002079	SAMEA3389034	PRJEB8624	2006	Australia	Resistant (*vanB*)
wtchgD00002080 ERX962708	SAMEA3389035	PRJEB8624	2012	Australia	Susceptible
wtchgD00002081	SAMEA3389036	PRJEB8624	2007	Australia	Susceptible
wtchgD00002082	SAMEA3389037	PRJEB8624	2013	Australia	Susceptible
wtchgD00002083	SAMEA3389038	PRJEB8624	2011	Australia	Resistant (*vanB*)
wtchgD00002084	SAMEA3389039	PRJEB8624	2013	Australia	Susceptible
wtchgD00002085	SAMEA3389040	PRJEB8624	2011	Australia	Resistant (*vanB*)
wtchgD00002086	SAMEA3389041	PRJEB8624	2012	Australia	Resistant (*vanB*)
wtchgD00002087	SAMEA3389042	PRJEB8624	2011	Australia	Susceptible
wtchgD00002088	SAMEA3389043	PRJEB8624	2012	Australia	Resistant (*vanB*)
wtchgD00002089	SAMEA3389044	PRJEB8624	2012	Australia	Resistant (*vanB*)
wtchgD00002090	SAMEA3389045	PRJEB8624	2012	Australia	Resistant (*vanB*)
wtchgD00002091	SAMEA3389046	PRJEB8624	2004	Australia	Resistant (*vanB*)
wtchgD00002092	SAMEA3389047	PRJEB8624	2011	Australia	Susceptible
wtchgD00002093	SAMEA3389048	PRJEB8624	2005	Australia	Resistant (*vanB*)
wtchgD00002095	SAMEA3389049	PRJEB8624	2006	Australia	Susceptible
wtchgD00002096	SAMEA3389050	PRJEB8624	2012	Australia	Resistant (*vanB*)

Table 2 continued overleaf

Sample ID	Sample Accession	Study Accession	Collection Date	Country of Isolation	Predicted vancomycin susceptibility[1]
wtchgD00002097	SAMEA3389051	PRJEB8624	2007	Australia	Susceptible
wtchgD00002098	SAMEA3389052	PRJEB8624	2013	Australia	Susceptible
wtchgD00002099 ERX962726	SAMEA3389053	PRJEB8624	2011	Australia	Susceptible
wtchgD00002100	SAMEA3389054	PRJEB8624	2013	Australia	Resistant (*vanB*)
wtchgD00002101 ERX962728	SAMEA3389055	PRJEB8624	2011	Australia	Susceptible
wtchgD00002102	SAMEA3389056	PRJEB8624	2012	Australia	Susceptible
wtchgD00002103	SAMEA3389057	PRJEB8624	2011	Australia	Resistant (*vanB*)
wtchgD00002104 ERX962731	SAMEA3389058	PRJEB8624	2012	Australia	Susceptible
wtchgD00002105	SAMEA3389059	PRJEB8624	2012	Australia	Resistant (*vanB*)
wtchgD00002106 ERX962733	SAMEA3389060	PRJEB8624	2012	Australia	Susceptible
wtchgD00002108	SAMEA3389062	PRJEB8624	2013	Australia	Susceptible
wtchgD00002109 ERX962736	SAMEA3389063	PRJEB8624	2005	Australia	Resistant (*vanB*)
wtchgD00002110	SAMEA3389064	PRJEB8624	2012	Australia	Susceptible
wtchgD00002111	SAMEA3389065	PRJEB8624	2007	Australia	Resistant (*vanB*)
wtchgD00002112	SAMEA3389066	PRJEB8624	2012	Australia	Resistant (*vanB*)
wtchgD00002113	SAMEA3389067	PRJEB8624	2005	Australia	Resistant (*vanB*)
wtchgD00002114	SAMEA3389068	PRJEB8624	2013	Australia	Susceptible
wtchgD00002115	SAMEA3389069	PRJEB8624	2011	Australia	Susceptible
wtchgD00002117	SAMEA3389070	PRJEB8624	2011	Australia	Susceptible
wtchgD00002118 ERX962744	SAMEA3389071	PRJEB8624	2011	Australia	Resistant (*vanB*)
wtchgD00002119	SAMEA3389072	PRJEB8624	2012	Australia	Susceptible
wtchgD00002120	SAMEA3389073	PRJEB8624	2004	Australia	Susceptible
wtchgD00002121	SAMEA3389074	PRJEB8624	2005	Australia	Resistant (*vanB*)

Table 2 continued overleaf

Sample ID	Sample Accession	Study Accession	Collection Date	Country of Isolation	Predicted vancomycin susceptibility[1]
wtchgD00002122	SAMEA3389075	PRJEB8624	2007	Australia	Resistant (*vanB*)
wtchgD00002123 ERX962749	SAMEA3389076	PRJEB8624	2007	Australia	Resistant (*vanB*)
wtchgD00002124	SAMEA3389077	PRJEB8624	2011	Australia	Susceptible
wtchgD00002125	SAMEA3389078	PRJEB8624	2011	Australia	Resistant (*vanB*)
wtchgD00002126	SAMEA3389079	PRJEB8624	2011	Australia	Susceptible
wtchgD00002127	SAMEA3389080	PRJEB8624	2012	Australia	Susceptible
wtchgD00002128 ERX962754	SAMEA3389081	PRJEB8624	2004	Australia	Susceptible
wtchgD00002129	SAMEA3389082	PRJEB8624	2005	Australia	Susceptible
wtchgD00002130 ERX962756	SAMEA3389083	PRJEB8624	2007	Australia	Resistant (*vanB*)
wtchgD00002131	SAMEA3389084	PRJEB8624	2007	Australia	Susceptible
wtchgD00002132	SAMEA3389085	PRJEB8624	2011	Australia	Resistant (*vanB*)
wtchgD00002133	SAMEA3389086	PRJEB8624	2011	Australia	Resistant (*vanB*)
wtchgD00002134	SAMEA3389087	PRJEB8624	2011	Australia	Susceptible
wtchgD00002135	SAMEA3389088	PRJEB8624	2012	Australia	Susceptible
wtchgD00002136	SAMEA3389089	PRJEB8624	2004	Australia	Susceptible
wtchgD00002137	SAMEA3389090	PRJEB8624	2006	Australia	Susceptible
wtchgD00002138	SAMEA3389091	PRJEB8624	2007	Australia	Resistant (*vanB*)
wtchgD00002140	SAMEA3389093	PRJEB8624	2011	Australia	Resistant (*vanB*)
wtchgD00002141	SAMEA3389094	PRJEB8624	2011	Australia	Susceptible
wtchgD00002142	SAMEA3389095	PRJEB8624	2012	Australia	Resistant (*vanB*)
wtchgD00002143	SAMEA3389096	PRJEB8624	2012	Australia	Resistant (*vanB*)
wtchgD00002145 ERX962770	SAMEA3389097	PRJEB8624	2006	Australia	Susceptible
wtchgD00002146	SAMEA3389098	PRJEB8624	2007	Australia	Resistant (*vanB*)

Table 2 continued overleaf

Sample ID	Sample Accession	Study Accession	Collection Date	Country of Isolation	Predicted vancomycin susceptibility[1]
wtchgD00002147 ERX962772	SAMEA3389099	PRJEB8624	2011	Australia	Susceptible
wtchgD00002148	SAMEA3389100	PRJEB8624	2011	Australia	Resistant (*vanB*)
wtchgD00002149 ERX962774	SAMEA3389101	PRJEB8624	2011	Australia	Susceptible
wtchgD00002150	SAMEA3389102	PRJEB8624	2011	Australia	Resistant (*vanB*)
wtchgD00002151 ERX962776	SAMEA3389103	PRJEB8624	2012	Australia	Susceptible
wtchgD00002152	SAMEA3389104	PRJEB8624	2004	Australia	Susceptible
wtchgD00002153	SAMEA3389105	PRJEB8624	2006	Australia	Susceptible
wtchgD00002154	SAMEA3389106	PRJEB8624	2007	Australia	Susceptible
wtchgD00002155	SAMEA3389107	PRJEB8624	2011	Australia	Susceptible
wtchgD00002156 ERX962781	SAMEA3389108	PRJEB8624	2011	Australia	Resistant (*vanB*)
wtchgD00002157	SAMEA3389109	PRJEB8624	2011	Australia	Susceptible
wtchgD00002158	SAMEA3389110	PRJEB8624	2012	Australia	Resistant (*vanB*)
wtchgD00002159	SAMEA3389111	PRJEB8624	2012	Australia	Susceptible
wtchgD00002160	SAMEA3389112	PRJEB8624	2006	Australia	Susceptible
wtchgD00002161 ERX962786	SAMEA3389113	PRJEB8624	2007	Australia	Resistant (*vanB*)
wtchgD00002162	SAMEA3389114	PRJEB8624	2011	Australia	Resistant (*vanB*)
wtchgD00002163	SAMEA3389115	PRJEB8624	2011	Australia	Resistant (*vanB*)
wtchgD00002164	SAMEA3389116	PRJEB8624	2011	Australia	Susceptible
wtchgD00002165	SAMEA3389117	PRJEB8624	2012	Australia	Resistant (*vanB*)
wtchgD00002166 ERX962791	SAMEA3389118	PRJEB8624	2012	Australia	Susceptible
5 ERX1546267	SAMEA4052459	PRJEB14625	2014	Denmark	Resistant (*vanA*)
7 ERX1546269	SAMEA4052461	PRJEB14625	2014	Denmark	Resistant (*vanA*)
8 ERX1546270	SAMEA4052462	PRJEB14625	2014	Denmark	Resistant (*vanA*)

Table 2 continued overleaf

Sample ID	Sample Accession	Study Accession	Collection Date	Country of Isolation	Predicted vancomycin susceptibility[1]
9 ERX1546271	SAMEA4052463	PRJEB14625	2013	Denmark	Resistant (*vanA*)
10 ERX1546272	SAMEA4052464	PRJEB14625	2014	Denmark	Resistant (*vanA*)
11 ERX1546273	SAMEA4052465	PRJEB14625	2014	Denmark	Resistant (*vanA*)
12 ERX1546274	SAMEA4052466	PRJEB14625	2014	Denmark	Resistant (*vanA*)
15 ERX1546277	SAMEA4052469	PRJEB14625	2013	Denmark	Resistant (*vanA*)
E6014 ERX2790691	SAMEA4884761	PRJEB28495	2010	Latvia	Resistant (*vanA*)
E6018 ERX2790695	SAMEA4884765	PRJEB28495	2010	Latvia	Resistant (*vanA*)
E6020 ERX2790697	SAMEA4884767	PRJEB28495	2010	Latvia	Resistant (*vanA*)
E6059 ERX2790735	SAMEA4884805	PRJEB28495	2010	Portugal	Resistant (*vanA*)
E6968 ERX2790784	SAMEA4884854	PRJEB28495	2010	Latvia	Resistant (*vanA*)
E7002 ERX2790817	SAMEA4884887	PRJEB28495	2010	Latvia	Resistant (*vanA*)
E7005 ERX2790820	SAMEA4884890	PRJEB28495	2009	France	Resistant (*vanB*)
E7008 ERX2790823	SAMEA4884893	PRJEB28495	2010	Slovenia	Resistant (*vanA*)
E7010 ERX2790825	SAMEA4884895	PRJEB28495	2009	France	Resistant (*vanA*)
E7053 ERX2790861	SAMEA4884931	PRJEB28495	2010	Portugal	Resistant (*vanA*)
E7100 ERX2790906	SAMEA4884976	PRJEB28495	2008	Slovenia	Resistant (*vanA*)
E7191 ERX2790962	SAMEA4885032	PRJEB28495	2010	Portugal	Resistant (*vanA*)
E7201 ERX2790972	SAMEA4885042	PRJEB28495	2009	Luxembourg	Resistant (*vanA*)
E7204 ERX2790975	SAMEA4885045	PRJEB28495	2009	Greece	Resistant (*vanA*)
E7205 ERX2790976	SAMEA4885046	PRJEB28495	2009	Greece	Resistant (*vanA*)
E7232 ERX2791001	SAMEA4885071	PRJEB28495	2010	Greece	Resistant (*vanA*)
E7237 ERX2791006	SAMEA4885076	PRJEB28495	2010	Greece	Resistant (*vanB*)
E7256 ERX2791025	SAMEA4885095	PRJEB28495	2009	Greece	Resistant (*vanA*)

Table 2 continued overleaf

Sample ID	Sample Accession	Study Accession	Collection Date	Country of Isolation	Predicted vancomycin susceptibility[1]
E7263 ERX2791032	SAMEA4885102	PRJEB28495	2009	Greece	Resistant (*vanA*)
E7308 ERX2791043	SAMEA4885113	PRJEB28495	2012	Netherlands	Resistant (*vanA*)
E7314 ERX2791049	SAMEA4885119	PRJEB28495	2012	Netherlands	Resistant (*vanB*)
E7414 ERX2791126	SAMEA4885198	PRJEB28495	2012	Netherlands	Resistant (*vanA*)
E7425 ERX2791135	SAMEA4885207	PRJEB28495	2009	Netherlands	Resistant (*vanB*)
E7429 ERX2791139	SAMEA4885211	PRJEB28495	2010	Netherlands	Resistant (*vanB*)
E7437 ERX2791145	SAMEA4885217	PRJEB28495	2011	Netherlands	Resistant (*vanA*)
E7474 ERX2791160	SAMEA4885232	PRJEB28495	2012	Netherlands	Resistant (*vanA*)
E7586 ERX2791245	SAMEA4885317	PRJEB28495	2012	Netherlands	Resistant (*vanA*)
E7590 ERX2791249	SAMEA4885321	PRJEB28495	2012	Netherlands	Resistant (*vanB*)
E7595 ERX2791254	SAMEA4885326	PRJEB28495	2012	Netherlands	Resistant (*vanA*)
E7607 ERX2791259	SAMEA4885331	PRJEB28495	2013	Netherlands	Resistant (*vanB*)
E7641 ERX2791267	SAMEA4885339	PRJEB28495	2013	Netherlands	Resistant (*vanA*)
E7672 ERX2791297	SAMEA4885369	PRJEB28495	2013	Netherlands	Resistant (*vanA*)
E7711 ERX2791335	SAMEA4885407	PRJEB28495	2013	Netherlands	Resistant (*vanB*)
E7861 ERX2791350	SAMEA4885422	PRJEB28495	2013	Netherlands	Resistant (*vanA*)
E7920 ERX2791390	SAMEA4885462	PRJEB28495	2013	Netherlands	Resistant (*vanB*)
E7935 ERX2791403	SAMEA4885475	PRJEB28495	2013	Netherlands	Resistant (*vanB*)
E7950 ERX2791418	SAMEA4885490	PRJEB28495	2013	Netherlands	Resistant (*vanB*)
E7965 ERX2791426	SAMEA4885498	PRJEB28495	2013	Netherlands	Resistant (*vanA*)
E7967 ERX2791428	SAMEA4885500	PRJEB28495	2013	Netherlands	Resistant (*vanA*)
E8022 ERX2791464	SAMEA4885536	PRJEB28495	2014	Netherlands	Resistant (*vanB*)
E8029 ERX2791471	SAMEA4885543	PRJEB28495	2014	Netherlands	Resistant (*vanB*)

Table 2 continued overleaf

Sample ID	Sample Accession	Study Accession	Collection Date	Country of Isolation	Predicted vancomycin susceptibility[1]
E8047 ERX2791489	SAMEA4885561	PRJEB28495	2014	Netherlands	Resistant (*vanA*)
E8219 ERX2791576	SAMEA4885648	PRJEB28495	2005	Netherlands	Resistant (*vanA*)
E8265 ERX2791597	SAMEA4885669	PRJEB28495	2015	Netherlands	Resistant (*vanB*)
E8339 ERX2791659	SAMEA4885731	PRJEB28495	2015	Netherlands	Resistant (*vanA*)
E8342 ERX2791662	SAMEA4885734	PRJEB28495	2015	Netherlands	Resistant (*vanA*)
E8344 ERX2791664	SAMEA4885736	PRJEB28495	2015	Netherlands	Resistant (*vanA*)
E8394 ERX2791696	SAMEA4885768	PRJEB28495	2015	Netherlands	Resistant (*vanA*)
E8402 ERX2791704	SAMEA4885776	PRJEB28495	2015	Netherlands	Resistant (*vanA*)
E8407 ERX2791709	SAMEA4885781	PRJEB28495	2015	Netherlands	Susceptible
E8413 ERX2791714	SAMEA4885786	PRJEB28495	2015	Netherlands	Resistant (*vanB*)
E8424 ERX2791724	SAMEA4885796	PRJEB28495	2015	Netherlands	Resistant (*vanB*)
E8459 ERX2791759	SAMEA4885831	PRJEB28495	2015	Netherlands	Resistant (*vanA*)
E9001 ERX2791867	SAMEA4885940	PRJEB28495	2015	Netherlands	Resistant (*vanA*)
E1193 ERX2791927	SAMEA4886000	PRJEB28495	Unknown	Spain	Susceptible
E1303 ERX2791932	SAMEA4886005	PRJEB28495	Unknown	Poland	Susceptible
V220 ERX2817757	SAMEA4937740	PRJEB28731	2013	Denmark	Resistant (*vanA*)
V1184	SAMEA4937746	PRJEB28731	2015	Denmark	Resistant (*vanA*)
V1075 ERX3199758	SAMEA5367834	PRJEB28731	2015	Denmark	Resistant (*vanA*)
V1076	SAMEA5367835	PRJEB28731	2015	Denmark	Resistant (*vanA*)
V1096	SAMEA5367854	PRJEB28731	2015	Denmark	Resistant (*vanA*)
V1115	SAMEA5367873	PRJEB28731	2015	Denmark	Resistant (*vanA*)
V1116	SAMEA5367874	PRJEB28731	2015	Denmark	Resistant (*vanA*)
V1123	SAMEA5367880	PRJEB28731	2015	Denmark	Resistant (*vanA*)

Table 2 continued overleaf

Sample ID	Sample Accession	Study Accession	Collection Date	Country of Isolation	Predicted vancomycin susceptibility[1]
V1156	SAMEA5367909	PRJEB28731	2015	Denmark	Resistant (*vanA*)
V1165 ERX3199800	SAMEA5367918	PRJEB28731	2015	Denmark	Resistant (*vanA*)
V1170	SAMEA5367922	PRJEB28731	2013	Denmark	Resistant (*vanA*)
V1206	SAMEA5367953	PRJEB28731	2015	Denmark	Resistant (*vanA*)
V139	SAMEA5368005	PRJEB28731	2013	Denmark	Resistant (*vanA*)
V140 ERX3199103	SAMEA5368007	PRJEB28731	2013	Denmark	Resistant (*vanA*)
V167	SAMEA5368026	PRJEB28731	2013	Denmark	Resistant (*vanA*)
V180	SAMEA5368039	PRJEB28731	2013	Denmark	Resistant (*vanA*)
V182 ERX3199086	SAMEA5368041	PRJEB28731	2013	Denmark	Resistant (*vanA*)
V194 ERX3199121	SAMEA5368053	PRJEB28731	2013	Denmark	Resistant (*vanA*)
V209	SAMEA5368059	PRJEB28731	2013	Denmark	Resistant (*vanA*)
V210	SAMEA5368060	PRJEB28731	2013	Denmark	Resistant (*vanA*)
V315	SAMEA5368098	PRJEB28731	2013	Denmark	Resistant (*vanA*)
V342	SAMEA5368114	PRJEB28731	2014	Denmark	Resistant (*vanA*)
V355	SAMEA5368119	PRJEB28731	2014	Denmark	Resistant (*vanA*)
V395	SAMEA5368154	PRJEB28731	2014	Denmark	Resistant (*vanA*)
V4	SAMEA5368158	PRJEB28731	2012	Denmark	Resistant (*vanA*)
V400 ERX3199345	SAMEA5368159	PRJEB28731	2014	Denmark	Resistant (*vanA*)
V499	SAMEA5368210	PRJEB28731	2014	Denmark	Resistant (*vanA*)
V531 ERX3199413	SAMEA5368221	PRJEB28731	2014	Denmark	Resistant (*vanA*)
V588	SAMEA5368253	PRJEB28731	2014	Denmark	Resistant (*vanA*)
V619	SAMEA5368269	PRJEB28731	2014	Denmark	Resistant (*vanA*)
V645 ERX3199486	SAMEA5368296	PRJEB28731	2014	Denmark	Resistant (*vanA*)

Table 2 continued overleaf

Sample ID	Sample Accession	Study Accession	Collection Date	Country of Isolation	Predicted vancomycin susceptibility[1]
V660	SAMEA5368310	PRJEB28731	2014	Denmark	Resistant (*vanA*)
V668 ERX3199519	SAMEA5368318	PRJEB28731	2014	Denmark	Resistant (*vanA*)
V706	SAMEA5368352	PRJEB28731	2015	Denmark	Resistant (*vanA*)
V71	SAMEA5368355	PRJEB28731	2013	Denmark	Resistant (*vanA*)
V744	SAMEA5368386	PRJEB28731	2013	Denmark	Resistant (*vanA*)
V746	SAMEA5368388	PRJEB28731	2014	Denmark	Resistant (*vanA*)
V779	SAMEA5368420	PRJEB28731	2015	Denmark	Resistant (*vanA*)
V848	SAMEA5368487	PRJEB28731	2014	Denmark	Resistant (*vanA*)
V905	SAMEA5368543	PRJEB28731	2015	Denmark	Resistant (*vanA*)
V932	SAMEA5368570	PRJEB28731	2015	Denmark	Resistant (*vanA*)
VS119	SAMEA5368654	PRJEB28731	2013	Denmark	Susceptible
VS122	SAMEA5368657	PRJEB28731	2013	Denmark	Susceptible
VS129	SAMEA5368664	PRJEB28731	2013	Denmark	Susceptible
VS135	SAMEA5368670	PRJEB28731	2013	Denmark	Susceptible
VS150	SAMEA5368685	PRJEB28731	2013	Denmark	Susceptible
VS203	SAMEA5368708	PRJEB28731	2015	Denmark	Susceptible
VS212	SAMEA5368717	PRJEB28731	2015	Denmark	Susceptible
VS229	SAMEA5368735	PRJEB28731	2015	Denmark	Susceptible
VS231	SAMEA5368738	PRJEB28731	2015	Denmark	Susceptible
VS24	SAMEA5368742	PRJEB28731	2014	Denmark	Susceptible
VRE1853	SAMEA6819260	PRJEB38219	2015	Denmark	Resistant (*vanA*)
VRE1859 ERX4096639	SAMEA6819264	PRJEB38219	2015	Denmark	Resistant (*vanA*)
VRE1957	SAMEA6819337	PRJEB38219	2015	Denmark	Resistant (*vanA*)

Table 2 continued overleaf

Sample ID	Sample Accession	Study Accession	Collection Date	Country of Isolation	Predicted vancomycin susceptibility[1]
VRE1960	SAMEA6819340	PRJEB38219	2015	Denmark	Resistant (*vanA*)
VRE1970	SAMEA6819348	PRJEB38219	2015	Denmark	Resistant (*vanA*)
VRE1986	SAMEA6819356	PRJEB38219	2015	Denmark	Resistant (*vanA*)
VRE2011	SAMEA6819368	PRJEB38219	2015	Denmark	Resistant (*vanA*)
VRE2047	SAMEA6819398	PRJEB38219	2015	Denmark	Resistant (*vanA*)
VRE2061	SAMEA6819408	PRJEB38219	2015	Denmark	Resistant (*vanA*)
VRE2064	SAMEA6819411	PRJEB38219	2015	Denmark	Resistant (*vanA*)
VRE2073	SAMEA6819416	PRJEB38219	2015	Denmark	Resistant (*vanA*)
VRE2119 ERX4096828	SAMEA6819454	PRJEB38219	2015	Denmark	Resistant (*vanA*)
VRE2127	SAMEA6819461	PRJEB38219	2015	Denmark	Resistant (*vanA*)
VRE2179 ERX4096875	SAMEA6819501	PRJEB38219	2015	Denmark	Resistant (*vanA*)
VRE2190	SAMEA6819509	PRJEB38219	2015	Denmark	Resistant (*vanA*)
VRE2215	SAMEA6819527	PRJEB38219	2015	Denmark	Resistant (*vanA*)
VRE2226	SAMEA6819534	PRJEB38219	2015	Denmark	Resistant (*vanA*)
VRE2237 ERX4096918	SAMEA6819544	PRJEB38219	2015	Denmark	Resistant (*vanA*)
VRE2323 ERX4096937	SAMEA6819563	PRJEB38219	2015	Denmark	Resistant (*vanA*)
E1133	SAMN00779802	PRJNA82431	2001	USA	Resistant (*vanB*)
E1392 SRX144239	SAMN00779806	PRJNA82439	2000	United Kingdom	Susceptible
AHXO00000000	SAMN00779827	PRJNA82477	2013	Tanzania	Susceptible
AHXV00000000	SAMN00779835	PRJNA82491	2001	USA	Resistant (*vanA*)
AHWL00000000	SAMN00779844	PRJNA82419	1997	Israel	Resistant (*vanA*)
AHYF00000000	SAMN00779846	PRJNA82511	1999	Italy	Susceptible
AHYG00000000	SAMN00779847	PRJNA82513	2002	Germany	Resistant (*vanA*)

Table 2 continued overleaf

Sample ID	Sample Accession	Study Accession	Collection Date	Country of Isolation	Predicted vancomycin susceptibility[1]
E2369 SRX144247	SAMN00779848	PRJNA82515	2006	Netherlands	Resistant (*vanA*)
AHYI00000000	SAMN00779849	PRJNA82517	2002	Netherlands	Susceptible
AHYK00000000	SAMN00779851	PRJNA82521	2010	Latvia	Resistant (*vanA*)
AHYL00000000	SAMN00779852	PRJNA82523	2010	Portugal	Resistant (*vanA*)
Efm NY2-1	SAMN00779856	PRJNA82525	Unknown	USA	Resistant (*vanA*)
EnGen0376 SRX145152	SAMN00779857	PRJNA82527	Unknown	USA	Resistant (*vanA*)
Efm NY2-3 SRX145185	SAMN00779858	PRJNA82529	Unknown	USA	Resistant (*vanA*)
HM1072	SAMN00808917	PRJNA88473	1994	France	Resistant (*vanA*)
UAA945 SRX180459	SAMN00808918	PRJNA88475	1996	USA	Resistant (*vanA*)
109 A1 SRX189799	SAMN00808943	PRJNA88259	1995	Denmark	Resistant (*vanA*)
841V03 SRX189802	SAMN00808953	PRJNA88277	2003	Denmark	Resistant (*vanA*)
H17243 SRX145145	SAMN00808974	PRJNA88317	1995	Denmark	Resistant (*vanA*)
H17494 SRX145181	SAMN00808975	PRJNA88319	1995	Denmark	Resistant (*vanA*)
H17575	SAMN00808976	PRJNA88321	1995	Denmark	Resistant (*vanA*)
HM1071	SAMN00808977	PRJNA88323	1994	France	Resistant (*vanA*)
HM1074 SRX145143	SAMN00808978	PRJNA88325	1994	France	Susceptible
UAA716 SRX149855	SAMN00808986	PRJNA88339	1994	France	Resistant (*vanA*)
UAA720 SRX145158	SAMN00808989	PRJNA88345	1993	France	Resistant (*vanA*)
UAA723	SAMN00808993	PRJNA88351	1993	France	Resistant (*vanA*)
UAA724 SRX149876	SAMN00808994	PRJNA88353	1993	France	Resistant (*vanA*)
UAA725	SAMN00808995	PRJNA88355	1994	France	Resistant (*vanA*)
UAA825	SAMN00808996	PRJNA88357	1996	France	Resistant (*vanA*)
UAA944 SRX145129	SAMN00808997	PRJNA88359	1996	USA	Resistant (*vanA*)

Table 2 continued overleaf

Sample ID	Sample Accession	Study Accession	Collection Date	Country of Isolation	Predicted vancomycin susceptibility[1]
VRE 108 SRX145136	SAMN00809005	PRJNA88373	2010	Denmark	Resistant (*vanA*)
VRE 110	SAMN00809006	PRJNA88375	2010	Denmark	Resistant (*vanA*)
VRE 13	SAMN00809007	PRJNA88377	2010	Denmark	Resistant (*vanA*)
VRE 84	SAMN00809008	PRJNA88379	2010	Denmark	Resistant (*vanA*)
UAA909 SRX145095	SAMN00809009	PRJNA88381	1996	Switzerland	Resistant (*vanA*)
UAA910 SRX145084	SAMN00809010	PRJNA88383	1996	Switzerland	Resistant (*vanA*)
UAA911 SRX155287	SAMN00809011	PRJNA88385	1996	Switzerland	Resistant (*vanA*)
UAA1023 SRX152336	SAMN00809098	PRJNA88817	1996	France	Resistant (*vanA*)
UAA1024 SRX152335	SAMN00809099	PRJNA88819	1996	France	Resistant (*vanA*)
UAA1025	SAMN00809100	PRJNA88821	1996	France	Resistant (*vanA*)
UAA1433 SRX152342	SAMN00809103	PRJNA88827	2000	France	Resistant (*vanA*)
UAA1484 SRX152319	SAMN00809104	PRJNA88829	1992	Belgium	Resistant (*vanA*)
UAA947 SRX152325	SAMN00809108	PRJNA88801	1996	USA	Resistant (*vanA*)
UAA951 SRX152383	SAMN00809130	PRJNA88805	1996	USA	Resistant (*vanA*)
UAA210 SRX152352	SAMN00809142	PRJNA88897	1986	France	Resistant (*vanA*)
UAA1022 SRX152350	SAMN00809146	PRJNA88815	1996	Switzerland	Resistant (*vanA*)
UAA949 SRX152446	SAMN00809200	PRJNA89009	1996	USA	Resistant (*vanA*)
UAA950 SRX158220	SAMN00809201	PRJNA89011	1996	USA	Resistant (*vanA*)
Efm NY1-1	SAMN00809203	PRJNA89015	Unknown	USA	Resistant (*vanA*)
Efm NY1-2 SRX172447	SAMN00809204	PRJNA89017	Unknown	USA	Resistant (*vanA*)
Efm NY1-3 SRX174114	SAMN00809205	PRJNA89019	Unknown	USA	Resistant (*vanA*)
Efm NY1-4 SRX170870	SAMN00809206	PRJNA89021	Unknown	USA	Resistant (*vanA*)
Efm NY1-5 SRX174118	SAMN00809207	PRJNA89023	Unknown	USA	Resistant (*vanA*)

Table 2 continued overleaf

Sample ID	Sample Accession	Study Accession	Collection Date	Country of Isolation	Predicted vancomycin susceptibility[1]
Efm NY1-6 SRX174113	SAMN00809208	PRJNA89025	Unknown	USA	Resistant (*vanA*)
Efm NY3-1 SRX174115	SAMN00809209	PRJNA89027	Unknown	USA	Resistant (*vanA*)
Ef aus0006 SRX349487	SAMN02318071	PRJNA205886	1999	Australia	Susceptible
Ef aus0015 SRX349491	SAMN02318073	PRJNA205886	2002	Australia	Susceptible
Ef aus0016 SRX349492	SAMN02318074	PRJNA205886	2003	Australia	Resistant (*vanB*)
Ef aus0018 SRX349493	SAMN02318075	PRJNA205886	2003	Australia	Susceptible
Ef aus0021 SRX349495	SAMN02318076	PRJNA205886	2004	Australia	Resistant (*vanB*)
Ef aus0029 SRX349496	SAMN02318077	PRJNA205886	2005	Australia	Susceptible
Ef aus0030 SRX349497	SAMN02318078	PRJNA205886	2005	Australia	Resistant (*vanB*)
Ef aus0038 SRX349499	SAMN02318079	PRJNA205886	2006	Australia	Susceptible
Ef aus0040 SRX349501	SAMN02318080	PRJNA205886	2006	Australia	Susceptible
Ef aus0048 SRX349504	SAMN02318081	PRJNA205886	2007	Australia	Resistant (*vanB*)
Ef aus0091 SRX349521	SAMN02318082	PRJNA205886	2009	Australia	Resistant (*vanB*)
Ef aus0094 SRX349523	SAMN02318084	PRJNA205886	2009	Australia	Susceptible
Ef aus0098 SRX349524	SAMN02318087	PRJNA205886	2003	Australia	Susceptible
Ef aus0100 SRX349525	SAMN02318088	PRJNA205886	2000	Australia	Susceptible
Ef RPH1 SRX349527	SAMN02318091	PRJNA205886	2009	Australia	Resistant (*vanB*)
Ef RPH3 SRX349529	SAMN02318092	PRJNA205886	2009	Australia	Resistant (*vanB*)
Ef aus0007 SRX349488	SAMN02318157	PRJNA205886	1999	Australia	Susceptible
Ef aus0012 SRX349490	SAMN02318158	PRJNA205886	2000	Australia	Resistant (*vanB*)
Ef aus0019 SRX349494	SAMN02318159	PRJNA205886	2004	Australia	Susceptible
Ef aus0031 SRX349498	SAMN02318160	PRJNA205886	2005	Australia	Resistant (*vanB*)
Ef aus0039 SRX349500	SAMN02318161	PRJNA205886	2006	Australia	Susceptible

Table 2 continued overleaf

Sample ID	Sample Accession	Study Accession	Collection Date	Country of Isolation	Predicted vancomycin susceptibility[1]
Ef aus0041 SRX349502	SAMN02318162	PRJNA205886	2006	Australia	Susceptible
Ef aus0045 SRX349503	SAMN02318163	PRJNA205886	2007	Australia	Resistant (*vanB*)
Ef aus0050 SRX349505	SAMN02318164	PRJNA205886	2007	Australia	Resistant (*vanB*)
Ef aus0053 SRX349506	SAMN02318166	PRJNA205886	2007	Australia	Susceptible
Ef aus0055 SRX349507	SAMN02318167	PRJNA205886	2007	Australia	Resistant (*vanB*)
Ef aus0057 SRX349508	SAMN02318169	PRJNA205886	2007	Australia	Susceptible
Ef aus0063 SRX349509	SAMN02318170	PRJNA205886	2008	Australia	Susceptible
Ef aus0064 SRX349510	SAMN02318171	PRJNA205886	2008	Australia	Susceptible
Ef aus0065 SRX349511	SAMN02318172	PRJNA205886	2008	Australia	Susceptible
Ef aus0069 SRX349512	SAMN02318174	PRJNA205886	2008	Australia	Resistant (*vanB*)
Ef aus0070 SRX349513	SAMN02318175	PRJNA205886	2008	Australia	Resistant (*vanB*)
Ef aus0071 SRX349514	SAMN02318176	PRJNA205886	2008	Australia	Resistant (*vanB*)
Ef aus0078 SRX349515	SAMN02318180	PRJNA205886	2008	Australia	Susceptible
Ef aus0080 SRX349516	SAMN02318181	PRJNA205886	2008	Australia	Susceptible
Ef aus0081 SRX349517	SAMN02318182	PRJNA205886	2009	Australia	Resistant (*vanB*)
Ef aus0084 SRX349518	SAMN02318183	PRJNA205886	2009	Australia	Resistant (*vanB*)
Ef aus0087 SRX349519	SAMN02318185	PRJNA205886	2009	Australia	Resistant (*vanB*)
Ef RPH2 SRX349528	SAMN02318189	PRJNA205886	2009	Australia	Susceptible
Case1VSE SRX1496320	SAMN04358603	PRJNA306646	2014	Norway	Resistant (*vanA*)
UW11590	SAMN05375116	PRJNA328573	2014	Germany	Resistant (*vanA*)
UW11733 SRX1934255	SAMN05375117	PRJNA328573	2014	Germany	Resistant (*vanB*)
UW11858	SAMN05375118	PRJNA328573	2014	Germany	Resistant (*vanA*)
UW12712	SAMN05375119	PRJNA328573	2015	Germany	Resistant (*vanA*)

Table 2 continued overleaf

Sample ID	Sample Accession	Study Accession	Collection Date	Country of Isolation	Predicted vancomycin susceptibility[1]
AUSMDU00003991 SRX1998502	SAMN05510547	PRJNA336433	2015	Australia	Resistant (*vanA*)
AUSMDU00003992 SRX1998503	SAMN05510548	PRJNA336433	2015	Australia	Resistant (*vanA*)
AUSMDU00003993 SRX1998514	SAMN05510549	PRJNA336433	2015	Australia	Resistant (*vanB*)
AUSMDU00003994 SRX1998525	SAMN05510550	PRJNA336433	2015	Australia	Resistant (*vanB*)
AUSMDU00003995 SRX1998536	SAMN05510551	PRJNA336433	2015	Australia	Resistant (*vanA*)
AUSMDU00003998 SRX1998547	SAMN05510552	PRJNA336433	2015	Australia	Resistant (*vanB*)
AUSMDU00004004 SRX1998558	SAMN05510553	PRJNA336433	2015	Australia	Resistant (*vanB*)
AUSMDU00004007 SRX1998569	SAMN05510554	PRJNA336433	2015	Australia	Resistant (*vanB*)
AUSMDU00004008 SRX1998580	SAMN05510555	PRJNA336433	2015	Australia	Resistant (*vanB*)
AUSMDU00004024 SRX1998591	SAMN05510556	PRJNA336433	2015	Australia	Resistant (*vanA*)
AUSMDU00004025 SRX1998504	SAMN05510557	PRJNA336433	2015	Australia	Resistant (*vanB*)
AUSMDU00004026 SRX1998505	SAMN05510558	PRJNA336433	2015	Australia	Resistant (*vanA*)
AUSMDU00004037 SRX1998506	SAMN05510559	PRJNA336433	2015	Australia	Resistant (*vanB*)
AUSMDU00004042 SRX1998507	SAMN05510560	PRJNA336433	2015	Australia	Resistant (*vanB*)
AUSMDU00004043 SRX1998508	SAMN05510561	PRJNA336433	2015	Australia	Resistant (*vanA*)
AUSMDU00004046 SRX1998509	SAMN05510562	PRJNA336433	2015	Australia	Resistant (*vanA*)
AUSMDU00004048 SRX1998510	SAMN05510563	PRJNA336433	2015	Australia	Resistant (*vanB*)
AUSMDU00004049 SRX1998511	SAMN05510564	PRJNA336433	2015	Australia	Resistant (*vanB*)
AUSMDU00004052 SRX1998512	SAMN05510565	PRJNA336433	2015	Australia	Resistant (*vanB*)
AUSMDU00004053 SRX1998513	SAMN05510566	PRJNA336433	2015	Australia	Resistant (*vanB*)
AUSMDU00004054 SRX1998515	SAMN05510567	PRJNA336433	2015	Australia	Resistant (*vanB*)
AUSMDU00004063 SRX1998516	SAMN05510568	PRJNA336433	2015	Australia	Resistant (*vanB*)
AUSMDU00004064 SRX1998517	SAMN05510569	PRJNA336433	2015	Australia	Resistant (*vanB*)

Table 2 continued overleaf

Sample ID	Sample Accession	Study Accession	Collection Date	Country of Isolation	Predicted vancomycin susceptibility[1]
AUSMDU00004067 SRX1998518	SAMN05510570	PRJNA336433	2015	Australia	Resistant (*vanB*)
AUSMDU00004078 SRX1998519	SAMN05510571	PRJNA336433	2015	Australia	Resistant (*vanB*)
AUSMDU00004081 SRX1998520	SAMN05510572	PRJNA336433	2015	Australia	Resistant (*vanB*)
AUSMDU00004082 SRX1998521	SAMN05510573	PRJNA336433	2015	Australia	Resistant (*vanA*)
AUSMDU00004083 SRX1998522	SAMN05510574	PRJNA336433	2015	Australia	Resistant (*vanB*)
AUSMDU00004085 SRX1998523	SAMN05510575	PRJNA336433	2015	Australia	Resistant (*vanB*)
AUSMDU00004086 SRX1998524	SAMN05510576	PRJNA336433	2015	Australia	Resistant (*vanB*)
AUSMDU00004087 SRX1998526	SAMN05510577	PRJNA336433	2015	Australia	Resistant (*vanB*)
AUSMDU00004090 SRX1998527	SAMN05510578	PRJNA336433	2015	Australia	Resistant (*vanA*)
AUSMDU00004095 SRX1998528	SAMN05510579	PRJNA336433	2015	Australia	Resistant (*vanB*)
AUSMDU00004101 SRX1998529	SAMN05510580	PRJNA336433	2015	Australia	Resistant (*vanB*)
AUSMDU00004113 SRX1998530	SAMN05510581	PRJNA336433	2015	Australia	Resistant (*vanB*)
AUSMDU00004124 SRX1998531	SAMN05510582	PRJNA336433	2015	Australia	Resistant (*vanB*)
AUSMDU00004131 SRX1998532	SAMN05510583	PRJNA336433	2015	Australia	Resistant (*vanA*)
AUSMDU00004134 SRX1998533	SAMN05510584	PRJNA336433	2015	Australia	Resistant (*vanA*)
AUSMDU00004143 SRX1998534	SAMN05510585	PRJNA336433	2015	Australia	Resistant (*vanB*)
AUSMDU00004146 SRX1998535	SAMN05510586	PRJNA336433	2015	Australia	Resistant (*vanB*)
AUSMDU00004148 SRX1998537	SAMN05510587	PRJNA336433	2015	Australia	Resistant (*vanB*)
AUSMDU00004160 SRX1998538	SAMN05510588	PRJNA336433	2015	Australia	Resistant (*vanA*)
AUSMDU00004162 SRX1998539	SAMN05510589	PRJNA336433	2015	Australia	Resistant (*vanB*)
AUSMDU00004164 SRX1998540	SAMN05510590	PRJNA336433	2015	Australia	Resistant (*vanB*)
AUSMDU00004165 SRX1998541	SAMN05510591	PRJNA336433	2015	Australia	Resistant (*vanB*)
AUSMDU00004166 SRX1998542	SAMN05510592	PRJNA336433	2015	Australia	Resistant (*vanA*)

Table 2 continued overleaf

Sample ID	Sample Accession	Study Accession	Collection Date	Country of Isolation	Predicted vancomycin susceptibility[1]
AUSMDU00004167 SRX1998543	SAMN05510593	PRJNA336433	2015	Australia	Resistant (*vanA*)
AUSMDU00004170 SRX1998544	SAMN05510594	PRJNA336433	2015	Australia	Resistant (*vanB*)
AUSMDU00004173 SRX1998545	SAMN05510595	PRJNA336433	2015	Australia	Resistant (*vanB*)
AUSMDU00004176 SRX1998546	SAMN05510596	PRJNA336433	2015	Australia	Resistant (*vanB*)
AUSMDU00004179 SRX1998548	SAMN05510597	PRJNA336433	2015	Australia	Resistant (*vanB*)
AUSMDU00004190 SRX1998549	SAMN05510598	PRJNA336433	2015	Australia	Resistant (*vanB*)
AUSMDU00004192 SRX1998550	SAMN05510599	PRJNA336433	2015	Australia	Resistant (*vanA*)
AUSMDU00004193 SRX1998551	SAMN05510600	PRJNA336433	2015	Australia	Resistant (*vanB*)
AUSMDU00004195 SRX1998552	SAMN05510601	PRJNA336433	2015	Australia	Resistant (*vanB*)
AUSMDU00004198 SRX1998553	SAMN05510602	PRJNA336433	2015	Australia	Resistant (*vanB*)
AUSMDU00004204 SRX1998554	SAMN05510603	PRJNA336433	2015	Australia	Resistant (*vanA*)
AUSMDU00004214 SRX1998555	SAMN05510604	PRJNA336433	2015	Australia	Resistant (*vanB*)
AUSMDU00004217 SRX1998556	SAMN05510605	PRJNA336433	2015	Australia	Resistant (*vanB*)
AUSMDU00004219 SRX1998557	SAMN05510606	PRJNA336433	2015	Australia	Resistant (*vanA*)
AUSMDU00004224 SRX1998559	SAMN05510607	PRJNA336433	2015	Australia	Resistant (*vanB*)
AUSMDU00004225 SRX1998560	SAMN05510608	PRJNA336433	2015	Australia	Resistant (*vanB*)
AUSMDU00004226 SRX1998561	SAMN05510609	PRJNA336433	2015	Australia	Resistant (*vanB*)
AUSMDU00004227 SRX1998562	SAMN05510610	PRJNA336433	2015	Australia	Resistant (*vanB*)
AUSMDU00004230 SRX1998563	SAMN05510611	PRJNA336433	2015	Australia	Resistant (*vanB*)
AUSMDU00004232 SRX1998564	SAMN05510612	PRJNA336433	2015	Australia	Resistant (*vanB*)
AUSMDU00004233 SRX1998565	SAMN05510613	PRJNA336433	2015	Australia	Resistant (*vanB*)
AUSMDU00004235 SRX1998566	SAMN05510614	PRJNA336433	2015	Australia	Resistant (*vanB*)
AUSMDU00004236 SRX1998567	SAMN05510615	PRJNA336433	2015	Australia	Resistant (*vanB*)

Table 2 continued overleaf

Sample ID	Sample Accession	Study Accession	Collection Date	Country of Isolation	Predicted vancomycin susceptibility[1]
AUSMDU00004237 SRX1998568	SAMN05510616	PRJNA336433	2015	Australia	Resistant (*vanB*)
AUSMDU00004241 SRX1998570	SAMN05510617	PRJNA336433	2015	Australia	Resistant (*vanB*)
AUSMDU00004244 SRX1998571	SAMN05510618	PRJNA336433	2015	Australia	Resistant (*vanB*)
AUSMDU00004245 SRX1998572	SAMN05510619	PRJNA336433	2015	Australia	Resistant (*vanB*)
AUSMDU00004248 SRX1998573	SAMN05510620	PRJNA336433	2015	Australia	Resistant (*vanB*)
AUSMDU00004250 SRX1998574	SAMN05510621	PRJNA336433	2015	Australia	Resistant (*vanB*)
AUSMDU00004252 SRX1998575	SAMN05510622	PRJNA336433	2015	Australia	Resistant (*vanB*)
AUSMDU00004253 SRX1998576	SAMN05510623	PRJNA336433	2015	Australia	Resistant (*vanB*)
AUSMDU00004259 SRX1998577	SAMN05510624	PRJNA336433	2015	Australia	Resistant (*vanA*)
AUSMDU00004260 SRX1998578	SAMN05510625	PRJNA336433	2015	Australia	Resistant (*vanB*)
AUSMDU00004263 SRX1998579	SAMN05510626	PRJNA336433	2015	Australia	Resistant (*vanB*)
AUSMDU00004273 SRX1998581	SAMN05510627	PRJNA336433	2015	Australia	Resistant (*vanB*)
AUSMDU00004274 SRX1998582	SAMN05510628	PRJNA336433	2015	Australia	Resistant (*vanA*)
AUSMDU00004276 SRX1998583	SAMN05510629	PRJNA336433	2015	Australia	Resistant (*vanB*)
AUSMDU00004280 SRX1998584	SAMN05510630	PRJNA336433	2015	Australia	Resistant (*vanB*)
AUSMDU00004281 SRX1998585	SAMN05510631	PRJNA336433	2015	Australia	Resistant (*vanB*)
AUSMDU00004283 SRX1998586	SAMN05510632	PRJNA336433	2015	Australia	Resistant (*vanB*)
AUSMDU00004286 SRX1998587	SAMN05510633	PRJNA336433	2015	Australia	Resistant (*vanB*)
AUSMDU00004287 SRX1998588	SAMN05510634	PRJNA336433	2015	Australia	Resistant (*vanB*)
AUSMDU00004292 SRX1998589	SAMN05510635	PRJNA336433	2015	Australia	Resistant (*vanB*)
AUSMDU00004294 SRX1998590	SAMN05510636	PRJNA336433	2015	Australia	Resistant (*vanA*)
AUSMDU00004298 SRX1998592	SAMN05510637	PRJNA336433	2015	Australia	Resistant (*vanB*)
AUSMDU00004299 SRX1998593	SAMN05510638	PRJNA336433	2015	Australia	Resistant (*vanB*)

Table 2 continued overleaf

Sample ID	Sample Accession	Study Accession	Collection Date	Country of Isolation	Predicted vancomycin susceptibility[1]
AUSMDU00004303 SRX1998594	SAMN05510639	PRJNA336433	2015	Australia	Resistant (*vanB*)
AUSMDU00004305 SRX1998595	SAMN05510640	PRJNA336433	2015	Australia	Resistant (*vanB*)
AUSMDU00004309 SRX1998596	SAMN05510641	PRJNA336433	2015	Australia	Resistant (*vanB*)
AUSMDU00004310 SRX1998597	SAMN05510642	PRJNA336433	2015	Australia	Resistant (*vanB*)
AUSMDU00004313 SRX1998598	SAMN05510643	PRJNA336433	2015	Australia	Resistant (*vanB*)
AUSMDU00004315 SRX1998599	SAMN05510644	PRJNA336433	2015	Australia	Resistant (*vanB*)
AUSMDU00004319 SRX1998600	SAMN05510645	PRJNA336433	2015	Australia	Resistant (*vanB*)
AUSMDU00004321 SRX1998601	SAMN05510646	PRJNA336433	2015	Australia	Resistant (*vanB*)
AUS0009 SRX2193697	SAMN05831040	PRJNA342552	2000	Australia	Resistant (*vanA*)
AUS0026 SRX2193709	SAMN05831042	PRJNA342552	2005	Australia	Susceptible
AUS0043 SRX2193732	SAMN05831044	PRJNA342552	2006	Australia	Susceptible
AUS0156 SRX2193743	SAMN05831045	PRJNA342552	2011	Australia	Susceptible
AUS0158 SRX2193747	SAMN05831046	PRJNA342552	2011	Australia	Susceptible
AUS0203 SRX2193749	SAMN05831048	PRJNA342552	2011	Australia	Resistant (*vanB*)
AUS0205 SRX2193750	SAMN05831049	PRJNA342552	2011	Australia	Susceptible
AUS0206 SRX2193699	SAMN05831050	PRJNA342552	2011	Australia	Susceptible
AUS0217 SRX2193701	SAMN05831052	PRJNA342552	2011	Australia	Susceptible
AUS0224 SRX2193703	SAMN05831054	PRJNA342552	2011	Australia	Susceptible
AUS0226 SRX2193704	SAMN05831055	PRJNA342552	2011	Australia	Susceptible
AUS0227 SRX2193705	SAMN05831056	PRJNA342552	2011	Australia	Resistant (*vanB*)
AUS0229 SRX2193707	SAMN05831058	PRJNA342552	2011	Australia	Resistant (*vanB*)
AUS0231 SRX2193708	SAMN05831059	PRJNA342552	2011	Australia	Resistant (*vanB*)
AUS0235 SRX2193710	SAMN05831060	PRJNA342552	2012	Australia	Resistant (*vanB*)

Table 2 continued overleaf

Sample ID	Sample Accession	Study Accession	Collection Date	Country of Isolation	Predicted vancomycin susceptibility[1]
AUS0236 SRX2193711	SAMN05831061	PRJNA342552	2012	Australia	Susceptible
AUS0237 SRX2193712	SAMN05831062	PRJNA342552	2012	Australia	Resistant (*vanB*)
AUS0245 SRX2193714	SAMN05831064	PRJNA342552	2012	Australia	Resistant (*vanB*)
AUS0247 SRX2193716	SAMN05831066	PRJNA342552	2012	Australia	Susceptible
AUS0248 SRX2193717	SAMN05831067	PRJNA342552	2012	Australia	Susceptible
AUS0249 SRX2193718	SAMN05831068	PRJNA342552	2012	Australia	Resistant (*vanB*)
AUS0251 SRX2193720	SAMN05831069	PRJNA342552	2012	Australia	Susceptible
AUS0252 SRX2193722	SAMN05831070	PRJNA342552	2012	Australia	Resistant (*vanB*)
AUS0253 SRX2193723	SAMN05831071	PRJNA342552	2012	Australia	Resistant (*vanB*)
AUS0255 SRX2193724	SAMN05831072	PRJNA342552	2013	Australia	Susceptible
AUS0256 SRX2193725	SAMN05831073	PRJNA342552	2013	Australia	Susceptible
AUS0259 SRX2193726	SAMN05831074	PRJNA342552	2013	Australia	Susceptible
AUS0260 SRX2193727	SAMN05831075	PRJNA342552	2013	Australia	Susceptible
AUS0261 SRX2193728	SAMN05831076	PRJNA342552	2013	Australia	Resistant (*vanB*)
AUS0263 SRX2193730	SAMN05831078	PRJNA342552	2013	Australia	Susceptible
AUS0316 SRX2193734	SAMN05831081	PRJNA342552	2013	Australia	Resistant (*vanB*)
AUS0701 SRX2193735	SAMN05831082	PRJNA342552	2014	Australia	Resistant (*vanB*)
AUS0705 SRX2193736	SAMN05831083	PRJNA342552	2014	Australia	Susceptible
AUS0728 SRX2193737	SAMN05831084	PRJNA342552	2014	Australia	Susceptible
AUS0732 SRX2193739	SAMN05831086	PRJNA342552	2014	Australia	Susceptible
AUS0733 SRX2193740	SAMN05831087	PRJNA342552	2014	Australia	Resistant (*vanB*)
AUS0735 SRX2193741	SAMN05831088	PRJNA342552	2014	Australia	Susceptible
AUS0736 SRX2193742	SAMN05831089	PRJNA342552	2015	Australia	Susceptible

Table 2 continued overleaf

Sample ID	Sample Accession	Study Accession	Collection Date	Country of Isolation	Predicted vancomycin susceptibility[1]
AUS0737 SRX2193744	SAMN05831090	PRJNA342552	2015	Australia	Resistant (*vanB*)
AUS0738 SRX2193745	SAMN05831091	PRJNA342552	2015	Australia	Resistant (*vanA*)
AUS0741 SRX2193746	SAMN05831092	PRJNA342552	2015	Australia	Resistant (*vanB*)
E0008 SRX8457633	SAMN15088040	PRJNA636894	2011	Spain	Susceptible
E0009 SRX8457644	SAMN15088041	PRJNA636894	2004	Spain	Susceptible
E0010 SRX8457655	SAMN15088042	PRJNA636894	2012	Spain	Susceptible
E0011 SRX8457347	SAMN15088043	PRJNA636894	2012	Spain	Susceptible
E0012 SRX8457358	SAMN15088044	PRJNA636894	2006	Spain	Susceptible
E0013 SRX8457369	SAMN15088045	PRJNA636894	2008	Spain	Susceptible
E0014 SRX8457380	SAMN15088046	PRJNA636894	2009	Spain	Susceptible
E0018 SRX8457424	SAMN15088050	PRJNA636894	2010	Spain	Susceptible
E0019 SRX8457435	SAMN15088051	PRJNA636894	2010	Spain	Susceptible
E0020 SRX8457446	SAMN15088052	PRJNA636894	2011	Spain	Susceptible
E0027 SRX8457524	SAMN15088059	PRJNA636894	2010	Spain	Susceptible
E0028 SRX8457535	SAMN15088060	PRJNA636894	2010	Spain	Susceptible
E0029 SRX8457546	SAMN15088061	PRJNA636894	2011	Spain	Resistant (*vanB*)
E0030 SRX8457557	SAMN15088062	PRJNA636894	2010	Spain	Susceptible
E0031 SRX8457569	SAMN15088063	PRJNA636894	2011	Spain	Resistant (*vanB*)
E0032 SRX8457580	SAMN15088064	PRJNA636894	2009	Spain	Susceptible
E0037 SRX8457596	SAMN15088069	PRJNA636894	2009	Spain	Susceptible
E0038 SRX8457597	SAMN15088070	PRJNA636894	2002	Portugal	Resistant (*vanA*)
E0039 SRX8457598	SAMN15088071	PRJNA636894	2004	Australia	Resistant (*vanB*)
E0040 SRX8457599	SAMN15088072	PRJNA636894	1997	Australia	Resistant (*vanA*)

Table 2 continued overleaf

Sample ID	Sample Accession	Study Accession	Collection Date	Country of Isolation	Predicted vancomycin susceptibility[1]
E0041 SRX8457601	SAMN15088073	PRJNA636894	2000	Argentina	Resistant (*vanA*)
E0042 SRX8457602	SAMN15088074	PRJNA636894	1992	USA	Resistant (*vanA*)
E0043 SRX8457603	SAMN15088075	PRJNA636894	1997	Argentina	Resistant (*vanA*)
E0044 SRX8457604	SAMN15088076	PRJNA636894	2009	Spain	Resistant (*vanA*)
E0045 SRX8457605	SAMN15088077	PRJNA636894	1996	Finland	Resistant (*vanA*)
E0046 SRX8457606	SAMN15088078	PRJNA636894	2003	Spain	Resistant (*vanA*)
E0047 SRX8457607	SAMN15088079	PRJNA636894	2000	Saudi Arabia	Resistant (*vanA*)
E0048 SRX8457608	SAMN15088080	PRJNA636894	2003	Tunisia	Resistant (*vanA*)
E0049 SRX8457609	SAMN15088081	PRJNA636894	Unknown	Brazil	Resistant (*vanA*)
E0050 SRX8457610	SAMN15088082	PRJNA636894	1991	USA	Resistant (*vanB*)
E0051 SRX8457612	SAMN15088083	PRJNA636894	2004	Spain	Resistant (*vanB*)
E0052 SRX8457613	SAMN15088084	PRJNA636894	2005	Spain	Resistant (*vanB*)
E0053 SRX8457614	SAMN15088085	PRJNA636894	2006	Spain	Resistant (*vanB*)
E0054 SRX8457615	SAMN15088086	PRJNA636894	2004	Spain	Resistant (*vanB*)
E0055 SRX8457616	SAMN15088087	PRJNA636894	2005	Poland	Resistant (*vanA*)
E0056 SRX8457617	SAMN15088088	PRJNA636894	2006	Germany	Resistant (*vanA*)
E0057 SRX8457618	SAMN15088089	PRJNA636894	2002	Italy	Resistant (*vanB*)
E0058 SRX8457619	SAMN15088090	PRJNA636894	2000	Saudi Arabia	Resistant (*vanA*)
E0059 SRX8457620	SAMN15088091	PRJNA636894	Unknown	Portugal	Resistant (*vanA*)
E0060 SRX8457621	SAMN15088092	PRJNA636894	2005	Denmark	Resistant (*vanA*)
E0061 SRX8457623	SAMN15088093	PRJNA636894	2005	Poland	Resistant (*vanA*)
E0062 SRX8457624	SAMN15088094	PRJNA636894	2003	Chile	Resistant (*vanB*)
E0063 SRX8457625	SAMN15088095	PRJNA636894	2004	Chile	Resistant (*vanB*)

Table 2 continued overleaf

Sample ID	Sample Accession	Study Accession	Collection Date	Country of Isolation	Predicted vancomycin susceptibility[1]
E0064 SRX8457626	SAMN15088096	PRJNA636894	1999	Portugal	Resistant (*vanA*)
E0065 SRX8457627	SAMN15088097	PRJNA636894	2002	Portugal	Resistant (*vanA*)
E0066 SRX8457628	SAMN15088098	PRJNA636894	2001	Australia	Resistant (*vanB*)
E0067 SRX8457629	SAMN15088099	PRJNA636894	1998	Argentina	Resistant (*vanA*)
E0068 SRX8457630	SAMN15088100	PRJNA636894	2001	Italy	Resistant (*vanA*)
E0069 SRX8457631	SAMN15088101	PRJNA636894	2005	Spain	Resistant (*vanA*)
E0070 SRX8457632	SAMN15088102	PRJNA636894	2006	Spain	Resistant (*vanA*)
E0071 SRX8457634	SAMN15088103	PRJNA636894	2005	Paraguay	Resistant (*vanA*)
E0072 SRX8457635	SAMN15088104	PRJNA636894	1998	Germany	Resistant (*vanA*)
E0073 SRX8457636	SAMN15088105	PRJNA636894	2008	Spain	Resistant (*vanA*)
E0074 SRX8457637	SAMN15088106	PRJNA636894	2004	Germany	Resistant (*vanA*)
E0075 SRX8457638	SAMN15088107	PRJNA636894	2004	USA	Resistant (*vanA*)
E0076 SRX8457639	SAMN15088108	PRJNA636894	2005	Germany	Resistant (*vanA*)
E0077 SRX8457640	SAMN15088109	PRJNA636894	2005	Denmark	Resistant (*vanB*)
E0079 SRX8457642	SAMN15088111	PRJNA636894	2005	Canada	Resistant (*vanA*)
E0080 SRX8457643	SAMN15088112	PRJNA636894	2006	Paraguay	Resistant (*vanA*)
E0082 SRX8457646	SAMN15088114	PRJNA636894	Unknown	Brazil	Resistant (*vanA*)
E0084 SRX8457648	SAMN15088116	PRJNA636894	1998	Spain	Resistant (*vanB*)
E0085 SRX8457649	SAMN15088117	PRJNA636894	1996	Finland	Resistant (*vanB*)
E0086 SRX8457650	SAMN15088118	PRJNA636894	2002	Spain	Resistant (*vanB*)
E0087 SRX8457651	SAMN15088119	PRJNA636894	2005	Spain	Resistant (*vanA*)
E0088 SRX8457652	SAMN15088120	PRJNA636894	Unknown	Spain	Susceptible
E0089 SRX8457653	SAMN15088121	PRJNA636894	2005	Spain	Resistant (*vanA*)

Table 2 continued overleaf

Sample ID	Sample Accession	Study Accession	Collection Date	Country of Isolation	Predicted vancomycin susceptibility[1]
E0090 SRX8457654	SAMN15088122	PRJNA636894	2005	Spain	Resistant (*vanA*)
E0091 SRX8457656	SAMN15088123	PRJNA636894	2009	Spain	Resistant (*vanA*)
E0092 SRX8457657	SAMN15088124	PRJNA636894	2003	Spain	Resistant (*vanB*)
E0093 SRX8457658	SAMN15088125	PRJNA636894	2004	Spain	Resistant (*vanB*)
E0094 SRX8457659	SAMN15088126	PRJNA636894	1999	Spain	Resistant (*vanA*)
E0095 SRX8457660	SAMN15088127	PRJNA636894	2005	Spain	Resistant (*vanA*)
E0249 SRX8457661	SAMN15088128	PRJNA636894	2015	Denmark	Resistant (*vanA*)
E0271 SRX8457662	SAMN15088129	PRJNA636894	2014	Denmark	Resistant (*vanA*)
E0303 SRX8457664	SAMN15088131	PRJNA636894	2013	Denmark	Susceptible
E0312 SRX8457350	SAMN15088135	PRJNA636894	2013	Denmark	Susceptible
E0327 SRX8457356	SAMN15088141	PRJNA636894	2013	Denmark	Susceptible
E0329 SRX8457359	SAMN15088143	PRJNA636894	2015	Denmark	Resistant (*vanA*)
E0330 SRX8457360	SAMN15088144	PRJNA636894	2015	Denmark	Resistant (*vanA*)
E0332 SRX8457361	SAMN15088145	PRJNA636894	2015	Denmark	Resistant (*vanA*)
E0333 SRX8457362	SAMN15088146	PRJNA636894	2015	Denmark	Resistant (*vanA*)
E0337 SRX8457363	SAMN15088147	PRJNA636894	2015	Denmark	Resistant (*vanA*)
E0341 SRX8457364	SAMN15088148	PRJNA636894	2015	Denmark	Resistant (*vanA*)
E0342 SRX8457365	SAMN15088149	PRJNA636894	2015	Denmark	Resistant (*vanB*)
E0345 SRX8457366	SAMN15088150	PRJNA636894	2015	Denmark	Resistant (*vanA*)
E0347 SRX8457367	SAMN15088151	PRJNA636894	2015	Denmark	Resistant (*vanA*)
E0352 SRX8457368	SAMN15088152	PRJNA636894	2015	Denmark	Resistant (*vanA*)
E0354 SRX8457370	SAMN15088153	PRJNA636894	2015	Denmark	Resistant (*vanA*)
E0356 SRX8457371	SAMN15088154	PRJNA636894	2015	Denmark	Resistant (*vanA*)

Table 2 continued overleaf

Sample ID	Sample Accession	Study Accession	Collection Date	Country of Isolation	Predicted vancomycin susceptibility[1]
E0358 SRX8457372	SAMN15088155	PRJNA636894	2015	Denmark	Resistant (*vanA*)
E0363 SRX8457373	SAMN15088156	PRJNA636894	2012	Norway	Susceptible
E0365 SRX8457374	SAMN15088157	PRJNA636894	2014	Norway	Susceptible
E0366 SRX8457375	SAMN15088158	PRJNA636894	2012	Norway	Susceptible
E0367 SRX8457376	SAMN15088159	PRJNA636894	2015	Norway	Susceptible
E0372 SRX8457379	SAMN15088162	PRJNA636894	2015	Norway	Susceptible
E0373 SRX8457381	SAMN15088163	PRJNA636894	2015	Norway	Resistant (*vanB*)
E0374 SRX8457382	SAMN15088164	PRJNA636894	2015	Norway	Resistant (*vanB*)
E0375 SRX8457383	SAMN15088165	PRJNA636894	2015	Norway	Resistant (*vanB*)
E0376 SRX8457384	SAMN15088166	PRJNA636894	2015	Norway	Resistant (*vanB*)
E0544 SRX8457386	SAMN15088168	PRJNA636894	1997	Israel	Resistant (*vanA*)
E0546 SRX8457387	SAMN15088169	PRJNA636894	Unknown	Italy	Susceptible
E0558 SRX8457392	SAMN15088173	PRJNA636894	2001	Tanzania	Susceptible
E0562 SRX8457394	SAMN15088175	PRJNA636894	2005	Hungary	Resistant (*vanA*)
E0773 SRX8457404	SAMN15088184	PRJNA636894	1998	Brazil	Susceptible
E0774 SRX8457405	SAMN15088185	PRJNA636894	2001	Tanzania	Susceptible
E0777 SRX8457408	SAMN15088188	PRJNA636894	2001	Tanzania	Susceptible
E0778 SRX8457409	SAMN15088189	PRJNA636894	2001	Tanzania	Susceptible
E0884 SRX8457411	SAMN15088191	PRJNA636894	2016	Germany	Susceptible
E0885 SRX8457412	SAMN15088192	PRJNA636894	2016	Germany	Resistant (*vanA*)
E0887 SRX8457415	SAMN15088194	PRJNA636894	2016	Germany	Resistant (*vanB*)
E0888 SRX8457416	SAMN15088195	PRJNA636894	2016	Germany	Resistant (*vanB*)
E0889 SRX8457417	SAMN15088196	PRJNA636894	2016	Germany	Resistant (*vanA*)

Table 2 continued overleaf

Sample ID	Sample Accession	Study Accession	Collection Date	Country of Isolation	Predicted vancomycin susceptibility[1]
E0890 SRX8457418	SAMN15088197	PRJNA636894	2016	Germany	Resistant (*vanA*)
E0891 SRX8457419	SAMN15088198	PRJNA636894	2016	Germany	Resistant (*vanB*)
E0892 SRX8457420	SAMN15088199	PRJNA636894	2016	Germany	Resistant (*vanB*)
E0893 SRX8457421	SAMN15088200	PRJNA636894	2016	Germany	Resistant (*vanB*)
E0894 SRX8457422	SAMN15088201	PRJNA636894	2016	Germany	Resistant (*vanB*)
E0895 SRX8457423	SAMN15088202	PRJNA636894	2016	Germany	Resistant (*vanA*)
E0897 SRX8457426	SAMN15088204	PRJNA636894	2016	Germany	Resistant (*vanB*)
E0899 SRX8457428	SAMN15088206	PRJNA636894	2016	Germany	Resistant (*vanB*)
E0900 SRX8457429	SAMN15088207	PRJNA636894	2016	Germany	Resistant (*vanB*)
E0901 SRX8457430	SAMN15088208	PRJNA636894	2016	Germany	Resistant (*vanB*)
E0902 SRX8457431	SAMN15088209	PRJNA636894	2016	Germany	Resistant (*vanB*)
E0903 SRX8457432	SAMN15088210	PRJNA636894	2016	Germany	Resistant (*vanB*)
E0904 SRX8457433	SAMN15088211	PRJNA636894	2016	Germany	Resistant (*vanB*)
E0905 SRX8457434	SAMN15088212	PRJNA636894	2016	Germany	Susceptible
E0906 SRX8457436	SAMN15088213	PRJNA636894	2016	Germany	Susceptible
E0907 SRX8457437	SAMN15088214	PRJNA636894	2016	Germany	Susceptible
E0908 SRX8457438	SAMN15088215	PRJNA636894	2016	Germany	Resistant (*vanB*)
E0909 SRX8457439	SAMN15088216	PRJNA636894	2016	Germany	Resistant (*vanB*)
E0910 SRX8457440	SAMN15088217	PRJNA636894	2016	Germany	Resistant (*vanA*)
E0912 SRX8457442	SAMN15088219	PRJNA636894	2016	Germany	Resistant (*vanA*)
E0913 SRX8457443	SAMN15088220	PRJNA636894	2016	Germany	Resistant (*vanA*)
E0914 SRX8457444	SAMN15088221	PRJNA636894	2016	Germany	Resistant (*vanA*)
E0915 SRX8457445	SAMN15088222	PRJNA636894	2016	Germany	Resistant (*vanB*)

Table 2 continued overleaf

Sample ID	Sample Accession	Study Accession	Collection Date	Country of Isolation	Predicted vancomycin susceptibility[1]
E0916 SRX8457447	SAMN15088223	PRJNA636894	2016	Germany	Susceptible
E0917 SRX8457448	SAMN15088224	PRJNA636894	2016	Germany	Resistant (*vanB*)
E0918 SRX8457449	SAMN15088225	PRJNA636894	2016	Germany	Resistant (*vanB*)
E0919 SRX8457450	SAMN15088226	PRJNA636894	2016	Germany	Resistant (*vanA*)
E0920 SRX8457451	SAMN15088227	PRJNA636894	2016	Germany	Resistant (*vanB*)
E0921 SRX8457452	SAMN15088228	PRJNA636894	2016	Germany	Resistant (*vanB*)
E0922 SRX8457453	SAMN15088229	PRJNA636894	2016	Germany	Resistant (*vanA*)
E0923 SRX8457454	SAMN15088230	PRJNA636894	2016	Germany	Resistant (*vanB*)
E0924 SRX8457455	SAMN15088231	PRJNA636894	2016	Germany	Resistant (*vanB*)
E0927 SRX8457460	SAMN15088234	PRJNA636894	2016	Germany	Resistant (*vanB*)
E0929 SRX8457462	SAMN15088236	PRJNA636894	2016	Germany	Resistant (*vanB*)
E0931 SRX8457464	SAMN15088238	PRJNA636894	2016	Germany	Resistant (*vanB*)
E0932 SRX8457465	SAMN15088239	PRJNA636894	2016	Germany	Susceptible
E0933 SRX8457466	SAMN15088240	PRJNA636894	2016	Germany	Resistant (*vanB*)
E0934 SRX8457467	SAMN15088241	PRJNA636894	2016	Germany	Resistant (*vanB*)
E0935 SRX8457468	SAMN15088242	PRJNA636894	2016	Germany	Resistant (*vanB*)
E0936 SRX8457470	SAMN15088243	PRJNA636894	2016	Germany	Resistant (*vanB*)
E0939 SRX8457473	SAMN15088246	PRJNA636894	2016	Germany	Susceptible
E0940 SRX8457474	SAMN15088247	PRJNA636894	2016	Germany	Resistant (*vanB*)
E0941 SRX8457475	SAMN15088248	PRJNA636894	2016	Germany	Resistant (*vanB*)
E0942 SRX8457476	SAMN15088249	PRJNA636894	2016	Germany	Resistant (*vanB*)
E0943 SRX8457477	SAMN15088250	PRJNA636894	2016	Germany	Susceptible
E0944 SRX8457478	SAMN15088251	PRJNA636894	2014	Japan	Susceptible

Table 2 continued overleaf

Sample ID	Sample Accession	Study Accession	Collection Date	Country of Isolation	Predicted vancomycin susceptibility[1]
E0947 SRX8457482	SAMN15088254	PRJNA636894	2014	Japan	Susceptible
E0948 SRX8457483	SAMN15088255	PRJNA636894	2014	Japan	Susceptible
E0949 SRX8457484	SAMN15088256	PRJNA636894	2014	Japan	Susceptible
E0951 SRX8457486	SAMN15088258	PRJNA636894	2014	Japan	Susceptible
E0952 SRX8457487	SAMN15088259	PRJNA636894	2014	Japan	Susceptible
E0953 SRX8457488	SAMN15088260	PRJNA636894	2014	Japan	Susceptible
E0954 SRX8457489	SAMN15088261	PRJNA636894	2014	Japan	Susceptible
E0955 SRX8457490	SAMN15088262	PRJNA636894	2014	Japan	Susceptible
E0956 SRX8457492	SAMN15088263	PRJNA636894	2014	Japan	Susceptible
E0958 SRX8457494	SAMN15088265	PRJNA636894	2014	Japan	Susceptible
E0959 SRX8457495	SAMN15088266	PRJNA636894	2014	Japan	Susceptible
E0960 SRX8457496	SAMN15088267	PRJNA636894	2014	Japan	Susceptible
E0961 SRX8457497	SAMN15088268	PRJNA636894	2014	Japan	Susceptible
E0962 SRX8457498	SAMN15088269	PRJNA636894	2014	Japan	Susceptible
E0963 SRX8457499	SAMN15088270	PRJNA636894	2014	Japan	Susceptible
E0964 SRX8457500	SAMN15088271	PRJNA636894	2014	Japan	Susceptible
E0965 SRX8457501	SAMN15088272	PRJNA636894	2014	Japan	Susceptible
E0966 SRX8457503	SAMN15088273	PRJNA636894	2014	Japan	Susceptible
E0968 SRX8457505	SAMN15088275	PRJNA636894	2014	Japan	Susceptible
E0969 SRX8457506	SAMN15088276	PRJNA636894	2014	Japan	Susceptible
E0970 SRX8457507	SAMN15088277	PRJNA636894	2014	Japan	Susceptible
E0971 SRX8457508	SAMN15088278	PRJNA636894	2014	Japan	Susceptible
E0972 SRX8457509	SAMN15088279	PRJNA636894	2014	Japan	Susceptible

Table 2 continued overleaf

Sample ID	Sample Accession	Study Accession	Collection Date	Country of Isolation	Predicted vancomycin susceptibility[1]
E0973 SRX8457510	SAMN15088280	PRJNA636894	2014	Japan	Susceptible
E0974 SRX8457511	SAMN15088281	PRJNA636894	2014	Japan	Susceptible
E0976 SRX8457514	SAMN15088283	PRJNA636894	2014	Japan	Susceptible
E0977 SRX8457515	SAMN15088284	PRJNA636894	2014	Japan	Susceptible
E0979 SRX8457517	SAMN15088286	PRJNA636894	2014	Japan	Susceptible
E0980 SRX8457518	SAMN15088287	PRJNA636894	2014	Japan	Susceptible
E0981 SRX8457519	SAMN15088288	PRJNA636894	2014	Japan	Susceptible
E0982 SRX8457520	SAMN15088289	PRJNA636894	2014	Japan	Susceptible
E0983 SRX8457521	SAMN15088290	PRJNA636894	2014	Japan	Susceptible
E0984 SRX8457522	SAMN15088291	PRJNA636894	2014	Japan	Susceptible
E0985 SRX8457523	SAMN15088292	PRJNA636894	2014	Japan	Susceptible
E0986 SRX8457525	SAMN15088293	PRJNA636894	2014	Japan	Susceptible
E0987 SRX8457526	SAMN15088294	PRJNA636894	2014	Japan	Susceptible
E0988 SRX8457527	SAMN15088295	PRJNA636894	2014	Japan	Susceptible
E0989 SRX8457528	SAMN15088296	PRJNA636894	2014	Japan	Susceptible
E0990 SRX8457529	SAMN15088297	PRJNA636894	2014	Japan	Susceptible
E0991 SRX8457530	SAMN15088298	PRJNA636894	2014	Japan	Susceptible
E0993 SRX8457532	SAMN15088300	PRJNA636894	2014	Japan	Susceptible
E0994 SRX8457533	SAMN15088301	PRJNA636894	2014	Japan	Susceptible
E0995 SRX8457534	SAMN15088302	PRJNA636894	2014	Japan	Susceptible
E0996 SRX8457536	SAMN15088303	PRJNA636894	2014	Japan	Susceptible
E0998 SRX8457538	SAMN15088305	PRJNA636894	2014	Japan	Susceptible
E0999 SRX8457539	SAMN15088306	PRJNA636894	2014	Japan	Susceptible

Table 2 continued overleaf

Sample ID	Sample Accession	Study Accession	Collection Date	Country of Isolation	Predicted vancomycin susceptibility[1]
E1000 SRX8457540	SAMN15088307	PRJNA636894	2014	Japan	Susceptible
E1001 SRX8457541	SAMN15088308	PRJNA636894	2014	Japan	Susceptible
E1002 SRX8457542	SAMN15088309	PRJNA636894	2014	Japan	Susceptible
E1003 SRX8457543	SAMN15088310	PRJNA636894	2014	Japan	Susceptible
E1004 SRX8457544	SAMN15088311	PRJNA636894	2014	Japan	Susceptible
E1007 SRX8457548	SAMN15088314	PRJNA636894	2014	Japan	Susceptible
E1008 SRX8457549	SAMN15088315	PRJNA636894	2014	Japan	Susceptible
E1009 SRX8457550	SAMN15088316	PRJNA636894	2014	Japan	Susceptible
E1010 SRX8457551	SAMN15088317	PRJNA636894	2014	Japan	Susceptible
E1011 SRX8457552	SAMN15088318	PRJNA636894	2014	Japan	Susceptible
E1012 SRX8457553	SAMN15088319	PRJNA636894	2014	Japan	Susceptible
E1013 SRX8457554	SAMN15088320	PRJNA636894	2014	Japan	Susceptible
E1014 SRX8457555	SAMN15088321	PRJNA636894	2015	Japan	Susceptible
E1015 SRX8457556	SAMN15088322	PRJNA636894	2015	Japan	Susceptible
E1017 SRX8457559	SAMN15088324	PRJNA636894	2015	Japan	Susceptible
E1018 SRX8457560	SAMN15088325	PRJNA636894	2015	Japan	Susceptible
E1020 SRX8457562	SAMN15088327	PRJNA636894	2015	Japan	Susceptible
E1021 SRX8457563	SAMN15088328	PRJNA636894	2015	Japan	Susceptible
E1022 SRX8457564	SAMN15088329	PRJNA636894	2015	Japan	Susceptible
E1023 SRX8457565	SAMN15088330	PRJNA636894	2015	Japan	Susceptible
E1024 SRX8457566	SAMN15088331	PRJNA636894	2015	Japan	Susceptible
E1025 SRX8457567	SAMN15088332	PRJNA636894	2015	Japan	Susceptible
E1026 SRX8457570	SAMN15088333	PRJNA636894	2015	Japan	Susceptible

Table 2 continued overleaf

Sample ID	Sample Accession	Study Accession	Collection Date	Country of Isolation	Predicted vancomycin susceptibility[1]
E1027 SRX8457571	SAMN15088334	PRJNA636894	2015	Japan	Susceptible
E1028 SRX8457572	SAMN15088335	PRJNA636894	2015	Japan	Susceptible
E1029 SRX8457573	SAMN15088336	PRJNA636894	2015	Japan	Susceptible
E1030 SRX8457574	SAMN15088337	PRJNA636894	2015	Japan	Susceptible
E1032 SRX8457576	SAMN15088339	PRJNA636894	2015	Japan	Susceptible
E1034 SRX8457578	SAMN15088341	PRJNA636894	2015	Japan	Susceptible
E1035 SRX8457579	SAMN15088342	PRJNA636894	2015	Japan	Susceptible
E1037 SRX8457582	SAMN15088344	PRJNA636894	2015	Japan	Susceptible
E1038 SRX8457583	SAMN15088345	PRJNA636894	2015	Japan	Susceptible
E1041 SRX8457586	SAMN15088348	PRJNA636894	2012	Belgium	Resistant (*vanA*)
E1057 SRX8457587	SAMN15088349	PRJNA636894	2014	Belgium	Resistant (*vanB*)
E1101 SRX8457592	SAMN15088353	PRJNA636894	2007	Belgium	Susceptible
BSAC_ec1016	ERR375078	PRJEB4344	2005	United Kingdom	Susceptible
BSAC_ec1031	ERR375046	PRJEB4344	2005	United Kingdom	Resistant (*vanA*)
BSAC_ec1032	ERR374834	PRJEB4344	2005	United Kingdom	Resistant (*vanB*)
BSAC_ec1033	ERR374832	PRJEB4344	2005	United Kingdom	Resistant (*vanB*)
BSAC_ec1034	ERR375056	PRJEB4344	2005	United Kingdom	Resistant (*vanA*)
BSAC_ec1057	ERR375258	PRJEB4344	2005	United Kingdom	Susceptible
BSAC_ec1061	ERR375033	PRJEB4344	2005	United Kingdom	Resistant (*vanB*)
BSAC_ec1063	ERR374856	PRJEB4344	2005	United Kingdom	Susceptible
BSAC_ec1065	ERR375100	PRJEB4344	2005	United Kingdom	Resistant (*vanB*)
BSAC_ec1066	ERR375165	PRJEB4344	2005	United Kingdom	Susceptible
BSAC_ec1067	ERR374966	PRJEB4344	2005	United Kingdom	Susceptible

Table 2 continued overleaf

Sample ID	Sample Accession	Study Accession	Collection Date	Country of Isolation	Predicted vancomycin susceptibility[1]
BSAC_ec1071	ERR375017	PRJEB4344	2005	United Kingdom	Resistant (*vanA*)
BSAC_ec1072	ERR374857	PRJEB4344	2005	United Kingdom	Resistant (*vanA*)
BSAC_ec1073	ERR374947	PRJEB4344	2005	United Kingdom	Resistant (*vanA*)
BSAC_ec1074	ERR374673	PRJEB4344	2005	United Kingdom	Resistant (*vanA*)
BSAC_ec1075	ERR375086	PRJEB4344	2005	United Kingdom	Resistant (*vanA*)
BSAC_ec1076	ERR375016	PRJEB4344	2005	United Kingdom	Resistant (*vanA*)
BSAC_ec1077	ERR375062	PRJEB4344	2005	United Kingdom	Resistant (*vanA*)
BSAC_ec1081	ERR375278	PRJEB4344	2005	United Kingdom	Susceptible
BSAC_ec1085	ERR375256	PRJEB4344	2005	United Kingdom	Susceptible
BSAC_ec1090	ERR375050	PRJEB4344	2005	United Kingdom	Resistant (*vanA*)
BSAC_ec1098	ERR374988	PRJEB4344	2005	United Kingdom	Resistant (*vanA*)
BSAC_ec1103	ERR374791	PRJEB4344	2005	United Kingdom	Susceptible
BSAC_ec1106	ERR375006	PRJEB4344	2005	United Kingdom	Susceptible
BSAC_ec1111	ERR374854	PRJEB4344	2005	United Kingdom	Susceptible
BSAC_ec1112	ERR375012	PRJEB4344	2005	United Kingdom	Susceptible
BSAC_ec1116	ERR374680	PRJEB4344	2005	United Kingdom	Susceptible
BSAC_ec1119	ERR374943	PRJEB4344	2005	United Kingdom	Susceptible
BSAC_ec1123	ERR375157	PRJEB4344	2005	United Kingdom	Resistant (*vanA*)
BSAC_ec1137	ERR375169	PRJEB4344	2005	United Kingdom	Resistant (*vanB*)
BSAC_ec1140	ERR374970	PRJEB4344	2005	United Kingdom	Susceptible
BSAC_ec1142	ERR374989	PRJEB4344	2005	United Kingdom	Resistant (*vanA*)
BSAC_ec1144	ERR375023	PRJEB4344	2005	United Kingdom	Resistant (*vanA*)
BSAC_ec1146	ERR374942	PRJEB4344	2005	United Kingdom	Susceptible

Table 2 continued overleaf

Sample ID	Sample Accession	Study Accession	Collection Date	Country of Isolation	Predicted vancomycin susceptibility[1]
BSAC_ec1148	ERR375099	PRJEB4344	2005	United Kingdom	Resistant (*vanA*)
BSAC_ec1150	ERR375083	PRJEB4344	2005	United Kingdom	Susceptible
BSAC_ec1153	ERR375246	PRJEB4344	2005	United Kingdom	Resistant (*vanA*)
BSAC_ec1154	ERR374923	PRJEB4344	2005	United Kingdom	Susceptible
BSAC_ec1161	ERR374737	PRJEB4344	2005	United Kingdom	Resistant (*vanA*)
BSAC_ec1162	ERR374876	PRJEB4344	2005	United Kingdom	Resistant (*vanA*)
BSAC_ec1163	ERR375203	PRJEB4344	2005	United Kingdom	Resistant (*vanA*)
BSAC_ec1167	ERR374689	PRJEB4344	2005	United Kingdom	Resistant (*vanA*)
BSAC_ec1168	ERR375002	PRJEB4344	2005	United Kingdom	Susceptible
BSAC_ec1177	ERR375029	PRJEB4344	2005	United Kingdom	Susceptible
BSAC_ec1179	ERR374732	PRJEB4344	2005	United Kingdom	Resistant (*vanA*)
BSAC_ec1180	ERR374664	PRJEB4344	2005	United Kingdom	Resistant (*vanA*)
BSAC_ec1201	ERR374823	PRJEB4344	2005	United Kingdom	Resistant (*vanA*)
BSAC_ec1203	ERR374929	PRJEB4344	2005	United Kingdom	Susceptible
BSAC_ec1205	ERR374660	PRJEB4344	2005	United Kingdom	Resistant (*vanA*)
BSAC_ec1207	ERR375044	PRJEB4344	2005	United Kingdom	Resistant (*vanA*)
BSAC_ec1212	ERR374705	PRJEB4344	2005	United Kingdom	Susceptible
BSAC_ec1217	ERR375121	PRJEB4344	2005	United Kingdom	Susceptible
BSAC_ec1223	ERR375173	PRJEB4344	2005	United Kingdom	Susceptible
BSAC_ec1227	ERR375089	PRJEB4344	2005	United Kingdom	Resistant (*vanA*)
BSAC_ec1231	ERR375255	PRJEB4344	2005	United Kingdom	Resistant (*vanA*)
BSAC_ec1234	ERR374771	PRJEB4344	2005	United Kingdom	Susceptible
BSAC_ec1241	ERR374882	PRJEB4344	2005	United Kingdom	Resistant (*vanA*)

Table 2 continued overleaf

Sample ID	Sample Accession	Study Accession	Collection Date	Country of Isolation	Predicted vancomycin susceptibility[1]
BSAC_ec1242	ERR374879	PRJEB4344	2005	United Kingdom	Resistant (*vanA*)
BSAC_ec1244	ERR374913	PRJEB4344	2005	United Kingdom	Susceptible
BSAC_ec1245	ERR375111	PRJEB4344	2005	United Kingdom	Susceptible
BSAC_ec1248	ERR375009	PRJEB4344	2005	United Kingdom	Susceptible
BSAC_ec1250	ERR375082	PRJEB4344	2005	United Kingdom	Resistant (*vanA*)
BSAC_ec1267	ERR375060	PRJEB4344	2006	United Kingdom	Susceptible
BSAC_ec1272	ERR375163	PRJEB4344	2006	United Kingdom	Susceptible
BSAC_ec1281	ERR375014	PRJEB4344	2006	United Kingdom	Resistant (*vanA*)
BSAC_ec1286	ERR375053	PRJEB4344	2006	United Kingdom	Susceptible
BSAC_ec1287	ERR375168	PRJEB4344	2006	United Kingdom	Susceptible
BSAC_ec1288	ERR375066	PRJEB4344	2006	United Kingdom	Resistant (*vanA*)
BSAC_ec1301	ERR374992	PRJEB4344	2006	United Kingdom	Susceptible
BSAC_ec1307	ERR374810	PRJEB4344	2006	United Kingdom	Resistant (*vanB*)
BSAC_ec1310	ERR374964	PRJEB4344	2006	United Kingdom	Resistant (*vanA*)
BSAC_ec1313	ERR374848	PRJEB4344	2006	United Kingdom	Resistant (*vanA*)
BSAC_ec1322	ERR374820	PRJEB4344	2006	United Kingdom	Resistant (*vanA*)
BSAC_ec1324	ERR375011	PRJEB4344	2006	United Kingdom	Resistant (*vanB*)
BSAC_ec1325	ERR374721	PRJEB4344	2006	United Kingdom	Resistant (*vanA*)
BSAC_ec1326	ERR374668	PRJEB4344	2006	United Kingdom	Resistant (*vanA*)
BSAC_ec1327	ERR375219	PRJEB4344	2006	United Kingdom	Resistant (*vanA*)
BSAC_ec1331	ERR388687	PRJEB4344	2006	United Kingdom	Resistant (*vanA*)
BSAC_ec1338	ERR374676	PRJEB4344	2006	United Kingdom	Susceptible
BSAC_ec1339	ERR374831	PRJEB4344	2006	United Kingdom	Susceptible

Table 2 continued overleaf

Sample ID	Sample Accession	Study Accession	Collection Date	Country of Isolation	Predicted vancomycin susceptibility[1]
BSAC_ec1340	ERR374769	PRJEB4344	2006	United Kingdom	Susceptible
BSAC_ec1349	ERR374974	PRJEB4344	2006	United Kingdom	Susceptible
BSAC_ec1352	ERR375124	PRJEB4344	2006	United Kingdom	Susceptible
BSAC_ec1353	ERR375070	PRJEB4344	2006	United Kingdom	Resistant (*vanA*)
BSAC_ec1356	ERR374933	PRJEB4344	2006	United Kingdom	Resistant (*vanA*)
BSAC_ec1357	ERR374774	PRJEB4344	2006	United Kingdom	Resistant (*vanA*)
BSAC_ec1358	ERR375081	PRJEB4344	2006	United Kingdom	Resistant (*vanA*)
BSAC_ec1359	ERR374663	PRJEB4344	2006	United Kingdom	Resistant (*vanA*)
BSAC_ec1361	ERR374751	PRJEB4344	2006	United Kingdom	Resistant (*vanA*)
BSAC_ec1369	ERR374744	PRJEB4344	2006	United Kingdom	Susceptible
BSAC_ec1382	ERR388696	PRJEB4344	2006	United Kingdom	Resistant (*vanA*)
BSAC_ec1388	ERR375037	PRJEB4344	2006	United Kingdom	Susceptible
BSAC_ec1392	ERR374779	PRJEB4344	2006	United Kingdom	Susceptible
BSAC_ec1394	ERR374833	PRJEB4344	2006	United Kingdom	Resistant (*vanA*)
BSAC_ec1395	ERR374743	PRJEB4344	2006	United Kingdom	Susceptible
BSAC_ec1399	ERR374805	PRJEB4344	2006	United Kingdom	Resistant (*vanA*)
BSAC_ec1406	ERR374939	PRJEB4344	2006	United Kingdom	Susceptible
BSAC_ec1416	ERR374977	PRJEB4344	2006	United Kingdom	Susceptible
BSAC_ec142	ERR374861	PRJEB4344	2001	United Kingdom	Resistant (*vanA*)
BSAC_ec1426	ERR374953	PRJEB4344	2006	United Kingdom	Resistant (*vanA*)
BSAC_ec143	ERR374863	PRJEB4344	2001	United Kingdom	Susceptible
BSAC_ec1430	ERR374696	PRJEB4344	2006	United Kingdom	Susceptible
BSAC_ec1439	ERR374851	PRJEB4344	2006	United Kingdom	Susceptible

Table 2 continued overleaf

Sample ID	Sample Accession	Study Accession	Collection Date	Country of Isolation	Predicted vancomycin susceptibility[1]
BSAC_ec144	ERR375276	PRJEB4344	2001	United Kingdom	Susceptible
BSAC_ec1451	ERR375001	PRJEB4344	2006	United Kingdom	Resistant (*vanA*)
BSAC_ec1452	ERR374811	PRJEB4344	2006	United Kingdom	Susceptible
BSAC_ec1454	ERR374725	PRJEB4344	2006	United Kingdom	Susceptible
BSAC_ec1455	ERR374829	PRJEB4344	2006	United Kingdom	Susceptible
BSAC_ec1483	ERR374962	PRJEB4344	2006	United Kingdom	Susceptible
BSAC_ec1484	ERR374754	PRJEB4344	2006	United Kingdom	Susceptible
BSAC_ec1485	ERR375268	PRJEB4344	2006	United Kingdom	Resistant (*vanA*)
BSAC_ec1489	ERR375188	PRJEB4344	2006	United Kingdom	Susceptible
BSAC_ec1491	ERR375167	PRJEB4344	2006	United Kingdom	Resistant (*vanA*)
BSAC_ec1496	ERR374875	PRJEB4344	2006	United Kingdom	Resistant (*vanA*)
BSAC_ec1497	ERR375130	PRJEB4344	2006	United Kingdom	Susceptible
BSAC_ec1498	ERR375019	PRJEB4344	2006	United Kingdom	Resistant (*vanA*)
BSAC_ec15	ERR374741	PRJEB4344	2001	United Kingdom	Susceptible
BSAC_ec1512	ERR375232	PRJEB4344	2007	United Kingdom	Resistant (*vanA*)
BSAC_ec1514	ERR374938	PRJEB4344	2007	United Kingdom	Susceptible
BSAC_ec1563	ERR374931	PRJEB4344	2007	United Kingdom	Susceptible
BSAC_ec1565	ERR374949	PRJEB4344	2007	United Kingdom	Resistant (*vanA*)
BSAC_ec1568	ERR374738	PRJEB4344	2007	United Kingdom	Resistant (*vanA*)
BSAC_ec1570	ERR375226	PRJEB4344	2007	United Kingdom	Susceptible
BSAC_ec1572	ERR374690	PRJEB4344	2007	United Kingdom	Resistant (*vanA*)
BSAC_ec1576	ERR375080	PRJEB4344	2007	United Kingdom	Resistant (*vanA*)
BSAC_ec1577	ERR375036	PRJEB4344	2007	United Kingdom	Resistant (*vanA*)

Table 2 continued overleaf

Sample ID	Sample Accession	Study Accession	Collection Date	Country of Isolation	Predicted vancomycin susceptibility[1]
BSAC_ec1582	ERR375178	PRJEB4344	2007	United Kingdom	Susceptible
BSAC_ec1589	ERR375286	PRJEB4344	2007	United Kingdom	Resistant (*vanA*)
BSAC_ec1602	ERR375273	PRJEB4344	2007	United Kingdom	Resistant (*vanA*)
BSAC_ec1603	ERR375015	PRJEB4344	2007	United Kingdom	Resistant (*vanA*)
BSAC_ec1608	ERR374683	PRJEB4344	2007	United Kingdom	Susceptible
BSAC_ec1609	ERR388688	PRJEB4344	2007	United Kingdom	Resistant (*vanA*)
BSAC_ec1618	ERR374956	PRJEB4344	2007	United Kingdom	Susceptible
BSAC_ec162	ERR374733	PRJEB4344	2001	United Kingdom	Resistant (*vanA*)
BSAC_ec1621	ERR375156	PRJEB4344	2007	United Kingdom	Resistant (*vanA*)
BSAC_ec1626	ERR374918	PRJEB4344	2007	United Kingdom	Susceptible
BSAC_ec1628	ERR374912	PRJEB4344	2007	United Kingdom	Susceptible
BSAC_ec1629	ERR374926	PRJEB4344	2007	United Kingdom	Resistant (*vanA*)
BSAC_ec163	ERR374885	PRJEB4344	2001	United Kingdom	Susceptible
BSAC_ec1651	ERR374849	PRJEB4344	2007	United Kingdom	Resistant (*vanA*)
BSAC_ec1653	ERR375257	PRJEB4344	2007	United Kingdom	Susceptible
BSAC_ec1658	ERR374945	PRJEB4344	2007	United Kingdom	Susceptible
BSAC_ec1660	ERR388689	PRJEB4344	2007	United Kingdom	Susceptible
BSAC_ec1662	ERR375288	PRJEB4344	2007	United Kingdom	Resistant (*vanA*)
BSAC_ec1666	ERR375250	PRJEB4344	2007	United Kingdom	Susceptible
BSAC_ec1671	ERR375264	PRJEB4344	2007	United Kingdom	Susceptible
BSAC_ec1684	ERR374784	PRJEB4344	2007	United Kingdom	Resistant (*vanB*)
BSAC_ec1687	ERR374719	PRJEB4344	2007	United Kingdom	Susceptible
BSAC_ec1688	ERR375241	PRJEB4344	2007	United Kingdom	Resistant (*vanB*)

Table 2 continued overleaf

Sample ID	Sample Accession	Study Accession	Collection Date	Country of Isolation	Predicted vancomycin susceptibility[1]
BSAC_ec1693	ERR375274	PRJEB4344	2007	United Kingdom	Susceptible
BSAC_ec1694	ERR374679	PRJEB4344	2007	United Kingdom	Susceptible
BSAC_ec1699	ERR388690	PRJEB4344	2007	United Kingdom	Resistant (*vanB*)
BSAC_ec1701	ERR375251	PRJEB4344	2007	United Kingdom	Susceptible
BSAC_ec1702	ERR374777	PRJEB4344	2007	United Kingdom	Susceptible
BSAC_ec1703	ERR375007	PRJEB4344	2007	United Kingdom	Susceptible
BSAC_ec1706	ERR374793	PRJEB4344	2007	United Kingdom	Resistant (*vanA*)
BSAC_ec1707	ERR375088	PRJEB4344	2007	United Kingdom	Resistant (*vanA*)
BSAC_ec1708	ERR375072	PRJEB4344	2007	United Kingdom	Resistant (*vanA*)
BSAC_ec1715	ERR388691	PRJEB4344	2007	United Kingdom	Susceptible
BSAC_ec1717	ERR388692	PRJEB4344	2007	United Kingdom	Resistant (*vanA*)
BSAC_ec1723	ERR375270	PRJEB4344	2007	United Kingdom	Susceptible
BSAC_ec1725	ERR388693	PRJEB4344	2007	United Kingdom	Susceptible
BSAC_ec1729	ERR375003	PRJEB4344	2007	United Kingdom	Resistant (*vanA*)
BSAC_ec1732	ERR374995	PRJEB4344	2007	United Kingdom	Susceptible
BSAC_ec1746	ERR375028	PRJEB4344	2007	United Kingdom	Resistant (*vanA*)
BSAC_ec1801	ERR375057	PRJEB4344	2008	United Kingdom	Susceptible
BSAC_ec1802	ERR374969	PRJEB4344	2008	United Kingdom	Susceptible
BSAC_ec1806	ERR375040	PRJEB4344	2008	United Kingdom	Resistant (*vanA*)
BSAC_ec1809	ERR375041	PRJEB4344	2008	United Kingdom	Susceptible
BSAC_ec1814	ERR374967	PRJEB4344	2008	United Kingdom	Susceptible
BSAC_ec1815	ERR374787	PRJEB4344	2008	United Kingdom	Susceptible
BSAC_ec1821	ERR375151	PRJEB4344	2008	United Kingdom	Resistant (*vanA*)

Table 2 continued overleaf

Sample ID	Sample Accession	Study Accession	Collection Date	Country of Isolation	Predicted vancomycin susceptibility[1]
BSAC_ec1822	ERR374884	PRJEB4344	2008	United Kingdom	Resistant (*vanA*)
BSAC_ec1824	ERR375183	PRJEB4344	2008	United Kingdom	Resistant (*vanA*)
BSAC_ec1825	ERR375271	PRJEB4344	2008	United Kingdom	Susceptible
BSAC_ec1829	ERR375253	PRJEB4344	2008	United Kingdom	Resistant (*vanA*)
BSAC_ec1840	ERR374959	PRJEB4344	2008	United Kingdom	Susceptible
BSAC_ec1902	ERR374887	PRJEB4344	2008	United Kingdom	Resistant (*vanA*)
BSAC_ec1903	ERR375284	PRJEB4344	2008	United Kingdom	Resistant (*vanA*)
BSAC_ec1906	ERR375138	PRJEB4344	2008	United Kingdom	Susceptible
BSAC_ec1908	ERR374776	PRJEB4344	2008	United Kingdom	Resistant (*vanA*)
BSAC_ec1910	ERR374864	PRJEB4344	2008	United Kingdom	Susceptible
BSAC_ec1935	ERR374703	PRJEB4344	2008	United Kingdom	Susceptible
BSAC_ec1937	ERR375140	PRJEB4344	2008	United Kingdom	Susceptible
BSAC_ec1949	ERR374815	PRJEB4344	2008	United Kingdom	Resistant (*vanA*)
BSAC_ec1951	ERR375048	PRJEB4344	2008	United Kingdom	Resistant (*vanA*)
BSAC_ec1952	ERR374866	PRJEB4344	2008	United Kingdom	Resistant (*vanA*)
BSAC_ec1971	ERR374674	PRJEB4344	2008	United Kingdom	Resistant (*vanA*)
BSAC_ec1972	ERR375277	PRJEB4344	2008	United Kingdom	Susceptible
BSAC_ec1973	ERR374836	PRJEB4344	2008	United Kingdom	Susceptible
BSAC_ec1984	ERR375022	PRJEB4344	2008	United Kingdom	Susceptible
BSAC_ec1993	ERR374991	PRJEB4344	2008	United Kingdom	Susceptible
BSAC_ec1997	ERR374731	PRJEB4344	2008	United Kingdom	Resistant (*vanA*)
BSAC_ec1998	ERR374752	PRJEB4344	2008	United Kingdom	Susceptible
BSAC_ec2000	ERR374702	PRJEB4344	2008	United Kingdom	Resistant (*vanA*)

Table 2 continued overleaf

Sample ID	Sample Accession	Study Accession	Collection Date	Country of Isolation	Predicted vancomycin susceptibility[1]
BSAC_ec2004	ERR375049	PRJEB4344	2009	United Kingdom	Susceptible
BSAC_ec2006	ERR375209	PRJEB4344	2009	United Kingdom	Resistant (*vanA*)
BSAC_ec2008	ERR374914	PRJEB4344	2009	United Kingdom	Resistant (*vanA*)
BSAC_ec2009	ERR374968	PRJEB4344	2009	United Kingdom	Resistant (*vanA*)
BSAC_ec2034	ERR374909	PRJEB4344	2009	United Kingdom	Resistant (*vanA*)
BSAC_ec2036	ERR375030	PRJEB4344	2009	United Kingdom	Susceptible
BSAC_ec2037	ERR374919	PRJEB4344	2009	United Kingdom	Susceptible
BSAC_ec2041	ERR375174	PRJEB4344	2009	United Kingdom	Susceptible
BSAC_ec2043	ERR375170	PRJEB4344	2009	United Kingdom	Susceptible
BSAC_ec2044	ERR374813	PRJEB4344	2009	United Kingdom	Susceptible
BSAC_ec2048	ERR375280	PRJEB4344	2009	United Kingdom	Resistant (*vanA*)
BSAC_ec2050	ERR375195	PRJEB4344	2009	United Kingdom	Susceptible
BSAC_ec2054	ERR374958	PRJEB4344	2009	United Kingdom	Resistant (*vanA*)
BSAC_ec2061	ERR374797	PRJEB4344	2009	United Kingdom	Resistant (*vanA*)
BSAC_ec2062	ERR375024	PRJEB4344	2009	United Kingdom	Resistant (*vanA*)
BSAC_ec2065	ERR374973	PRJEB4344	2009	United Kingdom	Resistant (*vanA*)
BSAC_ec2070	ERR374727	PRJEB4344	2009	United Kingdom	Resistant (*vanA*)
BSAC_ec2071	ERR375025	PRJEB4344	2009	United Kingdom	Resistant (*vanA*)
BSAC_ec2074	ERR374808	PRJEB4344	2009	United Kingdom	Susceptible
BSAC_ec2075	ERR374950	PRJEB4344	2009	United Kingdom	Susceptible
BSAC_ec2076	ERR374934	PRJEB4344	2009	United Kingdom	Resistant (*vanA*)
BSAC_ec2077	ERR374740	PRJEB4344	2009	United Kingdom	Resistant (*vanA*)
BSAC_ec2078	ERR375199	PRJEB4344	2009	United Kingdom	Resistant (*vanA*)

Table 2 continued overleaf

Sample ID	Sample Accession	Study Accession	Collection Date	Country of Isolation	Predicted vancomycin susceptibility[1]
BSAC_ec2080	ERR374961	PRJEB4344	2009	United Kingdom	Susceptible
BSAC_ec2084	ERR375026	PRJEB4344	2009	United Kingdom	Susceptible
BSAC_ec2085	ERR375224	PRJEB4344	2009	United Kingdom	Susceptible
BSAC_ec2087	ERR374993	PRJEB4344	2009	United Kingdom	Resistant (*vanA*)
BSAC_ec2090	ERR375260	PRJEB4344	2009	United Kingdom	Resistant (*vanA*)
BSAC_ec2101	ERR375079	PRJEB4344	2009	United Kingdom	Resistant (*vanA*)
BSAC_ec2114	ERR374723	PRJEB4344	2009	United Kingdom	Susceptible
BSAC_ec2124	ERR375071	PRJEB4344	2009	United Kingdom	Resistant (*vanA*)
BSAC_ec2125	ERR375087	PRJEB4344	2009	United Kingdom	Susceptible
BSAC_ec2127	ERR375091	PRJEB4344	2009	United Kingdom	Susceptible
BSAC_ec2129	ERR374895	PRJEB4344	2009	United Kingdom	Resistant (*vanA*)
BSAC_ec2133	ERR374972	PRJEB4344	2009	United Kingdom	Susceptible
BSAC_ec2149	ERR374979	PRJEB4344	2009	United Kingdom	Resistant (*vanA*)
BSAC_ec2150	ERR374963	PRJEB4344	2009	United Kingdom	Susceptible
BSAC_ec2155	ERR375217	PRJEB4344	2009	United Kingdom	Susceptible
BSAC_ec2183	ERR375227	PRJEB4344	2009	United Kingdom	Resistant (*vanB*)
BSAC_ec2184	ERR375215	PRJEB4344	2009	United Kingdom	Resistant (*vanA*)
BSAC_ec2194	ERR375248	PRJEB4344	2009	United Kingdom	Susceptible
BSAC_ec2198	ERR374807	PRJEB4344	2009	United Kingdom	Resistant (*vanA*)
BSAC_ec2201	ERR375281	PRJEB4344	2009	United Kingdom	Resistant (*vanA*)
BSAC_ec2204	ERR375027	PRJEB4344	2009	United Kingdom	Resistant (*vanA*)
BSAC_ec2210	ERR375018	PRJEB4344	2009	United Kingdom	Resistant (*vanB*)
BSAC_ec222	ERR374951	PRJEB4344	2001	United Kingdom	Susceptible

Table 2 continued overleaf

Sample ID	Sample Accession	Study Accession	Collection Date	Country of Isolation	Predicted vancomycin susceptibility[1]
BSAC_ec2220	ERR374889	PRJEB4344	2009	United Kingdom	Susceptible
BSAC_ec223	ERR374880	PRJEB4344	2001	United Kingdom	Resistant (*vanA*)
BSAC_ec224	ERR374998	PRJEB4344	2001	United Kingdom	Resistant (*vanA*)
BSAC_ec225	ERR375064	PRJEB4344	2001	United Kingdom	Resistant (*vanA*)
BSAC_ec2259	ERR374883	PRJEB4344	2010	United Kingdom	Susceptible
BSAC_ec2268	ERR374761	PRJEB4344	2010	United Kingdom	Susceptible
BSAC_ec227	ERR374688	PRJEB4344	2001	United Kingdom	Susceptible
BSAC_ec2271	ERR374940	PRJEB4344	2010	United Kingdom	Resistant (*vanA*)
BSAC_ec2281	ERR374837	PRJEB4344	2010	United Kingdom	Resistant (*vanA*)
BSAC_ec2284	ERR374753	PRJEB4344	2010	United Kingdom	Susceptible
BSAC_ec2285	ERR375285	PRJEB4344	2010	United Kingdom	Resistant (*vanA*)
BSAC_ec2286	ERR374910	PRJEB4344	2010	United Kingdom	Resistant (*vanA*)
BSAC_ec2288	ERR374760	PRJEB4344	2010	United Kingdom	Resistant (*vanA*)
BSAC_ec229	ERR374739	PRJEB4344	2001	United Kingdom	Resistant (*vanA*)
BSAC_ec2290	ERR374794	PRJEB4344	2010	United Kingdom	Resistant (*vanA*)
BSAC_ec2293	ERR374868	PRJEB4344	2010	United Kingdom	Resistant (*vanA*)
BSAC_ec2294	ERR375272	PRJEB4344	2010	United Kingdom	Susceptible
BSAC_ec2298	ERR375160	PRJEB4344	2010	United Kingdom	Resistant (*vanB*)
BSAC_ec2299	ERR375134	PRJEB4344	2010	United Kingdom	Susceptible
BSAC_ec2300	ERR375107	PRJEB4344	2010	United Kingdom	Resistant (*vanA*)
BSAC_ec2306	ERR374693	PRJEB4344	2010	United Kingdom	Resistant (*vanA*)
BSAC_ec2308	ERR374764	PRJEB4344	2010	United Kingdom	Resistant (*vanA*)
BSAC_ec2310	ERR374799	PRJEB4344	2010	United Kingdom	Susceptible

Table 2 continued overleaf

Sample ID	Sample Accession	Study Accession	Collection Date	Country of Isolation	Predicted vancomycin susceptibility[1]
BSAC_ec2311	ERR374800	PRJEB4344	2010	United Kingdom	Susceptible
BSAC_ec2312	ERR375074	PRJEB4344	2010	United Kingdom	Susceptible
BSAC_ec2314	ERR374735	PRJEB4344	2010	United Kingdom	Resistant (*vanA*)
BSAC_ec2318	ERR374694	PRJEB4344	2010	United Kingdom	Susceptible
BSAC_ec2329	ERR374685	PRJEB4344	2010	United Kingdom	Susceptible
BSAC_ec2334	ERR375177	PRJEB4344	2010	United Kingdom	Resistant (*vanA*)
BSAC_ec2335	ERR375143	PRJEB4344	2010	United Kingdom	Resistant (*vanA*)
BSAC_ec2338	ERR375135	PRJEB4344	2010	United Kingdom	Susceptible
BSAC_ec2340	ERR374982	PRJEB4344	2010	United Kingdom	Resistant (*vanA*)
BSAC_ec2341	ERR375031	PRJEB4344	2010	United Kingdom	Susceptible
BSAC_ec2346	ERR374921	PRJEB4344	2010	United Kingdom	Resistant (*vanA*)
BSAC_ec2351	ERR375231	PRJEB4344	2010	United Kingdom	Resistant (*vanA*)
BSAC_ec2352	ERR375090	PRJEB4344	2010	United Kingdom	Susceptible
BSAC_ec2353	ERR375042	PRJEB4344	2010	United Kingdom	Susceptible
BSAC_ec2355	ERR375136	PRJEB4344	2010	United Kingdom	Resistant (*vanA*)
BSAC_ec2356	ERR374952	PRJEB4344	2010	United Kingdom	Susceptible
BSAC_ec2357	ERR375193	PRJEB4344	2010	United Kingdom	Resistant (*vanA*)
BSAC_ec2364	ERR374986	PRJEB4344	2010	United Kingdom	Susceptible
BSAC_ec2365	ERR375076	PRJEB4344	2010	United Kingdom	Resistant (*vanA*)
BSAC_ec2380	ERR375179	PRJEB4344	2010	United Kingdom	Susceptible
BSAC_ec2382	ERR375158	PRJEB4344	2010	United Kingdom	Resistant (*vanA*)
BSAC_ec239	ERR374681	PRJEB4344	2001	United Kingdom	Susceptible
BSAC_ec2396	ERR374915	PRJEB4344	2010	United Kingdom	Resistant (*vanA*)

Table 2 continued overleaf

Sample ID	Sample Accession	Study Accession	Collection Date	Country of Isolation	Predicted vancomycin susceptibility[1]
BSAC_ec2409	ERR375161	PRJEB4344	2010	United Kingdom	Resistant (*vanA*)
BSAC_ec241	ERR374870	PRJEB4344	2001	United Kingdom	Resistant (*vanA*)
BSAC_ec2411	ERR375287	PRJEB4344	2010	United Kingdom	Susceptible
BSAC_ec242	ERR374976	PRJEB4344	2001	United Kingdom	Susceptible
BSAC_ec2420	ERR375238	PRJEB4344	2010	United Kingdom	Susceptible
BSAC_ec2441	ERR374925	PRJEB4344	2010	United Kingdom	Susceptible
BSAC_ec2442	ERR375182	PRJEB4344	2010	United Kingdom	Susceptible
BSAC_ec2443	ERR374990	PRJEB4344	2010	United Kingdom	Resistant (*vanA*)
BSAC_ec2444	ERR374905	PRJEB4344	2010	United Kingdom	Susceptible
BSAC_ec2446	ERR374789	PRJEB4344	2010	United Kingdom	Resistant (*vanB*)
BSAC_ec245	ERR374840	PRJEB4344	2001	United Kingdom	Resistant (*vanA*)
BSAC_ec246	ERR374742	PRJEB4344	2001	United Kingdom	Susceptible
BSAC_ec2482	ERR374697	PRJEB4344	2010	United Kingdom	Resistant (*vanA*)
BSAC_ec2484	ERR374944	PRJEB4344	2010	United Kingdom	Susceptible
BSAC_ec2485	ERR375162	PRJEB4344	2010	United Kingdom	Susceptible
BSAC_ec2486	ERR375204	PRJEB4344	2010	United Kingdom	Resistant (*vanA*)
BSAC_ec2496	ERR375265	PRJEB4344	2010	United Kingdom	Resistant (*vanA*)
BSAC_ec2498	ERR374726	PRJEB4344	2010	United Kingdom	Susceptible
BSAC_ec2499	ERR374686	PRJEB4344	2010	United Kingdom	Susceptible
BSAC_ec2500	ERR374920	PRJEB4344	2010	United Kingdom	Resistant (*vanA*)
BSAC_ec2502	ERR374877	PRJEB4344	2010	United Kingdom	Resistant (*vanA*)
BSAC_ec2503	ERR375092	PRJEB4344	2010	United Kingdom	Resistant (*vanA*)
BSAC_ec251	ERR374767	PRJEB4344	2002	United Kingdom	Resistant (*vanA*)

Table 2 continued overleaf

Sample ID	Sample Accession	Study Accession	Collection Date	Country of Isolation	Predicted vancomycin susceptibility[1]
BSAC_ec2511	ERR374941	PRJEB4344	2010	United Kingdom	Susceptible
BSAC_ec2513	ERR374978	PRJEB4344	2010	United Kingdom	Resistant (*vanA*)
BSAC_ec2515	ERR375145	PRJEB4344	2010	United Kingdom	Resistant (*vanA*)
BSAC_ec2516	ERR375137	PRJEB4344	2010	United Kingdom	Susceptible
BSAC_ec2529	ERR374718	PRJEB4344	2010	United Kingdom	Resistant (*vanA*)
BSAC_ec2532	ERR375097	PRJEB4344	2011	United Kingdom	Resistant (*vanB*)
BSAC_ec2535	ERR374927	PRJEB4344	2011	United Kingdom	Resistant (*vanA*)
BSAC_ec2559	ERR375120	PRJEB4344	2011	United Kingdom	Susceptible
BSAC_ec256	ERR374881	PRJEB4344	2002	United Kingdom	Susceptible
BSAC_ec2561	ERR375118	PRJEB4344	2011	United Kingdom	Resistant (*vanA*)
BSAC_ec2562	ERR374806	PRJEB4344	2011	United Kingdom	Susceptible
BSAC_ec2565	ERR375133	PRJEB4344	2011	United Kingdom	Resistant (*vanB*)
BSAC_ec2566	ERR374916	PRJEB4344	2011	United Kingdom	Resistant (*vanA*)
BSAC_ec2569	ERR375093	PRJEB4344	2011	United Kingdom	Susceptible
BSAC_ec2570	ERR375005	PRJEB4344	2011	United Kingdom	Resistant (*vanA*)
BSAC_ec2572	ERR375129	PRJEB4344	2011	United Kingdom	Resistant (*vanA*)
BSAC_ec2573	ERR375155	PRJEB4344	2011	United Kingdom	Susceptible
BSAC_ec2575	ERR375095	PRJEB4344	2011	United Kingdom	Resistant (*vanA*)
BSAC_ec2577	ERR374955	PRJEB4344	2011	United Kingdom	Resistant (*vanA*)
BSAC_ec2578	ERR375147	PRJEB4344	2011	United Kingdom	Resistant (*vanA*)
BSAC_ec2579	ERR374756	PRJEB4344	2011	United Kingdom	Resistant (*vanA*)
BSAC_ec2594	ERR375008	PRJEB4344	2011	United Kingdom	Susceptible
BSAC_ec2596	ERR374798	PRJEB4344	2011	United Kingdom	Resistant (*vanA*)

Table 2 continued overleaf

Sample ID	Sample Accession	Study Accession	Collection Date	Country of Isolation	Predicted vancomycin susceptibility[1]
BSAC_ec2597	ERR375164	PRJEB4344	2011	United Kingdom	Resistant (*vanA*)
BSAC_ec2599	ERR375149	PRJEB4344	2011	United Kingdom	Resistant (*vanA*)
BSAC_ec2600	ERR375154	PRJEB4344	2011	United Kingdom	Susceptible
BSAC_ec2610	ERR374835	PRJEB4344	2011	United Kingdom	Resistant (*vanA*)
BSAC_ec2611	ERR375192	PRJEB4344	2011	United Kingdom	Resistant (*vanA*)
BSAC_ec2614	ERR388694	PRJEB4344	2011	United Kingdom	Susceptible
BSAC_ec2622	ERR374928	PRJEB4344	2011	United Kingdom	Susceptible
BSAC_ec2629	ERR375240	PRJEB4344	2011	United Kingdom	Resistant (*vanA*)
BSAC_ec263	ERR374826	PRJEB4344	2002	United Kingdom	Susceptible
BSAC_ec2631	ERR375085	PRJEB4344	2011	United Kingdom	Susceptible
BSAC_ec2632	ERR375194	PRJEB4344	2011	United Kingdom	Susceptible
BSAC_ec2633	ERR374821	PRJEB4344	2011	United Kingdom	Resistant (*vanA*)
BSAC_ec2641	ERR374692	PRJEB4344	2011	United Kingdom	Susceptible
BSAC_ec2644	ERR374828	PRJEB4344	2011	United Kingdom	Susceptible
BSAC_ec2647	ERR374701	PRJEB4344	2011	United Kingdom	Resistant (*vanA*)
BSAC_ec265	ERR374728	PRJEB4344	2002	United Kingdom	Susceptible
BSAC_ec2660	ERR375247	PRJEB4344	2011	United Kingdom	Susceptible
BSAC_ec2668	ERR374865	PRJEB4344	2011	United Kingdom	Susceptible
BSAC_ec2685	ERR375039	PRJEB4344	2011	United Kingdom	Resistant (*vanA*)
BSAC_ec2690	ERR374922	PRJEB4344	2011	United Kingdom	Resistant (*vanA*)
BSAC_ec2700	ERR374763	PRJEB4344	2011	United Kingdom	Susceptible
BSAC_ec2701	ERR375131	PRJEB4344	2011	United Kingdom	Resistant (*vanA*)
BSAC_ec2708	ERR375013	PRJEB4344	2011	United Kingdom	Susceptible

Table 2 continued overleaf

Sample ID	Sample Accession	Study Accession	Collection Date	Country of Isolation	Predicted vancomycin susceptibility[1]
BSAC_ec2727	ERR375254	PRJEB4344	2011	United Kingdom	Resistant (*vanB*)
BSAC_ec2729	ERR375208	PRJEB4344	2011	United Kingdom	Susceptible
BSAC_ec2731	ERR375051	PRJEB4344	2011	United Kingdom	Susceptible
BSAC_ec2732	ERR374899	PRJEB4344	2011	United Kingdom	Resistant (*vanA*)
BSAC_ec2733	ERR374746	PRJEB4344	2011	United Kingdom	Resistant (*vanA*)
BSAC_ec2742	ERR374724	PRJEB4344	2011	United Kingdom	Susceptible
BSAC_ec2744	ERR374894	PRJEB4344	2011	United Kingdom	Resistant (*vanA*)
BSAC_ec2745	ERR374770	PRJEB4344	2011	United Kingdom	Resistant (*vanA*)
BSAC_ec2750	ERR375077	PRJEB4344	2011	United Kingdom	Susceptible
BSAC_ec2755	ERR375214	PRJEB4344	2011	United Kingdom	Susceptible
BSAC_ec2759	ERR375245	PRJEB4344	2011	United Kingdom	Resistant (*vanA*)
BSAC_ec2761	ERR375216	PRJEB4344	2011	United Kingdom	Susceptible
BSAC_ec2783	ERR374675	PRJEB4344	2011	United Kingdom	Susceptible
BSAC_ec2791	ERR375243	PRJEB4344	2011	United Kingdom	Susceptible
BSAC_ec289	ERR374814	PRJEB4344	2002	United Kingdom	Resistant (*vanA*)
BSAC_ec293	ERR374783	PRJEB4344	2002	United Kingdom	Susceptible
BSAC_ec295	ERR374707	PRJEB4344	2002	United Kingdom	Resistant (*vanA*)
BSAC_ec296	ERR375210	PRJEB4344	2002	United Kingdom	Susceptible
BSAC_ec300	ERR374816	PRJEB4344	2002	United Kingdom	Resistant (*vanA*)
BSAC_ec311	ERR374678	PRJEB4344	2002	United Kingdom	Susceptible
BSAC_ec312	ERR375075	PRJEB4344	2002	United Kingdom	Susceptible
BSAC_ec314	ERR375200	PRJEB4344	2002	United Kingdom	Susceptible
BSAC_ec316	ERR374908	PRJEB4344	2002	United Kingdom	Resistant (*vanA*)

Table 2 continued overleaf

Sample ID	Sample Accession	Study Accession	Collection Date	Country of Isolation	Predicted vancomycin susceptibility[1]
BSAC_ec318	ERR374765	PRJEB4344	2002	United Kingdom	Resistant (*vanA*)
BSAC_ec32	ERR374750	PRJEB4344	2001	United Kingdom	Susceptible
BSAC_ec332	ERR374803	PRJEB4344	2002	United Kingdom	Susceptible
BSAC_ec335	ERR374901	PRJEB4344	2002	United Kingdom	Susceptible
BSAC_ec336	ERR374749	PRJEB4344	2002	United Kingdom	Susceptible
BSAC_ec337	ERR375252	PRJEB4344	2002	United Kingdom	Susceptible
BSAC_ec34	ERR374971	PRJEB4344	2001	United Kingdom	Resistant (*vanA*)
BSAC_ec340	ERR374965	PRJEB4344	2002	United Kingdom	Susceptible
BSAC_ec342	ERR375235	PRJEB4344	2002	United Kingdom	Susceptible
BSAC_ec356	ERR375043	PRJEB4344	2002	United Kingdom	Susceptible
BSAC_ec361	ERR375021	PRJEB4344	2002	United Kingdom	Susceptible
BSAC_ec368	ERR375244	PRJEB4344	2002	United Kingdom	Resistant (*vanA*)
BSAC_ec383a	ERR375218	PRJEB4344	2002	United Kingdom	Resistant (*vanB*)
BSAC_ec384	ERR374804	PRJEB4344	2002	United Kingdom	Susceptible
BSAC_ec391	ERR375207	PRJEB4344	2002	United Kingdom	Susceptible
BSAC_ec411	ERR375073	PRJEB4344	2002	United Kingdom	Resistant (*vanB*)
BSAC_ec421	ERR374796	PRJEB4344	2002	United Kingdom	Susceptible
BSAC_ec426	ERR374669	PRJEB4344	2002	United Kingdom	Susceptible
BSAC_ec472	ERR374957	PRJEB4344	2002	United Kingdom	Susceptible
BSAC_ec474	ERR374786	PRJEB4344	2002	United Kingdom	Resistant (*vanA*)
BSAC_ec476	ERR374759	PRJEB4344	2002	United Kingdom	Susceptible
BSAC_ec479	ERR374772	PRJEB4344	2002	United Kingdom	Resistant (*vanA*)
BSAC_ec493	ERR374842	PRJEB4344	2002	United Kingdom	Susceptible

Table 2 continued overleaf

Sample ID	Sample Accession	Study Accession	Collection Date	Country of Isolation	Predicted vancomycin susceptibility[1]
BSAC_ec494	ERR374871	PRJEB4344	2002	United Kingdom	Susceptible
BSAC_ec495	ERR374844	PRJEB4344	2002	United Kingdom	Resistant (*vanA*)
BSAC_ec514	ERR375101	PRJEB4344	2003	United Kingdom	Resistant (*vanA*)
BSAC_ec516	ERR375067	PRJEB4344	2003	United Kingdom	Susceptible
BSAC_ec519	ERR375283	PRJEB4344	2003	United Kingdom	Resistant (*vanB*)
BSAC_ec531	ERR374859	PRJEB4344	2003	United Kingdom	Susceptible
BSAC_ec533	ERR374890	PRJEB4344	2003	United Kingdom	Resistant (*vanA*)
BSAC_ec537	ERR374682	PRJEB4344	2003	United Kingdom	Resistant (*vanA*)
BSAC_ec538	ERR374987	PRJEB4344	2003	United Kingdom	Resistant (*vanA*)
BSAC_ec547	ERR375069	PRJEB4344	2003	United Kingdom	Susceptible
BSAC_ec548	ERR374671	PRJEB4344	2003	United Kingdom	Resistant (*vanA*)
BSAC_ec562	ERR375279	PRJEB4344	2003	United Kingdom	Resistant (*vanB*)
BSAC_ec565	ERR374745	PRJEB4344	2003	United Kingdom	Susceptible
BSAC_ec566	ERR374845	PRJEB4344	2003	United Kingdom	Resistant (*vanB*)
BSAC_ec570	ERR374847	PRJEB4344	2003	United Kingdom	Susceptible
BSAC_ec577	ERR374812	PRJEB4344	2003	United Kingdom	Susceptible
BSAC_ec578	ERR374830	PRJEB4344	2003	United Kingdom	Susceptible
BSAC_ec582	ERR375213	PRJEB4344	2003	United Kingdom	Susceptible
BSAC_ec587	ERR374827	PRJEB4344	2003	United Kingdom	Resistant (*vanA*)
BSAC_ec603	ERR375032	PRJEB4344	2003	United Kingdom	Susceptible
BSAC_ec604	ERR374843	PRJEB4344	2003	United Kingdom	Susceptible
BSAC_ec650	ERR375055	PRJEB4344	2003	United Kingdom	Susceptible
BSAC_ec66	ERR375063	PRJEB4344	2001	United Kingdom	Resistant (*vanA*)

Table 2 continued overleaf

Sample ID	Sample Accession	Study Accession	Collection Date	Country of Isolation	Predicted vancomycin susceptibility[1]
BSAC_ec667	ERR374937	PRJEB4344	2003	United Kingdom	Resistant (*vanA*)
BSAC_ec668	ERR374907	PRJEB4344	2003	United Kingdom	Susceptible
BSAC_ec67	ERR374898	PRJEB4344	2001	United Kingdom	Resistant (*vanA*)
BSAC_ec673	ERR374873	PRJEB4344	2003	United Kingdom	Susceptible
BSAC_ec675	ERR375230	PRJEB4344	2003	United Kingdom	Susceptible
BSAC_ec676	ERR375201	PRJEB4344	2003	United Kingdom	Resistant (*vanA*)
BSAC_ec68	ERR375266	PRJEB4344	2001	United Kingdom	Resistant (*vanA*)
BSAC_ec680	ERR375035	PRJEB4344	2003	United Kingdom	Resistant (*vanA*)
BSAC_ec698	ERR375106	PRJEB4344	2003	United Kingdom	Resistant (*vanA*)
BSAC_ec71	ERR374897	PRJEB4344	2001	United Kingdom	Susceptible
BSAC_ec72	ERR375052	PRJEB4344	2001	United Kingdom	Resistant (*vanA*)
BSAC_ec725	ERR374762	PRJEB4344	2003	United Kingdom	Resistant (*vanA*)
BSAC_ec728	ERR374911	PRJEB4344	2003	United Kingdom	Resistant (*vanA*)
BSAC_ec73	ERR374792	PRJEB4344	2001	United Kingdom	Susceptible
BSAC_ec730	ERR374860	PRJEB4344	2003	United Kingdom	Susceptible
BSAC_ec739	ERR374734	PRJEB4344	2003	United Kingdom	Susceptible
BSAC_ec747	ERR374886	PRJEB4344	2003	United Kingdom	Susceptible
BSAC_ec748	ERR374722	PRJEB4344	2003	United Kingdom	Resistant (*vanA*)
BSAC_ec752	ERR375109	PRJEB4344	2004	United Kingdom	Resistant (*vanA*)
BSAC_ec754	ERR374714	PRJEB4344	2004	United Kingdom	Susceptible
BSAC_ec781	ERR374994	PRJEB4344	2004	United Kingdom	Susceptible
BSAC_ec782	ERR374755	PRJEB4344	2004	United Kingdom	Susceptible
BSAC_ec786	ERR375122	PRJEB4344	2004	United Kingdom	Susceptible

Table 2 continued overleaf

Sample ID	Sample Accession	Study Accession	Collection Date	Country of Isolation	Predicted vancomycin susceptibility[1]
BSAC_ec787	ERR375148	PRJEB4344	2004	United Kingdom	Susceptible
BSAC_ec79	ERR374867	PRJEB4344	2001	United Kingdom	Resistant (*vanB*)
BSAC_ec790	ERR374824	PRJEB4344	2004	United Kingdom	Susceptible
BSAC_ec80	ERR374855	PRJEB4344	2001	United Kingdom	Susceptible
BSAC_ec809	ERR374670	PRJEB4344	2004	United Kingdom	Resistant (*vanB*)
BSAC_ec814	ERR374924	PRJEB4344	2004	United Kingdom	Susceptible
BSAC_ec816	ERR375153	PRJEB4344	2004	United Kingdom	Susceptible
BSAC_ec819	ERR374930	PRJEB4344	2004	United Kingdom	Susceptible
BSAC_ec822	ERR375112	PRJEB4344	2004	United Kingdom	Resistant (*vanA*)
BSAC_ec823	ERR375114	PRJEB4344	2004	United Kingdom	Resistant (*vanA*)
BSAC_ec824	ERR374662	PRJEB4344	2004	United Kingdom	Resistant (*vanA*)
BSAC_ec827	ERR375105	PRJEB4344	2004	United Kingdom	Resistant (*vanA*)
BSAC_ec828	ERR375128	PRJEB4344	2004	United Kingdom	Susceptible
BSAC_ec832	ERR375187	PRJEB4344	2004	United Kingdom	Resistant (*vanA*)
BSAC_ec833	ERR374778	PRJEB4344	2004	United Kingdom	Susceptible
BSAC_ec835	ERR374698	PRJEB4344	2004	United Kingdom	Resistant (*vanA*)
BSAC_ec837	ERR374713	PRJEB4344	2004	United Kingdom	Resistant (*vanA*)
BSAC_ec852	ERR375094	PRJEB4344	2004	United Kingdom	Susceptible
BSAC_ec860	ERR374838	PRJEB4344	2004	United Kingdom	Susceptible
BSAC_ec871	ERR374917	PRJEB4344	2004	United Kingdom	Susceptible
BSAC_ec893	ERR375150	PRJEB4344	2004	United Kingdom	Susceptible
BSAC_ec902	ERR375146	PRJEB4344	2004	United Kingdom	Resistant (*vanA*)
BSAC_ec903	ERR375116	PRJEB4344	2004	United Kingdom	Susceptible

Table 2 continued overleaf

Sample ID	Sample Accession	Study Accession	Collection Date	Country of Isolation	Predicted vancomycin susceptibility[1]
BSAC_ec908	ERR374729	PRJEB4344	2004	United Kingdom	Resistant (*vanA*)
BSAC_ec909	ERR374809	PRJEB4344	2004	United Kingdom	Susceptible
BSAC_ec911	ERR375206	PRJEB4344	2004	United Kingdom	Susceptible
BSAC_ec917	ERR374782	PRJEB4344	2004	United Kingdom	Susceptible
BSAC_ec926	ERR374902	PRJEB4344	2004	United Kingdom	Susceptible
BSAC_ec929	ERR375144	PRJEB4344	2004	United Kingdom	Resistant (*vanA*)
BSAC_ec951	ERR374954	PRJEB4344	2004	United Kingdom	Resistant (*vanA*)
BSAC_ec956	ERR375172	PRJEB4344	2004	United Kingdom	Resistant (*vanA*)
BSAC_ec958	ERR375142	PRJEB4344	2004	United Kingdom	Resistant (*vanA*)
BSAC_ec959	ERR374780	PRJEB4344	2004	United Kingdom	Susceptible
BSAC_ec960	ERR375152	PRJEB4344	2004	United Kingdom	Resistant (*vanA*)
BSAC_ec967	ERR374850	PRJEB4344	2004	United Kingdom	Susceptible
BSAC_ec982	ERR374936	PRJEB4344	2004	United Kingdom	Susceptible
BSAC_ec986	ERR374893	PRJEB4344	2004	United Kingdom	Resistant (*vanA*)
BSAC_ec987	ERR375229	PRJEB4344	2004	United Kingdom	Resistant (*vanA*)
BSAC_ec994	ERR375010	PRJEB4344	2004	United Kingdom	Susceptible

Adapted from (Raven *et al.*, 2016; van Hal *et al.*, 2021).
Abbreviations: NCBI, National Center for Biotechnology Information.
[1] Vancomycin resistance genotypes were extracted in silico from short-read whole genome sequencing data using ABRicate (https://github.com/tseemann/abricate).

Appendix 2